U.S. DEPARTMENT OF ENERGY

PNNL-22420

Prepared for the U.S. Department of Energy
under Contract DE-AC05-76RL01830

Geochemical Impacts of Leaking CO_2 from Subsurface Storage Reservoirs to Unconfined and Confined Aquifers

NP Qafoku
CF Brown
G Wang
C Sullivan
AR Lawter
OR Harvey
M Bowden

April 2013

Pacific Northwest NATIONAL LABORATORY

Proudly Operated by Battelle Since 1965

PACIFIC NORTHWEST NATIONAL LABORATORY
operated by
BATTELLE
for the
UNITED STATES DEPARTMENT OF ENERGY
under Contract DE-AC05-76RL01830

Printed in the United States of America

Available to DOE and DOE contractors from the
Office of Scientific and Technical Information,
P.O. Box 62, Oak Ridge, TN 37831-0062;
ph: (865) 576-8401
fax: (865) 576-5728
email: reports@adonis.osti.gov

Available to the public from the National Technical Information Service
5301 Shawnee Rd., Alexandria, VA 22312
ph: (800) 553-NTIS (6847)
email: orders@ntis.gov <http://www.ntis.gov/about/form.aspx>
Online ordering: http://www.ntis.gov


This document was printed on recycled paper.
(8/2010)

PNNL-22420

Geochemical Impacts of Leaking CO_2 from Subsurface Storage Reservoirs to Unconfined and Confined Aquifers

NP Qafoku
CF Brown
G Wang
C Sullivan
AR Lawter
M Bowden[1]
OR Harvey[2]

April 2013

Prepared for
the U.S. Department of Energy
under Contract DE-AC05-76RL01830

Pacific Northwest National Laboratory
Richland, Washington 99352

---

[1] Environmental Molecular Science Laboratory, Richland, Washington.
[2] University of Southern Mississippi, Hattiesburg, Mississippi.

Executive Summary

Experimental research work has been conducted and continues at Pacific Northwest National Laboratory (PNNL) to address a variety of scientific issues and impacts related to the potential leakage of carbon dioxide (CO_2) from deep subsurface storage reservoirs. The main objectives of this work are as follows:

- Develop a systematic understanding of how CO_2 leakage is likely to influence pertinent geochemical processes (e.g., dissolution/precipitation, sorption/desorption and redox reactions) in the aquifer sediments.
- Identify prevailing environmental conditions that would dictate one geochemical outcome over another.
- Gather useful information to support site selection, risk assessment, policy-making, and public education efforts associated with geologic carbon sequestration.

In this report, we present results from experiments conducted at PNNL to address research issues related to the main objectives of this effort. A series of batch and column experiments and solid phase characterization studies (quantitative x-ray diffraction and wet chemical extractions with a concentrated acid) were conducted with representative rocks and sediments from an unconfined, oxidizing carbonate aquifer, i.e., the Edwards aquifer in Texas, and a confined aquifer, i.e., the High Plains aquifer in Kansas. These materials were exposed to a CO_2 gas stream to simulate CO_2 gas leakage scenarios, and changes in aqueous phase pH and chemical composition were measured in liquid samples (batch experiments) and effluent samples (column experiments) collected at pre-determined experimental times.

Results from these experimental efforts provide valuable insights for the development of site-specific, third generation reduced order models being developed under the National Risk Assessment Partnership (NRAP) Program. In addition, results will initially serve as input parameters during model calibration runs and, ultimately, will be used to test model predictive capability and competency. The results from these investigations will provide useful information to support site selection, risk assessment, and public education efforts associated with geologic, deep subsurface CO_2 storage and sequestration.

Acknowledgments

The U.S. Department of Energy's (DOE's) Office of Fossil Energy has established the National Risk Assessment Partnership (NRAP) Project. This multiyear project harnesses the breadth of capabilities across the DOE national laboratory system to develop a defensible, science-based quantitative methodology for determining risk profiles at carbon dioxide (CO_2) storage sites. As part of this effort, scientists from Lawrence Berkeley National Laboratory (LBNL), Lawrence Livermore National Laboratory (LLNL), Los Alamos National Laboratory (LANL), Pacific Northwest National Laboratory (PNNL), and the National Energy Technology Laboratory (NETL) are working to evaluate the potential for aquifer impacts should CO_2 or brine leak from deep subsurface storage reservoirs.

The research presented in this report was completed as part of the groundwater protection task of the NRAP Project. NRAP funding was provided to PNNL under DOE contract number DE-AC05-76RL01830.

The sediments samples from the High Plains aquifer in Kansas were provided by the Kansas Geological Survey Drill Core Library. We are grateful to David Laflen, Manager of the Kansas Geological Survey Geological Materials Archive and Laboratory, for his help and support.

The authors wish to thank Jeff Serne for his technical peer review, and Susan Ennor and Kathy Neiderhiser for editorial review and document production.

Acronyms and Abbreviations

°C	degree(s) Celsius
Al	aluminum
As	arsenic
AsFeS	arsenopyrite
Ba	barium
Ca	calcium
Cd	cadmium
cm	centimeter(s)
cm^3	cubic centimeter(s)
CO	carbon monoxide
CO_2	carbon dioxide
Cs	cesium
Cu	copper
DOE	U.S. Department of Energy
EMSL	Environmental Molecular Sciences Laboratory
EPA	U.S. Environmental Protection Agency
EQL	elemental quantification limit
fbg	(foot)feet below ground
Fe	iron
FeS_2	pyrite
g	gram(s)
ICP-MS	inductively coupled plasma mass spectrometry
ICP-OES	inductively coupled plasma optical emission spectrometry
ID	inner diameter
K	potassium
KOH	potassium hydroxide
L	liter(s)
LANL	Los Alamos National Laboratory
LBNL	Lawrence Berkeley National Laboratory
LLNL	Lawrence Livermore National Laboratory µm micron(s)
M	molar
MCL	maximum contaminant level
mg	milligram(s)
Mg	magnesium
min	minute(s)
mL	milliliter(s)

mm	millimeter(s)
mM	millimol
Mn	manganese
Mo	molybdenum
N	nitrogen
Na	sodium
NETL	National Energy Technology Laboratory
Ni	nickel
NRAP	National Risk Assessment Partnership
P	phosphorus
Pb	lead
PbS	galena
PNNL	Pacific Northwest National Laboratory
Pt	platinum
rpm	rotations per minute
S	sulfur
Sb	antimony
Se	selenium
SGW	synthetic groundwater
Si	silicon
SLiMEs	subsurface lithautotrophic microbial ecosystems
Sn	tin
Sr	strontium
TDS	total dissolved solids
USGS	U.S. Geological Survey
XRD	x-ray diffraction
Zn	zinc

Contents

1.0 Introduction

The U.S. Department of Energy's (DOE's) Office of Fossil Energy established the multiyear National Risk Assessment Partnership (NRAP) Project to engage the capabilities of its national laboratory system in developing a defensible, science-based quantitative methodology for determining risk profiles at carbon dioxide (CO_2) storage sites and to evaluate the potential for aquifer impacts if CO_2 or brine leak from deep subsurface storage reservoirs. Research in this area is relatively new and there is no consensus within the scientific community about whether the potential implications of CO_2 leakage from deep subsurface storage reservoirs are a major risk factor in terms of adversely affecting groundwater quality. Ongoing experimental research is being conducted at Pacific Northwest National Laboratory (PNNL) to address a variety of scientific issues related to the potential leakage of CO_2 from deep storage reservoirs. The results of this research will provide insights to further our understanding of the impacts from CO_2 leakage into potable aquifers.

1.1 Objectives of the Study

The main objectives of this research effort are as follows:

- Develop a systematic understanding of how CO_2 leakage is likely to influence pertinent geochemical processes (e.g., dissolution/precipitation, sorption/desorption and redox reactions) in the aquifer sediments.
- Identify prevailing environmental conditions that would dictate one geochemical outcome over another.
- Gather useful information to support site selection, risk assessment, policy-making, and public education efforts associated with geologic carbon sequestration.

The specific goals of this study are to gain an understanding of how the effects of CO_2 gas are likely to influence 1) the aqueous phase pH; 2) mobilization of major, minor, and trace elements (some of them potential contaminants) from mineral surfaces and/or their bulk structures via dissolution and/or exchange reactions; and 3) aqueous phase speciation, saturation indexes and precipitation reactions, and formation of new mineral phases. Geochemical modeling will be used in future efforts to address the third objective. The data from the kinetic batch experiments will be used in future efforts to calculate dissolution rates in representative materials and sediments of the aquifers under the condition when the CO_2 gas leakage rate and the subsequent dissolution of the CO_2 gas in the groundwater are not limiting the processes and reactions occurring during CO_2 gas exposure. These parameters may be used in generation III predictive models, which will be developed by the NRAP groundwater team in fiscal year 2013 (FY13).

Two experimental methodologies were used as part of this research effort: batch experiments to simulate sudden, fast and short-lived release of CO_2 as would occur in the case of well failure during injection, and column experiments to simulate more gradual leaks such as those occurring along undetected faults, fractures, or well linings. The experiments were conducted at room temperature and atmospheric pressure. Some of the batch experiments involving microbes and redox sensitive minerals were conducted in a controlled atmosphere chamber. Major variables of interest included in the experimental design were sediment type, particle size, solid-to-solution ratio, and brine concentrations.

Experiments were conducted to assess the role of these variables in mediating mineral dissolution/ precipitation and/or sorption/desorption reactions in the vadose zone or a potable aquifer affected by CO_2 migrating from deep geologic storage. Representative rocks from the Edwards Aquifer in Texas and sediment samples from the High Plains aquifer in Kansas were obtained for testing. Collectively, these two aquifers represent the two primary aquifer types (sand/sandstone and carbonate) overlying potential CO_2 sequestration repositories within the continental US. In terms of microbial processes, the study focused on the role of methanogenesis and anaerobic methane oxidation in mediating pure mineral dissolution/precipitation and/or sorption/desorption reactions in CO_2-rich conditions.

1.2 Report Contents and Organization

The ensuing sections of the report provide background information about carbon capture and storage and potential leakage issues (Section 2.0), describe the technical scope and approach (Section 3.0), present results (Section 4.0), and provide conclusions (Section 5.0). Appendixes contain maps and sample locations/coordinates (Appendix A); photos of apparatuses, systems, and sediment samples (Appendix B); tables (Appendix C); and figures (Appendix D).

2.0 Background Information

The capture and storage of CO_2 in deep geologic formations (or geologic CO_2 sequestration) is widely considered a feasible option for reducing anthropogenic CO_2 concentrations in the atmosphere. However, not all potential risk factors associated with this technology have been identified. For example, a possible risk factor and barrier to widespread deployment of geologic CO_2 sequestration is the potential leakage of CO_2 from the deep storage reservoirs into overlying aquifers, which may have a deleterious impact on groundwater quality.

To evaluate potential risks to groundwater quality if CO_2 leakage were to occur, a systematic understanding of how CO_2 leakage would affect the geochemistry of potable aquifers, and subsequently control or affect contaminant mobilization via dissolution, desorption, and/or redox reactions, is crucial to the maintenance of environmental quality. Potential negative impacts are an important public concern with respect to the wide-scale deployment of carbon capture and storage in deep geologic settings.

Knowledge of the environmental consequences associated with CO_2 leakage from deep subsurface storage reservoirs is continually evolving. Supercritical CO_2 will undergo exsolution (phase change from liquid to gas) as it migrates from deep geologic formations to shallower depths in the subsurface. Upon entering an aquifer, a portion of the CO_2 gas will dissolve into groundwater, which will cause a subsequent decrease in aqueous pH of approximately 1 to 3 units due to the formation of carbonic acid according to the reaction:

$$CO_2(g) + H_2O \leftrightarrow H_2CO_3 \leftrightarrow HCO_3^-(aq) + H^+(aq)$$

Reactions that may occur due to CO_2 intrusion include dissolution of different minerals, as well as ion exchange and competitive anionic and cationic desorption (Apps et al. 2010). Dissolution reactions for calcite and a representative 1:1 phyllosilicate are provided below:

$$CaCO_3 + CO_2(g) + H_2O \rightarrow Ca^{2+} + 2HCO_3^-$$

$$Al_2Si_2O_5(OH)_4 + 5H_2O + 6CO_2(g) \rightarrow 2Al^{3+} + 6HCO_3^- + 2H_4SiO_4$$

In addition to the usual structural elements, both these, and other minerals, may host sorbed species (adsorbed and/or precipitated) of potential contaminants. They may also have a variety of other minor or trace elements incorporated in their structures during formation. Changes in pH will likely promote the release of major and minor ions into the aqueous phase, such as Ca, Si, Fe, Al, K, Na, Mg, etc. The groundwater may therefore become oversaturated with respect to neophases of different types, which may precipitate under these conditions.

In addition to major and minor elements, the release of potentially toxic, carcinogenic trace metals, such as Pb, As, and Cd, that are naturally present in aquifer rocks and sediments may also occur. As a result, aqueous concentrations of these potential contaminants may reach levels close to or above the U.S. Environmental Protection Agency (EPA) maximum contaminant levels (MCLs) (Apps et al. 2010; Wang and Jaffe 2004).

Trace metals present in aquifer materials can be adsorbed on the surfaces of different sorbents, such as carbonates and (oxy)hydroxides, exchanged for other ions adsorbed within interlayers or on the edges of phyllosilicates, and/or incorporated into the lattice structure during formation of secondary neoprecipitates. The sequence and time-dependency of different release reactions and processes will vary and ion exchange and desorption will likely occur faster than dissolution. However, the degree of perturbation and responses to the changes would depend on the subsurface system's specific thermodynamic and kinetic attributes and the aquifer chemical, physical, hydrological, biological, and mineralogical characteristics.

Laboratory studies have been carried out to investigate the impacts of CO_2 leakage into shallow aquifer settings (Little and Jackson 2010; Lu et al. 2010; Smyth et al. 2009). Most of these studies used batch systems where aquifer sediments were exposed to enriched dissolved CO_2 solutions. The mixing time varied from 2 weeks to >300 days. Most of the experiments reported a decrease in pH, accompanied by increases in concentrations of some chemical elements such as Ba, Ca, Co, Fe, Mg, Mn, Ni, and Sr, etc. Batch experiments are useful because they provide a relatively simple and inexpensive means for determining the chemicals that can be mobilized by CO_2 leakage in a variety of aquifer settings. However, in batch settings the sediments are allowed to equilibrate with CO_2 over extended periods of time in well mixed, usually high surface area systems and the amount of metals released could be over-predicted (Gilfillan and Haszeldine 2011).

Several field experiments involving a controlled release of CO_2 gas-saturated waters into shallow aquifers were carried out to observe the geochemistry changes that may occur in aquifers under field conditions. Kharaka et al. (2010), conducted experiments with a perforated pipe that was used to release CO_2 below the groundwater table at the 2-m depth. They observed rapid and systematic changes in pH, alkalinity, and electrical conductivity, along with an increase in the concentrations of metals such as Ca,

Mg, Fe, Mn, and organics (benzene, toluene, ethylbenzene, and xylenes). However, the measured metal and organic concentrations were below EPA MCLs.

Recently, Trautz et al. (2013) conducted a controlled release experiment of dissolved CO_2 into a sandy aquifer, and monitored changes in groundwater quality through a monitoring well. They observed a sustained and easily detected decrease of about 3 pH units, but all the trace constituents measured during this experiment were below the EPA MCLs. However, they observed a pulse response for some constituents (Ba, Ca, Cr, Sr, Mg, Mn, and Fe), which suggested a fast-release mechanism (desorption, exchange, and/or fast dissolution of small finite amounts of metal bearing solids or coatings).

Compared to the well-mixed batch systems and expensive field experimental efforts, laboratory flow-through column experiments could be a cost-effective way to replicate field conditions. In the current literature, only a few column experiments on CO_2 intrusion-metal release assessment are reported. One of them is the investigation by Frye et al. (2012), who conducted column experiments to study trace metal release using artificially spiked samples. Frye et al. (2012) used column experiments packed with Cd-spiked illite mixed with quartz to quantify Cd desorption under varied CO_2 leakage conditions, including different leakage flow rates (0.05–1.0 mL/min) with varied CO_2 saturation fluids (0–43.79 mM). They found that fast leakage rates were responsible for earlier and larger amounts of Cd desorption. The long weathering time of Cd-laden clay led to low Cd desorption. They also suggested that calcite content as low as 10% can mitigate the effect of pH reduction and may result in zero Cd desorption (the calcite dissolution increased the solution pH values preventing Cd desorption). Increasing the salinity of the leaking fluid had a relatively minor effect in the experiments they conducted, primarily because of the offsetting impacts of an increased extent of ion exchange and the decrease in CO_2 solubility (and therefore acidity).

As part of the research effort at PNNL, we initially conducted a thorough review of the current literature on how CO_2 leakage (from storage reservoirs) would likely affect the geochemistry of overlying potable aquifers (Harvey et al. 2013). This review revealed the potential for both beneficial and deleterious effects resulting from exposure of subsurface sediments to CO_2 leaked from the deep reservoirs.

Among the most important beneficial effects are 1) the mineralogical trapping of CO_2 in carbonate minerals, which provides another potential mechanism for CO_2 re-sequestration in near surface environments, and 2) contaminant immobilization as a result of changes in sorption behavior of minerals and/or reactive secondary phase formation, after aquifer groundwater and sediments are exposed to the CO_2 gas. The most important deleterious effect (Harvey et al. 2013) is the CO_2-induced reactions leading to the degradation of water quality via mobilization of contaminants or changes in other water quality parameters such as alkalinity, salinity, or total dissolved solids (TDS).

Two CO_2 leakage scenarios are possible (Bachu 2008; Metz et al. 2005). The first is where there is a sudden, fast, and short-lived release of CO_2 as would occur in the case of well failure during injection or spontaneous blowouts (Damen et al. 2005; Holloway et al. 2007; Jordan and Benson 2009). The second local leakage scenario is where the leak is more gradual, occurring along undetected faults, fractures, or well linings (Annunziatellis et al. 2008; Bachu 2008; Celia and Nordbotten 2009; Damen et al. 2005; Lewicki et al. 2007; Nordbotten et al. 2005; Scherer et al. 2011). Such diffusive leakage has the greatest potential to cause broad-scale environmental impacts (Bachu 2008; Damen et al. 2005; Metz et al. 2005). However, the fate of the leaked CO_2 gas after migrating from the deep storage aquifer/reservoir will

depend largely on the physical, mineralogical, chemical, hydrological and biological properties and processes occurring in the overlying environment.

The review by Harvey et al. (2013) also revealed the urgent need for development of consistent experimental protocols and methodical experimental work because significant discrepancies exist between studies (most of them modeling studies) concerning the type of contaminants and the geochemical processes involved. These results also emphasized the need to consider important experimental factors, such as gas leakage rates, redox status, sediment type and water content, and the influence of co-transported gases as the most important and relevant factors controlling or significantly affecting the release and fate of contaminants, as well as the salinity and the total amount of dissolved solids in these systems. In addition, studies involving bacteria should be conducted and focus on how their activity may induce changes in the aqueous and gas phase chemistry of the aquifers. For example, autotrophic methanogenesis bacteria may consume CO_2 to convert it to CH_4, or they may promote methanogenesis-induced precipitation of carbonate neophase(s).

Currently, two different schools of thought exist about whether the potential implications of CO_2 leakage from deep subsurface storage reservoirs are a major risk factor in terms of adversely affecting aquifer and groundwater quality. Research in this area is relatively new and presently, there isn't a consensus within the scientific community regarding this topic. The results from our research effort will provide insights to further our understanding of potential impacts of CO_2 on potable aquifers.

3.0 Technical Scope and Approach

This study involved the use of particular sediments, sediment characterization techniques, and the preparation of synthetic groundwater prior to conducting batch and column experiments.

3.1 The Source and Nature of the Sediment Materials

Representative rocks and sediment samples were derived from the Edwards aquifer in Texas and the High Plains aquifer in Kansas.

3.1.1 Samples from the Edwards Aquifer, Texas

Two sets of representative samples from the Edwards aquifer were used in this study: Set A and Set B. There were seven samples in both sets (maps and sample collection locations and coordinates are included in Appendix A). These rock samples were from the ground surface but they were from the same stratigraphic unit (geological formation) and represented well the aquifer rocks although some of them were slightly weathered and, for this reason, they may be different from the subsurface aquifer materials. Some of the rock samples were ground and sieved to separate the <2-mm and the <53-μm size fractions. These fractions were characterized using x-ray diffraction (XRD) analyses and 8-M nitric acid extractions, and they were used in the batch and column experiments.

3.1.2 High Plains Sediments

We also received sediment samples from the High Plains aquifer in Kansas from the Drill Core Library at the Kansas Geological Survey (maps are included in Appendix A). These samples were from three different wells named CNG, CAL 121, and CAL 122. The samples arrived as loose sediments, mostly <2 mm. Some of the samples underwent sieving and were subsequently used in batch and column experiments of different types.

3.2 Sediment Characterization

The sediments were characterized using XRD analysis and acid extraction.

3.2.1 XRD Analyses

Most of the XRD analyses were conducted at the Environmental Molecular Sciences Laboratory (EMSL). Powder diffraction data were collected with a Panalytical X'Pert Bragg-Brentano diffractometer using Cu-Kα radiation (λ = 1.5418 Å), a graphite post-diffraction monochromator, and variable divergence and anti-scatter slits (illuminated length= 10 mm). The specimens were loaded into traditional well-type aluminum holders with a cavity measuring 20 x 15 x 2 mm. Patterns were collected between 5 and 75° 2θ, counting for 2s at 0.04° steps. Some analyses were conducted at the Radiological Processing Laboratory (Building 325, PNNL) using a Rigaku MSC Inc. X-ray diffractometer, model Ultima IV. All diffractograms produced were analyzed and fitted using JADE software package (Materials Data Inc., Livermore, CA.

3.2.2 Acid Extractions (8-M Nitric Acid)

Acid extractions were performed on select representative Edwards and High Plains aquifer materials using a concentrated acid. The samples were sieved to obtain the <2-mm size fraction. The sieving and acid extractions were done on samples as received (the samples were not dried). Some of the Edwards aquifer samples were ground to obtain the <2-mm size fraction. In some samples, size fractions such as 53 μm–2 mm and <53 μm were separated from the materials and were used in acid extractions. The moisture content of each material was measured in replicates.

Exactly one gram of sample was added to a 15-mL centrifuge tube, in duplicate. A pipette was used to add 5 mL of room temperature 8-M nitric acid. The sample and the acid were mixed, and then transferred to an acid extraction tube. To ensure all solid was transferred from the centrifuge tube, an additional 1 mL aliquot of 8-M nitric acid was used to rinse the centrifuge tubes; the rinse was added to the acid extraction tube. We used 0.5 g of sample and 3 mL of acid for the samples that did not have sufficient amounts of <53-μm size fraction.

The acid extraction tubes were heated to 95 °C for 2 hours. Each sample was then transferred back to the centrifuge tube to be centrifuged at 3500 rpm for 10 minutes. The supernatant was decanted into a 5-mL syringe and filtered through a 0.22-μm syringe filter. The liquid was then submitted for inductively coupled plasma mass spectrometry (ICP-MS) and ICP-optical emission spectrometry (OES) analyses. ICP-MS and ICP-OES analyses were performed using a Thermo Scientific, X-series II and Perkin Elmer Optima 3300 DV and 8300 DV, respectively. All analyses were performed following the strict quality

assurance guidelines specified in the quality assurance program of the Environmental Science Laboratory, Geosciences Group, PNNL (CAWSRP – conducting analytical work in support of regulatory programs).

3.3 Synthetic Groundwater Preparation

Synthetic groundwater was prepared to replicate that found at each aquifer site.

3.3.1 Edwards Aquifer Site

A synthetic groundwater (SGW) solution, which was similar in composition to the Edwards aquifer groundwater, based on U.S. Geological Survey groundwater data of the Edwards aquifer, was used in the batch and column studies. The moles of major anions and cations were balanced, and several similar batches of SGW were prepared for these experiments (recipe amounts listed below). The calcium carbonate was dissolved in 5 mL of 2% nitric acid, and then added to the solution. After dissolving all components of the SGW in 1 L poly bottles, the SGW was pH adjusted over several days to obtain a stable pH close to 6.99 (the average pH of the Edwards aquifer groundwater). The pH was adjusted with potassium hydroxide and nitric acid. The pH adjustments cause the amount of KOH and nitric acid to vary slightly between batches. Samples of the SGW used in each experiment underwent full chemical analysis to determine the final chemical composition of each batch.

Chemical Used	Amount per 1 L
$CaCO_3$	0.2770 g
Na_2SO_4	0.0242 g
$MgCl_2 \times 6H_2O$	0.0806 g
2% HNO_3	20 mL
1 M KOH	1.2 mL

3.3.2 Kansas Synthetic Groundwater

The same steps were taken to prepare a groundwater recipe to contact the Kansas sediments in the various experiments. USGS data for the High Plains aquifer was used to calculate the appropriate amount of major cations and anions to include in the High Plains SGW. $CaCO_3$ and $MgCO_3$ were dissolved in 2% nitric acid before being added to the groundwater to ensure complete dissolution of the salts. The following recipe has been used in all experiments with sediments from the High Plains aquifer. As with the Edwards SGW, the amount of KOH and nitric acid varied slightly with each batch due to differing pH adjustments.

Chemical Used	Amount per 1 L
$CaCO_3$	0.1201 g
$MgCO_3$	0.0691 g
Na_2SO_4	0.0568 g
NaCl	0.0269 g
2% HNO_3	15.03 mL
1 M KOH	1.23 mL

3.4 Batch Experiments

A series of batch experiments were conducted to study major, minor, and trace element mobilization from the representative Edwards aquifer materials and High Plains aquifer sediments. CO_2 gas was injected periodically or continuously in the batch reactors. The high purity (99.998 %) or industrial grade (99.9 %) CO_2 gas delivered by Oxarc was used in these experiments.

3.4.1 Periodic CO_2 Gas Exposure: Edwards Aquifer Sediments

3.4.1.1 The First Batch Experiment (Batch 1)

Pictures of the batch apparatus used in this experiment are included in Appendix B. Four tests were conducted under the name "Batch 1." The <2-mm air-dried fraction of four representative samples from the Edwards aquifer Set A, i.e., samples 3, 4, 5, and 6, were used in the tests. The batch reactors received periodic injections of CO_2 gas. The objective was to study subsurface system responses to periodic short-term CO_2 gas exposure and determine changes in liquid phase chemistry (pH and major, minor, and trace element concentrations) as a function of time.

Details about the first test are provided below.

Batch 1, Test 1
Solid material: 5 g Edwards aquifer Set A Sample 3, <2 mm, air dried
SGW: 25 mL Edwards aquifer SGW

Five grams of the representative Edwards aquifer sample was transferred together with 25 mL of SGW into batch reactors (poly bottles with lids) and were left overnight to equilibrate at room temperature. The next day (Day 1), lids with holes to accommodate a pH probe and a tube to inject CO_2 gas were put on the bottles; parafilm was used to seal the top of the bottles, although excess CO_2 gas was allowed to escape during injection. Liquid samples (2.5 mL) were taken out of the bottles at predetermined experimental times to follow time-dependent changes in the chemical composition of the aqueous phase in contact with the sediments. Anytime a 2.5-mL sample was taken out of the bottles, a 2.5-mL aliquot of the SGW solution was added back into the bottle to maintain a consistent solid-to-solution ratio. CO_2 was injected for 5 minutes and a liquid sample was taken after injection (a 2.5-mL aliquot of the SGW solution was immediately added to the bottles). The CO_2 injection continued for an additional 1 minute to ensure uniform CO_2 saturation in all liquid present inside bottles (total time of injection: 5+1 minutes). Liquid samples were taken at different times during this experiment, and before and after CO_2 gas injection. An average gas flow rate of 112.4 ± 3.1 mL/min was used in this experiment.

Three additional tests were conducted with three representative Edwards aquifer materials. Details on these experiments are provided below.

Batch 1, Test 2
Solid material: 5 g Edwards aquifer Set A Sample 4, <2 mm, air dried
SGW: 25 mL Edwards aquifer SGW

Batch 1, Test 3
Solid material: 5 g Edwards aquifer Set A Sample 5, <2 mm, ground, air dried
SGW: 25 mL Edwards aquifer SGW

Batch 1, Test 4
Solid material: 5 g Edwards aquifer Set A Sample 6, <2 mm, air dried
SGW: 25 mL Edwards aquifer SGW

Two replicates of exactly 5 g of the representative Edwards aquifer sample and 25 mL of SGW were added to a 50-mL centrifuge tube **(**sample 4, sample 5, and sample 6). The samples were left overnight on a shaker to equilibrate. The next day, the bottles were centrifuged at 3000 rpm for 10 minutes, and then a 2.5-mL sample was taken from each of them. The same amount of SGW was added to replace the 2.5 mL of liquid removed. The bottles were then vortexed to suspend the solid materials (this procedure was repeated after each sampling time). Then, the pH probe was inserted, and parafilm was used to seal the top.

The CO_2 flow rate was measured at the beginning and end of injection. The CO_2 gas injection lasted for 5 minutes. The pH was recorded during and after each CO_2 injection. The bottles were then sealed and left overnight. The same procedure was repeated the next day. After the second CO_2 injection, the bottles were centrifuged and the liquid phase was sampled. The same procedure was repeated on the following days: 3, 4, 5, 6, 7, 8, 9, 10, 14, 17, 23, 24, 29, 34, and 52. The CO_2 gas flow rate was similar in the three tests (overall average: 113.30 ± 2.23 mL/min).

3.4.2 Continuous CO_2 Gas Exposure: Representative Edwards Aquifer Materials and High Plains Aquifer Sediments

The objective was to study time-dependent release of major, minor, and trace elements or potential contaminants from materials representing the Edwards aquifer (ground unweathered or slightly weathered rocks in the form of powder), and sediments collected from the High Plains aquifer. The solid materials were mixed with their respective SGW and were exposed to a CO_2 gas stream and brine solutions. All these experiments had similar CO_2 gas intrusion rates of about 70 mL/min. The rates applied in these experiments were relatively high so that the rate of intrusion and the resulting CO_2 SGW saturation would not limit processes and reactions taking place in the course of these experiments. The gas rates were measured frequently during the experiments to ensure that similar conditions were applied in all experiments conducted under continuous CO_2 exposure.

3.4.2.1 Second Batch Experiment (Batch 2)

Three tests were conducted in the "Batch 2" experimental set.

Batch 2, Test 1
Solid material: 5 g Edwards aquifer, Set B Sample 4, <2 mm
SGW: 15 mL Edwards aquifer SGW

Batch 2, Test 2
Solid material: 5 g Edwards aquifer, Set B Sample 2, <2 mm
SGW: 15 mL Edwards aquifer SGW

Batch 2, Test 3
Solid material: 5 g Edwards aquifer, Set B Sample 7, <2 mm
SGW: 15 mL Edwards aquifer SGW

Variables: A) experiment time (0, 4, 8, 12, 24, 48 hours and 3, 7, and 14 days); B) sediment type.

Equilibration Period

Edward aquifer SGW was added to the 5 g of sediment for each sample and left overnight to equilibrate before beginning CO_2 continuous injection the following day. In each test, two additional bottles (batch reactors) were equilibrated overnight with the SGW and the liquid phase was separated from the solid the following day to measure aqueous phase chemical composition at experimental time zero.

Experimental Details

Twenty-four 125-mL bottles (batch reactors) were prepared for each test within Batch 2. The lids have an inlet valve for CO_2 gas entry and a small hole to allow gas to escape to avoid pressure buildup inside the batch reactor. Fifteen milliliters of Edwards aquifer SGW and 5 g of soil were added to each batch reactor. The elapsed experimental times were 0 hours (no gas injection), 4 hours, 8 hours, 12 hours, 1 day, 2 days, 3 days, 7 days, and 14 days. The experiments were run in two replicates and one blank was used for each respective time. CO_2 gas was continuously injected in the batch reactors for the entire pre-determined time. No gas was injected in the blanks. The total experimental time for these tests was 14 days. Four bottles at a time were injected with the CO_2 gas. The first four were the 14-day samples and the 4-hour samples. When the 4-hour samples were collected, the 8-hour samples were put in the gas line, and so on until the 7-day samples and the 14-day samples ended on the same day. Blanks were sampled at the same time their respective treated reactors were sampled.

The CO_2 gas was injected at a constant rate (72 ± 9 mL/min) in each of the batch reactors (plastic bottles). The CO_2 gas coming out of the gas tank flowed into a wash bottle (used to hydrate the gas), which was filled with the same SGW used in the batch reactors. From there the CO_2 gas flowed into the batch reactors. The flow rate was checked before it entered the hydration system as well as at each individual bottle before starting the experiment. Flow rates were measured frequently (once or twice a day).

At the end of the experimental time, the solid phase was separated from the liquid phase, which was transferred into centrifuge tubes for centrifugation. The supernatant was then filtered through a 0.22-µm filter and separated and acidified for analysis by ICP-MS. A subsample of the liquid phase in the reactors was taken immediately after the elapsed time for accurate pH measurement.

The solid materials used in these tests were crushed, representative Edwards aquifer rock in the form of powder. The release of chemical elements from the solids should be at their maximum under these conditions. The blank batch reactors were not perturbed with any gas flows. This was done purposely to

allow for comparison of the changes in the aqueous phase pH and chemical composition in the perturbed systems by CO_2 gas injection with the unperturbed blanks.

Liquid Mass Lost During Batch 2 Experiment

Test 1. All experiments started with 15.03 ± 0.02 g of liquid. The liquid mass in each batch reactor and in all tests was measured again at the end of the experiments. The changes were insignificant in most experiments with the exception of the 7-day experiments and the 14-day experiments which lost an average of 0.49 and 1.5 g, respectively. The liquid mass of the blanks did not vary more than 0.02 g.

Test 2. All experiments started with 15.00 ± 0.04 g of liquid. The changes in mass were insignificant during most experiments with the exception of the 7-day and 14-day experiments which lost an average of 3.1 and 2.6 g, respectively. The blank masses (including equilibration samples) did not change significantly.

Test 3. All experiments started with 14.98 ± 0.05 g of liquid. The changes in mass were insignificant during most experiments with the exception of the 7-day and 14-day experiments which lost 0.43 and 1.02 g, respectively. The blanks and equilibration experiments masses did not change significantly.

3.4.2.2 Third Batch Experiment (Batch 3)

One long–term test (119 days) was conducted under Batch 3.

Batch 3
Solid material: 8 g Edwards aquifer, Set B Sample 2, <2 mm
SGW: 24 mL Edwards aquifer SGW

Variable: Experimental time.

Equilibration Period

Edwards aquifer SGW was added into the batch reactors (60-mL plastic bottles) and which were equilibrated overnight before beginning CO_2 injection at a rate of about 69 ± 4 mL/min.

Experimental Details

Two replicates and one blank were run in this experiment. The lids had an inlet valve for CO_2 gas entry and an outlet to allow gas to escape to avoid pressure buildup inside the batch reactor. Twenty-four milliliters of SGW and 8 g of the material, ground and sized to <2 mm, were added in each batch reactor. Every 6 to 8 days, both replicates and the blank were sampled. For each bottle, 4 mL of liquid was removed and 4 mL of fresh SGW solution was added to the bottles to maintain a constant solid-to-solution ratio. Weights were measured before and after to determine the exact amount of liquid removed and added. Of the 4-mL aliquot, 1.5 mL was used for pH measurements. The remaining 2.5 mL was diluted/acidified with 2.5 mL of 2% nitric acid and submitted for ICP-OES and ICP-MS analyses.

Liquid Mass Lost During Experiment

The changes in liquid mass were followed and an appropriate amount of SGW was added to each reactor at the time of sampling to make the liquid mass similar to that at the beginning of the experiment.

3.4.2.3 Fourth Batch Experiment (Batch 4)

Four tests were conducted under Batch 4; the specifics are given below.

Batch 4, Test 1
Solid material: 5 g Edwards aquifer, Set B Sample 7, <2 mm
SGW: 15 mL Edwards aquifer SGW

Batch 4, Test 2
Solid material: 5 g Edwards aquifer, Set B Sample 7, >2 mm
SGW: 15 mL Edwards aquifer SGW

Batch 4, Test 3
Solid material: 5 g Edwards aquifer, Set B Sample 7, <2 mm, brine: 1 M NaCl
SGW: 15 mL Edwards aquifer SGW

Batch 4, Test 4
Solid material: 5 g Edwards aquifer, Set B Sample 7, <2 mm, brine: 0.1 M NaCl
SGW: 15 mL Edwards aquifer SGW

Variables: A) time (0, 4, 8, 12, 24, 48 hours and 3, 7, and 14 days); B) size fraction (greater and smaller than 2 mm); C) brine concentration (0.1 and 1 M NaCl).

Equilibration Period

SGW was added to the 5 g of sediment for each sample and left overnight before beginning continuous CO_2 injection. This experiment was conducted in a way similar to that for Batch 2.

Experimental Details

This experiment was conducted in a way similar to that for Batch 2. The only difference was that twenty four 60-mL bottles were used in this experiment. The lids again had an inlet valve for CO_2 gas entry and a small hole to allow gas to escape to avoid pressure buildup inside the batch reactor. The CO_2 gas injection rate was 71 ± 7 mL/min.

Liquid Mass Lost During Experiment

Test 1. Each experiment in Test 1 started with 15.01 ± 0.03 g of liquid. The changes in liquid mass were insignificant during most experiments with the exception of the 7-day and 14-day experiments which lost an average of 0.38 and 0.95 g, respectively. The liquid mass of the blanks (including equilibration experiments) did not change more than 0.01 g.

Test 2. Test 2 experiments started with 14.98 ± 0.02 g of liquid. The changes in mass were insignificant during most experiments with the exception of the 7-day and 14-day experiments which lost 0.51 and 1.08 g, respectively. The mass of the blanks and equilibration experiments changed less than 0.02 g.

Test 3. Test 3 sample experiments started with 15.58 ± 0.03 g of liquid; the liquid weight in Set 3 was higher than the other sets because the groundwater contained 1 M NaCl. The changes in mass were insignificant during most experiments with the exception of the 7-day and 14-day experiments which lost 0.61 and 0.99 g, respectively. The mass in the blanks and equilibration experiments changed by less than 0.02 g.

Test 4. These experiments started with 14.99 ± 0.15 g of liquid. The changes in mass were insignificant during most experiments with the exception of the 14-day experiments which lost an average of 0.65 g. The changes in mass in the blanks and equilibration experiments were insignificant.

3.4.2.4 Fifth Batch Experiment (Batch 5)

Four tests were conducted in Batch 5; the specifics are given below.

Batch 5, Test 1
Solid material: 5 g Edwards aquifer, Set B Sample 2, <2 mm
SGW: 15 mL Edwards aquifer SGW

Batch 5, Test 2
Solid material: 5 g Edwards aquifer, Set B Sample 2, >2 mm
SGW: 15 mL Edwards aquifer SGW

Batch 5, Test 3
Solid material: 5 g Edwards aquifer, Set B Sample 2, <2 mm, brine: 1 M NaCl
SGW: 15 mL Edwards aquifer SGW

Batch 5, Test 4
Solid material: 5 g Edwards aquifer, Set B Sample 2, <2 mm, brine: 0.1 M NaCl
SGW: 15 mL Edwards aquifer SGW

Variables: A) time (0, 4, 8, 12, 24, 48 hours and 3, 7, and 14 days); B) size fraction (greater and smaller than 2 mm); C) brine concentration (0.1 and 1 M NaCl).

Equilibration Period

SGW was added to the 5 g of sediment for each sample and left overnight before beginning continuous CO_2 injection at a rate of 73 ± 9 mL/min. This experiment was conducted in a way similar to that for Batch 2.

Liquid Mass Lost During Experiments

Test 1. Test 1 started with 15.00 ± 0.04 g of liquid. The changes in mass were insignificant during most experiments with the exception of the 14-day experiments which lost 0.88 g. The changes in mass in the blanks and equilibration experiments were insignificant.

Test 2. Test 2 started with 14.99 ± 0.04 g of liquid. The changes in mass were insignificant during most experiments with the exception of the 7-day experiments which lost 1.1 g. The changes in mass in the blanks and equilibration experiments were insignificant.

Test 3. Test 3 started with 15.59 ± 0.05 g of liquid. The liquid weight in Set 3 was higher than the other sets because the groundwater was 1 M in NaCl. The changes in mass were insignificant during most experiments with the exception of the 7-day and 14-day experiments which lost 0.94 1.42 g, respectively. The changes in mass in the blanks and equilibration experiments were insignificant.

Test 4. Test 4 started with 15.06 ± 0.06 g of liquid. The changes in mass were insignificant during most experiments with the exception of the 14-day experiments lost about 0.50 g. The changes in mass in the blanks and equilibration experiments were insignificant.

3.4.2.5 Sixth Batch Experiment (Batch 6)

Three tests were conducted in Batch 6.

Batch 6, Test 1
Solid material: 5 g Edwards aquifer, Set A Sample 1, <2 mm
SGW: 15 mL Edwards aquifer SGW

Batch 6, Test 2
Solid material: 5 g Edwards aquifer, Set A Sample 4, <2 mm
SGW: 15 mL Edwards aquifer SGW

Batch 6, Test 3
Solid material: 5 g Edwards aquifer, Set A Sample 6, <2 mm
SGW: 15 mL Edwards aquifer SGW

Variables: A) time (0, 4, 8, 12 hours and 1, 2, 3, 7, and 14 days); B) sediment type.

Equilibration Period

SGW was added to the 5 g of sediment for each sample and left overnight before beginning the continuous CO_2 injection at a rate of 72 ± 8 mL/min. This experiment was conducted in a way similar to that for Batch 2.

Liquid Mass Lost During Experiment

Test 1. Test 1 experiments started with 15.00 ± 0.06 g of liquid. The changes in mass were insignificant during most experiments with the exception of the 7-day and 14-day experiments which lost 0.8 and 0.88 g, respectively. The changes in liquid mass in the blanks and equilibration experiments were insignificant.

Test 2. Test 2 experiments started with 15.01 ± 0.02 g of liquid. The changes in mass were insignificant during most experiments with the exception of the 14-day experiments which lost an average of 0.77 g. The changes in liquid mass in the blanks and equilibrium experiments were insignificant.

Test 3. Test 3 experiments started with 14.99 ± 0.02 g of liquid. The changes in mass were insignificant in all experiments and the blanks.

3.4.2.6 Seventh Batch Experiment (Batch 7)

Four tests were conducted in Batch 7.

Batch 7, Test 1
Solid material: 5 g Edwards aquifer, Set A Sample 1, <2 mm
SGW: 15 mL Edwards aquifer SGW
Bacterial biomass: 127.5 µL of the bacterial suspension added in each batch reactor

Batch 7, Test 2
Solid material: 5 g Edwards aquifer, Set A Sample 1, <2 mm
SGW: 10 mL Edwards aquifer SGW
Bacterial biomass: 85 µL of the bacterial suspension added in each batch reactor

Batch 7, Test 3
Solid material: 5 g Edwards aquifer, Set B Sample 4, <2 mm
SGW: 10 mL Edwards aquifer SGW
Bacterial biomass: 85 µL of the bacterial suspension added in each batch reactor

Batch 7, Test 4
Solid material: 5 g Edwards aquifer, Set B Sample 7, <2 mm
SGW: 10 mL Edwards aquifer SGW
Bacterial biomass: 85 µL of the bacterial suspension added in each batch reactor

Variables: A) time (0, 4, 8, 12 hours and 1, 2, 3, 7, and 14 days); B) solid-to-solution ratio (1:3 vs. 1:2). A microbial protein solution (which contained 700 µg/mL protein and was added at the amount of 85 µL of solution per 10 mL of SGW. The objective was to simulate microbial activity in the batch reactors and study differences in the chemical composition of the aqueous phase. Microbial characterization studies were not conducted in the liquid and solid materials of these experiments.

Equilibration Period

SGW was added to the 5 g of sediment for each sample and left overnight before beginning continuous CO_2 injection at a rate of 70 ± 7 mL/min. This experiment was conducted in a way similar to that for Batch 2.

Liquid Mass Lost During Experiment

Test 1. Test 1 started with 15.02 ± 0.04 g of SGW and 0.13±0.01 g of biomass. The changes in mass were insignificant during most experiments with the exception of the 14-day experiments which lost 0.67 g. The changes in liquid mass of the blanks and equilibration experiments were insignificant.

Test 2. Test 2 experiments started with 10.00 ± 0.05 g of SGW and 0.09 ±0.01 g of biomass material. The changes in mass were insignificant during most experiments with the exception of the 7-day and 14-day experiments which lost 0.65 and 1.27 g, respectively. The changes in liquid mass of the blanks and equilibration experiments were insignificant.

Test 3. Test 3 experiments started with 9.98 ± 0.04 g of SGW and 0.08 ± 0.01 g of biomass material. The changes in mass were insignificant during most experiments with the exception of the 14-day experiment which lost 0.54 g. The changes in liquid mass of the blanks and equilibration experiments were insignificant.

Test 4. Test 4 experiments started with 9.99 ± 0.02 g of SGW and 0.08 ± 0.01 g of DvH material. The changes in mass were insignificant during most experiments with the exception of the 14-day experiments which lost 0.56 g. The changes in liquid mass of the blanks and equilibration experiments were insignificant.

3.4.2.7 Eighth Batch Experiment (Batch 8) High Plains Sediments

Four tests were conducted in Batch 8.

Batch 8, Test 1
Solid material: 5 g High Plains sediment CNG 110–111, <2 mm
SGW: 15 mL High Plains SGW

Batch 8, Test 2
Solid material: 5 g High Plains sediment CNG 60–61, <2 mm
SGW: 15 mL High Plains SGW

Batch 8, Test 3
Solid material: 5 g High Plains sediment CAL 121 151–152, <2 mm
SGW: 15 mL High Plains SGW

Batch 8, Test 4
Solid material: 5 g High Plains sediment CAL 122 29–30, <2 mm
SGW: 15 mL High Plains SGW

Variables: A) time (0, 4, 8, 12 hours and 1, 2, 3, 7 and 14 days); B) sediment type.

Equilibration Period

High Plains aquifer SGW was added to the 5 g of sediment for each sample and left overnight before beginning continuous CO_2 injection at a rate of 70 ± 7 mL/min. This experiment was conducted in a way similar to that for Batch 2.

Liquid Mass Lost During Experiment

Test 1. Test 1 experiments started with 15.01 ± 0.04 g of liquid. The changes in mass were insignificant during most experiments with the exception of the 14-day experiments which lost 0.9 g. The changes in liquid mass of the blanks and equilibration experiments were insignificant.

Test 2. Test 2 experiments started with 14.99 ± 0.03 g of liquid. The changes in mass were insignificant during most experiments with the exception of the 7-day and 14-day experiments which lost 0.84 and 1.75 g, respectively. The changes in liquid mass of the blanks and equilibration experiments were insignificant.

Test 3. Test 3 experiments started with 14.99 ± 0.06 g of liquid. The changes in mass were insignificant in all experiments and blanks.

Test 4. Test 4 experiments started with 14.98 ± 0.05 g of liquid. The changes in mass were insignificant during most experiments with the exception of the 14-day experiments which lost 0.78 g. The changes in liquid mass of the blanks and equilibration experiments were insignificant.

3.4.2.8 Ninth Batch Experiment (Batch 9) High Plains Sediments

Four tests were conducted in Batch 9.

Batch 9, Test 1
Solid material: 5 g High Plains sediment CNG 8–9, <2 mm
SGW: 15 mL High Plains SGW

Batch 9, Test 2
Solid material: 5 g High Plains sediment CNG 150–151, <2 mm
SGW: 15 mL High Plains SGW

Batch 9, Test 3
Solid material: 5 g High Plains sediment CAL 121 91–92, <2 mm
SGW: 15 mL High Plains SGW

Batch 9, Test 4
Solid material: 5 g High Plains sediment CAL 122 4–4.5, <2 mm
SGW: 15 mL High Plains SGW

Variables: A) time (0, 4, 8, 12 hours and 1, 2, 3, 7, and 14 days); B.) sediment type.

Equilibration Period

SGW was added to the 5 g of sediment for each sample and left overnight before beginning continuous CO_2 injection at a rate of 71 ± 5 mL/min. This experiment was conducted in a way similar to that for Batch 2.

Liquid Mass Lost During Experiment

Test 1. Test 1 started with 15.01 ± 0.03 g of liquid. The changes in mass were insignificant during most experiments with the exception of the 14-day experiments which lost 1.15 g. The changes in liquid mass of the blanks and equilibration experiments were insignificant.

Test 2. Test 2 started with 15.00 ± 0.03 g of liquid. The changes in mass were insignificant during most experiments with the exception of the 14-day experiments which lost an average of 1.39 g. The changes in liquid mass of the blanks and equilibration experiments were insignificant.

Test 3. Test 3 started with 15.00 ± 0.05 g of liquid. The changes in liquid mass were insignificant during all experiments and in all blanks.

Test 4. Test 4 started with 14.99 ± 0.03 g of liquid. The changes in mass were insignificant during most experiments with the exception of the 14-day experiments which lost 0.62 g. The changes in liquid mass in the blanks and equilibration experiments were insignificant.

Liquid Sample Preservation and Analyses

Liquid samples from all batch tests were acidified with a 2% nitric acid and stored in a refrigerator (+4°C) prior to ICP-OES and ICP-MS analysis.

3.5 Column Experiments

Pictures of the apparatus used in the experiments are included in Appendix B. In this study, we used column experiments to investigate major, minor, and trace element released from the crushed rock or sediments when they are exposed to CO_2 gas-saturated SGW. Changes in effluent pH, Eh, and chemical concentration with time were followed in these experiments. The objective of the study was to investigate the impacts on the potable aquifer pH and chemical composition caused by the CO_2 gas intrusion.

All materials selected and column experimental details are provided in Table C.1 (in Appendix C). A total of six sediments from the two aquifers (the Edwards aquifer in Texas and High Plains aquifer in

Kansas) were used in this study. A control column was packed with Accusand and was leached under conditions similar to those containing the crushed rocks or sediments from the two study sites.

All the Edwards aquifer rock samples were crushed with a hammer and then sieved through a <2-mm size sieve. The High Plains sediments were also sieved to separate the <2-mm size fraction. These <2-mm materials were then packed into the columns and were leached with the respective SGW.

Four sets, each with two column experiments, were conducted as part of this study, as described below.

Set 1 used a column packed exclusively with Accusand and another one packed half with Accusand and half with dry-sieved, <2-mm size fraction Edward aquifer Set B sample 4. This material was dry packed into a glass column with an inner diameter (ID) of 2.49 cm and length of 15.2 cm. The Edwards aquifer material was packed in the middle portion of the column (7.8 cm in length), while the remaining volume of the column was filled with Accusand (2.5 cm and 5 cm lengths on the top and bottom end portion of the column, respectively). The Accusand column was run in parallel as a control experiment. A 0.45-µm Millipore filter was used at both ends of each column to hold the packed materials in place and to filter the effluent solutions. Based on the mass of the packed material and density (2.65 and 2.71 g/cm^3 for Accusand and calcite, respectively), the estimated porosity for the packed Accusand column was 0.17, and in the column portion that was packed with the Set B sample 4 material it was 0.27.

Set 2 of the column experiments used smaller columns that were packed with the dry-sieved, <2-mm size fraction Edwards aquifer, Set B, samples 4 and 7.

Set 3 of the column experiments used small columns as the ones used in Set 2. The columns were packed with the dry-sieved, <2-mm size fraction Edwards aquifer, Set A, samples 1 and 4.

Set 4 of the column experiments again used small columns that were packed with the dry-sieved, <2-mm size fraction of two sediments from the High Plains aquifer, sediments CNG 60 and 110.

The Edward aquifer SGW (pH = 6.99) or the High Plains aquifer SGW (pH = 7.50) was used as the influent in these column experiments. The SGW used in these experiments was boiled for half an hour to cause de-aeration, and then it was stored inside an anaerobic chamber overnight before usage. All experiments were conducted under hydraulically saturated condition.

The de-aerated SGW was injected continuously into the columns from the bottom inlet using a KLOEHN V6 syringe pump at a relatively slow flow rate of about 0.03 mL/min. The experiments were conducted at room temperature (about 21°C), and the effluent pH and Eh was continuously measured on line using an Accumet benchtop XL15 pH and Eh meter. The buffer solutions used for pH electrode calibration were the ERA pH 4 and 7 solutions; the pH calibration and the electrode responses were checked periodically with a different set of standards, i.e., Fisher pH 4 and 7 buffer solutions. The solution Eh was determined by following the PNNL Technical Procedure (Document No.: AGG-Eh-001) in which the standard potential of the Pt electrode is determined using quinhydrone.

Frequent pH measurements were taken (usually, one measurement per hour during continuous flow, and one measurement per 15 minutes immediately after the stop-flow events). In addition, the effluent samples were collected more frequently after the stop-flow events. During the experiment, about one

sample per pore volume (PV) was collected. At the end of the experiments selected effluent samples were analyzed with both ICP-OES and -MS to determine the concentrations of major, minor, and trace elements.

The columns were initially leached with the appropriate SGW for several hours to achieve hydrological equilibrium (i.e., full saturation) and then they were leached with either the N_2-purged SGW (e.g., Set 1) or the CO_2 gas-saturated SGW (e.g., Sets 2, 3, and 4). The CO_2 gas was continuously purged in the influent bottle at a rate of 0.5 mL/min. The stop-flow condition was applied twice after the CO_2 gas-saturated SGW was used as the influent solution.

Only the column experiments of Set 1 were initially leached with a N_2-purged SGW (pH = 6.95) for about 200 hours until steady pH values were recorded in the column effluent. The N_2 gas was continuously purged into a SGW reservoir that had an initial volume of 2 L, under a gas flow rate of 0.5 mL/min during the entire 200-hour leaching process. Then the purging gas was switched from N_2 to CO_2 in the input solution reservoir while the column was continuously run for another 215 hours. During the entire 215 hours of CO_2 purging fluid injection, one stop-flow event, which lasted for 146 hours, was applied after the initial 125 hours of CO_2 purging fluid injection, after steady pH values were recorded in the effluents. The pH of the SGW in the inflow reservoir was monitored frequently with the Accumet AR25 bench-top pH meter.

3.6 Experiments with Pure Minerals and Microbes: The Impact of CO_2 to CH_4 Transformation on Metal Mobility

Under anaerobic conditions, CO_2 in the subsurface may be converted to CH_4 via autotrophic methanogenesis. The objective of this study was to understand how such a transformation would influence trace metal mobility in CO_2-affected aquifers. A series of batch incubation experiments was conducted to assess changes in the aqueous concentration of Fe, As, and Pb in sulfidic systems with and without autotrophic methanogenesis. Sources of Fe, As, and Pb were pyrite (FeS_2), arsenopyrite (AsFeS), and galena (PbS). Natural pyrite and galena samples were obtained from Dr. Kirk Cantrell's collection (PNNL) and arsenopyrite was purchased from Ward Scientific (Rochester, NY). The mineralogy of the samples was confirmed by XRD analysis and the elemental composition was determined through microwave digestion and subsequent analysis of the digest by ICP-OES (Figure D.41 [Appendix D] and Table C.8 [Appendix C]). Prior to use, these minerals were crushed, sieved (3 fractions: <150, 150−250, and 250−500 µm), rinsed (1% HCl), and air dried under anaerobic conditions (Coy glovebox). Portions of the less than 150-µm fraction were crushed (under anaerobic conditions) to a fine powder for XRD and microwave digestion while the 150- to 250-µm fraction was used for the batch experiments.

Batch incubation experiments were conducted under anaerobic conditions, using 15-mL crimp vials as batch reactors, a mineral:solution ratio of 1:20 (0.25 g:5 mL), and an incubation temperature of 37°C. A temperature of 37°C was chosen based on recommendations for the optimal growth of the methanogen (*Methanococcus* maripaludis) used in experiments with methanogenesis.

Preparation for and setup of the incubation experiments were done in an anaerobic glovebox. First, 0.25 ± 0.01 g of the mineral was placed in each crimp vial with 5 mL of microbial growth media (without methanogen inoculums), or 4.5 mL of growth media + 0.5 mL methanogen inoculum. The vials were then covered with a rubber septum, crimped, and the headspace flushed and filled with a H_2:CO_2 gas mix

(80% H_2:20% CO_2). After filling with the H_2:CO_2 gas mix, the vials were incubated in the dark at 37°C for 1, 3, 5, 7, or 14 days. Each batch reactor was prepared in duplicate (without methanogenesis) or triplicate (with methanogenesis).

After incubation, a syringe (+ needle) was used to sample the headspace of each vial and the sample analyzed immediately for CO_2 and CH_4 using gas chromatography. Vials were then returned to the glovebox, decrimped, destoppered, the pH of the solution measured, the solutions filtered (0.22 μm) and the solids washed/dried under anaerobic conditions. The filtered solutions were stored inside the glove box before they were analyzed for Fe, As, and Pb using ICP-OES/ICP-MS.

4.0 Results and Discussion

4.1 Sediment Characterization

Characterization of the sediments involved XRD analysis and acid extraction.

4.1.1 XRD Analyses

The Edwards aquifer Set A and B samples and High Plains aquifer samples were analyzed using XRD.

4.1.1.1 Edwards Aquifer Set A samples

The mineralogy of this sample set was dominated by calcite, quartz, and montmorillonite (Table C.2 [Appendix C] and Figure D.1 [Appendix D]). We were able to identify montmorillonite, which apparently had variable interlayer spacing because of the presence of interlayer water content and cations. This explains why the low angle peak is very broad and hard to see. However, montmorillonite was more difficult to quantify than expected. None of the crystal structures in the database or literature gave an adequate fit to the peaks present in this sample set, although the peaks seen in many of the samples had a good match to several of the montmorillonite patterns in the International Centre for Diffraction Data (ICDD) database.

To determine the quantity of montmorillonite in these samples, the following technique was used: We chose the sample with the most apparent montmorillonite (sample 4, <2 mm) and added Al_2O_3 as a standard to quantify the amount of calcite and quartz on an absolute scale (i.e., not just relative to each other). We fitted the montmorillonite peaks matching the ICDD patterns using a structure-less phase. Then we adjusted the absolute intensity of this phase so that the amounts of calcite, quartz, and montmorillonite totaled 100%. This assumed that there was no other amorphous material in the sample; we believe that this is the best way to tackle this issue. The amount of montmorillonite that results (58%) is high, but not at odds with the poor fits from the crystal structures we were getting (around 40% montmorillonite). There is no obvious evidence for amorphous material in the materials analyzed.

Having done that, we could use the structure-less phase to quantify montmorillonite in the other samples. Al_2O_3 was added to two other samples, and the results were reasonable; one sample had about 2% amorphous material, and the other had 9.5% (indicating some uncertainties of the method).

4.1.1.2 Edwards Aquifer Set B and High Plains Aquifer Samples

Again, crystalline Al_2O_3 was added to the original samples to estimate the abundance of the amorphous materials. The Edwards aquifer samples were predominantly calcite; no other compounds observed (Table C.3). The amorphous content came out between -3.5% and +0.6%. Clearly negative numbers are meaningless and so this is most likely a consequence of small errors. A relative error of a few percent (so less than 1% absolute for a compound present at 10% concentration) is not surprising.

The High Plains aquifer samples were mostly quartz and feldspar (Table C.3). Some had montmorillonite, most had a small amount of calcite, and all had small amounts of mica. A couple of samples gave negative amounts of amorphous material. For example, CAL 122 4-4.5' gave -1.5% amorphous material, which can be considered zero and the remaining phases scaled accordingly. CNG 150-151' gave -5.8% amorphous material. Because this was a bit more than what is considered acceptable, we re-ran this sample and the sample gave -0.2% amorphous material, which is quite acceptable.

Again, there was no crystal structure for montmorillonite which worked well with these samples. We used the same empirically derived set of peaks for this sample set, which could be a source of error. Feldspars are also difficult to identify because they have a wide variety of compositions and structures, that give rise to a wide range of similar (but not easily modeled) XRD patterns.

4.1.2 Acid Extractions

To determine the amount of major, minor, and trace elements present in the aquifer sediments (i.e., solid-phase chemical composition) that may potentially be released from aquifer sediments at different sites when they are exposed to leaking CO_2, a series of concentrated acid extractions was conducted. These extractions were conducted with representative Edwards and High Plains materials that were subsequently used in batch and column experiments.

We conducted extractions similar to a set of sediment materials collected at other sites, such as Wallula (Washington), FutureGen (Morgan County, Illinois), and the Electric Power Research Institute site (Mississippi). The results from these other sites will be presented in the report that will be published next year because these sediment materials will be used to test whether trace element contaminants are released in significant amounts from aquifer materials of different types.

Our goal in this effort was not to determine whether the Edwards aquifer materials and the High Plains aquifer sediments were hazardous; a more common approach to determining whether a solid is hazardous is to perform the EPA SW-846 Method 1311 test. The main objective for conducting the 8-M acid extractions was to demonstrate that the aquifer rocks and sediments used in the batch and column experiments contained appreciable amounts of potential contaminants, which may or may not be mobilized when these solid materials are exposed to a CO_2 gas stream or CO_2 saturated SGW.

4.1.2.1 Edwards Aquifer Materials

The results from the 8-M acid extractions of the Edwards aquifer samples (Table C.4) clearly show that the materials had significant amounts of important trace elements and potential contaminants, such as As, Cd, Cr, Pb, and, in some samples, Zn (included in the first column of Table C.4). Although the

conditions of these tests were extreme in terms of pH and temperature, the results confirmed that the Edwards aquifer samples may potentially release into the contacting aqueous phase significant amounts of trace elements following desorption and dissolution reactions.

4.1.2.2 High Plains Materials

Similar results were obtained from the 8-M acid extractions performed with the High Plains materials. The results are included in Table C.5.

4.2 Results from Batch Experiments

The results from a series of batch experiments are presented below. The data from the experiments conducted under periodic CO_2 gas exposure conditions is presented first, following by the data from the experiments conducted under continuous CO_2 gas exposure conditions.

4.2.1 Periodic CO_2 Gas Exposure

The pH of the aqueous phase decreased significantly and immediately from about 8.2 to slightly below 6 during the CO_2 gas injection (Figure D.2A and B). However, the aqueous pH rebounded considerably when gas injection was stopped; it reached values of 6.5 or greater within the first 4 hours. This occurred after each short-term (6-minute) CO_2 injection event, clearly demonstrating the ability of the Edwards aquifer material to buffer the effect of the intruding gas. If the system was left unperturbed, the pH increased further towards neutral pH values.

The analyses of select liquid samples collected during this experiment showed that the concentrations of Ca changed with pH (Figure D.3A), most likely indicating a calcite control on aqueous Ca concentration (via dissolution and re-precipitation). In addition, concentrations of Ba and K (Figure D.3B and E) increased compared to the blank concentrations, indicating that their release reaction was also pH dependent. On the other hand, the concentrations of other elements, such as Mg, Si, and Na (Figure D.3D, G, and F) were apparently not significantly affected by the short-term CO_2 intrusions. The aqueous concentration of Cs (Figure D.3C) decreased slightly in response to decreasing pH. The aqueous concentrations of other elements were below the detection limits.

The other Set A materials used in Tests 2, 3, and 4 behaved similarly. In addition to Ca, Ba, Mg, K, Si, and Na, which were mobilized in Tests 2, 3, and 4, the following elements were also detected at different times during these experiments (the EPA's MCLs are included in Table C.6):

- Test 2: Al = 778 µg/L was measured by 143 hours of experimental time (pH = 6.17); Cu = 16.4 µg/L was measured by 167 hours (pH = 6.19); Fe = 5.94 mg/L was measured at time zero (pH = 7.21), Mo = 6.68 and 3.94 µg/L was measured by 69 and 675 hours (the respective pH values were 6.38 and 6.20).
- Test 3: Mo = 3.84, 3.08, 6.28 and 4.23 µg/L were measured by 383, 528, 675, and 790 hours of experimental time (the respective pH values were 6.31, 6.28, 6.24, and 6.23).

- Test 4: Mo = 7.82 and 4.4 µg/L were measured by 120 and 528 hours (the respective pH values were 6.18 and 6.27); S was also released in the aqueous phase from time zero until 315 hours at concentrations that decreased from 20 to 13.4 mg/L.

4.2.2 Constant CO_2 Gas Exposure

4.2.2.1 Tests with Different Materials from the Edward Aquifer (Batch 2 and 6)

Two experimental sets, Batch 2 and Batch 6 with three tests each, were conducted with a total of six representative solid materials, either rocks or slightly weathered rocks, from the Edwards aquifer. Samples 4, 2, and 7 from Set B were used in the tests of Batch 2, and samples 1, 4, and 6 from Set A were used in the tests of Batch 6.

The initial pH value varied in the range of 7.5 and 8 in all tests of Batches 2 and 6, and remained in this range or decreased slightly as demonstrated by the measurements performed in the blanks at each experimental time (Figures D.4A, D.5A, D.6A, D.16A, D.17A, and D.18A). However, the pH of the CO_2 gas-treated samples decreased significantly and varied in the range 6.03 to 6.16 in these six tests. The aqueous Ca concentration also increased significantly and followed similar trends in all these tests (Figures D.4B, D.5B, D.6B, D.16B, D.17B, and D.18B).

In the six materials tested in Batches 2 and 6, the average Ca concentration in the treated samples varied by about 130 mg/L, from a minimum of about 456 mg/L (sample 4, Set B) to a maximum of about 588 mg/L (sample 6, Set A). The average Ca concentration in blanks varied from a minimum of 110 mg/L (sample 4, Set B) to a maximum of 223 mg/L (sample 6, Set A).

Si concentrations increased significantly in the samples of Batch 6 (Figures D.16C, D.17C, and D.18C); a maximum of about 17 mg/L was measured in sample 4, Set A. Si-bearing minerals, such as quartz and montmorillonite, were present in the Set A materials, in addition to calcite. On the other hand, the aqueous Si concentration was below the instrument detection limit in all tests of Batch 2. This is consistent with the results from the mineralogical analyses of the materials used in Batch 2 (the <2-mm fraction of the Set B materials was basically only calcite).

The concentration of divalent cations other than Ca, such as Ba (Figures D.4C, D.5C, D.6C, D.16D, D.17D, and D.18D), Mg (Figures D.4E, D.5D, D.6D, D.16E, D.17E, and D.18E), and Sr (Figures D.4D, D.5E, D.16F, D.17F, and D.18F) increased significantly in the CO_2-treated samples of all tests. The Set A samples (Batch 6) were richer in Ba than the Set B samples (Batch 2). An average Ba concentration of 501 mg/L and a maximum concentration of about 600 µg/L were measured in sample 4, Set A; a minimum of about 30 µg/L was measured in sample 4, Set B.

Sr concentrations were greater in sample 2, Set B (the average in the gas-treated samples was 574 mg/L and aqueous concentrations of over 600 µg/L were measured after 3 days), although the average Sr concentration measured in blanks was 376 µg/L in this sample; the lowest concentrations were measured in sample 4, Set A (about 160 µg/L). The concentrations of Mg were similar in all tests; the average of the treated samples varied from about 10 mg/L (sample 6, Set A) to about 16 mg/L (sample 4, Set A).

The concentrations of Na (Figures D.4G, D.5G, D.6F, D.16H, D.17H, and D.18H) and K (Figures D.4F, D.5F, D.6E, D.16G, D.17G, and D.18G) changed little in the CO_2-treated samples vs. blanks in all tests. However, consistently greater concentrations were found in the treated samples than those of blanks in samples 4 and 6, Set A for K, and sample 4, Set A for Na.

Detectable concentrations of S were measured in all tests of Batch 2 (Figures D.4H, D.5H, and D.6G) and in test 1 of Batch 6 (sample 4, Set B); the CO_2-exposed samples had consistently greater concentrations than the corresponding blanks. All samples of Batch 2 released substantial concentrations of Sn (Figures D.4I, D.5I, and D.6I) in the aqueous phase of the treated samples; sample 7 had the greatest average Sn concentration of about 1.2 mg/L. Concentrations of about 1.5 mg/L were measured after 1 day of experimental time in the test conducted with this sample. The only sample that released Sn in Batch 6 (Figure D.18J) was sample 6, Set A (maximum concentration of about 1000 µg/L).

Aqueous Mn concentrations were significantly greater in the CO_2-exposed samples in two tests of Batch 6 (samples 1 and 4, Set A) (Figures D.16I and D.17I). The average Mn concentration was about 2 mg/L in sample 1, Set A; the maximum Mn concentration measured in this test was over 3 mg/L.

In addition to the chemical elements mentioned above, inconsistent detectable concentrations of minor or trace elements were also measured in these tests. All measurements found to be above instrument detection limits can be summarized as follows:

- Batch 2, Test 1 (sample 4, Set B): Cu = 9.15 µg/L (2 days); Mo = 2.74 µg/L (4 hours), 0.74 µg/L (1 day), and 0.73 µg/L (2 days).
- Batch 2, Test 2 (sample 2, Set B): Cs = 1.2 µg/L (4 hours) and 0.311 µg/L (12 hours); Fe = 131 µg/L (4 hours); Pb = 7.94 µg/L (4 hours: blank concentration = 15 µg/L).
- Batch 2, Test 3 (sample 7, Set B): Si ~3 mg/L (day 2, 3, 7), ~5.6 mg/L (14 days, blank 3.3 mg/L); Sr = 210 µg/L (4, 8, and 12 hours).
- Batch 6, Test 1 (sample 1, Set A): S ~7.1 and 5.7 in the treated and blanks of all times except 7 and 14 days; Sn = 930 and 858 µg/L by 7 and 14 days; Al was detected in blanks (87 and 104 µg/L, 2 and 3 days); Cr = 1.96 and 3.06 µg/L by 4 hours and 3 days; Cu = 2.56, 2.31 and 2.21 at 4 hours, 8 hours, and 3 days, respectively.
- Batch 6, Test 2 (sample 4, Set A): S = 8 mg/L (7 mg/L in the blanks) from 4 hours to 3 days; Cd = 7.6 µg/L (8 hours); Cs = 0.06 µg/L (4 hours through 3 days).
- Batch 6, Test 3 (sample 6, Set A): Mn was detected only at 14 days (Mn = 188 µg/L).

4.2.2.2 The Long Term Effect of the Constant CO_2 Gas Exposure (Batch 3)

This experiment, which was conducted with the representative Edwards aquifer Set B, sample 2, lasted for 119 days; it was an extension of the Batch 2, Test 2. The trend of decreasing pH values with time observed in the blanks of Batch 2, Test 2, continued in the first days of Batch 3 but then stabilized at a pH value of 7.27 (Figure D.7A). The pH values in the treated reactors remained unchanged with time; the average pH was 6.13, which was similar to the average 6.10 of Test 2 of Batch 2.

The average Ca concentration (Figure D.7B) did not change significantly and it remained at 488 mg/L for the rest of the Batch 3 experiment. Low and similar Si concentrations (Figure D.7C) which decreased

with time were measured in both blanks and the CO_2-exposed samples. Decreasing trends in Ba (Figure D.7D), Mg (Figure D.7E), and Sr (Figure D.7F) concentration were also observed with time; the decrease in Ba and especially Sr concentration with time was more rapid than that of Mg.

The concentrations of K (Figure D.7G) and Na (Figure D.7I) either remained unchanged or changed slightly and in a similar way in both blanks and the CO_2-exposed samples. The S concentrations (Figure D.7J) changed within a narrow range of 7 and 8 mg/L during the experiment (with only a few exceptions).

The Sn concentration decreased from a concentration of about 1300 µg/L measured in 7 days, to about 1000 µg/L in 14, 21, and 28 days, and continued to decrease to a concentration of about 680 µg/L by 35 and 42 days, and Sn concentrations were not detected after 42 days. In addition to Sn, inconsistent detectable concentrations of Cu (ranging from 11 to 17 µg/L) were measured in the time interval of 64 to 92 days.

4.2.2.3 The Effects of Particle Size and Brine Concentrations (Batches 4 and 5)

We tested the effect of particle size and brine concentration in Batch 4 and 5 experimental sets. The following Edward aquifer materials were used: Set B, sample 7 and Set B, sample 2, respectively.

Four tests were conducted in each of these experimental sets. T tests that had materials with different size fractions, i.e., <2 mm and >2 mm, were used in the first two tests; two SGW brine solutions were used in the other tests, which simulated two different brine concentrations (1 and 0.1 M in NaCl).

There were no significant differences in the pH values of the CO_2-exposed samples of the four tests of Batch 4 (Figures D.8A, D.9A, D.10A, and D.11A). The average pH values were similar and varied within a narrow range, from 6.07 to 6.13.

The concentrations of Ca, on the other hand, were significantly greater in the brine-exposed samples than in the samples that were not exposed to the brine solutions (Figures D.8B, D.9B, D.10B, and D.11B). For example, the average Ca concentration was about 503 ± 20 mg/L in Test 1 (<2 mm fraction), decreased slightly to 488 ± 35 mg/L in Test 2 (>2 mm fraction), but increased significantly to 748 ± 38 mg/L in Test 3 (1 M NaCl). The average Ca concentration was significantly greater (590 ± 20 mg/L) in Test 4 (0.1 M NaCl) compared to that of Test 1. The differences in Ca concentration in the experiments conducted with different size fractions were insignificant (Tests 1 and 2).

While the concentrations of Ba followed the same trends as the ones of Ca (Figures D.8C, D.9C, D.10C, and D.11C), i.e., they increased in the brine exposed samples, the concentrations of Mg did not change in the four tests of Batch 4 (Figures D.8D, D.9D, D.10D, and D.11D). The average concentration of Ba was about 85 ± 19 µg/L in Test 1 (<2 mm fraction), 68 ± 20 µg/L in Test 2 (>2 mm fraction), almost doubled to 168 ± 44 µg/L in Test 3 (1 M NaCl), and it was again greater (112 ± 23 µg/L) in Test 4 (0.1 M NaCl) compared to Test 1.

The concentrations of K (Figures D.8E, D.9E, and D.11E) and Na (Figures D.8F, D.9F, D.10F, and D.11F) were not different in the Tests 1 and 2, indicating that they were not controlled by the solid-phase particle size. Less aqueous K was present in Test 4, which was conducted with the 0.1-M NaCl SGW

brine solution. The aqueous concentrations of S (Figures D.8G and D.9G) and Sn (Figures D.8I and D.8J) were similar in Tests 1 and 2, which were conducted with solid materials that had two different particle sizes.

One observation made in Test 3 was that Cu was detected in the 1-M NaCl SGW brine at a concentration of approximately 255 µg/L (most likely, it was an impurity in the NaCl salt used to make the 1-M NaCl SGW brine solution). Importantly, the Cu concentration was detected in all experiments and blanks of Test 3 and remained unchanged with time throughout the duration of the experiment, indicating the insignificant effect of the CO_2 gas stream on the fate of this potential contaminant, when brine was also present in the system.

The four tests of Batch 5 were conducted in a similar way to those of Batch 4. The difference was that a different Edward aquifer material (Sample 2, Set B) was used in Batch 5.

Again, there were no significant differences in the pH values of the treated samples of the four tests of Batch 5 (Figures D.12A, D.13A, D.14A, and D.15A). The average pH value varied within a narrow range, from 6.04 to 6.14.

The concentrations of Ca (Figures D.12B, D.13B, D.14B, and D.15B), were again significantly greater in the brine exposed samples. For example, the average Ca concentration was about 503 ± 8 mg/L in Test 1 (<2 mm fraction), decreased by about 50 mg/L to 453 ± 35 mg/L in Test 2 (>2 mm fraction), increased significantly in response to brine exposure to 747 ± 31 mg/L in Test 3 (1 M NaCl), and, again, was greater (569 ± 14 mg/L) in Test 4 (0.1 M NaCl) compared to Test 1.

Importantly, the responses of the two Edwards aquifer materials used in Batch 4 and Batch 5 to the brine exposure were almost identical. The differences of the average Ca concentrations of Tests 1 and 2 were significant only in Batch 5, indicating that the size fraction effect was significant in this material.

The Si aqueous concentrations were detected only in Tests 1 and 2 (Figures D.12C and D.13C). They were not affected by the particle size. Aqueous concentrations of Ba, on the other hand, were significantly different in Test 1 vs. Test 2, indicating a significant effect of the solid phase particle size on the concentration of this chemical element (Figures D.12D and D.13D).

The average concentrations of Mg (Figures D.12E, D.13E, D.14C, and D.15C) were not different in the four tests of Batch 5. The concentrations of Sr (Figures D.12F, D.13F, and D.15F), on the other hand, were dramatically (more than three times) different in Tests 1 and 2 (the average Sr concentration in the gas treated experiments of Test 1 was 689 ± 72 µg/L, while the average Sr concentration of the gas treated experiments of Test 2 was only 196 ± 16 µg/L).

The Sr concentration of Test 4 were similar to those of Test 1 (the average Sr concentration in Test 4 was 657 ± 65 µg/L) and the trends of changes in concentration with time were almost identical, indicating that the less concentrated SGW brine solution (0.1 M NaCl) did not have an effect on the aqueous Sr concentration. The Sr concentration was not detected in the Test 3 that used a more concentrated SGW brine solution. This is most likely due to a higher dilution used to prepare the liquid samples for chemical analyses for this particular test because of the much higher Na concentration in the SGW brine solution.

The concentrations of K (Figures D.12G, D.13G, and D.15E) and Na (Figures D.12H, D.13H, D.14D, and D.15F) were not different in Tests 1 and 2, indicating that these concentrations were not controlled by the solid-phase particle size. The aqueous K concentration measured in the experiments of Test 4, which was conducted with the 0.1-M NaCl SGW brine solution, was similar to that of Test 1.

Detectable and similar concentrations of S were present in the aqueous phase of experiments conducted in Tests 1 and 2 (Figures D.12I and D.13I) and Test 4 (S = 7.37 ± 0.27 mg/L in the CO_2 gas-treated experiments), indicating that the effect of different particle sizes and that of the brine were not significant.

The concentrations of Sn were different in Tests 1 and 2 (481 ± 20 mg/L vs. 447 ± 14 mg/L) (Figures D.12J, D.13J, and D.14G). Significantly greater amounts of Sn were released in Test 4 clearly indicating the combined effects of the CO_2 gas intrusion and brine (Sn average concentration in the experiments exposed to the CO_2 gas was 1085 ± 76 mg/L, which is more than double of the Sn average concentration of Test 1).

The concentrations of Bi (Figures D.12K and D.13K) and P (Figures D.12L and D.13L), which were detected only in the experiments of Tests 1 and 2, where not significantly affected by the differences in particle sizes used in these tests.

Irregular detectable concentrations of minor or trace elements were measured in the tests of Batch 5. Examples are given below:

- Batch 5, Test 1: Al concentrations of ~280 µg/L were present in the blanks of the following experiments: 4, 8, and 12 hours, and 1, 2, 3, and 7 days. The concentration decreased steadily with time from about 308 µg/L (4 hours) to 97 µg/L (7 days).
- Cs concentrations of 0.06–0.14 µg/L were measured in the 12-hour, 1-day, 2-day, and 3-day experiments.
- Cu concentrations of about 5 µg/L were measured in all blanks except for the blank of the 14-day experiment (a maximum Cu of 7.61 was measured in the 4-hour blank).
- Fe concentrations of about 69 µg/L were detected after 8 hours; they slightly increased by 1 day to 146 µg/L. In addition, aqueous Fe concentrations were also measured in one replicate of the 7-day experiment (117 µg/L) and on replicate of the 14-day experiment (448 µg/L).
- Batch 5, Test 2: A concentration of Mo = 2.12 µg/L was measured in the 8-hour experiment.
- Batch 5, Test 3: K concentrations were similar in the gas-treated samples and blanks (32 ± 1 mg/L and 31 ± 1 mg/L); Cu concentration varied between 44–75 µg/L in the experiments where CO_2 gas was injected; similar Cu concentrations were measured in the blanks (48–82 µg/L).
- Batch 5, Test 4: Cu was detected in blanks and in the experiments at a concentration of about 13 µg/L; concentrations of Al varying between 422–758 µg/L were measured in the equilibration, 4-, 8-, 12-hour and 1-, 2-, 3-day experiments; concentrations of Bi (~1800 µg/L) were measured in the 1- and 2-day experiments.

4.2.2.4 The Effect of the Solid-to-Solution Ratio (Batch 7)

The Batch 7 experimental set was conducted with three representative materials from the Edward aquifer: sample 1 of Set A was used in Tests 1 and 2; sample 4 of Set B was used in Test 3, and sample 7 of Set B was used in Test 4. Tests 1 and 2 were conducted at a different solid-to-solution ratio (1:3 and 1:2, respectively). Tests 3 and 4 were conducted at a solid-to-solution ratio of 1:2, and the results from these tests are being compared to the results obtained in Batch 2, Tests 1 and 3 presented above, which used the same solid materials.

Identical pH values were measured in Tests 1 and 2 (pH = 6.12) (Figures D.19A and D.20A). The pH values measured in Tests 3 and 4 were also similar to the ones measured in Tests 1 and 3 of Batch 2, respectively (Figures D.21A and D.22A). A smaller solid-to-solution ratio was used in the latter tests.

The Ca concentration was slightly (but not significantly) greater in Test 2 compared to Test 1 (Figures D.19B and D.20B). The same is true for the other two solid materials used in Tests 3 and 4 (Figures D.21B and D.22B); the Ca concentration in these tests were slightly lower than the Ca concentrations measured in Batch 2, Tests 1 and 3, respectively.

Slight differences or no differences at all were found in the results of Tests 1 and 2 for Si, Ba, Sr, Mg, K, Na, and Sn. The average concentration of Mn was greater in Test 1 than Test 2 (419 vs. 281 µg/L) (these are included in Figures D.19 and D.20, C, D, E, F, G, H, and J).

Concentrations of Si were not measured in Batch 2, Tests 1 and 3, but Si concentrations of about 2 mg/L were measured in Tests 3 and 4 (Batch 7) suggesting that the solid–to-solution ratio is important when dealing with elements with low aqueous concentrations.

When comparing Batch 2, Test 1 (1:3 solid-to-solution ratio) vs. Batch 7, Test 3 (1:2 solid-to-solution ratio) significant differences were observed for Ba, Sr, K (Figures D.21D, E, and G). There were no differences for Mg, Na, and S (Figures D.21F, H, and I). Sn was not detected at all in Batch 7, Tests 3, but it was detected in Batch 2, Test 1.

When comparing Batch 2, Test 3 (1:3 solid-to-solution ratio) vs. Batch 7, Test 4 (1:2 solid-to-solution ratio) the following differences were observed: 1) less K was released in Batch 7, Test 4 (Figure D.22G); 2) more Na and Sr were released in Batch 7, Test 4 (Figure D.22H and E); 3) Sn was released only in Batch 2, Test 3. The concentrations of Ba, Mg, and S were similar in both tests (Figures D.22D, F, and J).

Other measurements taken during these tests were:

- Batch 7, Test 1: Fe = 542 µg/L was detected in the 7-day experiment; Cr = 4.87 µg/L was detected in the 2-day experiment.
- Batch 7, Test 4: Cr concentrations of 4.7 and 5.72 µg/L were detected in the 4-hour and 2-day experiments; Cu concentrations of 4.85 and 4.72 µg/L were detected in the 4-hour and 8-hour blanks, and concentrations of 5.54 and 4.42 µg/L were measured in the equilibration and 14-day experiments; Mo concentrations of 1.93, 2.83, and 1.39 were measured in the 1-day, 14-day, and equilibration experiments.

4.2.2.5 High Plains Aquifer: Sediments from the CNG Well (Batches 8 and 9)

Batch 8 and Batch 9 experimental sets were conducted to determine major, minor, and trace elements released from different sediment materials collected at the High Plains aquifer in Kansas, when these materials were exposed to a CO_2 gas stream. Eight sediment materials were used in Batches 8 and 9.

Sediment materials from the same well but from different depths were used in Test 1 and Test 2 of Batch 8 and Test 1 and Test 2 of Batch 9 as described below:

- Batch 8, Test 1: CNG well, depth 110−111 fbg (hereafter named sediment CNG 110)
- Batch 8, Test 2: CNG well, depth 60−61 fbg (hereafter named sediment CNG 60)
- Batch 9, Test 1: CNG well, depth 8−9 fbg (hereafter named sediment CNG 8)
- Batch 9, Test 2: CNG well, depth 150−151 fbg (hereafter named sediment CNG 150).

The aqueous pH of the experiments conducted in Test 1 (Batch 8) (Figure D.23A) decreased significantly after CO_2 injection from about 7.80 to 6.09 and remained unchanged for the duration of experiment. The pH values measured in the blanks exhibited a slight decreasing trend with time.

The aqueous Ca concentration changed significantly from about 82 to about 300 mg/L in the first 4 hours of the experiment (Figure D.23B). The Ca concentration continued to increase with time. The aqueous Ca concentration of blanks was greater than that of the SGW and it increased slightly during the experiment.

The aqueous Si concentration increased initially at a faster rate (4 hours to 1 day) and continued to increase at a slower rate until the end of the experiment (Figure D.23C). The Si concentration in the blanks, which was greater than that in the SGW, also increased during the experiment, but it was consistently lower than the concentration measured in the CO_2 gas-exposed sediments, indicating that Si-bearing minerals underwent dissolution releasing Si into the aqueous phase.

The aqueous concentration of other divalent cations, i.e., Ba (Figure D.23D), Sr (Figure D.23E) and Mg (Figure D.23F) followed similar nonlinear increasing trends with time to the ones observed for Ca. These concentrations increased significantly after CO_2 exposure (more than three times for Ba and Sr, and two times for Mg). Monovalent cations, such as Na and K exhibited similar behaviors to divalent cations (Figures D.23G and H).

Importantly, the aqueous concentration of Mn increased significantly from zero in the blanks and SGW to almost 500 µg/L by 14 days (Figure D.23I). The concentrations of S were similar in the blanks and the CO_2 gas-treated reactors (Figure D.23J).

Other observations and measurements performed during this test include detectable concentrations of Mo (2.40 µg/L) being present in all blanks and at the equilibration experiments (time zero). However, Mo concentrations above instrument detection limit were not measured in the experiments conducted in the presence of the CO_2 gas, with the exception of the 4-hour experiment where an average Mo concentration of 1.43 ± 0.06 µg/L was measured in both replicates. In addition to Mo, Fe was detected in the 12-hour experiment at a concentration of 208 µg/L suggesting that some Fe was released in these experiments. The concentrations of all other major, minor, or traces elements were below the detection limits.

Batch 8, Test 2 was conducted with sediment CNG 60, which originated from a shallower depth. Both similarities and differences were observed between the data sets generated in Tests 1 and 2 in terms of the way these two sediment materials responded to the CO_2 gas exposure.

Some differences were as follows:

1. Sediment CNG 60 exhibited less buffering capacity than the deeper sediment; aqueous pH decreased from 7.70 to 5.37 (Figure D.24A) (which was about 0.7 pH units more acidic than the aqueous pH of CNG 110).
2. The Ca concentrations were much lower in the experiments conducted with sediment CNG 60 (Figure D.24B) than those in the experiments conducted with sediment CNG 110 (average Ca concentration of 113 ± 15 mg/L vs. 393 ± 39, respectively). Sediment CNG 60 was calcite free although calcite coatings might have been present.
3. Aqueous concentrations of divalent cations were lower in experiments conducted with sediment CNG 60 than in the experiments conducted with sediment CNG 110 [Ba: 452 ± 63 vs. 632 ± 91; Sr: 0.35 ± 0.05 vs. 0.64 ± 0.06; Mg: 14 ± 1.8 vs. 21 ± 2) (Figures D.24D, E, and F).
4. The deeper sediment CNG 110 released a greater amount of Mn into the aqueous phase after CO_2 exposure; Mn concentrations were measured only in the 12-hour experiment (96 µg/L), 7-day experiment (171 µg/L), and 14-day experiment (243.5 µg/L) of Test 2 conducted with the CNG 60 sediment.
5. While in the experiments conducted with sediment CNG 110 only two elements were mobilized, one minor and one trace elements (i.e., Fe and Mo), in the experiments conducted with sediment CNG 60 other elements were mobilized in addition to As (Figure D.24J) that was present in detectable concentrations in all CO_2 gas treated experiments, such as the following:
    a. P was released in all experiments except for the 14-day experiments (the average P concentration was 1068 µg/L)
    b. Al (227 µg/L) in the 8-hour experiment
    c. Cr (3.77 µg/L) in the equilibration experiment (time zero)
    d. Cu (16.8, 6.31 and 30.7 µg/L in the 2-day experiment, 7-day and equilibration experiments, respectively)
    e. Fe (249 and 221 µg/L in the 8-hour and 14-day experiment, respectively)
    f. Pb (5.31 and 4.03 µg/L in the 14-day and equilibration experiments, respectively)
    g. Mo with concentrations that varied between 1.93–3.66 µg/L in all blanks and equilibration experiment.

Some similarities were:

1. Si concentrations were not significantly different in Tests 1 and 2 (Figure D.24C).
2. The concentration of the monovalent cations, such as Na and K (Figures D.24G and H), and S (Figure D.24I) were similar in both sediments.
3. Mo was present in all blanks of both tests.

Two additional tests were conducted with the sediments from the CNG wells. Batch 9, Test 1 was conducted with a shallow sediment material (sediment CNG 8). This sediment behaved similarly to the previous ones in terms of pH change immediately after CO_2 gas exposure, from about 7.70 to 6.11 (Figure D.27A). However, much more Ca was mobilized in the experiments conducted with this sediment. The aqueous Ca concentration increased from about 152 to more than 400 mg/L in the first 4 hours of the experiment. The Ca concentration continued to increase with time to more than 500 mg/L, which was the highest concentration measured in the experiments conducted with the CNG sediments. (Figure D.27B). The Ca concentration of blanks was about three times greater than that of the SGW and did not change significantly during the experiment. This most likely indicated that soluble Ca salts were transported down from shallower horizons, or unstable Ca-bearing solids were present in this shallow sediment.

The aqueous Si concentration was the highest measured in the CNG sediments (a maximum of about 30 mg/L was measured on day 14 and it followed a nonlinear increasing trend (Figure D.27C). The concentration in the blanks changed little during the experiment, although the Si concentration of about 13 mg/L measured in the blanks was greater than the Si concentration of the SGW (0 mg/L).

The aqueous concentration of other divalent cations than Ca, i.e., Ba (Figure D.27D), Sr (Figure D.27E), and Mg (Figure D.27F) followed similar nonlinear increasing trends with time. These concentrations increased significantly after CO_2 exposure (more than three times for Ba [average Ba = 792 ± 63 µg/L]) and two times for Sr (average Sr = 2.8 ± 0.3 mg/L) and Mg (average Mg = 70 ± 9 mg/L). Monovalent cations, such as Na and K exhibited similar behaviors (average K = 27 ± 1 mg/L and average Na = 45 ± 1 mg/L) (Figures D.27G and H).

The aqueous concentration of Mn increased significantly from zero in the blanks and SGW to about 300 µg/L by 14 days (average Mn = 158 ± 104) (Figure D.27I). The concentrations of S did not change during the experiments although they were consistently greater in the CO_2 gas-treated samples than in blanks (average S = 26 ± 0.1) (Figure D.27J).

Detectable concentrations of Mo of about 2.5 µg/L were present in the blanks and in the equilibration experiments at time zero. In addition, Sb concentrations of about 0.70 µg/L were detected in the 8- and 12-hour experiments. The concentrations of all other major, minor, or traces elements were below the detection limits.

Another test was conducted with sediment CNG 150 (Batch 9, Test 2). The results were similar to those of sediment CNG 110 and 8 in terms of changes in pH and Ca and Si concentrations (Figures D.28A, B, and C). The maximum concentrations for Ca and Si were about 400 and 20 mg/L, respectively. Appreciable amounts of divalent cations were also released (average Ba = 670 ± 81 µg/L; average Sr = 1.7 ± 0.2 mg/L and average Mg = 33.2 ± 6 mg/L) (Figures D.28D, E, and F). Monovalent cations, such as Na and K exhibited similar behaviors (average K = 24 ± 2 mg/L and average Na = 35 ± 2 mg/L) (Figures D.28G and H). Both dissolution and exchange reactions may have contributed to these increases in concentration.

The concentrations of Mo decreased significantly after CO_2 exposure and were consistently lower than the concentrations measured in the blanks (Figure D.28I). Similar to other CNG sediments, the aqueous concentration of Mn increased significantly from zero in the blanks and SGW to more

than 300 µg/L by 14 days (Figure D.28K). The concentrations of S were similar in the blanks and in the CO_2-treated reactors (Figure D.28L).

A detectable concentration of Cu of about 5.83 µg/L was present in one of the CO_2 gas-treated reactors. A concentration of about 1 mg/L of Fe was also measured in one of the treatments. The concentrations of all other major, minor, or traces elements were below the detection limits.

4.2.2.6 High Plains Aquifer: Sediments from the CAL 121 Well (Batches 8 and 9)

Batch 8, Test 3 was conducted with a sediment material collected during drilling of well CAL 121 at a depth of 151 to 152 fbg (hereafter called sediment CAL 1 151). Another test (Test 3 of Batch 9) was conducted with a sediment from the same well that was collected at a depth of 91−92 fbg (hereafter called sediment CAL 1 91). We will initially present the results of Batch 9, Test 3 conducted with sediment CAL 1 91 (that contains no calcite) and will compare these results to those of Batch 8, Test 3 conducted with sediment CAL 1 151 (that contains calcite). Otherwise, these two sediments had similar mineralogy as determined by the quantitative XRD results.

The aqueous pH decreased significantly from about 7.87 to 5.78 in Batch 9, Test 3 (Figure D.29A). The pH values measured in the blanks changed little during the 14 days of the experiment.

The aqueous Ca concentration changed significantly from about 70 mg/L in the blanks to more than 160 mg/L in the first 4 hours of the experiment reaching a maximum of about 280 mg/L by 14 days (Figure D.29B) (average Ca concentration was 239 ± 46 mg/L). Ca concentration of blanks was greater than that of the SGW and remained unchanged during the experiment.

The aqueous Si concentration increased nonlinearly in the first 3 days, but then followed an apparent linear increasing trend reaching a maximum of more than 8 mg/L by day 14 (Figure D.29C). Si average concentration in the CO_2-treated experiments was 5.7 ± 1.8 mg/L. The concentration in the blanks increased as well but reached an apparent new equilibrium at around 4 mg/L.

The aqueous concentration of other divalent cations than Ca, i.e., Ba (Figure D.29D), Sr (Figure D.29E), and Mg (Figure D.29F), and monovalent cations, i.e., Na and K (Figures D.29G and H) followed similar increasing trends to the ones observed in previous experiments. These concentrations increased significantly after CO_2 exposure (more than two times for Ba [average Ba concentration = 255 ± 23 mg/L) and two times for Sr (average Sr concentration = 0.71 ± 0.13 mg/L) and Mg (average Mg = 19 ± 2 mg/L]). Monovalent cations, such as Na and K exhibited similar behaviors (average K concentration = 33 ± 1 mg/L and average Na concentration = 30 ± 1 mg/L) (Figures D.29G and H). Both dissolution and exchange reactions may have contributed to these increases in concentration.

The aqueous concentrations of Mo were consistently smaller in the aqueous phase of the sediments exposed to the CO_2 gas, while steadily increased in the blanks up to about 15 µg/L by 14 days (Figure D.29I).

The aqueous concentration of Mn increased significantly from zero in the blanks and SGW to almost 1500 µg/L by 14 days (Figure D.29K). The average Mn concentration in the CO_2 gas-treated experiments was 774 ± 342 µg/L. The concentrations of S were similar in the blanks and CO_2 gas-treated experiments; average S concentration was 16 ± 1 µg/L (Figure D.29L).

A detectable concentration of Cd of about 1.12 µg/L was first measured in the 12-hour experiment. Similar Cd concentrations (varying from 1.07 to 1.43 µg/L) were measured in the time interval from 2 to 14 days. A Cu concentration of about 4.70 µg/L was detected in the 4- and 8-hour experiments, and a slightly greater Cu concentration (5–6 µg/L) was measured in the 7- and 14-day experiments. The concentrations of all other major, minor, or traces elements were below the detection limits.

We will now compare these results with those of the experiments conducted with sediment CAL 121 1 151 (that contained calcite). The aqueous pH decreased significantly from about 7.87 to 6.11 in Batch 8, Test 3 (Figure D.25A), indicating a better buffering capacity of this sediment than the shallower sediment CAL 1 91.

Greater amounts of Ca were released in sediment CAL 1 151. The aqueous Ca concentration changed significantly from about 86 mg/L in the blanks to almost 200 mg/L in the first 4 hours of the experiment reaching a maximum of more than 400 mg/L by 14 days (Figure D.25B) (average Ca concentration was 379 ± 80 mg/L vs. 239 ± 46 mg/L in sediment CAL 1 91). The average Si concentration was 7 ± 2.5 mg/L (Figure D.25C), which was comparable to the average Si concentration of 5.7 ± 1.8 mg/L in sediment CAL 1 91.

The concentrations of other ions in the CO_2-treated experiments were as follows: average Ba concentration = 311 ± 82 vs. 255 ± 23 mg/L in sediment CAL 1 91) (Figure D.25D); average Sr concentration = 0.86 ± 0.2 vs. 0.71 ± 0.13 mg/L in sediment CAL 1 91 (Figure D.25E); average Mg = 21 ± 5 vs. 19 ± 2 mg/L in CAL 1 91) (Figure D.25F); average K concentration = 29 ± 6 vs. 33 ± 1 mg/L in sediment CAL 1 91 (Figure D.25G); average Na concentration = 30 ± 46 vs. 30 ± 1 mg/L in sediment CAL 1 91) (Figure D.25H); average Mn concentration 427 ± 225 vs. 774 ± 342 µg/L in sediment CAL 1 91 (Figure D.25K); average S concentration = 15 ± 3 vs. 16 ± 1 µg/L of sediment CAL 1 91 (Figure D.25I); average Mo concentration = 13 ± 1.5 µg/L vs. 13 ± 1.7 µg/L in sediment CAL 1 91 (Figure D.25L).

Only one trace metal was detected in the experiments conducted with sediment CAL 1 151 (Batch 8, Test 3) (Pb =1.16 ± 0.30 µg/L in the 1-day experiment), compared to a few others detected in the experiments conducted with sediment CAL 1 91 (such as Cd and Cu), although they were detected at particular experiments and not in all of them. The concentrations of all other major, minor, or trace elements were below the detection limits.

4.2.2.7 High Plains Aquifer: Sediments from the CAL 122 Well (Batches 8 and 9)

Two additional batch experiments were conducted with the High Plains aquifer sediments. Batch 8, Test 4 was conducted with a sediment from the well CAL 122 collected at a depth of 29 to 30 fbg (hereafter called sediment CAL 2 29). Another test, (Test 4 of Batch 9) was conducted with a sediment from the same well but different depth, 4–4.5 fbg (hereafter called sediment CAL 2 4).

The sediments CAL 2 4 and CAL 2 29 contained 4.7 and 1.6% calcite, and 5.2 and 2.6% mica, respectively. The other mineralogical components were present in similar amounts.

The aqueous pH of the CO_2-treated experiments of Batch 9, Test 4 (shallow sediment CAL 2 4) decreased significantly and almost instantaneously with about two units, from 8.16 to 6.17 (Figure D.30A). The aqueous Ca concentration increased from about 48 mg/L (in the blanks) to greater

than 300 mg/L in less than 4 hours (Figure D.30B). The average Ca concentration was 338 ± 18 mg/L. The aqueous Si concentration increased significantly as well (Figure D.30C); the average Si concentration was 24 ± 6 mg/L.

The concentrations of divalent cations, such as Ba (Figure D.30D), Sr (Figure D.30E), and Mg (Figure D.30F) also changed significantly in the experiments after CO_2 exposure. This change was either instantaneous similar to that of Ca (e.g., Ba) or followed an increasing nonlinear trend as a function of time (e.g., Sr and Mg). The maximum Mg concentration measured was about 130 mg/L. The average concentrations of Ba, Sr, and Mg were 306 µg/L, 3.6 mg/L, and 107 mg/L, respectively. Monovalent cations, such as Na and K, manifested similar behavior (Figures D.30H and G). The average concentration of Na and K were 64 and 45 mg/L, respectively. The concentration of S was similar in the experiments and blanks (average S concentration was 22 ± 1.5 mg/L).

Importantly, the concentration of Mn increased dramatically in the experiments exposed to the CO_2 gas and the maximum Mn concentration was more than 400 µg/L (the average Mn concentration was 196 ± 102 mg/L) (Figure D.30L). The reason for this increase is still under investigation, although one would argue that the dramatic release of Mn into the aqueous phase might be attributed to the changes in system's Eh (redox conditions) induced by the CO_2 gas injection.

Detectable concentrations of Mo, Cu, and As were also present in the aqueous phase (Figures D.30I, J, K). The Mo concentration in the blanks changed little (remained around 15 µg/L during the experimental time of 14 days) while the Mo concentration in the CO_2-treated experiments decreased significantly to nondetectable levels by 2 days. The Cu concentration followed the same trend in the first 2 days, but increased slightly by 7 and 14 days. The As concentration increased and remained unchanged at 5 µg/L in the first 2 days, but decreased to below detection limit values for the rest of the experiment.

A Sb concentration of 0.75 was measured in the 4- and 12-hour treatments and in some blanks. The concentrations of all other major, minor, and trace elements were below the detection limits of the instruments.

The other sediment (sediment CAL 2 29) behaved similarly. The aqueous pH of the CO_2-treated experiments of Batch 8, Test 4 (deeper sediment) decreased to 6.06 (about 0.11 pH unit more than the shallow sediment) (Figure D.26A). Both Ca concentration increasing trends and average concentration were similar in both sediments; the average Ca concentration was 316 ± 85 (CAL 2 29) (Figure D.26B) vs. 338 ± 18 mg/L (CAL 2 4); the average Si concentration was 15 ± 5 mg/L (Figure D.26C) (sediment CAL 2 29) vs. 24 ± 6 mg/L (sediment CAL 2 4).

Sediment CAL 2 29 had more Ba than sediment CAL 2 4 (average Ba concentration was 481 ± 131 vs. 306 ± 13 µg/L in the shallow sediment), but had less Mg and Sr (average Mg concentration was 46 ± 13 vs. 107 ± 27 mg/L and average Sr concentration was 1.7 ± 0.4 vs. 3.6 ± 0.6 mg/L) (Figures D.26D, F, and E). The concentrations of Na were similar in both sediments 59 vs. 64 mg/L (Figure D.26H), but the shallow sediment had more K (45 vs. 22 mg/L) (Figure D.26G). The concentration of S was also similar in both sediments (about 16 in the deep and 22 mg/L in the shallow sediment) (Figure D.26I).

Mn concentrations above detection limits were found in the 2-day, 3-day, 7–day, and 14-day experiments (the respective Mn concentrations were 132.5 ± 6.36, 161.5 ± 2.12, 125.0 ± 4.24, and 249.0 ± 12.7 µg/L). Clearly, sediment CAL 2 29 released less Mn than sediment CAL 2 4.

Mo was detected in the equilibration experiment (time zero) (Mo = 10.08 ± 0.14 µg/L) and in one replicate of the 4-hour experiment (6.54 µg/L), 1-day experiment (1.72 µg/L), and 2-day experiment (3.83 ± µg/L). Mo was also present in all blanks; the concentration in the blanks varied between 3.98 and 5.16 µg/L. Cd was detected in one replicate of the 3-day experiment (Cd = 2.79 µg/L). The concentrations and the variety of trace elements (Mo, Cu, As, Sb) detected in the shallow sediment (CAL 2 4, Batch 9, Test 4 discussed above) were greater than those of the deeper sediment.

The results from all batch tests presented in this section of the report showed that potential contaminants confirmed to be present in both Edwards aquifer rocks and High Plains sediments as determined by the 8-M acid extractions, were only occasionally mobilized into the contacting aqueous phase when these solid materials were exposed to the CO_2 gas stream and to the CO_2-saturated SGW. In addition, their detectable concentrations were low.

The results of the chemical analyses presented above were not corrected based on the liquid mass loss measured at the end of the experiments, which were presented in the Technical Scope and Approach section of this report, because the liquid mass losses were not significant in the majority of the experiments conducted with both Edwards aquifer rocks and High Plains aquifer sediments.

4.3 Results from Column Experiments

The results from the four sets of column experiments will be presented below. Representative Edwards aquifer materials and High Plains sediments were used to pack the columns. All column experiments were conducted under hydraulically saturated conditions.

4.3.1 Results from Set 1

Two column experiments were conducted in Set 1 (Figures D.31, D.32, and D.33). The first column was packed with Accusand and the second one was packed half with the Accusand and half with the Edward aquifer Set B sample 4. The Edward aquifer SGW purged with N_2 gas was initially used to leach the columns. A CO_2 gas-saturated SGW was also used in these experiments; it was prepared by injecting CO_2 gas into the influent solution (i.e., SGW). A gas flow rate of ~0.52 mL/min was applied and the SGW container had 2 L of the Edward SGW solution. The changes in pH during the CO_2 purging time are presented in Figure D.31. The pH was stabilized at a value of about 4 after about 100 hours. The pH was monitored frequently in the influent bottle during all the time.

The pH and Eh of the columns' effluent, which were measured continuously online, followed a similar decreasing (pH) or increasing (Eh) trend when a N_2-saturated SGW was leached through the columns of Accusand and Accusand plus the sediment (Figure D.32). When the inlet solution was switched to the CO_2 gas-saturated SGW, the pH of the effluent collected in the Accusand column decreased significantly to about 5, while the pH of the effluent of the column that was partially packed with the Edward aquifer material decreased to a pH about 6.5 right before the 146 stop-flow event. The pH increased during the stop-flow to about 7, but it followed again a decreasing trend as soon as the flow was reestablished. Clearly, the Edward aquifer material manifested a greater buffering capacity than the Accusand. Importantly, the Eh values in both columns increased with leaching time, indicating that the conditions in the column turned increasingly oxidizing.

Calcium concentration increased significalty as soon the CO_2 gas-saturated SGW was used as the leaching solution (as expected, Ca concentration did not change in the Accusand column's effluent) (Figure D.33). The Ca concentration decreased during the 146-hour stop-flow event, most likely in response to increasing pH, and then continued the increasing trend as soon as the flow restarted. A Ca concentration steady state (usually, indicative of pseudo equilibrium condition) was not observed during this experiment.

Other observations that were based on the effluent concentration data presented in Figure D.33 are as follows:

- Some elements had effluent concentrations below the elemental quantification limit (EQL) but were detectable by the equipment used to run the analyses. Examples: As, Al, Mn, Sn, Zn, P, Ni, Se, and Cd.
- Some elements had effluent concentrations above detection limits only during leaching with the N_2-saturated SGW and/or during the stop-flow events. Examples: Cu, Cs, Si, Sr, S, Cr, Mo, Pb.
- Some elements had effluent concentrations above detection limits in the effluents of the column packed partially with the Edwards aquifer material that followed different trends than those observed in the Accusand column. Examples: Na, Ba, Mg, K.
- Some elements had effluent concentrations above detection limits that followed similar trends in both columns. Example: Cs.

Based on the data collected from these experiments we conclude that the Edwards aquifer material was able to buffer the aqueous phase pH to values well above (approxiamtely 2.5 pH units) the CO_2 laden SGW influent pH (which was about 4).

One important conclusion derived from these observations is that important potential contaminants, such as Pb, Cs, Cu, and Mo, were detected in the aqueous phase only during the time the columns were leached with the N_2-saturated SGW, thereby confirming that these releases were not a consequence of the CO_2 gas exposure of the Edward aquifer material.

Another important conclusion is that some of the potential contaminants were released into the aqueous phase during the stop-flow events indicating that the reaction controlling their release was either time-dependent or pH-dependent, because an increase in liquid phase pH was also observed during the stop-flow events.

4.3.2 Results from Set 2: Edwards Aquifer Material, Set B, Samples 4 and 7

Effluent pH changed little during leaching with the SGW (the first 30 hours) in the experiment conducted with sample 4 (Figure D.34). The pH in the effluent of the other column initially decreased slightly, but then increased to values similar to the initial pH. When the CO_2 gas-saturated SGW was injected in both columns, the effluent pH decreased fast (within the first 10 hours) and then stabilized to about 6.4 and 6.5 in the experiments conducted with samples 4 and 7, respectively. The pH measured in the batch experiments conducted with the same sediments (Batch 2, Test 1 and Test 3) were lower (6.10 and 6.09, respectively), suggesting that the lower solid-to-solution ratio in batch tests allowed the dissolved CO_2 gas to overpower more of the Edwards aquifer materials buffering capacity.

The effluent chemical composition changed significantly during the column experiments (Figure D.35). For example, the Ca concentration increased immediately after the CO_2 gas-saturated SGW was injected into the columns, and it continued to increase for the duration of the experiment without establishing a steady-state concentration (a maximum concentration of about 250 mg/L was reached at the end of this experiment). The increasing trend, however, was irregular (i.e., not smooth), most likely indicating that more than one reaction (either simultaneous or sequential), with fast or slow kinetics, was affecting and/or controlling the aqueous Ca concentration as the liquid phase moved through the packed column.

The Ca concentration was significantly perturbed in both columns during the two stop-flow events of 143 and 69 hours applied in these column experiments, reinforcing the idea that either multiple or time-dependent reactions were controlling Ca concentration in the column liquid phase. The Ca concentrations measured in the batch experiments conducted with the same materials (Set B, samples 4 and 7) reached relatively fast (within the first hours of experiment) an apparent equilibrium concentration of 456 and 528 mg/L, although one should realize that the two systems, the column and batch systems, are fundamentally different in terms of solid-to-solution ratio and the fluid residence time, which is much shorter in the column experiments where CO_2 gas-saturated SGW was continuously injected into the columns.

Other observations based on the effluent concentration data from both column experiments presented in Figure D.35 are as follows:

- Some elements had effluent concentrations below the EQL but were detectable by the equipment used to run the analyses. Examples: Al, Ni, Zr.
- Some elements had effluent concentrations above the EQL only during leaching with SGW and during the stop-flow events. Examples: Cu, Mo, Se, and Ag.
- Some elements had effluent concentrations above detection limits in both columns (in addition to Ca). Examples: Sb, Ba, Mg, Cs, Si, Na, Sr, and S.

See Table C.7 in Appendix C for additional relevant data.

These results were consistent with the results from the batch experiments presented in the sections above, which used the same solid materials (Edwards aquifer Set B, samples 4 and 7) as the ones used in these column experiments (Batch 2, Tests 1 and 3).

The following elements were also detected in the batch experiments: Ba, Mg, Sr, Na, and S in addition to Ca. K was measured in the column effluents but its concentration was affected by the online pH electrode of the column apparatus and for this reason it was not reported.

The column effluent concentrations of Si and Cs were close to the detection limit and, most likely, for this reason they were not detected consistently in the batch experiments. Silicon was detected only in the 2-, 3-, and 7-day experiments of the test conducted with solid material Set B, sample 7. In addition, Sb was not detected in the batch experiments and Sn was not detected in the column experiments.

The concentrations of other elements and potential contaminants such as Cu, Mo, Se, and Ag were most likely controlled by pH-dependent reactions because their concentrations were detected only during

leaching with SGW and during the stop-flow events when a rebound in the aqueous phase pH was observed. Cu and Mo were also detected in the contacting aqueous phase in a few of the batch tests.

4.3.3 Results from Set 3: Edwards Aquifer Material, Set A, Samples 1 and 4

The changes in influent reservoir pH during CO_2 gas injection are presented in Figure D.36. The graph shows that injection of CO_2 gas caused the SGW pH to drop to about 4.2 after the first 25 hours of injection. Column effluent pH increased significantly in sample 1 and slightly in sample 4 during leaching with the SGW (the first 110 hours) (Figure D.37). When the CO_2 gas-saturated SGW was injected into the columns, the effluent pH decreased fast (within the first 10 hours) and then stabilized to about 6.2 and 6.3 in the experiments conducted with the Edwards aquifer material, samples 1 and 4, respectively. The pH measured in the batch experiments conducted with the same sediments (Batch 6, Test 1 and Test 2) were lower (6.10 and 6.03, respectively).

The effluent chemical composition changed significantly during these two column experiments (Figure D.38). The Ca concentration decreased in both columns during leaching with SGW (from 150 to 120 mg/L in sample 1 and from 260 to 160 mg/L in sample 4. It then increased significantly in sample 1 (from 120 to about 200 mg/L) and slightly in sample 4 (from 160 to 180 mg/L) immediately after the CO_2 gas-saturated SGW was injected. The Ca concentration continued to increase for the duration of the experiment following a slowly increasing trend and reaching a maximum of about 250 mg/L before the end of the experiment. The increasing trend was again irregular and similar to the one observed in the previous column experiments, most likely indicating that more than one reaction (dissolution, precipitation, adsorption, desorption) was affecting and/or controlling the aqueous Ca concentration as the liquid phase moved through the column.

The Ca concentration decreased significantly during the 118- and 195-hour stop-flow events, reaching low concentrations well below the pseudo steady-state concentrations established in both columns at the beginning of the experiments during leaching with the SGW most likely in response to increases in pH observed during the 118- and 195-hour stop-flow events, assuming that calcite dissolution and precipitation were the primary controls on Ca concentration in these systems. The Ca concentrations measured in the batch experiments conducted with the same materials (Set A, samples 1 and 4) reached relatively fast (within the first hours of experiment) apparent equilibrium concentrations of 508 and 466 mg/L, respectively.

The Si concentration followed two well-distinguished trends in the two solid materials tested in the Set 3, Edwards aquifer Set A, samples 1 and 4. In sample 1, Si concentrations decreased nonlinearly from about 7 to 1 mg/L in the first 110 hours of experiment when the SGW was used to leach the columns; afterwards, it reached a peak maximum of about 9 mg/L immediately after the CO_2 gas-saturated SGW was injected into the column and the relatively short stop-flow event, but then decreased to values close to the detection limit. Finally, it peaked again during the 118- and 195-hour stop-flow events, but the peak concentrations decreased even though the stop-flow duration increased. This behavior is consistent with the fact that the solid source that was controlling and contributing to the Si concentration in solution was limited in mass. This solid source was most likely distributed throughout the sample matrix because the effluent concentration was a function of the fluid residence time; i.e., it increased during the stop-flow events, indicating that additional time was needed for contributions of the remote sites within sample matrix to travel through the diffusive pores to the advective pores within the column. The results from

this column experiment were also consistent with the results of Batch 6, Test 1 (conducted with the same material), which showed that the Si accumulated in the aqueous phase during 14 days was barely greater than 6 mg/L.

In sample 2, the Si concentration decreased only slightly and established a pseudo steady-state concentration during the first 110 hours of leaching with the SGW; the effluent pH changed insignificantly during this period of time. However, effluent Si concentration increased to a new pseudo steady state of about 11.5 mg/L as soon as the CO_2 gas-saturated SGW was injected into the column. The Si concentration decreased significantly during the 118- and 195-hour stop-flow events, most likely in response to changes in pH during the stop-flows. Most likely, a dissolving Si-bearing phase (silicate or phyllosilicate) was controlling the aqueous Si concentration. This phase (or phases) was able to release Si continuously into the aqueous phase (the influent fluid was Si-free), and sustain relatively constant Si effluent concentrations for the duration of the experiment (about 500 hours). The results from this column experiment are also consistent with the results of Batch 6, Test 2 (conducted with the same material), which showed that the Si concentration reached an apparent equilibrium at a concentration of about 18 mg/L.

Ba exhibited similar behavior to that of Si during these column experiments. Again, the results for Ba generated from the column experiments are consistent with the results obtained from Batch 6, Tests 1 and 2. Ba was much more abundant in sample 4 than in sample 1; the average Ba concentration in the experiments of Test 2 was 501 µg/L, while the average Ba concentration in the experiments of Test 1 (sample 1) was 177 µg/L.

Other observations made during these column experiments and the results presented in Figure D.38 are as follows:

- Some elements had effluent concentrations below the EQL but were detectable by the equipment used to run the analyses. Examples: Al, Bi, Cd, Li, P, U, Ni, and Zr.
- Some elements had effluent concentrations above the EQL only during leaching with SGW and during the stop-flow events. Examples: As, Cr, Cu, Pb, Mn, Se, and Zn.
- Some elements hadeffluent concentrations above detection limits in both columns (in addition to Ca). Examples: Sb, Ba, Mg, Si, Ag, Na, Sr, Sn, and S.
- Some elements had effluent concentrations above detection limits in one column. Examples: Cs, Mo, (Set A, sample 1), Hg (Set A, sample 4).

Cs and Mo were released in the column experiment conducted with sample 1: the maximum concentration measured in these experiments was of 0.5 µg/L and 11 µg/L, respectively. Hg was mobilized in the column experiment conducted with sample 4; the maximum concentration was 30 µg/L.

The results from these column experiments are consistent with the previously presented results of the batch experiments, which used the same solid materials (Edwards aquifer Set A, samples 1 and 4) as the ones used in these column experiments (Batch 6, Tests 1 and 2).

The following elements were also detected in all Batch 6 experiments, Tests 1 and 2: Si, Ba, Mg, Sr, and Na in addition to Ca. K was measured in the column effluents but its concentrations were affected by

the online pH electrode of the column apparatus and for this reason it was not reported. In addition, S and Sn were detected in some Batch 6 experiments of Tests 1 and 2.

Sb and Ag were not detected in the batch experiments and Mn was detected in the column experiments only during leaching with the SGW (the first 110 hours).

The concentration of other elements and potential contaminants in column effluents such as As, Cr, Cu, Pb, Mn, Se, and Zn, were mobilized only during leaching with SGW or during the stop-flow events when a rebound in the aqueous phase pH was observed. These intermittent detections most likely were controlled by pH-dependent reactions. Concentration of Cr, Cd, and Cu were detected inconsistently, i.e., only in few experiments of Batch 6, Tests 1 and 2).

4.3.4 Results from Set 4: High Plains Aquifer Sediment CNG

The effluent pH of both columns initially increased and reached values between 7.2 and 7.4, which were similar to the pH of the inlet solution (7.5), but then decreased significantly to pH values of about 5 and 6.5 after the CO_2 gas-saturated SGW was injected into the column (Figure D.39). The pH measured in the batch experiments conducted with the same sediments (Batch 8, Tests 2 and 1) were similar (5.37 and 6.09, respectively).

The effluent chemical composition of these columns changed significantly during the experiments (Figure D.40). The Ca concentration decreased slightly in both columns during leaching with SGW. It then increased significantly in the experiment conducted with CNG 60 (up to about 200 mg/L) but then decreased reaching an apparent steady state at about 50 mg/L. The effluent Ca concentration in the column packed with sediment CNG 110 was variable during leaching with CO_2 gas-saturated SGW, but it was consistently higher than the Ca concentration in the effluent of the column packed with the sediment CNG 60. The Ca concentration did not change significantly during the stop-flow events, most likely indicating that cation exchange reaction rather than dissolution was controlling the effluent Ca concentration in this column (sediment CNG 60).

The Si concentration followed a similar trend as that observed in the column experiment of Set 3 conducted with Edwards aquifer material Set A, sample 1. This behavior is again consistent with the fact that the solid source that was controlling and contributing to the Si concentration in both sediments' pore water was mass limited and distributed throughout the sample matrix.

Other observations made during these column experiments and the results presented in Figure D.40 are:

- Some elements had effluent concentrations below the EQL but were detectable by the instrument used to run the analyses. Examples: Bi, Cd, Li, Ni, and Zr.
- Some elements had effluent concentrations above the EQL only during leaching with SGW and during the stop-flow events. Examples: Sb, Cr, Cu, Se, and Zn.
- Some elements had effluent concentrations above detection limits in both columns (in addition to Ca). Examples: As, Ba, Pb, Mg, Mn, Hg, Mo, P, Si, Ag, Na, Sr and S.
- Some elements had effluent concentrations above detection limits in one column. Examples: Al and Cs, (sediment CNG 60).

Differences among these two sediments based on data collected from Batch 8, Tests 1 and 2, and the two column experiments of Set 4, are presented below:

- Sediment CNG 60 exhibited less buffering capacity than the deeper sediment (CNG 110); pH in the batch experiment aqueous contacting phase was 5.37 in CNG 60 vs. 6.09 in CNG 110; in the column experiments, the effluent pH was about 5 in CNG 60 and about 6.5 in CNG 110.
- The Ca concentrations in the batch experiments were lower in CNG 60 (113 mg/L) than in CNG 110 (393). The column effluent Ca concentration was about 60 mg/L in CNG 60 and very variable in CNG 110, but it was consistently and significantly greater than Ca concentration in CNG 60.
- Si concentrations were not significantly different in Batch 8, Tests 1 and 2, although the Si concentration was greater in the Test 2 conducted with sediment CNG 60. Similarly, the effluent Si concentrations were greater in the column experiment conducted with sediment CNG 60.
- Aqueous concentrations of divalent cations were lower in Batch 8, Tests 1 and 2 experiments conducted with sediment CNG 60 than in the experiments conducted with sediment CNG 110 (Ba: 452 ± 63 vs. 632 ± 91; Sr: 0.35 ± 0.05 vs. 0.64 ± 0.06; Mg: 14 ± 1.8 vs. 21 ± 2). In the column experiments Sr effluent concentration was definitely greater in CNG 110; the changes in column effluent concentrations of Ba and Mg followed similar trends.
- The deeper sediment CNG 110 released a greater amount of Mn in batch experiments. The maximum effluent concentration of Mn was greater in CNG 110 than in CNG 60, in the column experiments conducted with these two sediments.
- Mo (2.40 µg/L) and Fe (208 µg/L) were detected in the Batch 8, Tests 1 and 2 experiments conducted with sediment CNG 110. Other elements were detected in the batch experiments conducted with sediment CNG 60, such as P (average of 1068 µg/L), Al (227 µg/L), Cr (3.77 µg/L in the equilibration experiment: time zero), Cu (30.7 µg/L), As (average 8.28 µg/L), Fe (249 µg/L), Pb (5.31 µg/L), Mo (1.93–3.66 µg/L). Greater effluent concentrations were observed in the column experiments: Sb (10.5 µg/L); As (65 µg/L); Ba (1000 µg/L); Pb (150 µg/L); Mg (50 mg/L); Mn (500 µg/L); Hg (2 mg/L); Mo (10 to a maximum of 100 µg/L); P (3.1 mg/L); Si (25 mg/L); Ag (30 µg/L); Na (42 mg/L); Sr (740 µg/L); S (14 mg/L).

4.4 Results from Experiments with Select Minerals and Microbes

The conversion of CO_2 to CH_4 over the course of the study is shown in Figure D.42. After a week of incubation, the concentration of CO_2 in the methanogen-inoculated tests decreased by 88% and remained relatively constant thereafter. About 95% of the decrease in CO_2 was directly attributed to methanogenesis. With the exception of day 3 treatments containing PbS, no significant difference in methanogenesis was observed across mineral phases. The reason for the lower initial methanogenesis in the PbS, compared to FeS_2 and AsFeS treatments, was not confirmed but could be plausibly associated with a general higher affinity of microbes for Fe-bearing minerals that could provide Fe—an important element in many biological processes. The eventual rebounding of methanogenesis in PbS treatments to the same levels as the Fe-bearing sulfides suggests that any initial limitations to CO_2 conversion was eventually overcome.

Methanogenesis was accompanied by an increase in solution pH consistent with the consumption of hydrogen as CO_2 is biochemically reduced to CH_4 (Figure D.43). The trends in pH were also similar to

those observed for CH_4 production across the minerals. That is, despite a lower initial increase in solution pH for PbS treatments on day 3, pH was comparable across all minerals for incubation times greater than 3 days. These findings suggest that the methanogenic conversion of CO_2 in CO_2-affected aquifers will likely result in very different chemical environments than would be present if such microbial processes were not considered.

Data on the elemental composition of the minerals indicated that in addition to being present in proportions consistent with the chemical formula of the minerals, the targeted elements were also the dominant metallic species present in the sulfides. That is, Fe was dominant in pyrite, Fe and As in arsenopyrite, and Pb in galena. Potential short-term impacts on the aqueous concentration of these metals in the different chemical environments associated with methanogenic versus non-methanogenic CO_2-impacted systems were reflected in Figure D.44. Despite the lack of a consistent trend in aqueous Pb concentrations evidence indicates the mobility of As and Fe will differ in methanogenic versus non-methanogenic CO_2-affected aquifers. For example, in both the pyrite and arsenopyrite treatments the aqueous concentration of Fe was much lower in the methanogenic than the comparable non-methanogenic CO_2-affected system. Conversely, despite an increase in the aqueous concentrations of As in both systems over time, concentrations were generally lower in the non-methanogenic than in the equivalent methanogenic system.

The lower aqueous concentrations of Fe in the methanogenic system indicated a sequestering of Fe and points to one of two scenarios: 1) the solubility of the mineral is less under methanogenic than non-methanogenic conditions or 2) some of the Fe that is mobilized in the microenvironment of the methanogens is precipitated once it is exposed to the bulk methanogenic conditions. The latter scenario appeared to be the most likely in our experiments. For example, during the dissolution of arsenopyrite, As and Fe would be co-released resulting in similar trends in aqueous concentrations for both species. The fact that the aqueous concentration of As generally increased while aqueous Fe decreased in our methanogenic experiments suggested the subsequent precipitation of aqueous Fe as a crucial mechanism in explaining the lower aqueous Fe concentrations. Evidence from scanning electron microscopy-energy dispersive spectroscopy (SEM-EDS) analysis showing the formation of a neophase on the surface of pyrite samples from methanogenic experiments were also consistent with a precipitation driven decrease in aqueous Fe (Figure D.45). Qualitative EDS of the precipitate in Figure D.4 indicated that it was indeed Fe-rich. However, efforts to ascertain its exact identity were inconclusive.

5.0 Summary

This report described the experimental research accomplished under an ongoing program at PNNL to address a variety of scientific issues related to potential leakage of CO_2 gas from deep storage reservoirs. It presented the results from a series of experiments PNNL conducted to address research issues related to the development of a systematic understanding of how CO_2 leakage might influence pertinent geochemical processes in the aquifer sediments.

At the onset, a thorough review of the current literature on how CO_2 leakage (from storage reservoirs) would likely affect the geochemistry of overlying potable aquifers was conducted (Harvey et al. 2013), and revealed the potential for both beneficial and deleterious effects resulting from the exposure of subsurface sediments to CO_2 gas leaking from the deep reservoirs. One important beneficial effect is

contaminant immobilization as a result of changes induced by the CO_2 gas intrusion (i.e., increased reactivity of the existing minerals via dissolution of nonreactive coatings on the surface of reactive minerals, or formation of neophases with highly reactive surface groups). The most important deleterious effect as described by Harvey et al. (2013) are the CO_2-induced reactions leading to the degradation of water quality via mobilization of contaminants or changes in other water quality parameters, such as alkalinity, salinity, or TDS. The experimental research reported herein focused on the effects of CO_2 gas and brine solutions on the aqueous phase chemistry of aquifer sediments.

5.1 Recap of Research Findings

The study results are recapped below in terms of the changes induced by CO_2 gas and brine exposure; the subsequent release of major chemical elements into the contacting aqueous phase (such as Ca, Mg, Ba, Sr, Si, Na, and K); the release and consumption of minor elements (such as Fe, Al, and Mn), which are able to form highly reactive secondary phases; and the mobilization or immobilization of trace elements (such as As, Cd, Pb, Cu, Zn, Mo, etc.), which may potentially contaminate the groundwater.

1. The results from solid-phase characterization studies show that the mineralogy of the Edwards aquifer Set A samples is dominated by calcite, quartz, and montmorillonite, while the mineralogy of Set B samples is dominated by calcite. The High Plains aquifer sediments are abundant in quartz and feldspars and contain about 15 to 20 wt% montmorillonite, and up to 5 wt% micas. Some of the High Plains aquifer sediments contain no calcite, while others contain up to about 7 wt% calcite.
2. The strong acid extraction tests confirm that in addition to the usual elements present in most soils, rocks, and sediments, the Edward aquifer materials and High Plains aquifer sediments contain As, Cd, Pb, Cu, and occasionally Zn, which potentially may be mobilized from the solid to the aqueous phase during or after exposure to CO_2.
3. The results from the batch tests conducted under periodic CO_2 gas exposure demonstrate that:
    a. The pH of the aqueous phase decreases significantly (more than 2 pH units) during CO_2 gas exposure, but it rebounds considerably after gas injection is stopped. Rebounding occurred after each short-term (6-minute) CO_2 injection, clearly demonstrating the ability of the Edwards aquifer material to buffer the effect of the intruding gas.
    b. If the system is left unperturbed, the pH increases further towards neutral pH values.
    c. Aqueous Ca concentrations are most likely controlled by calcite dissolution/precipitation because they follow the pH changes.
    d. Other major elements mobilized during the batch periodic CO_2 gas exposure experiments are Ba, Mg, K, Si, and Na. The mechanisms of their release could be either dissolution or ion exchange reactions.
    e. Al and Fe are occasionally present in the aqueous phase after periodic CO_2 gas exposure, suggesting aqueous phase mediated transformation of Al/Fe-bearing solid phases. The oxidized Fe may disappear fast from the aqueous phase (and probably for this reason is not frequently detected) to form insoluble secondary phases.
    f. Potential contaminants, such as Cu and Mo, are rarely present in the aqueous phase after periodic CO_2 gas exposure, and they occur at low concentrations (about 16 and 8 µg/L, respectively).
    g. Other potential contaminants were not detected in these periodic CO_2 gas exposure tests.

4. The results from the batch tests conducted under constant CO_2 gas exposure, that used six representative Edward aquifer materials, demonstrate that:
    a. pH decreases by about two pH units immediately after CO_2 injection into the batch reactors.
    b. As a result, Ca concentrations increase significantly in the aqueous phase (it varies between 456 and 588 mg/L in the solutions contacting the six representative Edward aquifer materials).
    c. Si concentrations increase in the aqueous phase of tests with Edwards aquifer materials that were abundant in montmorillonite and quartz.
    d. Ba and Sr concentrations as high as 600 µg/L are also present in the aqueous phase of some aquifer materials.
    e. Other elements, such as Mg, Na, K, S, Sn, and Mn, are mobilized as well.
    f. Low concentrations of minor and trace elements are also present in the aqueous phase, but only irregularly; they are Cu = 9.15 µg/L; Mo = 2.74 µg/L; Cs = 1.2 µg/L; Fe = 131 µg/L; Pb = 7.94 µg/L; Cr = 3.06 µg/L; and Cd = 7.6 µg/L.
5. The results obtained in the long-term constant CO_2 gas exposure experiment (119 days) show the following:
    a. pH remains unchanged with time at 6.13.
    b. Similarly, the average Ca concentration does not change with time and remains at 488 mg/L.
    c. The aqueous phase concentrations of Ba, Mg, Sn, and Sr decrease with time, and the aqueous phase concentrations of S, K, and Na either remain unchanged or change slightly in a similar way in both blanks and the CO_2-exposed samples.
    d. Detectable concentrations of Cu (ranging from 11 to 17 µg/L) are measured occasionally in the time interval of 64 to 92 days.
6. The results from the batch tests conducted with simulated brine solutions and with two representative Edwards aquifer materials under constant CO_2 gas exposure, show that:
    a. The pH decreases equally in the batch tests with or without brine solutions; it varies within a narrow range, between 6.04 and 6.14, in both materials tested.
    b. The responses of the two representative materials to the brine exposure are almost identical and the concentrations of Ca are significantly greater in the brine-exposed samples (the greatest Ca concentration of 748 mg/L was measured in the test conducted with a 1-M NaCl SGW brine solution).
    c. Ba and Sn aqueous concentrations increase almost two times with the brine concentration.
    d. The aqueous concentrations of other elements, such as Mg, S, and K do not change with the brine concentration.
    e. Al concentrations (between 422 and 758 µg/L) are present in the test conducted with the 0.1-M NaCl brine solution.
    f. Cu concentrations are detected in all experiments and blanks of the tests conducted with the 1-M brine solution (most likely Cu is an impurity in the NaCl salt). Its concentration remains

unchanged with time throughout the duration of the experiment, indicating an insignificant effect of the CO_2 gas stream on the fate of this potential contaminant, when brine is was also present in the system.

7. The results from the batch tests conducted with two size fractions separated from two representative Edwards Aquifer materials under constant CO_2 gas exposure, show the following:
   a. The effect of particle size is insignificant in one of the materials (Edwards aquifer Set B, sample 7) (no significant differences are observed for Ca, Ba, Mg, K, Na, S, and Sn in the test conducted with less than and greater than 2-mm size fractions, respectively).
   b. In the test conducted with the second material (Edwards aquifer Set B, sample 2), significant differences are observed only for the Ca, Sr, Sn, and Ba aqueous concentrations.
   c. The aqueous concentrations of Si, S, Mg, Bi, P, K, and Na are not affected by the particle size in this test.
8. The solid-to-solution ratio in batch tests is an important variable because some elements occur at low concentrations that can only be detected when the tests are conducted at a high solid-to-solution ratio.
9. Results from batch tests conducted under constant CO_2 gas exposure with four sediments from the High Plains aquifer (sediments CNG), demonstrate the following:
   a. pH decreases significantly in three tests conducted with sediments that contained calcite (pH = 6.08–6.11), and it is even more acidic (pH = 5.37) in the test conducted with the High Plains sediment that do not contain calcite.
   b. The changes in aqueous Ca concentrations in response to CO_2 gas exposure are more pronounced in the sediments that contain calcite (average Ca concentration varied between 385 and 483 mg/L) than in the sediment that did not contain calcite (Ca average concentration of 113 mg/L), although calcite coatings and adsorbed exchangeable Ca may have been present in this sediment.
   c. The dissolution of Si-bearing solid phases is also demonstrated in these experiments because the Si concentration increases significantly in the experiments conducted in the presence of the CO_2 gas. The greatest amount of Si is measured in the shallower sediment (a maximum of about 30 mg/L).
   d. Appreciable amounts of Ba, Sr, Mg, Na, and K are mobilized in all sediments; their aqueous concentrations follow a non-linear increasing trend as a function of time. Importantly, the aqueous concentrations of divalent cations, such Ba, Sr, and Mg, were smaller in experiments conducted with the calcite-free sediment.
   e. Mn is mobilized from all sediments; the maximum Mn concentration measured is about 500 µg/L. Slightly (but not significantly) greater S concentrations are present in the experiments exposed to CO_2 gas.
   f. Detectable aqueous concentrations of Mo (about 2.5 µg/L) are present in all blanks and at the equilibration experiments (time zero) in three sediments. However, Mo concentrations above the instrument detection limit are not measured in the experiments conducted in the presence of the CO_2 gas. In the fourth sediment sample used in these batch tests, the Mo concentration decreases significantly after CO_2 exposure and is consistently lower than the concentrations measured in the blanks. This Mo aqueous phase decrease suggests a beneficial effect of the CO_2 gas exposure.

g. Aqueous phase Fe is also detected in some experiments conducted with these sediments, suggesting that changes in Fe mineralogy may have occurred during these experiments.

h. The CNG sediments mobilize only low concentrations of trace elements (potential contaminants), which are detected occasionally in the aqueous phase. Importantly, these occurrences are more frequent in the calcite-free sediment.

10. Two additional batch tests were conducted under constant CO_2 gas exposure with two sediments from the High Plains aquifer that have similar mineralogies (sediment CAL 1 91 and CAL 1 151). The only difference is that one sediment contains an appreciable amount of calcite and the other does not contain calcite. The results from these tests demonstrate the following:

    a. The pH decreases significantly from 7.87 to 5.78 in the calcite-free sediment, but pH is buffered to a less acidic value (i.e., pH = 6.11) in the sediment that contains calcite.

    b. The aqueous concentrations of elements such as Ca, Ba, Sr, Mg, Na (in one sediment: sediment CAL 1 91), K, Si, and Mn all increased significantly in the CO_2 gas-treated experiments.

    c. The aqueous concentrations of Mo are consistently lower in the sediments exposed to the CO_2 gas, while they steadily increased in the blanks to about 15 µg/L by 14 days.

    d. The aqueous S concentrations are similar in the blanks and in the experiments that were exposed to CO_2 gas.

    e. Greater amounts of Ca are released in the calcite sediment (average Ca concentration in this sediment was 379 mg/L vs. 239 mg/L in calcite-free sediment).

    f. Similar amounts of Si are released in both sediments, but greater amounts of Ba are mobilized in the calcite-bearing sediment.

    g. The amounts of Sr, Mg, K, Na, S, and Mo mobilized in both sediments are similar.

    h. Mn is present at higher aqueous concentrations in the calcite-free sediment.

    i. During these batch experiments, both CAL 1 sediments released only low concentrations of a few trace elements (potential contaminants), which are detected occasionally in the aqueous phase. Importantly, these occurrences are more frequent in the experiments conducted with the calcite-free sediment.

11. Two batch experiments are conducted under constant CO_2 gas exposure with the High Plains aquifer sediments CAL 2 4 and CAL 2 29. These sediments contained 4.7 and 1.6% calcite, and 5.2 and 2.6% mica, respectively. The other mineralogical components are present in similar amounts in both sediments. The results from these tests demonstrate the following:

    a. The pH in the CO_2-treated sediments decreases significantly and almost instantaneously from 8.16 to 6.17 in sediment CAL 2 4 and to 6.06 in sediment CAL 2 29.

    b. Aqueous concentrations of Ca, Ba, Mg, Sr, Na, and K are greater in the CO_2 gas-treated experiments. The change in concentration is either instantaneous, similar to that of Ca (e.g., Ba), or follows an increasing nonlinear trend as a function of time (e.g., Sr and Mg). The concentration of S is similar in the experiments and blanks.

    c. Importantly, the aqueous concentration of Mn increases significantly in the experiments conducted with sediment CAL 2 4 exposed to CO_2 gas (the maximum Mn concentration is about

400 µg/L). The reason for this increase is still under investigation although the release of Mn in the aqueous phase may be attributed to changes in Eh (redox conditions) induced by the CO_2 gas injection.

d. Aqueous concentrations of Ca Na, S, and Si are similar in both sediments. However, the aqueous phase from sediment CAL 2 29 contains more Ba than sediment CAL 2 4, but less Mg, Sr, K, and Mn.

e. Few trace metals are released in the aqueous phase in these experiments. For example, aqueous phase Mo is present in the blanks (sediment CAL 2 29), but it occurs at much lower concentrations in the CO_2-exposed experiments. Aqueous phase Cd is also detected in one experiment but its concentration is low (Cd = 2.79 µg/L). The concentrations and the variety of trace elements (such as, Mo, Cu, As, Sb) detected in the aqueous phase from the shallow sediment CAL 2 4 are greater.

12. The results from Set 1 of column experiments (a control column packed with sand and another column packed with sand and a material from the Edward aquifer [Set B, sample 4]), demonstrate the following:

a. The effluent pH in the sand column decreases significantly to about 5 during leaching with the CO_2 gas-saturated SGW, while the effluent pH of the column packed with sand and the representative Edward aquifer material decreased to about 6.5. This material is able to buffer the aqueous phase pH to values well above (approximately 2.5 pH units) the CO_2-laden influent solution pH (which is about 4).

b. The pH increases to about 7 during the stop-flow events and follows a decreasing trend as soon as the flow is re-established.

c. Effluent Ca concentrations change with pH and increase significantly as soon as the CO_2 gas-saturated SGW is injected into both columns packed with Accusand and the representative Edwards aquifer material. Ca concentration decreases during the 146-hour stop-flow event, most likely in response to increasing pH, and then continued the increasing trend as soon as the flow restarted. A steady-state Ca conentration, which is usually indicative of a pseudo-equilibrium condition, was not observed during this experiment.

d. Elements with effluent concentrations above detection limits in the column containing both Accusand and the Edward aquifer material follow different trends than those observed in the Accusand column are Na, Ba, Mg, and K.

e. Important potential contaminants, such as Pb, Cs, Cu, and Mo, are detected in the aqueous phase only during the time the columns are leached with the N_2-saturated SGW, confirming that these releases are not caused by CO_2 gas exposure.

f. Some of the potential contaminants are released into the aqueous phase during the stop-flow events, indicating that the reaction controlling their release is either time-dependent or pH-dependent, because an increase in liquid-phase pH is also observed during the stop-flow events.

13. The results from the Set 2 column experiments, conducted with two representative Edwards aquifer materials (Set B, sample 4 and 7), demonstrate the following:

    a. When the CO_2 gas-saturated SGW is injected into the columns, the effluent pH decreases fast (within the first 10 hours) and stabilizes to about 6.4 and 6.5 in the experiments conducted with samples 4 and 7, respectively. The pH measured in the batch experiments conducted with the same sediments (Batch 2, Test 1 and Test 3) are lower (6.10 and 6.09, respectively).

    b. The effluent Ca concentration increases immediately after the CO_2 gas-saturated SGW is injected into the columns, and continues to increase for the duration of the experiment without establishing a steady-state concentration (a maximum concentration of about 250 mg/L is reached at the end of this experiment). The increasing trend, however, is irregular (i.e., not smooth), most likely indicating that more than one reaction (either simultaneous or sequential) with fast or slow kinetics is affecting and/or controlling the aqueous Ca concentration as the liquid phase moved through the packed column with the solid materials.

    c. The Ca concentration is significantly perturbed in both columns during the two stop-flow events of 143 and 69 hours, reinforcing the idea that either multiple or time-dependent reactions are controlling Ca concentrations in the column liquid phase. The Ca concentrations measured in the batch experiments conducted with the same materials (Set B, samples 4 and 7) peak relatively fast (within the first hours of experiment), with an apparent equilibrium concentration of 456 and 528 mg/L, although the column and batch systems are fundamentally different.

    d. Cu, Mo, Se, and Ag have effluent concentrations above the EQL only during leaching with CO_2-free SGW and during the stop-flow events, indicating that their aqueous concentrations are controlled by pH-dependent processes or reactions that occur at higher pH levels than the one induced by the CO_2 gas stream.

    e. In addition to Ca, the following elements have effluent concentrations above detection limits in both columns: Ba, Mg, Cs, Si, Na, Sr, Sb, and S.

    f. The results of these column experiments are consistent with the results of the batch experiments, which used the same solid materials (Edwards aquifer Set B, samples 4 and 7).

14. The results from the Set 3 column experiments conducted with two representative Edwards aquifer materials (Set A, samples 1 and 4), demonstrate the following:

    a. The effluent pH decreases fast (within the first 10 hours) immediately after the CO_2 gas-saturated SGW is injected into the columns and then stabilizes at about 6.2 and 6.3 in the experiments conducted with sample 1 and 4, respectively. The pH measured in the batch experiments conducted with the same sediments (Batch 6, Test 1 and Test 2) were lower (6.10 and 6.03, respectively).

    b. Effluent Ca concentrations increase significantly in the column packed with sample 1 (from 120 to about 200 mg/L) and slightly in the column packed with sample 4 (from 160 to 180 mg/L) immediately after the CO_2 gas-saturated SGW is injected into the columns, reaching a maximum of about 250 mg/L before the end of the experiment. The Ca concentrations measured in the batch experiments conducted with the same materials (Set A, samples 1 and 4) peaked relatively quickly (within the first hours of experiment), with apparent equilibrium concentrations of 508 and 466 mg/L, respectively. The increasing effluent Ca trend in Set 3 columns is again irregular and similar to the one observed in the previous column experiments, most likely indicating that

more than one reaction (dissolution, precipitation, adsorption, desorption) is affecting and/or controlling aqueous Ca concentrations.

c. Effluent Ca concentrations decrease significantly during the 118- and 195-hour stop-flow events, reaching low concentrations well below the pseudo steady-state concentrations established in both columns at the beginning of the experiments during leaching with the SGW, most likely in response to the increase in pH observed during the 118- and 195-hour stop-flow events. This most likely indicates that calcite dissolution and precipitation are the primary controls on aqueous Ca concentration in these systems.

d. The effluent Si concentration follows two well-distinguished trends in the two solid materials tested in the Set 3 column experiments. In sample 1, the changes in Si concentration with time are consistent with the fact that the solid source controlling and contributing to the Si concentration in solution was limited in mass. The results from this column experiment are also consistent with the results of Batch 6, Test 1 (conducted with the same material), which show that the Si accumulated in the aqueous phase during 14 days is barely 6 mg/L. In sample 2, effluent Si concentrations increase to a pseudo steady-state concentration of about 11.5 mg/L as soon as the CO_2 gas-saturated SGW is injected into the column. Most likely, a dissolving Si-bearing phase (silicate or phyllosilicate) is controlling the aqueous Si concentration. This phase (or phases) is able to continuously release Si in the aqueous phase (the influent fluid was Si-free), and sustain relatively constant Si effluent concentrations for the duration of the experiment (about 500 hours). The results from this column experiment are also consistent with the results of Batch 6, Test 2 (conducted with the same material), which show that the Si concentration reaches an apparent equilibrium at a concentration of about 18 mg/L.

e. Effluent Ba exhibits behavior similar to that of Si, and these results are consistent with the results of Batch 6, Tests 1 and 2 conducted with the same materials. Ba is much more abundant in sample 4 than in sample 1; the average Ba aqueous concentration in the batch experiments of Test 2 was of 501 µg/L while the average Ba concentration in the experiments of Test 1 (sample 1) was of 177 µg/L.

f. The column effluent concentrations of As, Cr, Cu, Pb, Mn, Se, and Zn are above the detection limit only during leaching with SGW and during the stop-flow events when a rebound in the aqueous phase pH is observed.

g. The column effluent concentrations of Sb, Ba, Mg, Si, Ag, Na, Sr, Sn, and S are above detection limits in both columns (in addition to Ca).

h. Cs and Mo are released in the column experiment conducted with sample 1; however, the maximum concentrations measured in these experiments are low (0.5 µg/L and 11 µg/L, respectively). Hg is mobilized in the column experiment conducted with sample 4 (the maximum concentration is 30 µg/L).

i. The results from these column experiments are consistent with the results of the batch experiments, which used the same solid materials (Edwards aquifer Set A, samples 1 and 4) as the ones used in these column experiments (Batch 6, Tests 1 and 2).

15. The results from the Set 4 column experiments conducted with two sediments from the High Plains aquifer (calcite-free sediment CNG 60 and sediment CNG 110), demonstrate the following:

    a. Effluent pH in both columns decreases significantly after the CO_2 gas-saturated SGW is injected into the column, reaching pH values of about 5 and 6.5. The pH measured in the batch experiments conducted with the same sediments (Batch 8, Test 2 and 1) were similar (5.37 and 6.09, respectively).

    b. The effluent Ca concentration initially peaks at about 200 mg/L in the experiment conducted with the calcite-free sediment CNG 60, but then decreases, reaching an apparent steady state at about 60 mg/L. The effluent Ca concentration does not change significantly during the stop-flow most likely indicating that a cation exchange reaction rather than calcite dissolution is controlling the effluent Ca concentration in this column (sediment CNG 60). The effluent Ca concentration in the column packed with sediment CNG 110 is variable during leaching with CO_2 gas-saturated SGW, but it is consistently higher than Ca concentrations in the effluent of the column packed with the sediment CNG 60.

    c. The effluent Si concentrations follow a similar trend to the one observed in Set 3, Set A, sample 1. This behavior is again consistent with the fact that the solid source that is controlling and contributing to the Si concentration in both sediments' pore water is mass limited and distributed throughout the sample matrix.

    d. The effluent concentrations of Sb, Cr, Cu, Se, and Zn are above detection limits only during leaching with SGW and during the stop-flow events.

    e. The effluent concentrations of As, Ba, Pb, Mg, Mn, Hg, Mo, P, Si, Ag, Na, Sr, and S were above detection limits in both columns (in addition to Ca).

    f. The effluent concentrations of Al and Cs are above detection limit in one of the column experiments (sediment CNG 60).

16. Our findings from the microbial experiments indicate that in the presence of a viable population of autotrophic methanogens (and optimal methanogenic conditions), elevated CO_2 concentrations in the subsurface could stimulate methanogenesis, resulting in the conversion of up to 95% of the CO_2 to CH_4. We found sufficient evidence to conclude that the geochemical impact of elevated CO_2 levels will differ significantly in methanogenic versus non-methanogenic systems. Such differences should be reflected and considered in efforts aiming to monitor, assess, predict, or mitigate CO_2 effects on subsurface environments. For example, the sequestration of Fe (as neophases) and concomitant mobilization of As under anaerobic conditions point to a direct impact of methanogenesis on the mineral dissolution/precipitation reactions as controls of the geochemical outcome of elevated CO_2 levels.

6.0 References

Annunziatellis A, SE Beaubien, S Bigi, et al. 2008. "Gas migration along fault systems and through the vadose zone in the Latera caldera (central Italy): Implications for CO_2 geological storage." *International Journal of Greenhouse Gas Control* 2(3):353–372.

Apps JA, L Zheng, Y Zhang, T Xu, and JT Birkholzer. 2010. "Evaluation of potential changes in groundwater quality in response to CO_2 leakage from deep geologic storage." *Transport in Porous Medis* 82(1):215–246.

Bachu S. 2008. "CO_2 storage in geological media: Role, means, status, and barriers to deployment." *Progress in Energy and Combustion Science* 34(2):254–273.

Celia MA and JM Nordbotten. 2009. "Practical modeling approaches for geological storage of carbon dioxide." *Ground Water* 47(5):627–638.

Damen K, AFaaij, F van Bergen, J Gale, and E Lysen. 2005. "Identification of early opportunities for CO2 sequestration-worldwide screening for CO_2-EOR and CO_2-ECBM projects." *Energy* 30(10):1931–1952.

Frye E, C Bao, L Li, and S Blumsack. 2012. "Environmental Controls of Cadmium Desorption during CO_2 Leakage." *Environmental Science & Technology* 46(8):4388–4395.

Gilfillan SMV and RS Haszeldine. 2011. "Comment on "Potential Impacts of Leakage from Deep CO_2 Geosequestration on Overlying Freshwater Aquifers." *Environmental Science & Technology* 45(7):3171–3174.

Harvey OR, NP Qafoku, KJ Cantrell, et al. 2013. "Geochemical Implications of Gas Leakage associated with Geologic CO_2 Storage-A Qualitative Review." *Environmental Science & Technology* 47(1):23–36.

Holloway S, JM Pearce, VL Hards, T Ohsumi, and J Gale. 2007. "Natural emissions of CO_2 from the geosphere and their bearing on the geological storage of carbon dioxide." *Energy* 32(7):1194–1201.

Jordan P and S Benson. 2009. "Well blowout rates and consequences in California Oil and Gas District 4 from 1991 to 2005: Implications for geological storage of carbon dioxide." *Environmental Geology* 57(5):1103–1123.

Kharaka YK, JJ Thorsden, E Kakouros, et al., 2010. "Changes in the chemistry of shallow groundwater related to the 2008 injection of CO_2 at the ZERT field site, Bozeman, Montana." *Environmental Earth Sciences* 60(2):273–284.

Lewicki JL, J Birkholzer, and CF Tsang. 2007. "Natural and industrial analogues for leakage of CO_2 from storage reservoirs: Identification of features, events, and processes and lessons learned." *Environmental Geology* 52(3):457–467.

Little MG and RB Jackson. 2010. "Potential impacts of leakage from deep CO_2 geosequestration on overlying freshwater aquifers." *Environmental Science and Technology* 44(23):9225–9232.

Lu J, J Partin, S Hovorka, and C Wong. 2010. "Potential risks to freshwater resources as a result of leakage from; geological storage: A batch-reaction experiment." *Environmental Earth Sciences* 60(2):335–348.

Metz B, O Davidson, H de Coninck, M Loos, and L Meyer. 2005. *Carbon Dioxide Capture and Storage-Special Report of the Intergovernmental Panel on Climate Change*. Cambridge University Press, Cambridge.

Nordbotten JM, MA Celia, S Bachu, and HK Dahle. 2005. "Semianalytical solution for CO_2 leakage through an abandoned well." *Environmental Science and Technology* 39(2):602–611.

Scherer GW, B Kutchko, N Thaulow, A Duguid, and B Mook. 2011. "Characterization of cement from a well at Teapot Dome Oil Field: Implications for geological sequestration." *International Journal of Greenhouse Gas Control* 5(1):115–124.

Smyth RC, SD Hovorka, J Lu, et al. 2009. "Assessing risk to fresh water resources from long term CO_2 injection-laboratory and field studies." *Energy Procedia* 1(1):1957–1964.

Trautz RC, JD Pugh, C Varadharajan, et al. 2013. "Effect of Dissolved CO_2 on a Shallow Groundwater System: A Controlled Release Field Experiment." *Environmental Science and Technology* 47(1):298–305.

Wang S and PR Jaffe. 2004. "Dissolution of a mineral phase in potable aquifers due to CO_2 releases from deep formations; effect of dissolution kinetics." *Energy Conversion and Management* 45(18–19):2833–2848.

Appendix A

Maps, Sample Locations, and Coordinates

Appendix A

Maps, Sample Locations, and Coordinates

Information, maps, and photos pertaining to the Edwards aquifer were provided by Charlotte Sullivan, PNNL.

Unconfined Edwards aquifer samples San Antonio, Texas, Set A. The read circles or ellipsoids show the location where sample was collected.

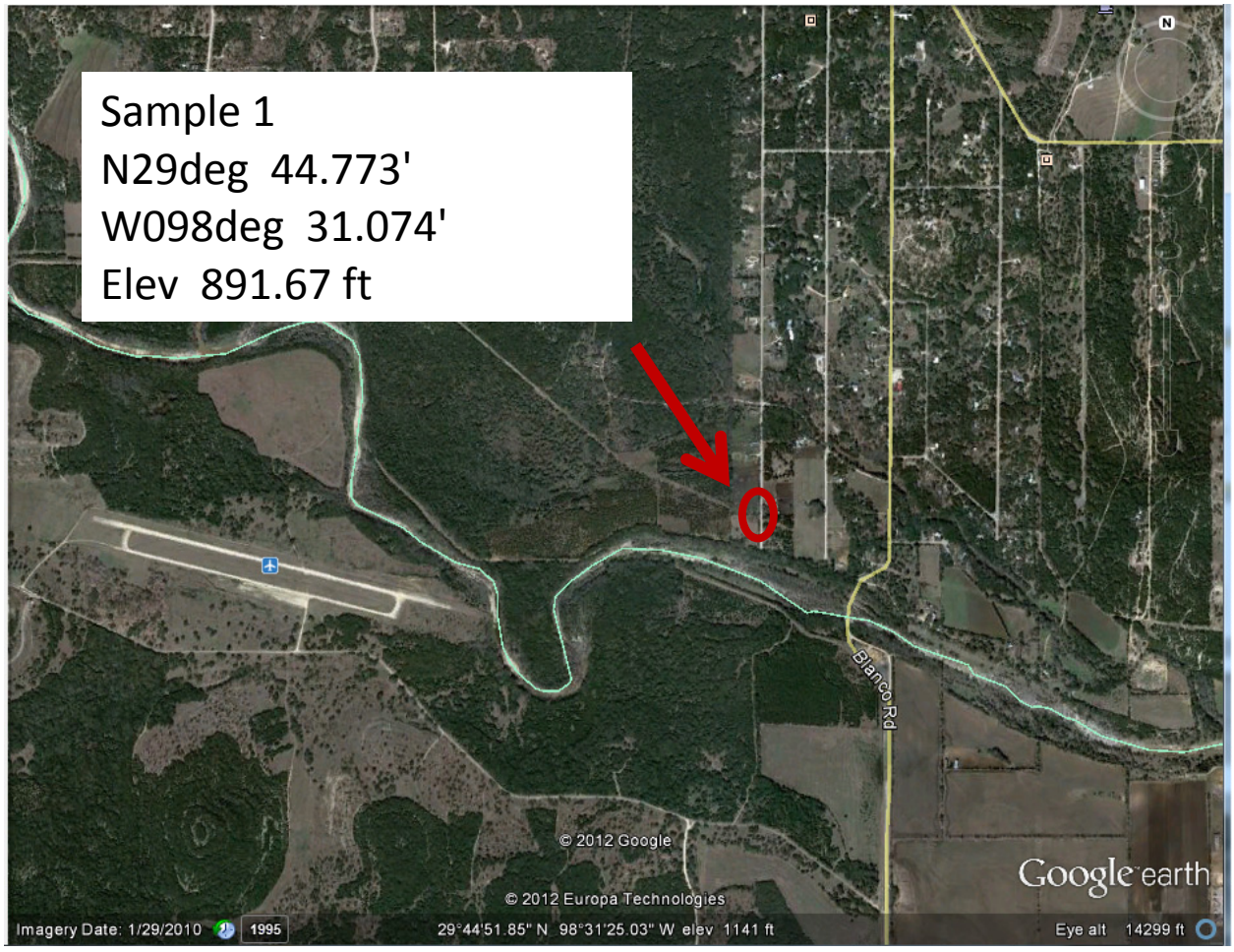

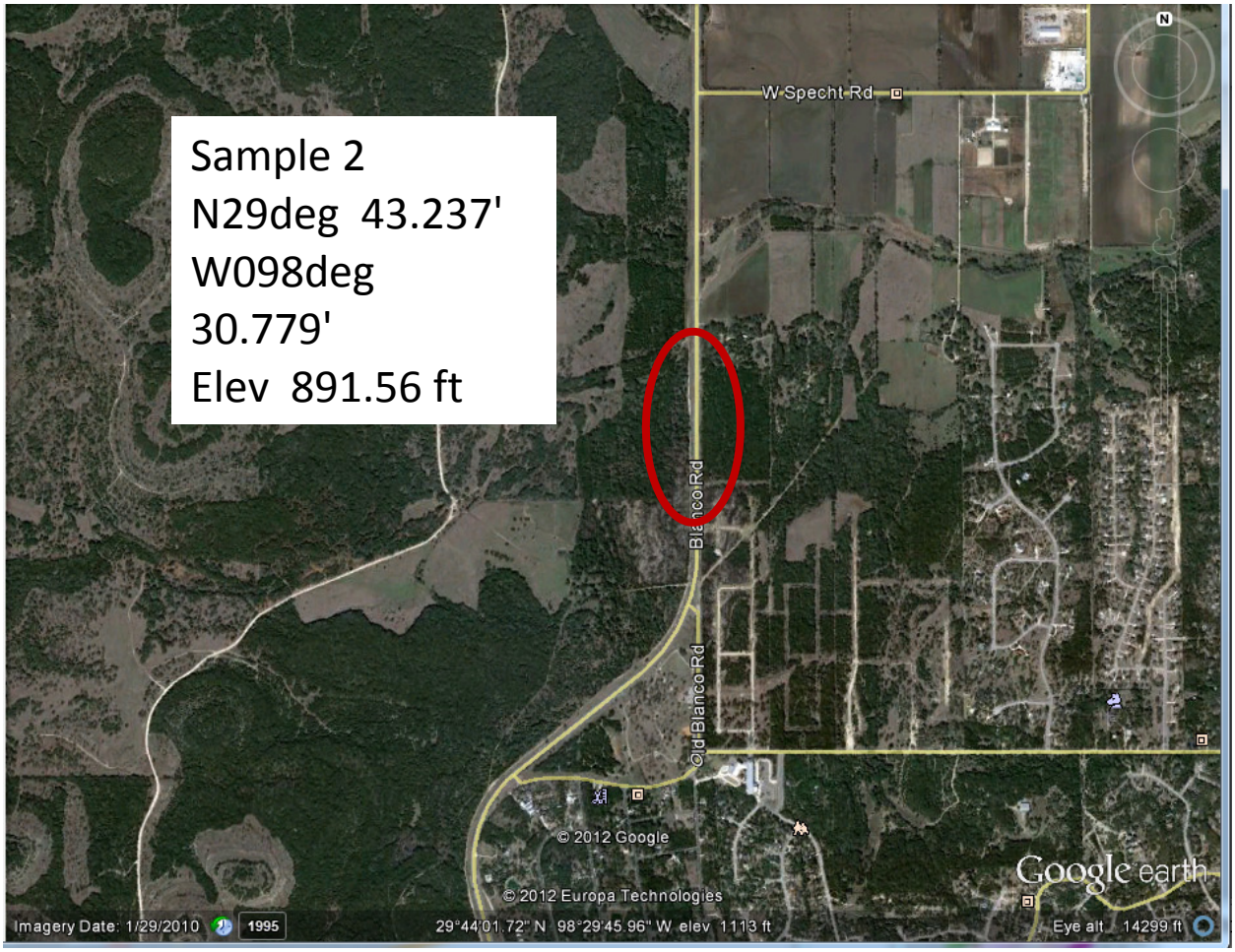
Sample 2
N29deg 43.237'
W098deg
30.779'
Elev 891.56 ft
W Specht Rd
Old Blanco Rd
© 2012 Google
© 2012 Europa Technologies
Google earth
Imagery Date: 1/29/2010
1995
29°44'01.72" N 98°29'45.96" W elev 1113 ft
Eye alt 14299 ft

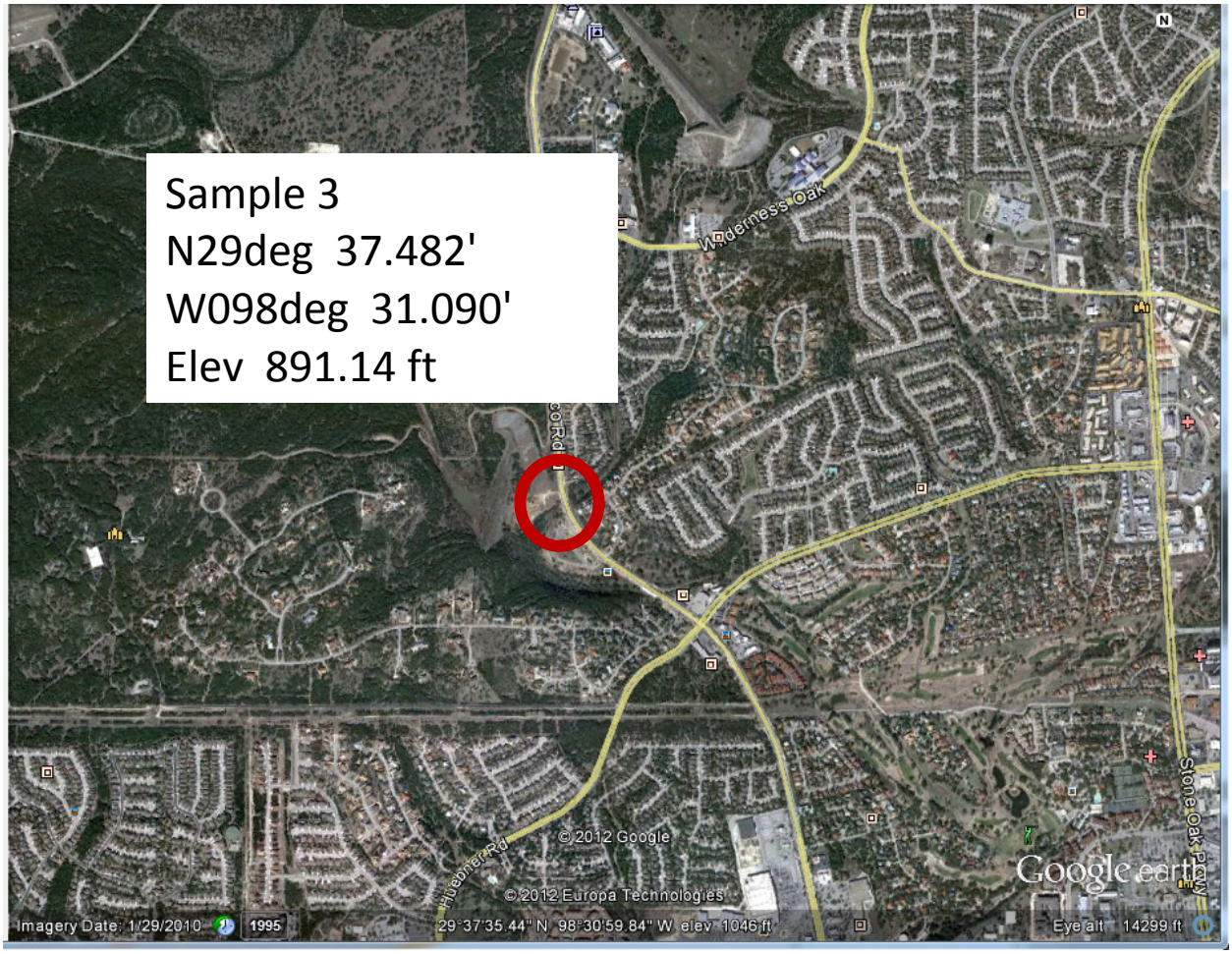
Sample 3
N29deg 37.482'
W098deg 31.090'
Elev 891.14 ft
Wilderness Oak
Huebner Rd
Stone Oak Pkwy
© 2012 Google
© 2012 Europa Technologies
Google earth
Imagery Date: 1/29/2010
1995
29°37'35.44" N 98°30'59.84" W elev 1046 ft
Eye alt 14299 ft

Sample 4; N29deg 36.672'; W098deg 32.850'; Elev 891.04 ft
Sample 5; N29deg 36.690'; W098deg 32.842'; Elev 891.04 ft
Sample 6; N29deg 36.846'; W098deg 32.636'; Elev 891.04 ft

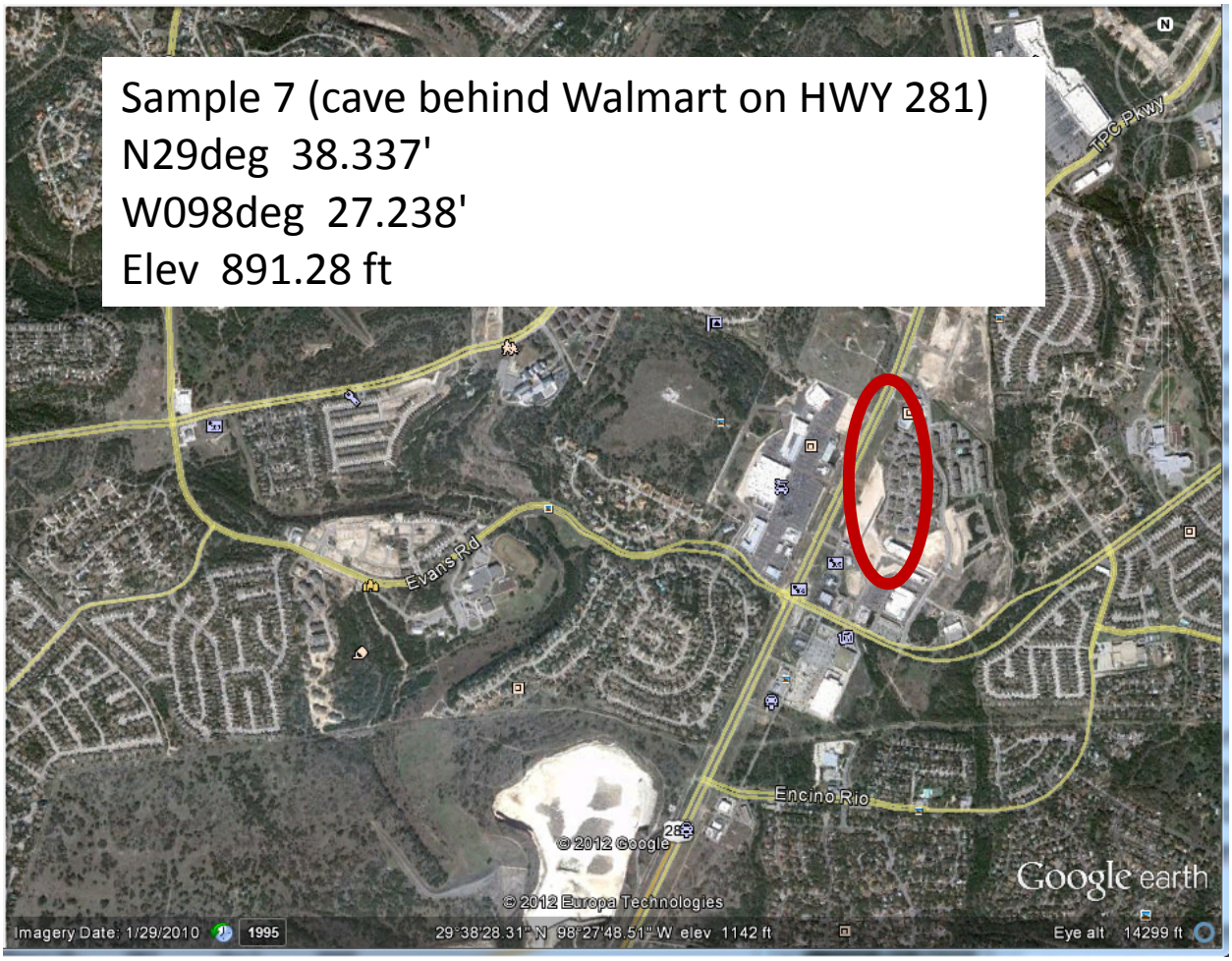
Sample 7 (cave behind Walmart on HWY 281)
N29deg 38.337'
W098deg 27.238'
Elev 891.28 ft
TPC Pkwy
Evans Rd
Encino Rio
© 2012 Google
© 2012 Europa Technologies
Google earth
Imagery Date: 1/29/2010
1995
29°38'28.31" N 98°27'48.51" W elev 1142 ft
Eye alt 14299 ft

Shallow unconfined Edwards aquifer San Antonio

Collection of 7 Samples May 2012

Close-up views of outcrops to follow

Edwards aquifer Set B

Sample1 29 46.878' N, 98 13.211'W

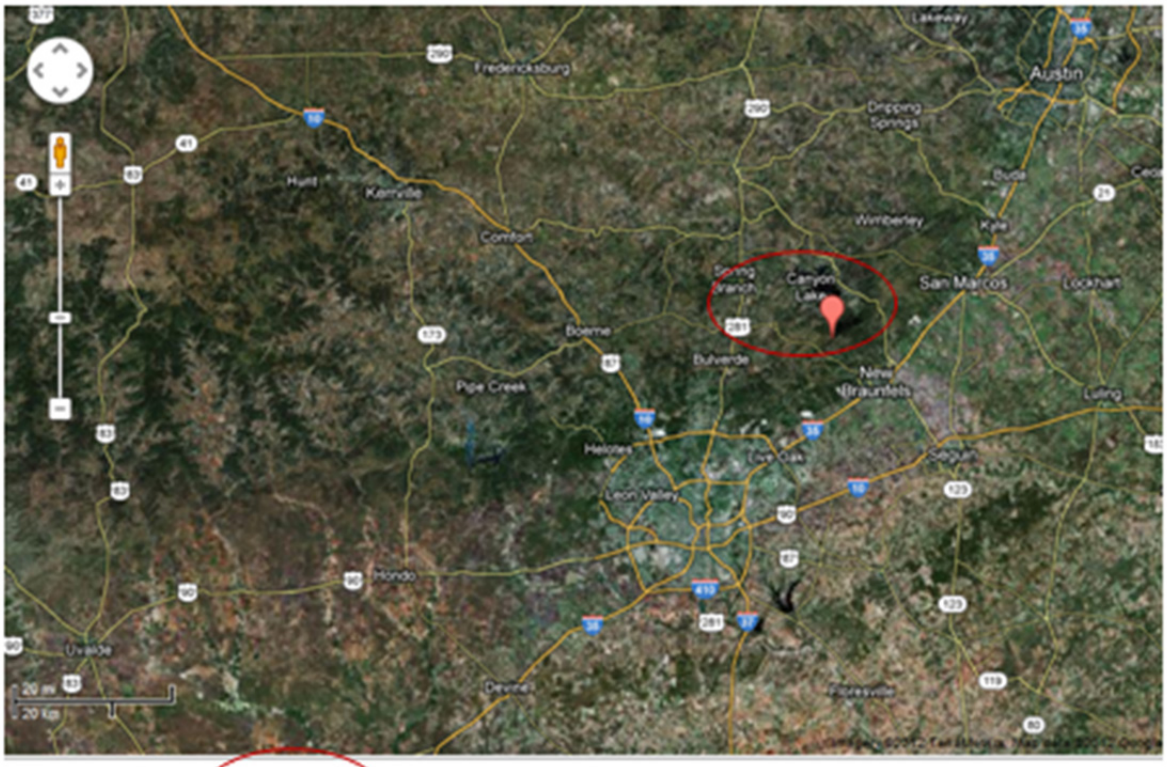

All May samples were collected from this area

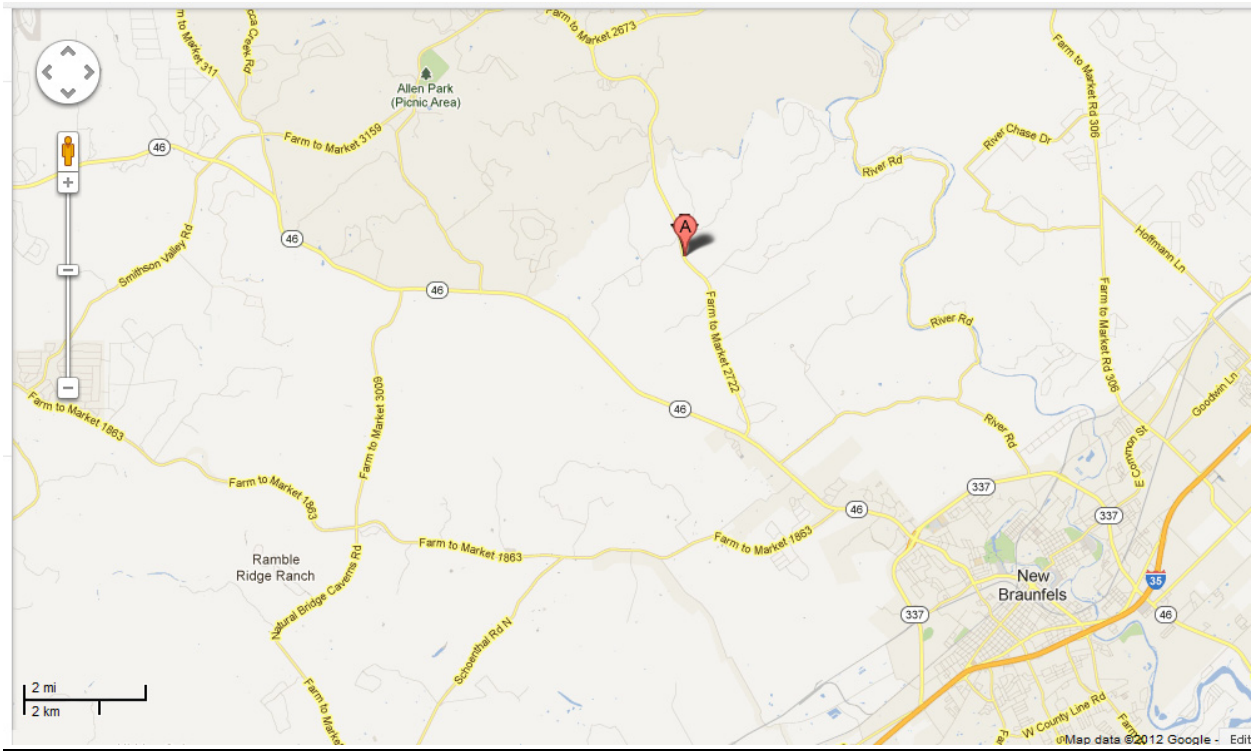

Sample 1 29 46.878' N, 98 13.211'W

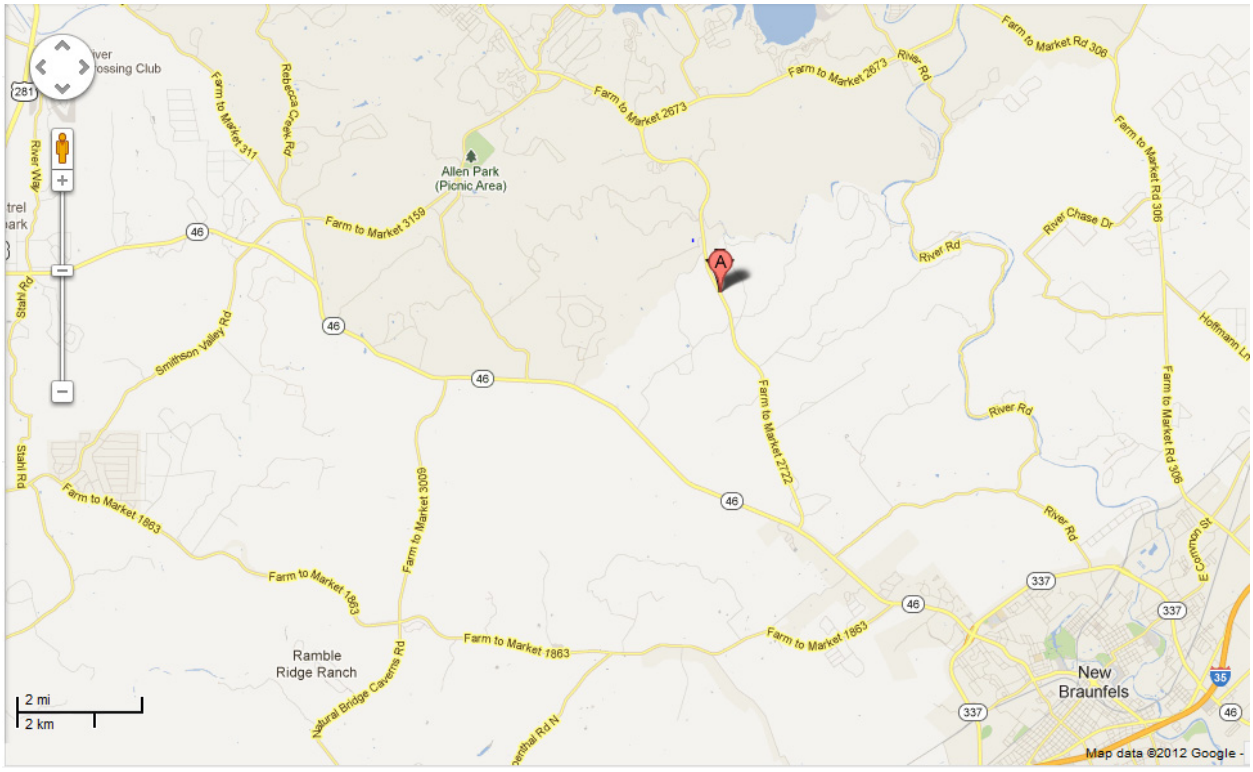

Sample 2 29 47.603'N, 98 13.479'W 1067' ELEVATION

https://maps.google.com/maps?hl=en&q=san+antonio+texas&ie=UTF-8

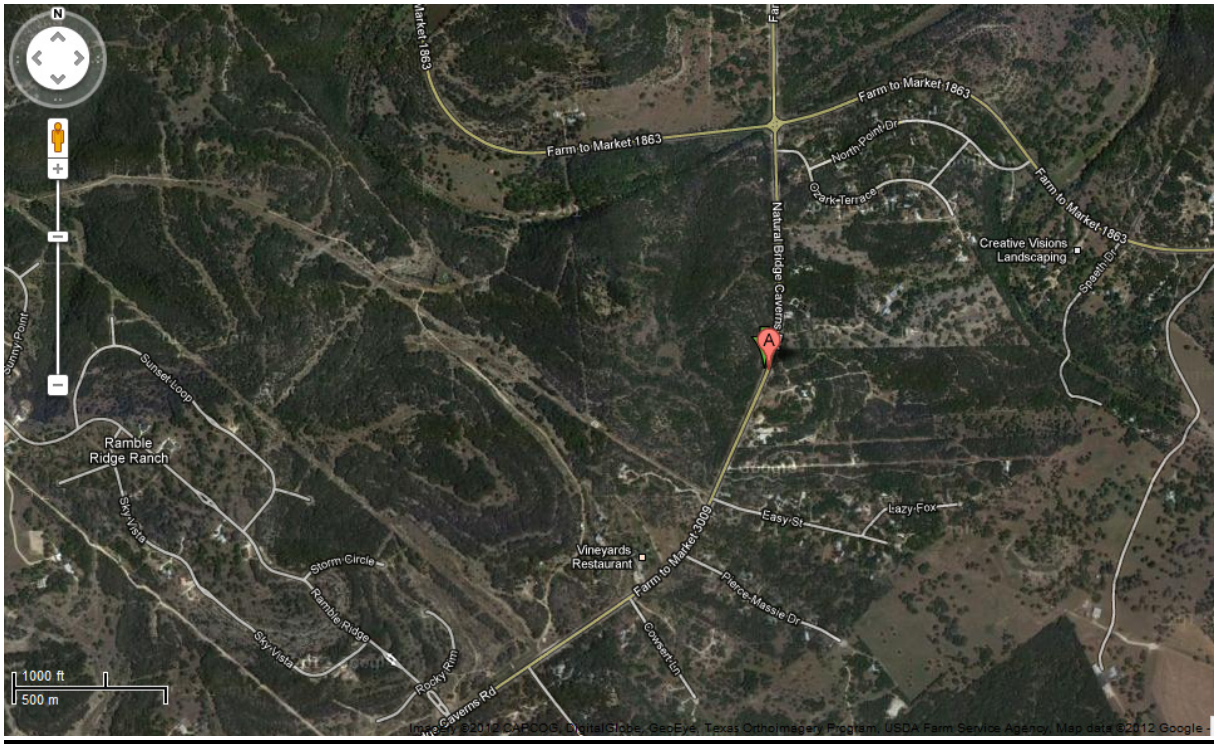

Sample 3 29 42.584 N , 98 18.622'W 1103' ELEVATION

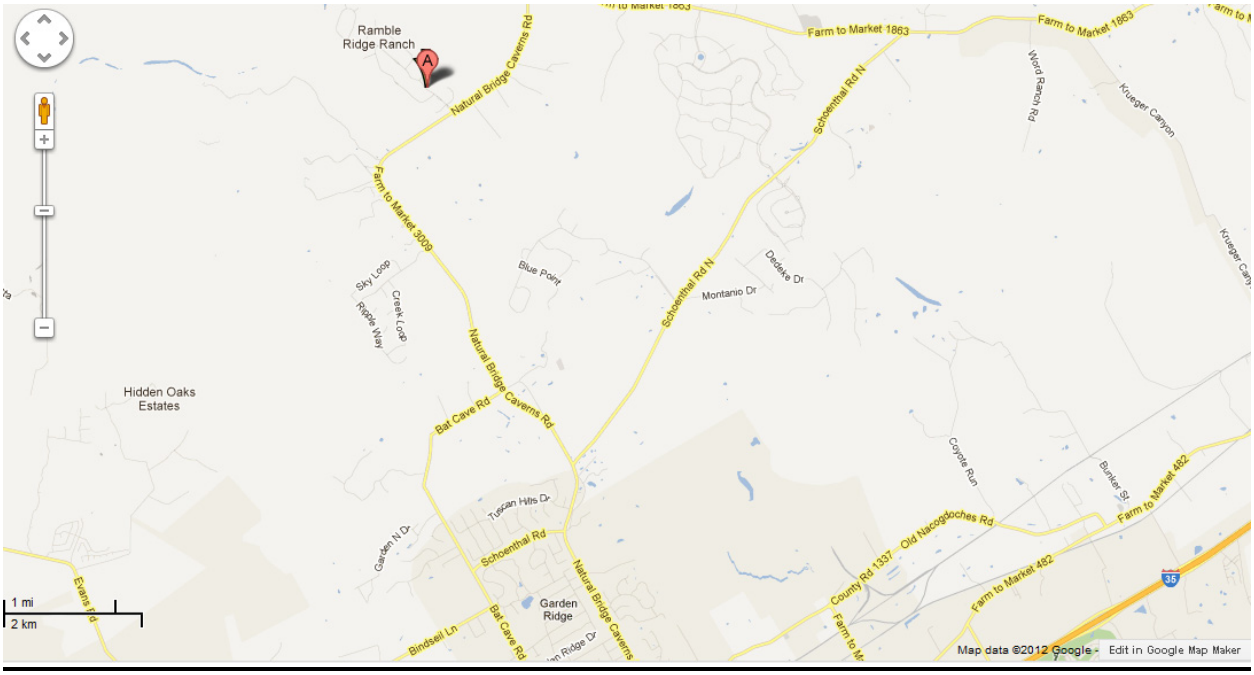

Sample 4 29 42 09.24' N, 98 19.51'W 1038' ELEVATION

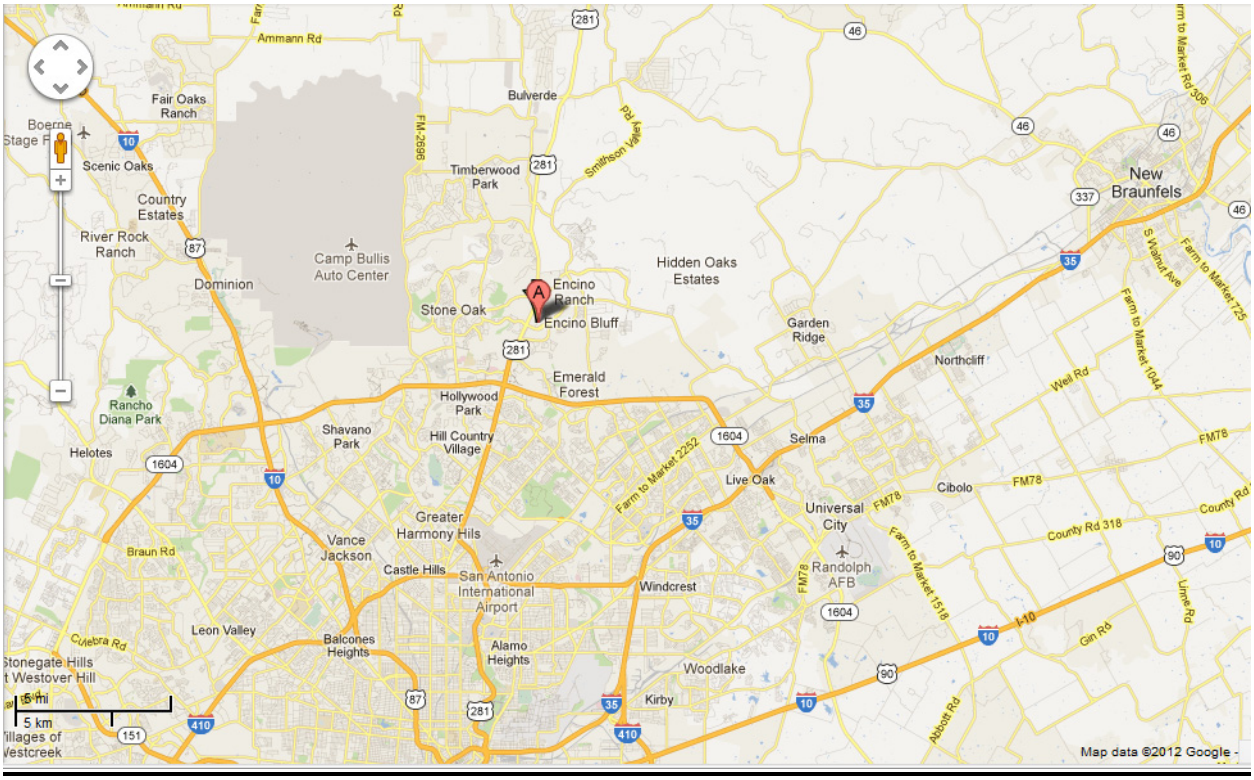

Sample 5 29 38.277' N, 98 27.069' W 1052' ELEVATION

Sample 6 29 38 24.08 N, 98 27' 10.85 W 1064' ELEVATION

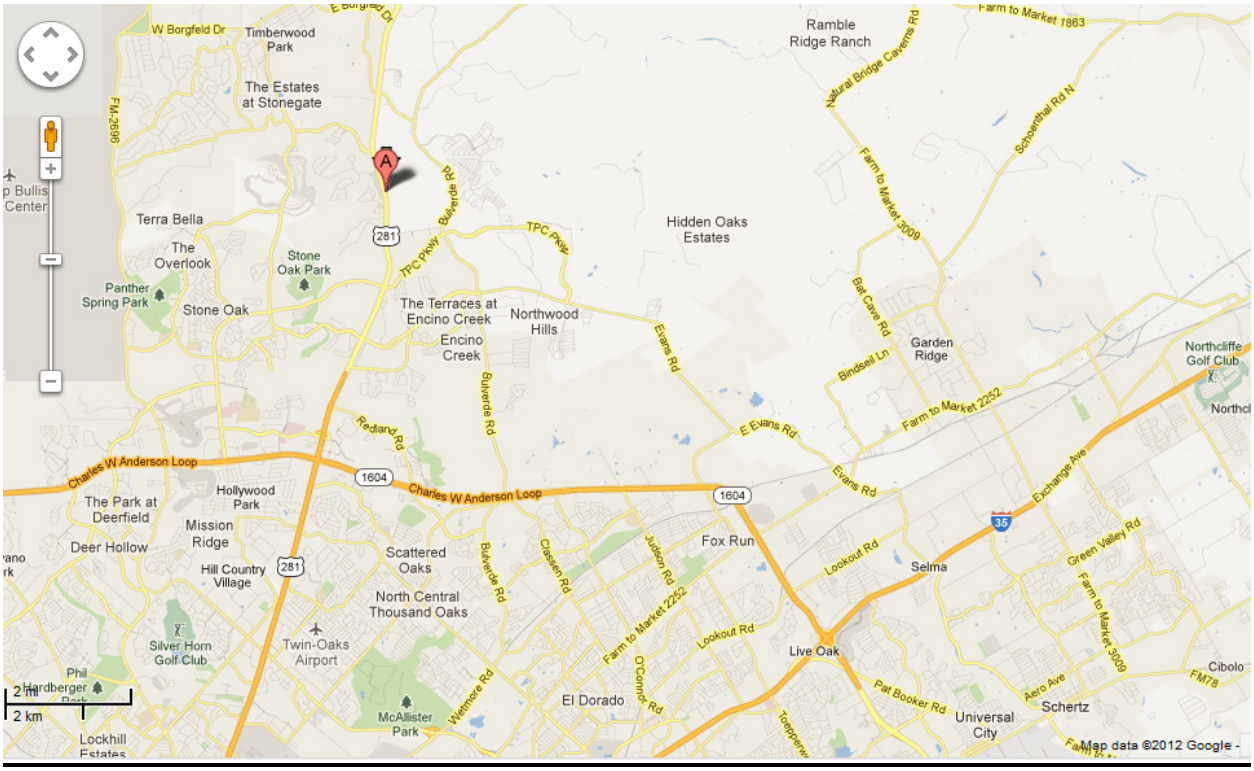

Sample 7 29 40.255N, 98 27.022W 1052' ELEVATION

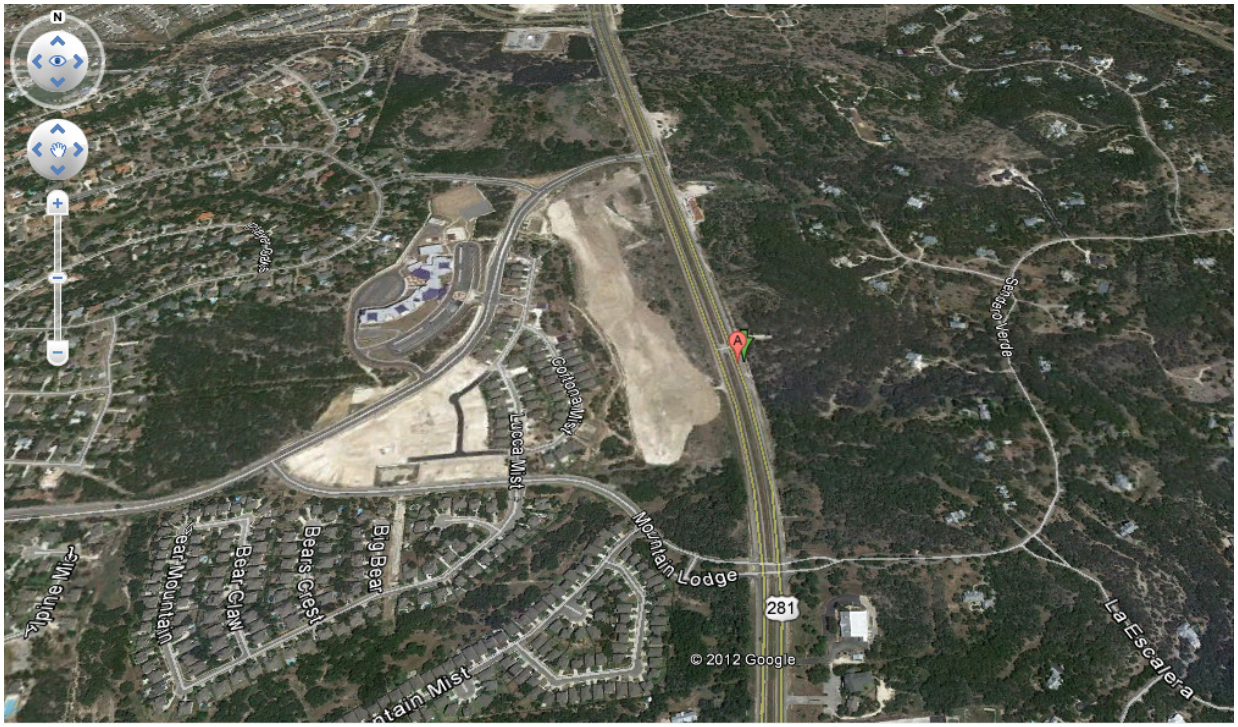

Sample 7 29 40.255' N, 98 27.022' W 1052' ELEVATION

Central High Plains Aquifer Maps

These maps show the location of wells where the samples were collected.

State level:

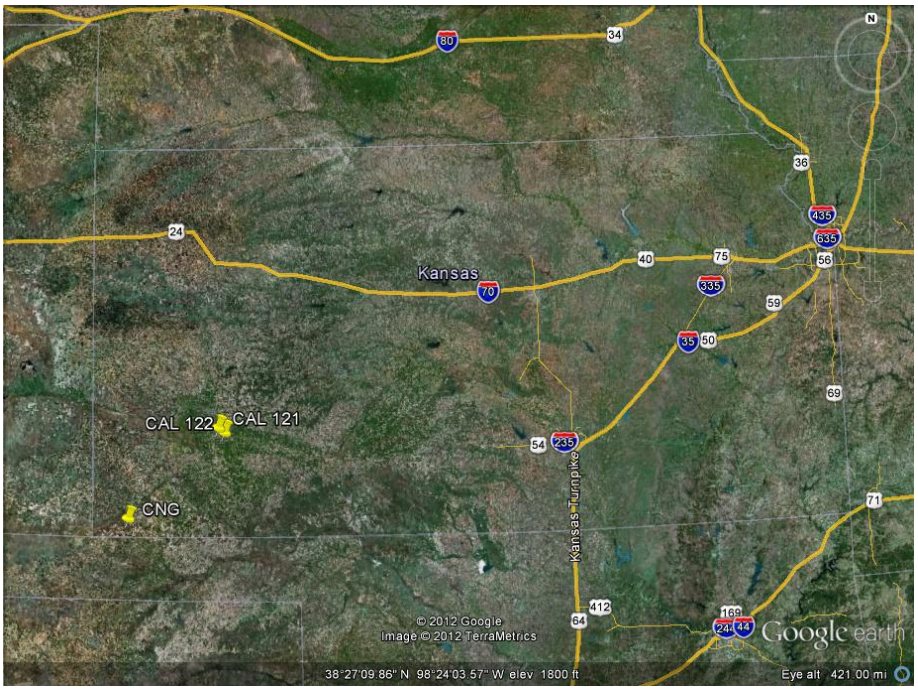

County level:

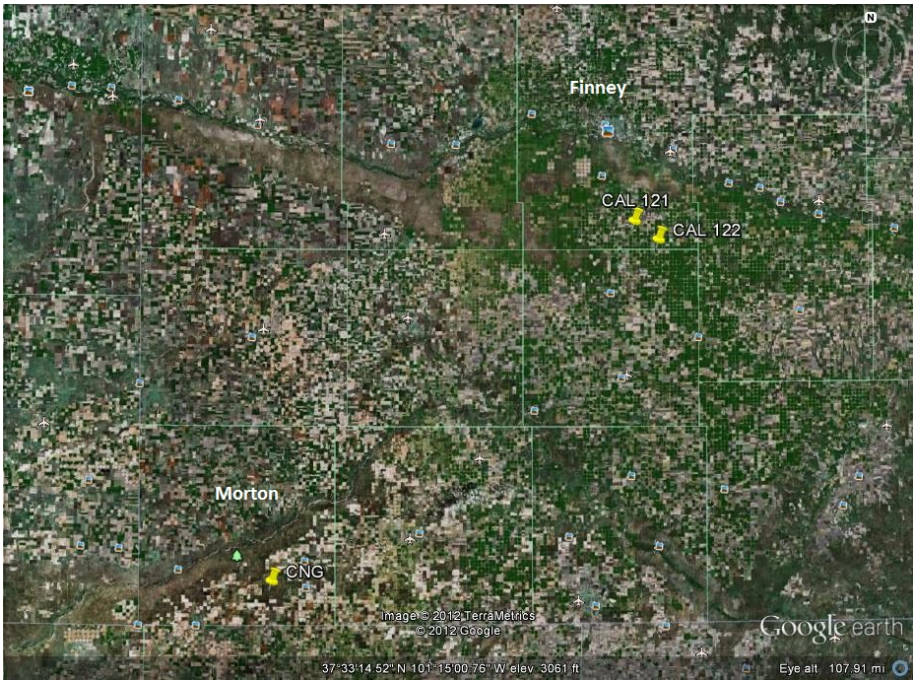

Appendix B

Apparatus, Pictures of the Systems, and Pictures of the Sediment Samples

Appendix B

Apparatus, Pictures of the Systems, Pictures of the Sediments Samples

Apparatus used in the batch experimental studies.

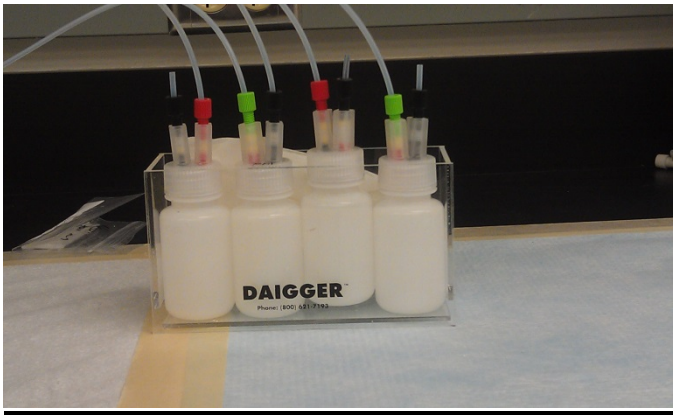

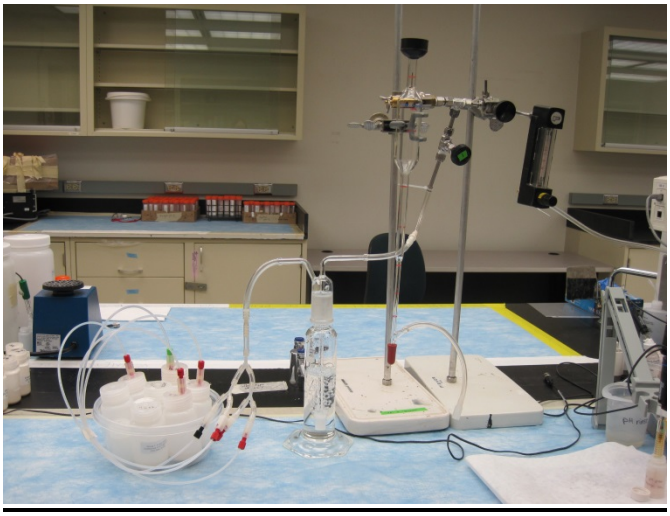

Separated size fractions of Edwards Sample 3 and Edwards Sample 7.

Experimental setup for 1-D saturated flow experiment involving aquifer sediments with simulated groundwater with or without gas intrusion.


oxarc

Appendix C

Tables

Table C.1. Selected column parameters and the aquifer sediments used in each column experiments.

Experiment Set	Material	Column Dimension	Porosity [-]	Flow Rate [mL/min]	Sample Preparation	Flow Fluid
Set 1	Accusand	ID2.49 * 15.2 cm	0.17		<2 mm	Synthesized Edwards ground water with N_2/CO_2 purging (0.5 mL/min] under 2 PSI headspace pressure in reservoir
	Accusand and Ed-Set B S4	ID2.49 * 15.2 cm	0.17/0.27*		Hammer-crashed to <2 mm	
Set 2	Ed-Set B S4	ID2.4 * 5.7 cm	0.25	0.024		
	Ed-Set B S7	ID2.4 * 5.7 cm	0.27	0.03		
Set 3	Ed-Set A S1	ID2.4 * 5.7 cm	0.26	0.031		
	Ed-Set A S4	ID2.4 * 5.7 cm	0.36	0.022	Sieved to <2 mm	
Set 4	K-CNG60-61’	ID2.4 * 5.7 cm	0.31	0.027		Synthesized Kansas ground water with CO_2 purging under 2 PSI headspace pressure in reservoir
	K-CNG110-111’	ID2.4 * 5.7 cm	0.31	0.026		

Table C.2. QXRD results from Edwards aquifer Set A samples.

Sample	Diffractometer	Calcite	Quartz	Montmorillonite
Sample 1 -2 mm	RPL	19.9%	36.4%	43.8%
Sample 1 -53 µm	RPL	54.5%	33.3%	12.1%
Sample 2 -2 mm	RPL	83.1%	6.9%	10.0%
Sample 2 -53 µm	RPL	69.2%	17.9%	12.9%
Sample 3 -2 mm	RPL	57.4%	17.4%	25.2%
Sample 3 -53 µm	RPL	71.3%	12.9%	15.8%
	EMSL	73.0%	10.1%	16.9%
Sample 4 -2 mm	RPL	1.0%	44.3%	54.7%
	EMSL	3.0%	37.3%	59.6%
Sample 4 -53 µm	RPL	37.8%	38.6%	23.7%
	EMSL	36.9%	36.9%	24.3%
Sample 5 -2 mm	RPL	57.5%	25.1%	17.4%
	EMSL	66.4%	14.1%	19.5%
Sample 5 -53 µm	RPL	61.4%	22.1%	16.5%
	EMSL	63.8%	18.7%	17.5%
Sample 6 -2 mm	RPL	77.9%	7.9%	14.2%
	EMSL	75.0%	8.0%	17.0%
Sample 6 -53 µm	RPL	98.1%	1.9%	
	EMSL	98.3%	1.7%	

Table C.3. QXRD results from Edwards aquifer Set B, samples 2, 4 and 7 and High Plains aquifers sediments used in batch and column experiments.

Sample	Calcite	Dolomite	Quartz	Montmorillonite	Feldspar	Kaolinite	Mica
Edwards New Set B, sample 2	100.0%						
Edwards New Set B, sample 4	100.0%						
Edwards New Set B, sample 7	100.0%						
Kansas CAL 121 91-92			64.1%		33.9%		2.2%
Kansas CAL 121 151-152	7.1%		60.0%		30.4%		2.4%
Kansas CAL 122 4-4.5	4.7%		41.3%	20.4%	27.3%	1.1%	5.2%
Kansas CAL 122B 29-30	1.6%		51.8%	17.8%	26.2%		2.6%
Kansas CNG 8-9	2.6%	1.0%	66.7%	13.8%	12.5%		3.5%
Kansas CNG 60-61			83.7%		14.5%		1.8%
Kansas CNG 110-111	1.0%		76.5%		20.3%		2.3%
Kansas CNG 150-151	4.1%		49.0%	14.8%	29.6%		2.6%

Table C.4. Results from the 8 M acid extraction in the <2-mm size fraction; Edwards Aquifer Materials, Set A, Samples 1–7, Set B, sample 2.

	µg/L	µg/L		µg/L	µg/L		µg/L	µg/L		µg/L	µg/L	
	Set A Sample 1			Set A Sample 2			Set A Sample 3			Set A Sample 4		
Elements	Average	Standard Deviation	Coefficent of Variation	Average	Standard Deviation	Coefficent of Variation	Average	Standard Deviation	Coefficent of Variation	Average	Standard Deviation	Coefficent of Variation
Aluminum	2.73E+06	1.96E+05	0.07	9.32E+05	7.95E+03	0.01	1.90E+06	2.70E+04	0.01	4.01E+06	1.62E+05	0.04
Arsenic	7.21E+02	5.56E+01	0.08	7.21E+02	2.34E+02	0.32	6.61E+02	5.93E+01	0.09	8.30E+02	1.75E+02	0.21
Barium	1.67E+04	1.20E+03	0.07	7.24E+03	2.53E+02	0.03	1.09E+04	1.64E+02	0.01	2.40E+04	1.47E+03	0.06
Beryllium										3.08E+02	1.51E+01	0.05
Bismuth	8.59E+03	9.39E+01	0.01	1.46E+04	4.82E+02	0.03	1.30E+04	3.69E+02	0.03			
Cadmium	6.08E+01	3.43E+00	0.06	3.25E+01	6.65E+00	0.20	4.63E+01	7.96E-01	0.02	4.64E+01	1.01E+00	0.02
Calcium	2.75E+07	5.01E+06	0.18	5.37E+07	1.07E+06	0.02	4.64E+07	2.29E+06	0.05	8.13E+06	7.05E+05	0.09
Cesium	2.56E+02	1.80E+01	0.07	1.28E+02	2.27E+01	0.18	1.98E+02	3.56E+00	0.02	4.44E+02	5.84E+01	0.13
Chromium	2.66E+03	2.35E+02	0.09	9.85E+02	2.29E+01	0.02	1.46E+03	4.89E+01	0.03	3.79E+03	1.87E+02	0.05
Chromium	2.83E+03	1.59E+02	0.06	1.32E+03	1.95E+01	0.01	1.85E+03	2.02E+01	0.01	4.07E+03	1.32E+02	0.03
Copper	1.51E+03	1.22E+02	0.08	6.89E+02	4.85E-01	0.00	1.31E+03	1.04E+01	0.01	1.99E+03	1.12E+02	0.06
Iron	2.47E+06	2.16E+05	0.09	1.04E+06	6.46E+02	0.00	1.55E+06	2.43E+04	0.02	3.74E+06	1.86E+05	0.05
Lead	2.87E+03	1.33E+02	0.05	1.16E+03	8.22E+01	0.07	2.13E+03	5.17E+01	0.02	2.82E+03	3.32E+01	0.01
Magnesium	3.98E+05	3.44E+04	0.09	4.17E+05	6.00E+03	0.01	3.22E+05	1.58E+04	0.05	3.24E+05	1.24E+04	0.04
Manganese	1.13E+05	5.90E+03	0.05	3.54E+04	1.64E+03	0.05	5.99E+04	2.16E+03	0.04	9.87E+04	4.08E+03	0.04
Molybdenum				6.78E+01	2.21E+00	0.03						
Nickel	2.51E+03	2.20E+02	0.09				2.49E+03	5.69E+01	0.02	2.94E+03	1.31E+02	0.04
Phosphorus	4.61E+04	3.72E+03	0.08	3.29E+04	1.93E+03	0.06	3.23E+04	1.42E+03	0.04	2.13E+04	4.17E+02	0.02
Potassium	3.97E+05	2.66E+04	0.07	1.96E+05	8.06E+01	0.00	2.46E+05	4.02E+03	0.02	1.96E+05	1.10E+04	0.06
Sodium				1.59E+04	4.83E+02	0.03						
Strontium	8.73E+03	1.91E+03	0.22	1.99E+04	3.80E+02	0.02	5.64E+03	8.77E+02	0.16	1.99E+03	1.04E+02	0.05
Sulfur	2.88E+05	4.07E+04	0.14	5.40E+05	1.04E+04	0.02	4.73E+05	2.12E+04	0.04	9.61E+04	7.16E+03	0.07
Tin	7.49E+03	6.60E+01	0.01	1.09E+04	2.60E+01	0.00	9.99E+03	1.36E+02	0.01			
Vanadium	3.75E+03	3.21E+02	0.09				2.77E+03	2.46E+01	0.01	7.76E+03	2.05E+02	0.03
Zinc	2.39E+04	1.64E+03	0.07	2.50E+03	3.57E+00	0.00	4.13E+03	6.16E+01	0.01	5.47E+03	1.88E+02	0.03

Table C.4. (contd)

	µg/L	µg/L		µg/L	µg/L		µg/L	µg/L	
	Set A Sample 5			Set A Sample 6			Set A Sample 7	K Sample 7	
Elements	Average	Standard Deviation	Coefficent of Variation	Average	Standard Deviation	Coefficent of Variation	Average	Standard Deviation	Coefficent of Variation
Aluminum	1.40E+06	8.42E+04	0.06	1.39E+06	1.31E+04	0.01	4.72E+05	8.11E+03	0.02
Arsenic	4.70E+02	2.06E+01	0.04	5.44E+02	2.03E+01	0.04			
Barium	1.26E+04	1.14E+03	0.09	7.95E+03	3.22E+02	0.04	3.66E+03	6.32E+01	0.02
Beryllium									
Bismuth	1.33E+04	5.21E+02	0.04	1.56E+04	3.21E+02	0.02	1.76E+04	5.24E+02	0.03
Cadmium	2.72E+01	1.34E-01	0.00	3.28E+01	3.90E-01	0.01	3.98E+01	6.35E-01	0.02
Calcium	4.67E+07	2.80E+06	0.06	5.63E+07	1.97E+06	0.04			
Cesium	1.62E+02	5.37E+00	0.03	1.25E+02	3.71E+00	0.03	4.96E+01	2.93E+00	0.06
Chromium	1.31E+03	6.60E+01	0.05	7.77E+02	6.30E+00	0.01			
Chromium	1.67E+03	9.46E+01	0.06	1.25E+03	4.82E+01	0.04	8.74E+02	2.01E+01	0.02
Copper	7.21E+02	2.68E+01	0.04	6.32E+02	1.58E+01	0.02	1.06E+03	1.41E+02	0.13
Iron	1.40E+06	5.25E+04	0.04	1.12E+06	2.91E+04	0.03	3.83E+05	1.53E+04	0.04
Lead	1.83E+03	5.02E+01	0.03	1.11E+03	1.50E+01	0.01	1.97E+03	1.38E+03	0.70
Magnesium	1.67E+05	3.78E+03	0.02	1.16E+05	6.45E+02	0.01	3.11E+05	1.00E+04	0.03
Manganese	2.73E+04	1.52E+03	0.06	1.36E+04	4.39E+02	0.03	2.68E+04	1.36E+03	0.05
Molybdenum				1.15E+02					
Nickel							2.84E+03	1.19E+02	0.04
Phosphorus	1.63E+04	5.21E+01	0.00	1.42E+04	5.74E+02	0.04	1.57E+05	6.35E+03	0.04
Potassium	7.76E+04	1.65E+03	0.02	8.42E+04	7.25E+02	0.01	5.88E+04	2.05E+03	0.03
Sodium	1.61E+04	#DIV/0!		2.03E+04	9.52E+02	0.05			
Strontium	5.62E+03	5.43E+02	0.10	2.72E+03	2.41E+02	0.09	5.96E+03	4.74E+00	0.00
Sulfur	4.97E+05	3.85E+04	0.08	5.62E+05	2.45E+04	0.04	6.36E+05	1.38E+04	0.02
Tin	9.80E+03	4.03E+02	0.04	1.11E+04	5.30E+01	0.00	1.23E+04	6.80E+02	0.06
Vanadium	2.59E+03	1.98E+01	0.01	2.82E+03	9.25E+01	0.03			
Zinc	2.42E+03	2.84E+01	0.01	2.40E+03	8.18E+01	0.03	4.88E+03	9.44E+01	0.02

Table C.4. (contd)

Edwards aquifer	LIMS ID	Edwards <53um Set B Sample 2		Edwards 53um-2mm Set B Sample 2	
		Average	St Dev	Average	St Dev
Aluminum	ug/L	1.76E+04	9.88E+02	1.44E+04	4.06E+03
Arsenic	ug/L	7.50E+01	4.30E+00	5.95E+01	
Barium	ug/L				
Bismuth	ug/L	1.10E+04	1.05E+03	1.31E+04	
Cadmium	ug/L				
Calcium	ug/L	8.54E+07	8.38E+06	7.84E+07	1.17E+07
Cesium	ug/L	6.15E+00	6.22E-02	4.75E+00	9.20E-01
Chromium	ug/L				
Chromium	ug/L	1.50E+02	8.15E+00	1.43E+02	2.46E+01
Copper	ug/L				
Iron	ug/L	4.07E+04	3.21E+03	3.16E+04	7.61E+03
Lead	ug/L				
Lead	ug/L	1.21E+03	6.00E+01	6.98E+01	1.24E+01
Magnesium	ug/L	2.69E+05	8.61E+03	2.84E+05	5.36E+04
Manganese	ug/L	5.51E+03	4.24E+02	4.38E+03	9.52E+02
Molybdenum	ug/L				
Nickel	ug/L				
Phosphorus	ug/L				
Potassium	ug/L				
Sodium	ug/L				
Strontium	ug/L	1.36E+04	4.03E+02	1.52E+04	2.39E+03
Sulfur	ug/L	6.94E+05	2.47E+04	7.37E+05	1.09E+05
Vanadium	ug/L				
Zinc	ug/L				

Table C.5. Results from the 8 M acid extraction; Kansas (High Plains) Aquifer Materials.

CNG Sediments		CNG 8'-9' <2mm		CNG 60'-61' <2mm		CNG 110'-111' <2mm		CNG 150'-151' <2mm		CNG 194'-195' <2mm	
	Units	Average	St Dev	Average	St Dev	Average	St Dev	Average	St Dev	Average	St Dev
Aluminum	µg/L	1.10E+06	9.19E+03	4.35E+05	5.04E+03	3.84E+05	1.49E+05	3.91E+05	1.73E+05	1.24E+06	1.27E+05
Arsenic	µg/L	3.68E+02	2.64E+01	2.79E+02	2.82E+01	1.67E+02	7.22E-01	1.83E+02	5.37E-01	3.07E+02	1.58E+01
Barium	µg/L	2.95E+04	1.39E+03	4.17E+03		1.17E+04		1.14E+04		1.82E+04	7.94E+02
Bismuth	µg/L										
Cadmium	µg/L	2.92E+01	2.59E+00							1.47E+01	1.20E+00
Calcium	µg/L	3.33E+06	1.47E+05	3.96E+05	7.41E+03	1.63E+06	7.51E+05	1.65E+06	8.09E+05	2.87E+06	2.40E+05
Cesium	µg/L	1.97E+02	1.05E+01	6.11E+01	4.78E+00	5.51E+01	1.26E+00	6.34E+01	1.79E+00	1.52E+02	7.49E+00
Chromium	µg/L									1.05E+03	
Chromium	µg/L	1.21E+03	7.30E+01	5.63E+02	6.26E+01	4.63E+02	1.94E+00	7.99E+02	1.42E+01	1.28E+03	8.31E+01
Copper	µg/L										
Iron	µg/L	1.39E+06	2.17E+04	7.65E+05	1.10E+04	5.74E+05	1.88E+05	5.83E+05	2.16E+05	1.33E+06	1.30E+05
Lead	µg/L										
Lead	µg/L	1.07E+03	6.75E+01	4.18E+02	4.35E+01	2.58E+02	5.29E+00	3.91E+02	9.18E+00	7.87E+02	1.79E+01
Magnesium	µg/L	6.64E+05	2.22E+04	1.46E+05	2.55E+03	2.13E+05	9.99E+04	2.14E+05	1.11E+05	6.38E+05	5.08E+04
Manganese	µg/L	3.79E+04	1.34E+03	7.88E+03	1.85E+02	1.53E+04	1.08E+04	1.56E+04	1.14E+04	3.95E+04	4.02E+03
Molybdenum	µg/L										
Nickel	µg/L										
Phosphorus	µg/L	6.34E+04	1.79E+03	8.91E+04	2.26E+03	2.79E+04	8.16E+03	2.89E+04	9.77E+03	5.87E+04	7.70E+03
Potassium	µg/L	2.64E+05	2.32E+03	1.19E+05	9.81E+02	7.15E+04	2.09E+04	7.24E+04	2.24E+04	2.27E+05	1.52E+04
Sodium	µg/L										
Strontium	µg/L	1.02E+04	3.50E+02			4.31E+03		4.45E+03		8.35E+03	5.79E+02
Sulfur	µg/L										
Vanadium	µg/L										
Zinc	µg/L	4.81E+03	1.18E+01							4.80E+03	4.22E+02

Table C.5. (contd)

CAL 121		CAL 121 2'-2.5' <53um		CAL121 2'-2.5' 53um-2mm		CAL 121 2'-2.5' <2mm		CAL 121 33'-33.5' <53um		CAL121 33'-33.5' 53um-2mm		CAL 121 33'-33.5' <2mm	
	LIMS ID	Average	St Dev	Average	St Dev	Average	St Dev	Average	St Dev	Average	St Dev	Average	St Dev
Aluminum	ug/L	2.24E+06	9.22E+04	1.38E+06	3.36E+03	1.91E+06	1.09E+05	1.77E+06	1.95E+05	9.70E+05	4.11E+04	1.44E+06	1.40E+04
Arsenic	ug/L	8.05E+02	2.16E+01	4.88E+02	9.01E+00	6.28E+02	4.57E+01	1.08E+03	6.30E+01	5.85E+02	8.96E+00	8.10E+02	8.64E+00
Barium	ug/L	4.56E+04	2.37E+03	2.80E+04	2.15E+03	3.61E+04	4.49E+03	2.59E+04	1.95E+03	1.93E+04	2.10E+03	2.24E+04	5.33E+03
Bismuth	ug/L												
Cadmium	ug/L	5.50E+01	1.39E+00	3.39E+01	1.04E+00	4.32E+01	2.28E+00	1.16E+02	5.34E+00	6.38E+01	7.77E-01	8.45E+01	3.06E-01
Calcium	ug/L	6.59E+06	3.43E+05	3.77E+06	3.56E+03	5.24E+06	2.41E+05	8.20E+06	6.82E+05	4.21E+06	2.11E+05	5.84E+06	9.46E+03
Cesium	ug/L	3.40E+02	8.52E+00	2.26E+02	3.56E+00	2.78E+02	2.09E+01	2.69E+02	1.60E+01	1.92E+02	1.23E-01	2.38E+02	5.43E+00
Chromium	ug/L	2.27E+03	7.88E+01	1.22E+03	1.77E+01	1.81E+03	1.20E+02	1.75E+03	2.69E+02			1.25E+03	1.00E+02
Chromium	ug/L	2.50E+03	9.06E+01	1.58E+03	3.14E+01	2.04E+03	1.57E+02	2.00E+03	1.55E+02	1.19E+03	4.64E-01	1.66E+03	3.08E+01
Copper	ug/L	3.56E+03	9.74E+01			3.08E+03	2.39E+01	4.09E+03	2.48E+02			3.30E+03	#DIV/0!
Iron	ug/L	2.82E+06	1.15E+05	1.74E+06	5.81E+03	2.36E+06	1.15E+05	3.02E+06	2.93E+05	1.68E+06	6.73E+04	2.43E+06	6.96E+04
Lead	ug/L												
Lead	ug/L	3.07E+03	4.97E+02	1.26E+03	6.34E+01	3.12E+03	2.43E+03	3.34E+03	2.15E+02	1.18E+03	5.93E+01	1.57E+03	4.95E+01
Magnesium	ug/L	1.09E+06	4.63E+04	6.50E+05	1.11E+03	8.61E+05	3.76E+04	8.76E+05	8.39E+04	4.90E+05	3.99E+03	6.77E+05	1.77E+04
Manganese	ug/L	5.74E+04	2.56E+03	4.35E+04	2.63E+03	5.44E+04	2.81E+03	7.70E+04	6.86E+03	3.90E+04	1.74E+03	5.43E+04	9.99E+02
Molybdenum	ug/L							1.13E+02	2.83E+00	8.20E+01	1.77E+00	1.12E+02	7.21E+00
Nickel	ug/L	3.27E+03						3.79E+03	3.14E+02				
Phosphorus	ug/L	1.16E+05	3.26E+03	6.12E+04	2.07E+03	8.27E+04	4.68E+03	2.55E+05	1.93E+04	1.27E+05	1.55E+03	1.75E+05	1.36E+03
Potassium	ug/L	4.84E+05	2.09E+04	3.06E+05	2.89E+03	3.99E+05	2.17E+04	3.43E+05	3.37E+04	2.09E+05	6.26E+03	2.77E+05	6.75E+03
Sodium	ug/L							6.24E+04	5.95E+03	3.12E+04	4.15E+03	4.27E+04	3.72E+02
Strontium	ug/L	2.22E+04	1.19E+03	1.31E+04	4.59E+01	1.71E+04	8.05E+02	1.91E+04	1.51E+03	1.21E+04	3.14E+02	1.51E+04	6.66E+02
Sulfur	ug/L							8.08E+04	5.32E+03				
Vanadium	ug/L							5.02E+03	5.66E+02				
Zinc	ug/L	9.08E+03	2.36E+02	5.74E+03	8.89E+01	7.60E+03	3.30E+02	1.12E+04	1.15E+03	6.07E+03	2.49E+02	8.54E+03	6.17E+01

Table C.5. (contd)

CAL 121		CAL 121 91'-92' <53um		CAL 121 91'-92' 53um-2mm		CAL 121 91'-92' <2mm		CAL 121 151'-152' <53um		CAL 121 151'-152' 53um-2mm		CAL 121 151'-152' <2mm	
	LIMS ID	Average	St Dev	Average	St Dev	Average	St Dev	Average	St Dev	Average	St Dev	Average	St Dev
Aluminum	ug/L	6.90E+05	5.16E+04	1.49E+05	1.72E+04	1.80E+05	6.06E+03	6.26E+05	1.93E+03	1.68E+05	8.70E+03	2.10E+05	3.03E+04
Arsenic	ug/L	7.40E+02	3.40E+01	1.53E+02	8.46E+00	1.82E+02	1.65E+01	7.96E+02	8.51E+00	3.04E+02	2.66E+01	3.98E+02	1.98E+01
Barium	ug/L	2.52E+05	9.33E+03	1.75E+04	2.14E+02	1.97E+04	4.82E+02	4.17E+04	3.93E+01	6.42E+03	1.01E+03	7.21E+03	7.48E+02
Bismuth	ug/L												
Cadmium	ug/L	6.53E+01	3.21E+00					6.90E+01	1.31E+00	1.48E+01		1.42E+01	1.56E+00
Calcium	ug/L	2.89E+06	2.75E+05	2.40E+05	3.55E+04	2.82E+05	5.38E+04	1.79E+07	5.48E+04	2.55E+06	3.96E+05	2.90E+06	3.81E+05
Cesium	ug/L	7.66E+01	2.45E+00	2.32E+01	4.43E-01	2.60E+01	2.26E+00	7.21E+01	3.96E-01	2.66E+01	8.23E-01	3.16E+01	7.20E-01
Chromium	ug/L	3.17E+03	3.23E+02					1.46E+03	1.60E+01				
Chromium	ug/L	3.36E+03	2.37E+02	3.73E+02	4.92E+01	4.30E+02	6.39E+00	1.78E+03	1.31E+01	3.24E+02	2.46E+01	3.90E+02	5.89E+01
Copper	ug/L	6.43E+03	9.34E+02					4.33E+03	8.82E+01				
Iron	ug/L	2.20E+06	1.27E+05	4.40E+05	3.02E+04	5.43E+05	4.09E+04	1.58E+06	1.03E+04	5.45E+05	1.59E+04	7.20E+05	4.43E+04
Lead	ug/L	1.41E+04	3.27E+03					6.05E+03	3.02E+02				
Lead	ug/L			4.32E+02	9.71E+00	5.51E+02	2.04E+01			3.64E+02	4.28E+01	4.93E+02	1.87E+01
Magnesium	ug/L	2.60E+05	1.84E+04	6.11E+04	9.68E+03	7.08E+04	3.94E+03	3.29E+05	1.58E+03	7.97E+04	2.97E+03	9.78E+04	2.23E+04
Manganese	ug/L	1.51E+05	1.08E+04	1.72E+04	1.42E+03	1.95E+04	4.78E+02	1.14E+05	9.77E+01	2.37E+04	5.15E+03	2.55E+04	2.60E+03
Molybdenum	ug/L	6.23E+02	6.00E+00	7.61E+01	6.05E+00	8.33E+01	9.95E-01	3.49E+02	2.77E+00	7.24E+01	1.06E+01	8.97E+01	6.45E+00
Nickel	ug/L	6.93E+03	2.93E+02										
Phosphorus	ug/L	1.14E+05	9.60E+03	2.25E+04		3.29E+04	1.62E+04	1.00E+05	1.67E+03	2.94E+04	7.66E+03	3.20E+04	7.14E+02
Potassium	ug/L	9.73E+04	1.22E+04					1.03E+05	2.09E+03				
Sodium	ug/L												
Strontium	ug/L	1.33E+04	8.98E+02					1.40E+04	8.38E+01	3.12E+03		3.47E+03	1.59E+01
Sulfur	ug/L	1.34E+05	1.12E+04					1.68E+05	1.63E+03				
Vanadium	ug/L												
Zinc	ug/L	7.10E+03	6.43E+02					4.24E+03	1.38E+02				

Table C.5. (contd)

CAL 122		CAL 122 4'-4.5' <53um		CAL 122 4'-4.5' 53um-2mm		CAL 122 4'-4.5' <2mm		CAL 122 29'-30' <53um		CAL 122 29'-30' 53um-2mm		CAL 122 29'-30' <2mm	
	LIMS ID	Average	St Dev	Average	St Dev	Average	St Dev	Average	St Dev	Average	St Dev	Average	St Dev
Aluminum	ug/L	2.02E+06	8.34E+04	1.74E+06	3.97E+04	2.00E+06	2.51E+05	1.42E+06	7.74E+03	6.48E+05	6.40E+03	6.82E+05	1.67E+04
Arsenic	ug/L	7.41E+02	2.58E+01	6.22E+02	1.59E+00	6.61E+02	2.26E+01	6.61E+02	1.48E+01	3.17E+02	1.08E+00	3.09E+02	8.35E+00
Barium	ug/L	5.85E+04	3.58E+02	5.64E+04	2.34E+03	5.26E+04	1.35E+04	2.66E+04	7.55E+02	7.82E+03	3.51E+02	7.41E+03	1.42E+02
Bismuth	ug/L												
Cadmium	ug/L	6.02E+01	6.25E-01	4.92E+01	2.22E-01	5.27E+01	1.15E+00	1.90E+01	2.48E+00				
Calcium	ug/L	5.87E+06	3.59E+04	4.61E+06	9.43E+04	5.09E+06	2.21E+05	3.31E+06	1.99E+04	6.85E+05	1.97E+04	7.68E+05	5.24E+04
Cesium	ug/L	3.32E+02	9.14E+00	2.93E+02	1.03E-01	3.15E+02	1.10E+01	2.25E+02	3.57E+00	1.13E+02	5.77E-01	1.14E+02	3.21E+00
Chromium	ug/L	2.09E+03	1.61E+02	1.71E+03	1.26E+01	1.90E+03	2.63E+02	1.53E+03	8.86E+00				
Chromium	ug/L	2.31E+03	1.08E+02	2.01E+03	1.54E+01	2.28E+03	7.80E+01	1.96E+03	3.64E+01	7.77E+02	5.15E-01	8.30E+02	1.01E+01
Copper	ug/L	3.60E+03	1.40E+01	2.97E+03	#DIV/0!	3.12E+03	1.62E+02	3.26E+03	4.71E+01				
Iron	ug/L	2.56E+06	9.43E+04	2.18E+06	3.44E+04	2.44E+06	2.80E+05	2.11E+06	4.57E+03	9.45E+05	1.17E+04	9.75E+05	8.56E+03
Lead	ug/L												
Lead	ug/L	3.57E+03	5.13E+01	1.72E+03	3.44E+02	4.09E+03	7.05E+02	8.70E+03	4.12E+02	8.07E+02	5.89E+00	7.28E+02	3.61E+00
Magnesium	ug/L	1.04E+06	1.81E+04	8.63E+05	1.49E+04	9.55E+05	1.08E+05	5.23E+05	1.13E+03	2.28E+05	4.52E+03	2.33E+05	6.36E+03
Manganese	ug/L	6.93E+04	8.67E+00	5.74E+04	2.83E+03	6.25E+04	7.09E+03	3.94E+04	1.85E+02	1.36E+04	5.19E+02	1.31E+04	4.41E+02
Molybdenum	ug/L												
Nickel	ug/L												
Phosphorus	ug/L	1.18E+05	2.67E+03	8.19E+04	1.84E+03	8.89E+04	8.56E+03	7.22E+04	1.20E+03	2.17E+04	1.15E+03	2.29E+04	
Potassium	ug/L	5.02E+05	2.02E+04	4.39E+05	1.69E+03	4.96E+05	3.78E+04	2.98E+05	2.00E+03	1.40E+05	2.07E+03	1.45E+05	4.14E+03
Sodium	ug/L	4.12E+04	1.07E+03	3.02E+04	9.94E+02	3.64E+04	5.10E+03	5.73E+04	1.34E+03				
Strontium	ug/L	1.95E+04	7.60E+01	1.58E+04	3.28E+02	1.68E+04	1.40E+03	1.32E+04	6.62E+01	4.08E+03	3.20E+01	4.05E+03	7.06E+01
Sulfur	ug/L	7.42E+04	5.11E+03										
Vanadium	ug/L												
Zinc	ug/L	8.78E+03	4.09E+02	7.14E+03	9.35E+01	8.06E+03	9.00E+02	5.29E+03	2.06E+00				

Table C.5. (contd)

CAL 121		CAL 122 99'-100' <53um #1		CAL 122 99'-100' 53um-2mm #1		CAL 122 99'-100' <2mm #1		CAL 122 151'-152' 53um-2mm		CAL 122 151'-152' <2mm #1	
	LIMS ID	Average	St Dev	Average	St Dev	Average	St Dev	Average	St Dev	Average	St Dev
Aluminum	ug/L	2.48E+06	2.08E+05	1.69E+06	3.64E+03	2.06E+06	3.94E+03	2.62E+06	5.53E+04	2.82E+06	2.85E+05
Arsenic	ug/L	1.32E+03	5.11E+01	1.04E+03	5.07E+01	1.18E+03	4.48E+00	1.45E+03	4.95E+01	1.41E+03	7.64E+01
Barium	ug/L	7.24E+04	3.66E+03	3.91E+04	1.66E+03	4.51E+04	3.80E+03	2.14E+04	5.63E+00	1.98E+04	2.48E+03
Bismuth	ug/L										
Cadmium	ug/L	6.74E+01	6.16E-01	5.67E+01	2.25E-02	6.44E+01	1.06E+00	1.62E+02	4.26E+00	1.73E+02	6.17E+00
Calcium	ug/L	1.72E+07	6.53E+05	1.61E+07	1.25E+06	1.86E+07	6.35E+05	7.84E+06	2.67E+05	8.19E+06	5.17E+05
Cesium	ug/L	3.03E+02	1.33E+01	2.18E+02	5.60E+00	2.49E+02	1.96E+00	3.63E+02	4.19E+00	3.47E+02	6.30E+00
Chromium	ug/L	2.49E+03	2.21E+02	1.38E+03	6.66E+01	1.74E+03	3.95E+01	2.96E+03	3.41E+01	3.19E+03	4.35E+02
Chromium	ug/L	2.73E+03	1.17E+02	1.76E+03	5.56E+01	2.12E+03	2.54E+01	3.22E+03	8.75E+01	3.27E+03	1.84E+02
Copper	ug/L	7.13E+03	5.42E+02	3.23E+03	6.71E+01	3.45E+03	5.89E+00	6.62E+03	7.63E+01	6.56E+03	5.33E+02
Iron	ug/L	3.16E+06	2.43E+05	2.23E+06	1.39E+04	2.61E+06	1.31E+04	4.23E+06	8.65E+04	4.53E+06	4.74E+05
Lead	ug/L	1.96E+04	2.50E+02								
Lead	ug/L			2.24E+03	1.11E+03	2.60E+03	7.85E+02	4.01E+03	4.19E+01	4.17E+03	5.06E+00
Magnesium	ug/L	1.17E+06	7.79E+04	7.81E+05	1.60E+04	9.31E+05	4.25E+03	1.06E+06	1.73E+04	1.15E+06	1.16E+05
Manganese	ug/L	7.97E+04	5.21E+03	6.14E+04	1.80E+03	7.32E+04	2.50E+03	1.28E+05	2.68E+03	1.33E+05	1.50E+04
Molybdenum	ug/L	1.07E+02	1.21E+00	1.20E+02	6.88E+00	1.27E+02	8.58E+00	1.75E+02	2.14E+00	1.67E+02	6.77E+00
Nickel	ug/L	4.23E+03	2.60E+02			3.59E+03	9.36E+01	6.24E+03	9.18E+01	6.70E+03	7.15E+02
Phosphorus	ug/L	1.06E+05	7.62E+03	6.17E+04	2.96E+02	6.60E+04	1.55E+02	1.50E+05	2.23E+03	1.64E+05	1.73E+04
Potassium	ug/L	5.31E+05	3.30E+04	3.60E+05	6.08E+03	4.33E+05	3.37E+02	4.07E+05	1.85E+04	4.27E+05	3.02E+04
Sodium	ug/L										
Strontium	ug/L	3.26E+04	1.58E+03	2.71E+04	1.21E+03	3.14E+04	1.08E+03	3.29E+04	1.14E+03	3.51E+04	2.41E+03
Sulfur	ug/L	1.69E+05	7.18E+03	1.41E+05	1.08E+04	1.66E+05	2.88E+03				
Vanadium	ug/L	5.51E+03	3.92E+02			4.82E+03	3.10E+02	6.49E+03	2.38E+02	6.94E+03	6.84E+02
Zinc	ug/L	1.08E+04	8.37E+02	5.75E+03	6.21E+01	6.53E+03	8.47E+01	1.81E+04	8.23E+01	1.99E+04	2.10E+03

Table C.6. EPA maximum contaminant levels (MCLs) and secondary drinking water standards for selected contaminants in drinking water for public supply systems. Limits in µg/L except as indicated; ND indicates no data.

Contaminant	Maximum Contaminant Level (MCL in µg/L)	Secondary Drinking Water Standards
Arsenic (As)	10	
Barium (Ba)	2000	
Cadmium (Cd)	5	
Chloride (Cl)		250000
Chromium (Cr)	100	
Copper (Cu)		1000
Iron (Fe)		300
Lead (Pb)	15	
Manganese (Mn)		50
Mercury (Hg)	2	
Nickel (Ni)	ND	ND
Nitrate (NO3 as N)	10000	
Selenium (Se)	50	
Silver (Ag)	50	
Sulfate (SO4)		250000
Thallium (TI)	2	
Uranium	30	
Zinc		5000
Total Dissolved Solids		500000
pH		6.5–8.5 standard pH units
Benzene	5	
Ethylbenzene	700	
Benzo(a)pyrene (PAHs)	0.2	

Table C.7. Data from the second set of column experiments conducted with Edwards Aquifer Sediments Set B, samples 4 and 7. The ND are nondetects.

Contaminant	EPA Maximum Contaminant Level (MCL in µg/L)	Set B Ed4	Set B Ed7	ICP-EOS/MS Experimental Quantitative Limit (=detection limit *dilution factor)
Aluminum	(50–200)	2–37	4–88	165
Arsenic (As)	10	0.2–24	0.2–45	4.68 (As75)
Barium (Ba)	2000	3.8–203	5.1–166	0.624 (Ba137)
Beryllium	4	ND	ND	23.7
Cadmium (Cd)	5	<0.14	<0.16	1.01 (Cd111)
Chloride (Cl)	(250000)	ND	ND	
Chromium (Cr)	100	0.4–12.4	0.4–18.1	1.92 (Cr52)
Copper (Cu)	(1000)	0.5–5.4	0.7–58.2	4.37 (Cu63)
Iron (Fe)	(300)	ND	ND	100
Lead (Pb)	15	0.1–97	0.1–817	0.93 (Pb208)
Manganese (Mn)	(50)	5.3–13	0–11.9	94.1
Mercury (Hg)	2	ND	ND	1.5 (Hg200)
Nickel (Ni)	ND	3.9–75	37–93	227
Nitrate (NO3 as N)	10000	ND	ND	
Selenium (Se)	50	0.2–81	0.4–150	13.6 (Se82)
Silver (Ag)	50; (100)	2.4–918	4.7–11.2	179
Sulfate (SO4)	(250000)	ND	ND	
Thallium (TI)	2	ND	ND	
Uranium	30	ND	ND	
Zinc	(5000)	0–154	0–750	299

Table C.8. Elemental composition of the pyrite (FeS_2), arsenopyrite (AsFeS) and galena (PbS) samples used in experiments. Samples were digested (microwave digestion) and the digest was analyzed by ICP-OES. Only species with concentrations exceeding 1 mg/g were considered.

	Pyrite-1	Pyrite-2	Pyrite-3	Avg	SD	Avg	Elemental
Analyte	µg/g	µg/g	µg/g	mg/g	mg/g	mmol/g	ratio
Iron	449000	446000	444000	446	2.52	7.97	Fe
Sulfur	500000	498000	494000	497	3.06	15.5	$S_{1.95}$

	Galena-1	Galena-2	Galena-3	Avg	SD	Avg	Elemental
Analyte	µg/g	µg/g	µg/g	mg/g	mg/g	mmol/g	ratio
Iron	1590	1800	2090	1.83	0.25	0.03	$Fe_{0.01}$
Lead	852000	768000	825000	815	42.9	3.94	Pb
Silicon	21300	28300	19900	23.2	4.50	0.83	$Si_{0.21}$
Sulfur	129000	122000	126000	126	3.51	3.93	S

	As-Pyrite-1	As-Pyrite-2	As-Pyrite-3	Avg	SD	Avg	Elemental
Analyte	µg/g	µg/g	µg/g	mg/g	mg/g	mmol/g	ratio
Arsenic	402000	395000	408000	402	6.51	5.36	$As_{0.87}$
Iron	335000	326000	339000	333	6.66	5.95	$Fe_{0.96}$
Lead	2210	2450	2340	2.33	0.12	0.01	$Pb_{0.002}$
Sulfur	198000	196000	200000	198	2.00	6.19	S

Appendix D

Figures

Appendix D

Figures

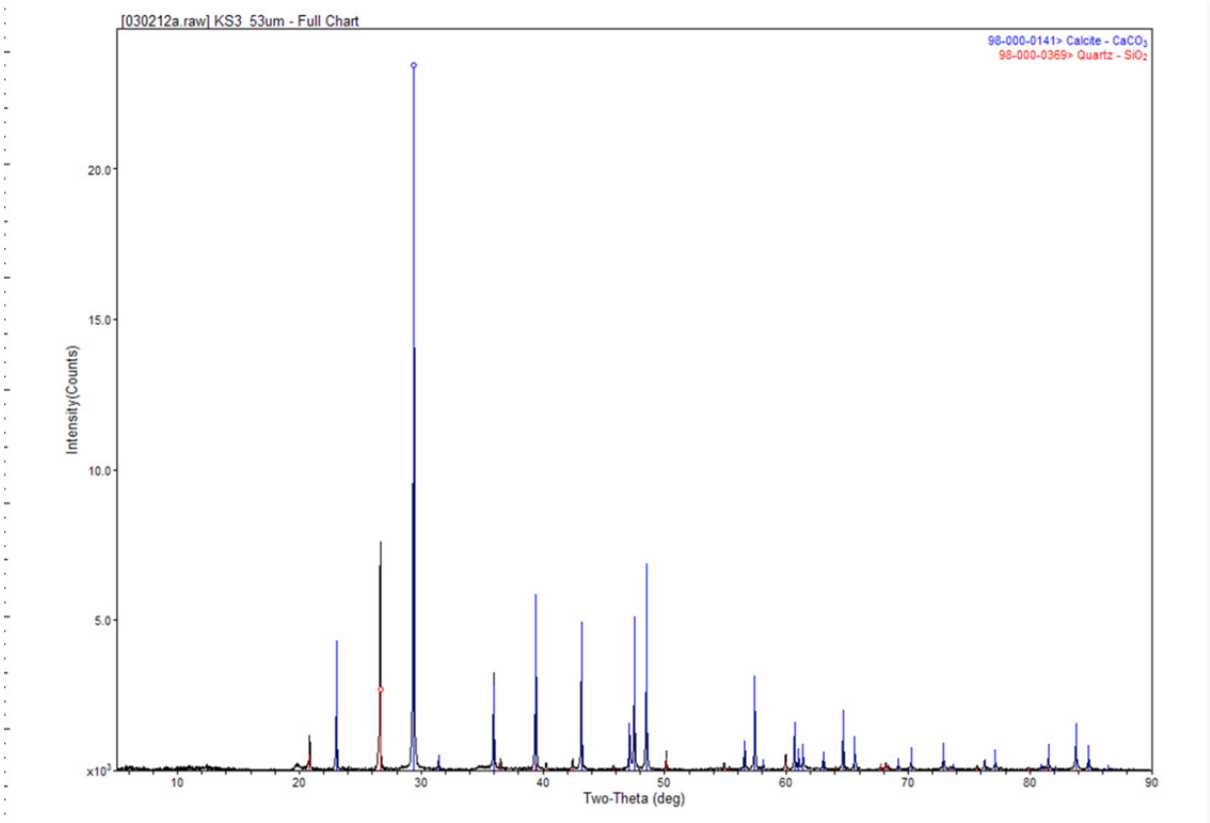

Figure D.1. XRD pattern of one of the Edwards aquifer samples (Set A Sample 3, <53 µm size fraction).

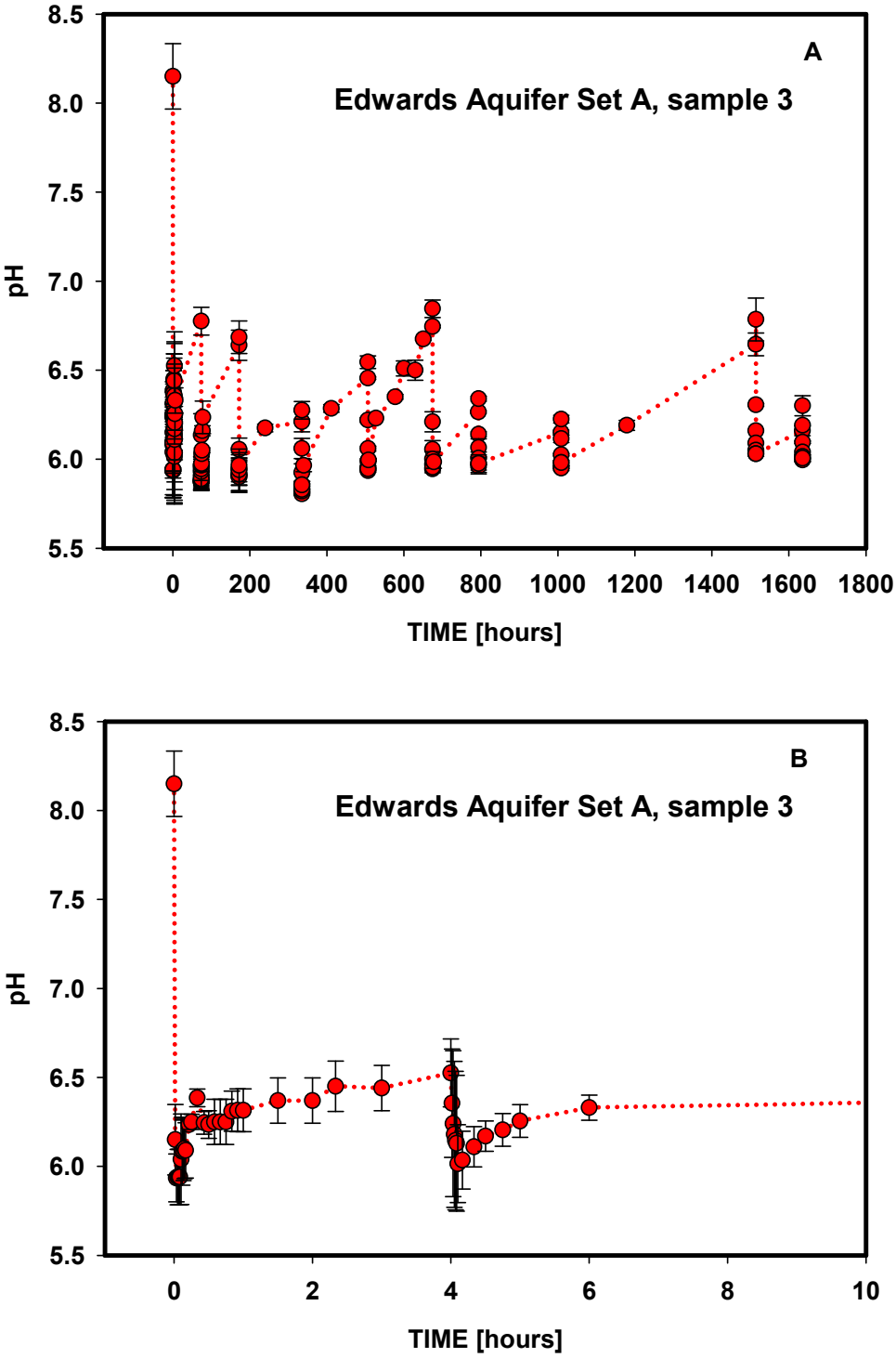

Figure D.2. Aqueous pH changes in response to periodic CO_2 injections (Batch 1, Test 1). The pH minima occur periodically at the time of the CO_2 gas periodic injection during the experiment.

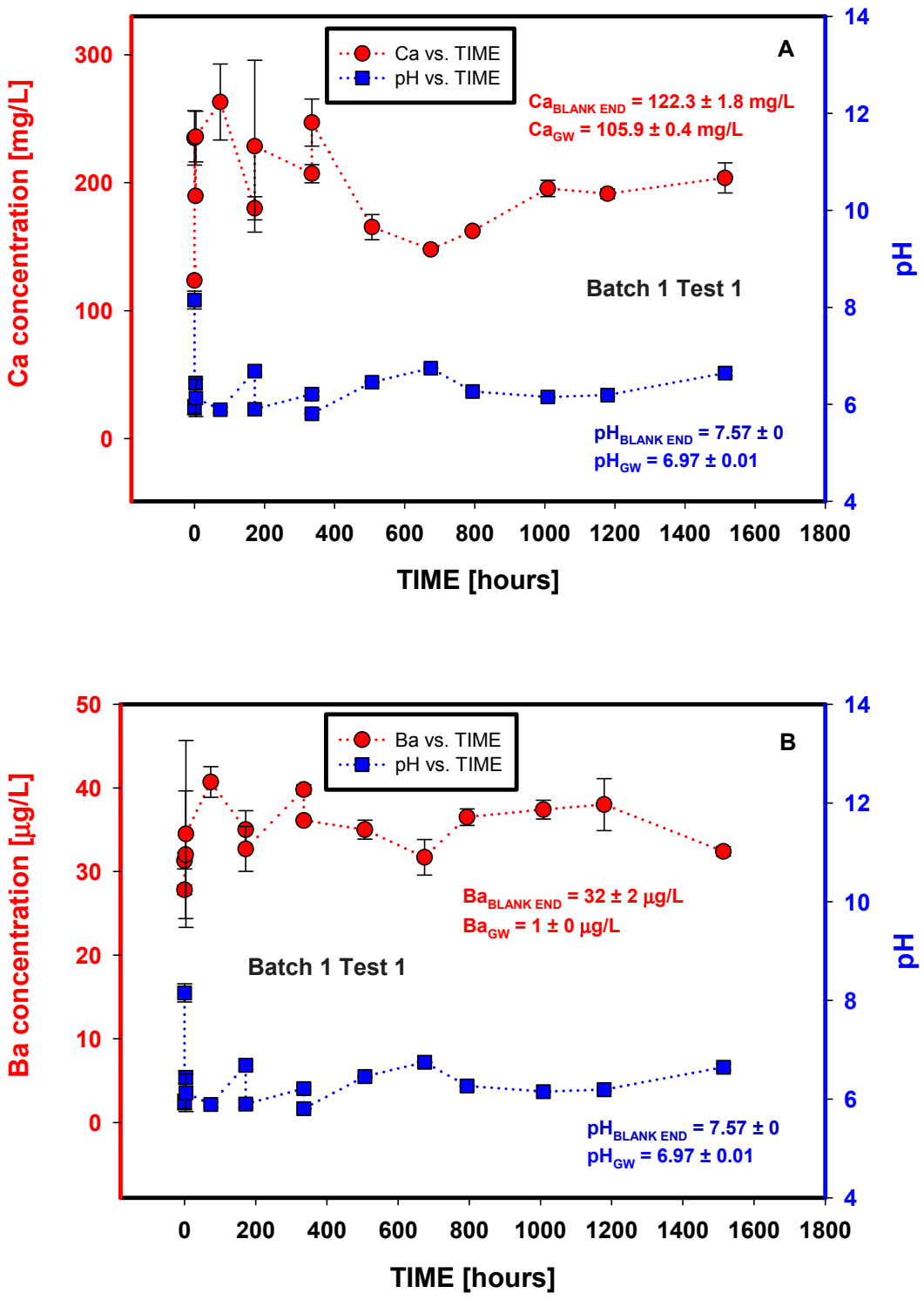

Figure D.3. Changes in pH and elemental composition as a function of time (Batch 1, Test 1, representative Edwards Aquifer Set A, sample 3).

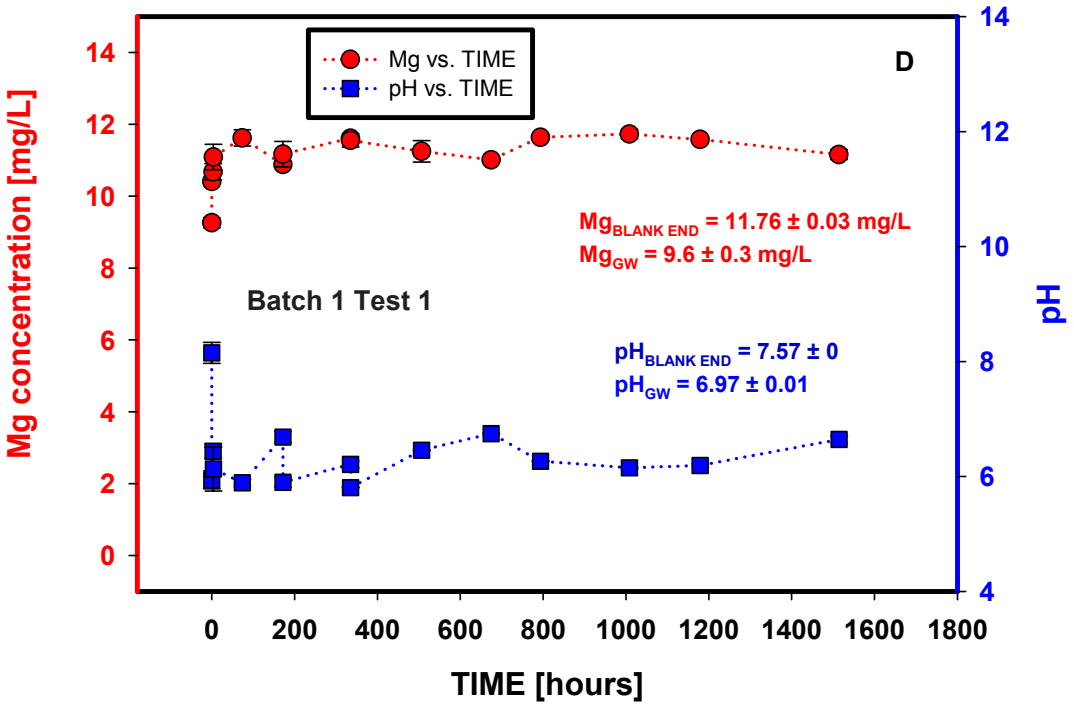

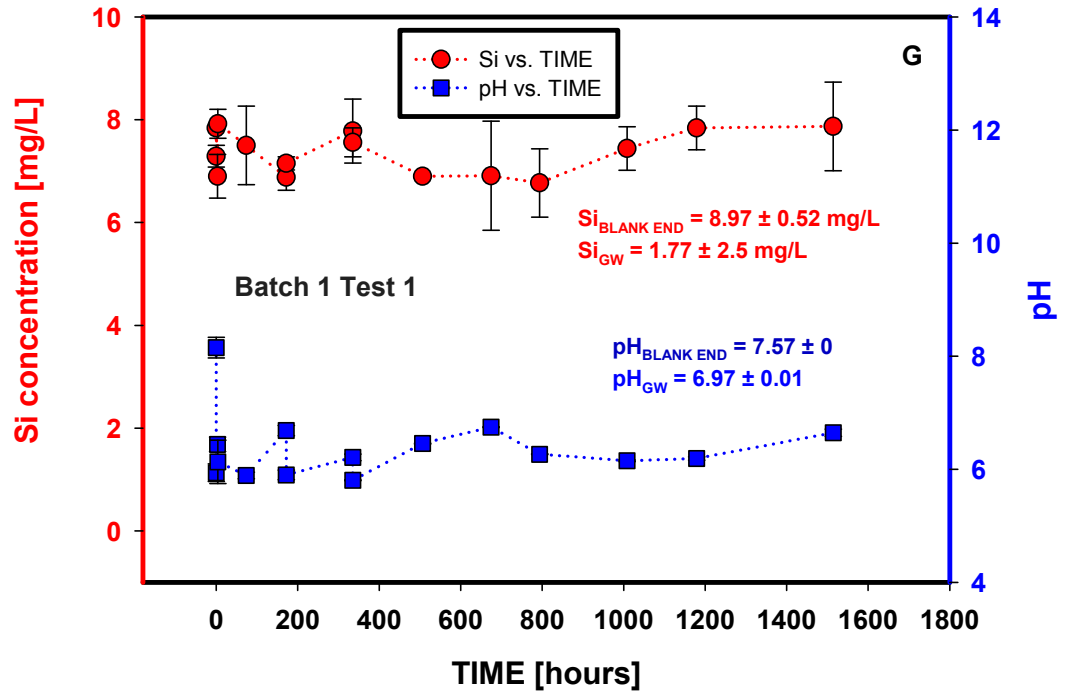

Figure D.3. (contd)

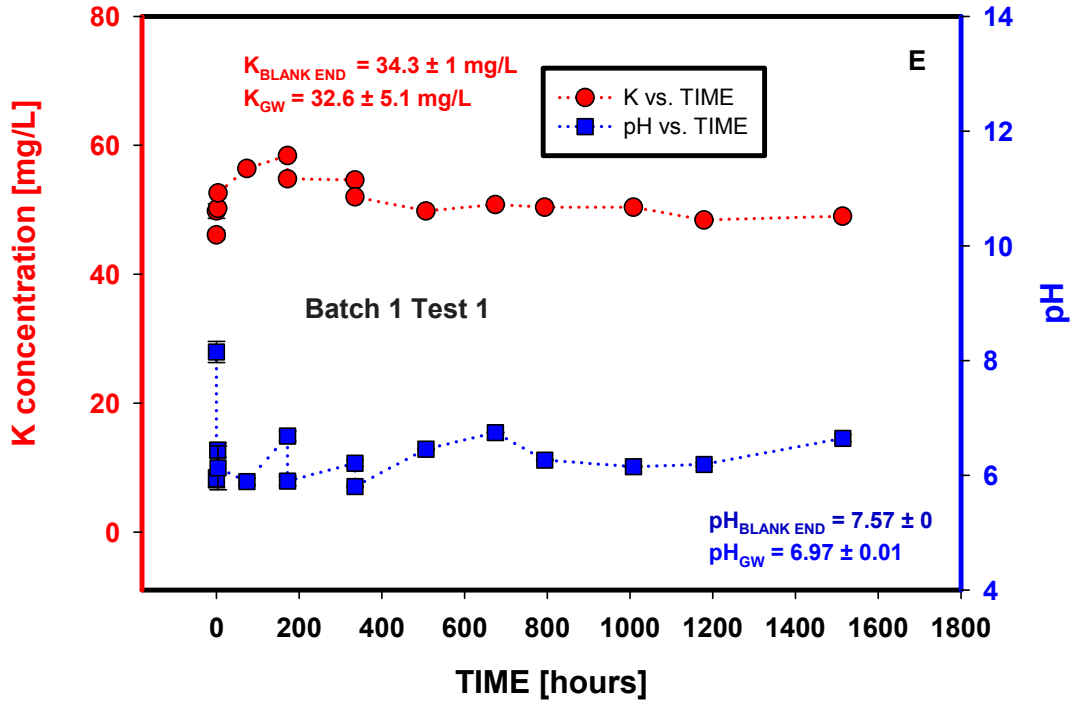

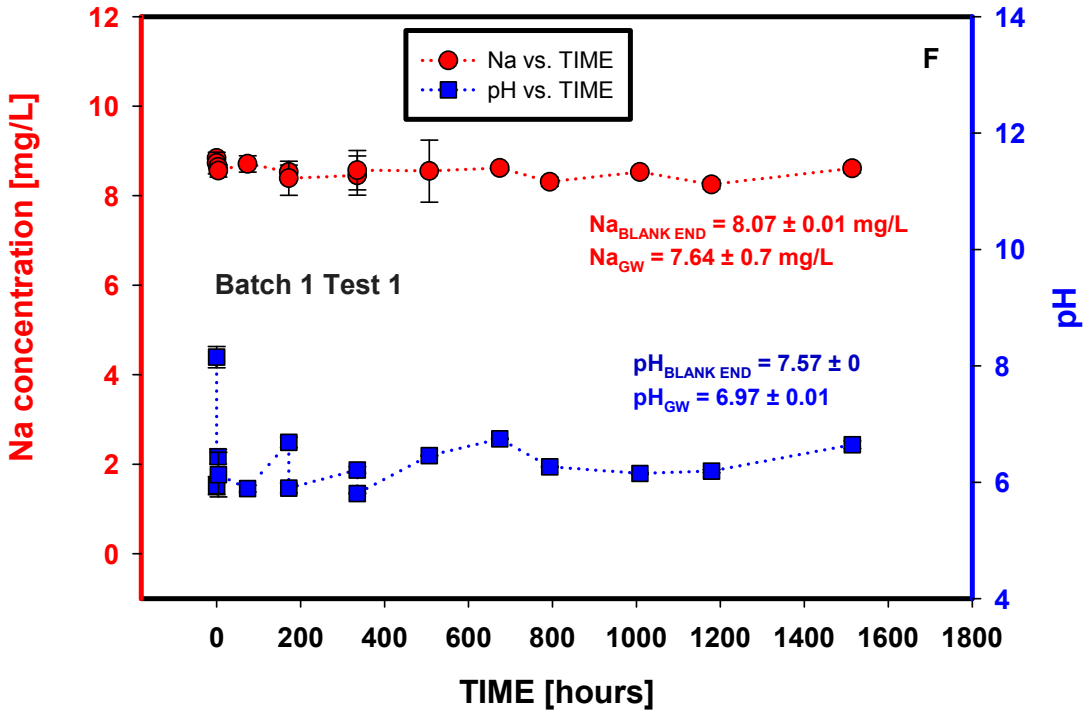

Figure D.3. (contd)

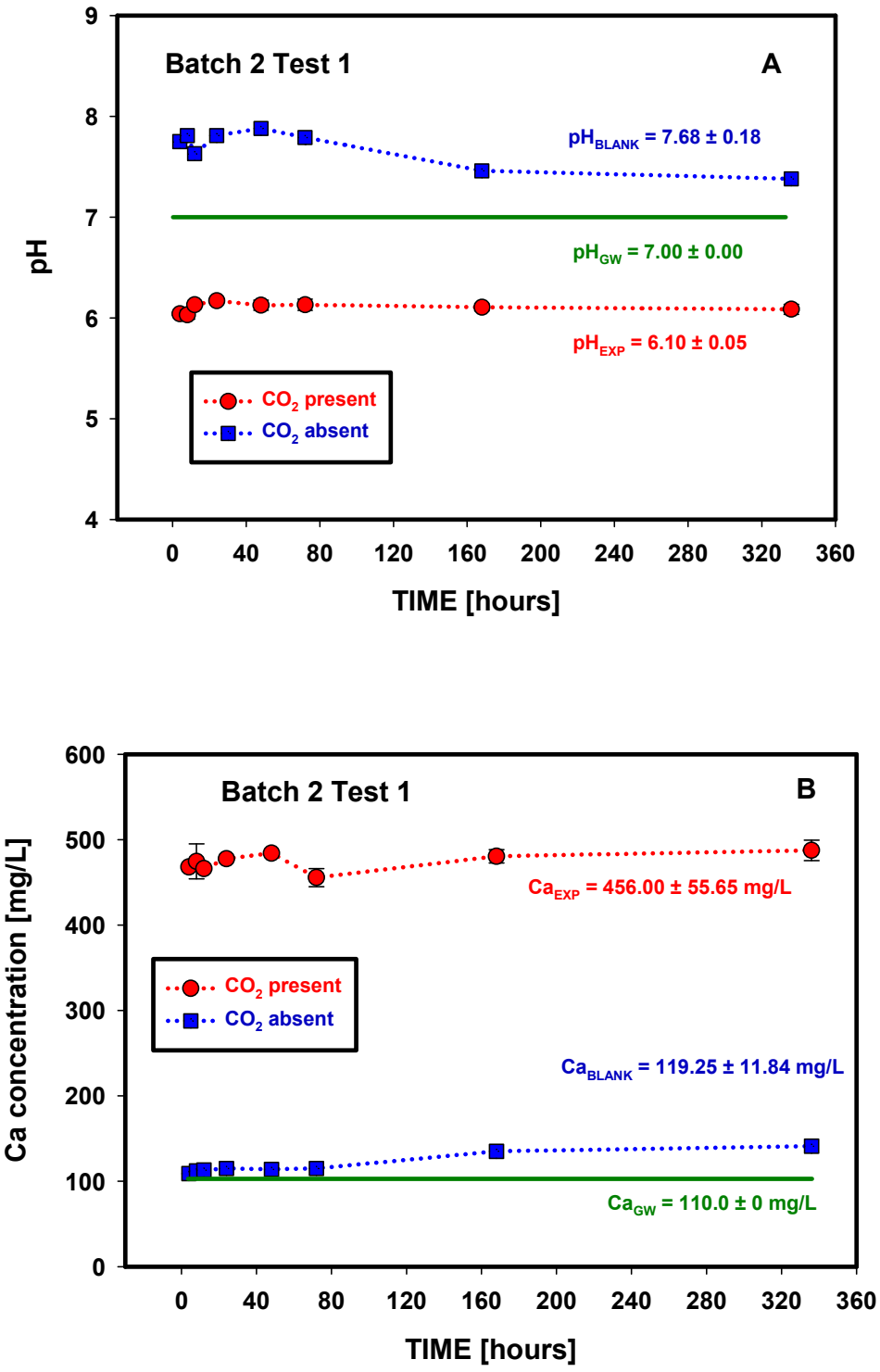

Figure D.4. Changes in pH and elemental composition as a function of time (Batch 2, Test 1, Edwards Aquifer Set B, sample 4).

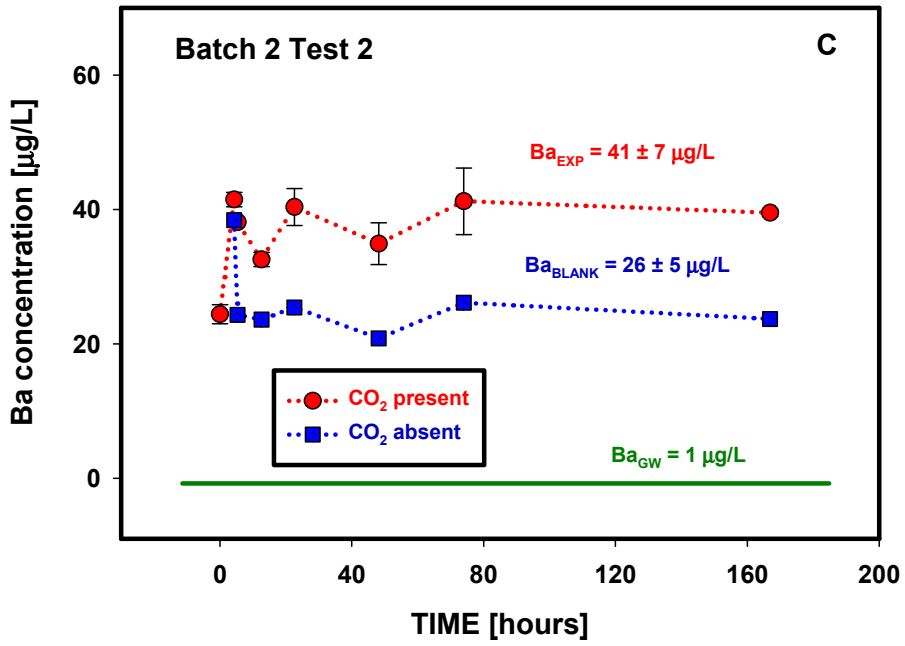

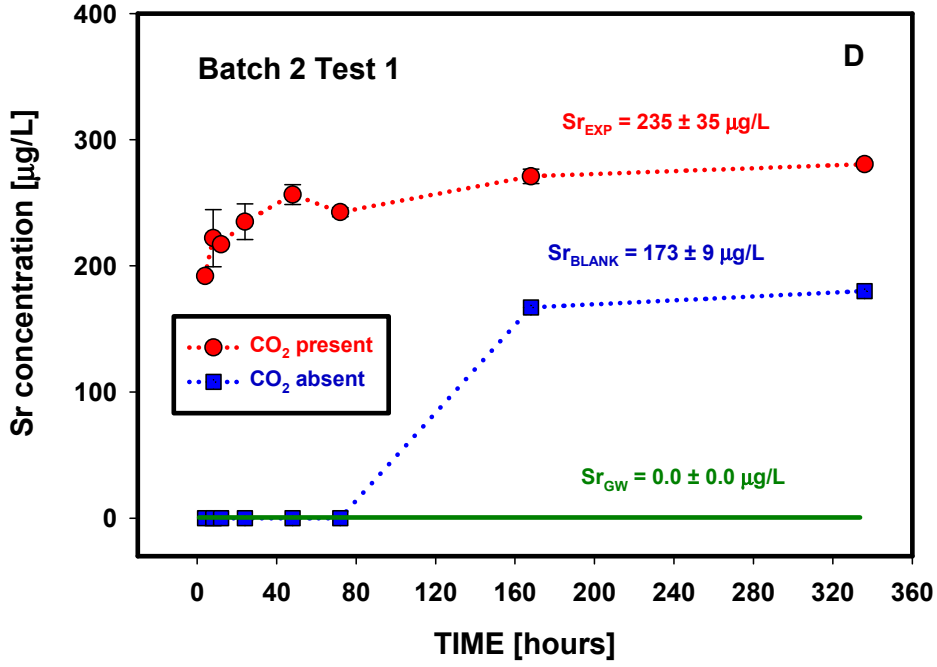

Figure D.4. (contd)

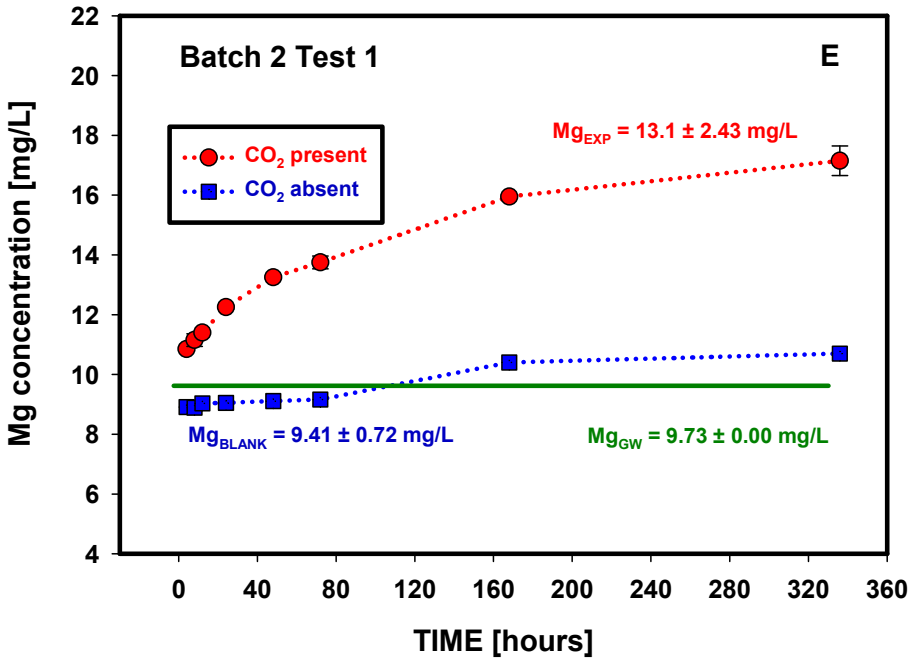

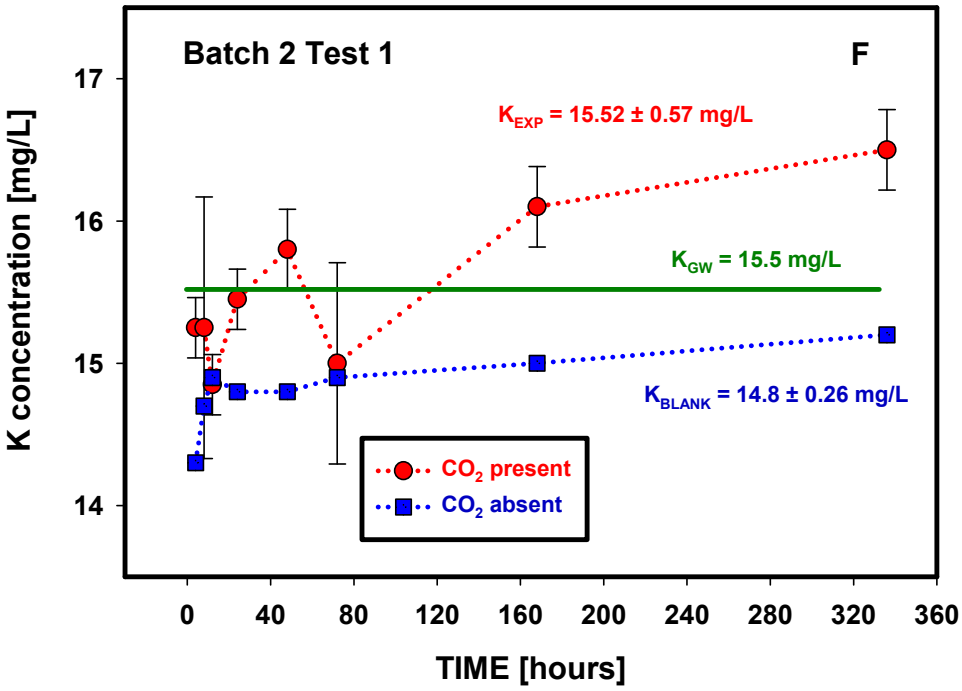

Figure D.4. (contd)

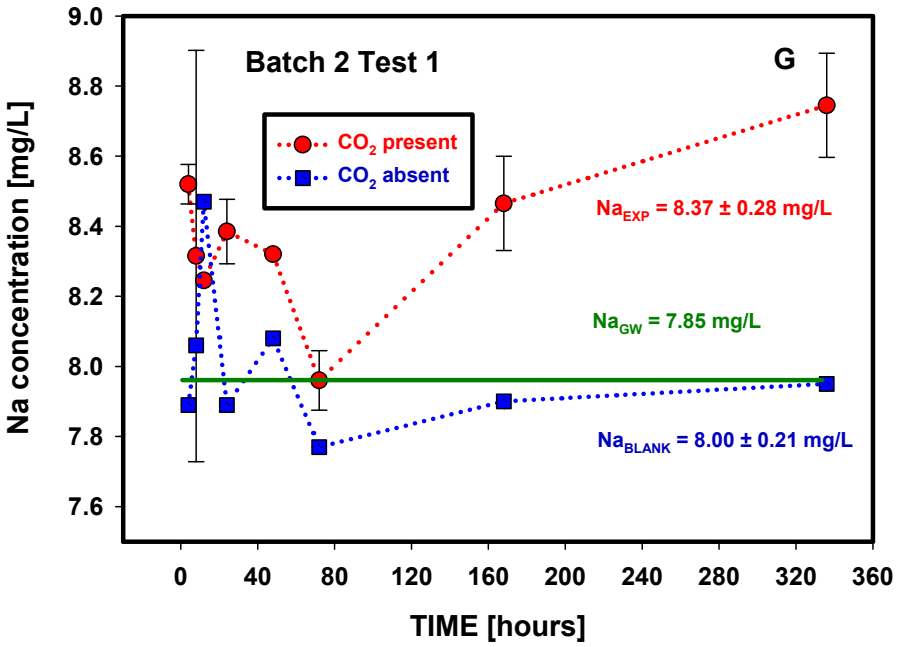

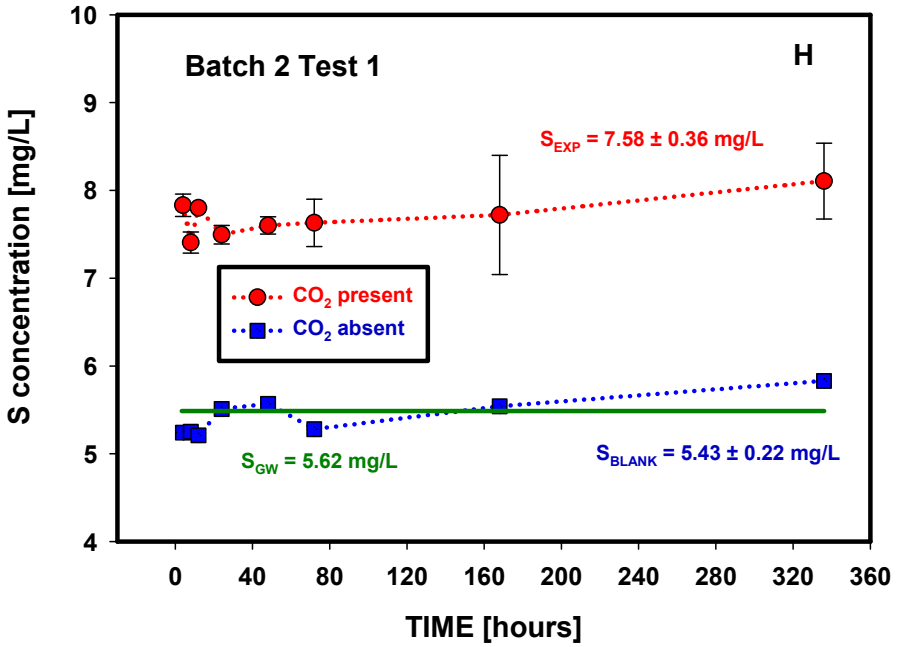

Figure D.4. (contd)

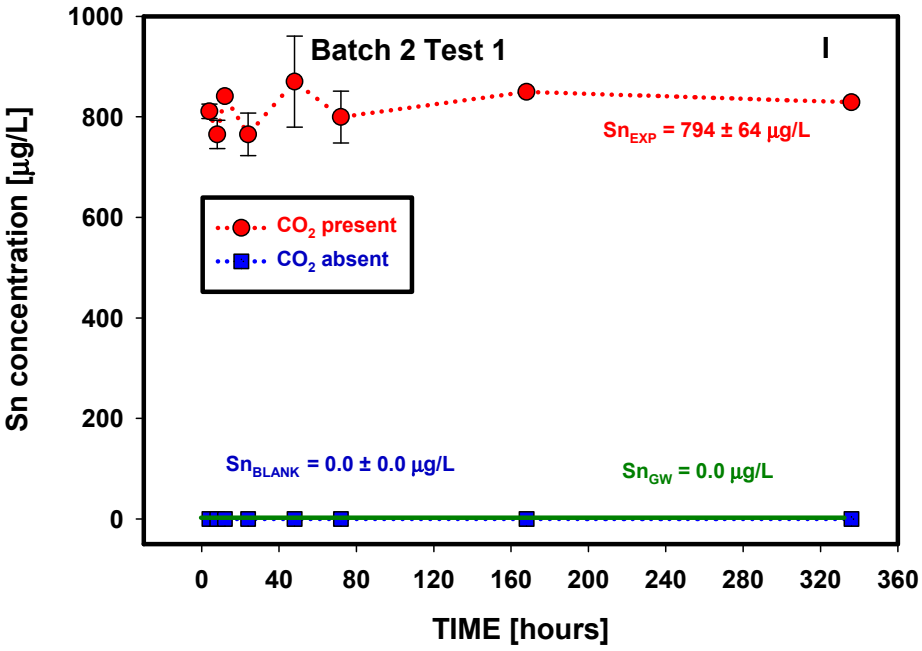

Figure D.4. (contd)

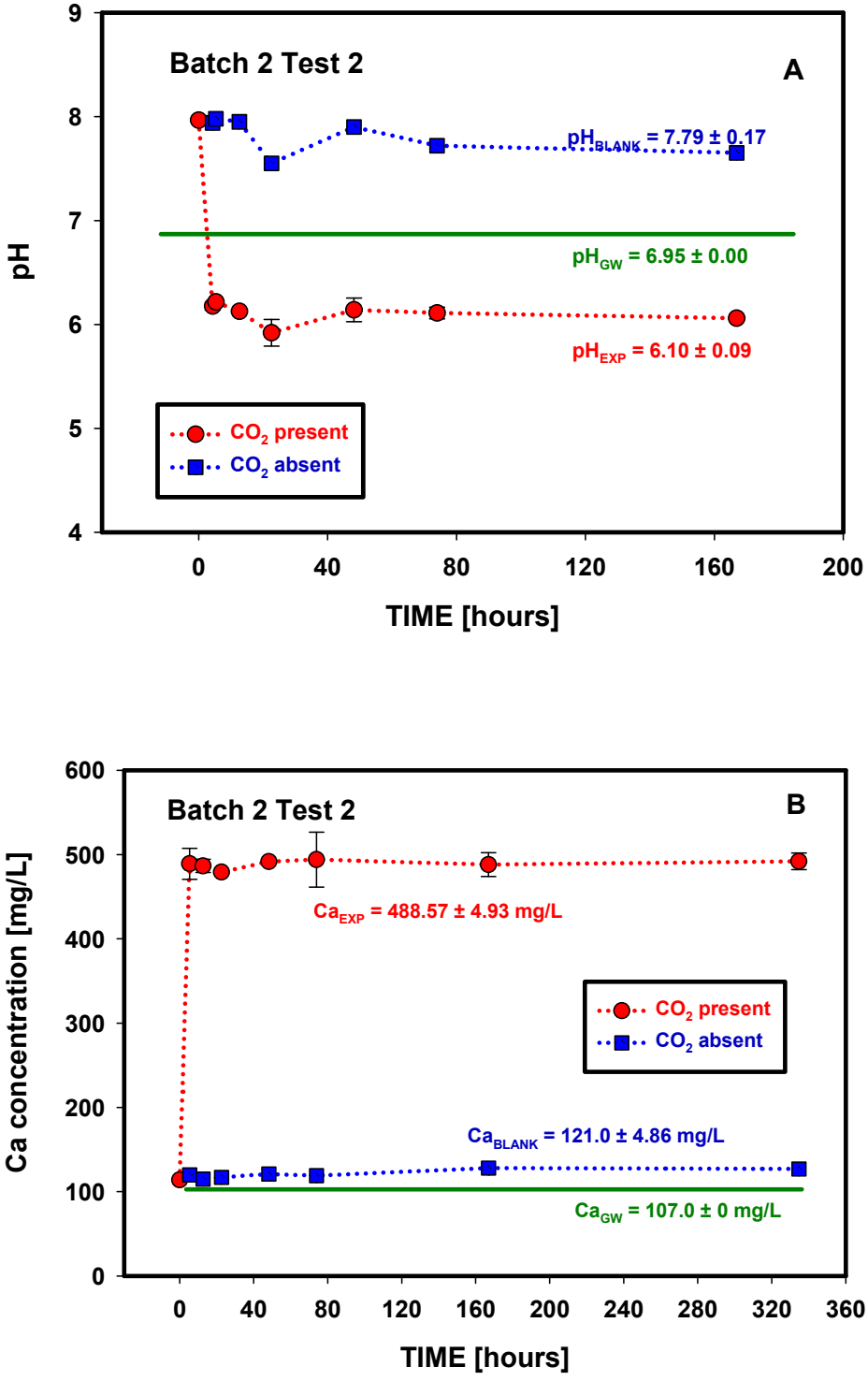

Figure D.5. Changes in pH and elemental composition as a function of time (Batch 2, Test 2, Edwards Aquifer Set B sample 2).

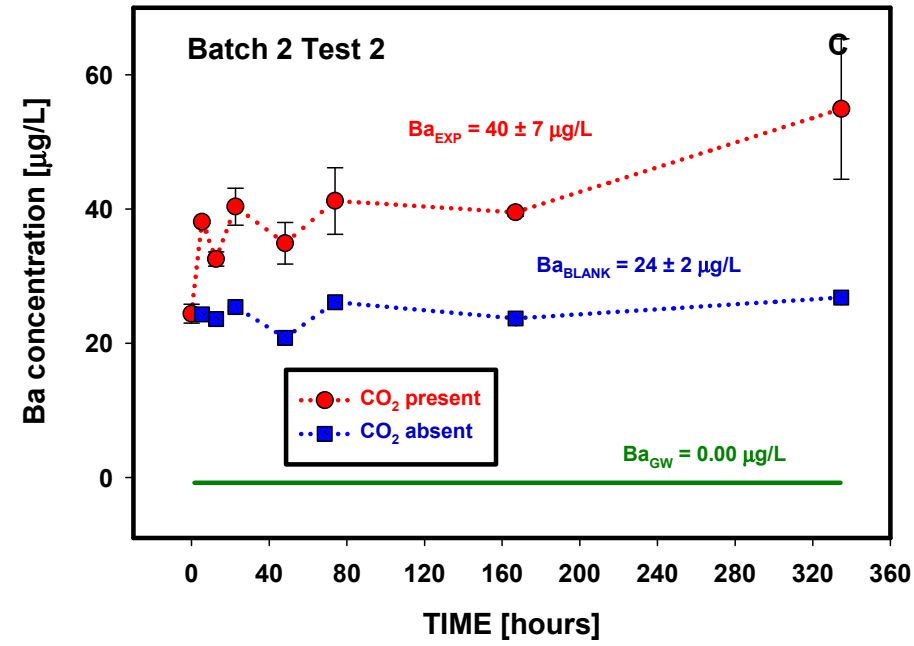

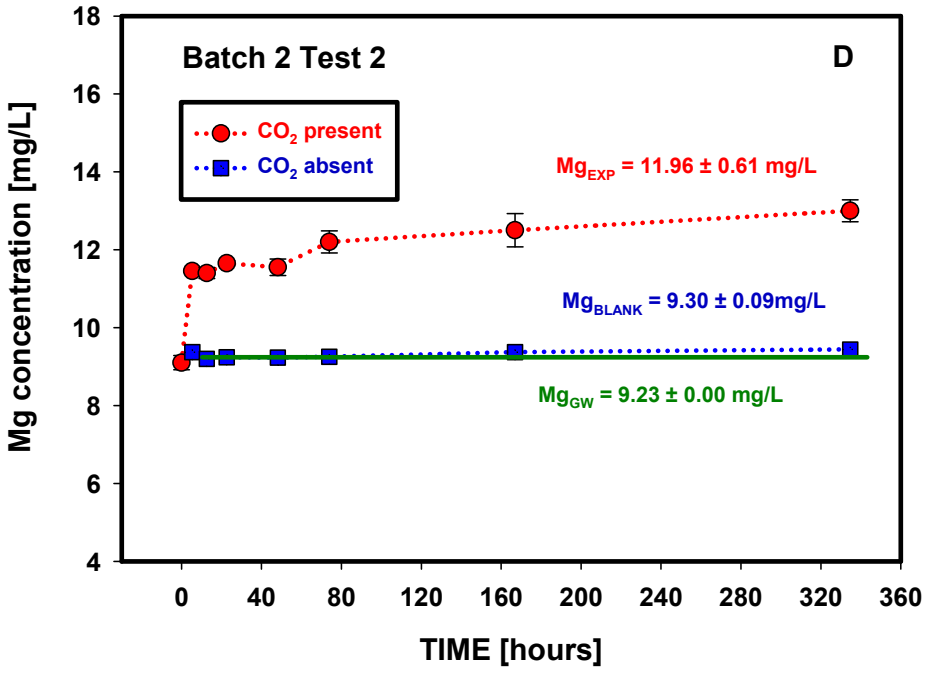

Figure D.5. (contd)

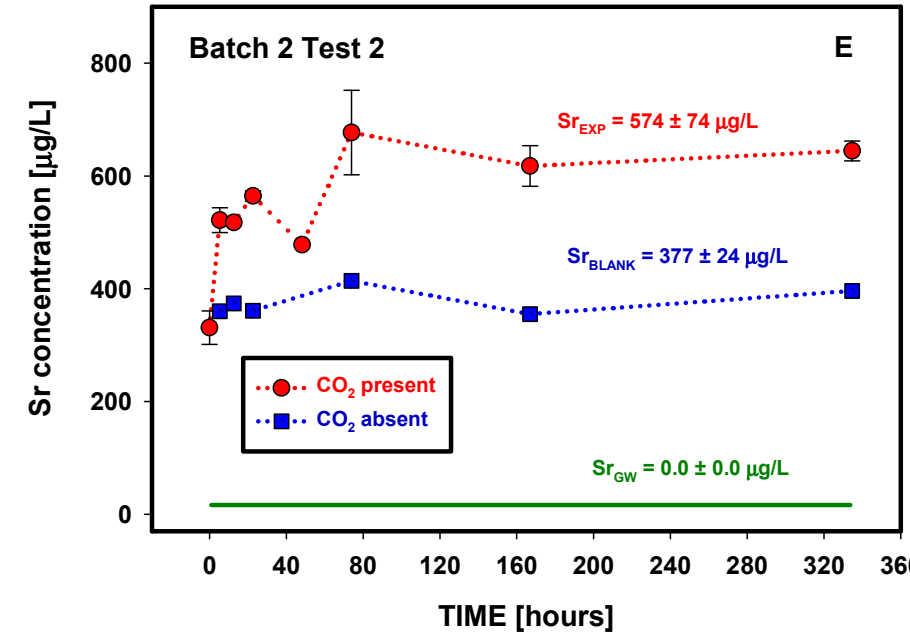

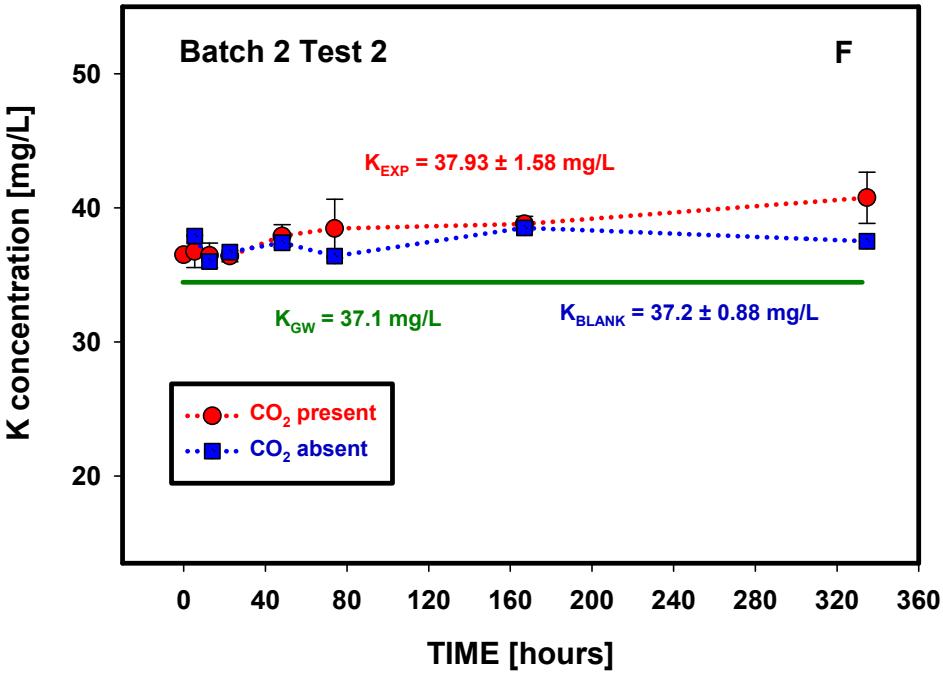

Figure D.5. (contd)

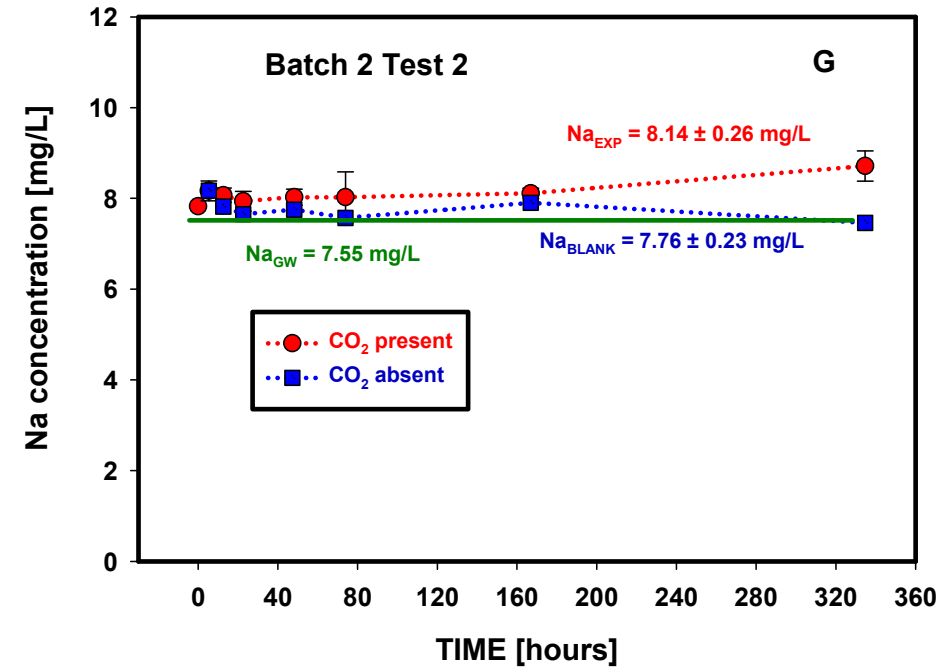

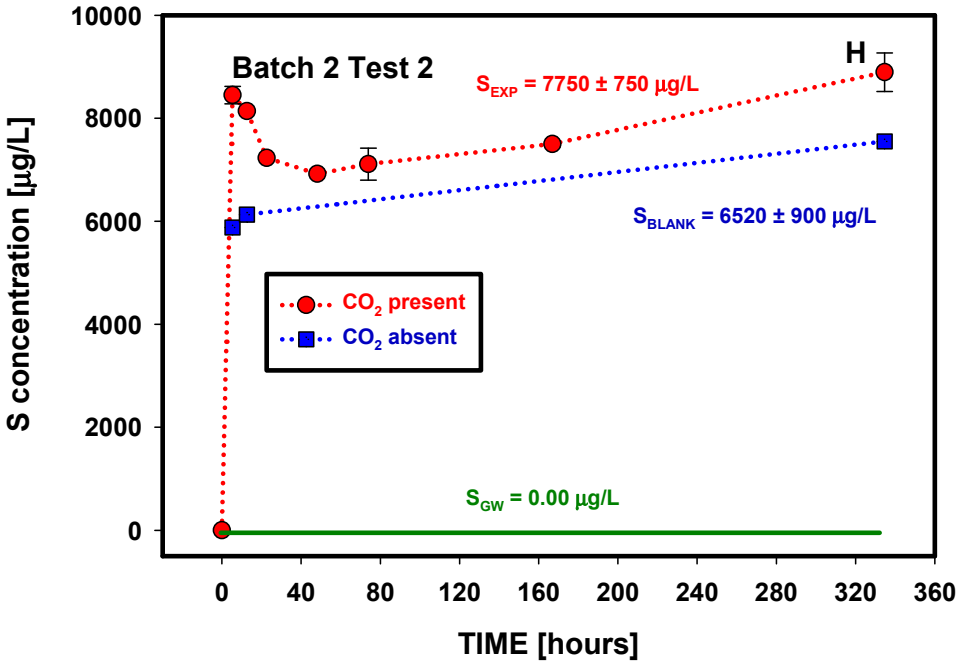

Figure D.5. (contd)

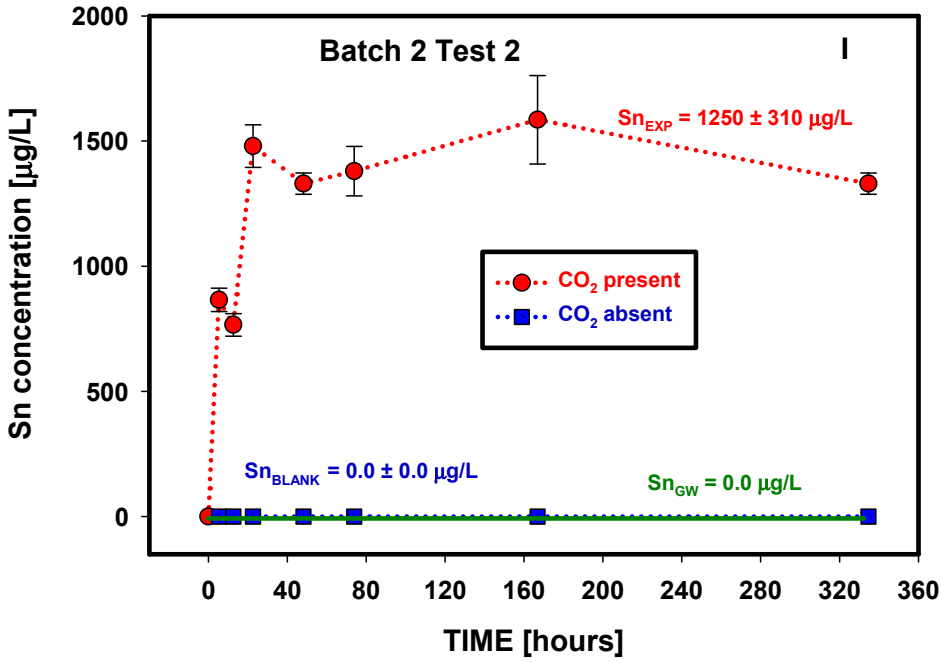

Figure D.5. (contd)

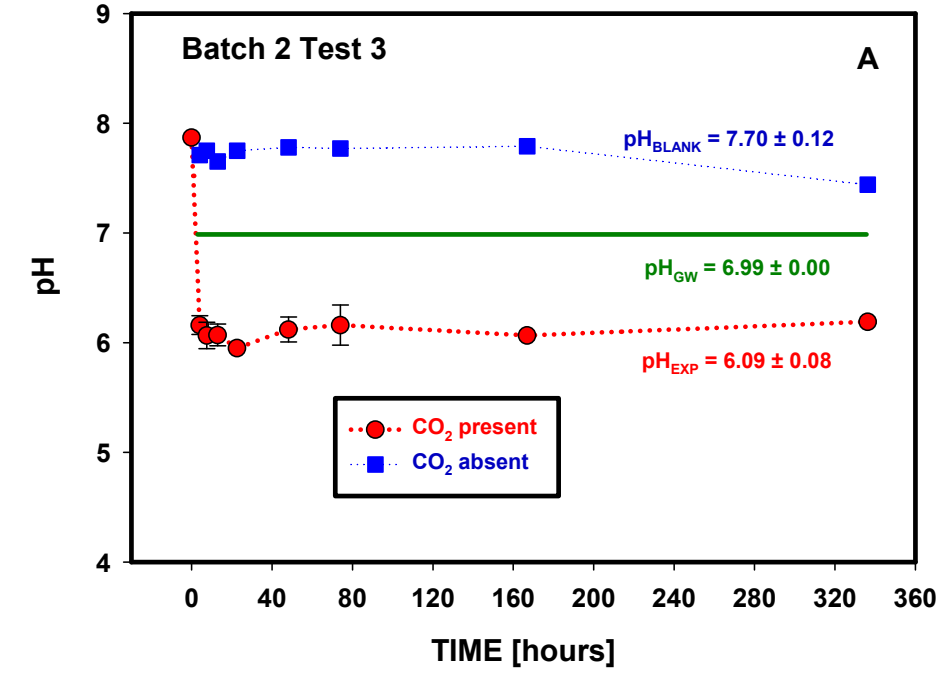

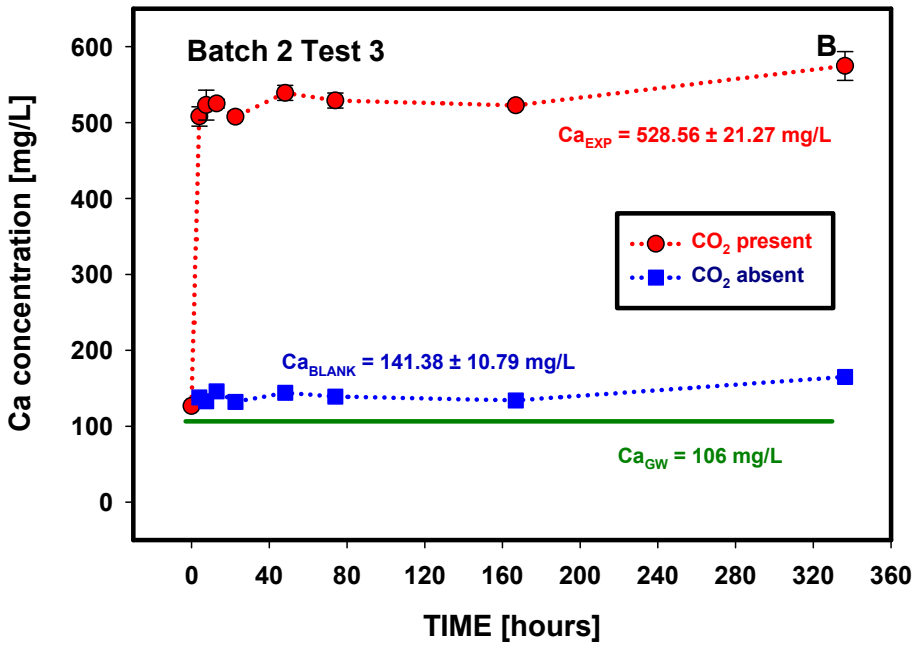

Figure D.6. Changes in pH and elemental composition as a function of time (Batch 2, Test 3, Edwards Aquifer Set B sample 7).

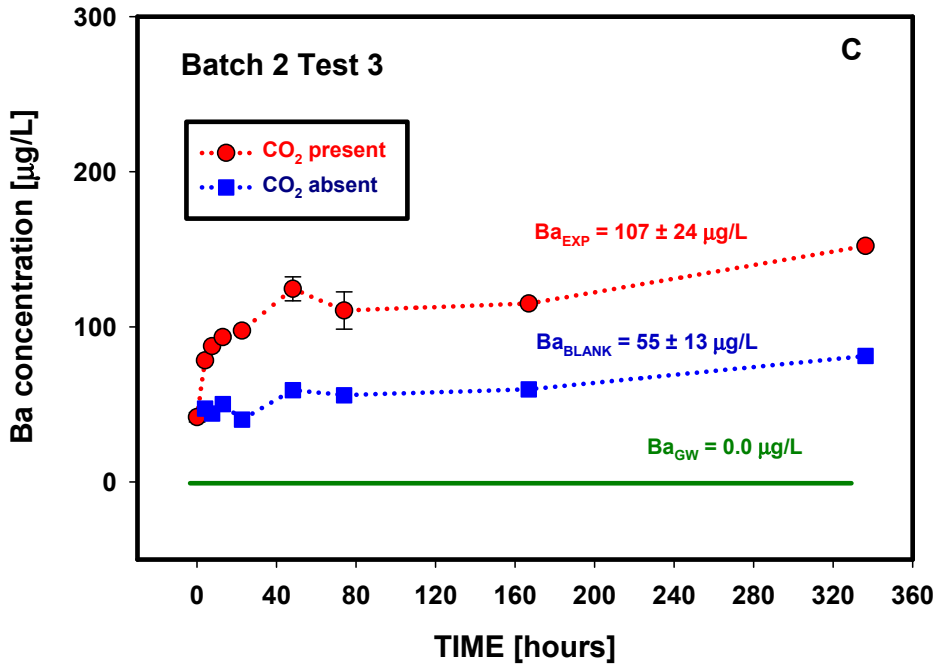

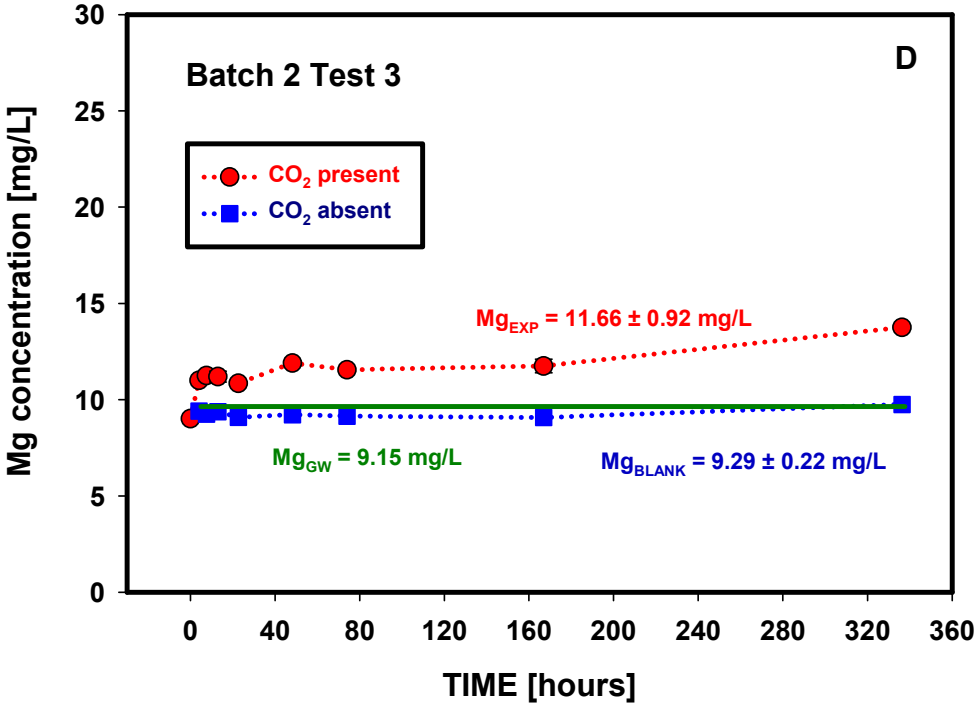

Figure D.6. (contd)

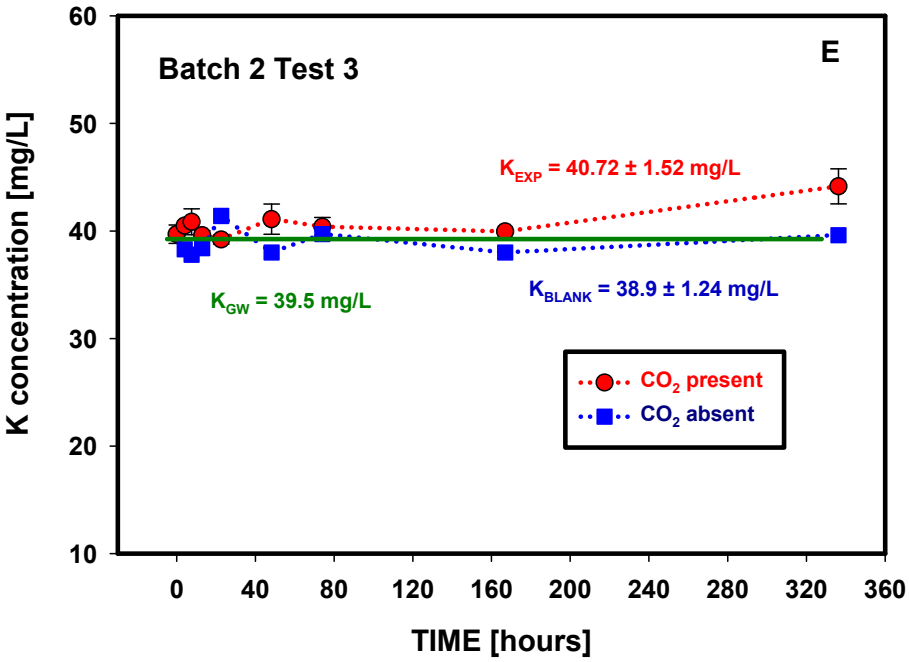

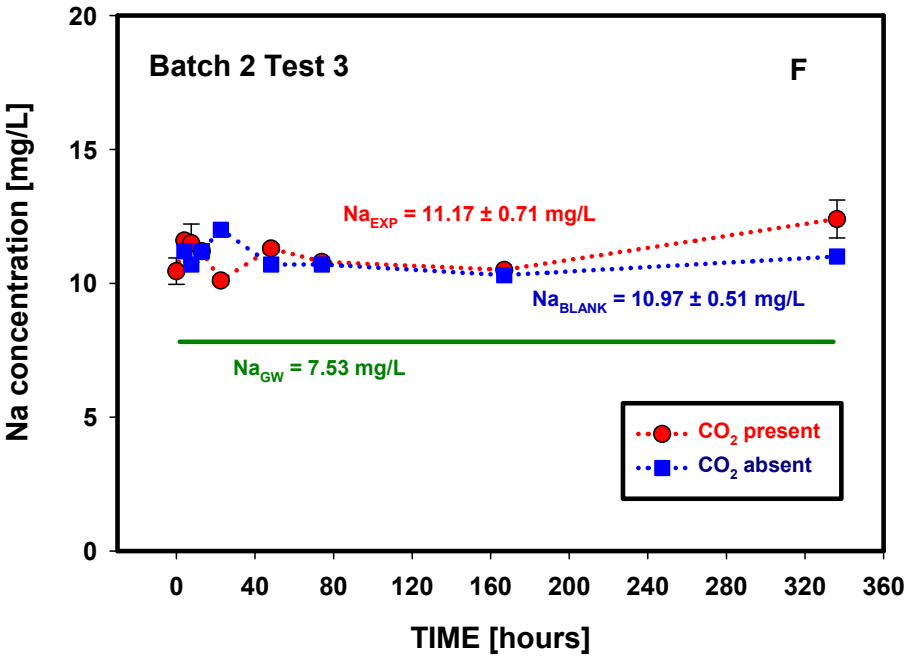

Figure D.6. (contd)

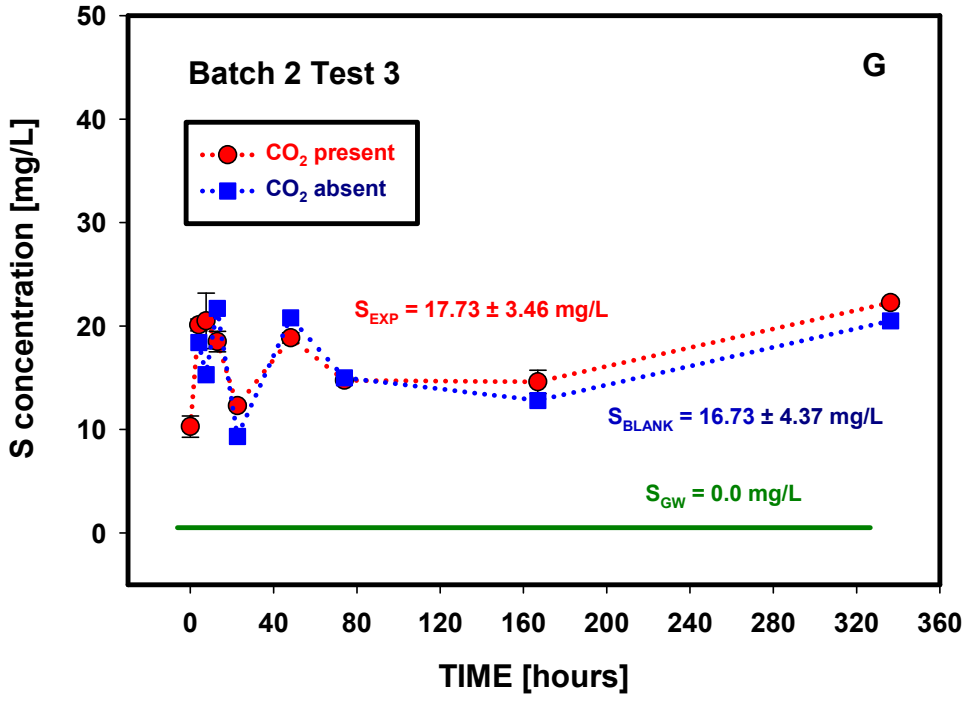

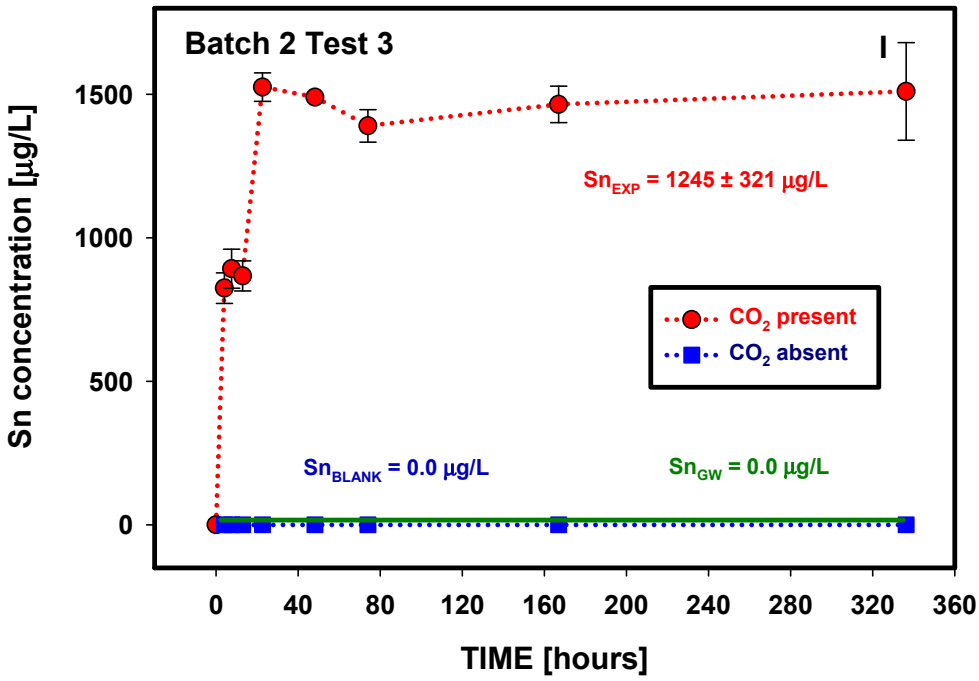

Figure D.6. (contd)

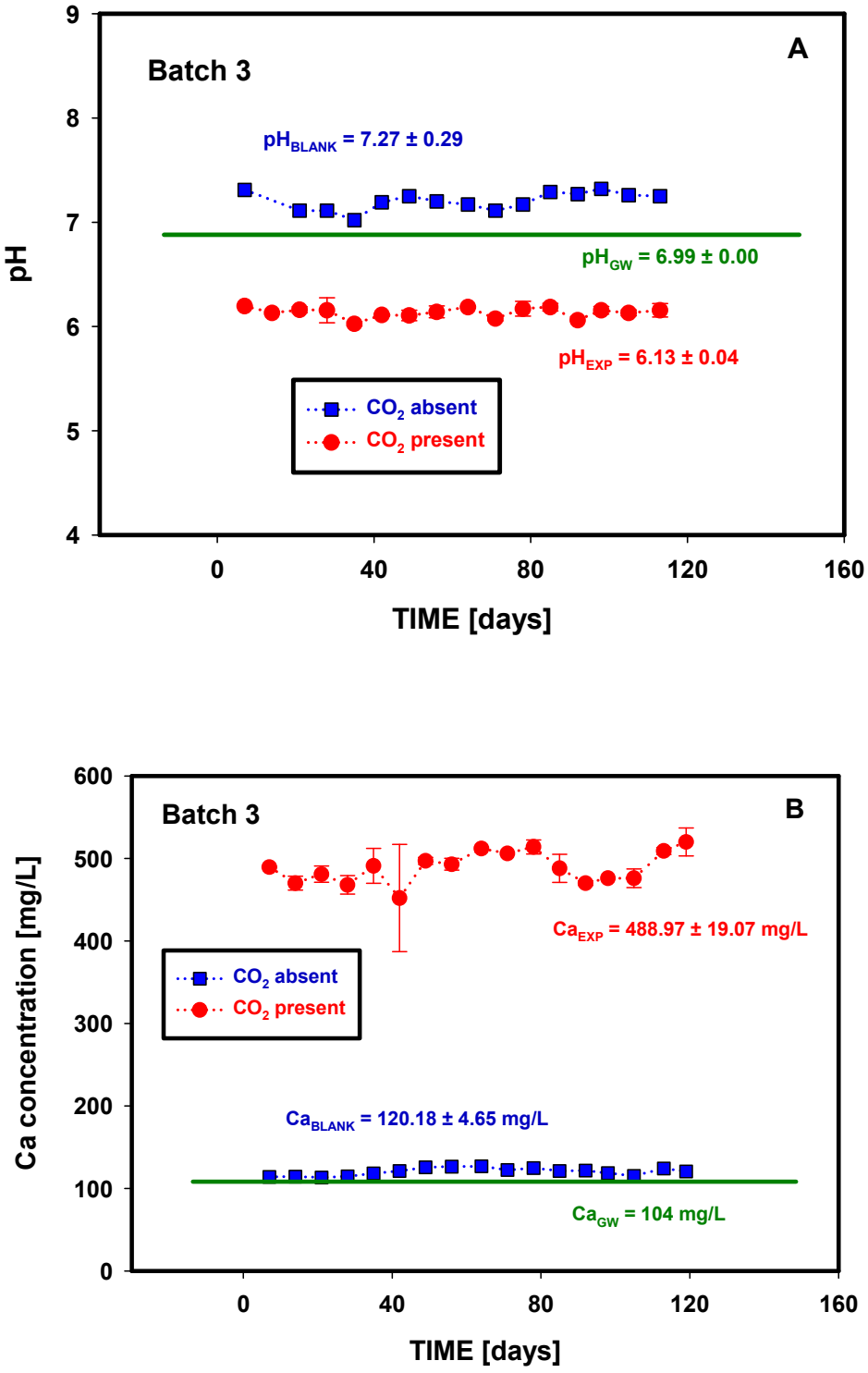

Figure D.7. Changes in pH and elemental composition as a function of time (Batch 3, Edwards Aquifer Set B sample 2).

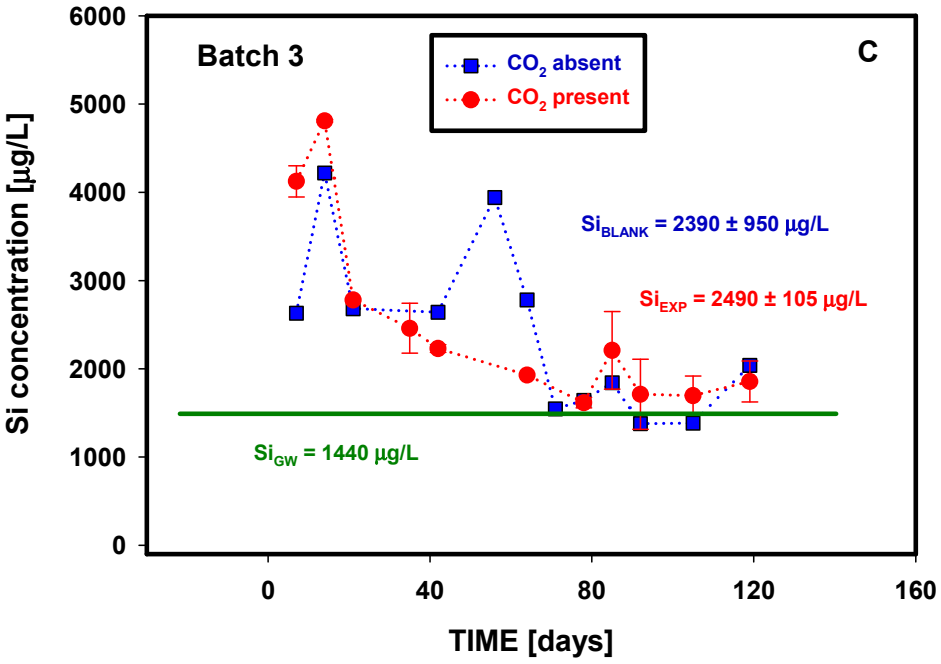

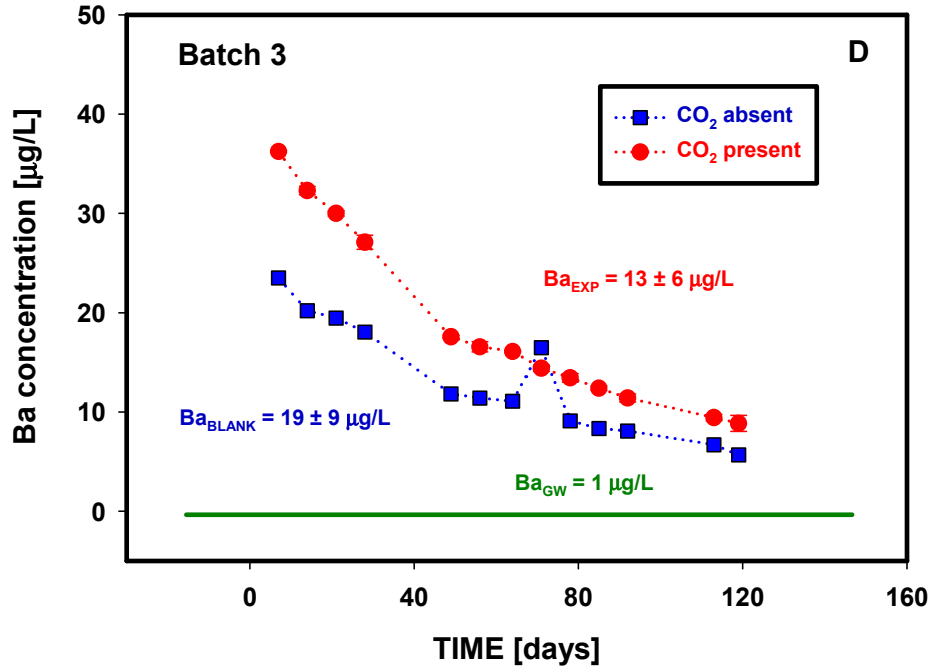

Figure D.7. (contd)

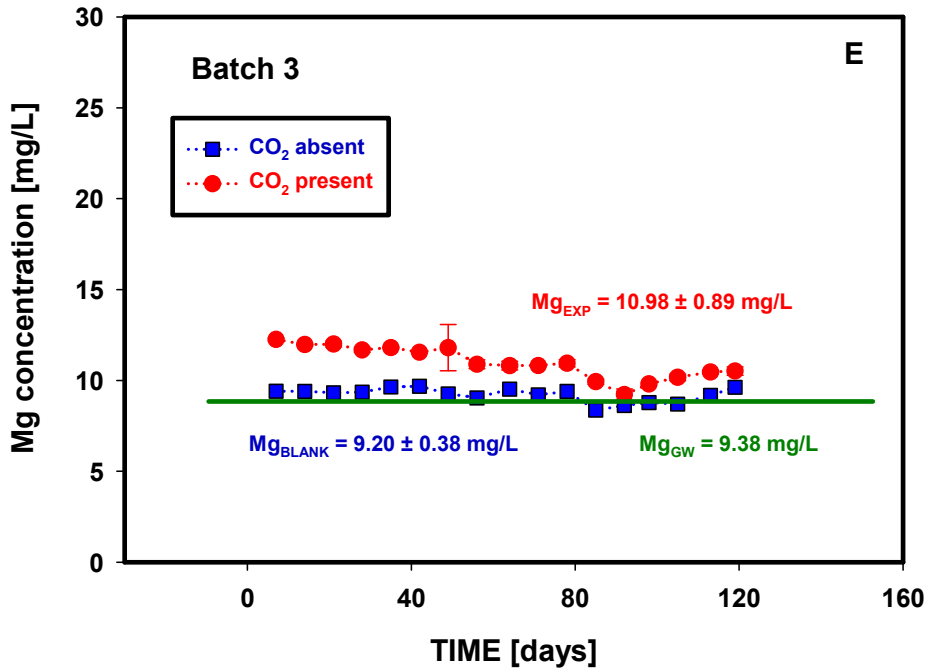

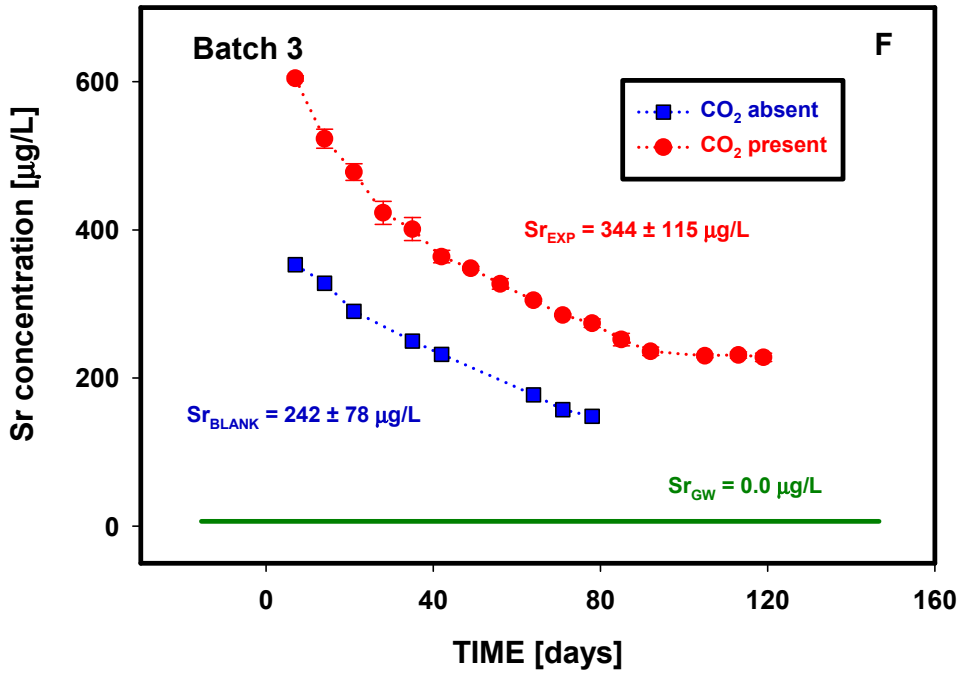

Figure D.7. (contd)

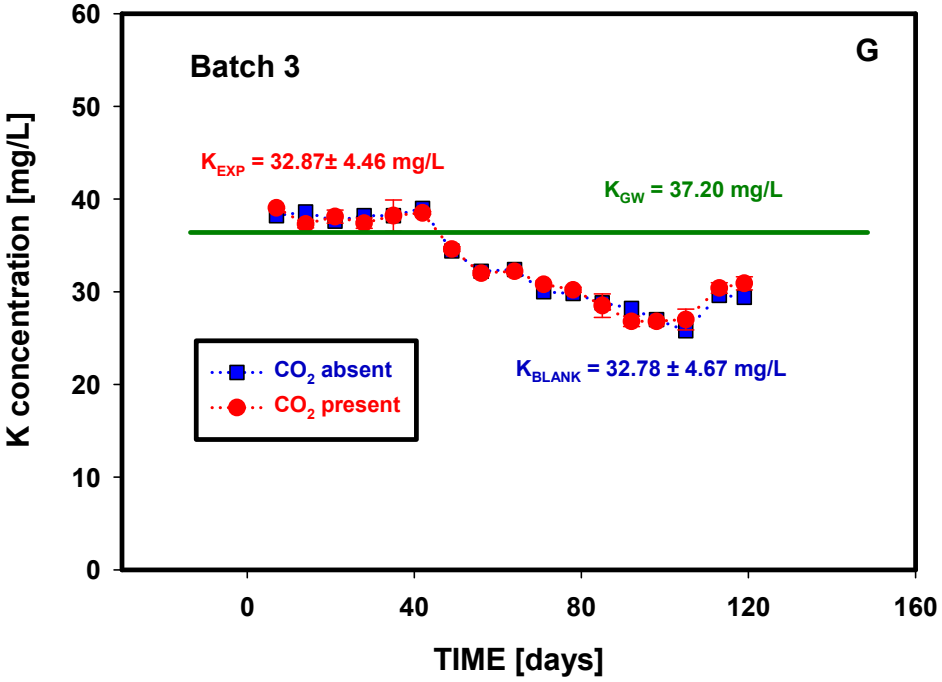

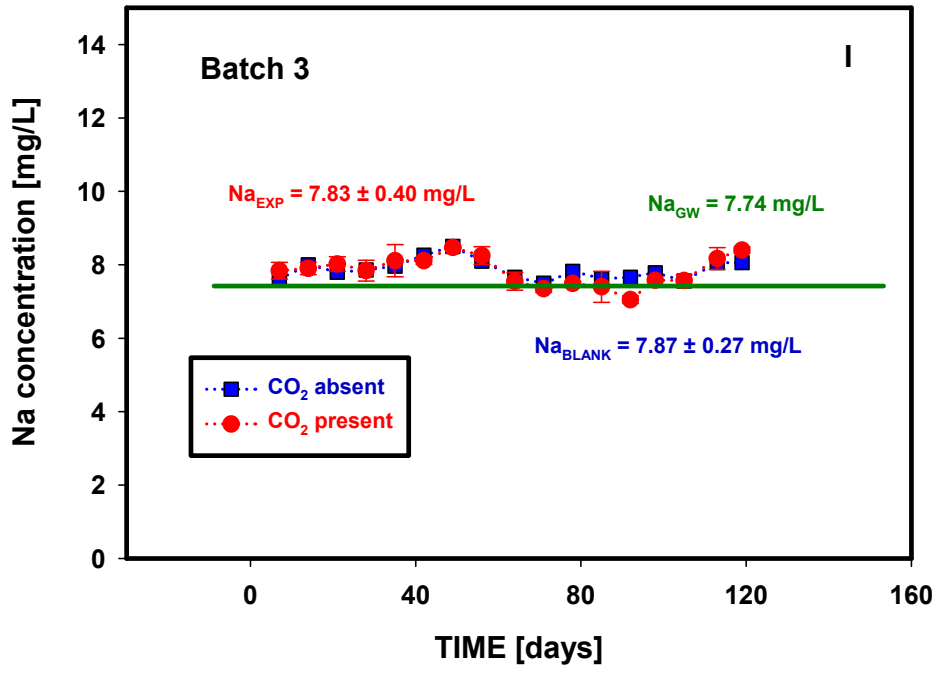

Figure D.7. (contd)

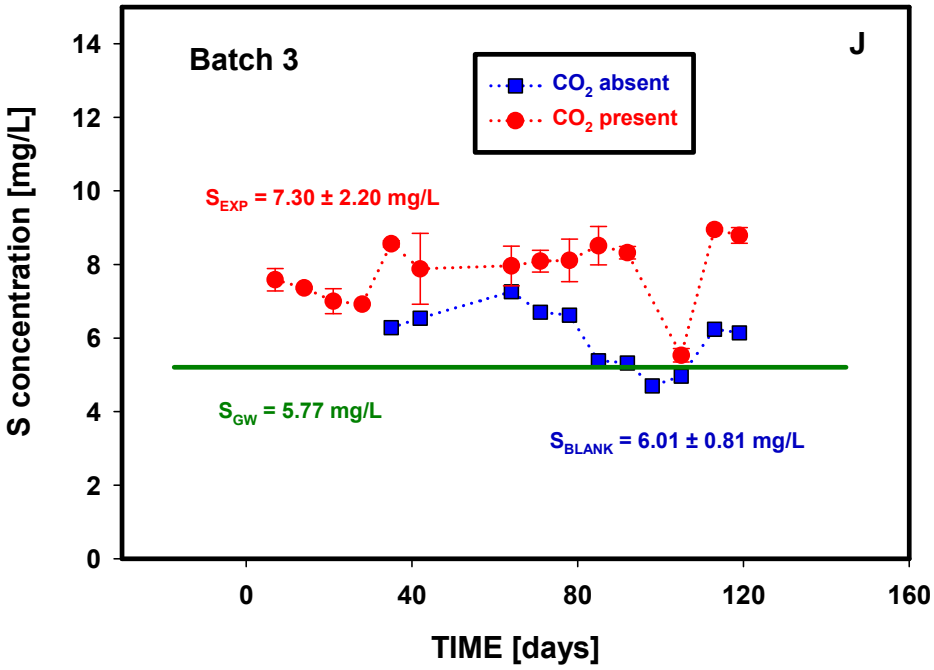

Figure D.7. (contd)

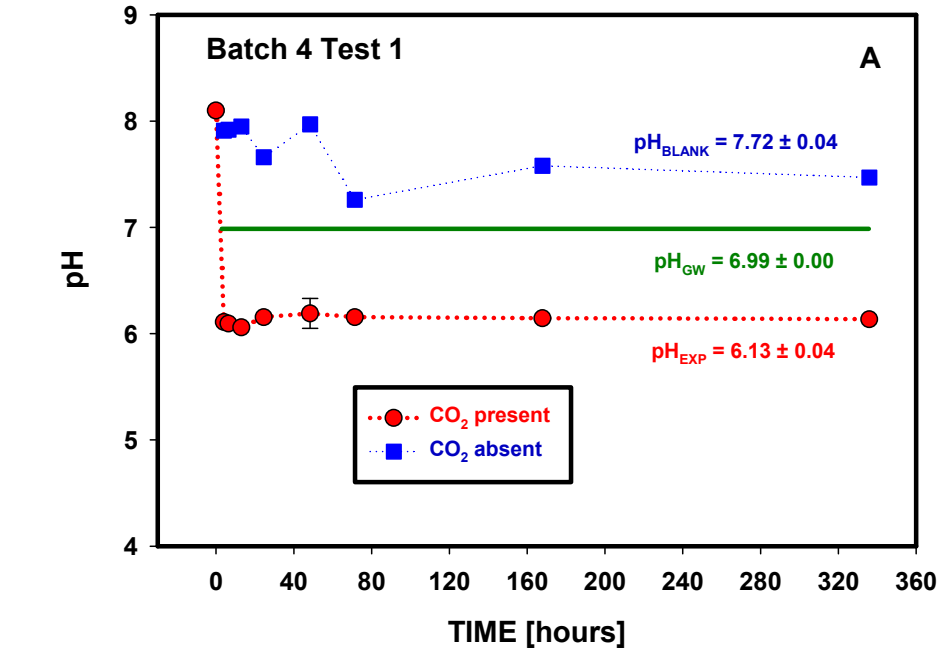

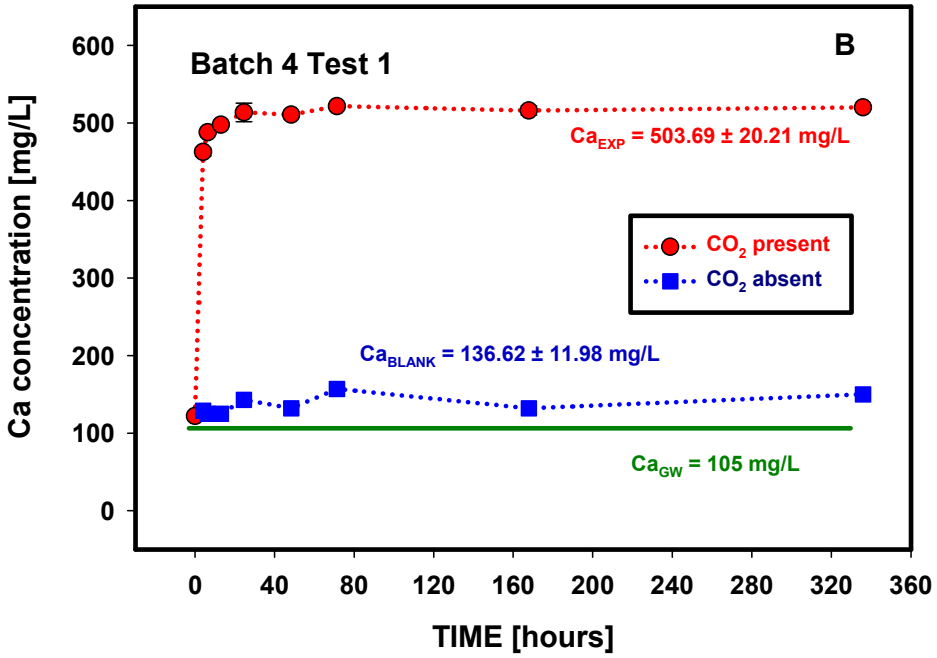

Figure D.8. Changes in pH and elemental composition as a function of time (Batch 4, Test 1, Edwards Aquifer Set B sample 7, <2 mm).

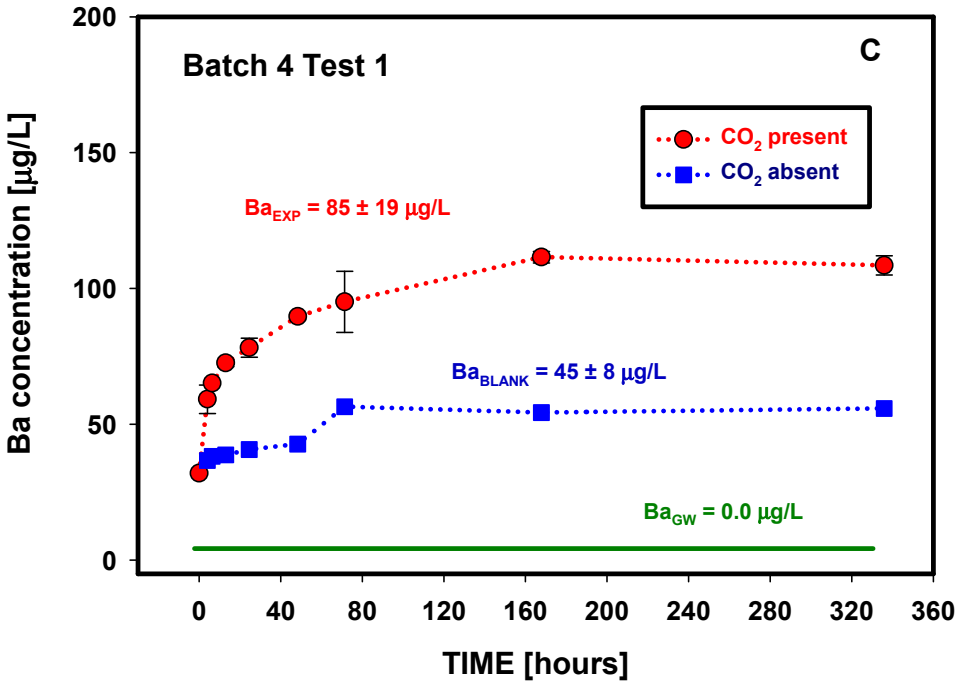

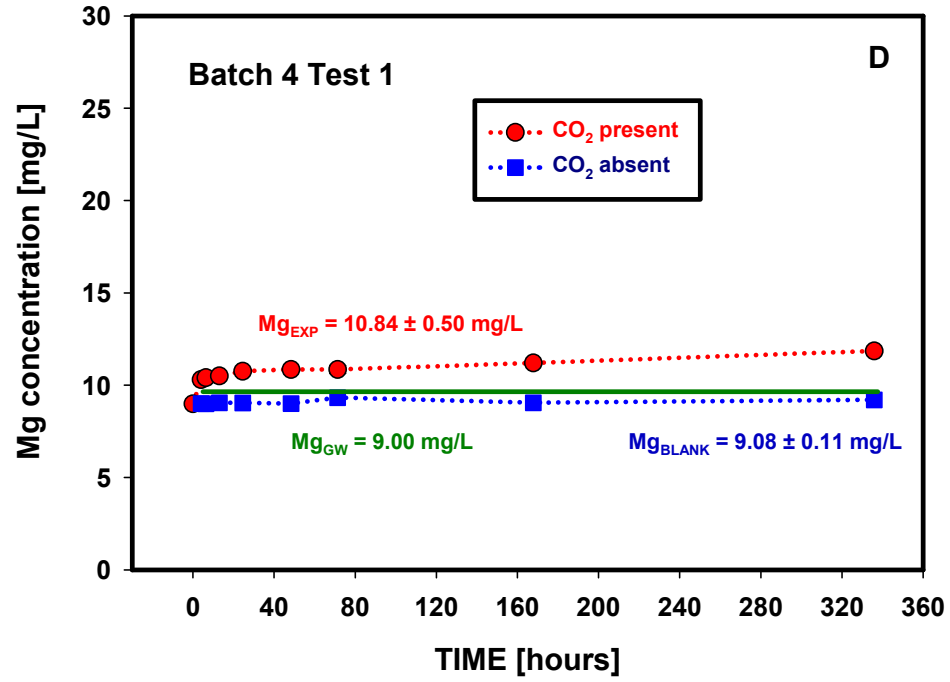

Figure D.8. (contd)

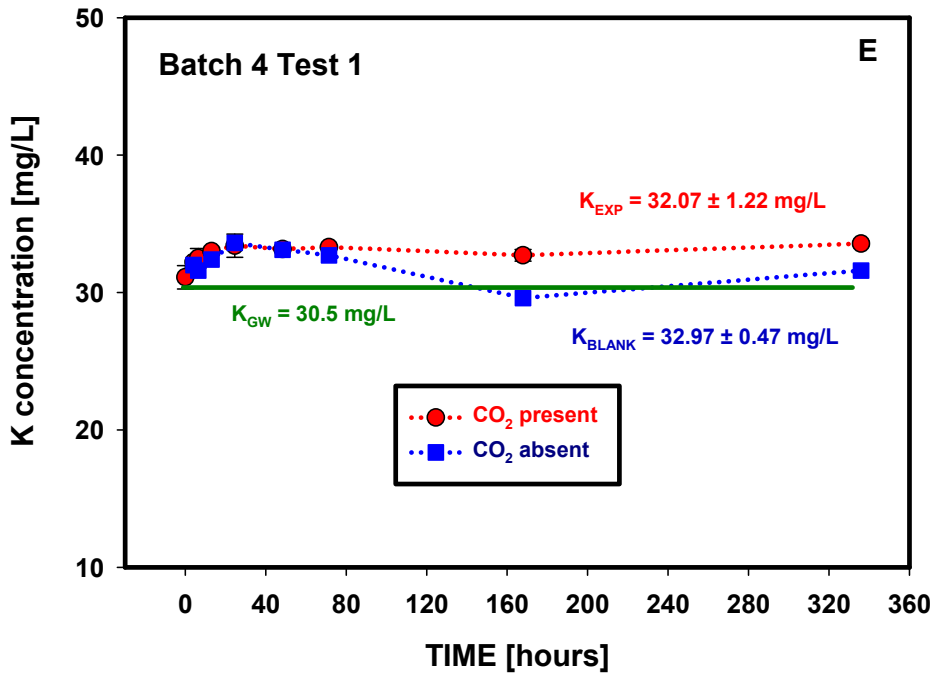

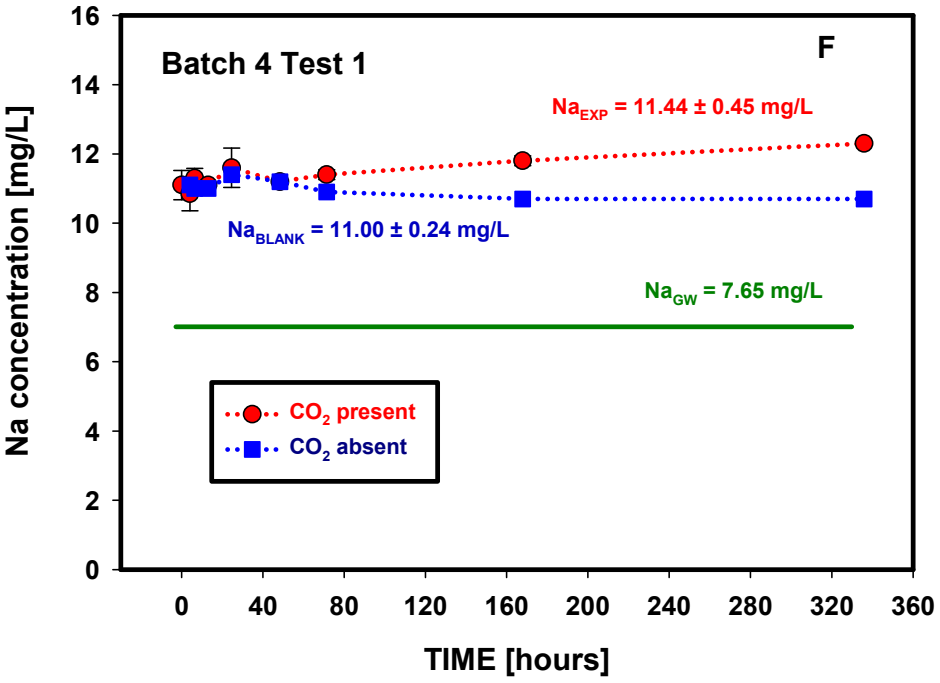

Figure D.8. (contd)

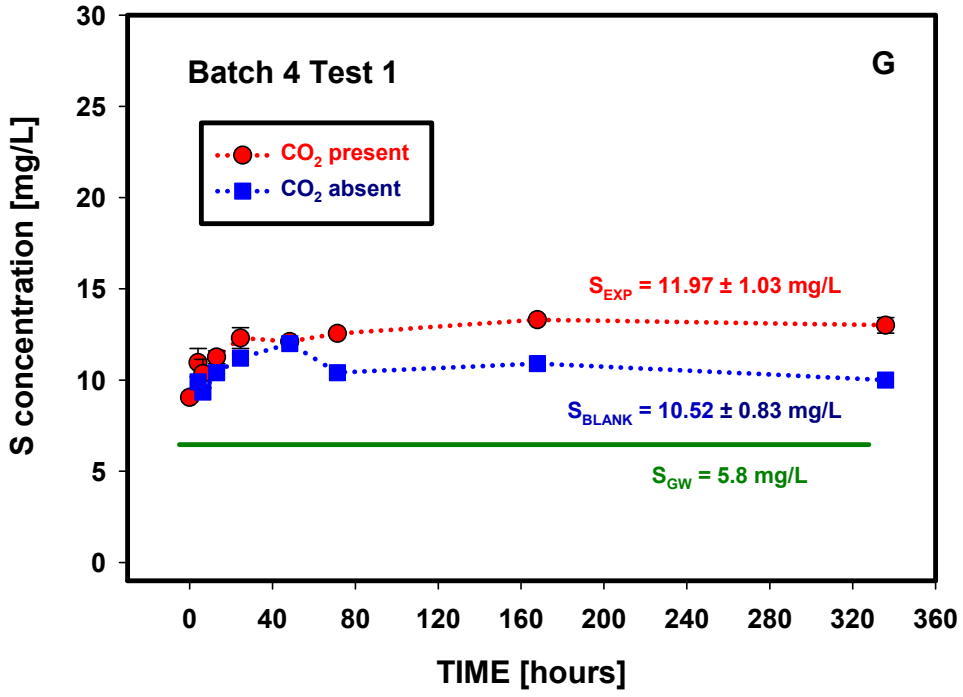

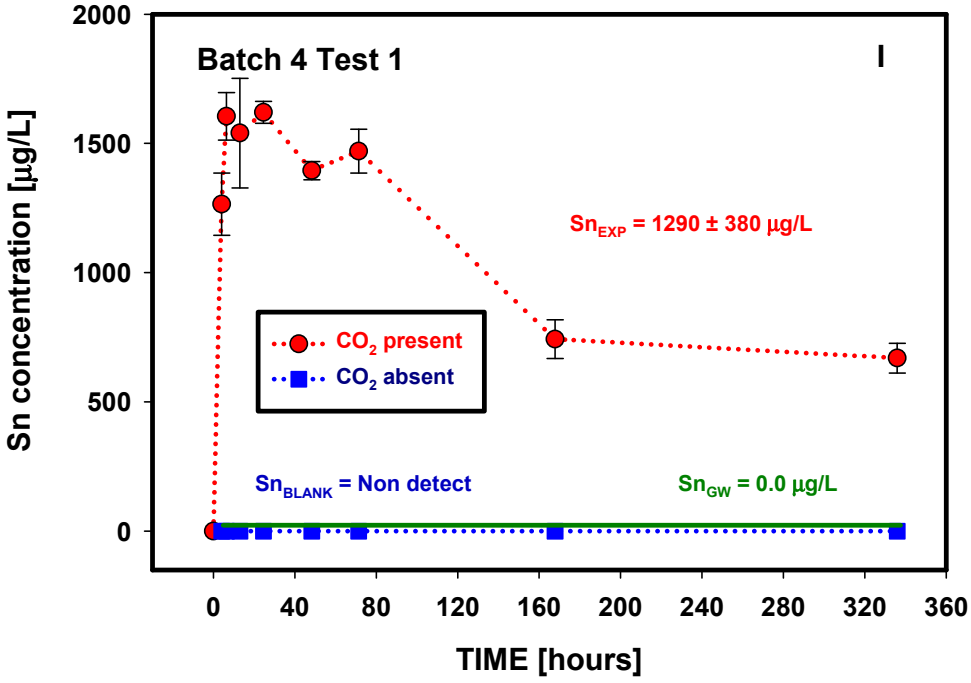

Figure D.8. (contd)

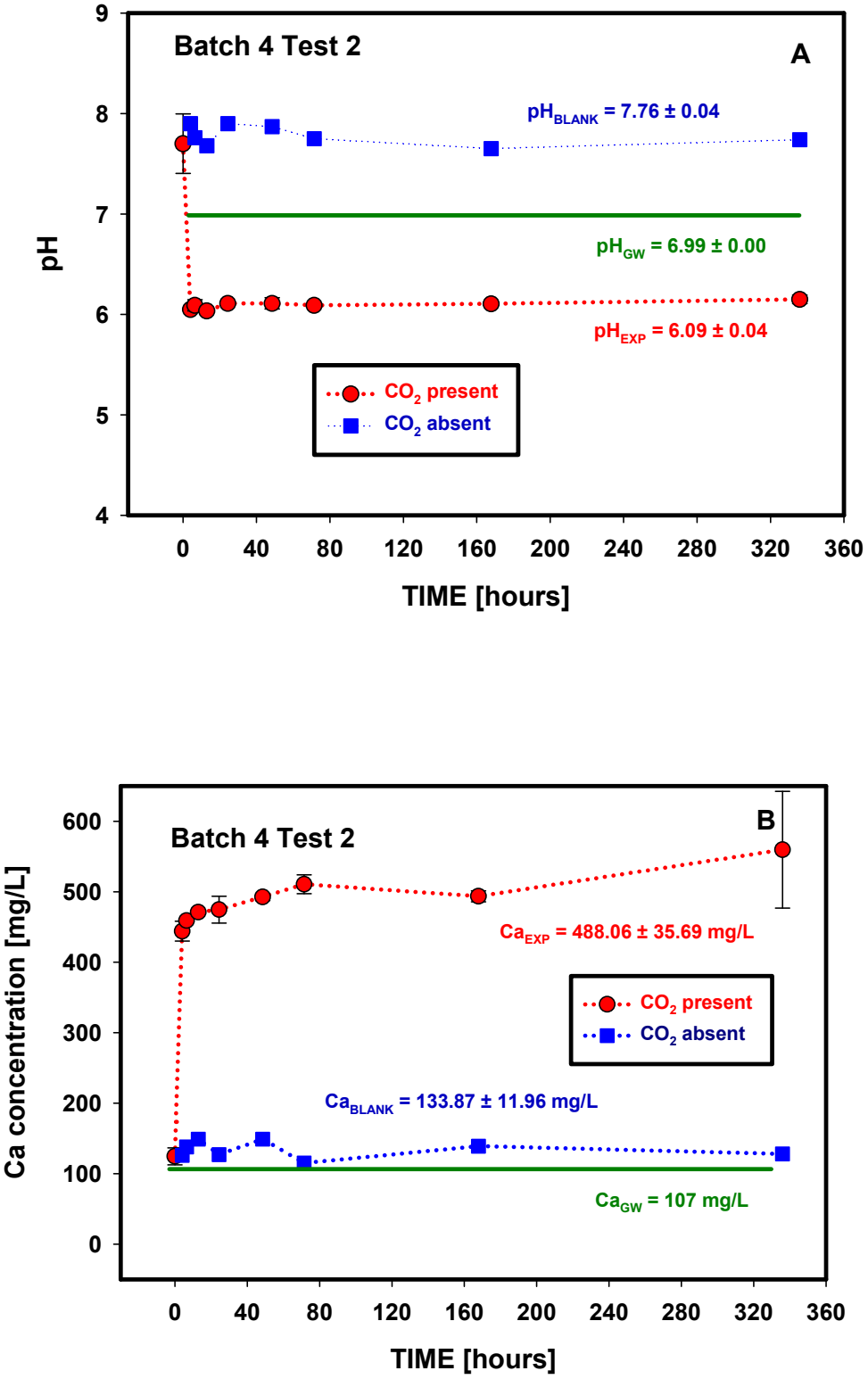

Figure D.9. Changes in pH and elemental composition as a function of time (Batch 4, Test 2, Edwards Aquifer Set B sample 7, >2 mm).

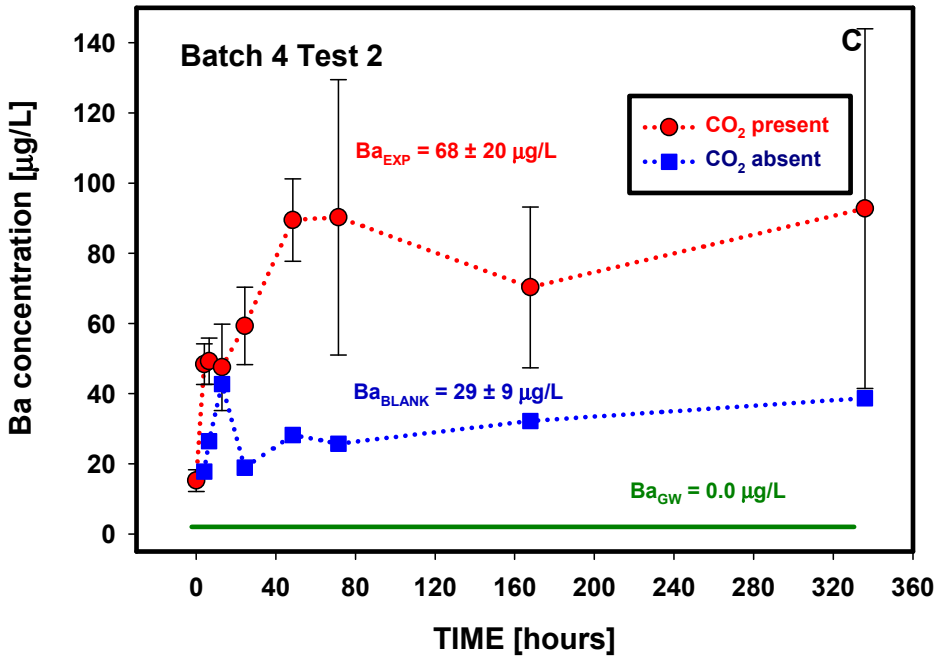

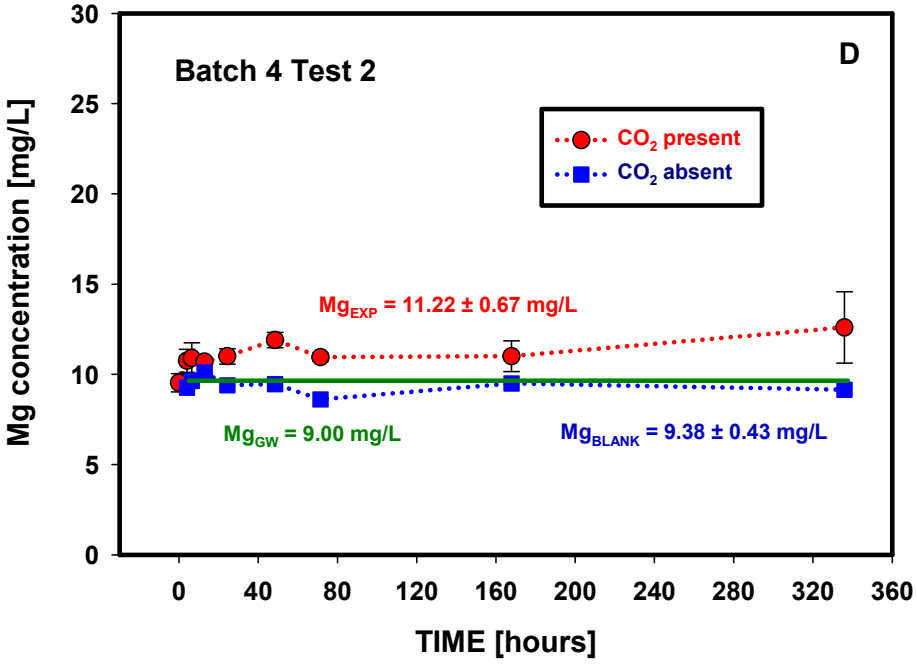

Figure D.9. (contd)

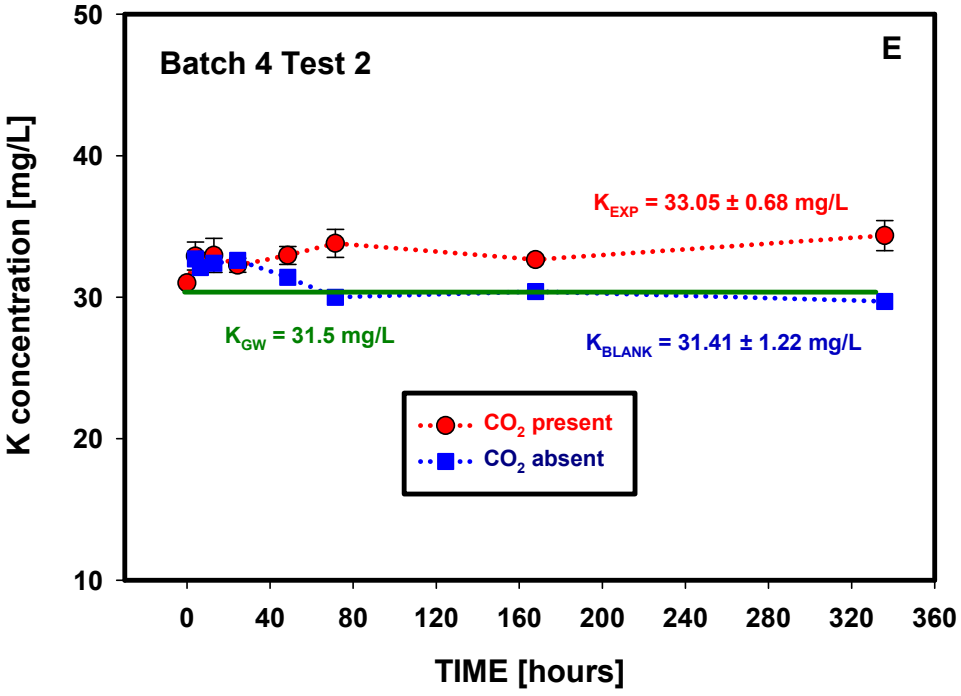

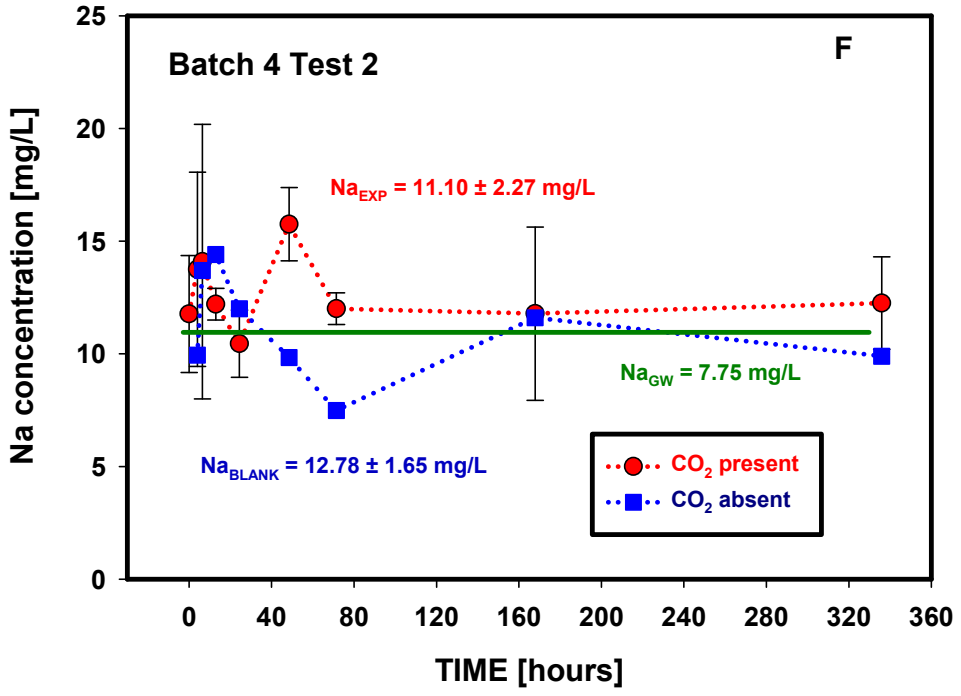

Figure D.9. (contd)

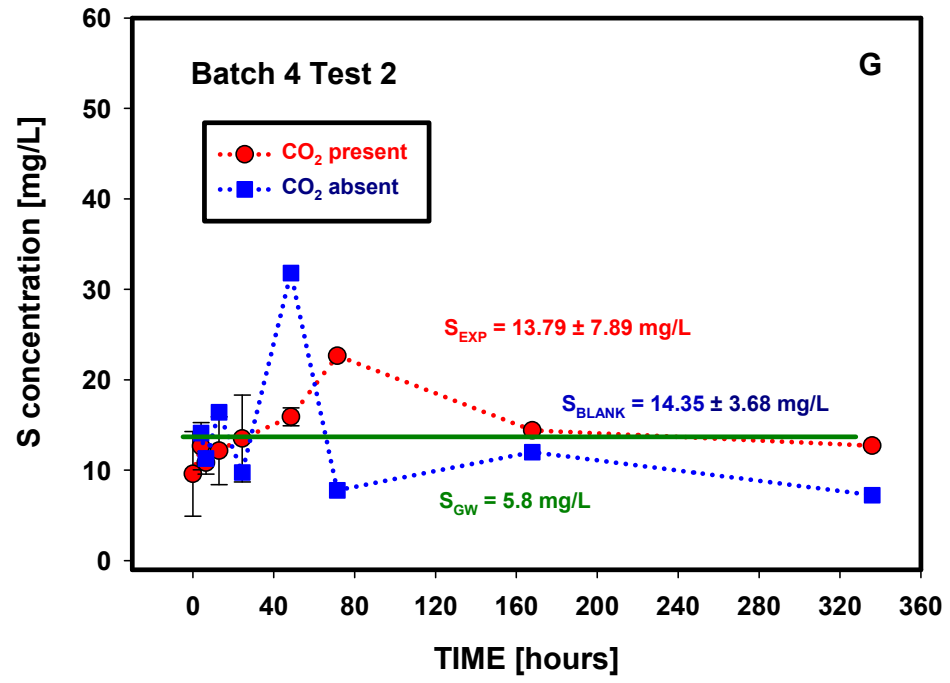

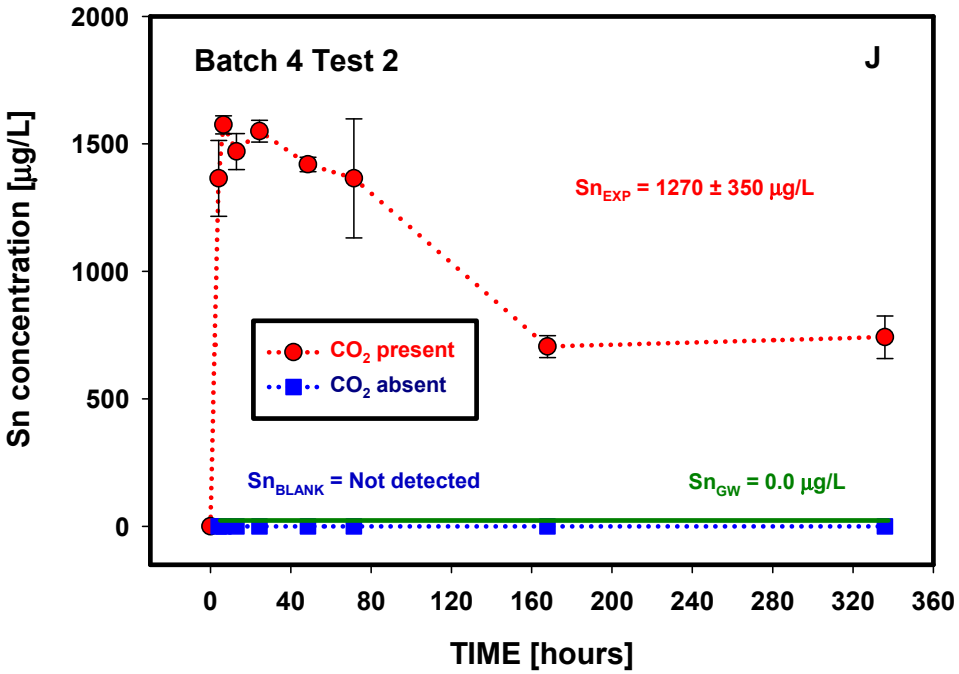

Figure D.9. (contd)

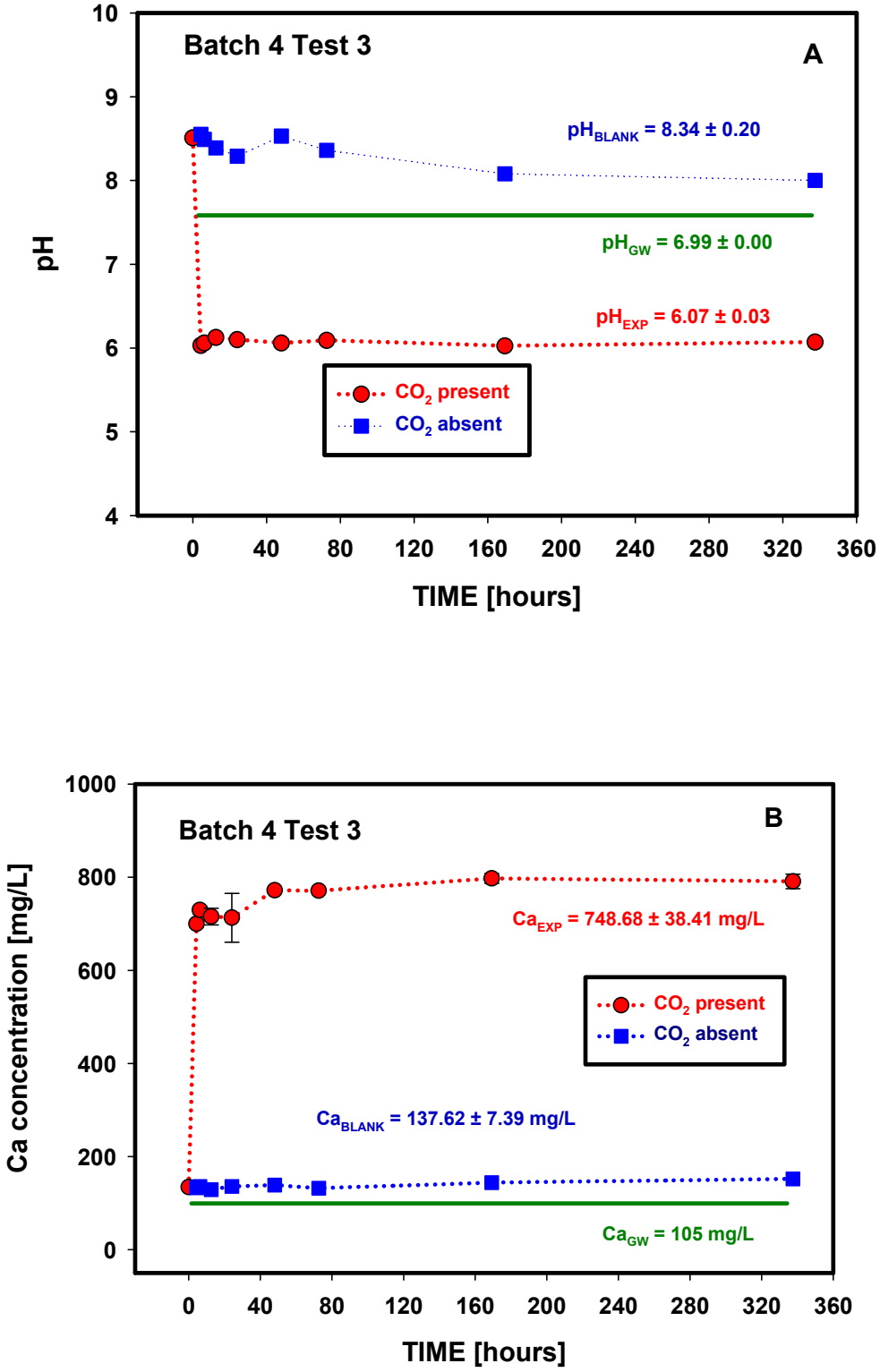

Figure D.10. Changes in pH and elemental composition as a function of time (Batch 4, Test 3, Edwards Aquifer Set B sample 7, <2 mm, 1 M NaCl).

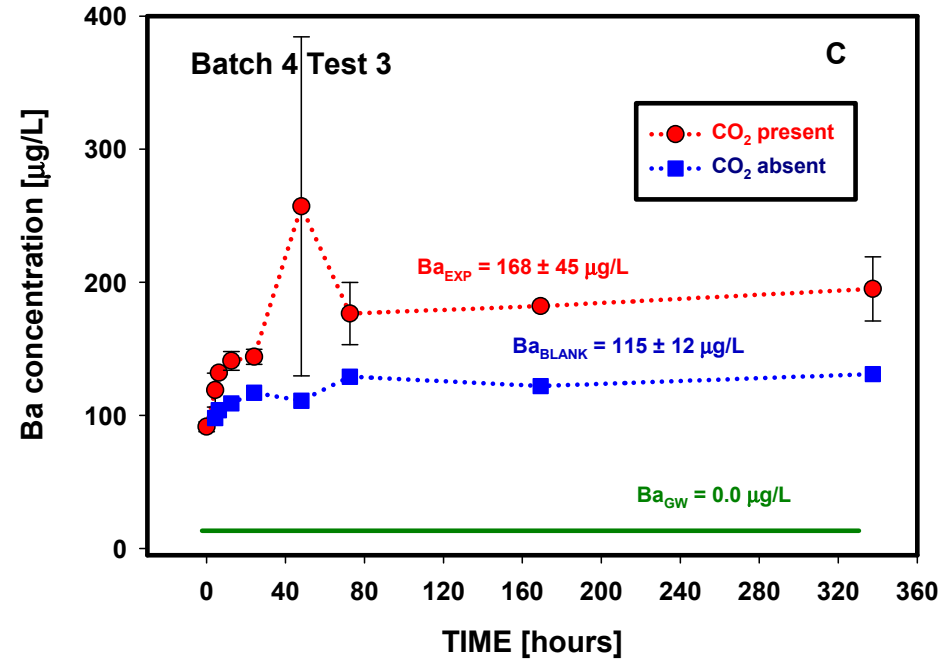

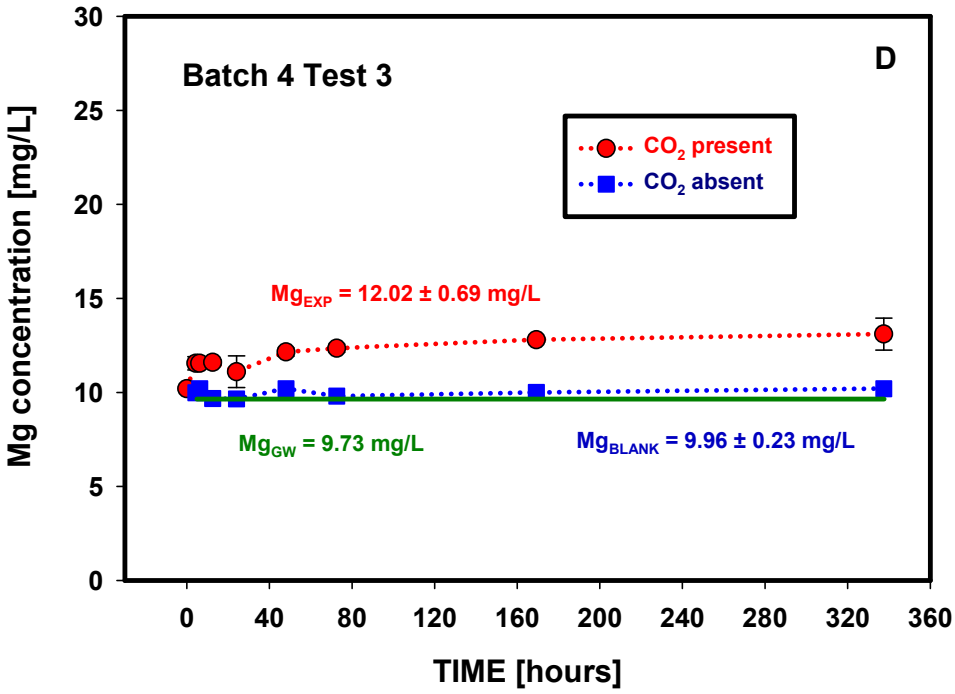

Figure D.10. (contd)

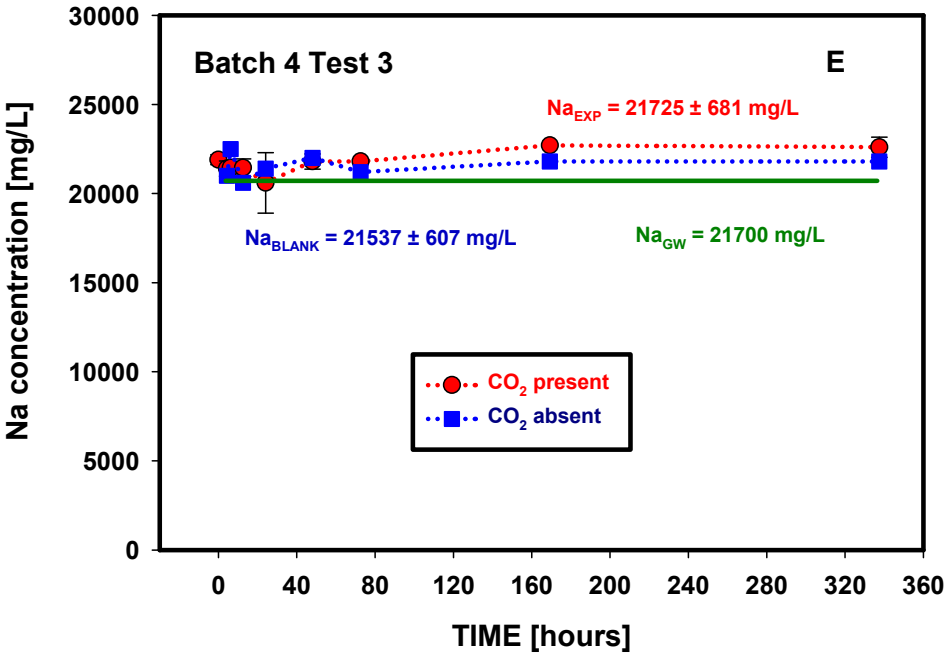

Figure D.10. (contd)

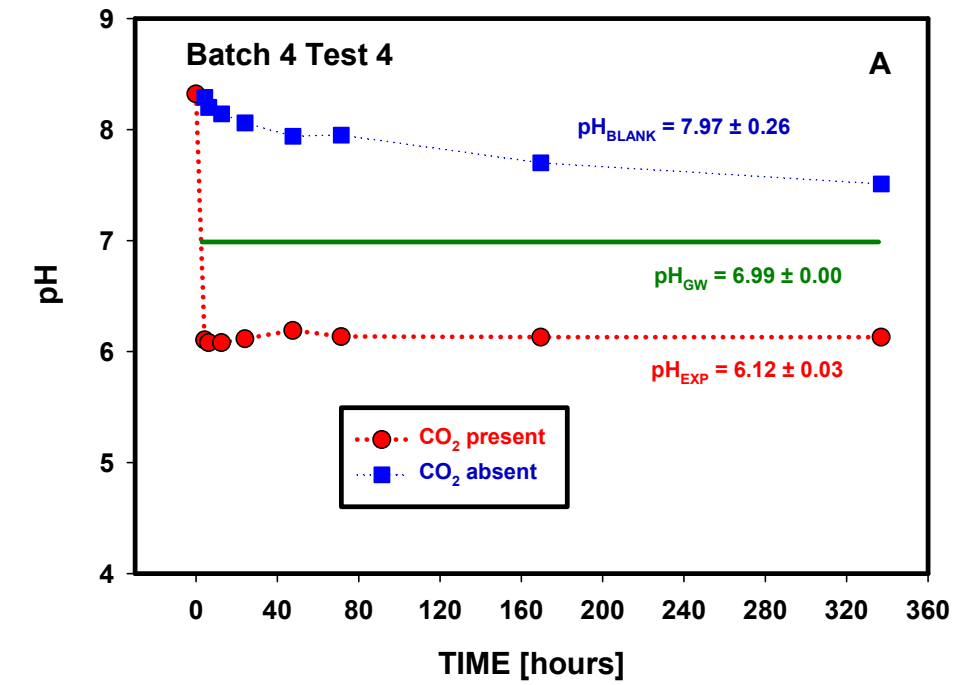

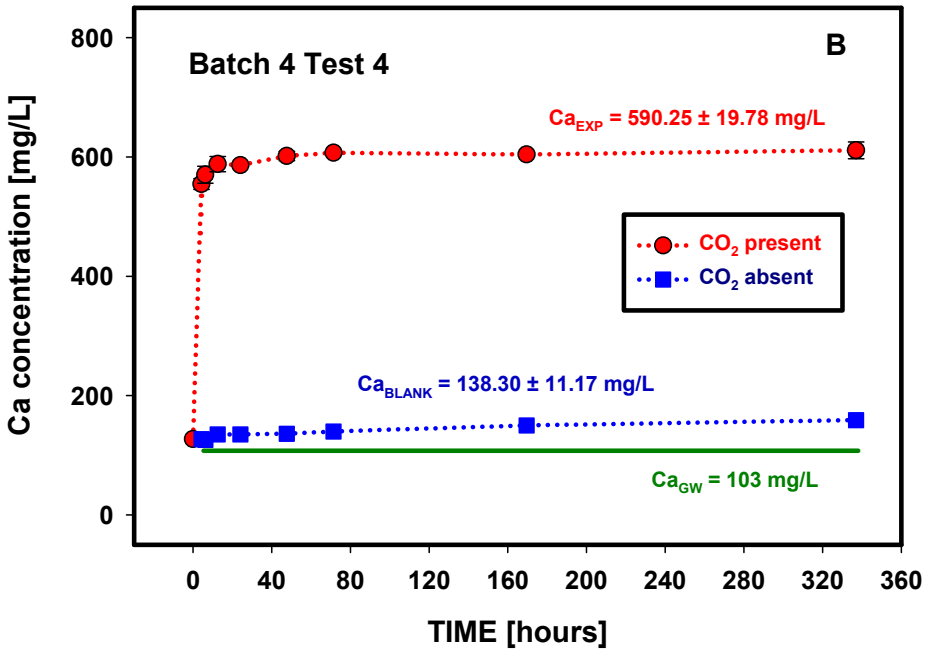

Figure D.11. Changes in pH and elemental composition as a function of time (Batch 4, Test 4, Edwards Aquifer Set B sample 7, <2 mm, 0.1 M NaCl).

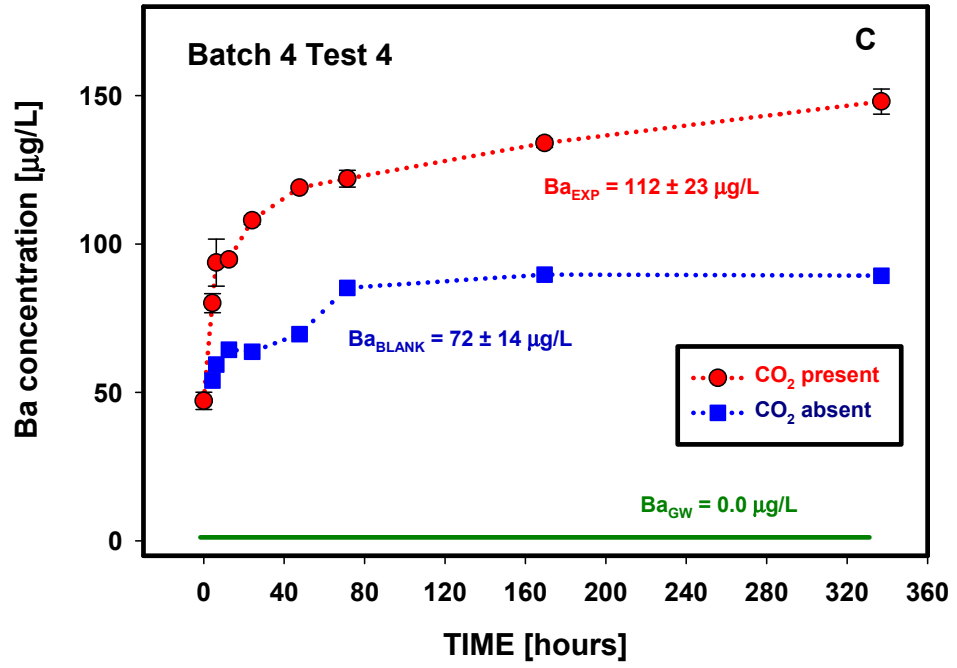

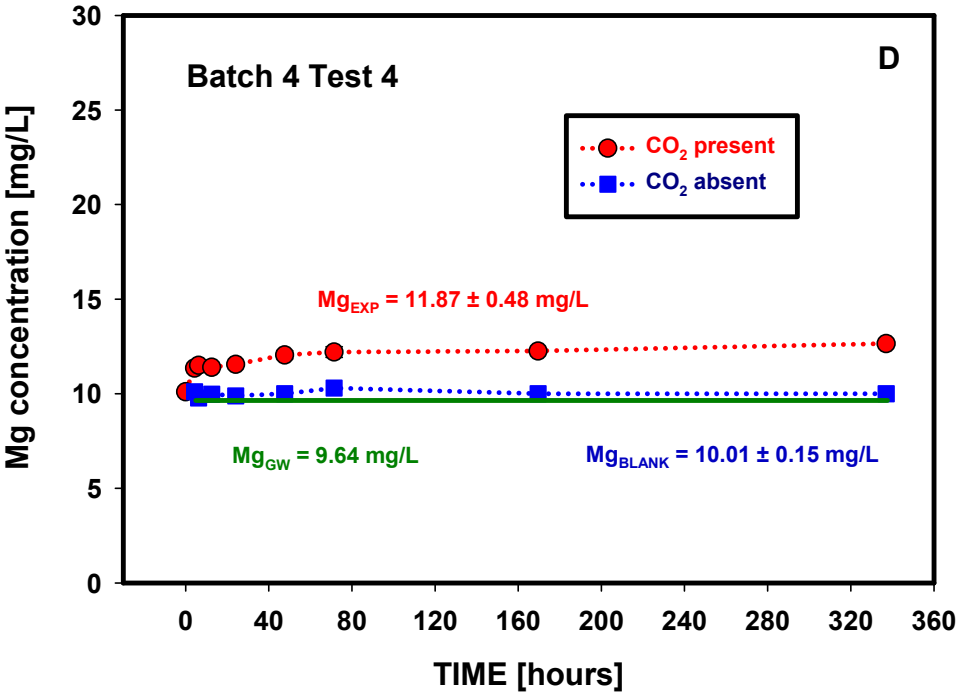

Figure D.11. (contd)

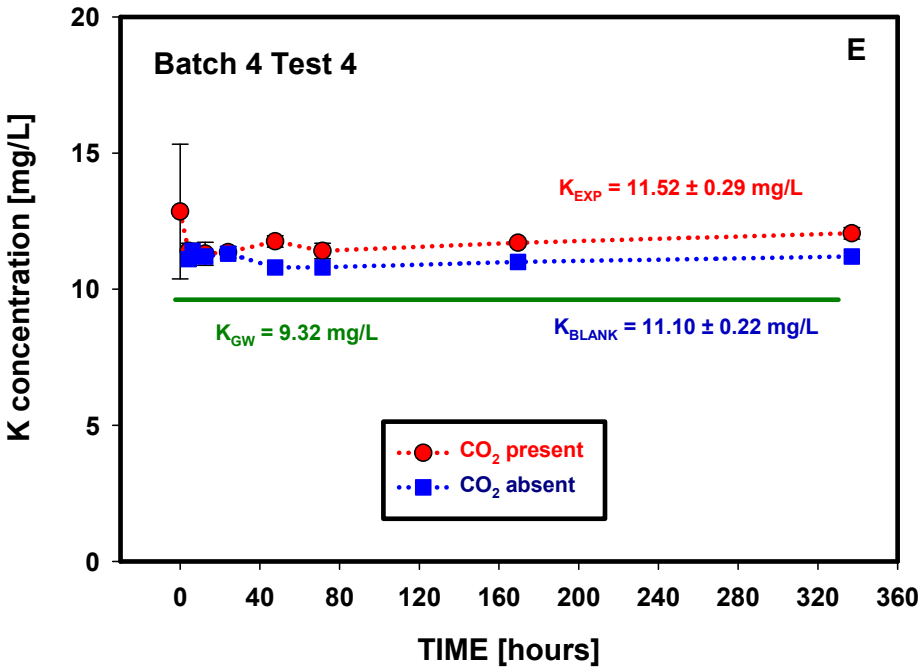

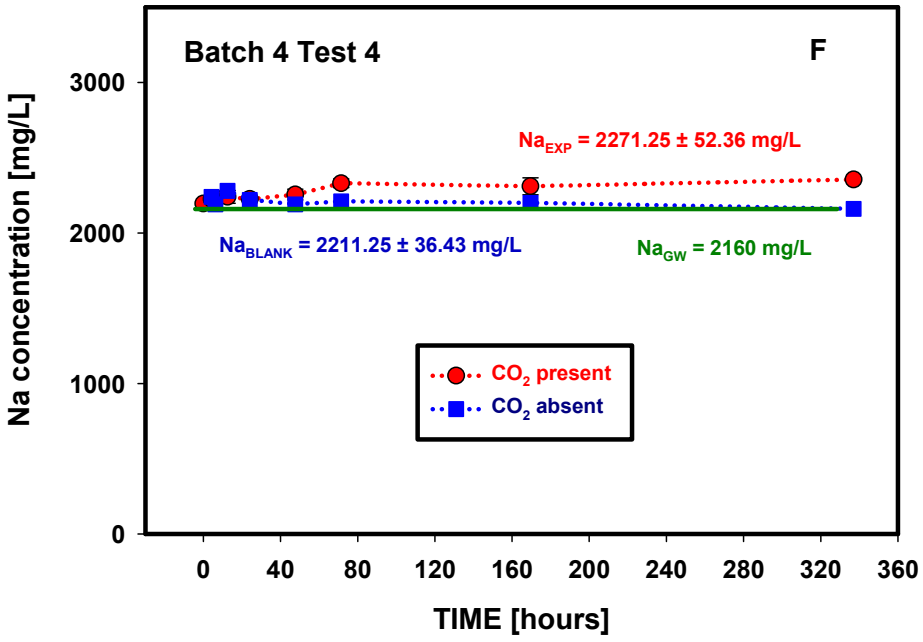

Figure D.11. (contd)

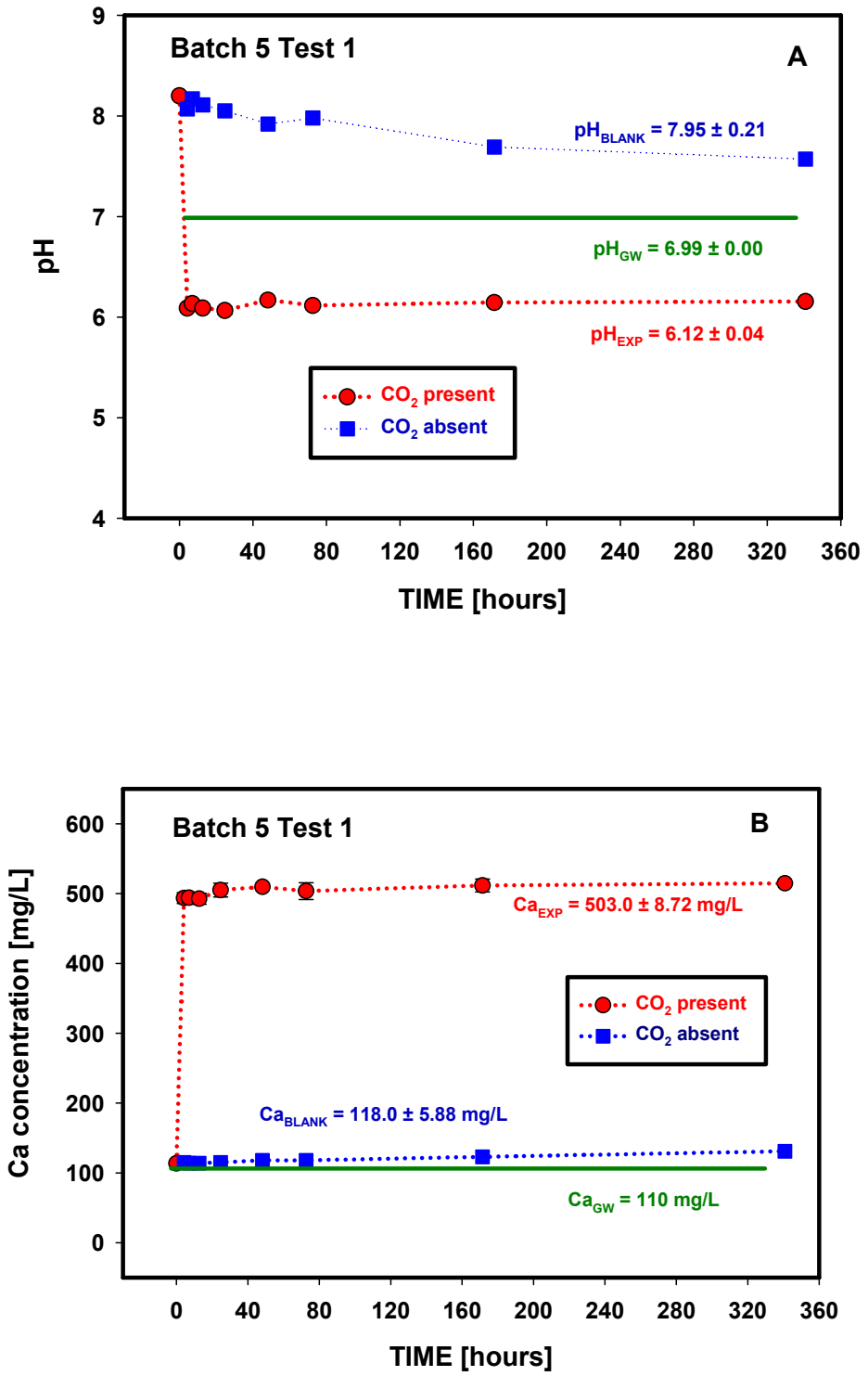

Figure D.12. Changes in pH and elemental composition as a function of time (Batch 5, Test 1, Edwards Aquifer Set B sample 2, <2 mm).

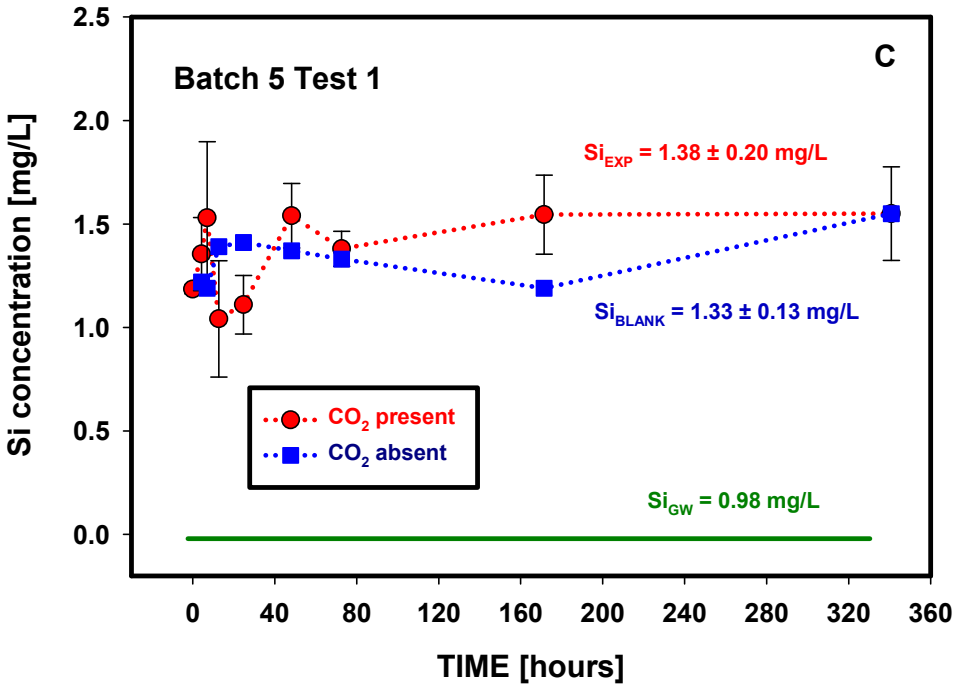

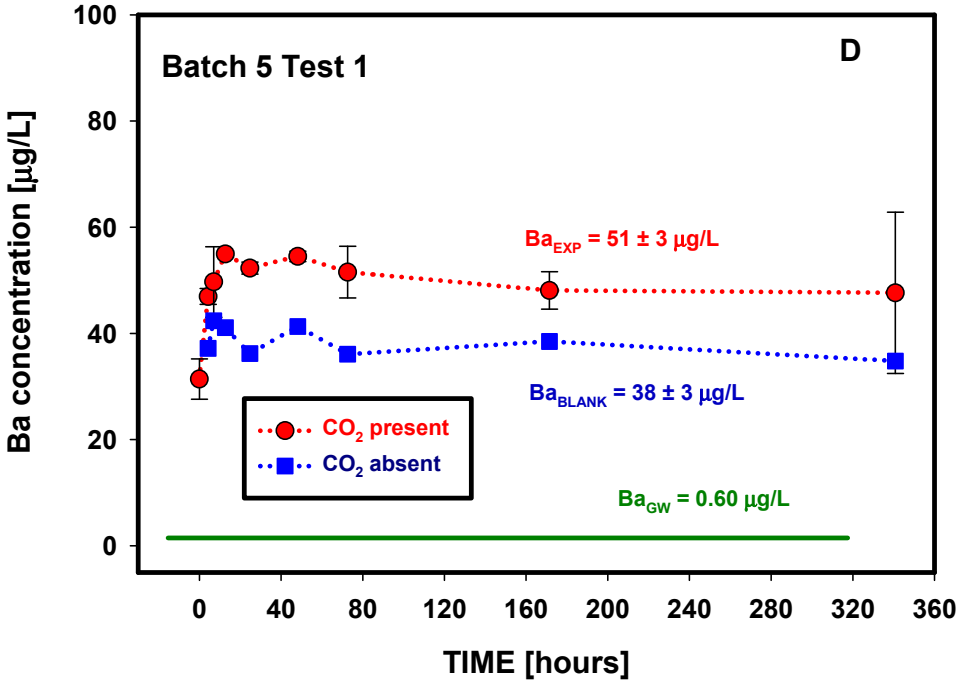

Figure D.12. (contd)

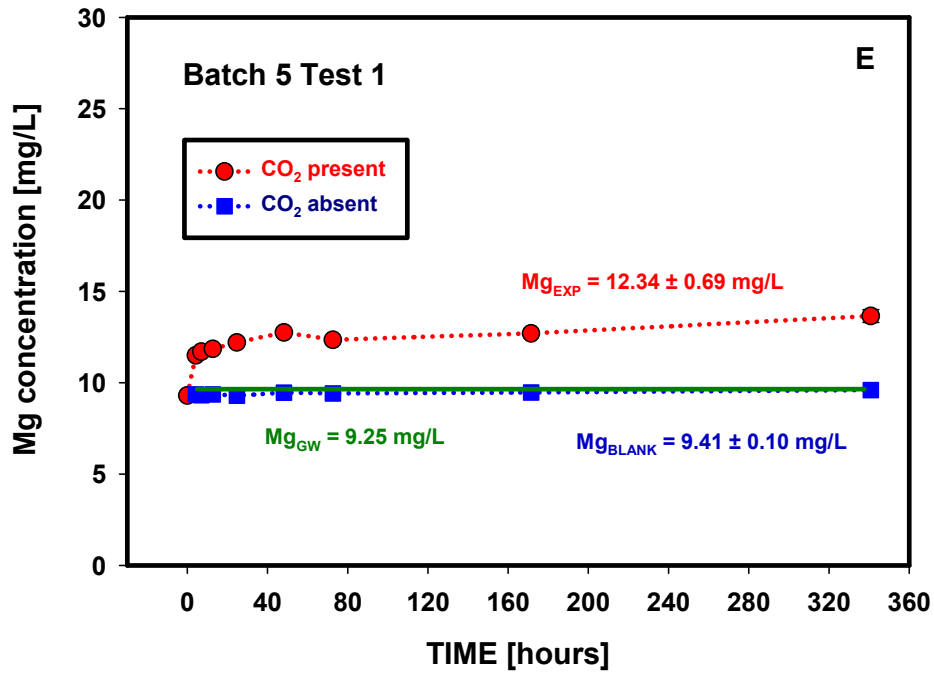

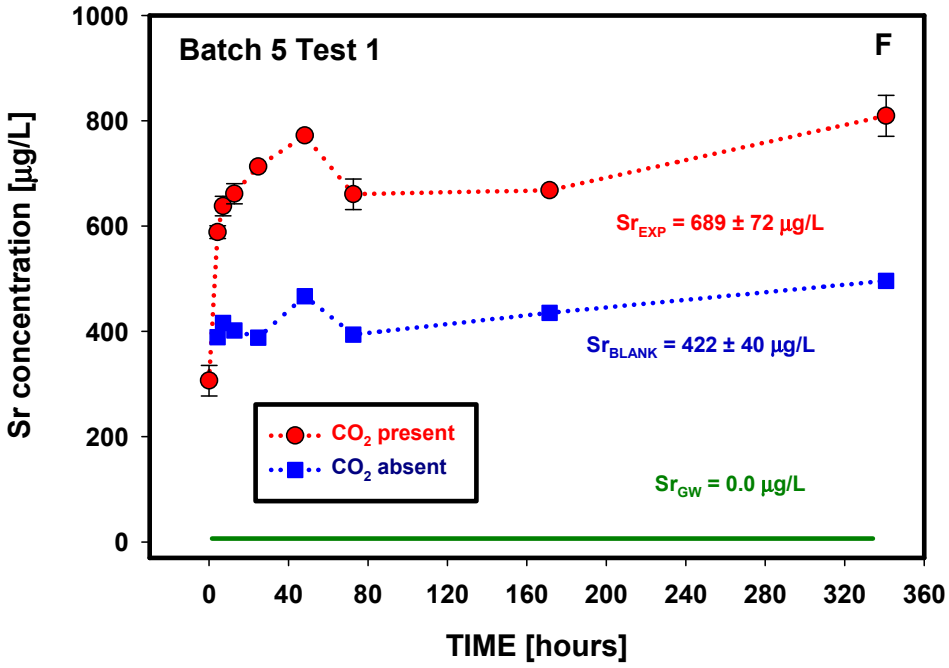

Figure D.12. (contd)

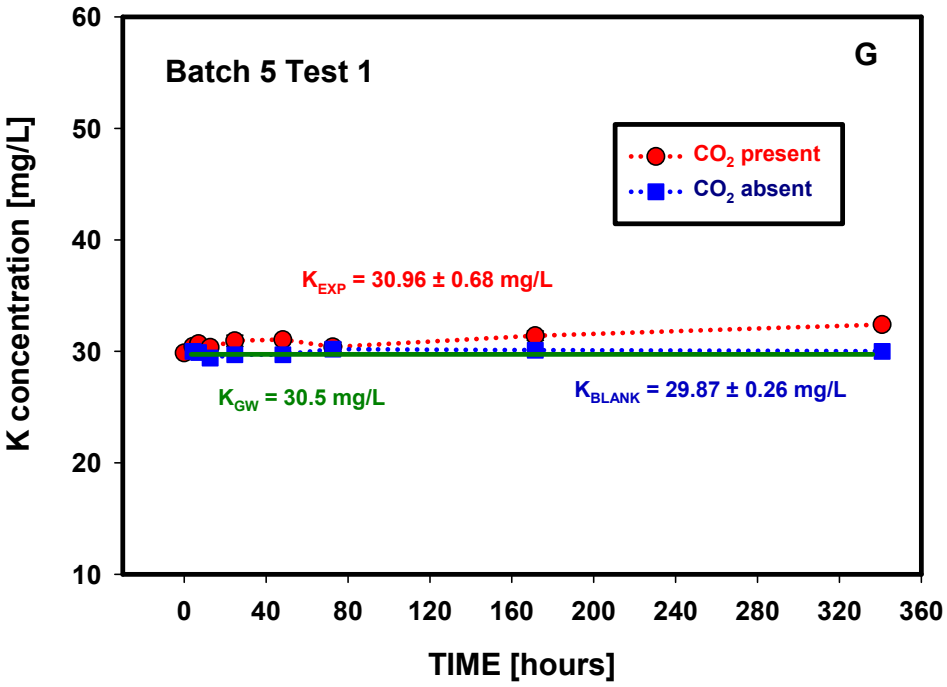

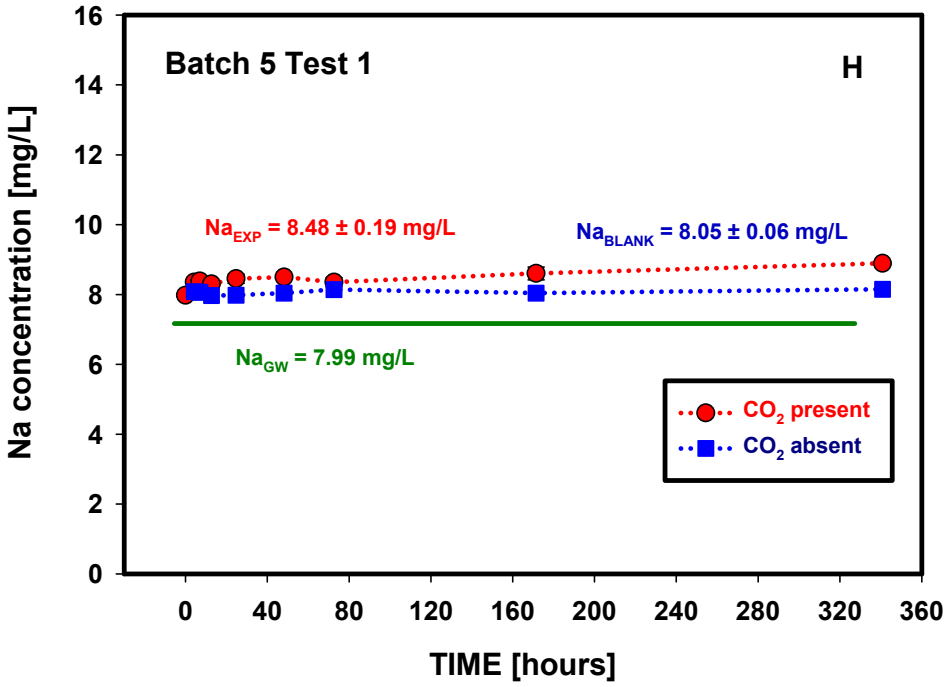

Figure D.12. (contd)

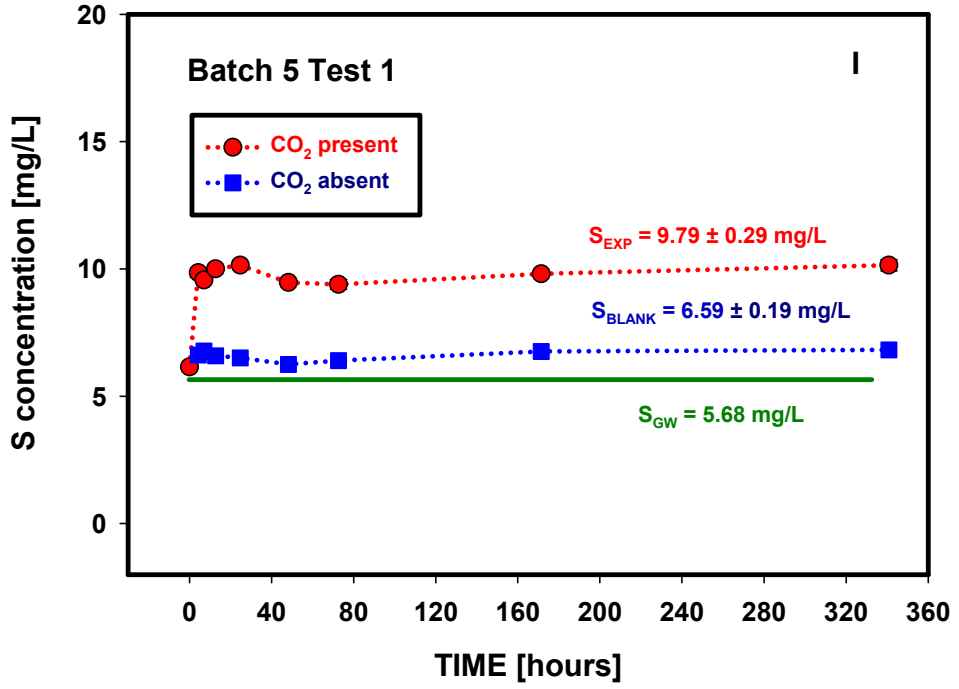

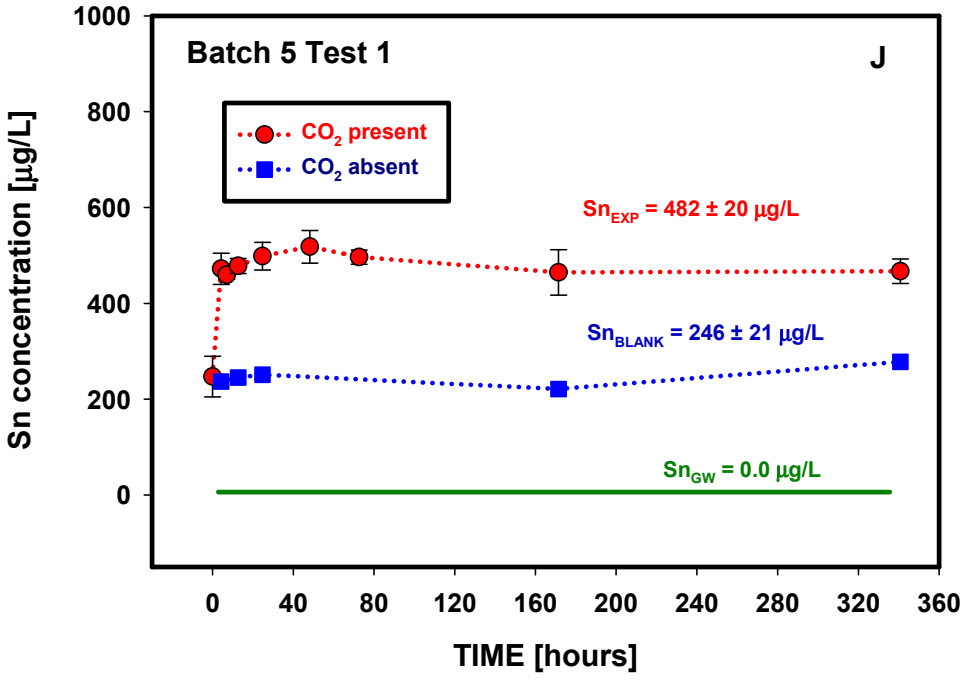

Figure D.12. (contd)

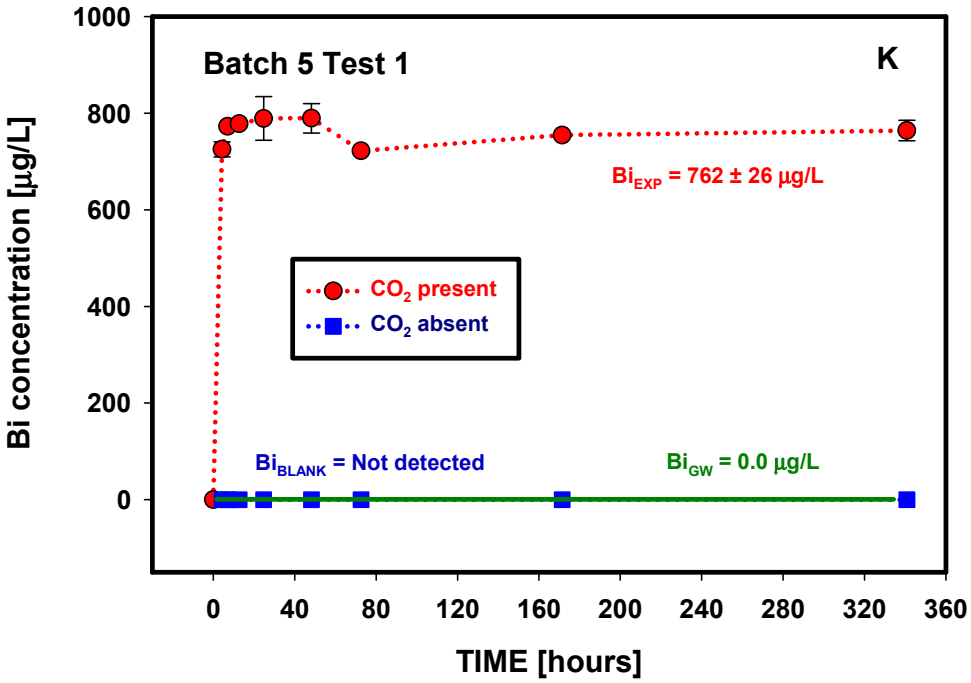

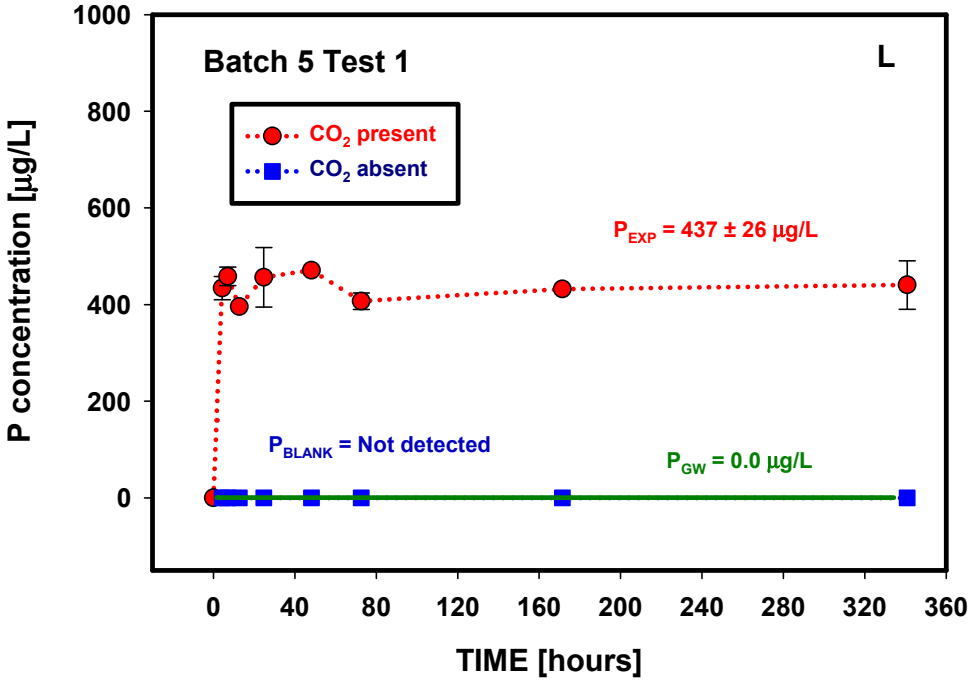

Figure D.12. (contd)

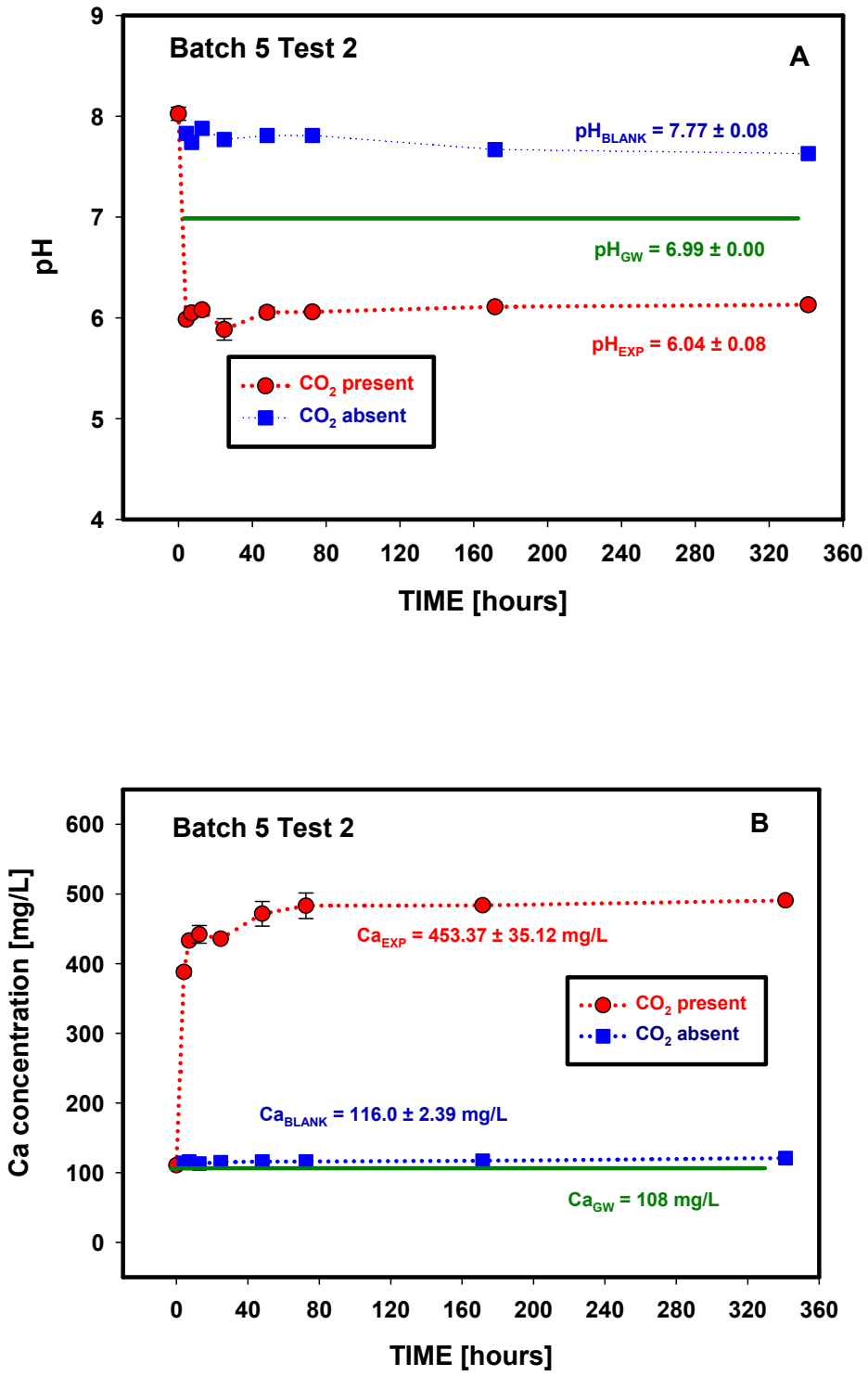

Figure D.13. Changes in pH and elemental composition as a function of time (Batch 5, Test 2, Edwards Aquifer Set B sample 2, >2 mm).

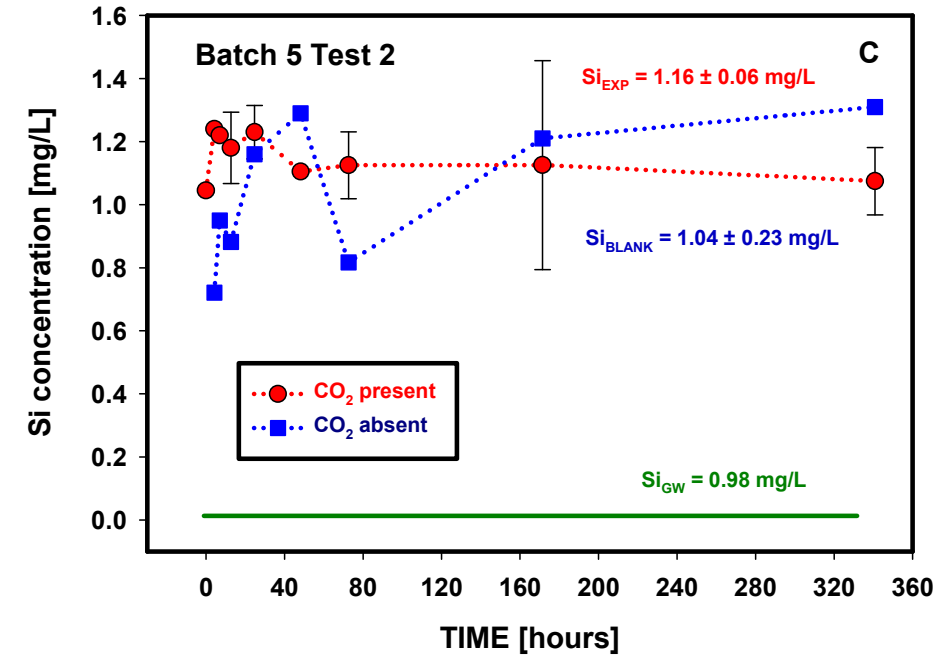

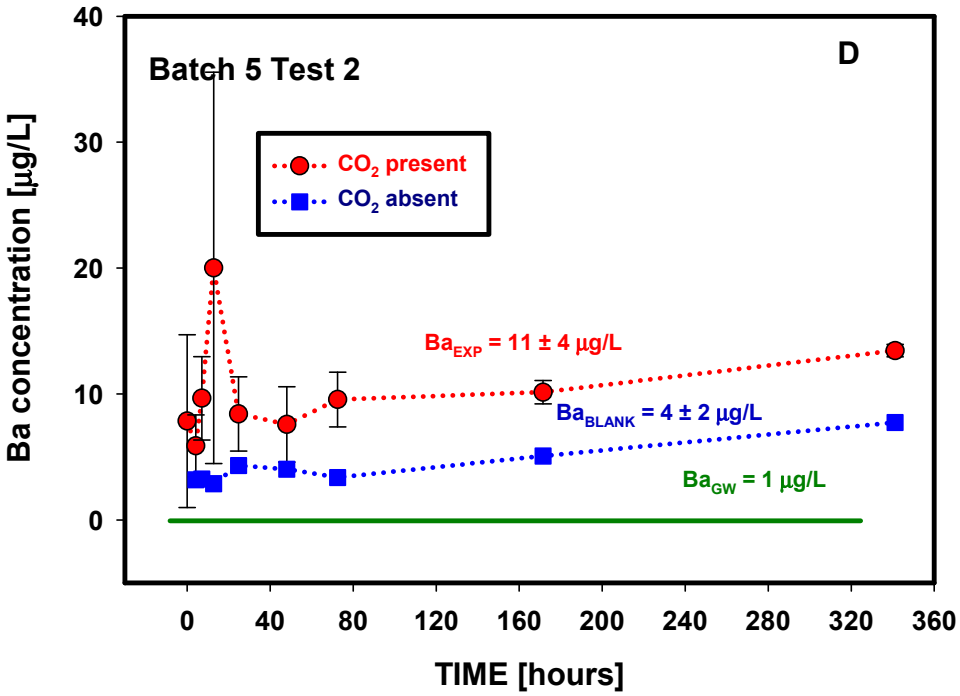

Figure D.13. (contd)

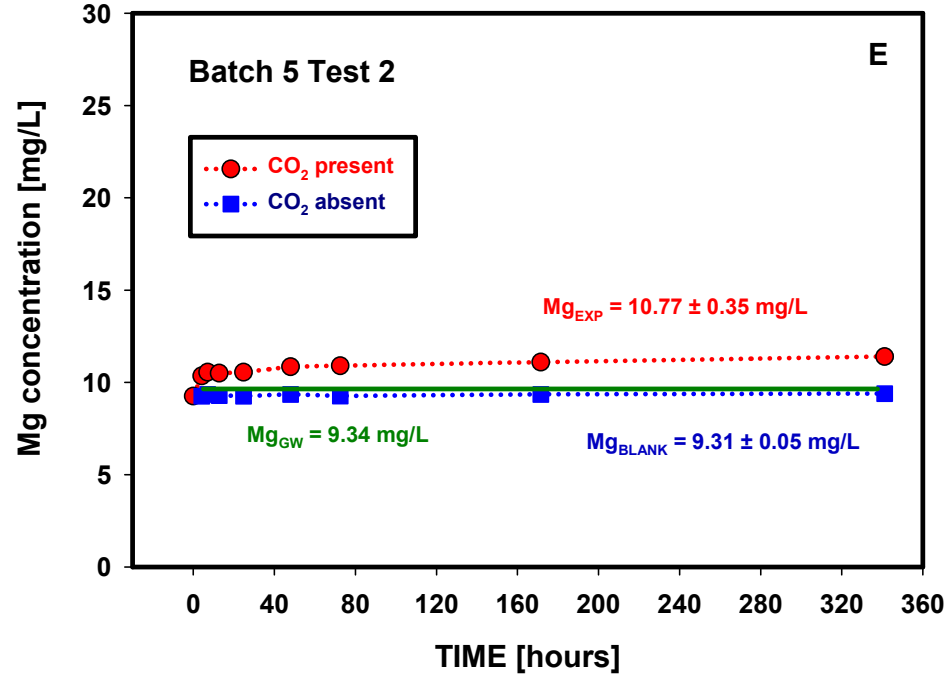

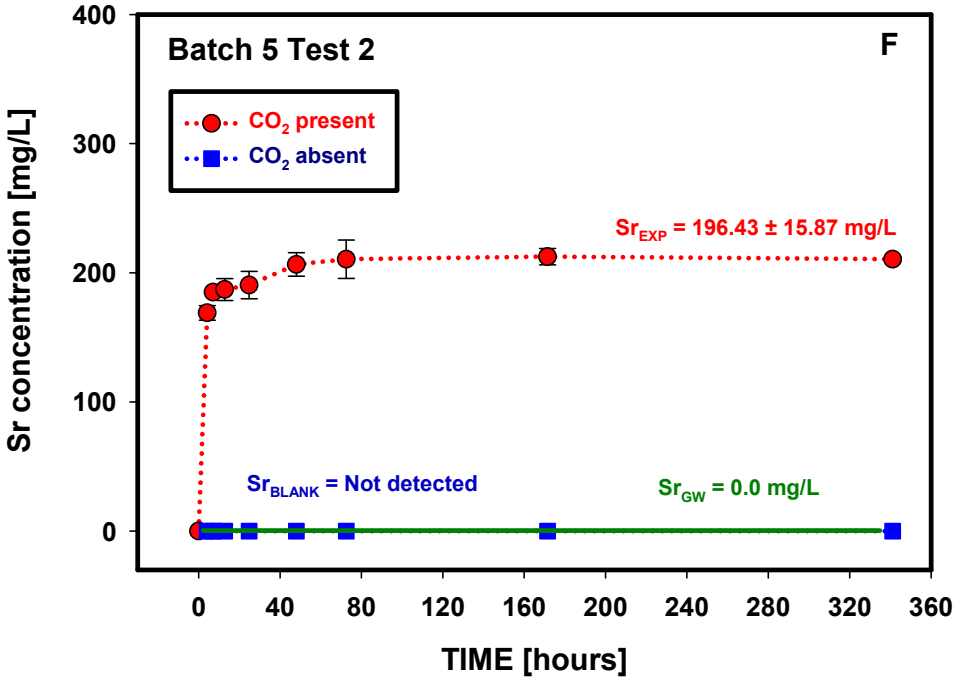

Figure D.13. (contd)

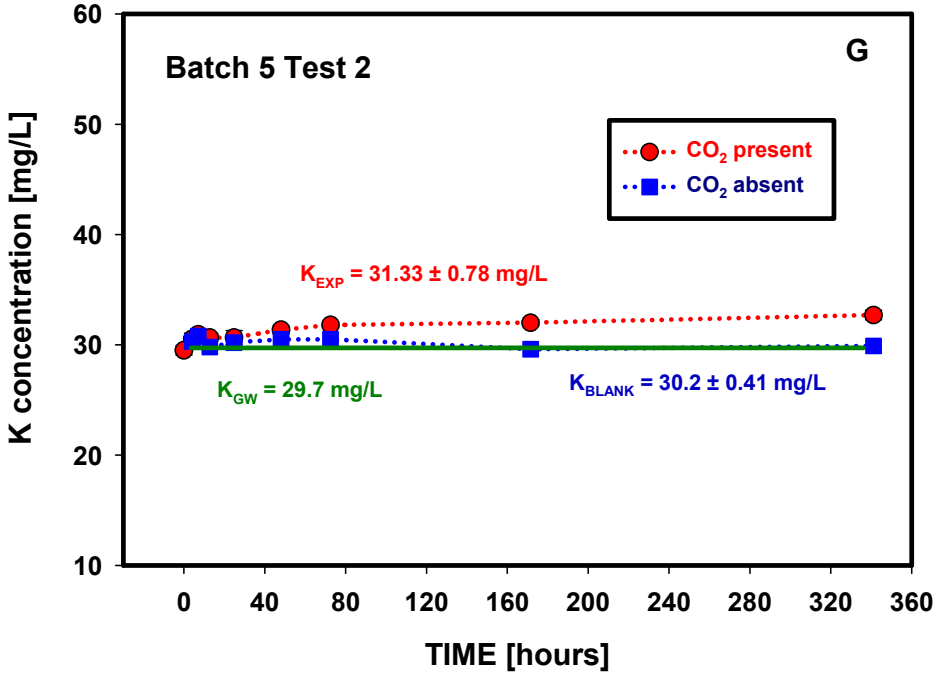

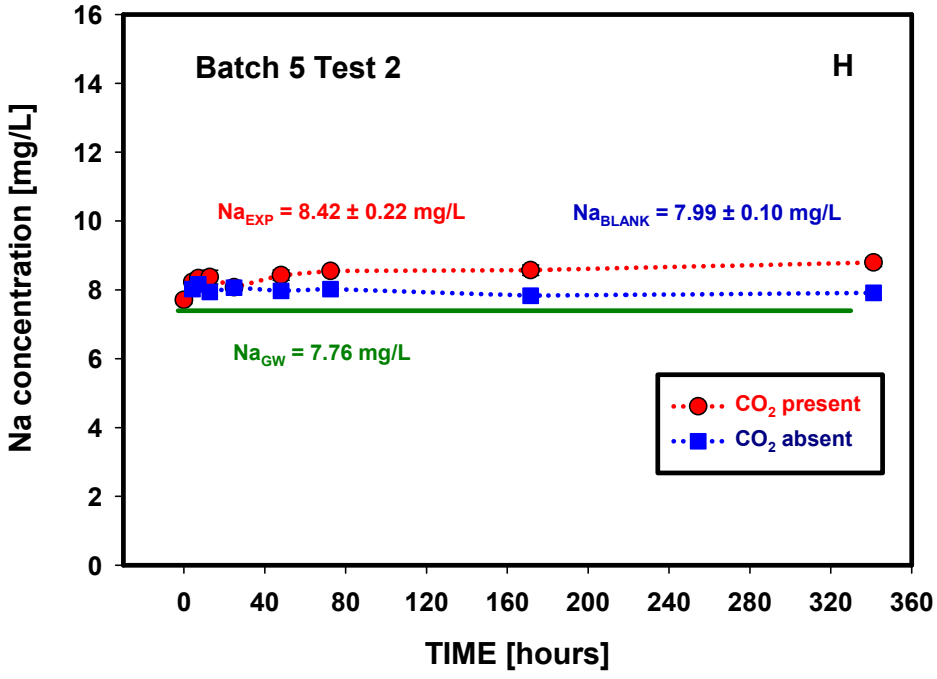

Figure D.13. (contd)

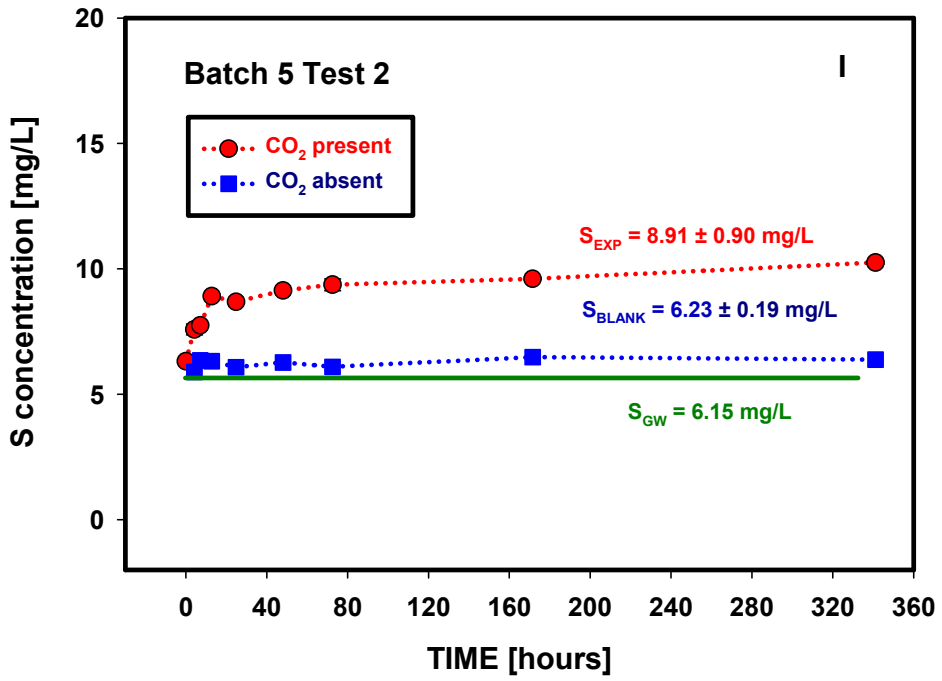

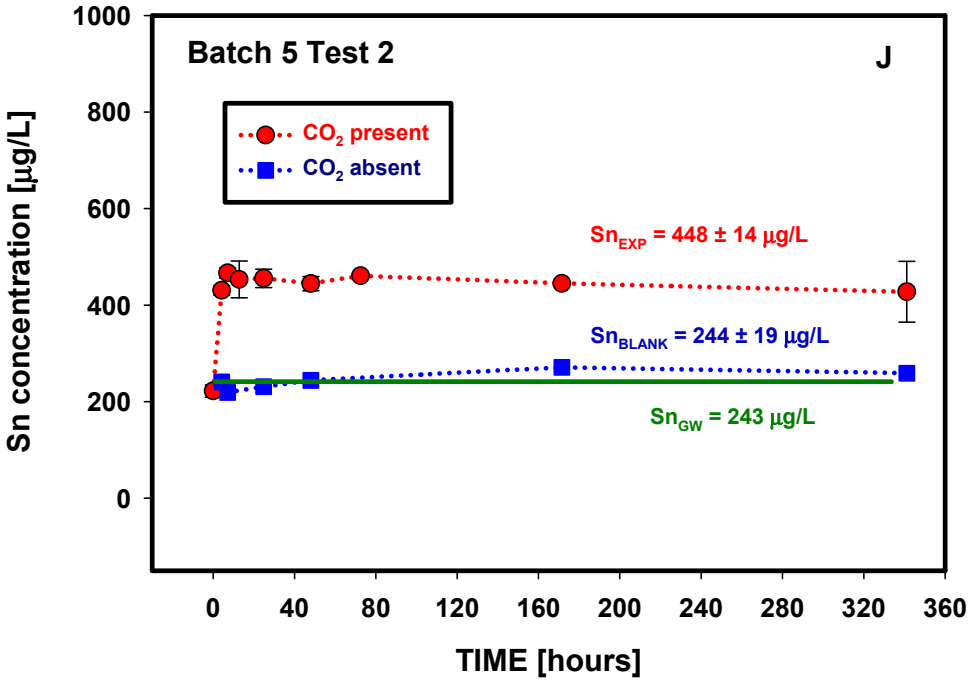

Figure D.13. (contd)

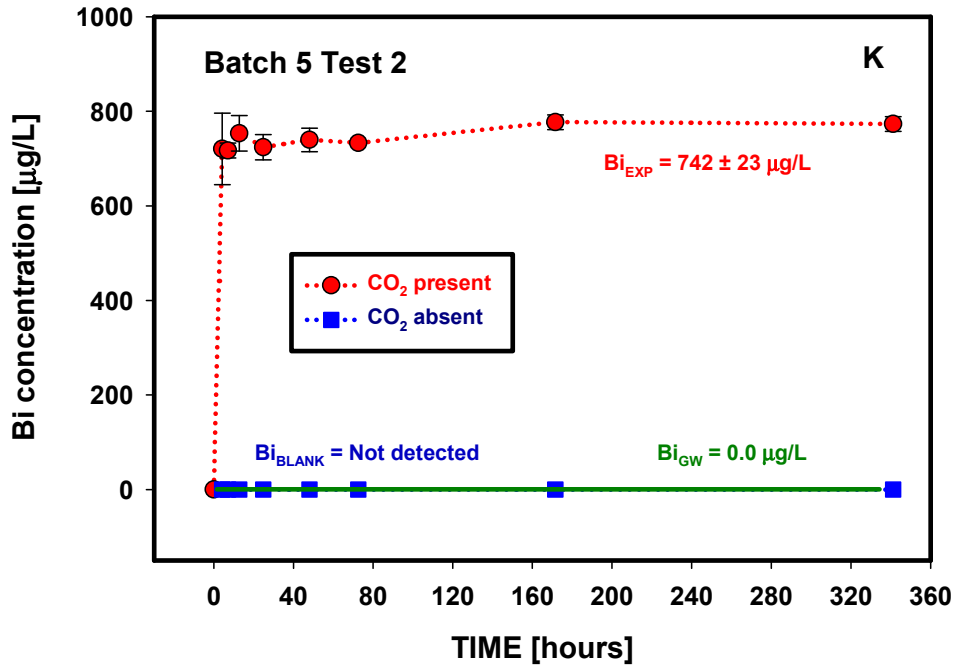

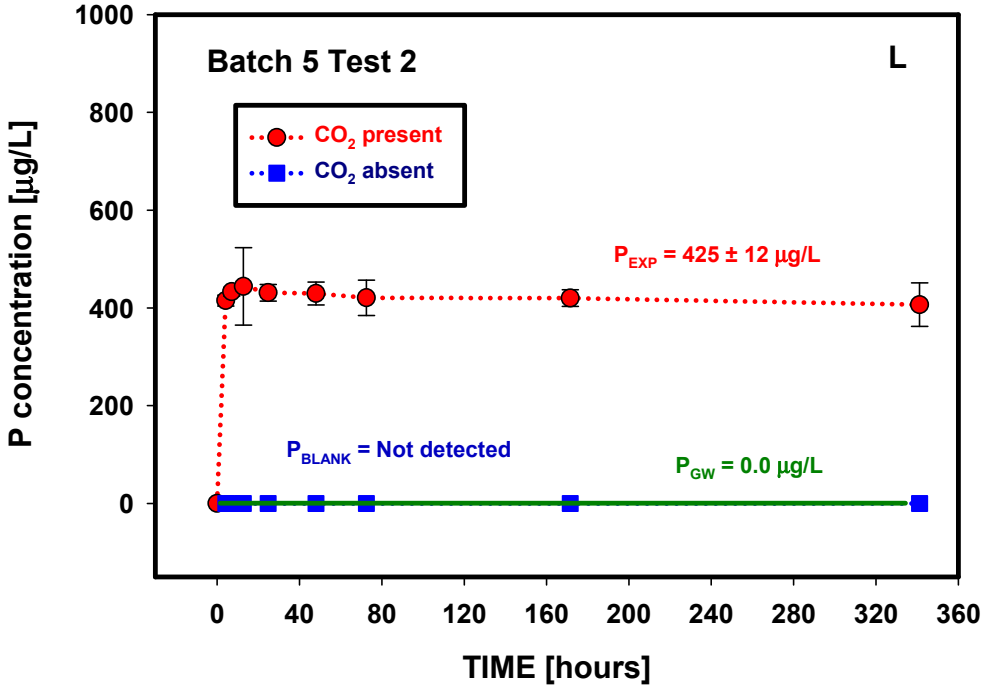

Figure D.13. (contd)

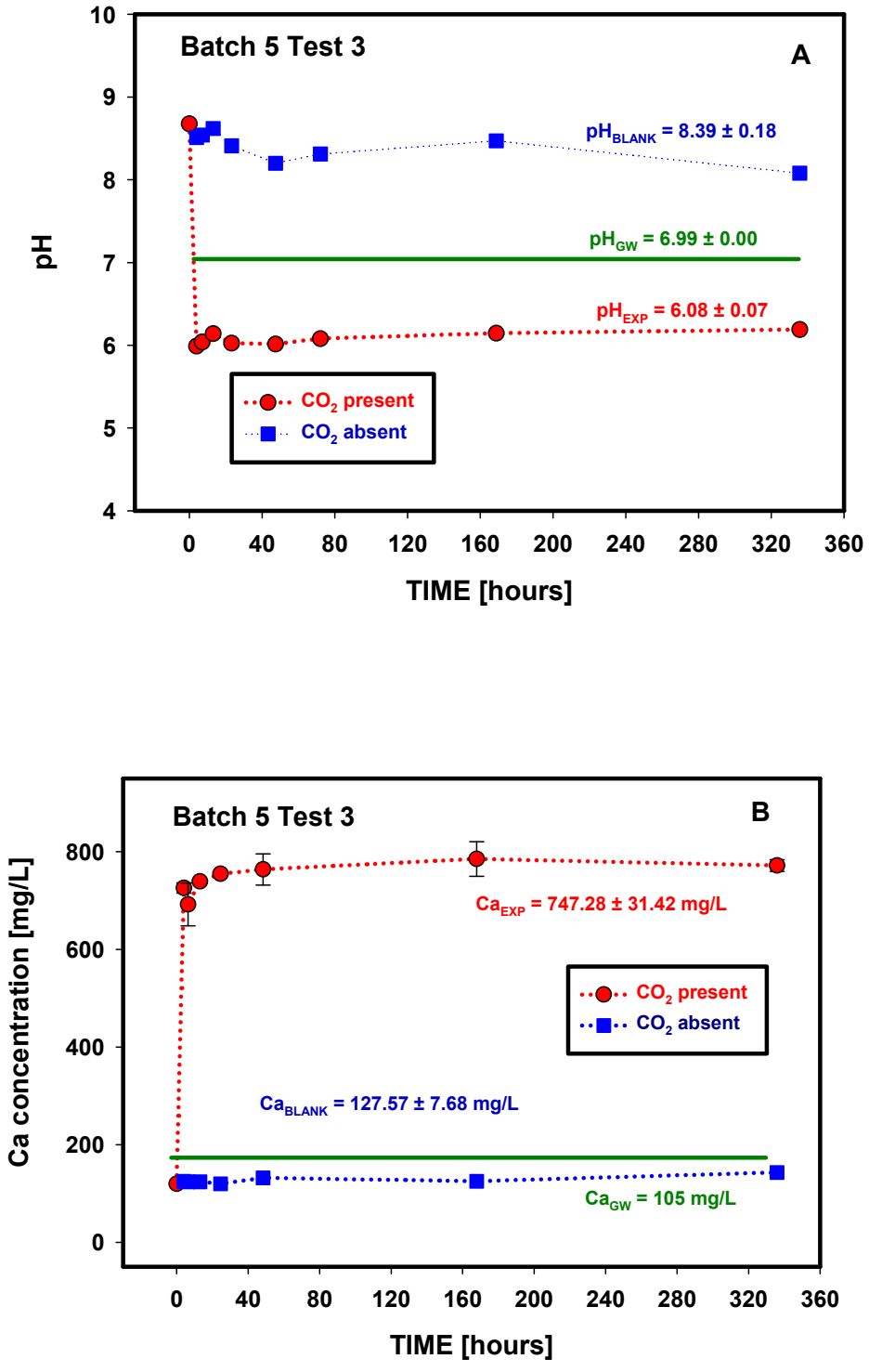

Figure D.14. Changes in pH and elemental composition as a function of time (Batch 5, Test 3, Edwards Aquifer Set B sample 2, <2 mm, 1 M NaCl).

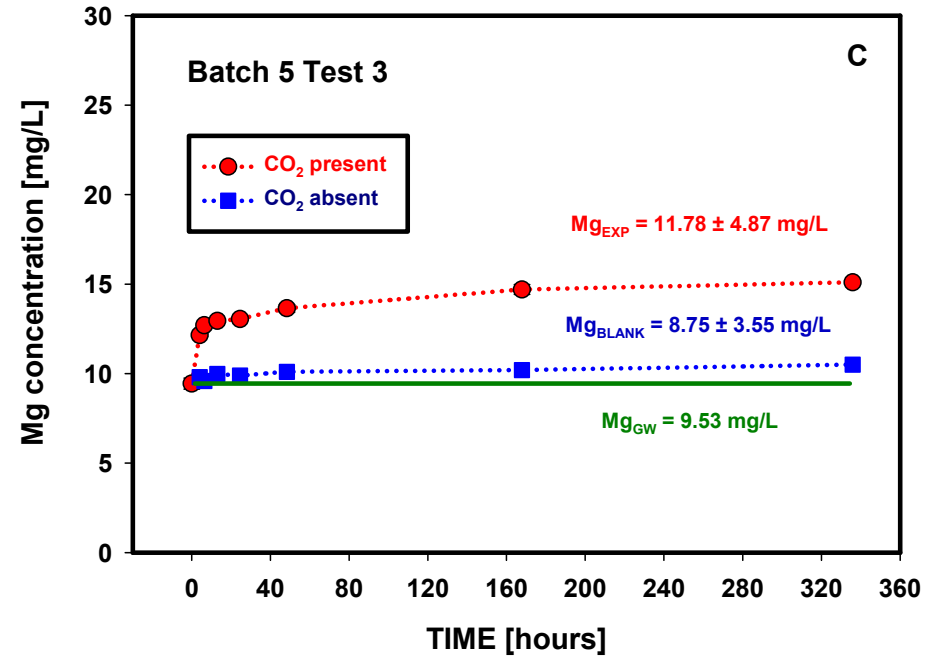

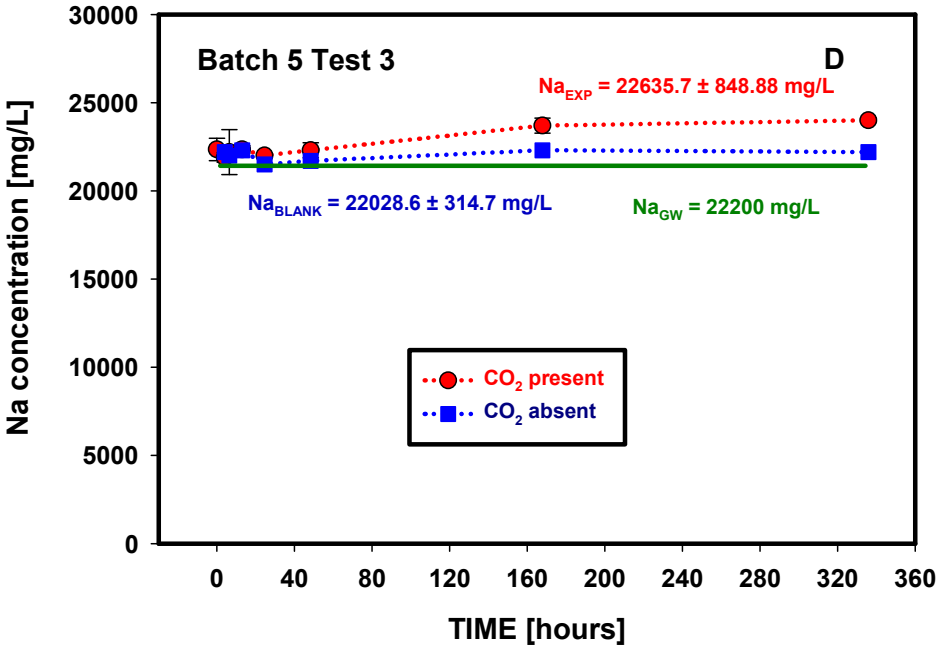

Figure D.14. (contd)

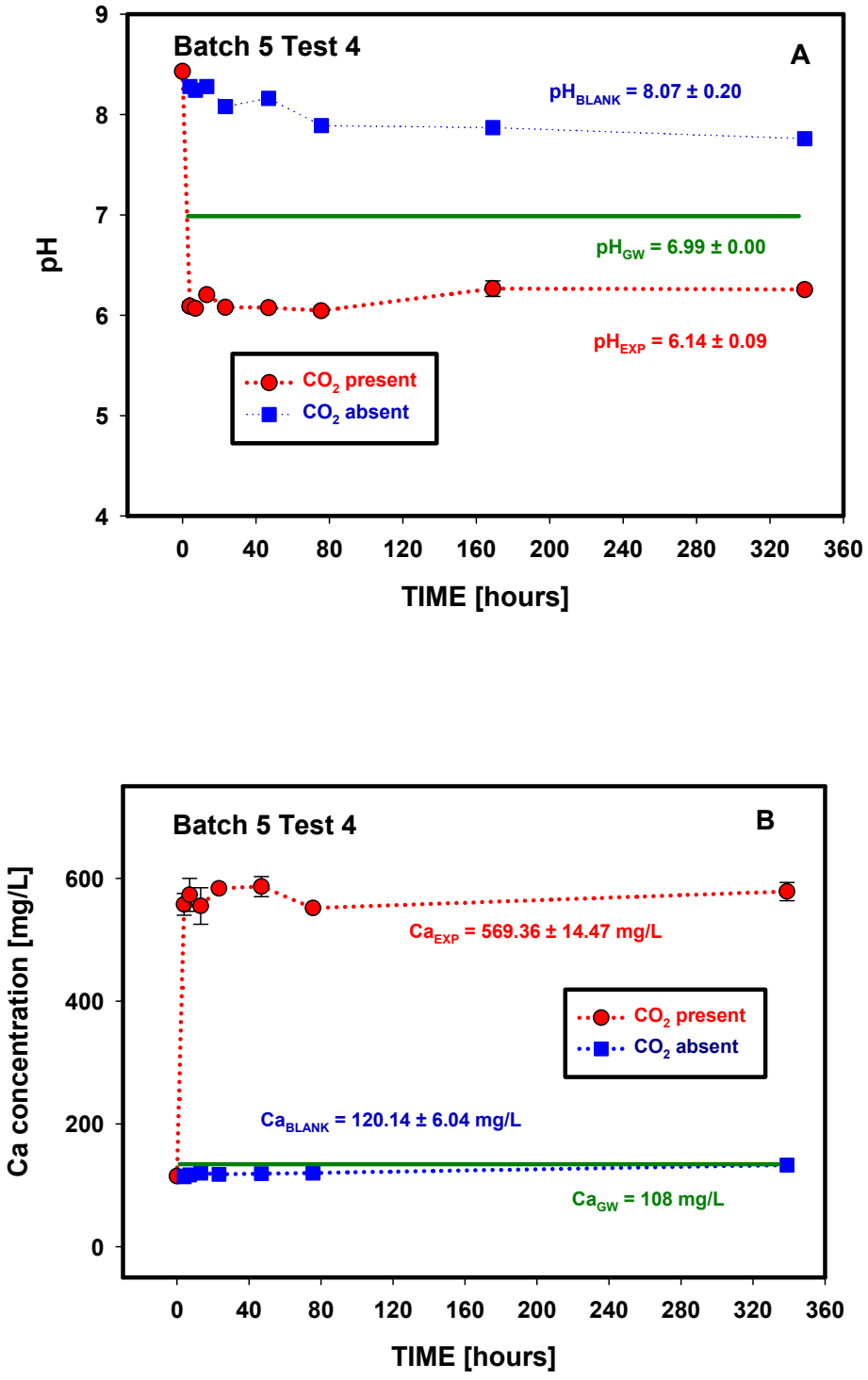

Figure D.15. Changes in pH and elemental composition as a function of time (Batch 5, Test 4, Edwards Aquifer Set B sample 2, <2 mm, 0.1 M NaCl).

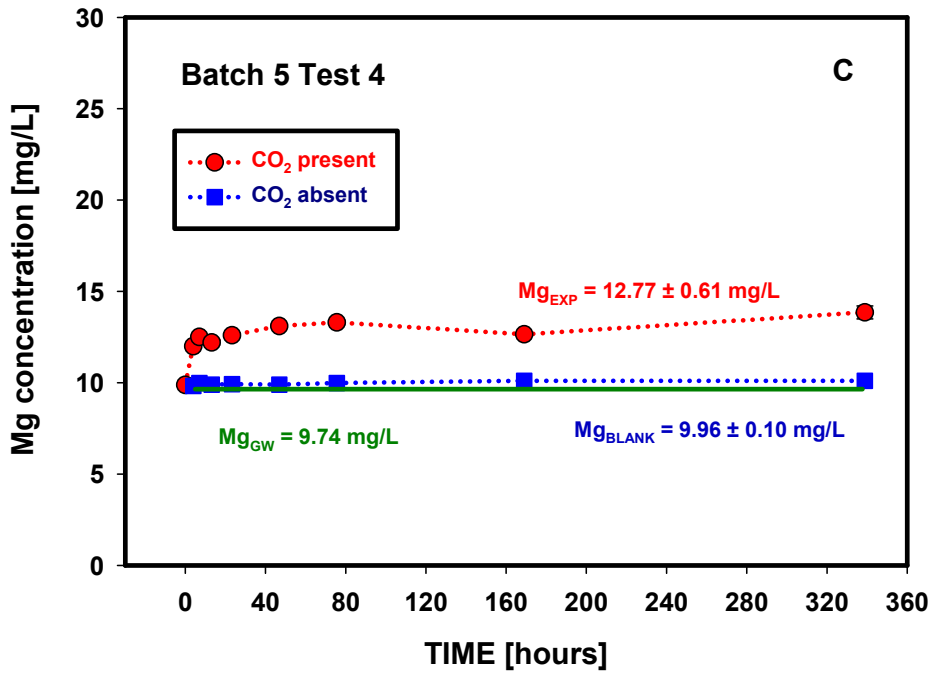

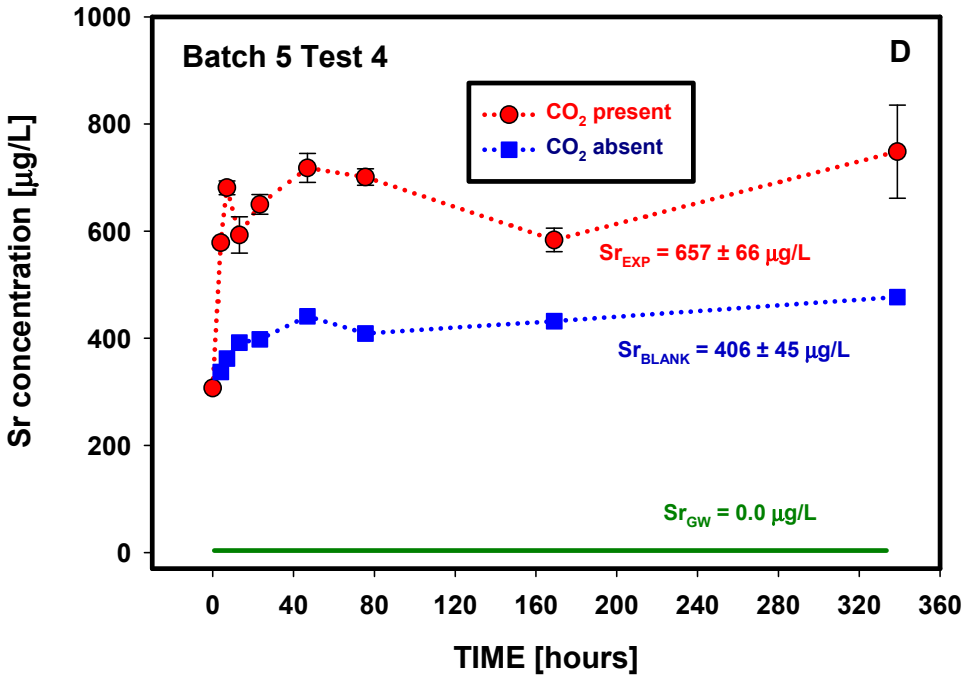

Figure D.15. (contd)

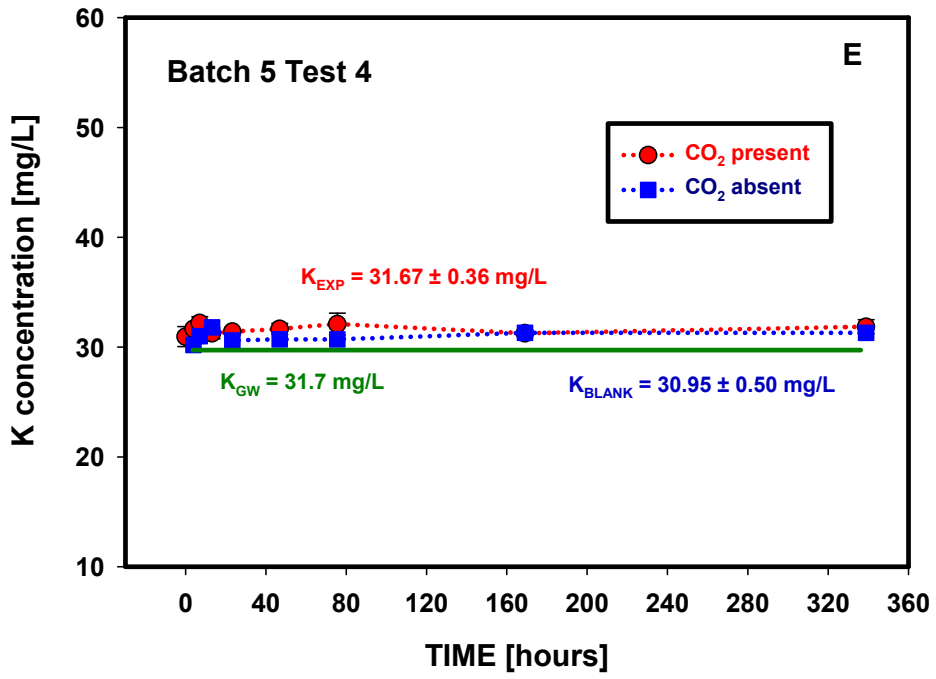

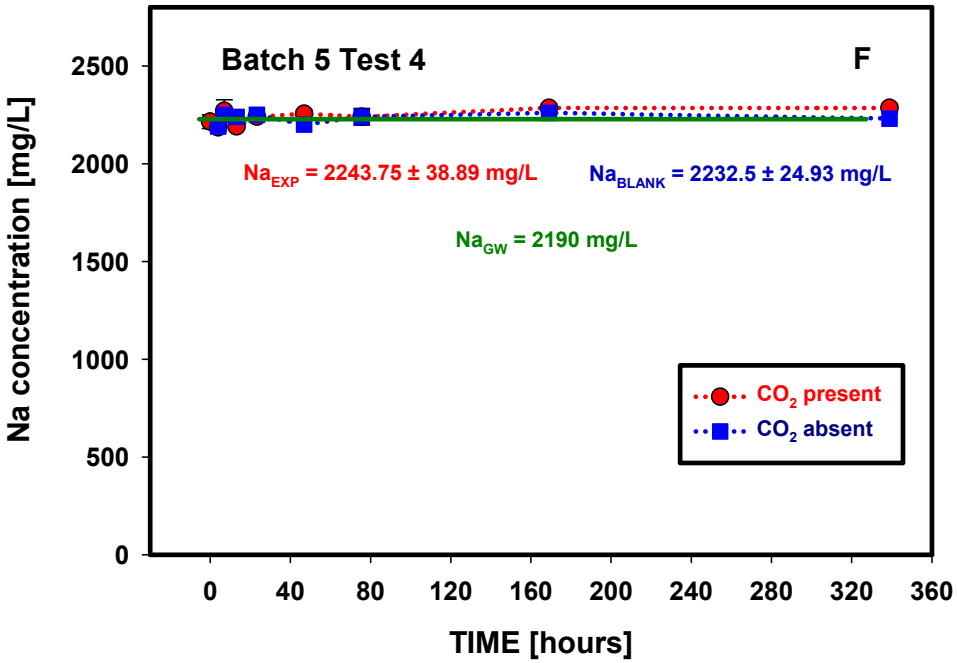

Figure D.15. (contd)

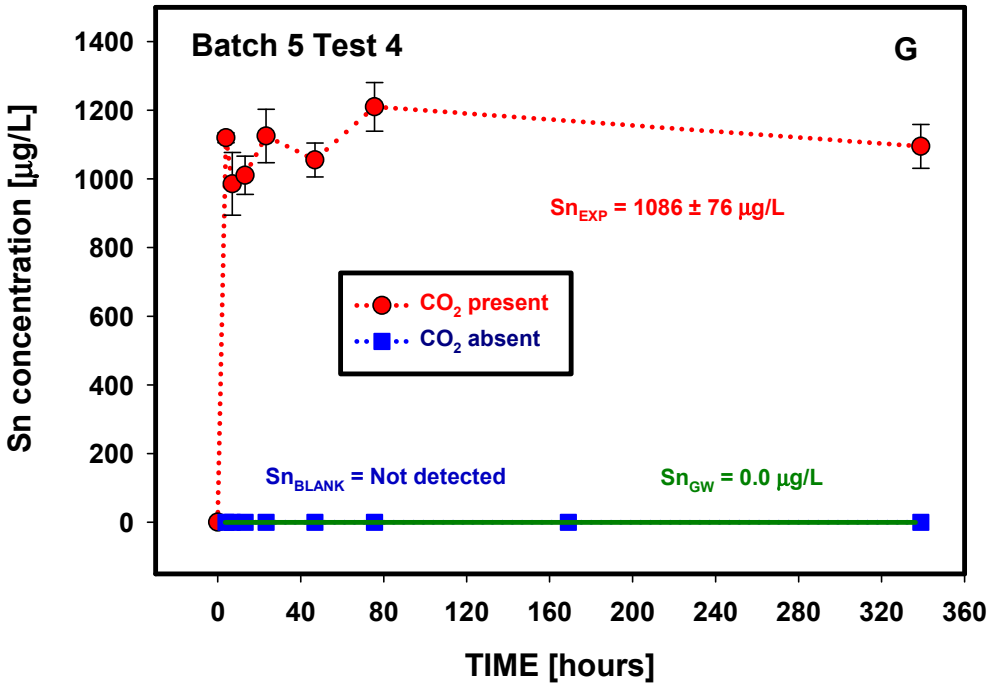

Figure D.15. (contd)

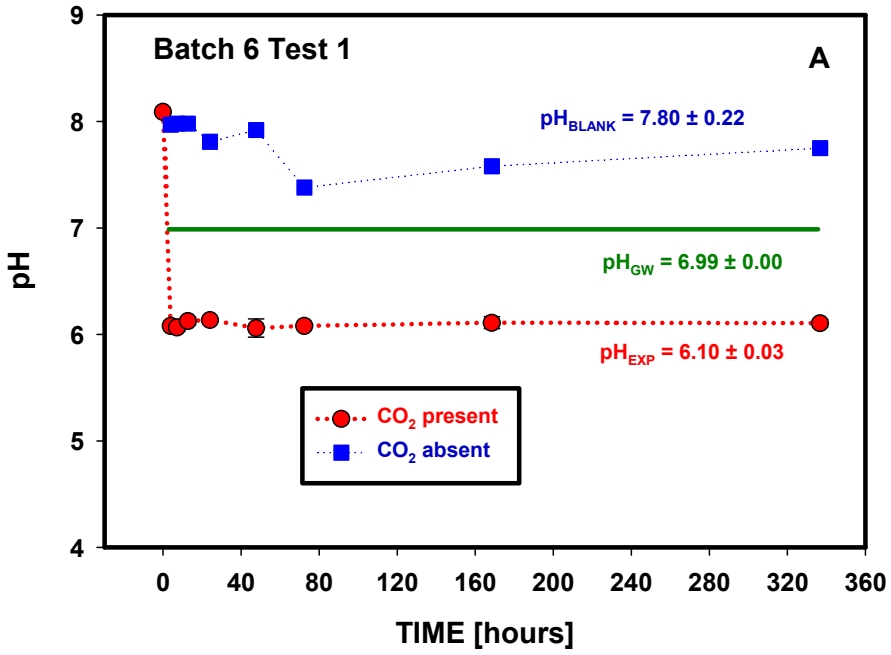

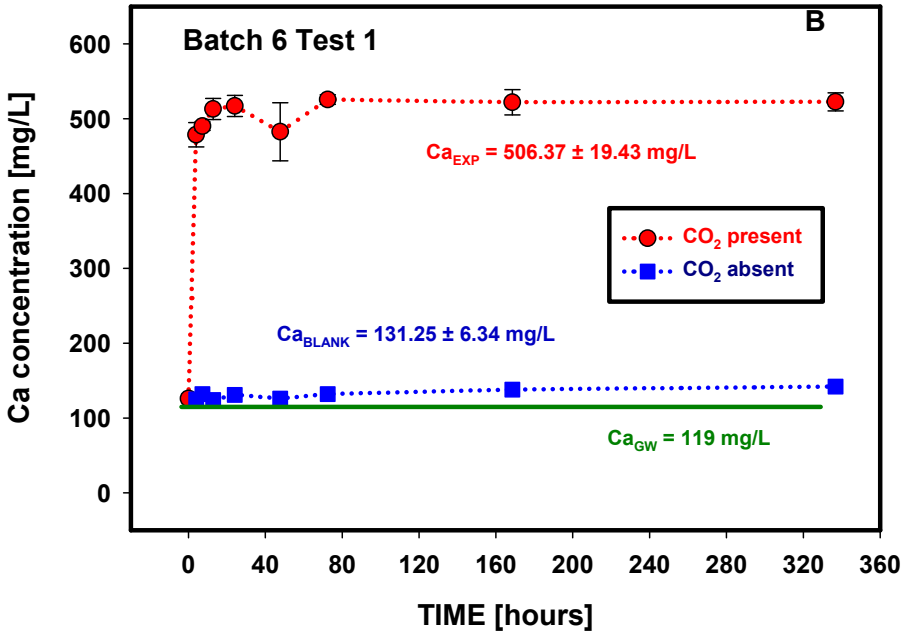

Figure D.16. Changes in pH and elemental composition as a function of time (Batch 6, Test 1, Edwards Aquifer Set A sample 1).

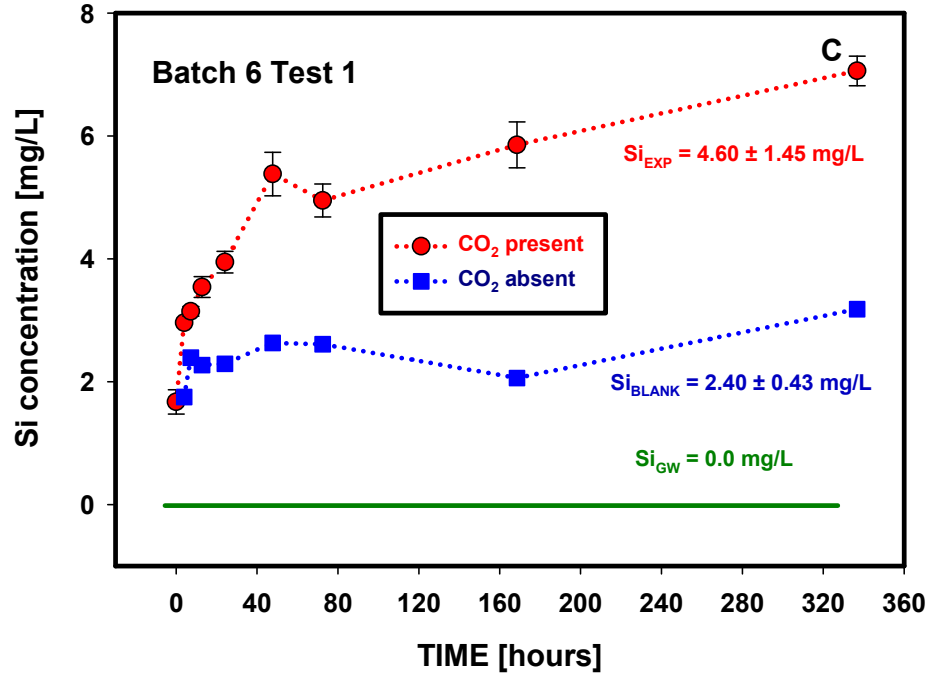

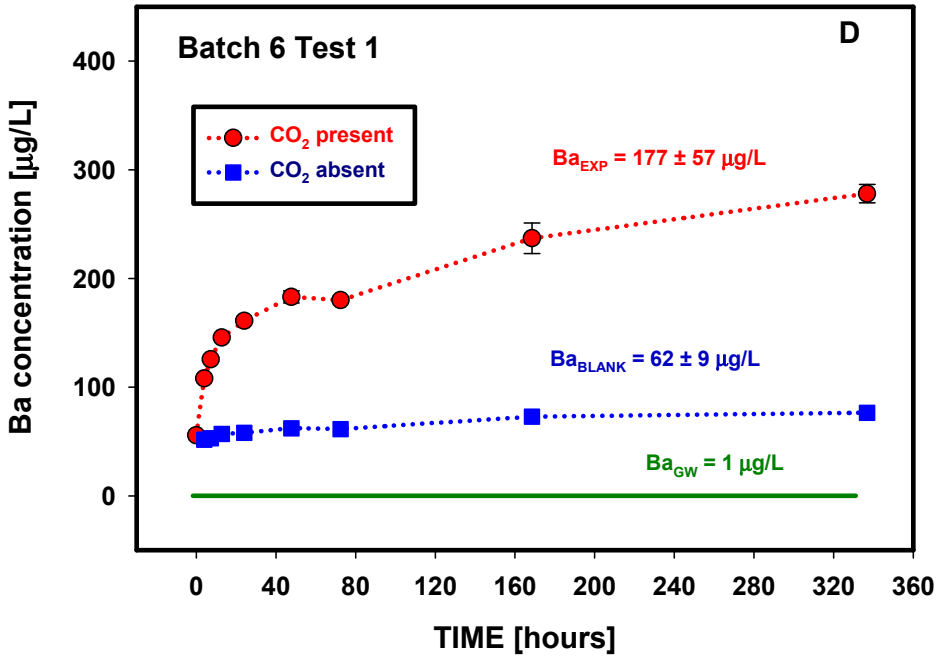

Figure D.16. (contd)

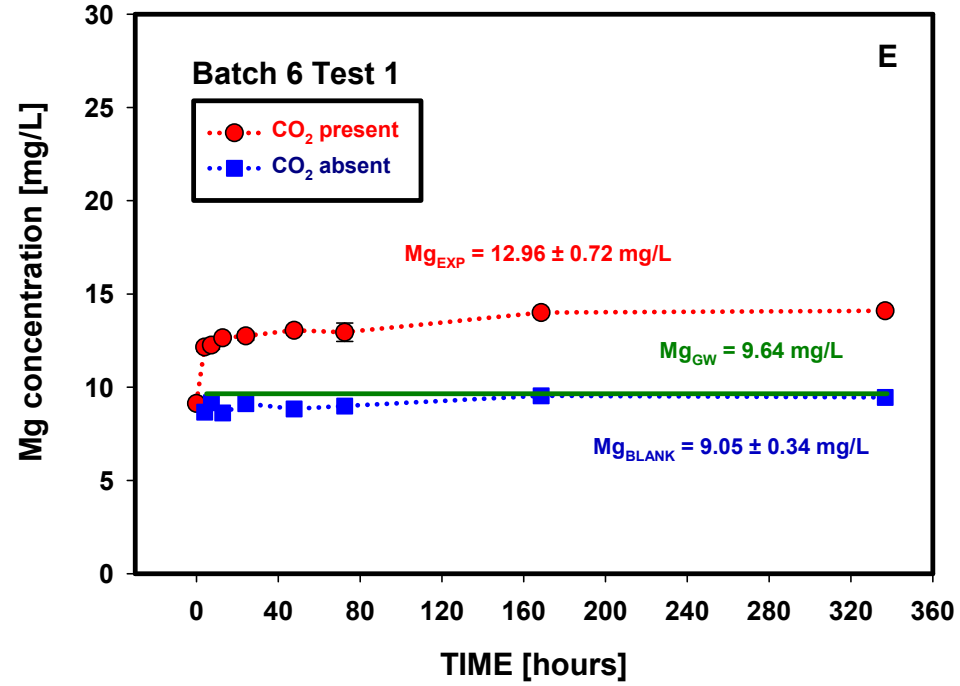

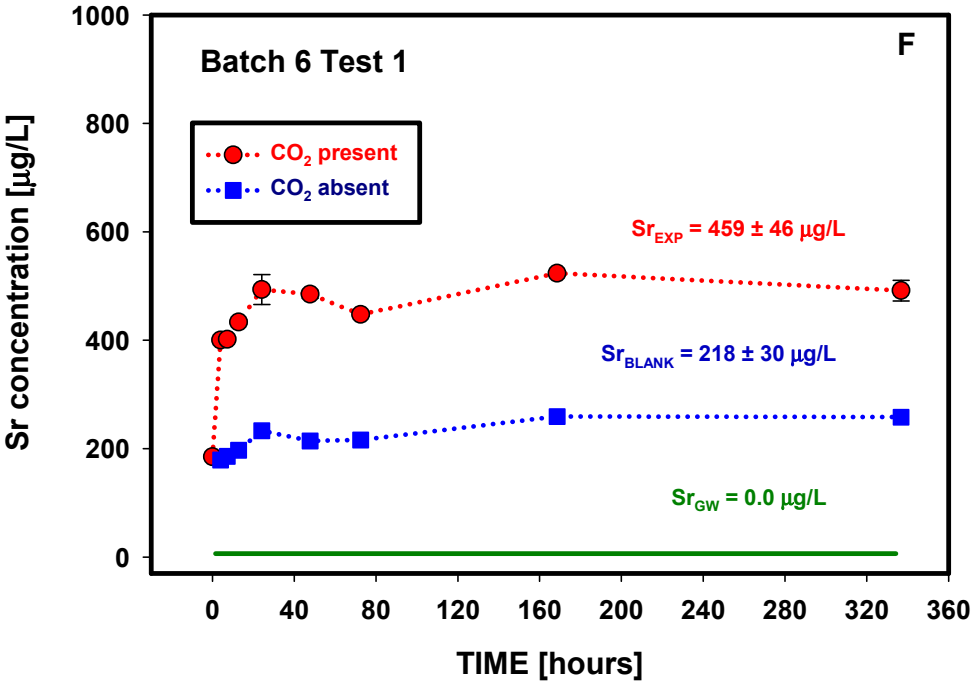

Figure D.16. (contd)

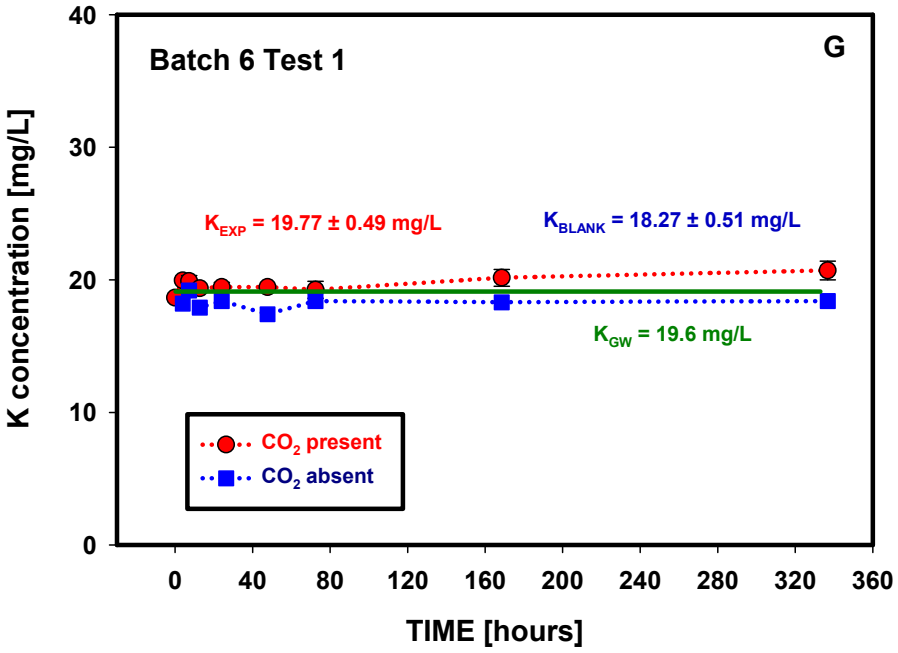

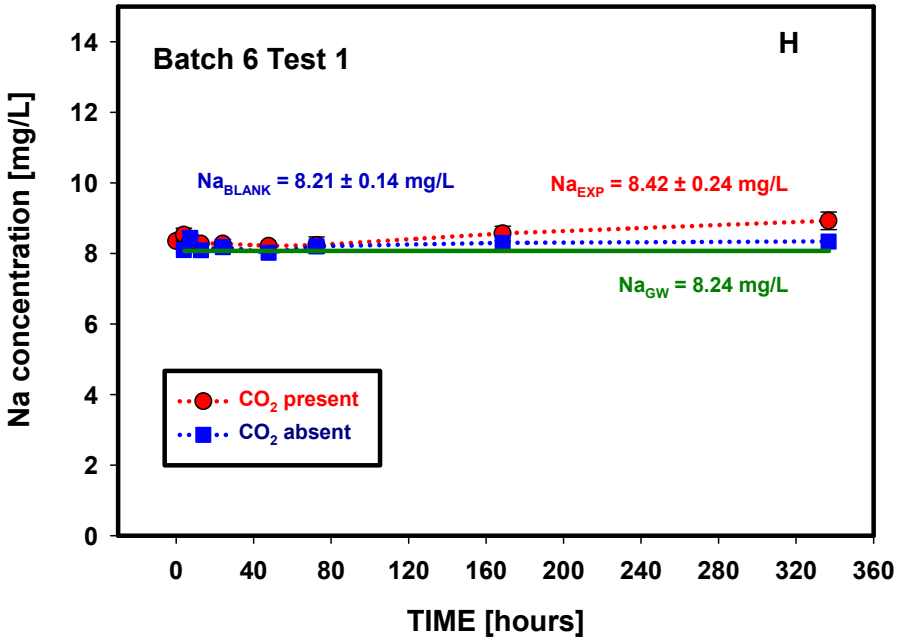

Figure D.16. (contd)

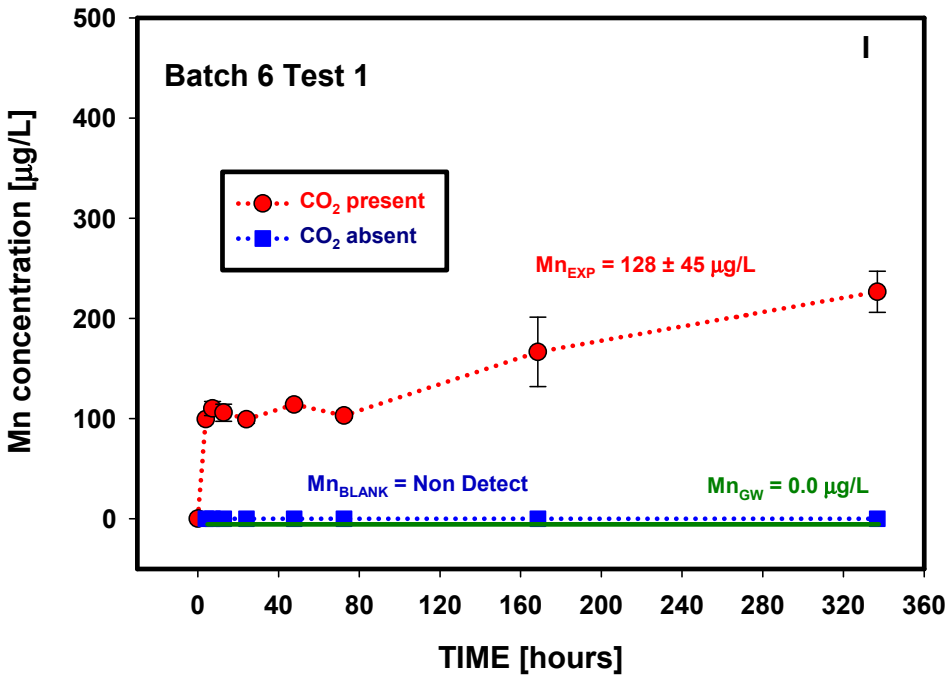

Figure D.16. (contd)

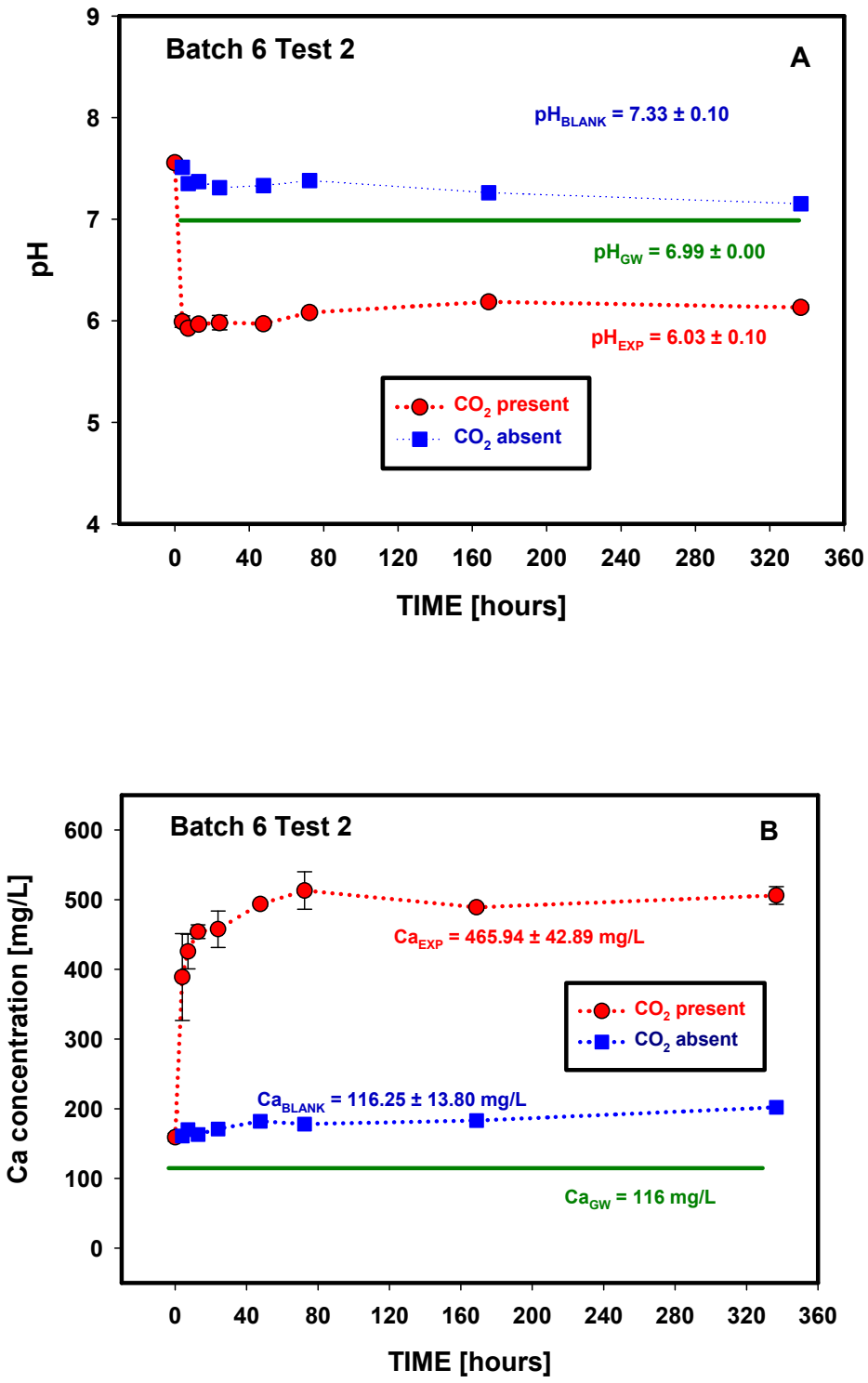

Figure D.17. Changes in pH and elemental composition as a function of time (Batch 6, Test 2, Edwards Aquifer Set A sample 4).

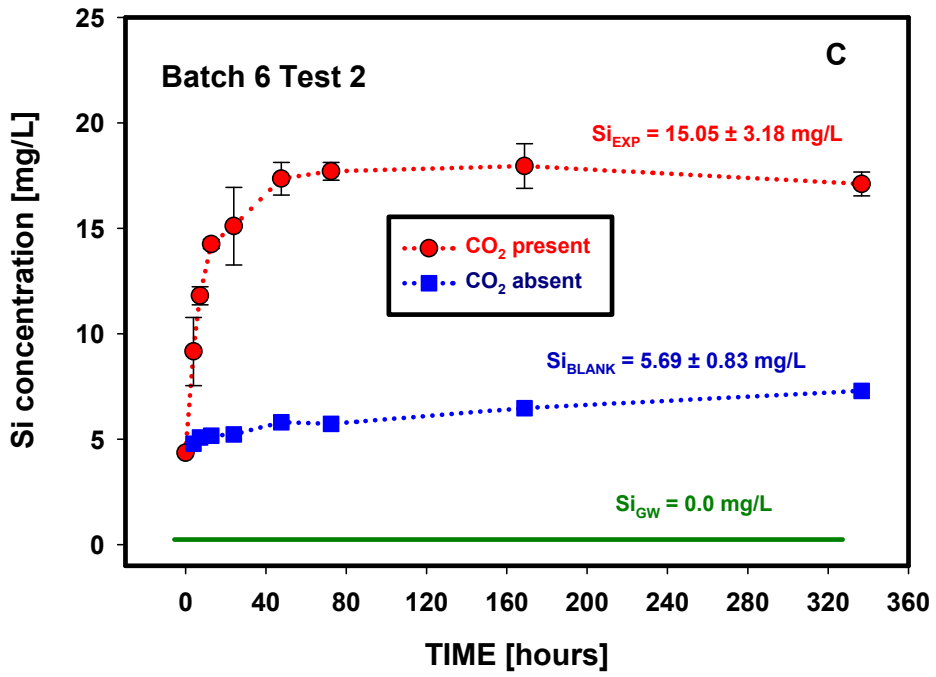

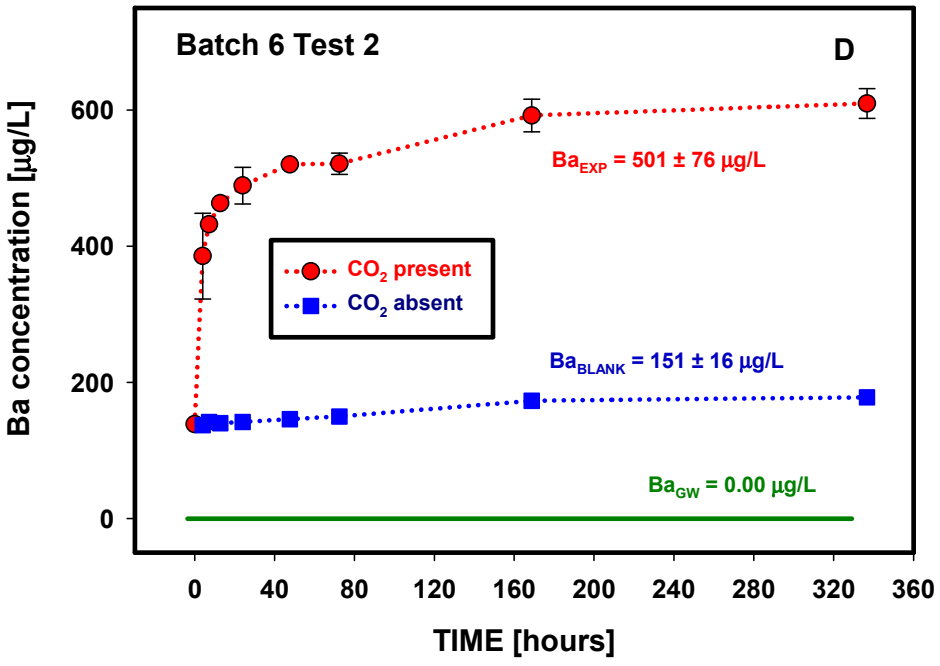

Figure D.17. (contd)

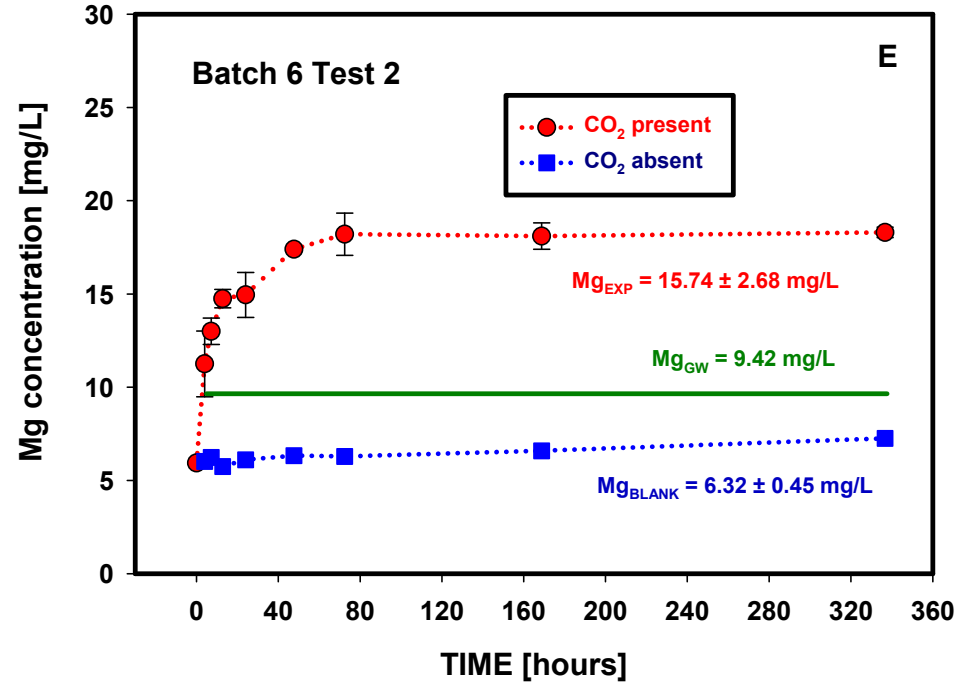

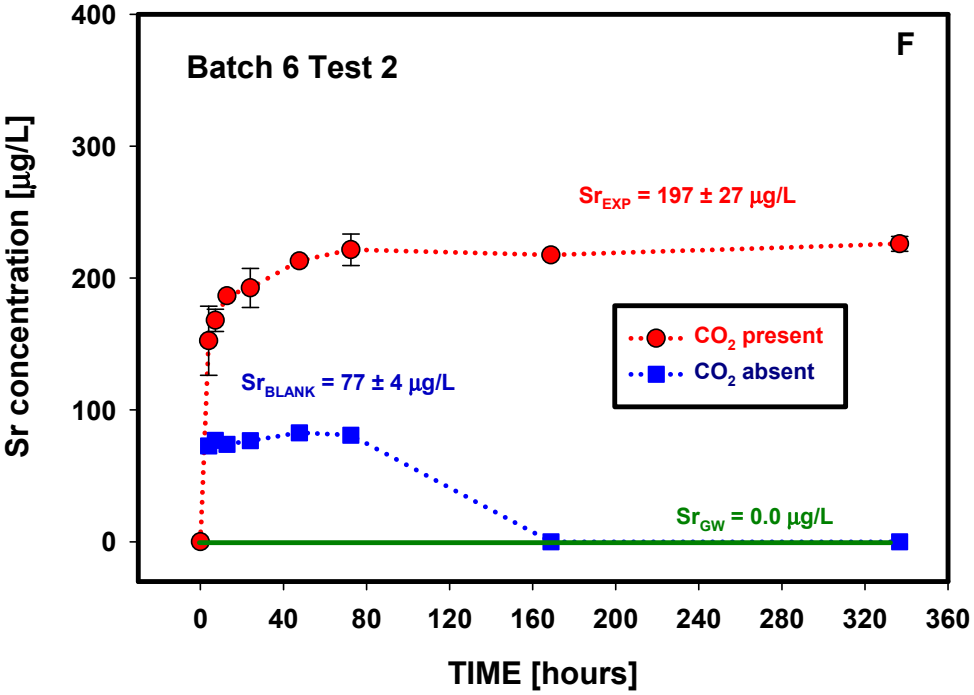

Figure D.17. (contd)

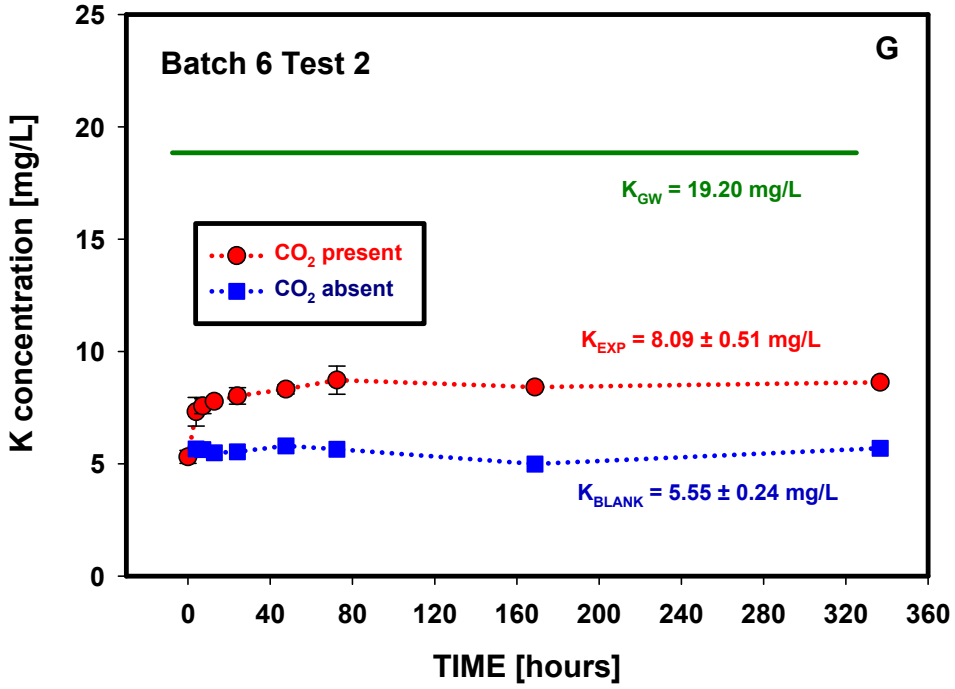

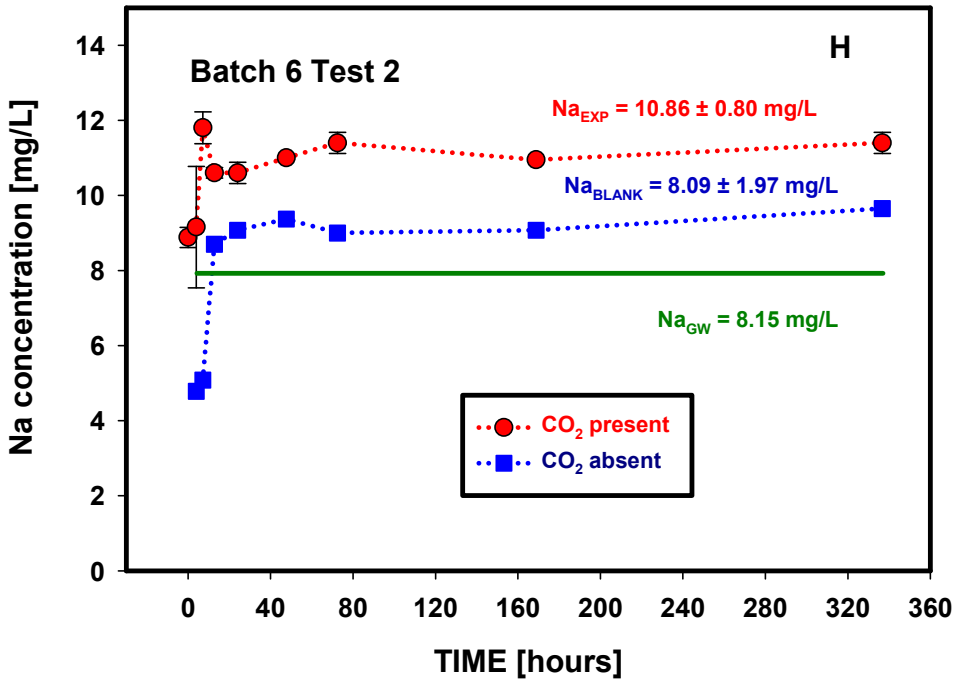

Figure D.17. (contd)

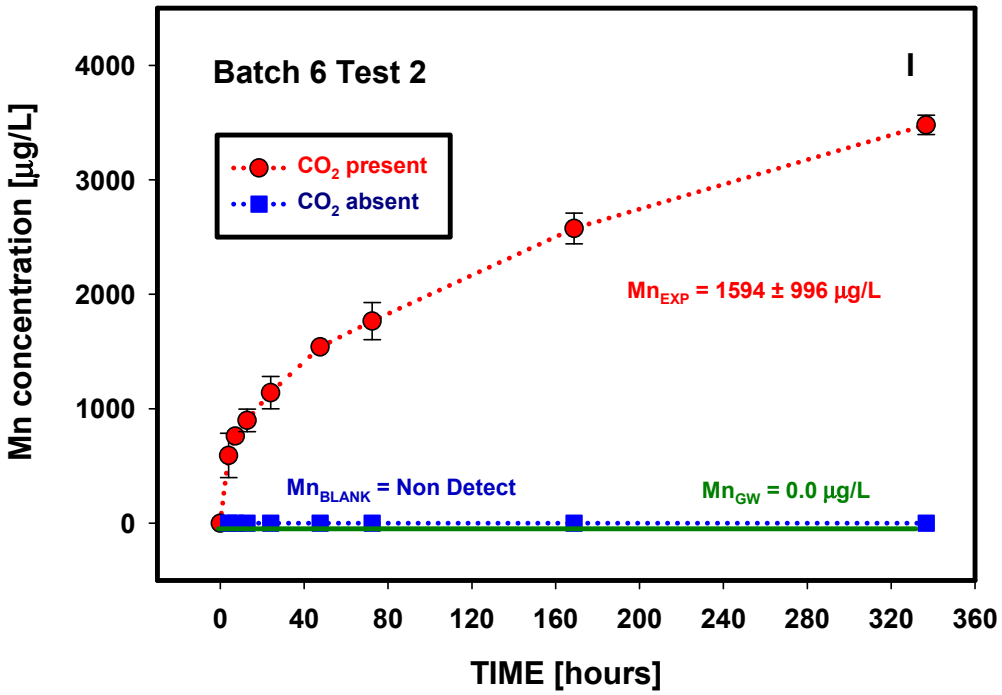

Figure D.17. (contd)

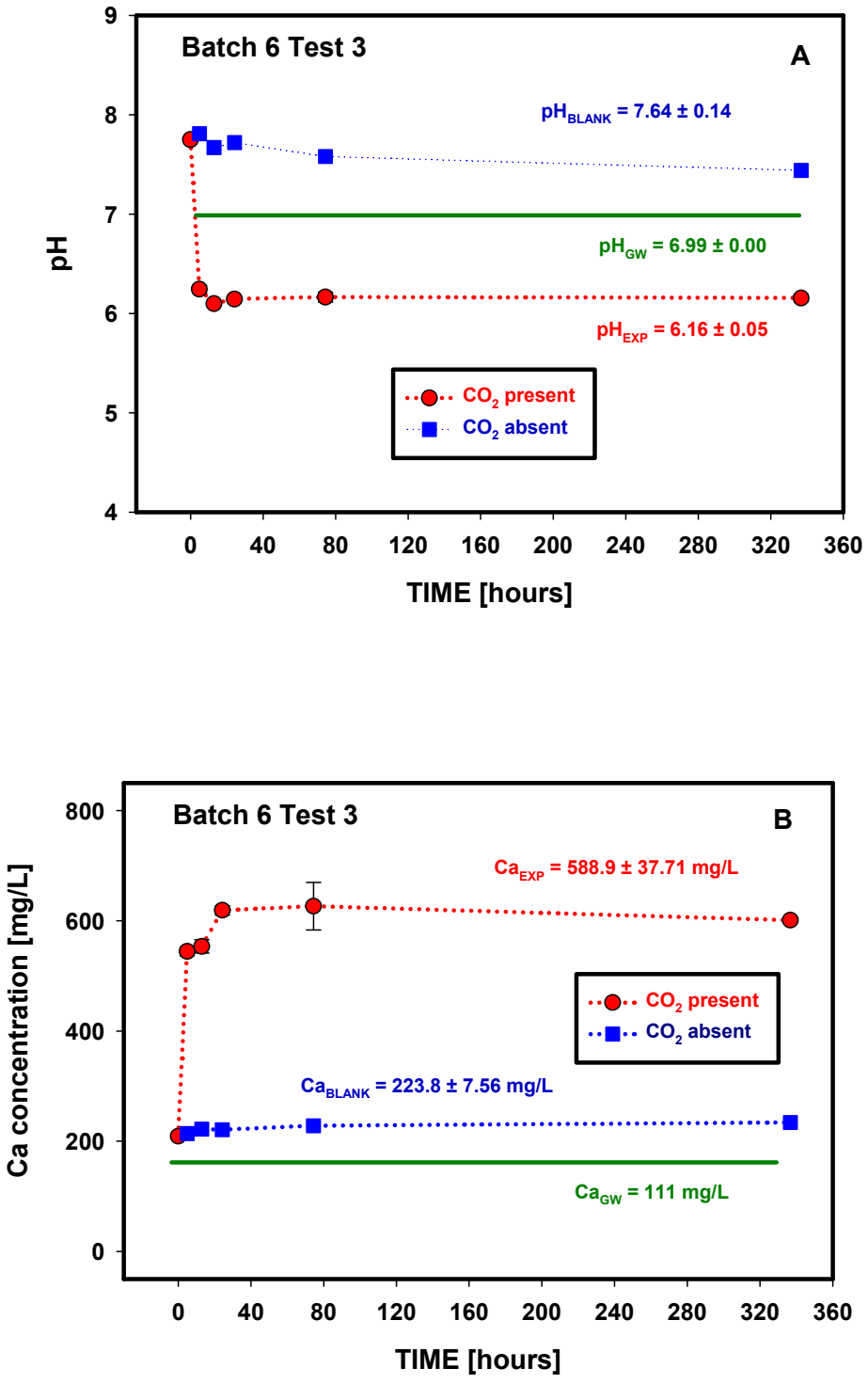

Figure D.18. Changes in pH and elemental composition as a function of time (Batch 6, Test 3, Edwards Aquifer Set A sample 6).

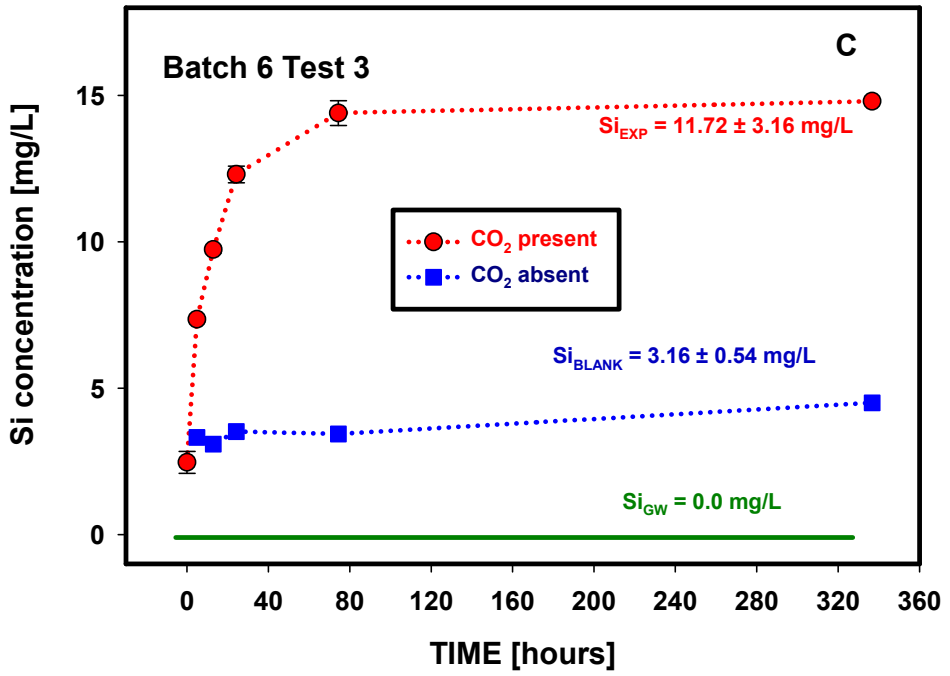

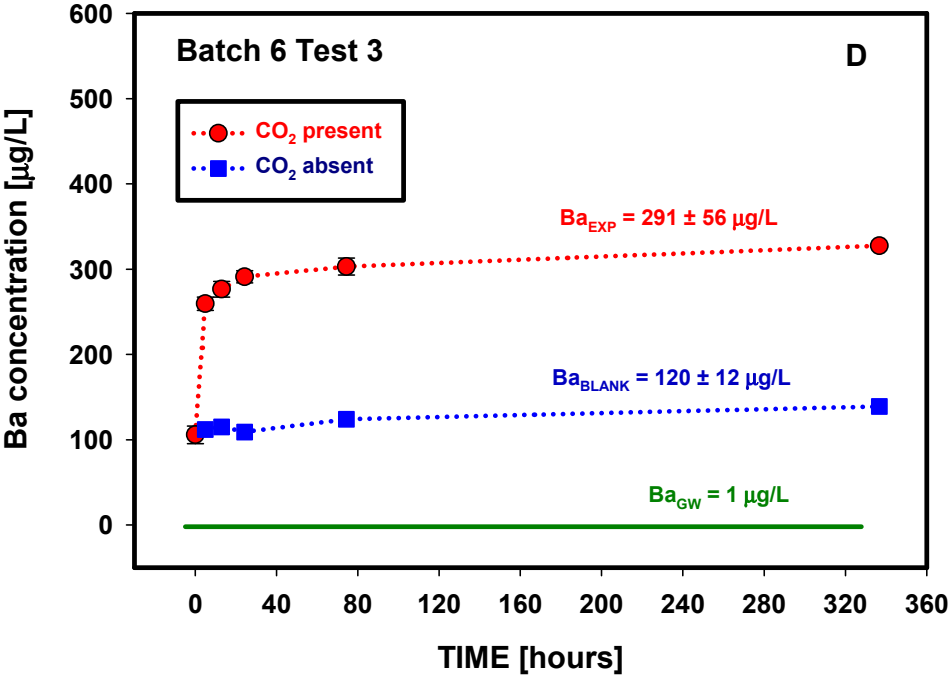

Figure D.18. (contd)

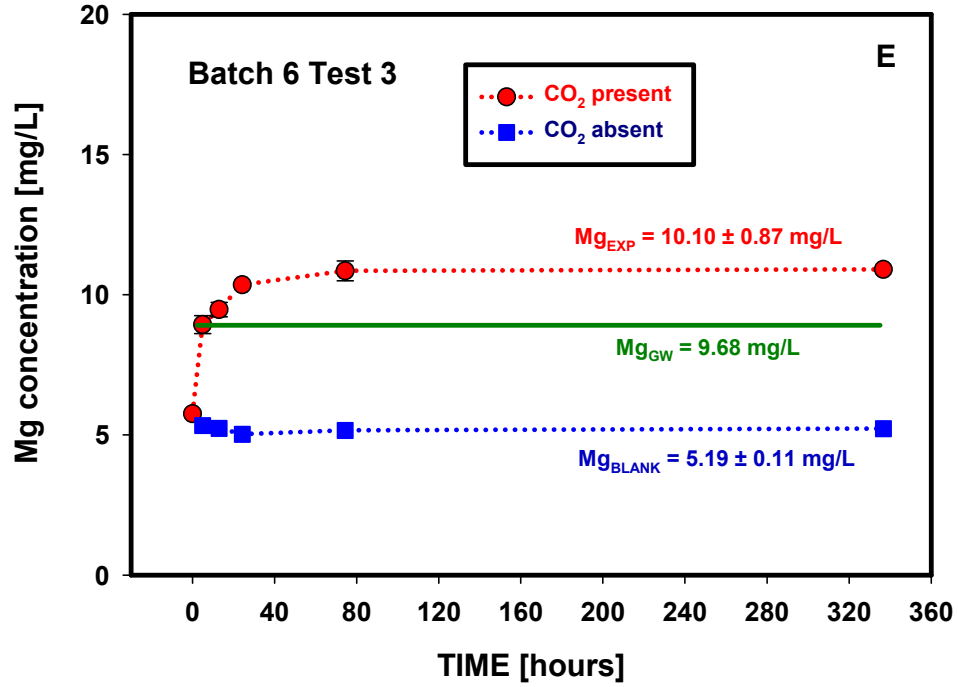

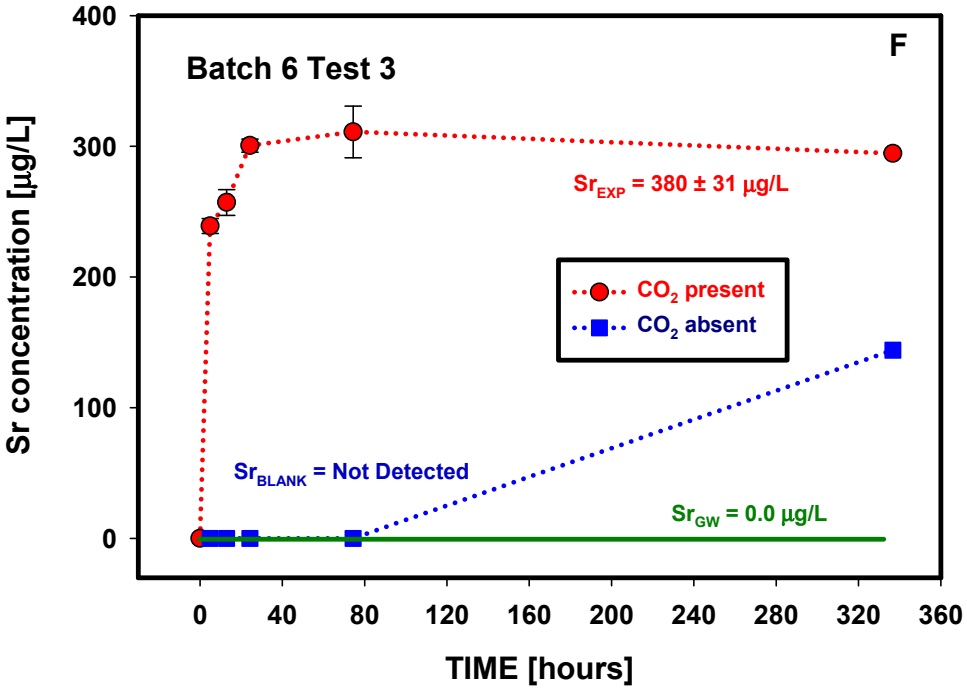

Figure D.18. (contd)

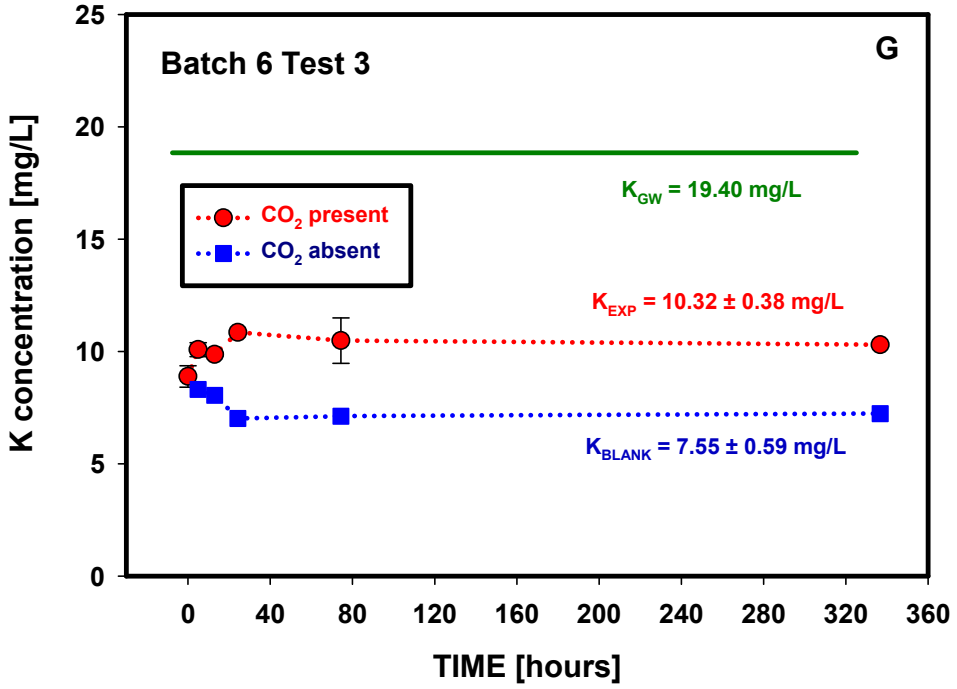

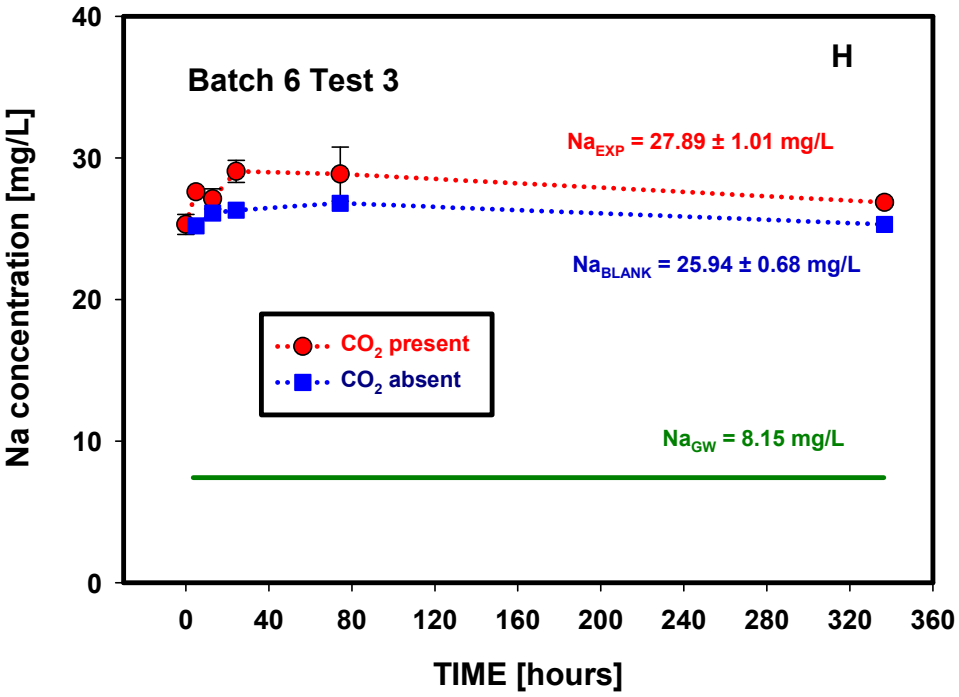

Figure D.18. (contd)

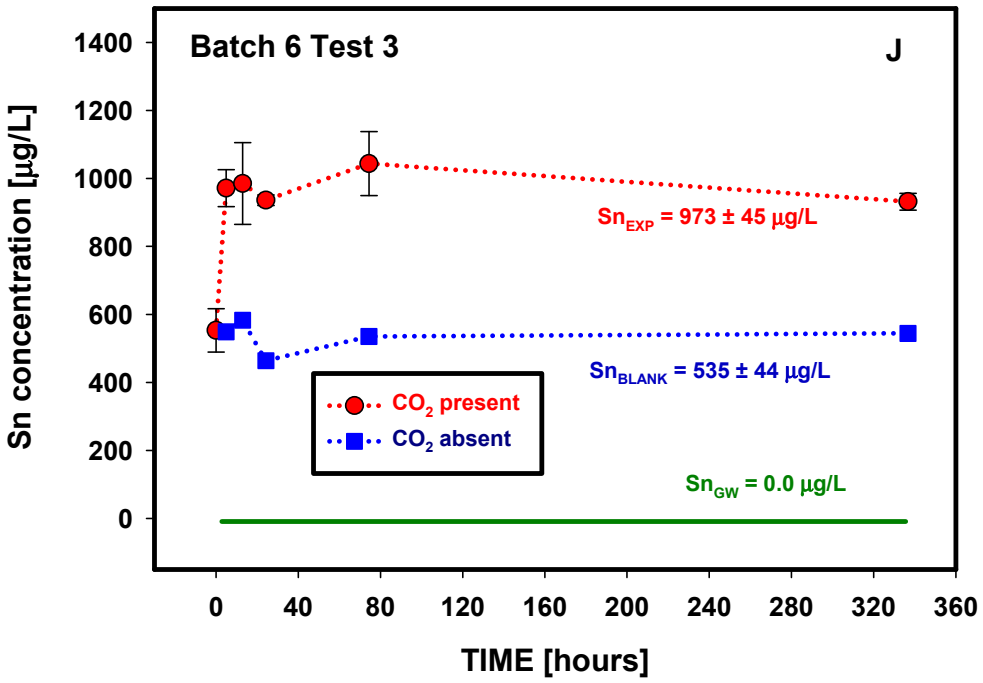

Figure D.18. (contd)

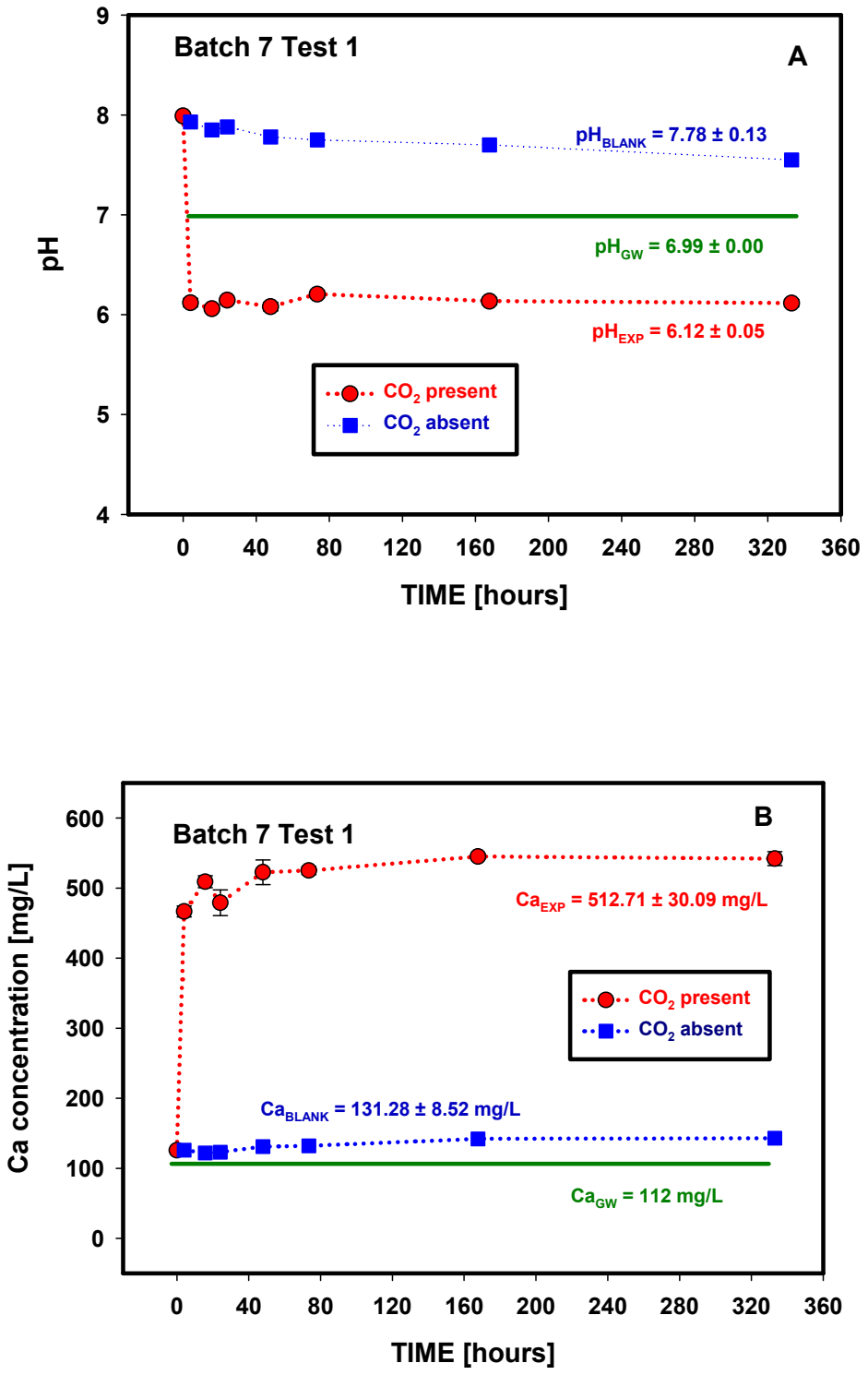

Figure D.19. Changes in pH and elemental composition as a function of time (Batch 7, Test 1, Edwards Aquifer Set A sample 1).

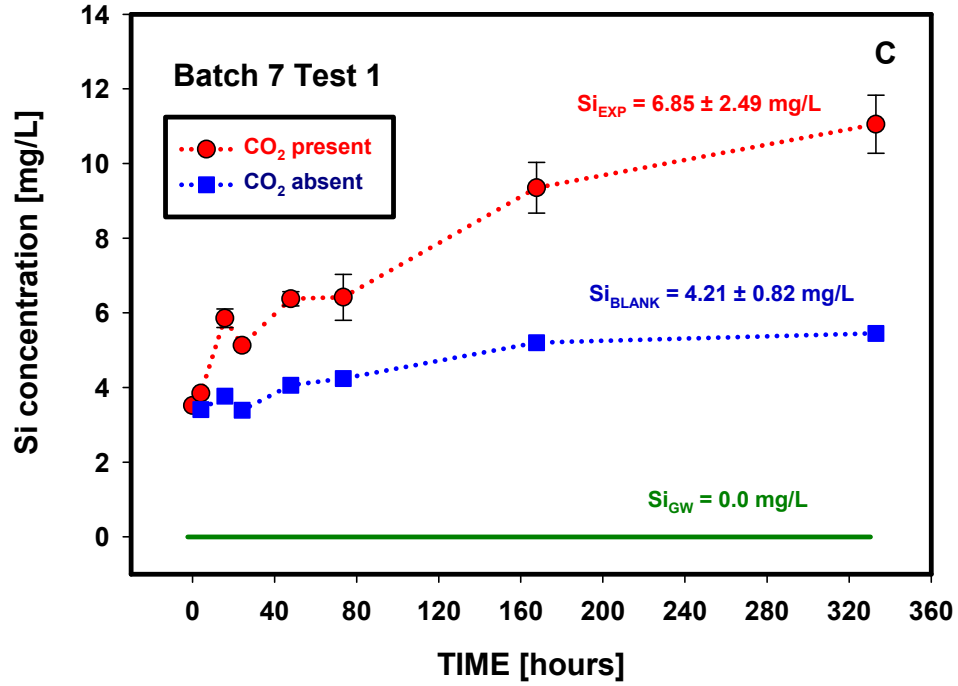

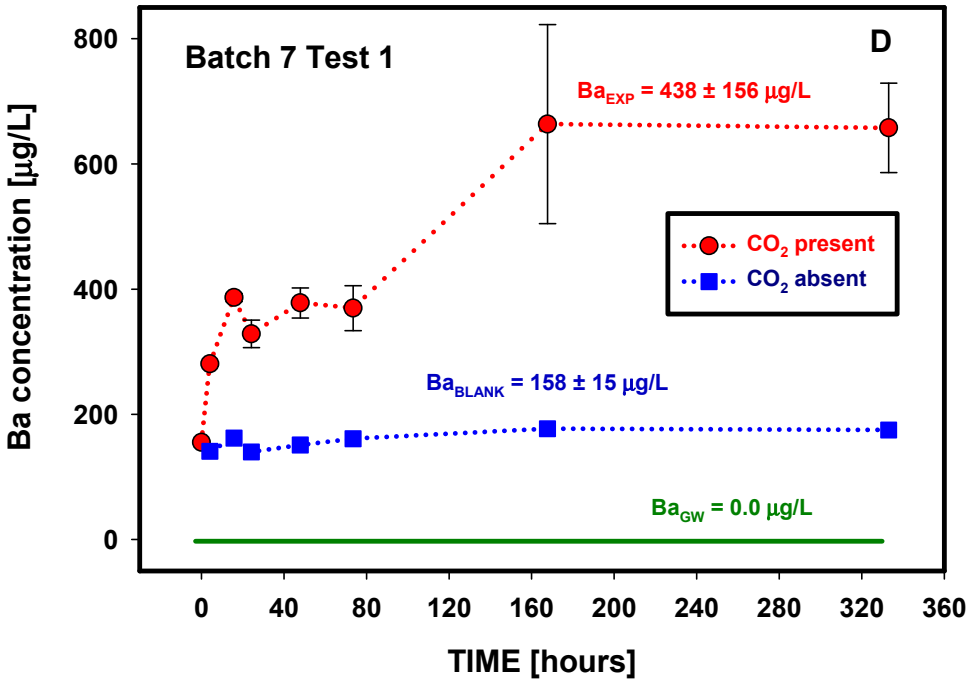

Figure D.19. (contd)

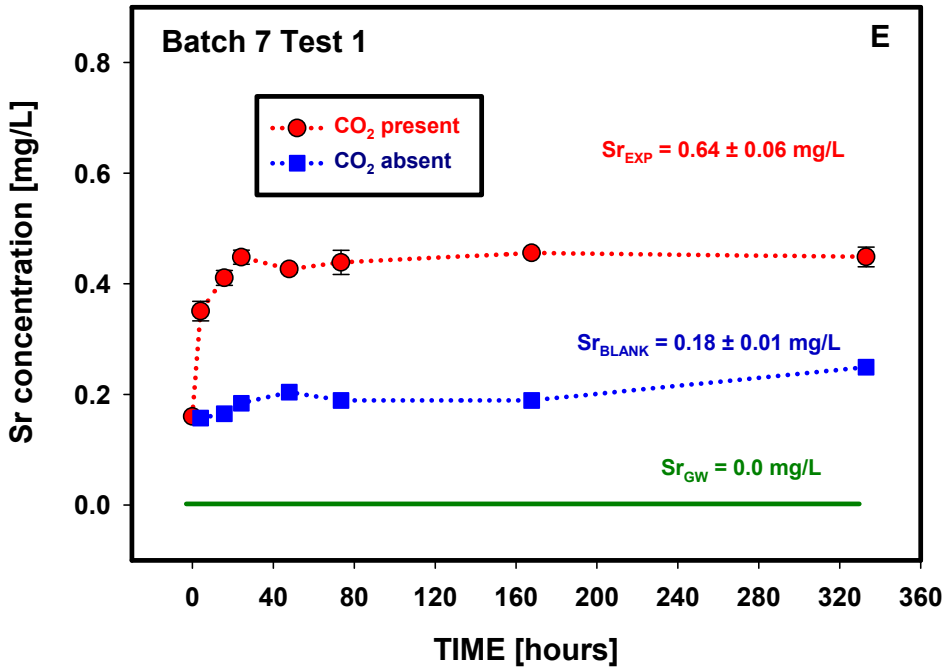

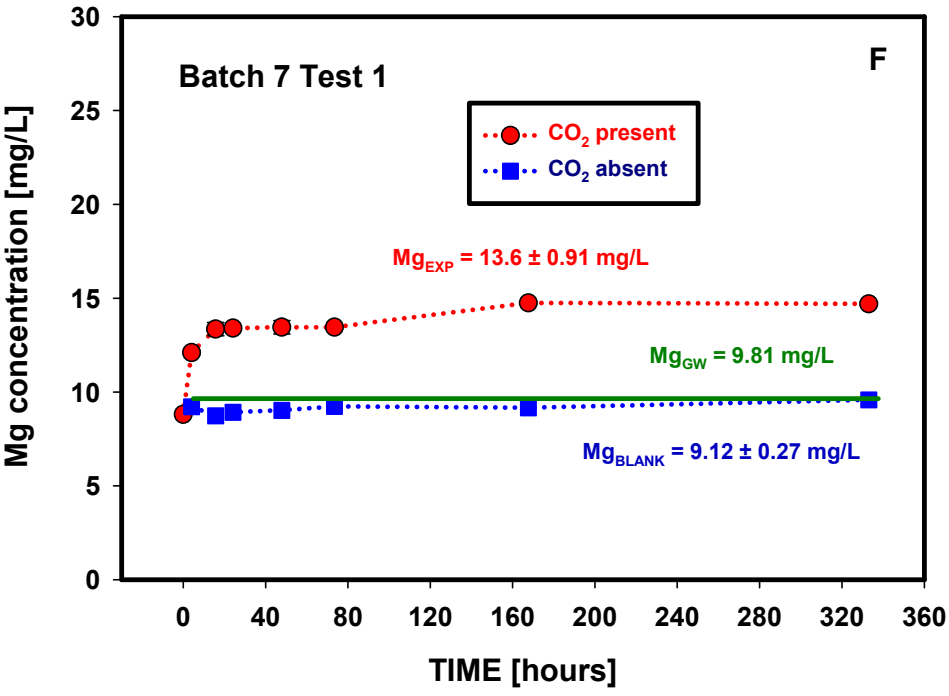

Figure D.19. (contd)

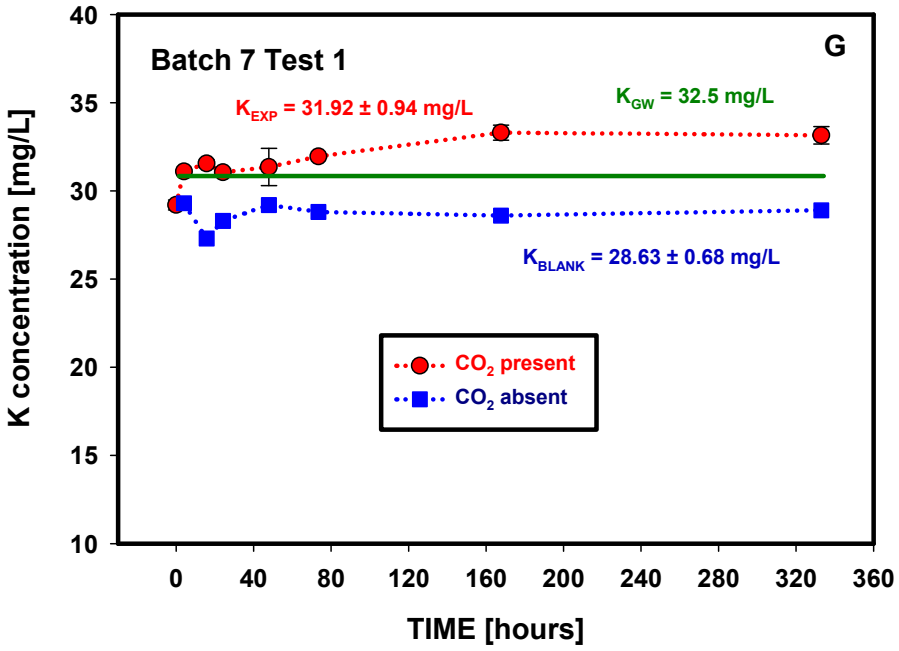

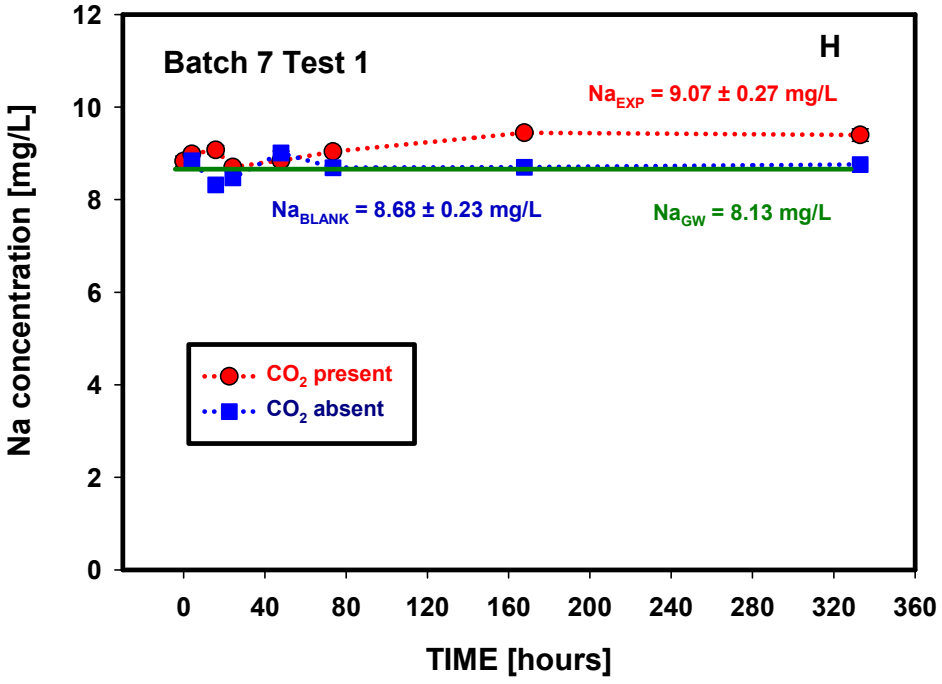

Figure D.19. (contd)

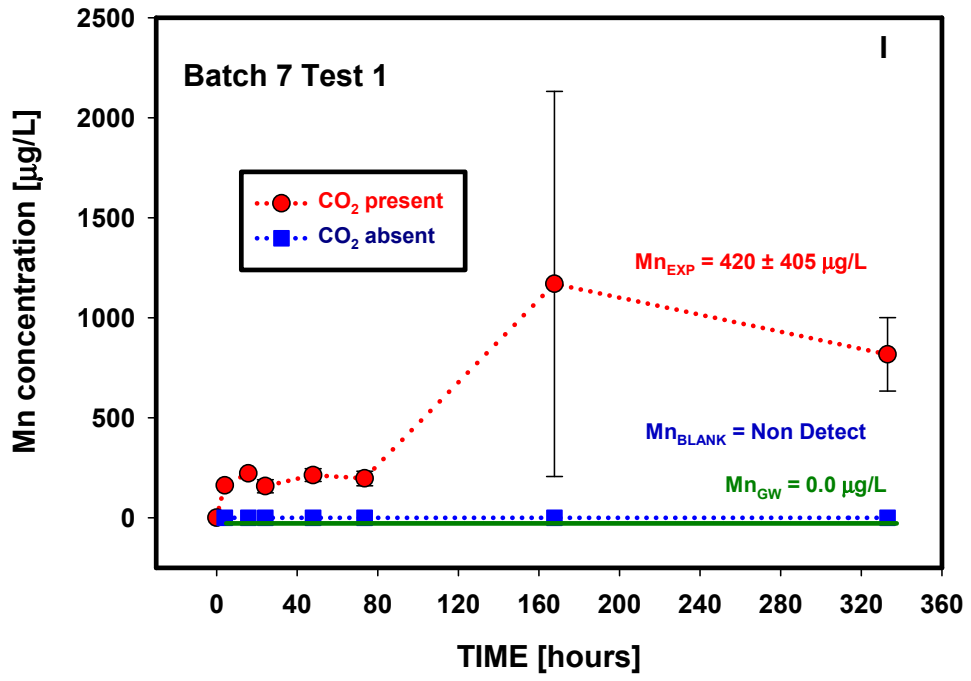

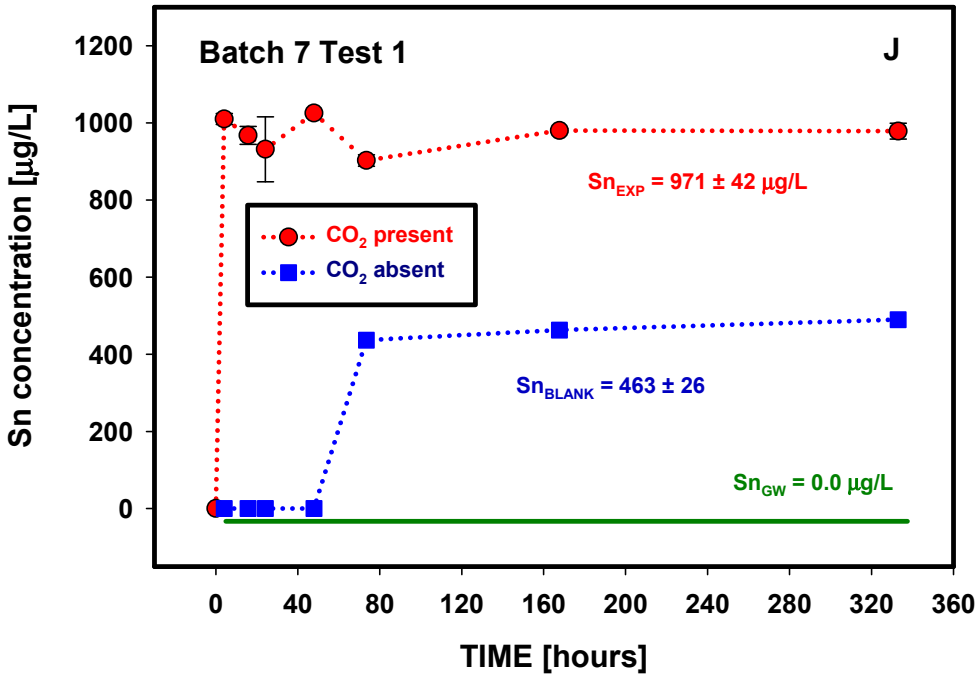

Figure D.19. (contd)

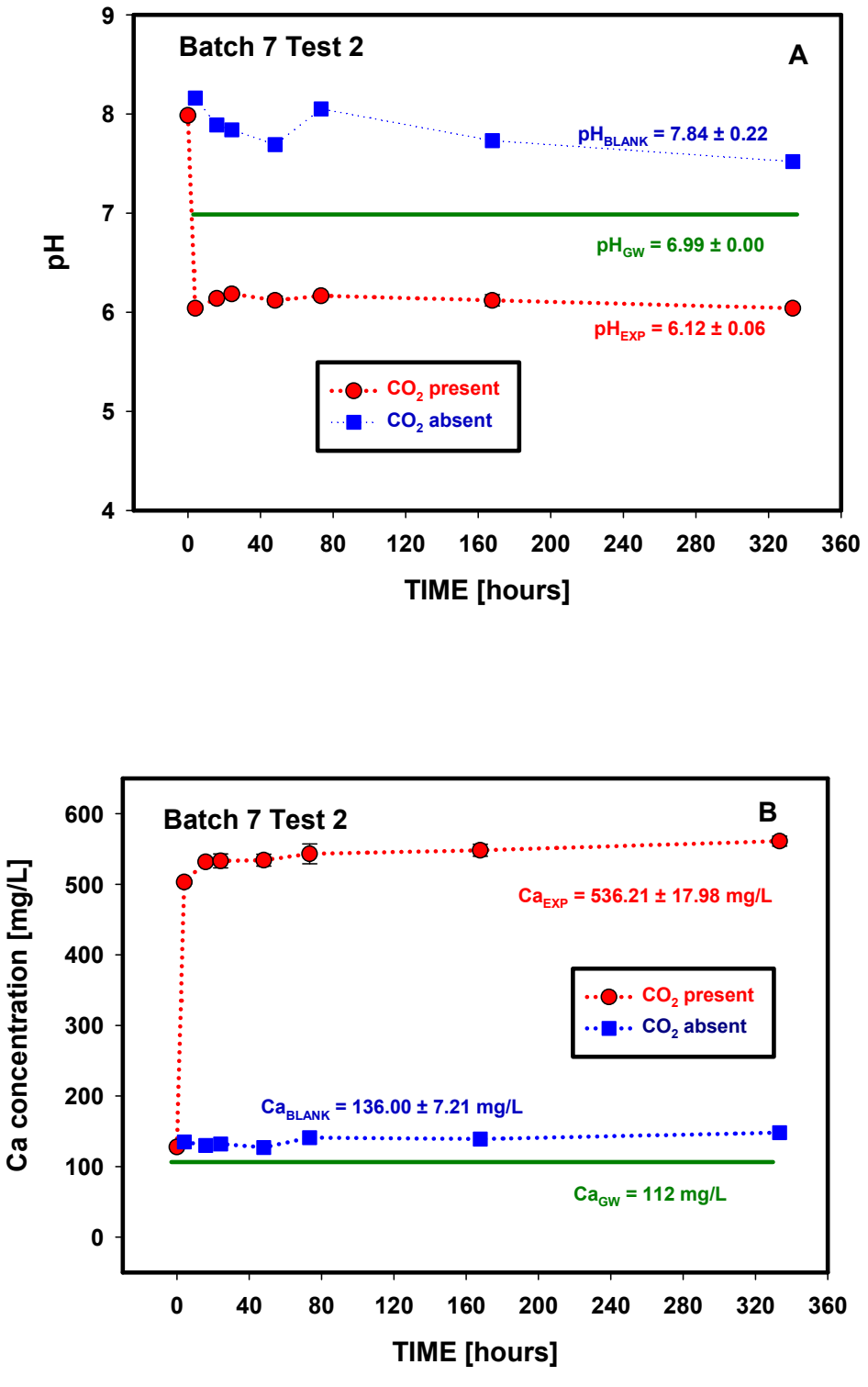

Figure D.20. Changes in pH and elemental composition as a function of time (Batch 7, Test 2, Edwards Aquifer Set A sample 1, 1:2 solid to solution ratio).

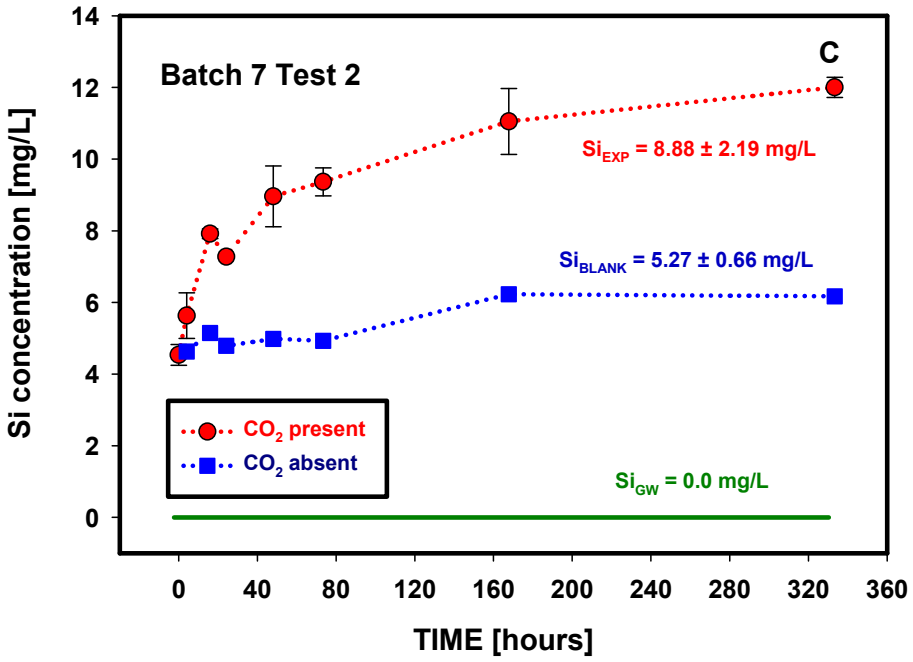

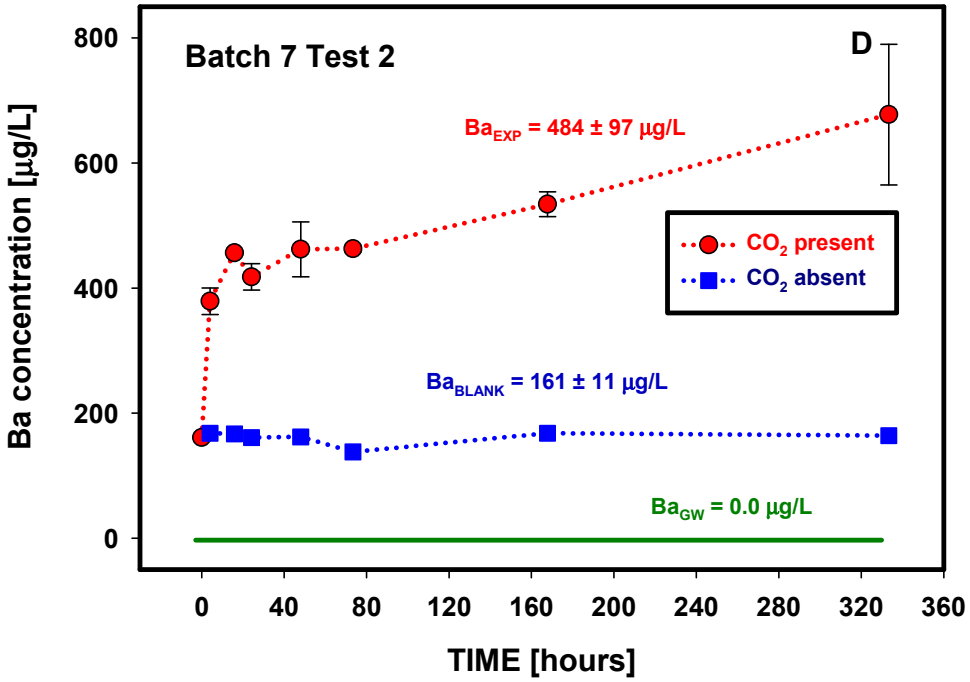

Figure D.20. (contd)

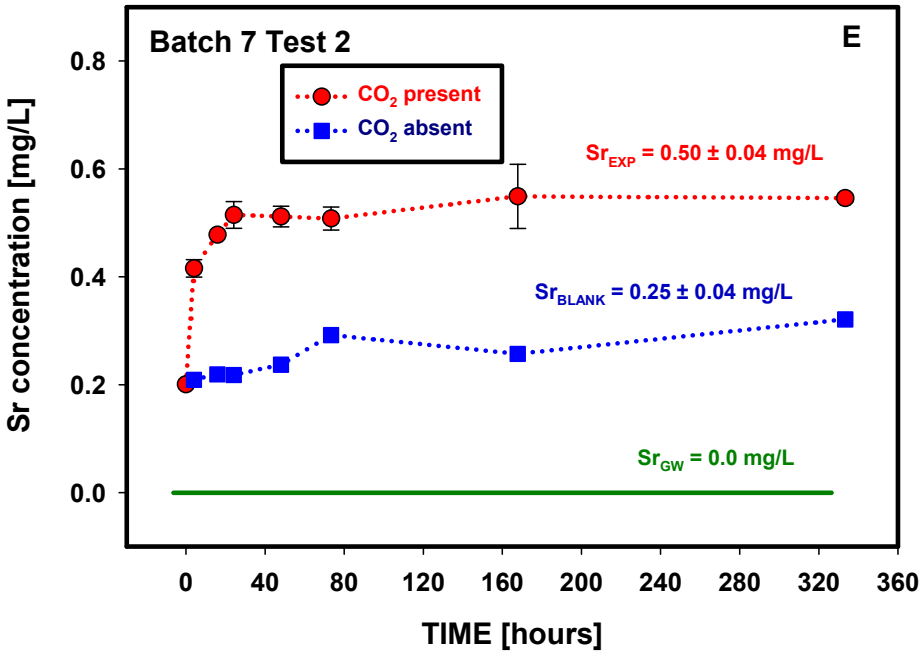

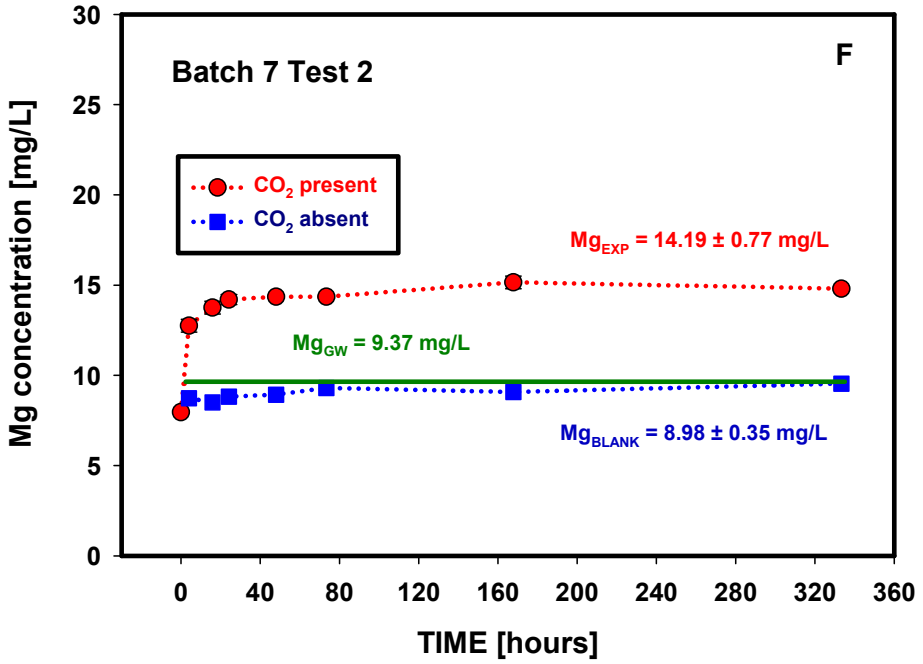

Figure D.20. (contd)

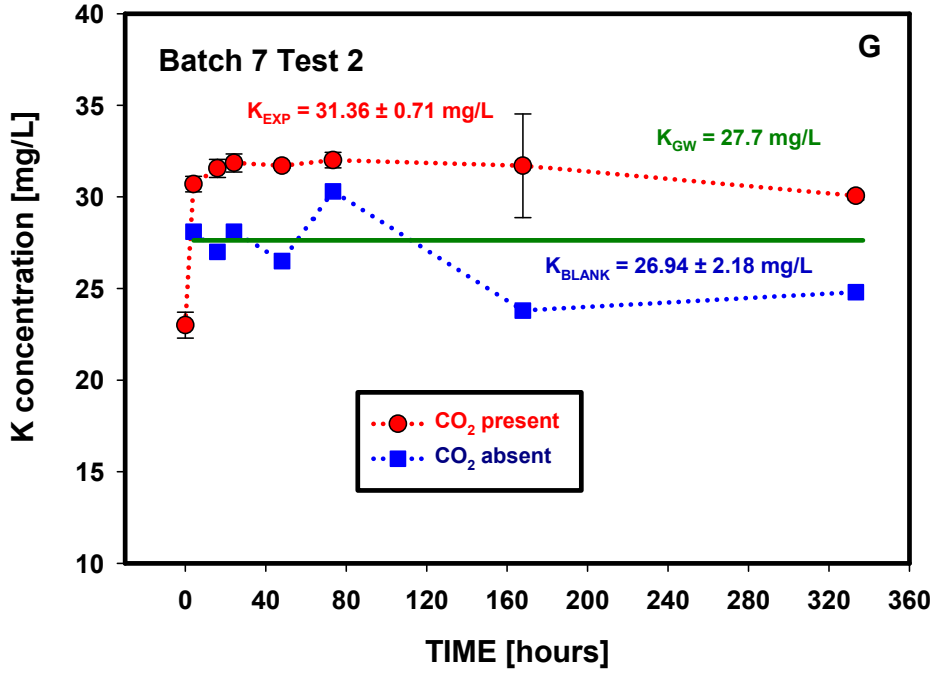

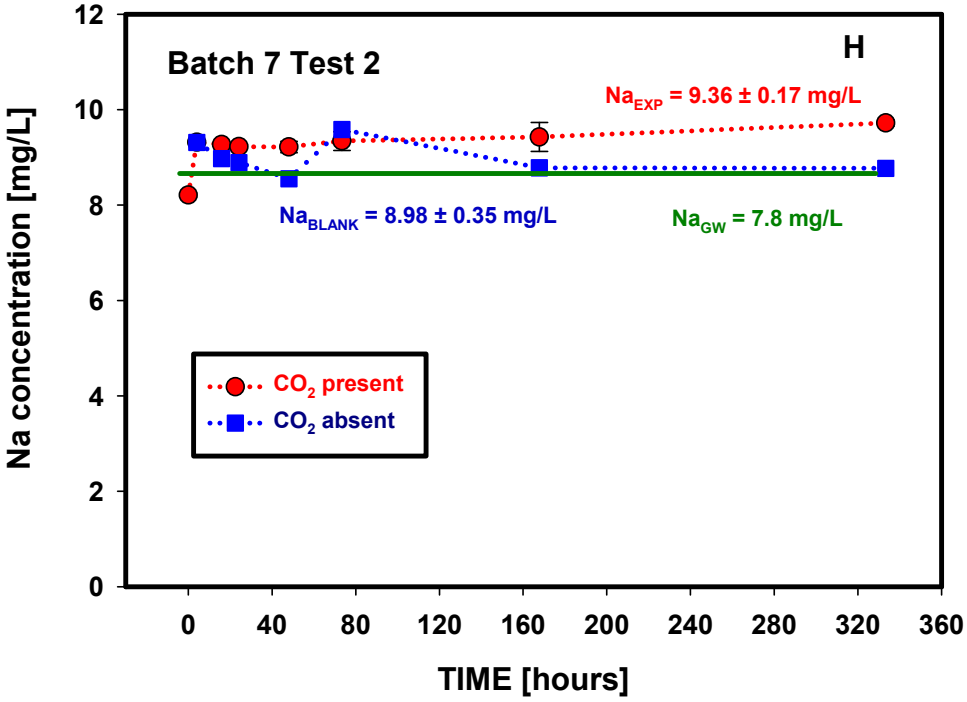

Figure D.20. (contd)

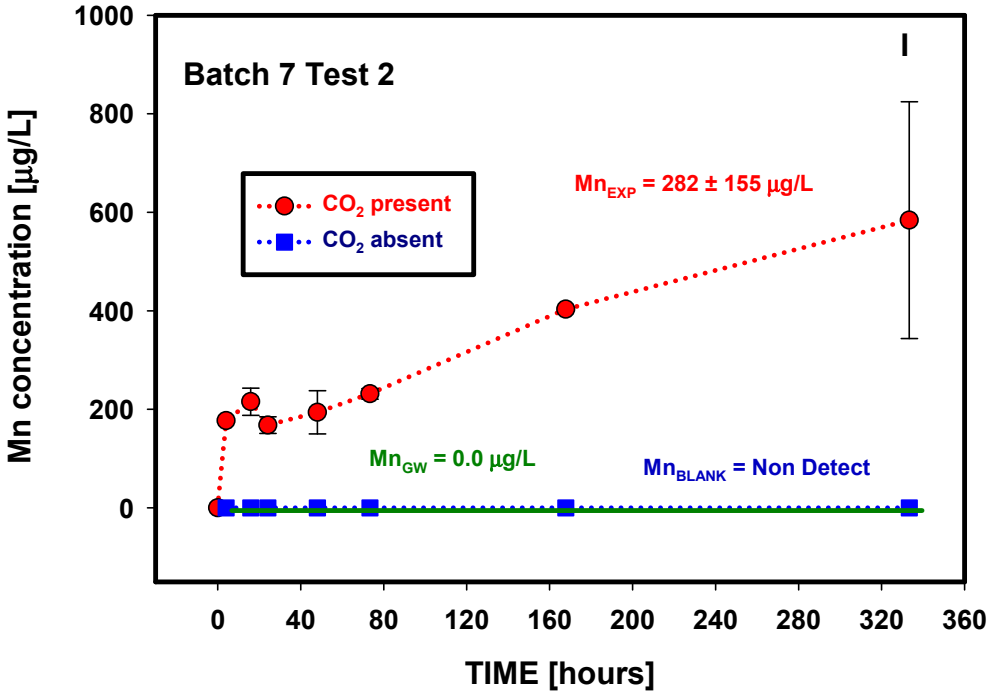

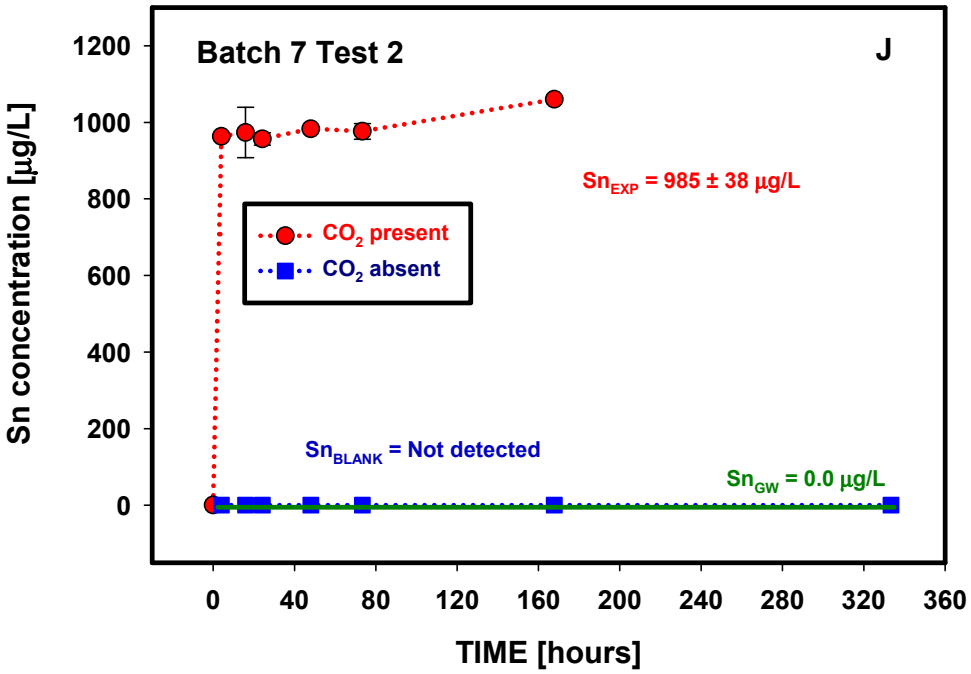

Figure D.20. (contd)

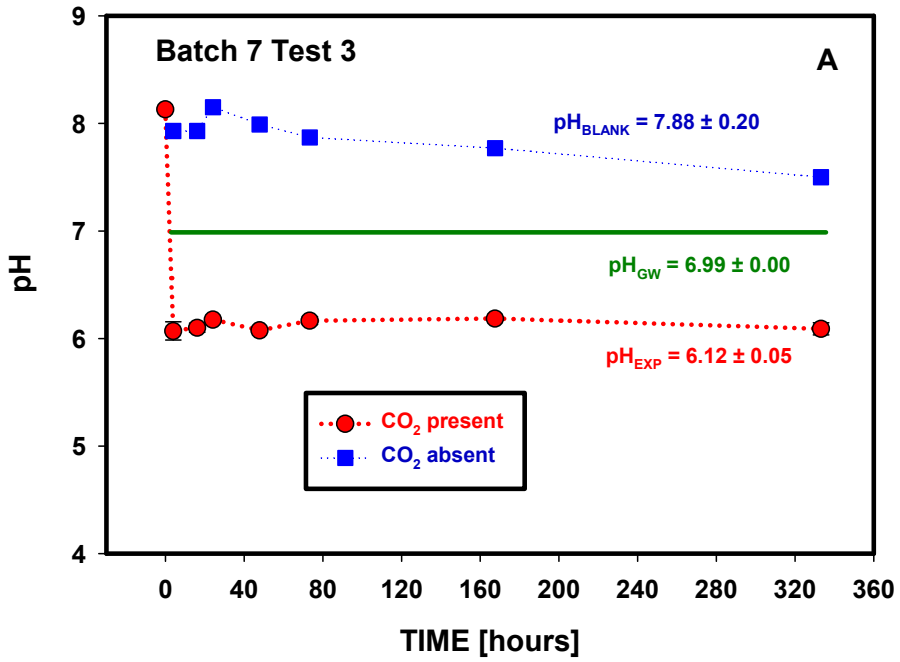

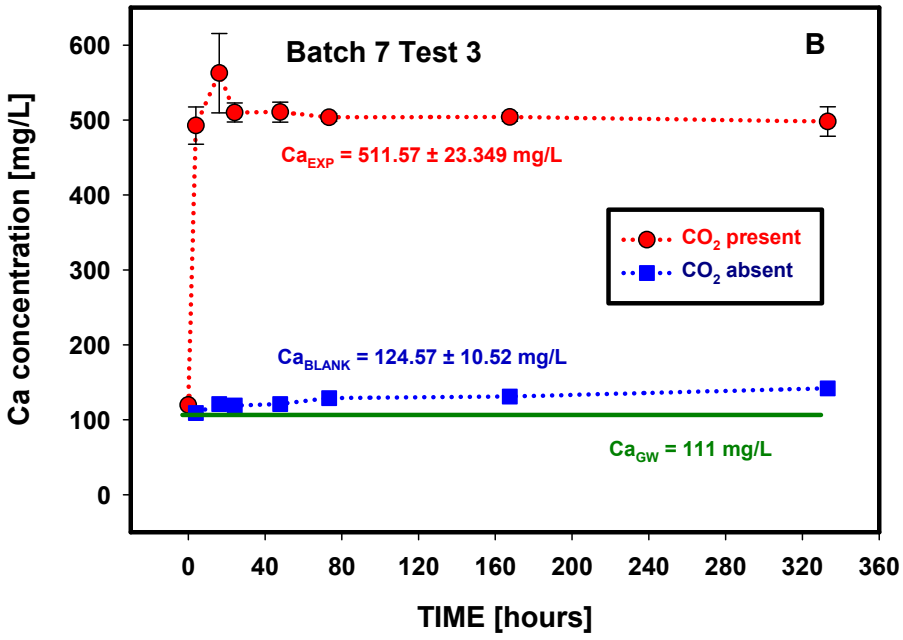

Figure D.21. Changes in pH and elemental composition as a function of time (Batch 7, Test 3, Edwards Aquifer Set B sample 4, 1:2 solid to solution ratio).

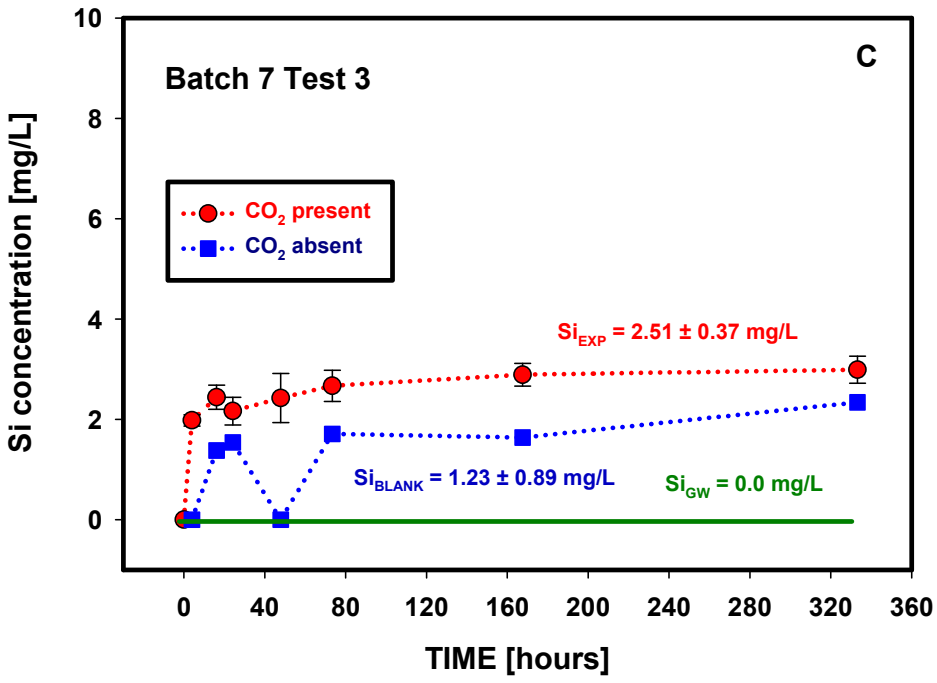

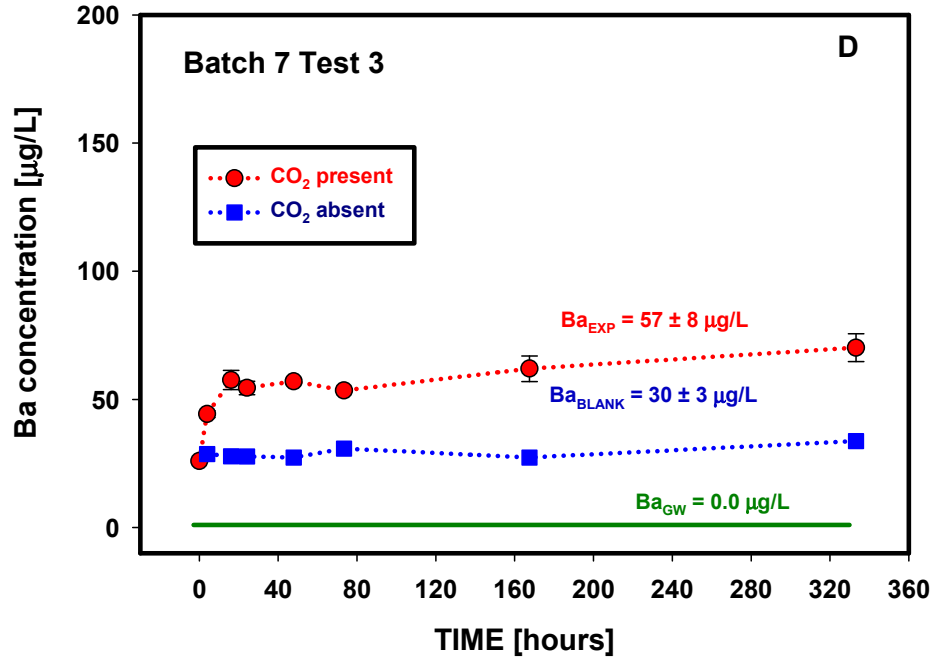

Figure D.21. (contd)

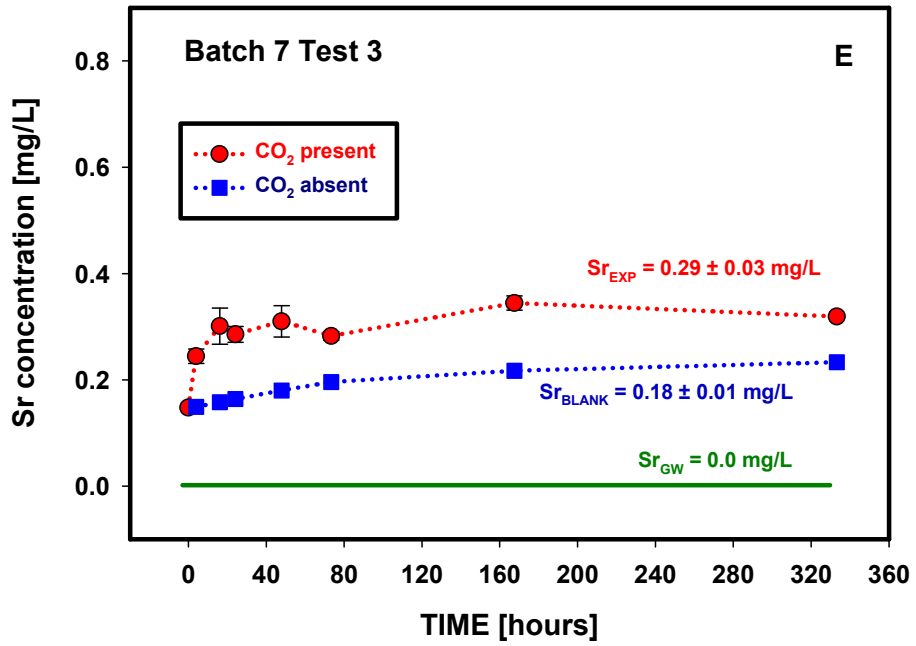

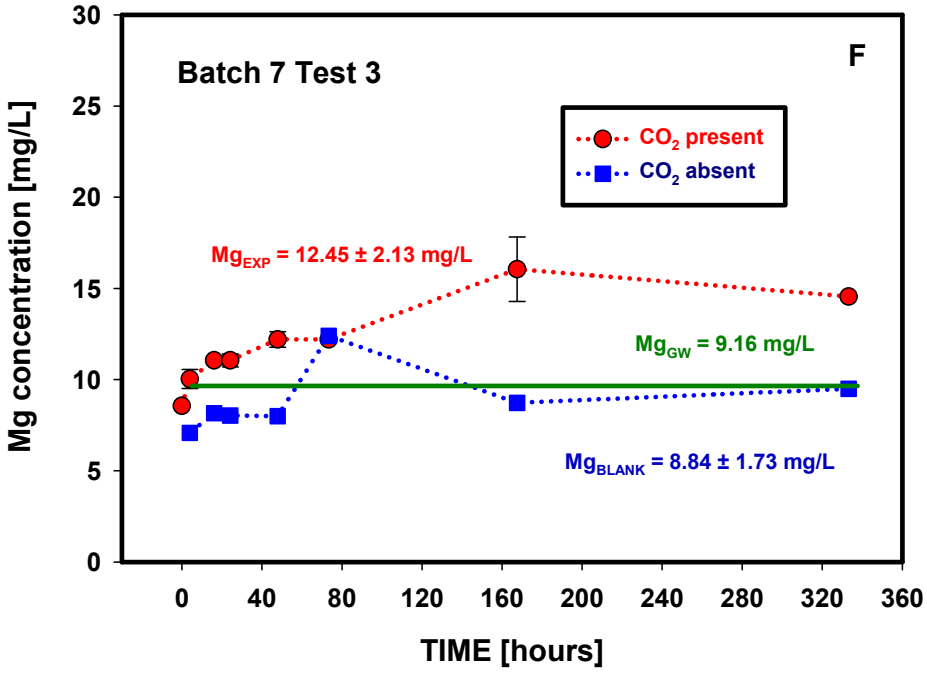

Figure D.21. (contd)

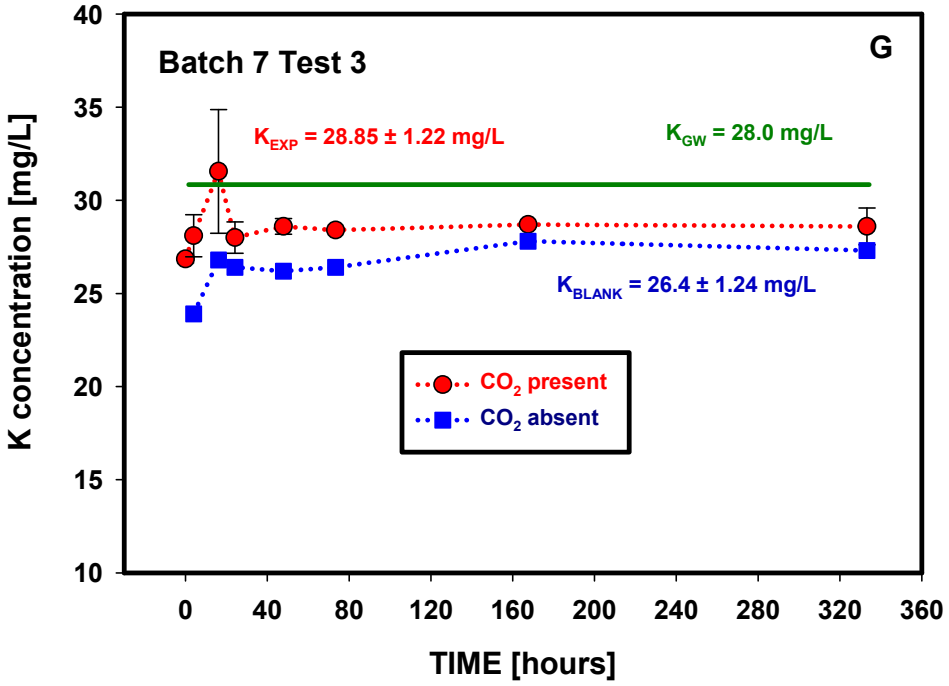

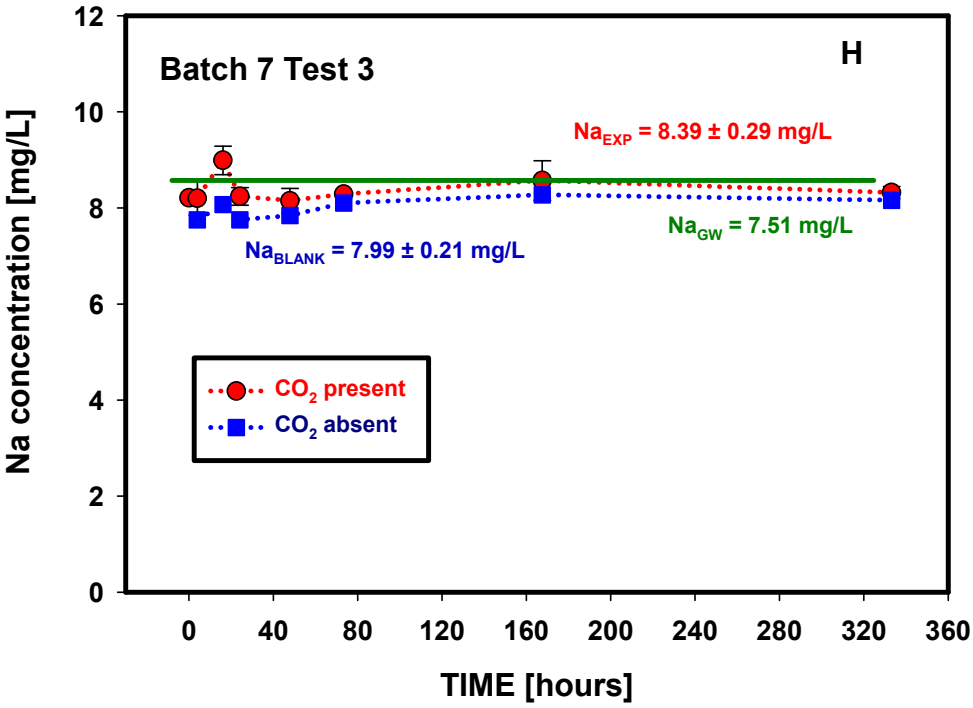

Figure D.21. (contd)

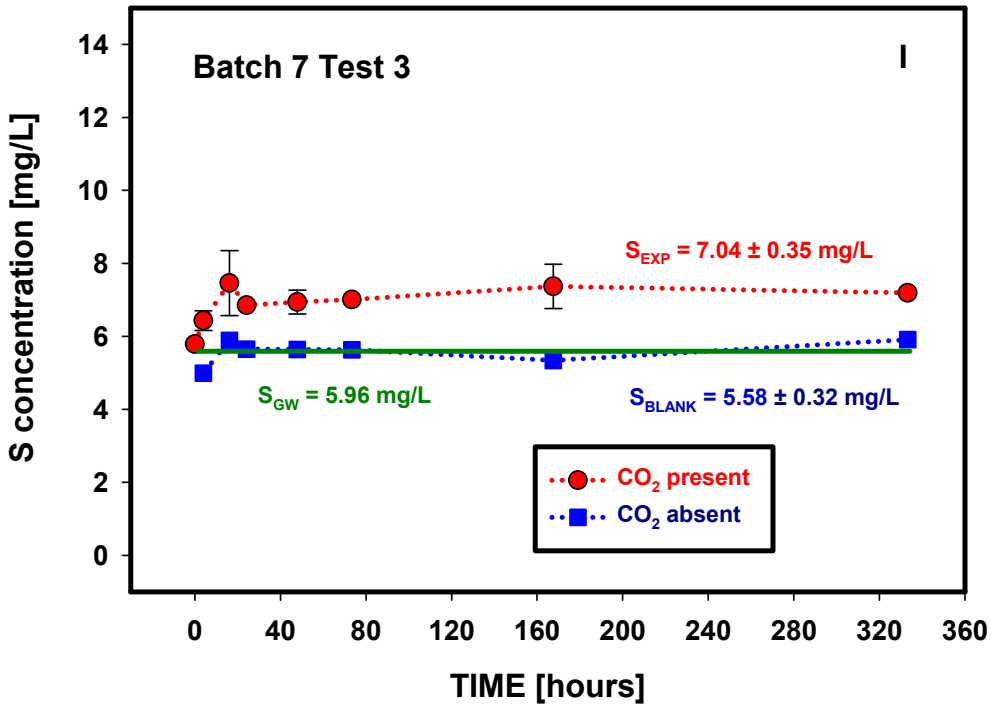

Figure D.21. (contd)

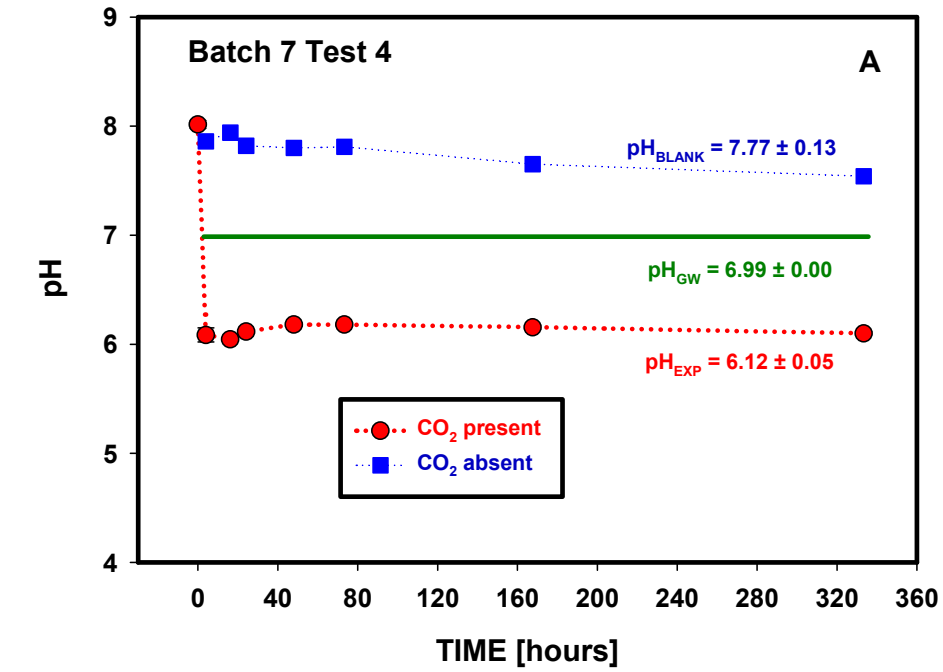

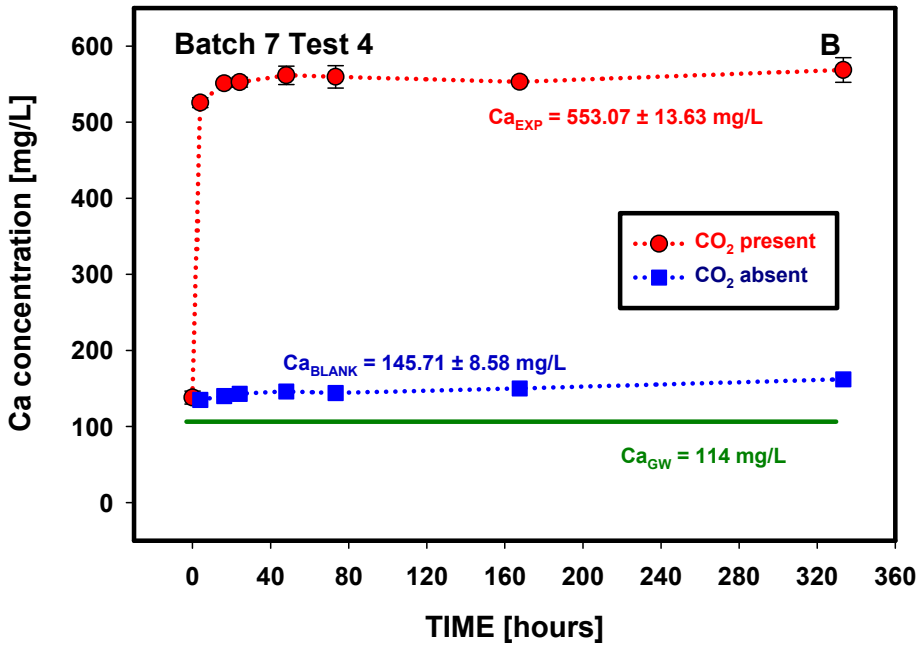

Figure D.22. Changes in pH and elemental composition as a function of time (Batch 7, Test 4, Edwards Aquifer Set B sample 7, 1:2 solid to solution ratio).

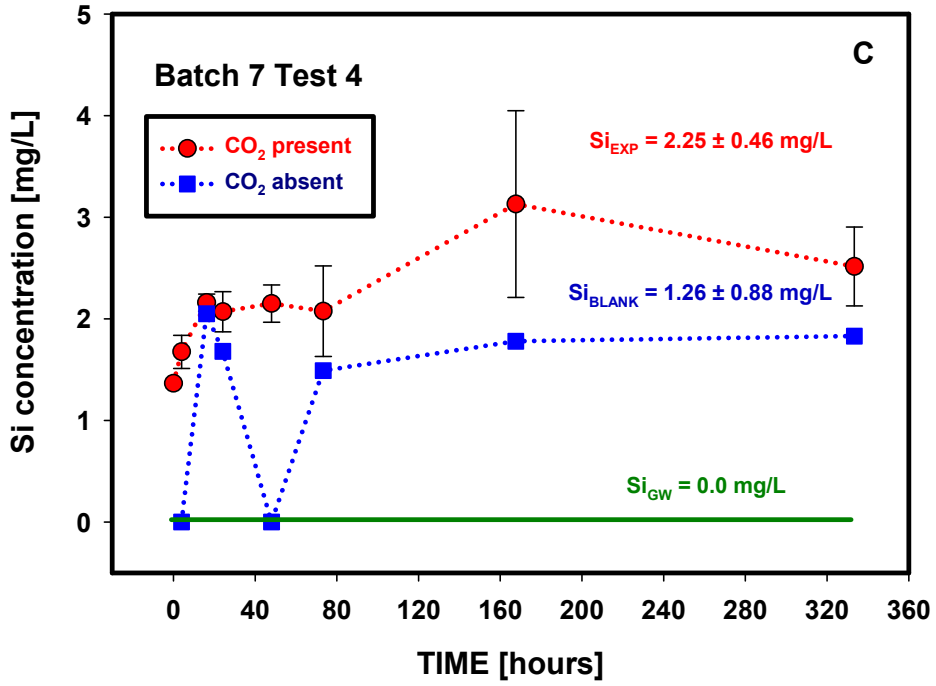

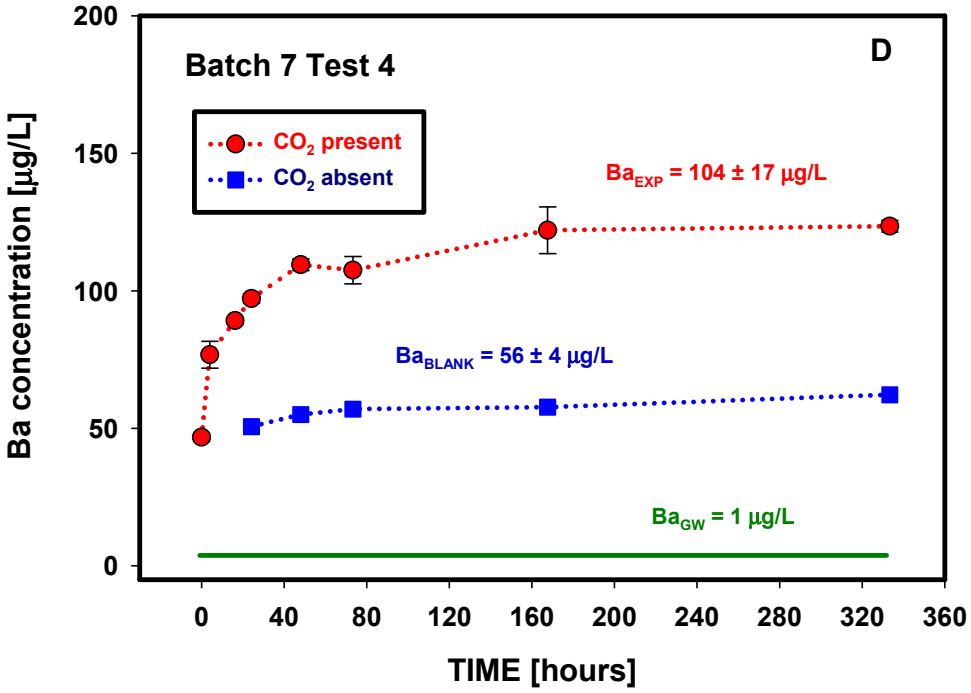

Figure D.22. (contd)

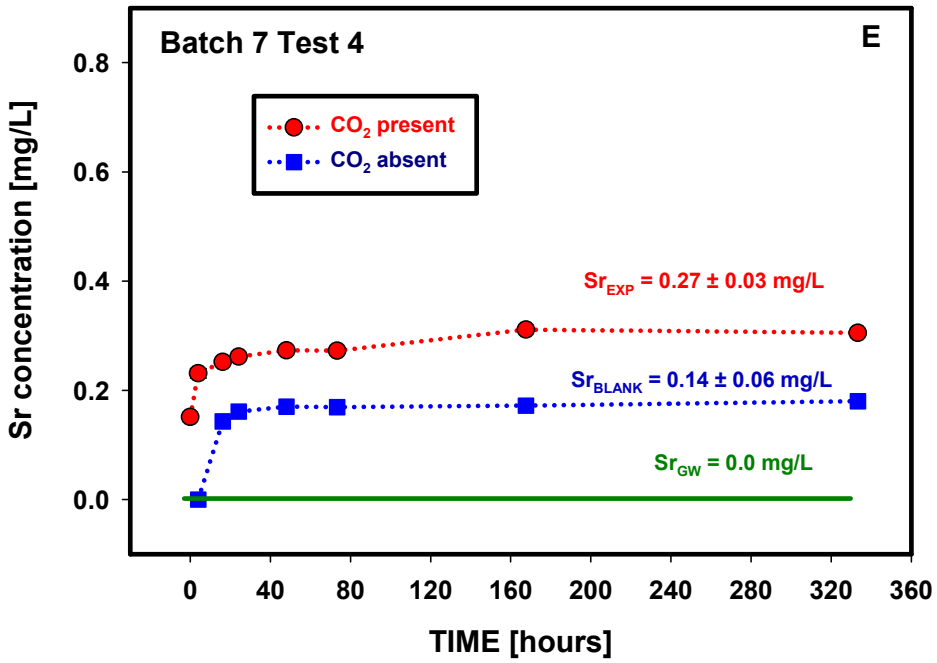

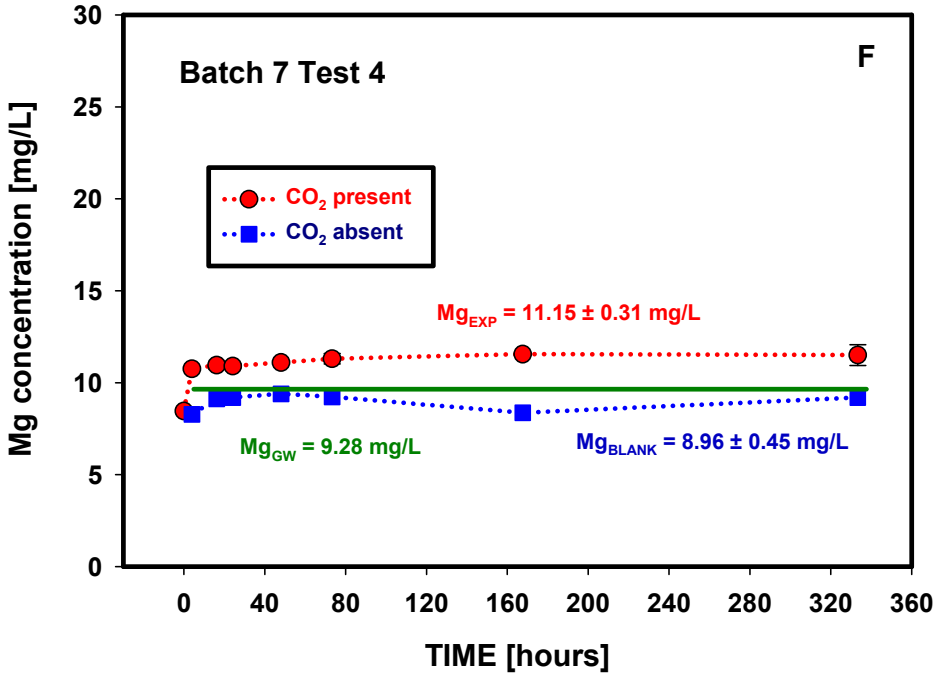

Figure D.22. (contd)

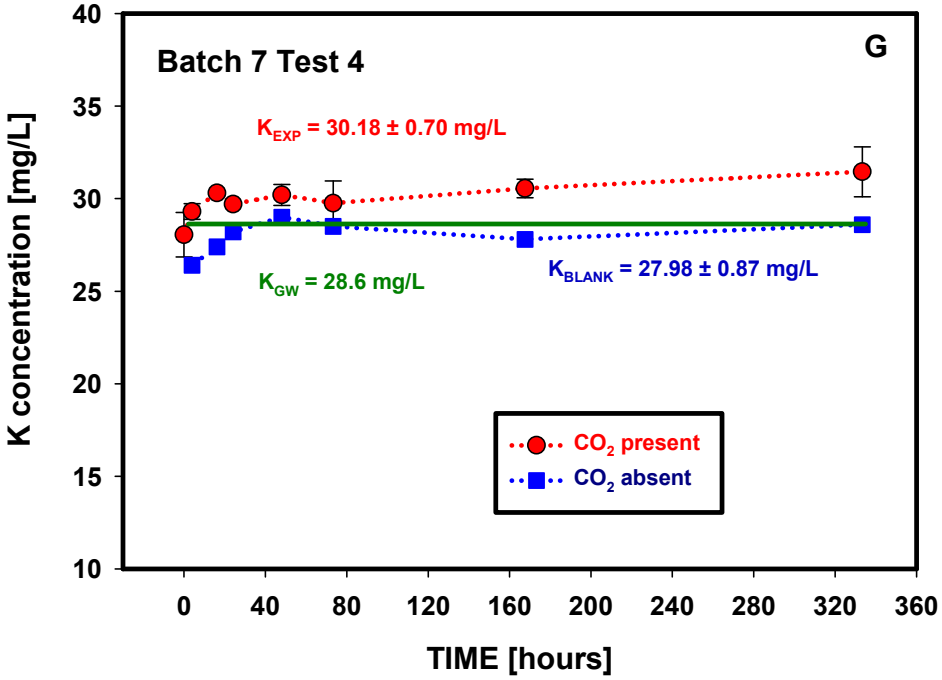

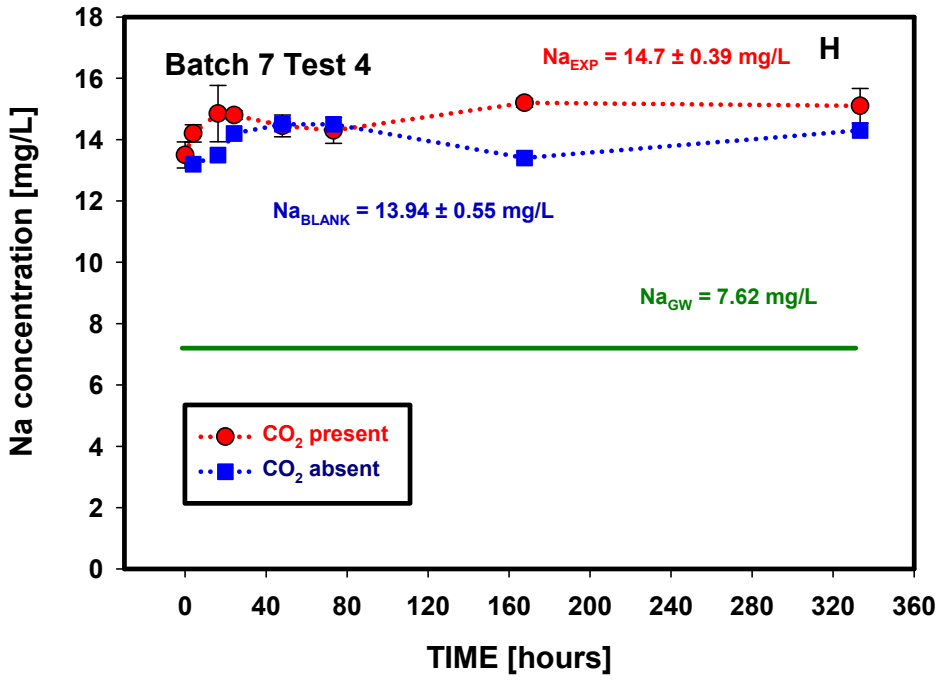

Figure D.22. (contd)

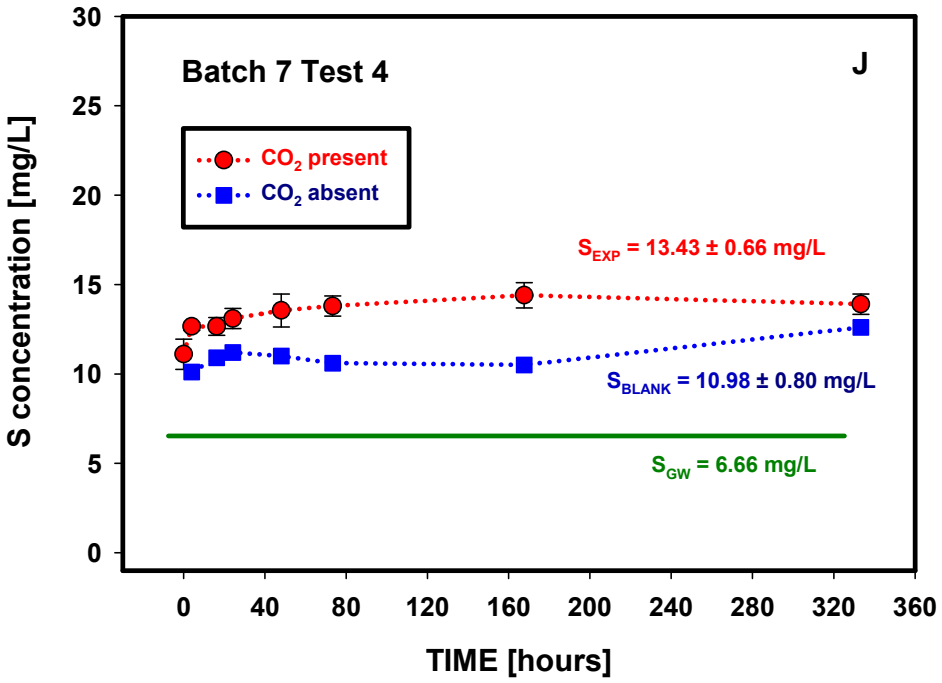

Figure D.22. (contd)

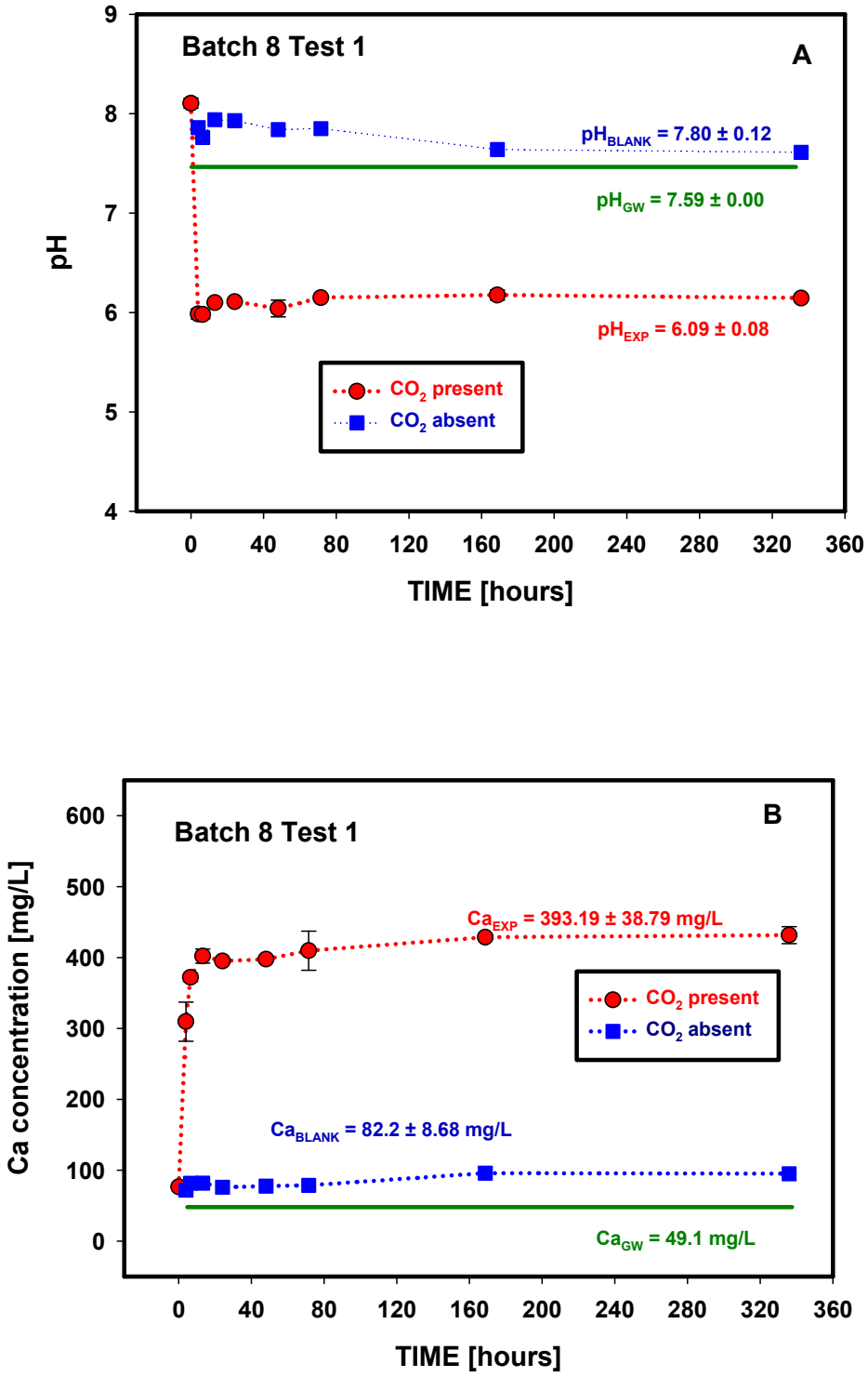

Figure D.23. Changes in pH and elemental composition as a function of time (Batch 8, Test 1, High Plains Aquifer, sediment CNG 110).

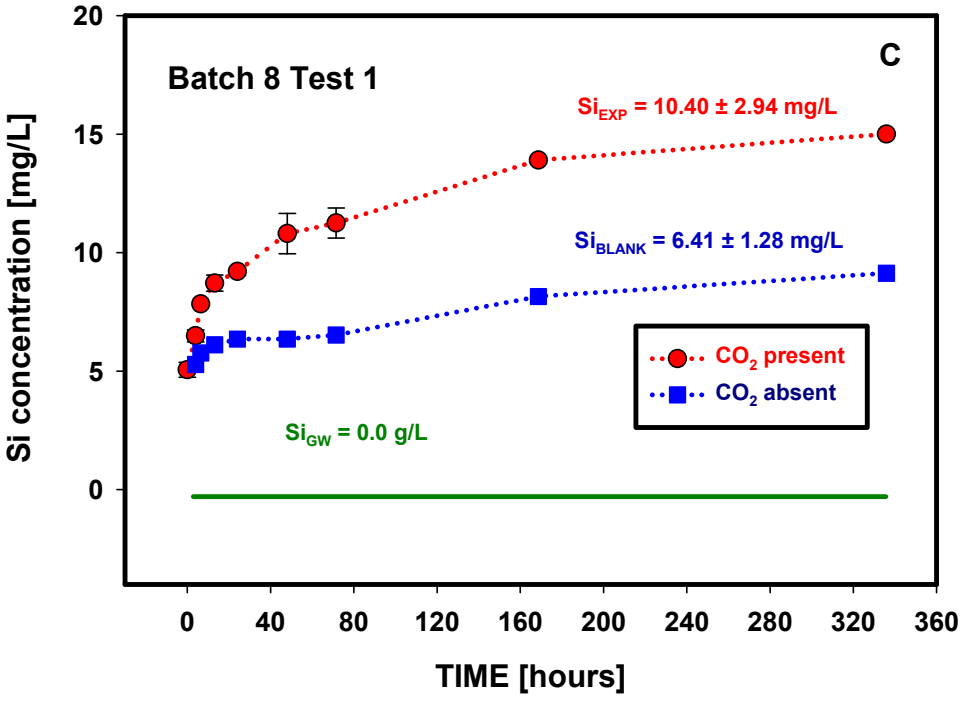

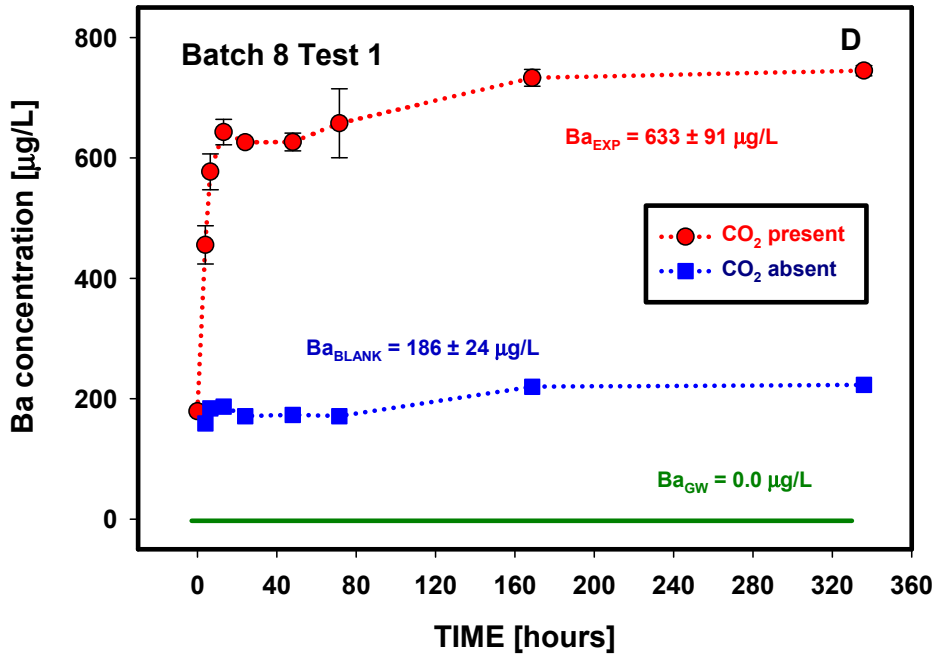

Figure D.23. (contd)

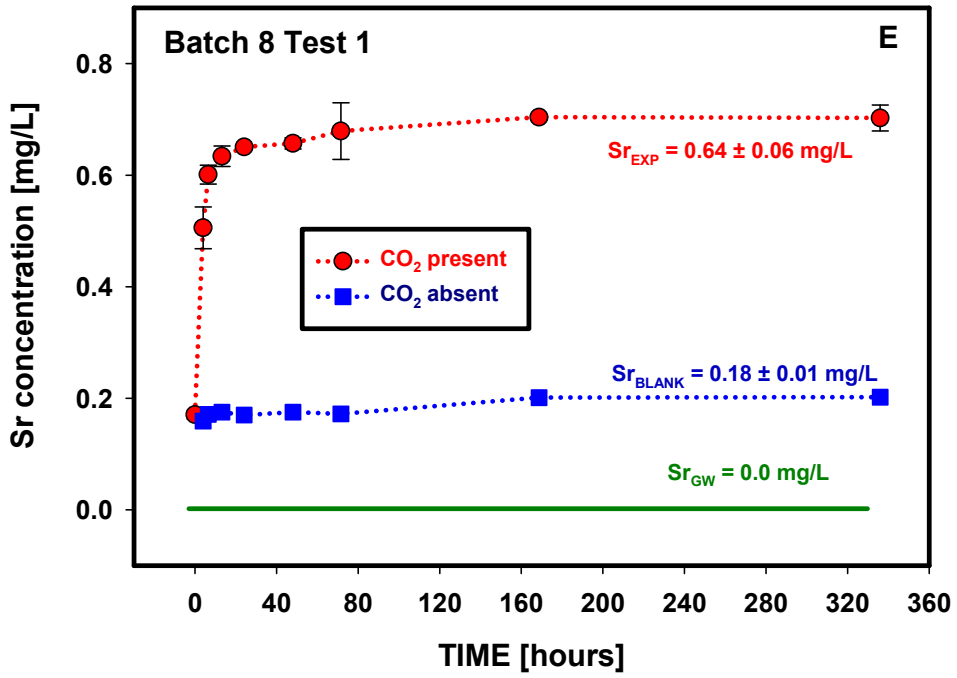

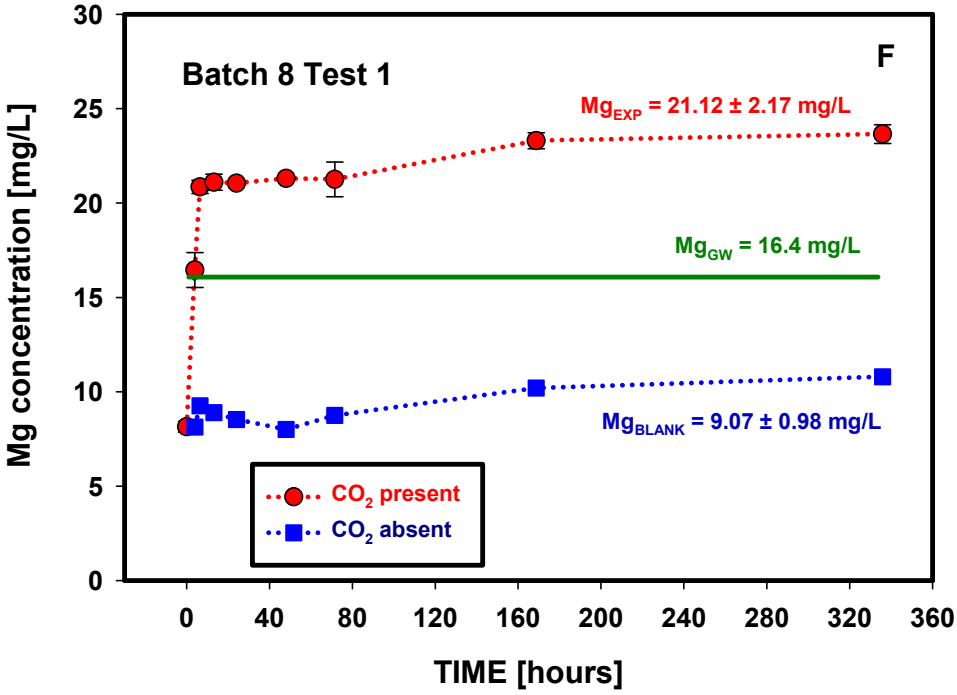

Figure D.23. (contd)

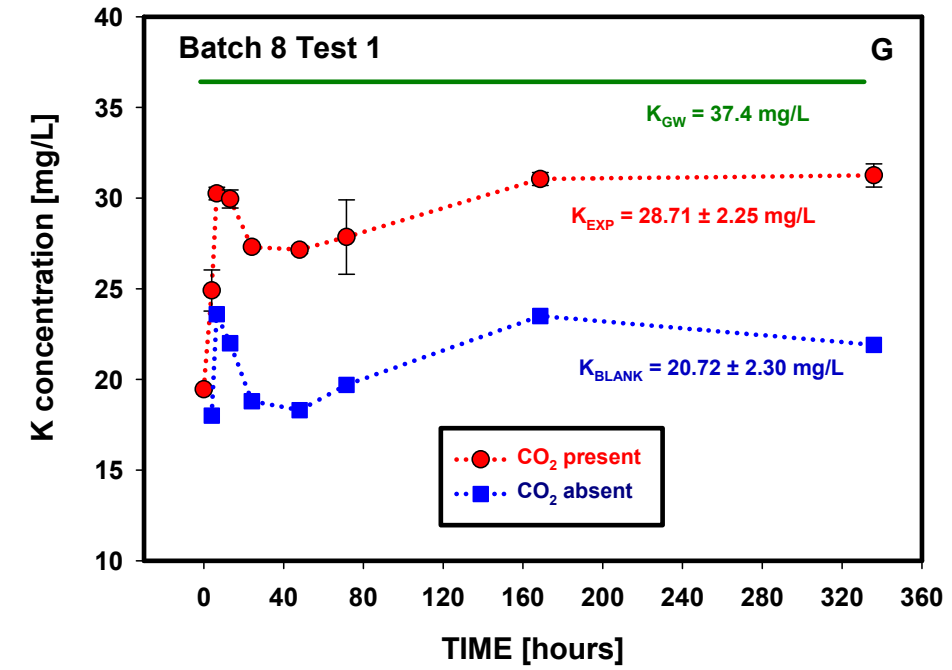

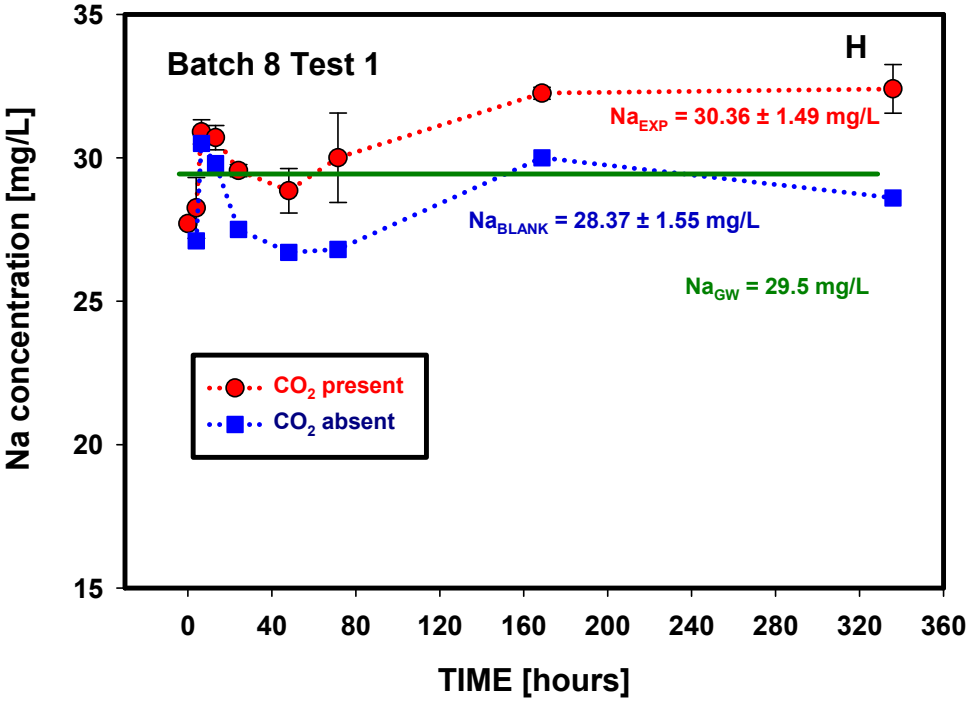

Figure D.23. (contd)

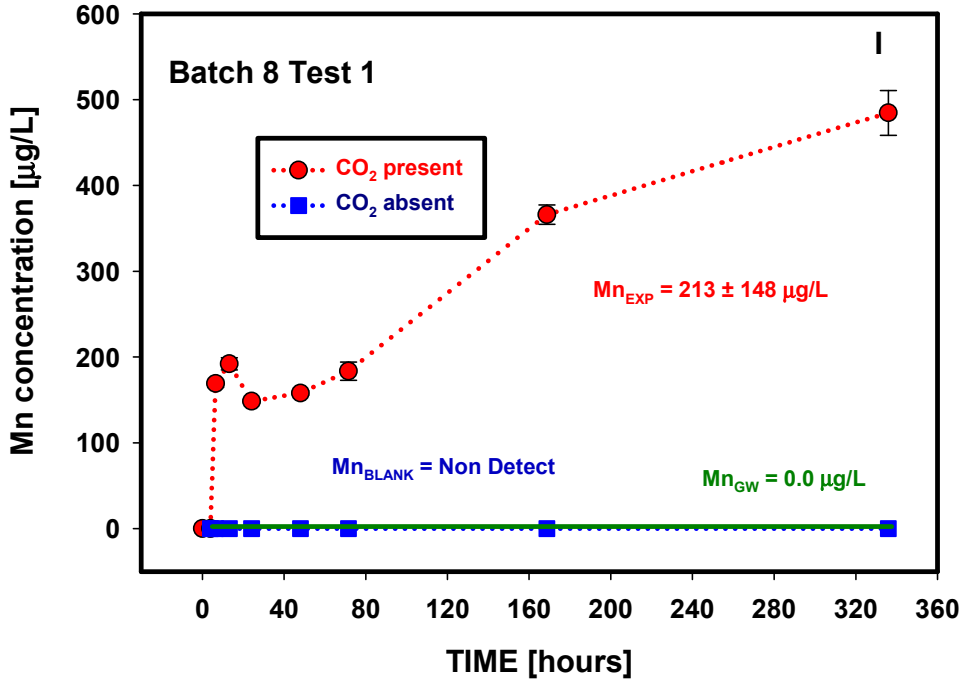

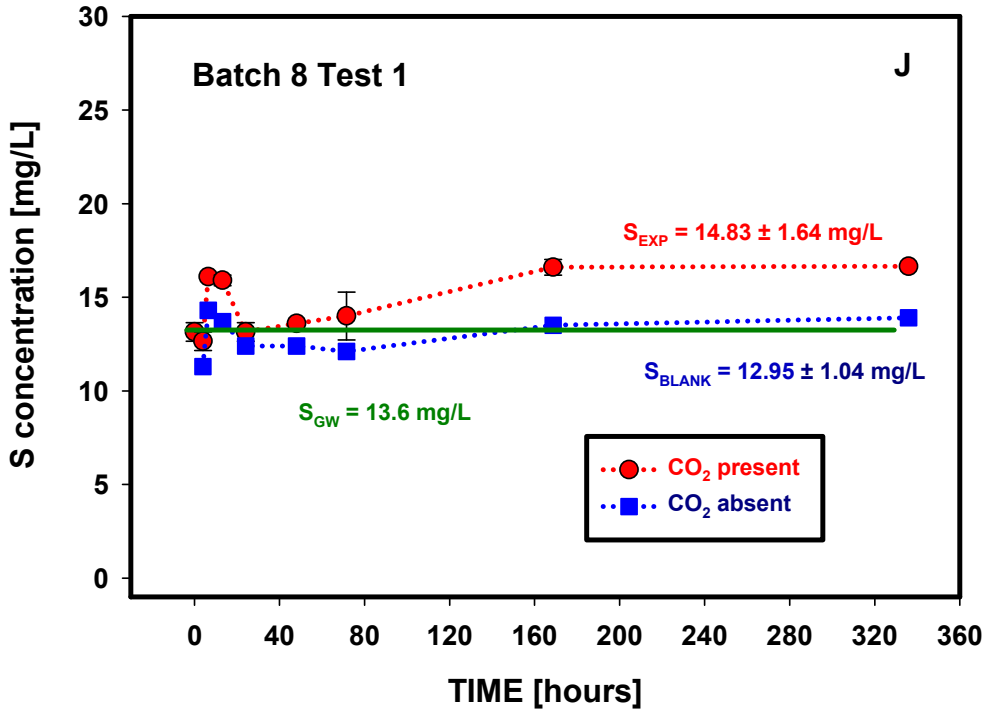

Figure D.23. (contd)

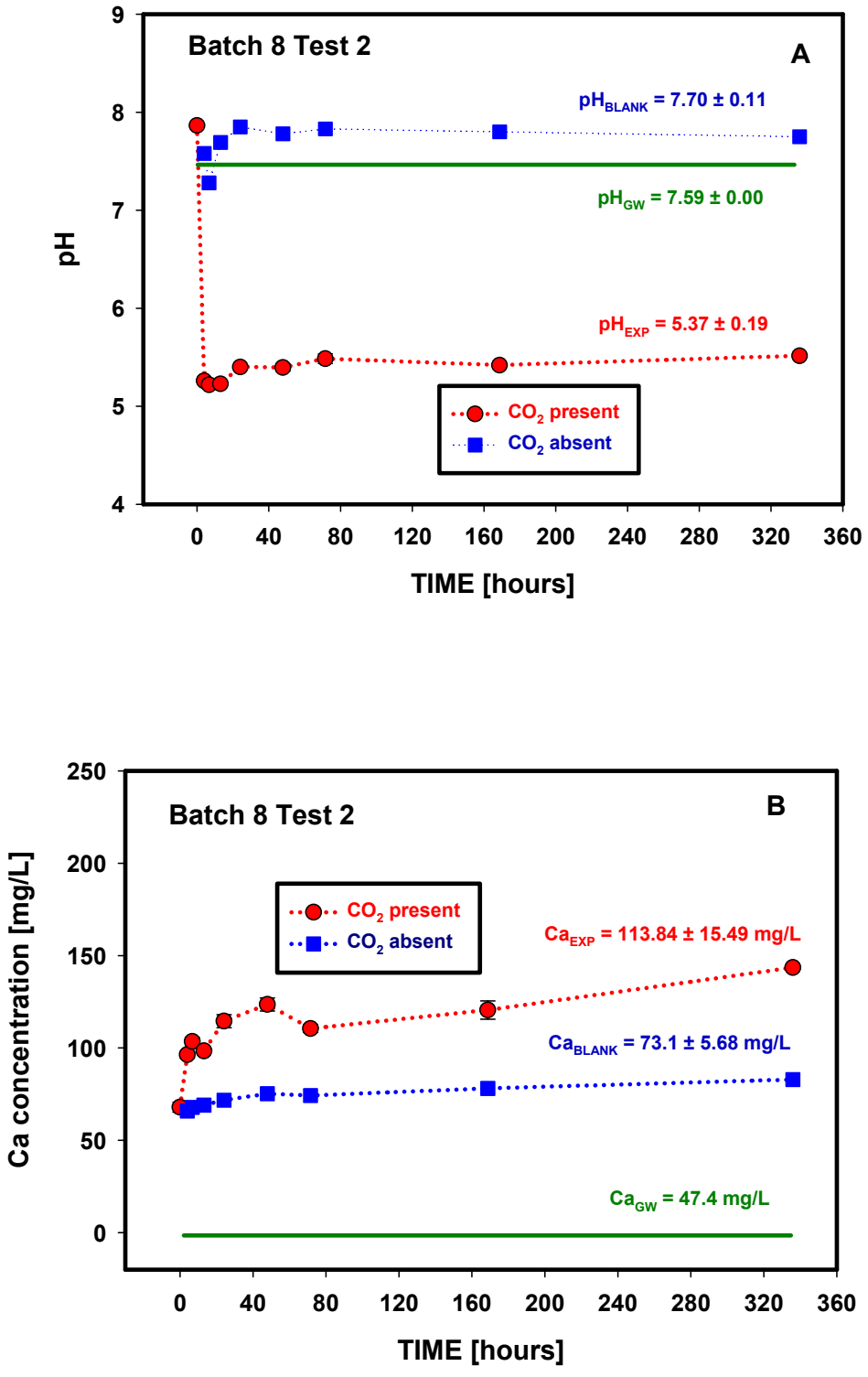

Figure D.24. Changes in pH and elemental composition as a function of time (Batch 8, Test 2, High Plains Aquifer, sediment CNG 60).

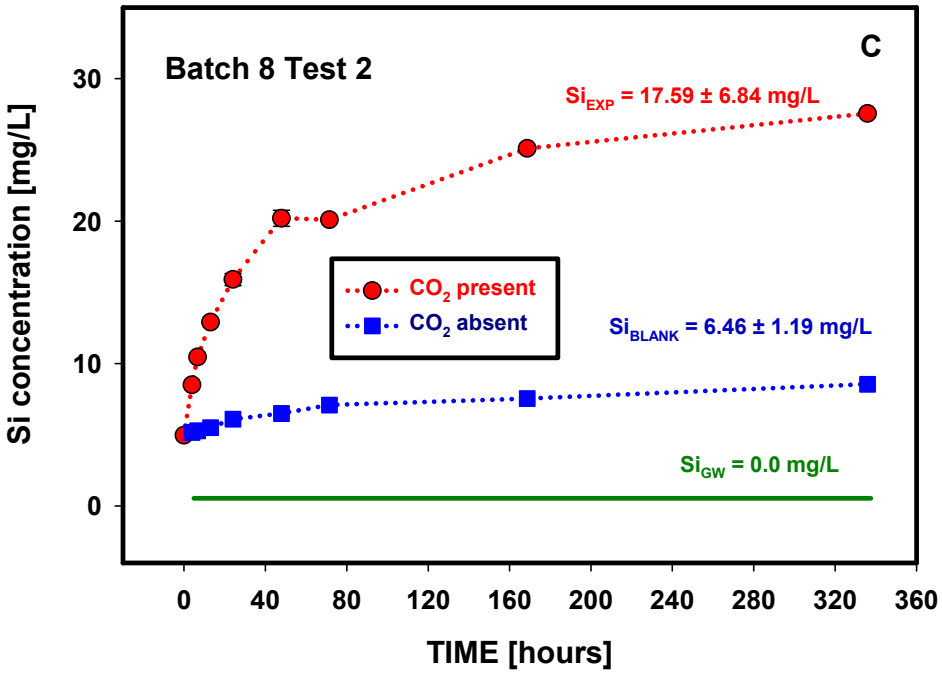

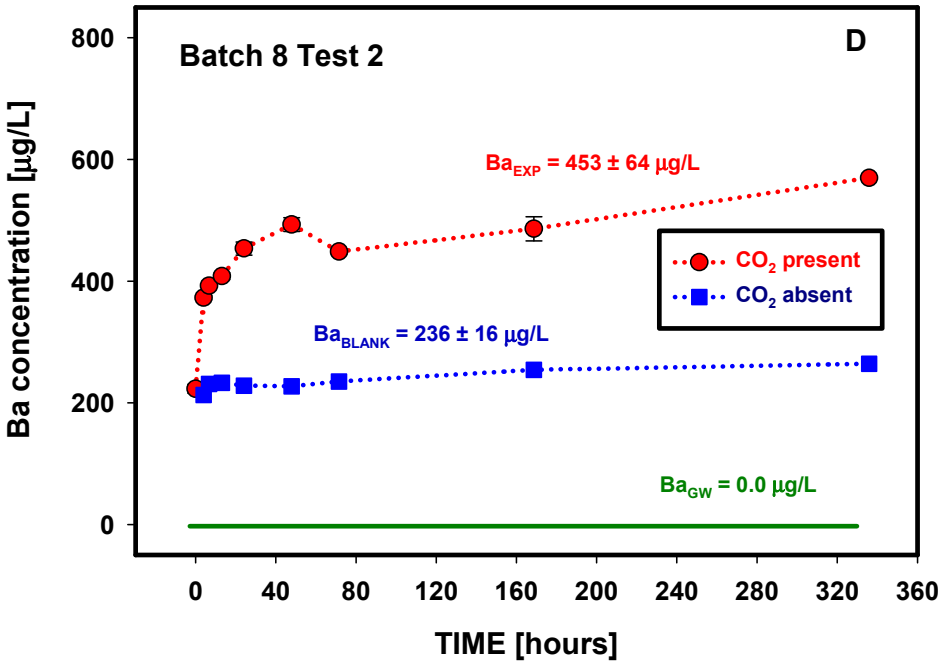

Figure D.24. (contd)

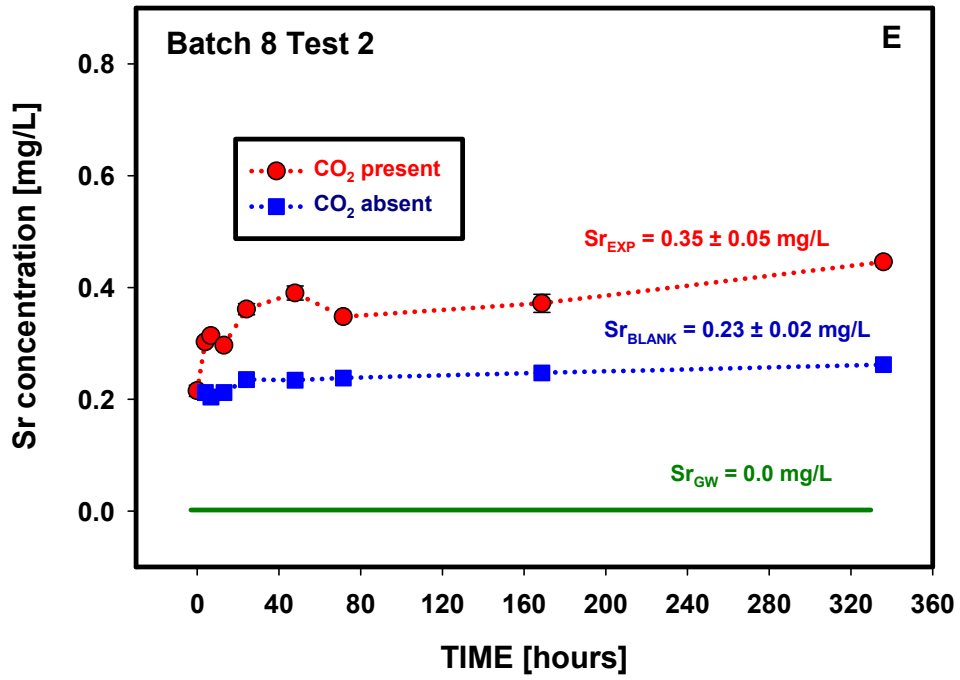

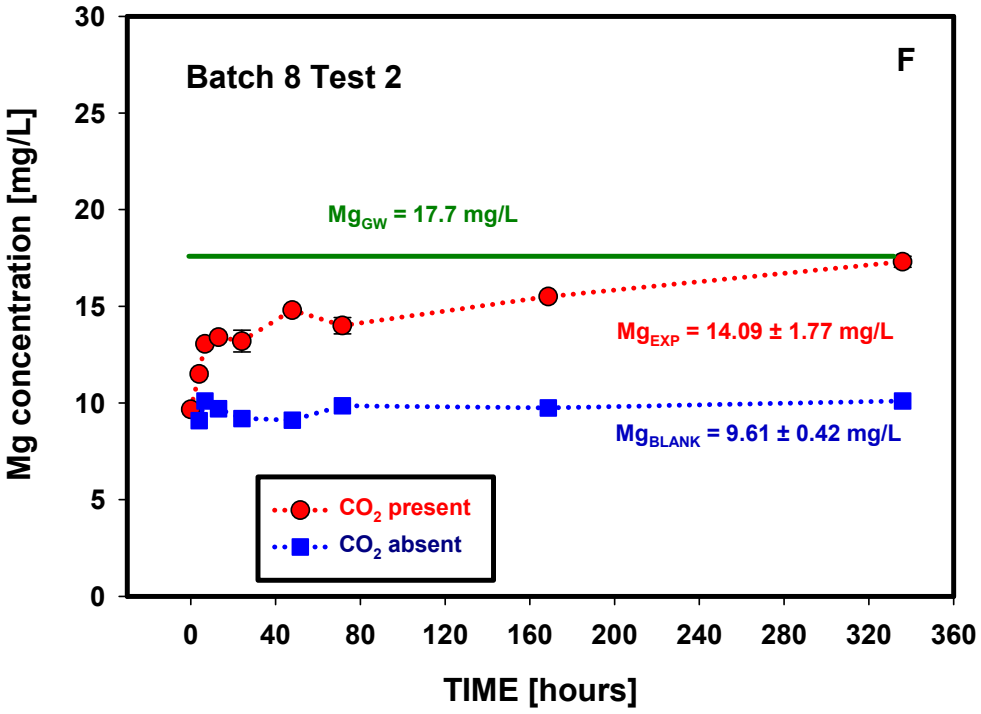

Figure D.24. (contd)

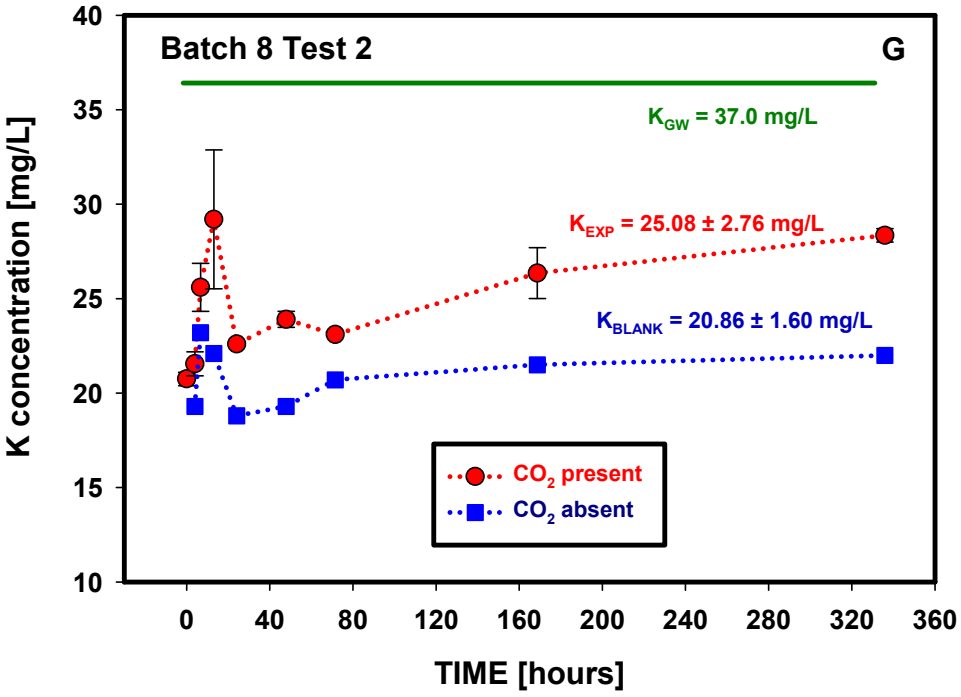

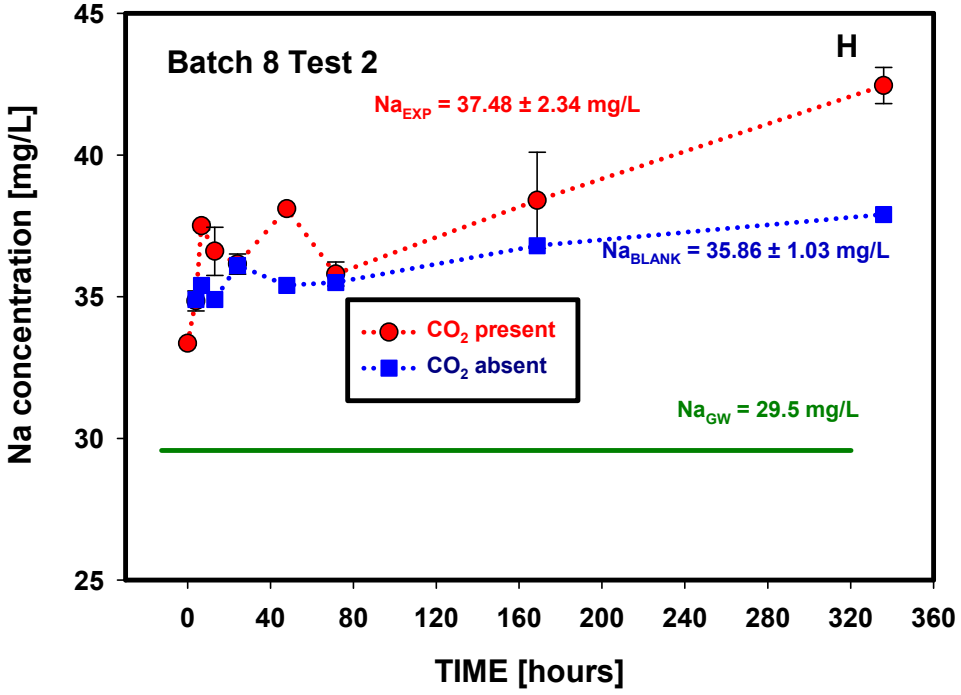

Figure D.24. (contd)

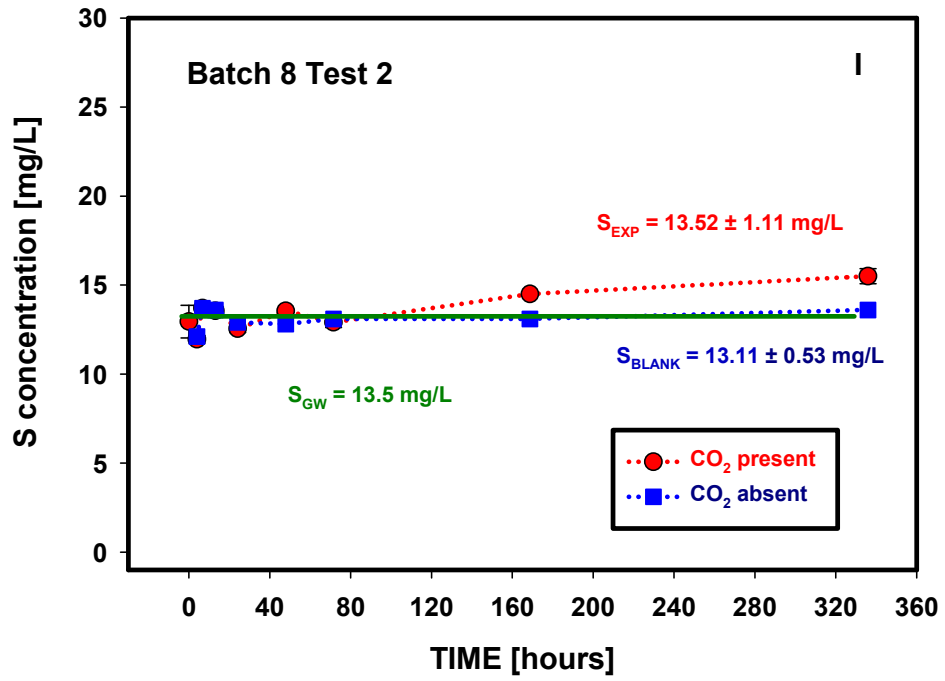

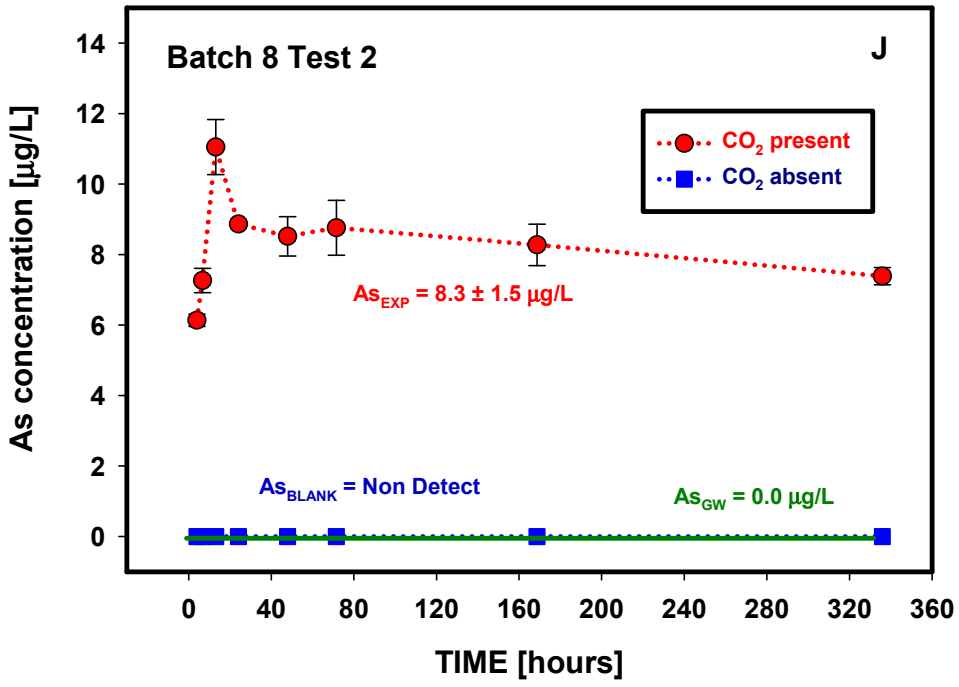

Figure D.24. (contd)

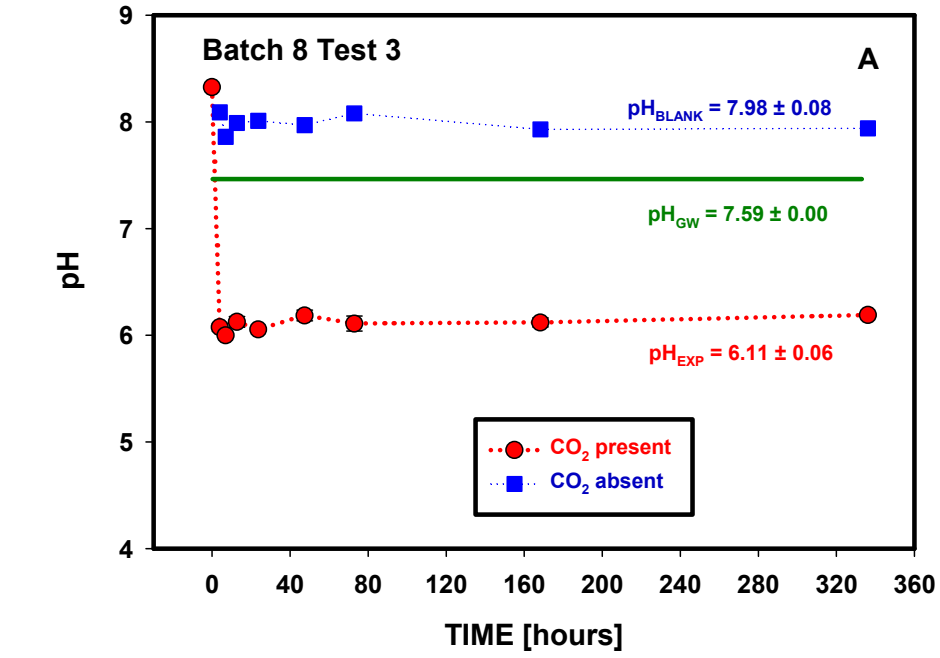

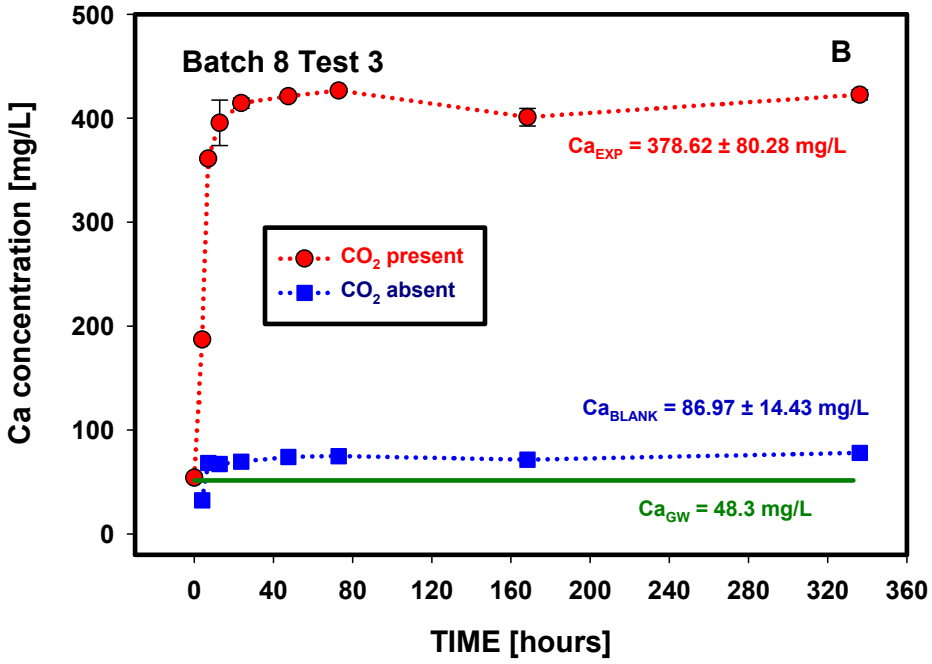

Figure D.25. Changes in pH and elemental composition as a function of time (Batch 8, Test 3, High Plains Aquifer, sediment CAL 1 151).

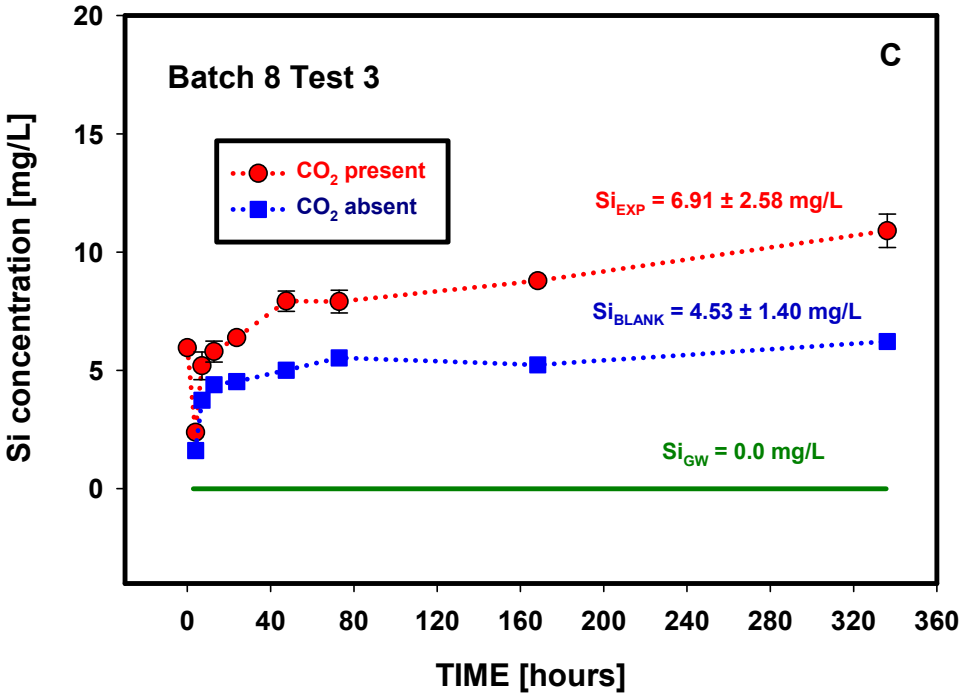

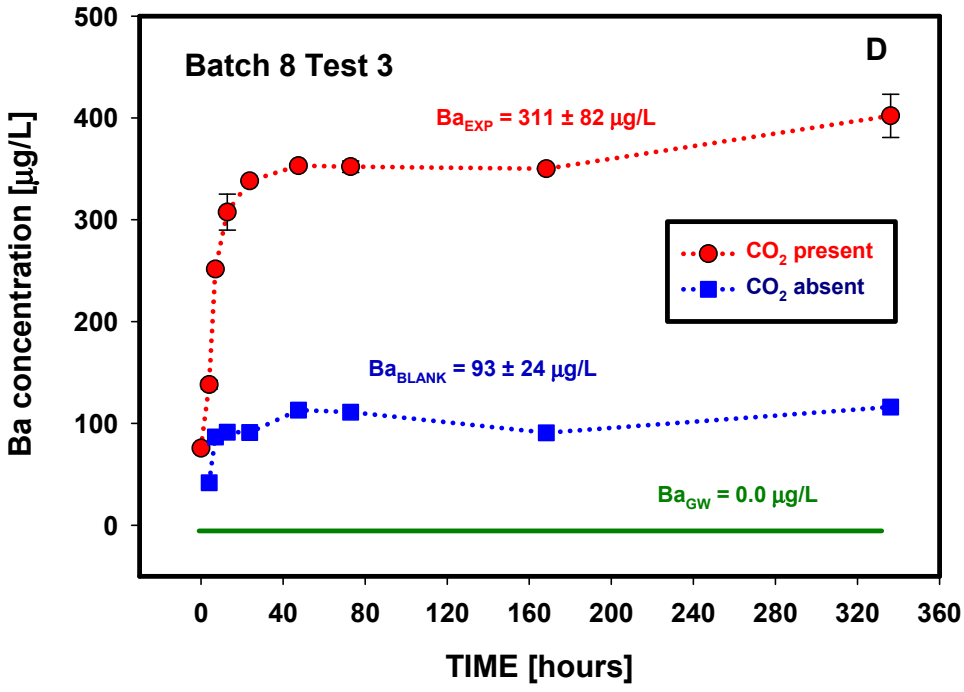

Figure D.25. (contd)

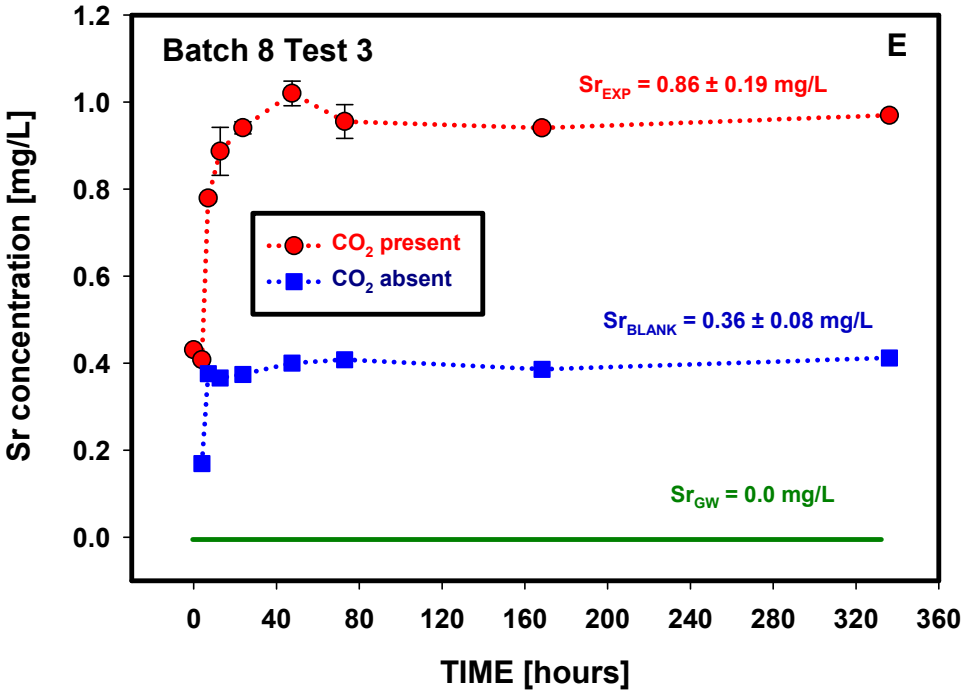

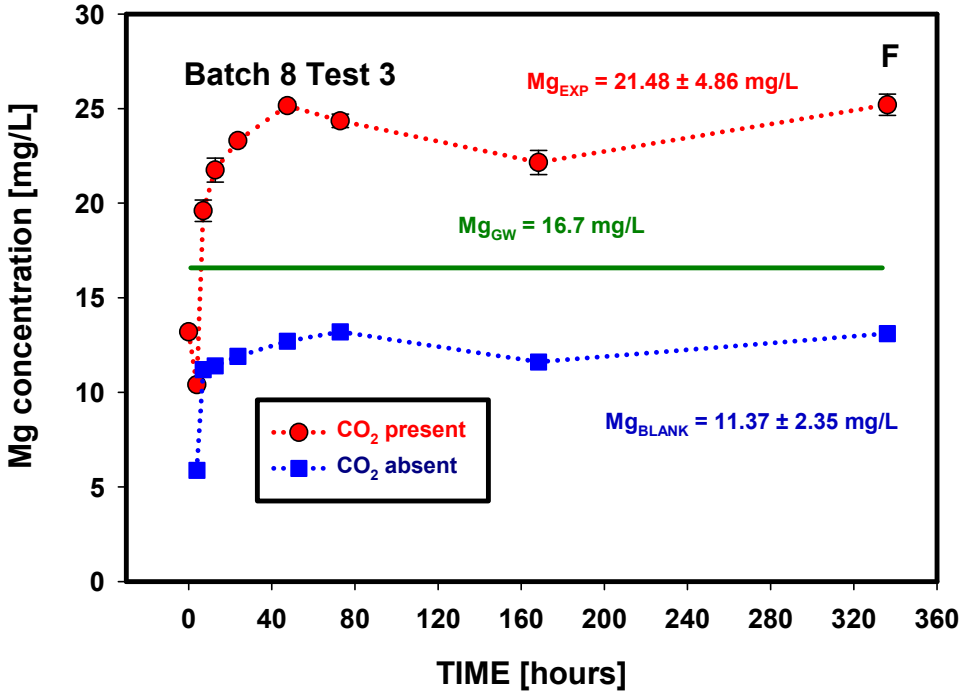

Figure D.25. (contd)

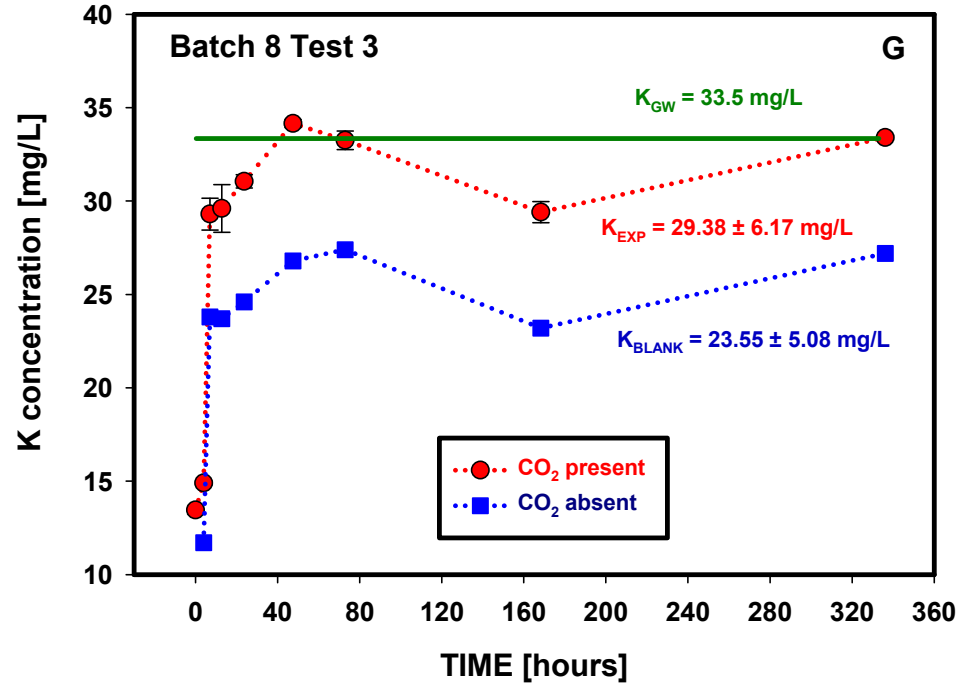

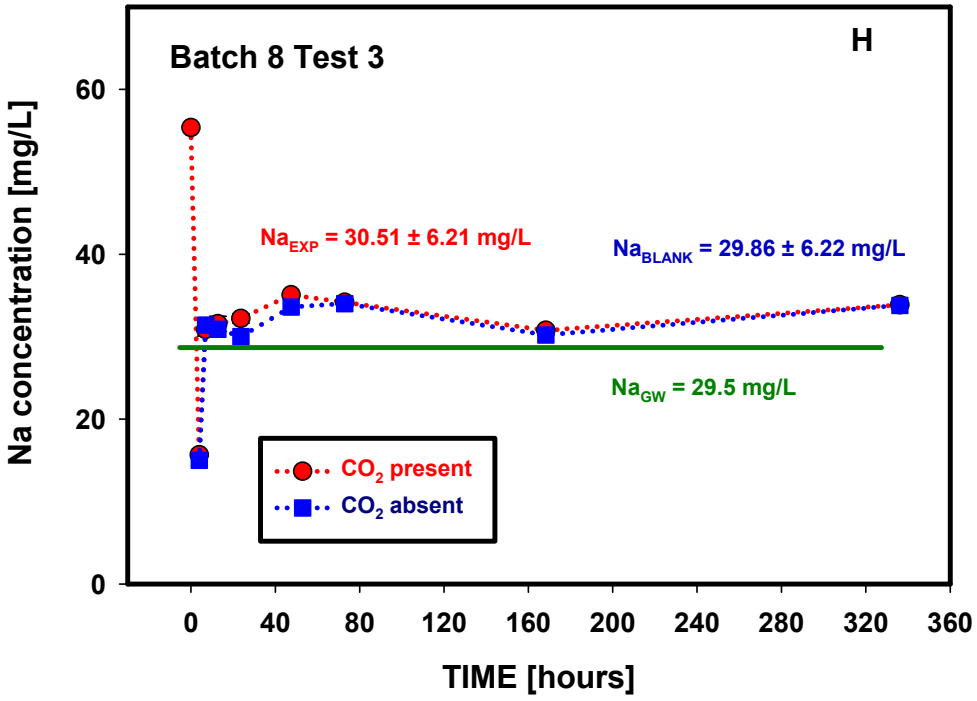

Figure D.25. (contd)

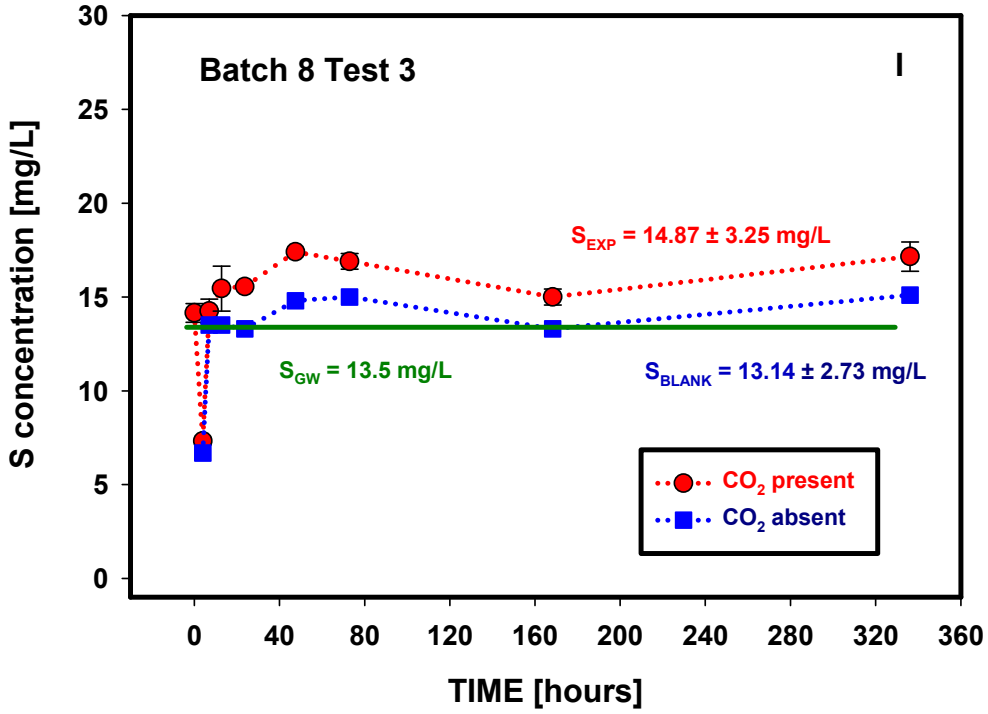

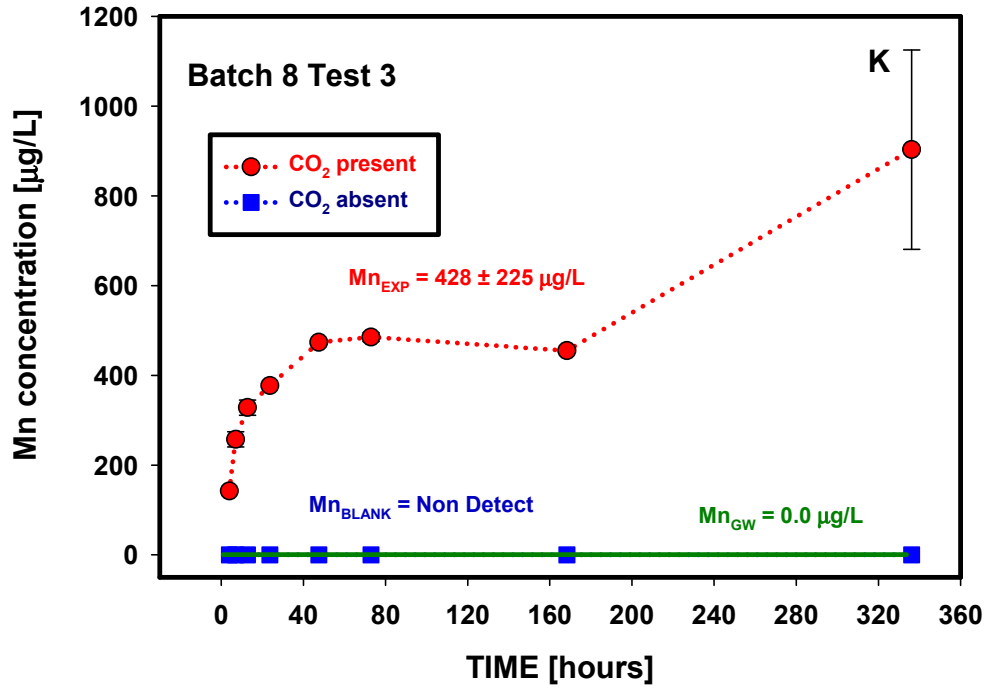

Figure D.25. (contd)

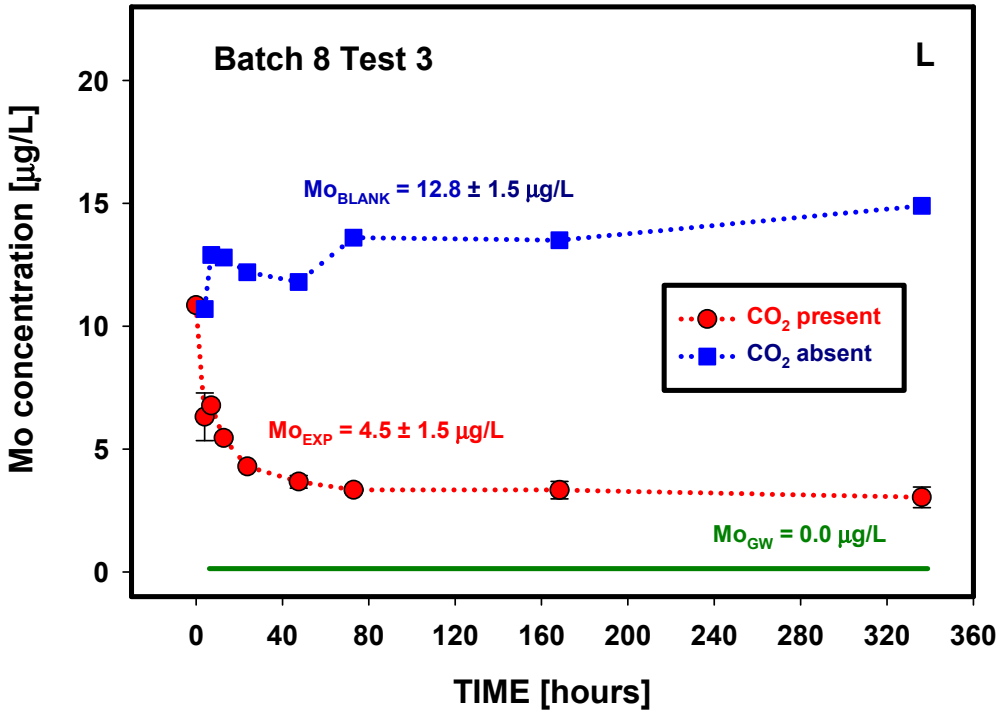

Figure D.25. (contd)

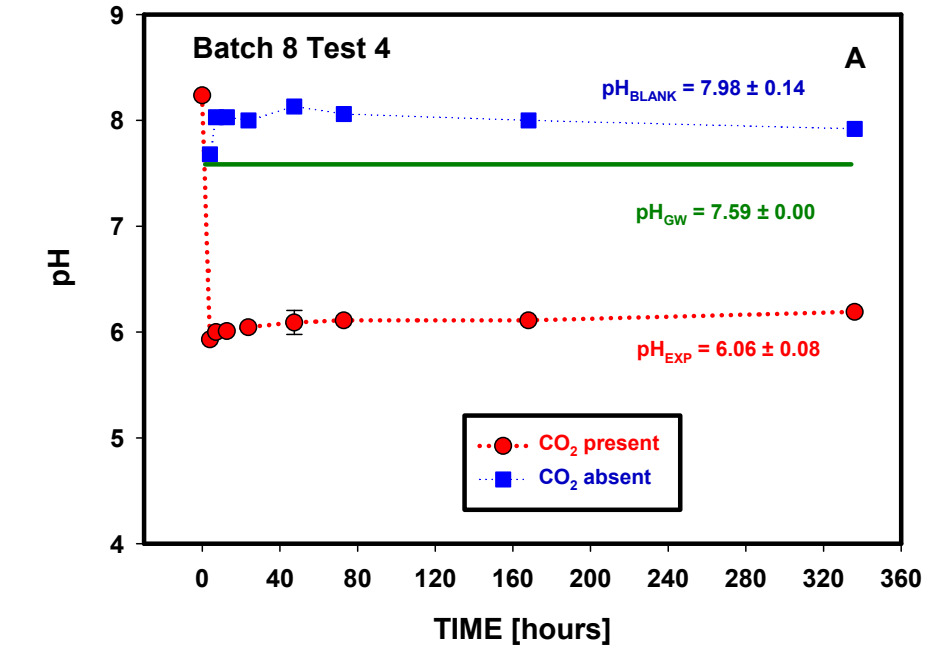

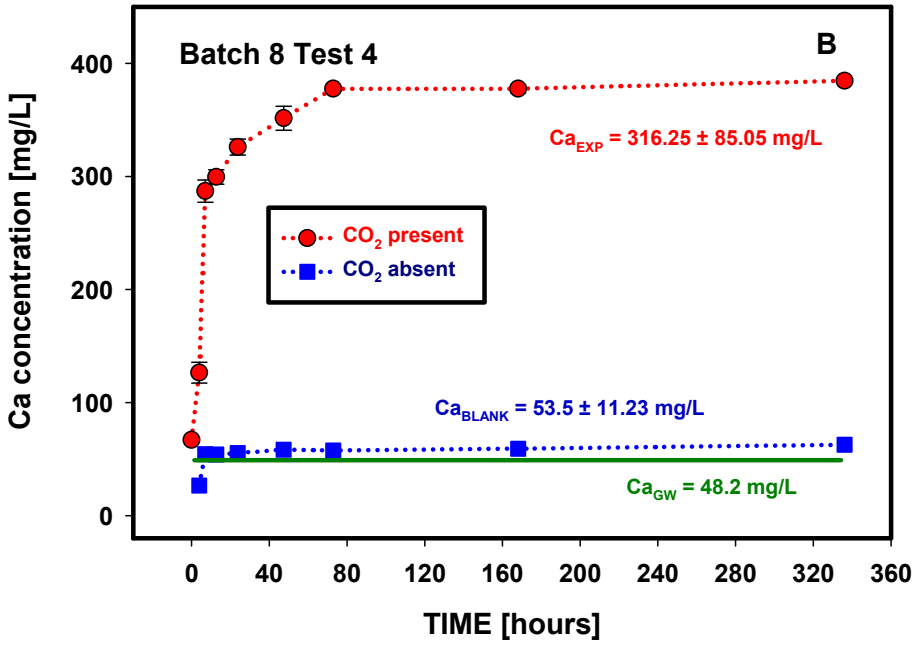

Figure D.26. Changes in pH and elemental composition as a function of time (Batch 8, Test 4, High Plains Aquifer, sediment CAL 2 29).

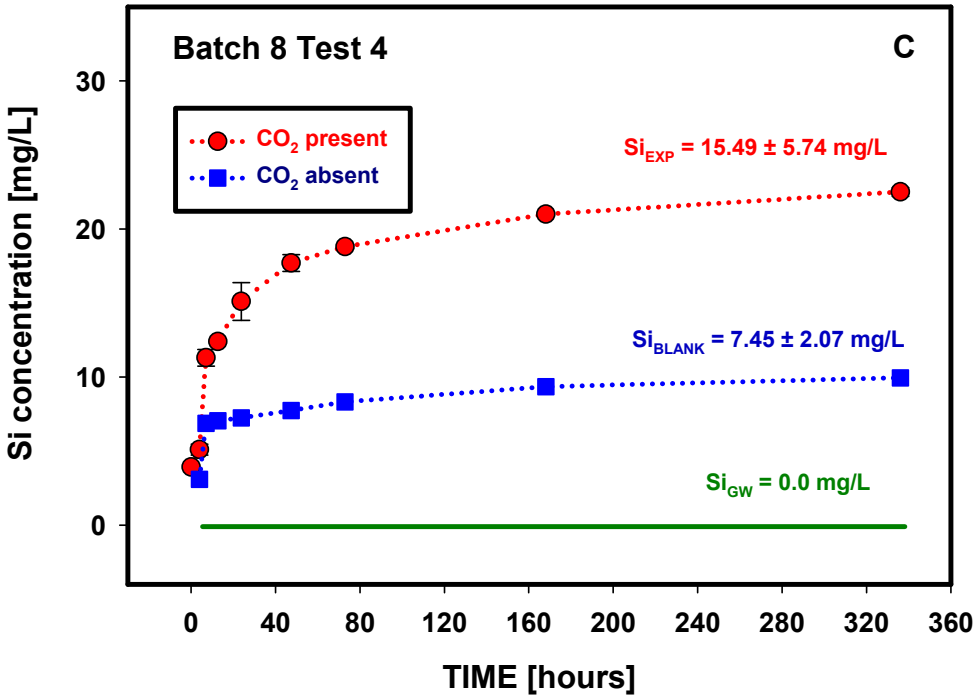

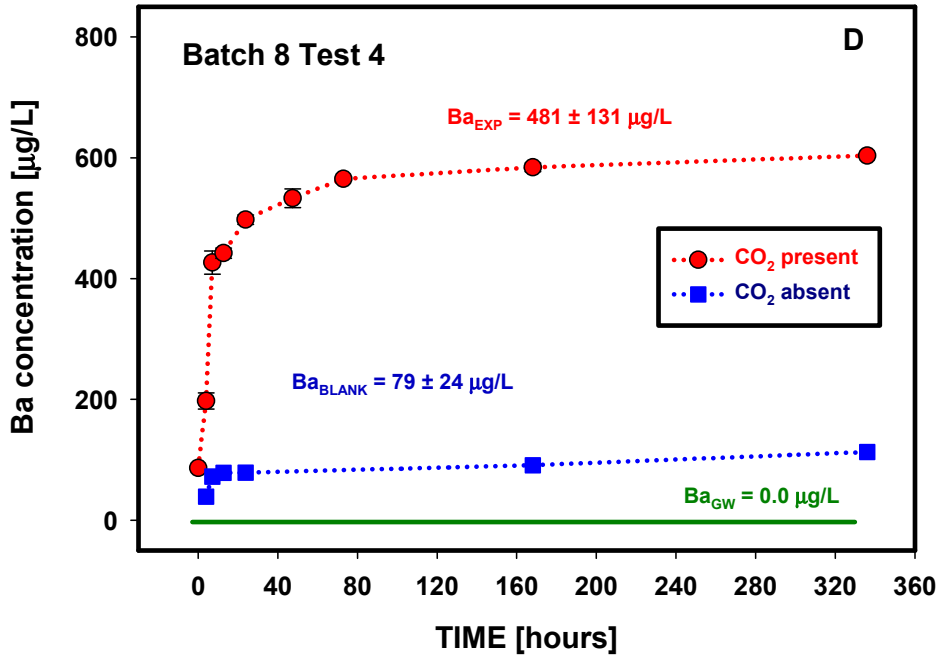

Figure D.26. (contd)

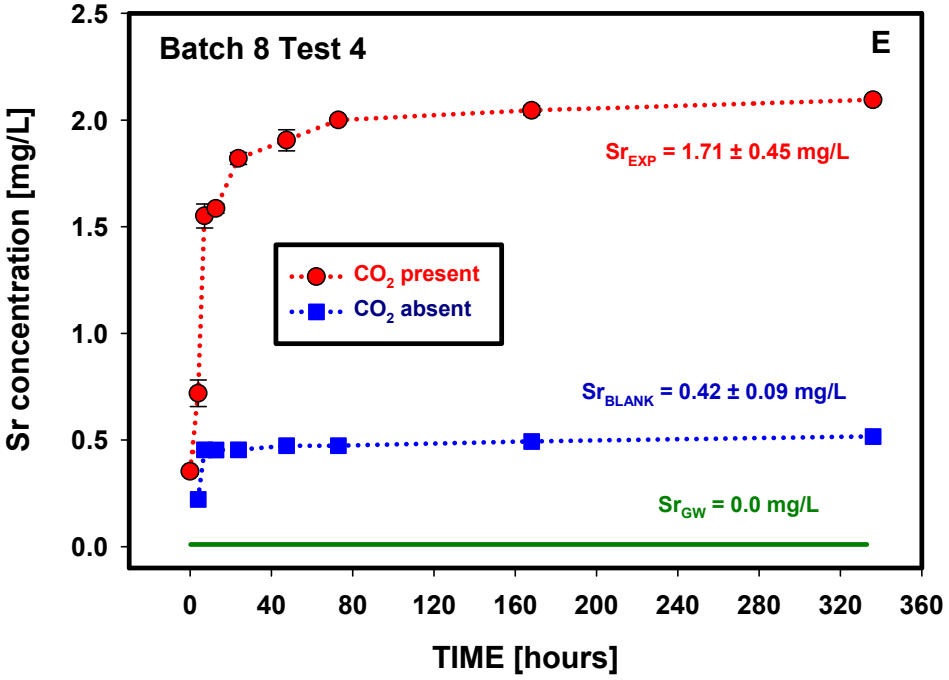

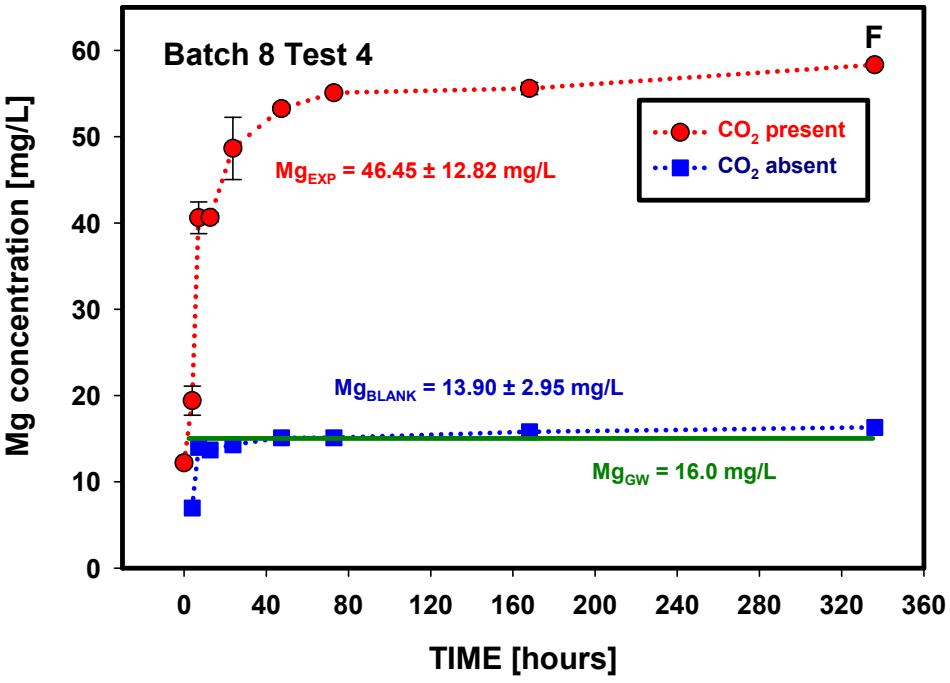

Figure D.26. (contd)

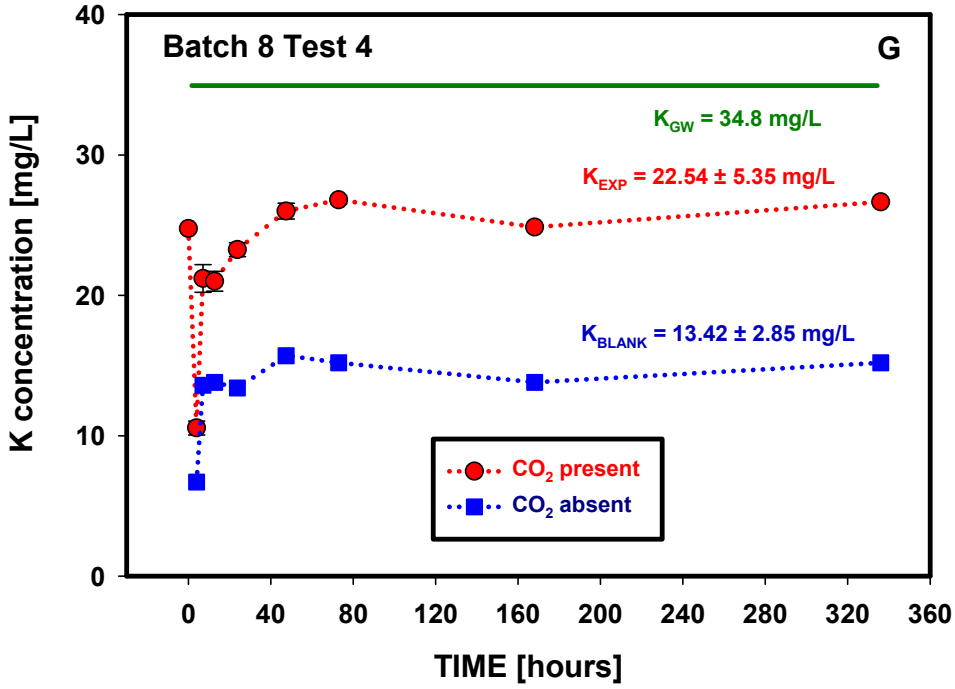

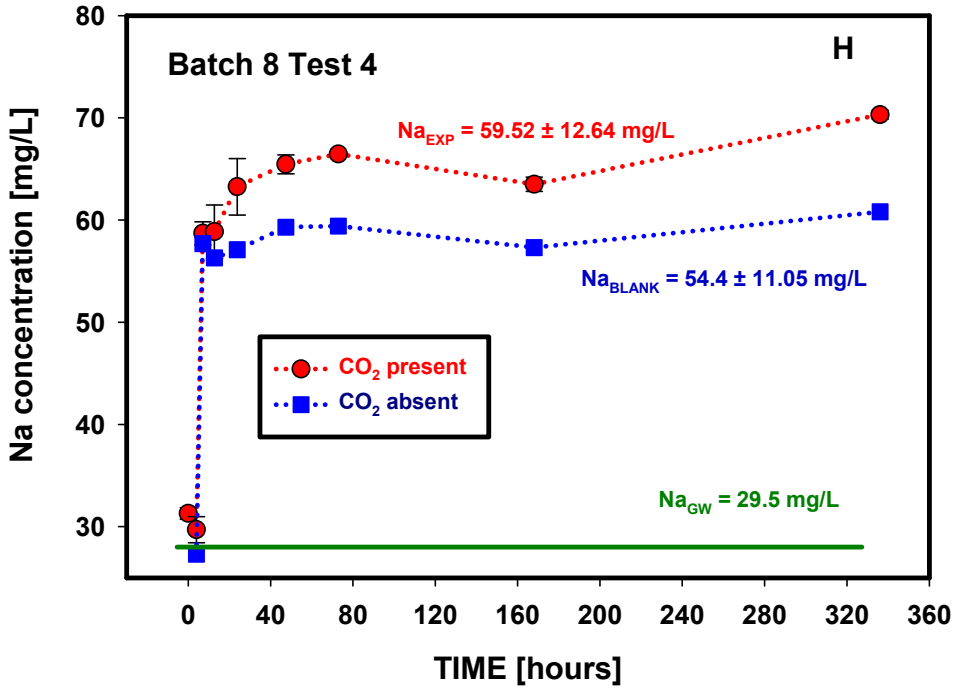

Figure D.26. (contd)

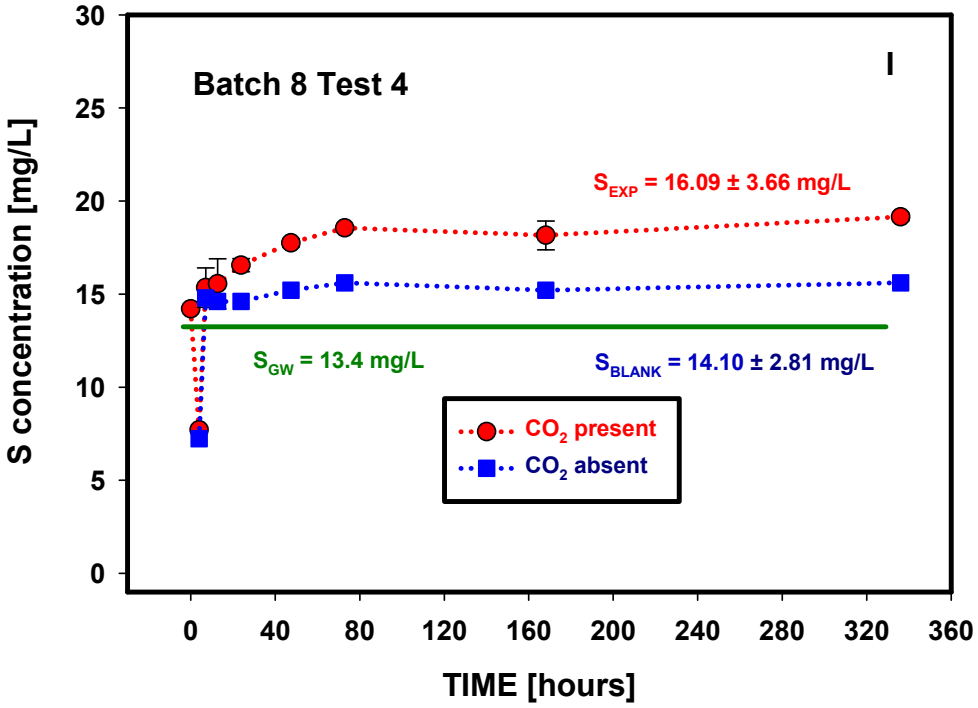

Figure D.26. (contd)

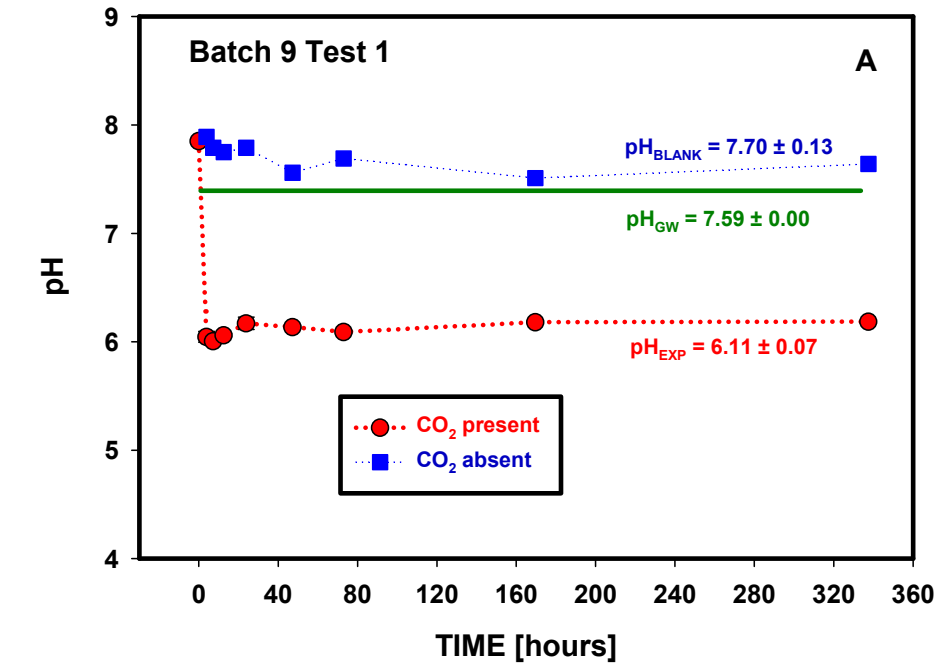

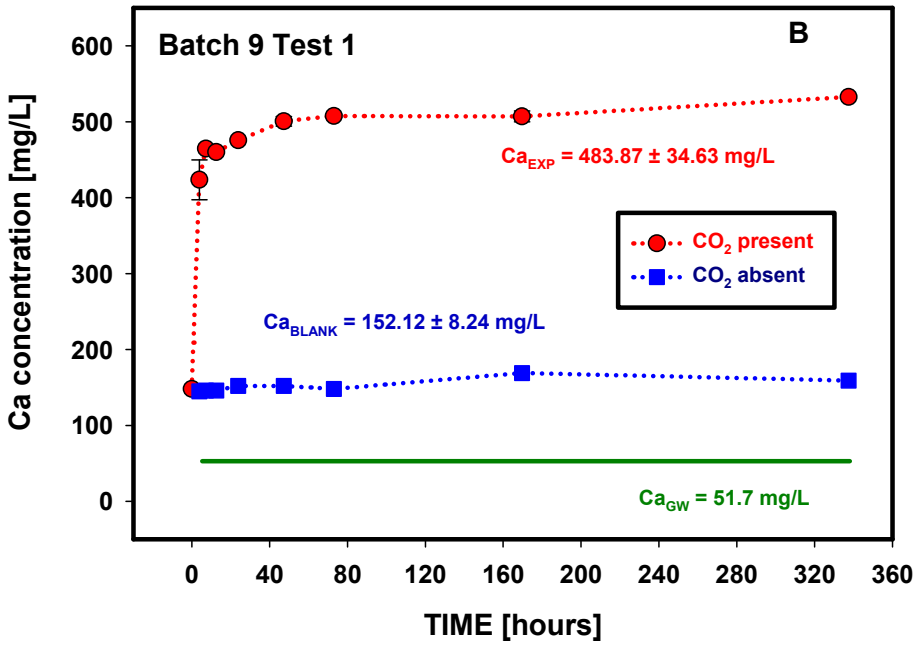

Figure D.27. Changes in pH and elemental composition as a function of time (Batch 9, Test 1, High Plains Aquifer, sediment CNG 8).

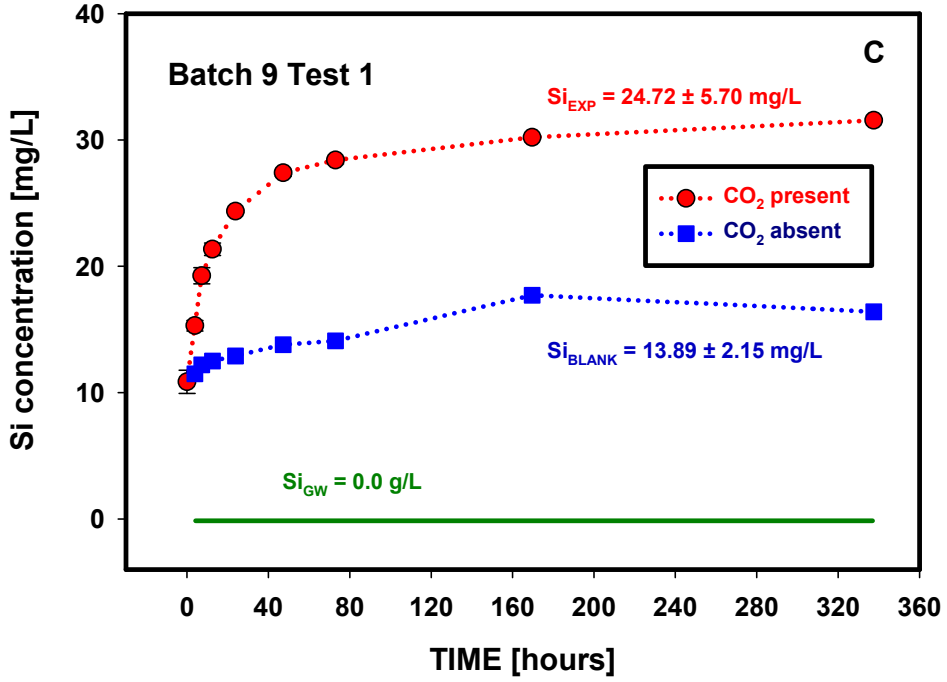

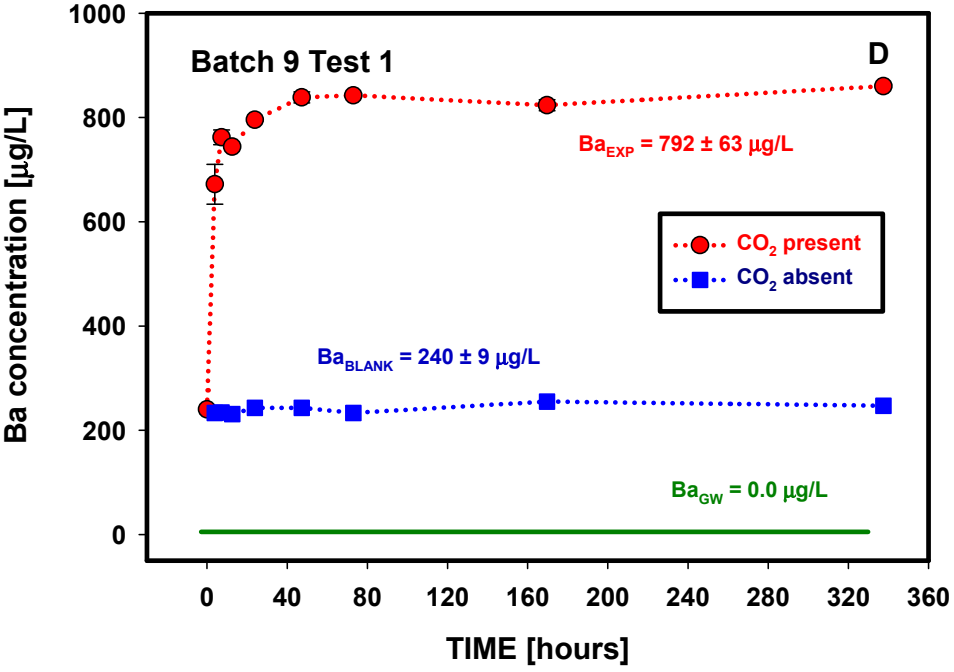

Figure D.27. (contd)

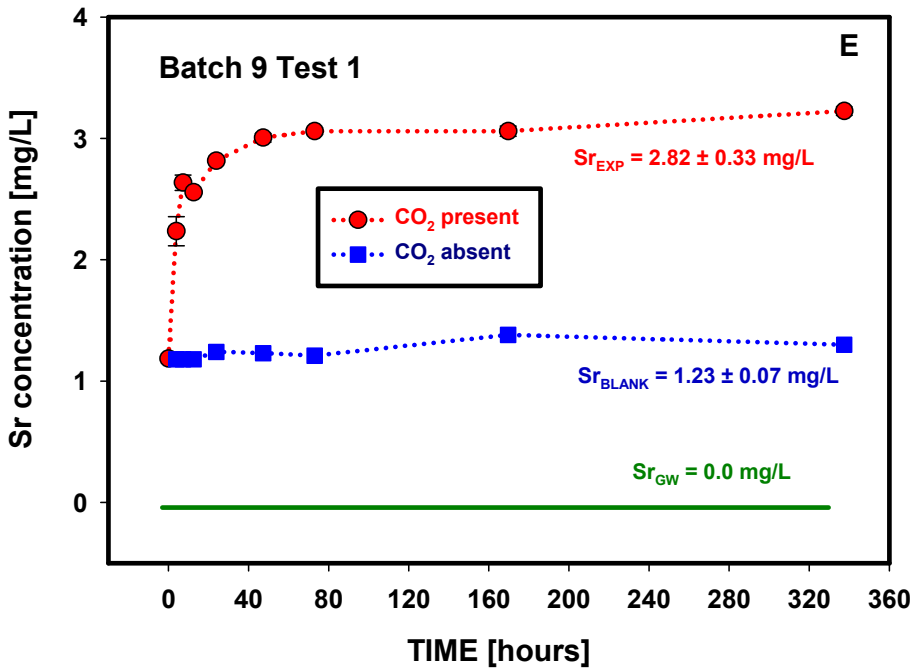

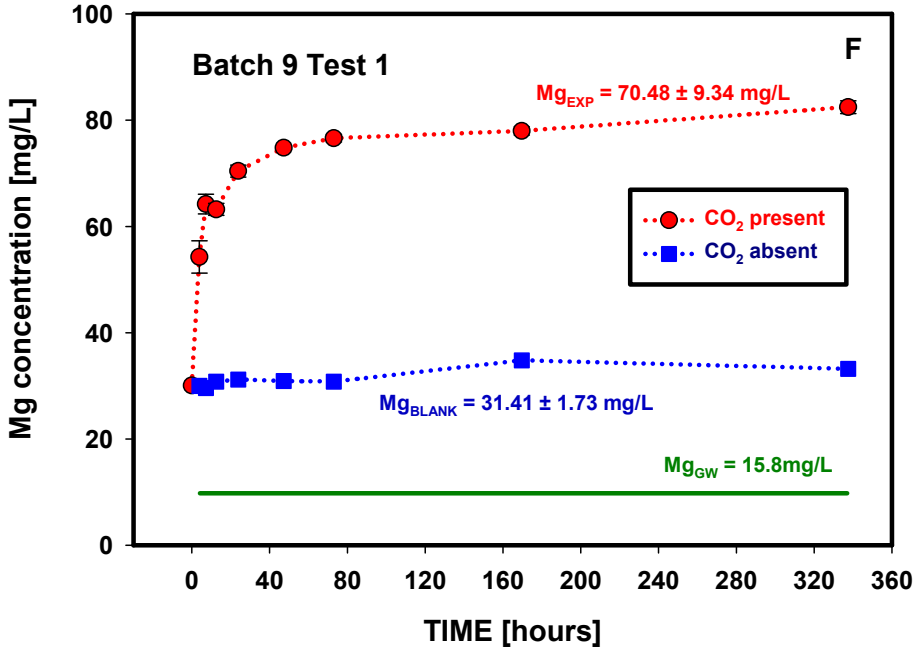

Figure D.27. (contd)

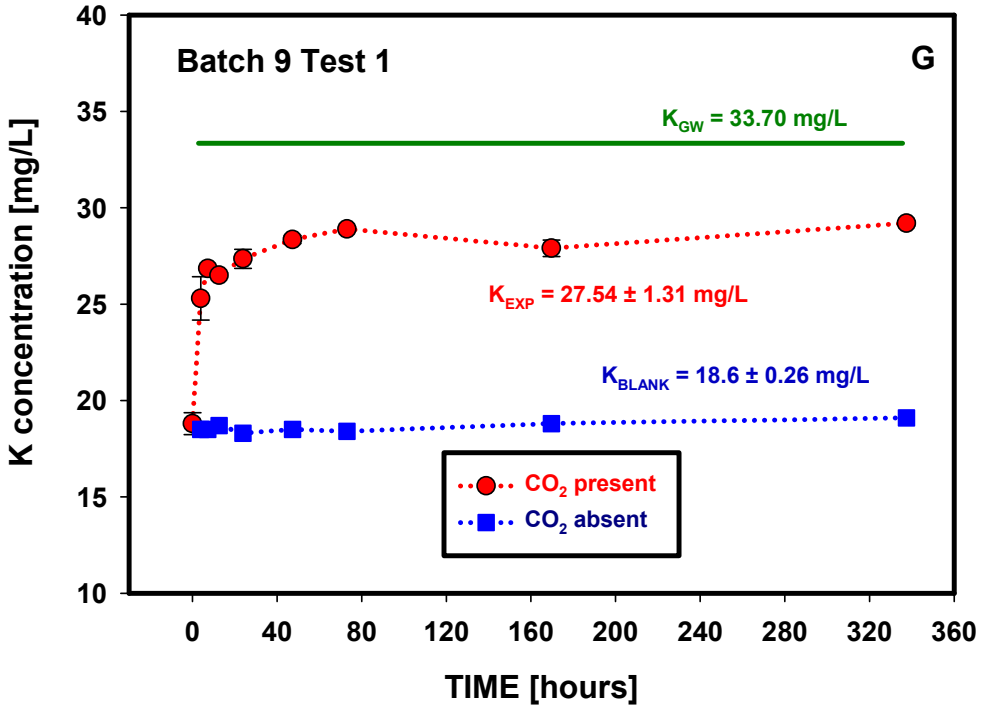

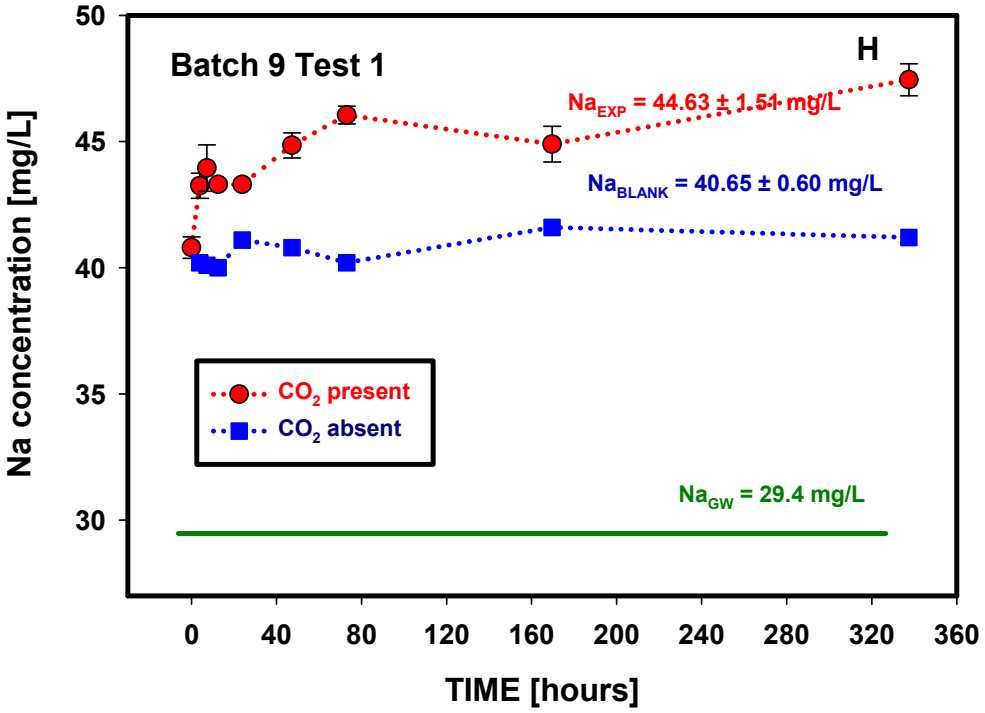

Figure D.27. (contd)

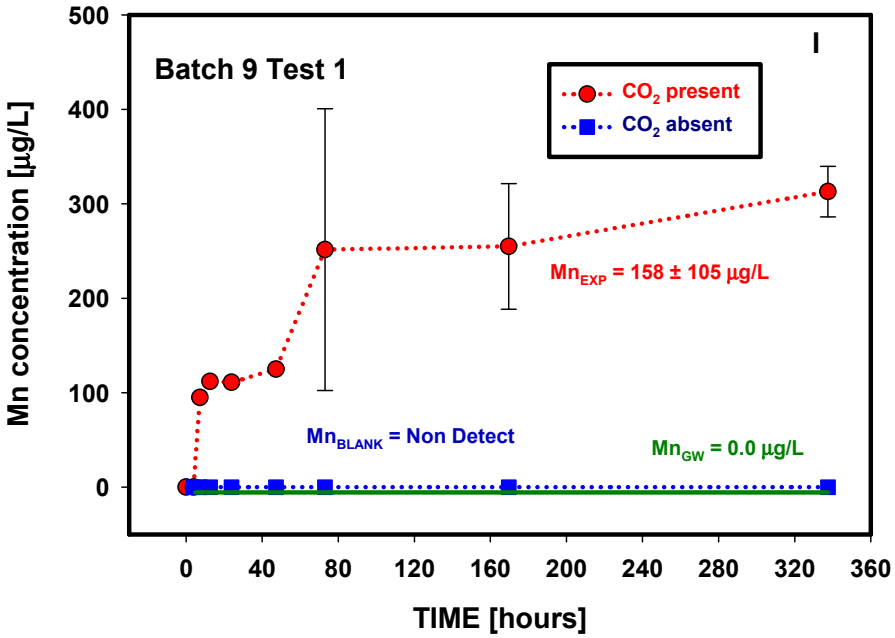

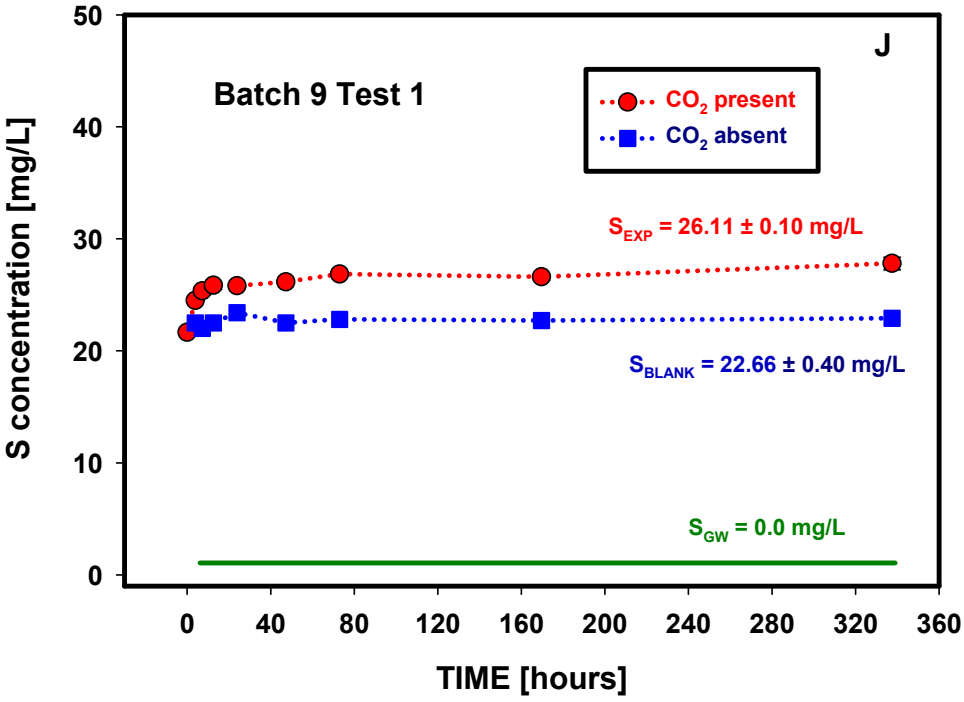

Figure D.27. (contd)

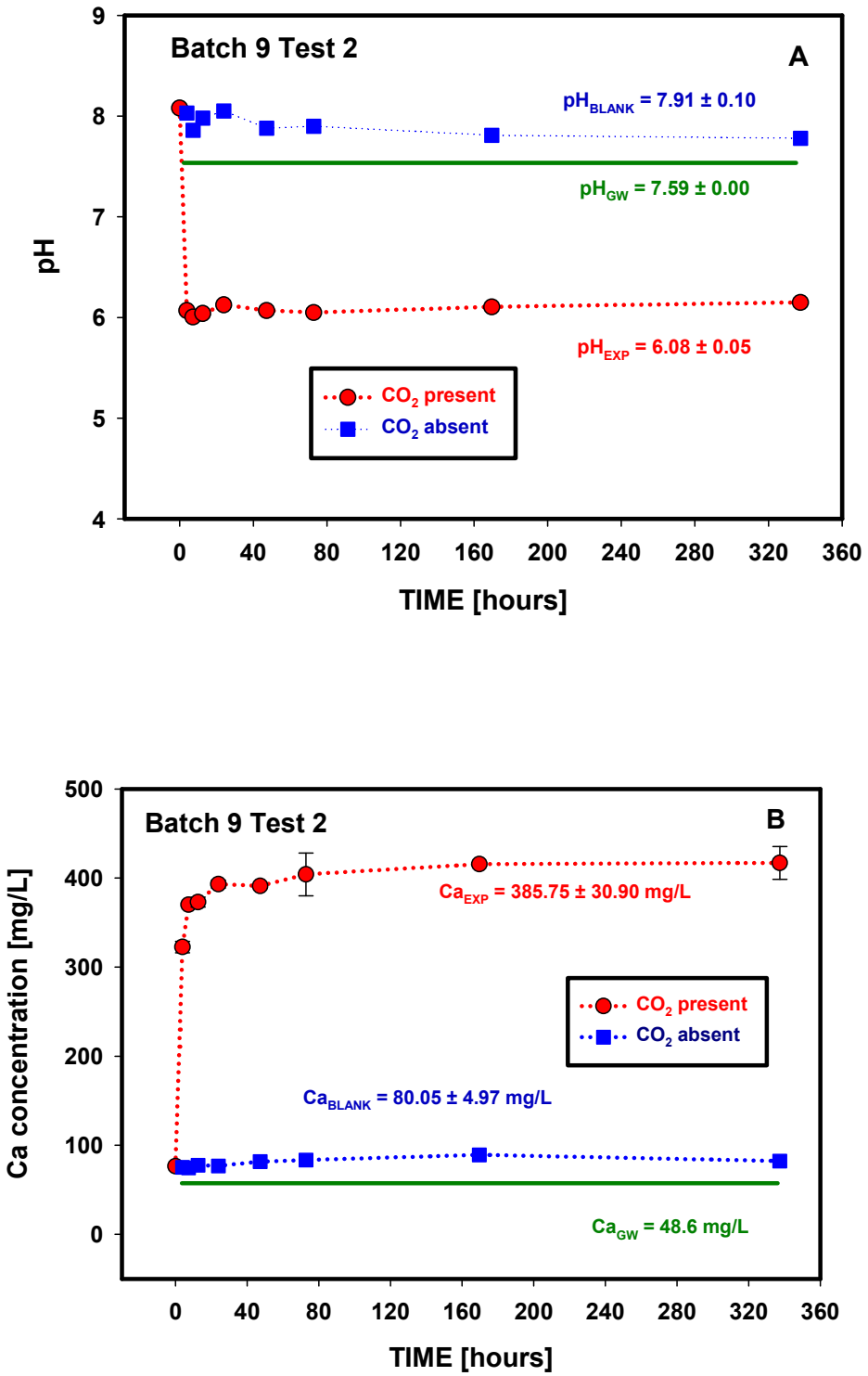

Figure D.28. Changes in pH and elemental composition as a function of time (Batch 9, Test 2, High Plains Aquifer, sediment CNG 150).

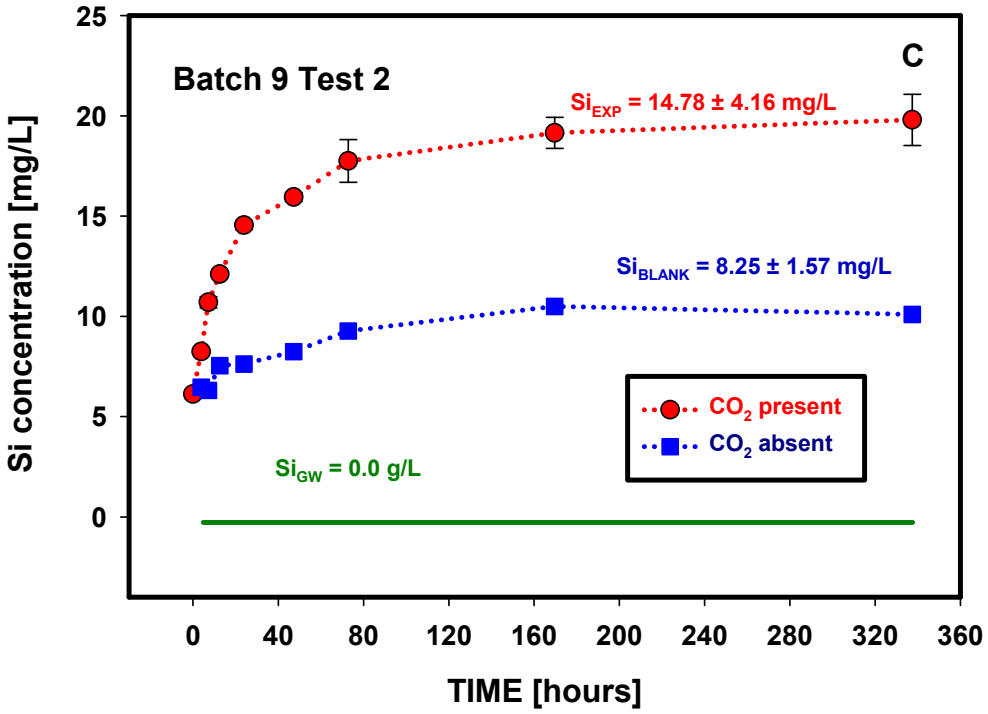

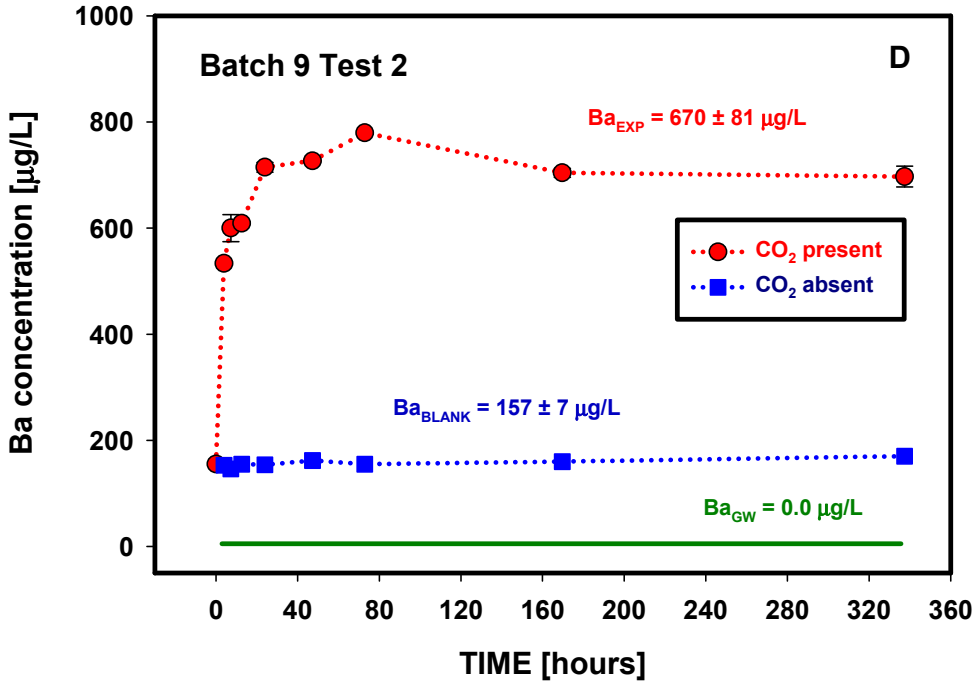

Figure D.28. (contd)

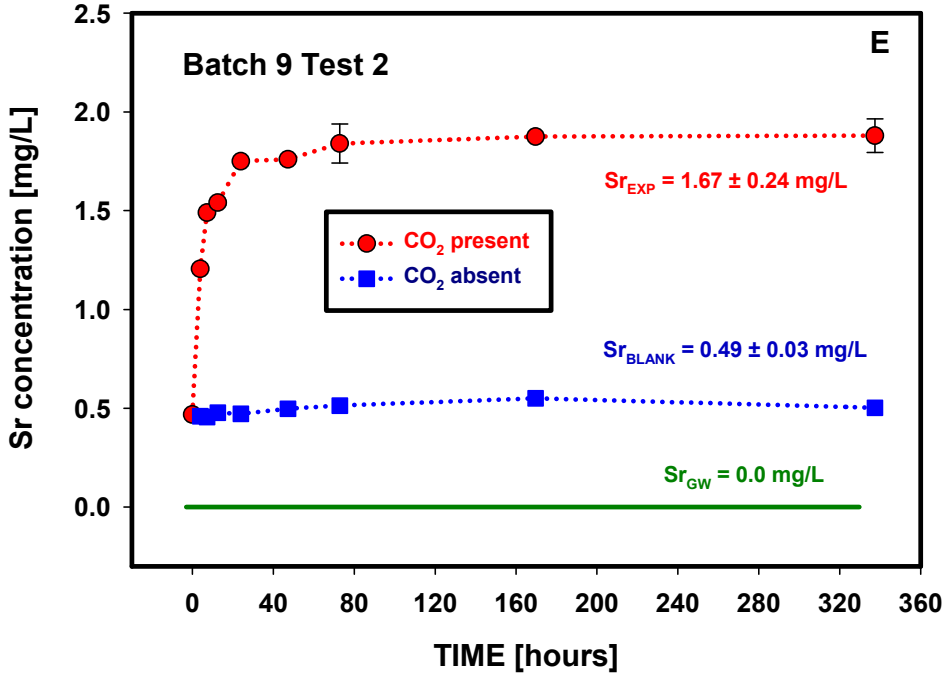

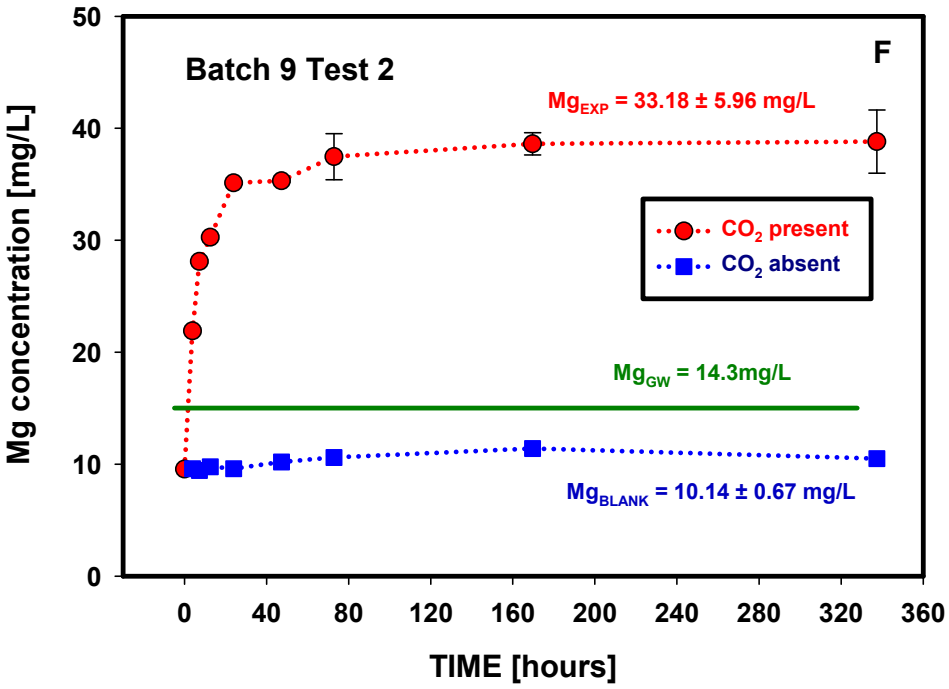

Figure D.28. (contd)

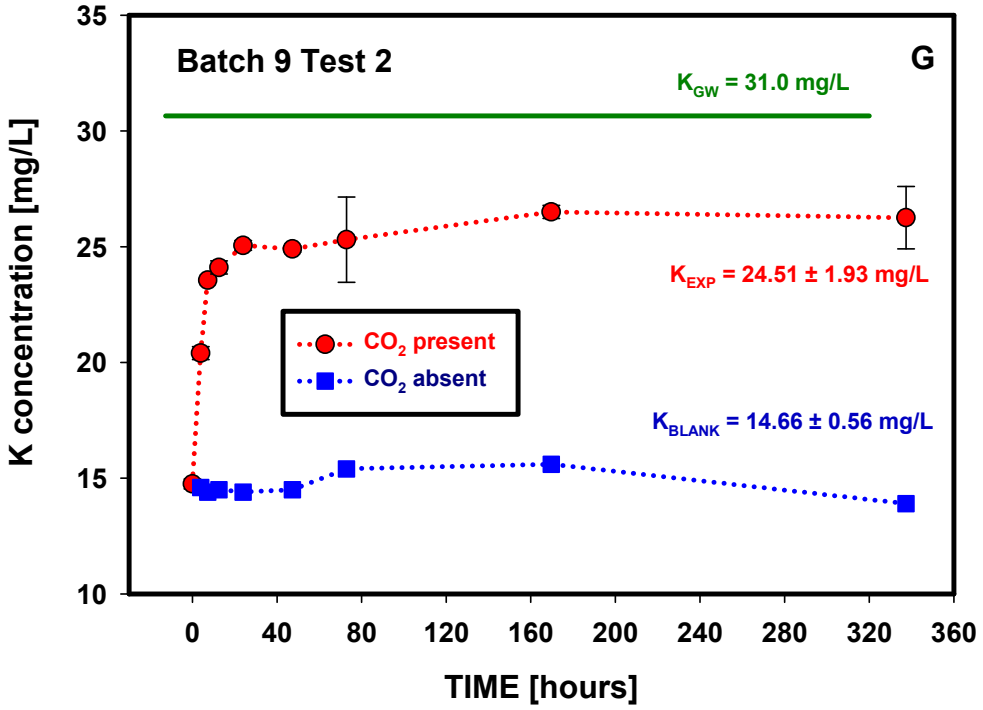

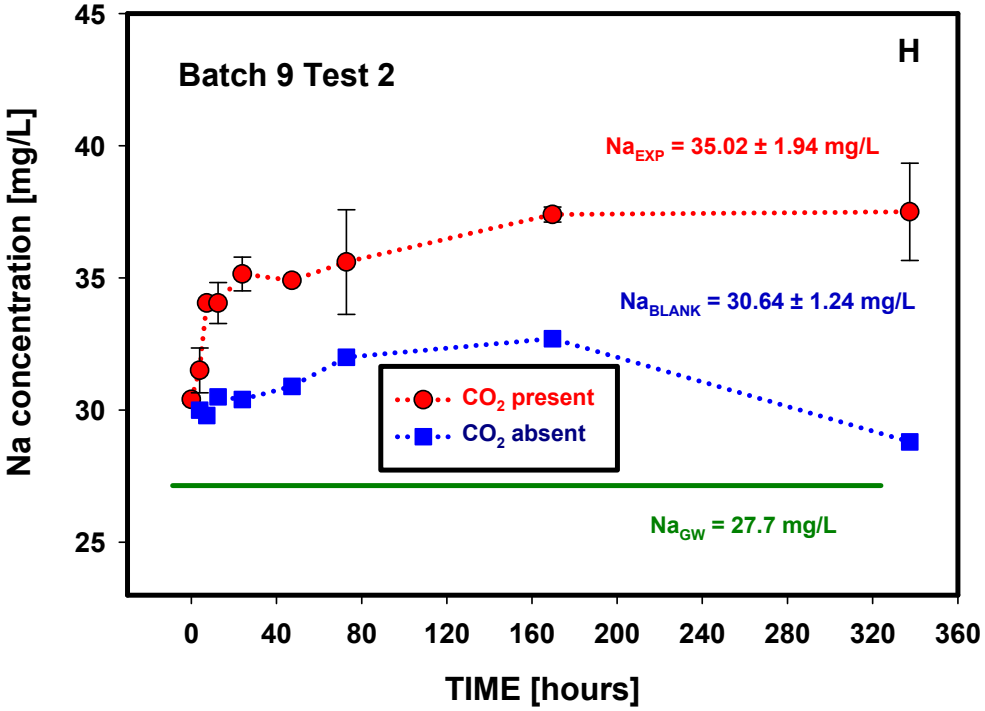

Figure D.28. (contd)

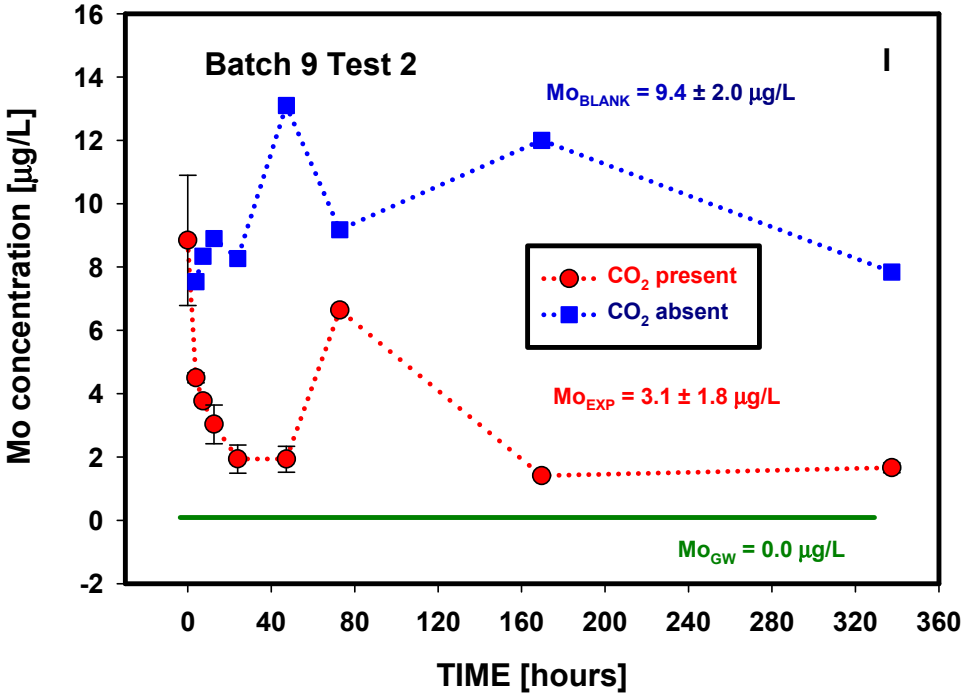

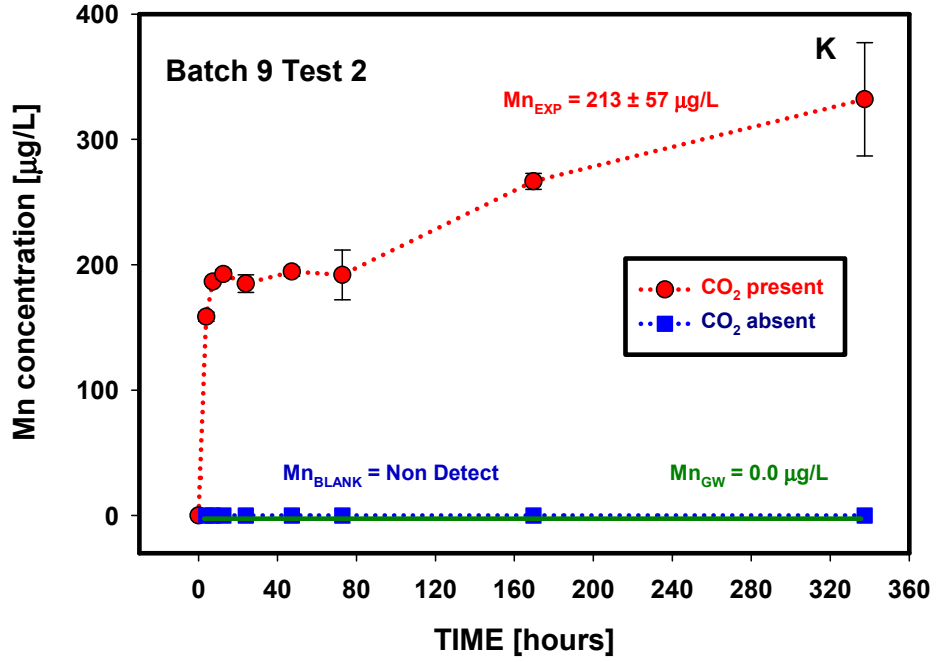

Figure D.28. (contd)

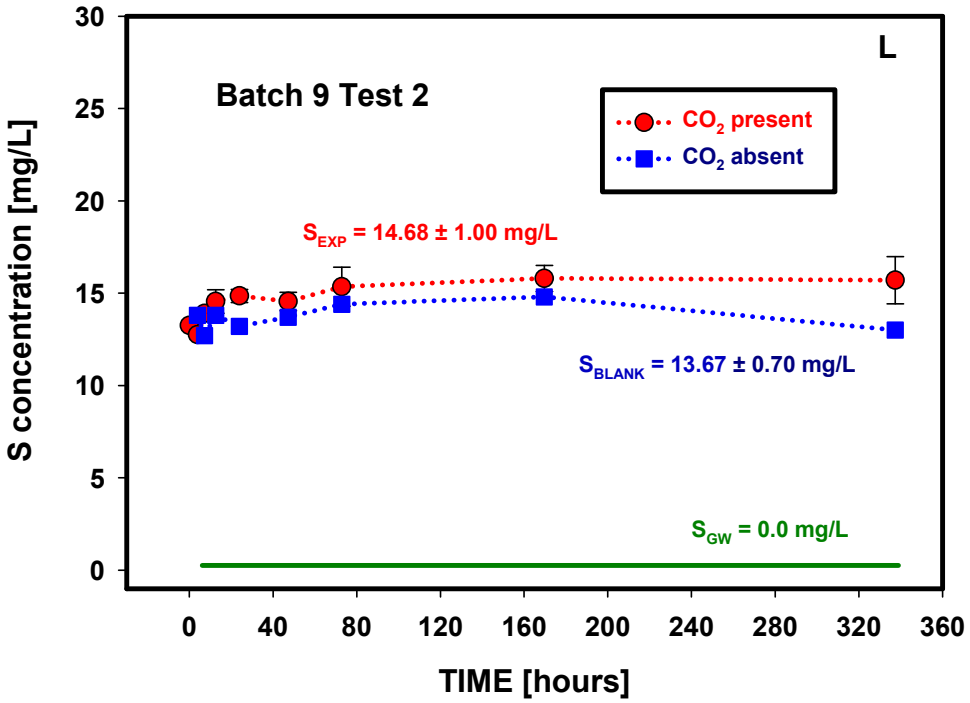

Figure D.28. (contd)

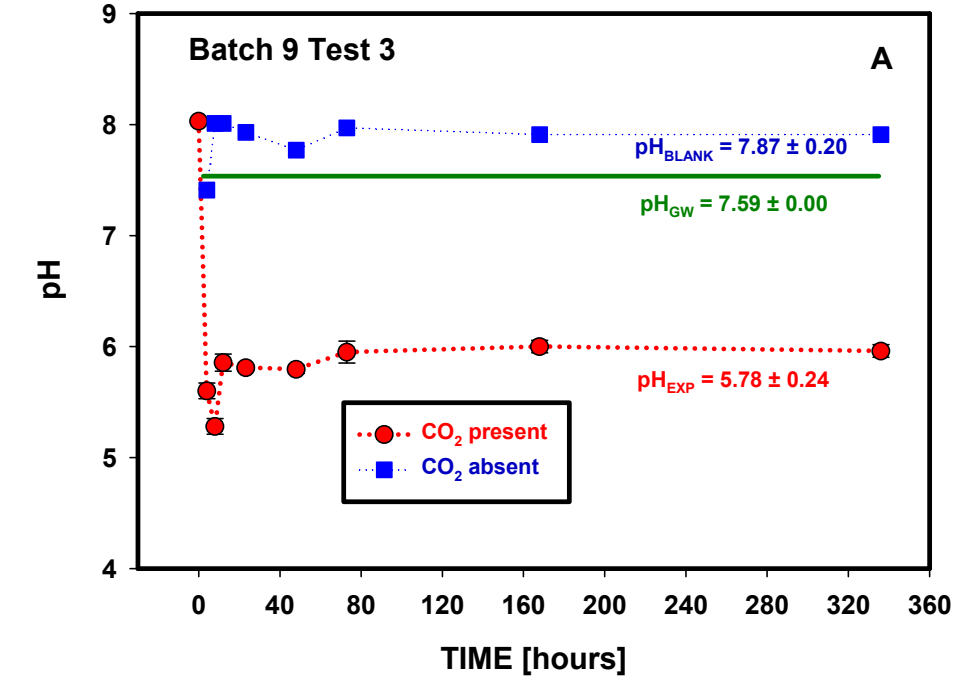

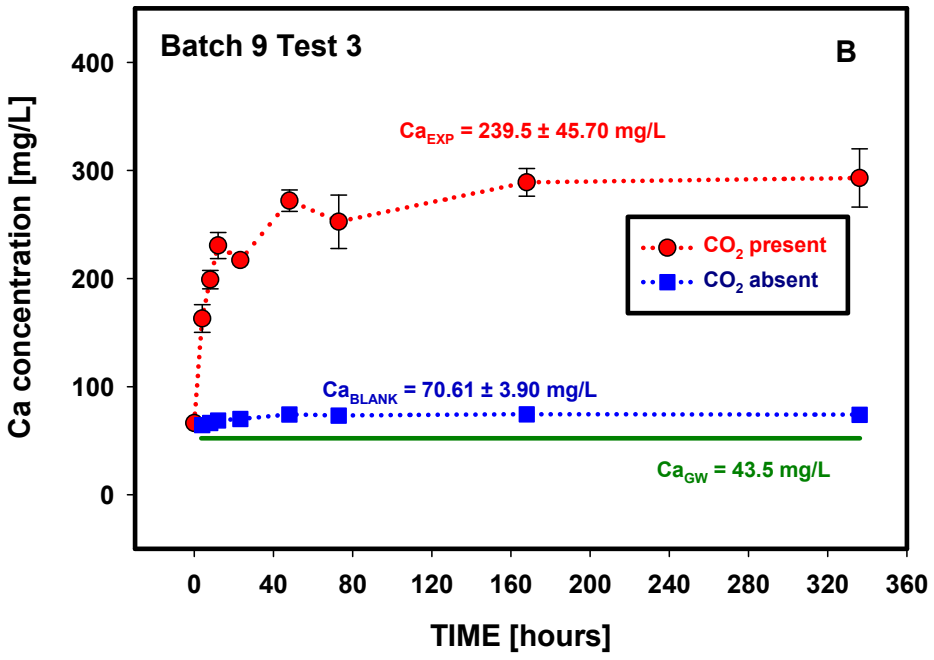

Figure D.29. Changes in pH and elemental composition as a function of time (Batch 9, Test 3, High Plains Aquifer, sediment CAL 1 91).

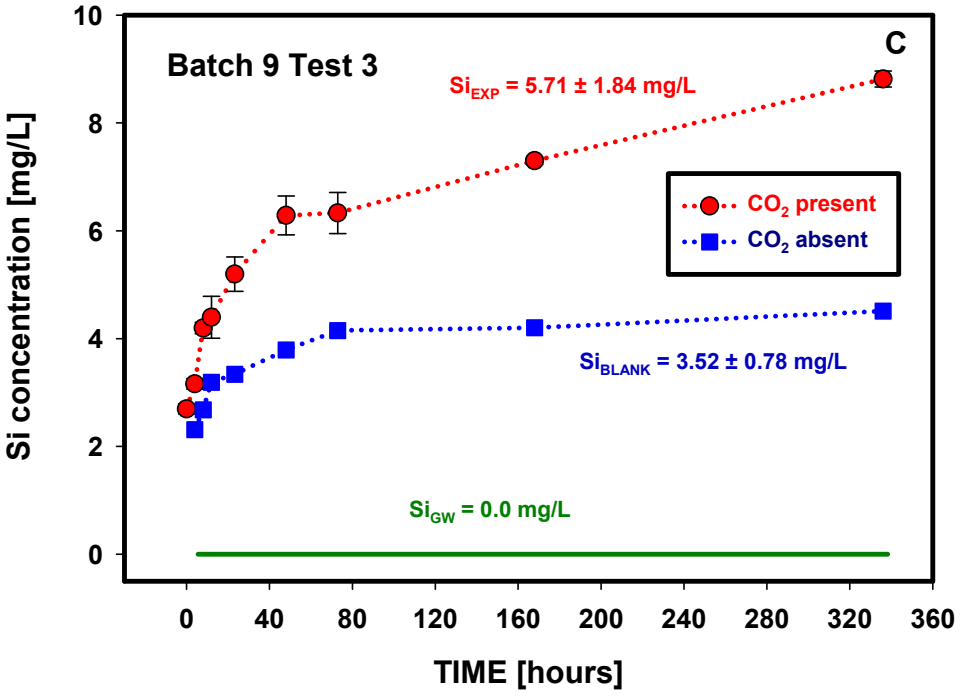

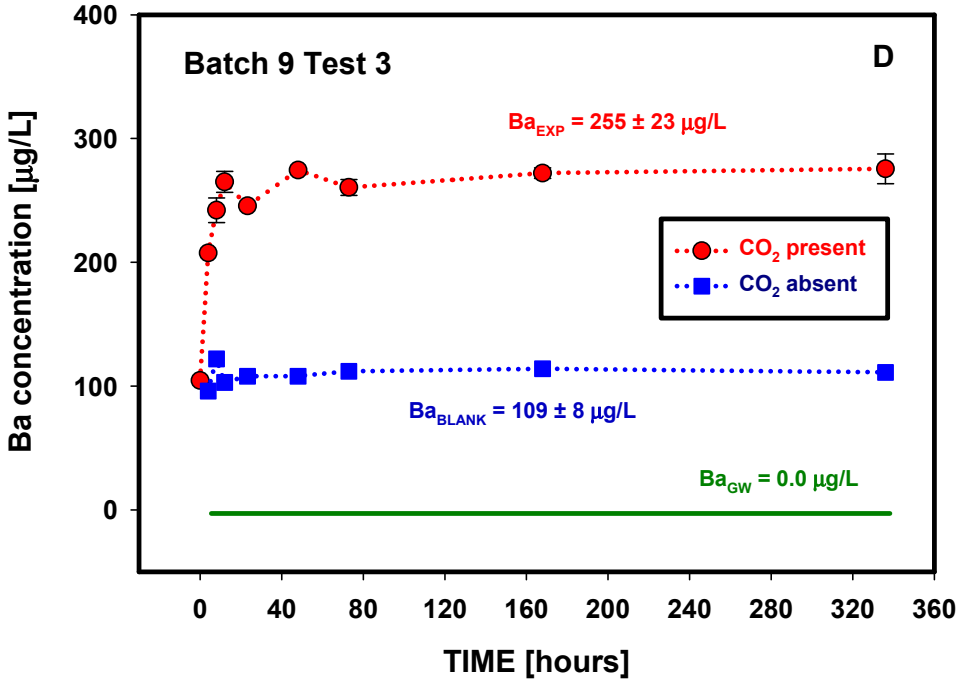

Figure D.29. (contd)

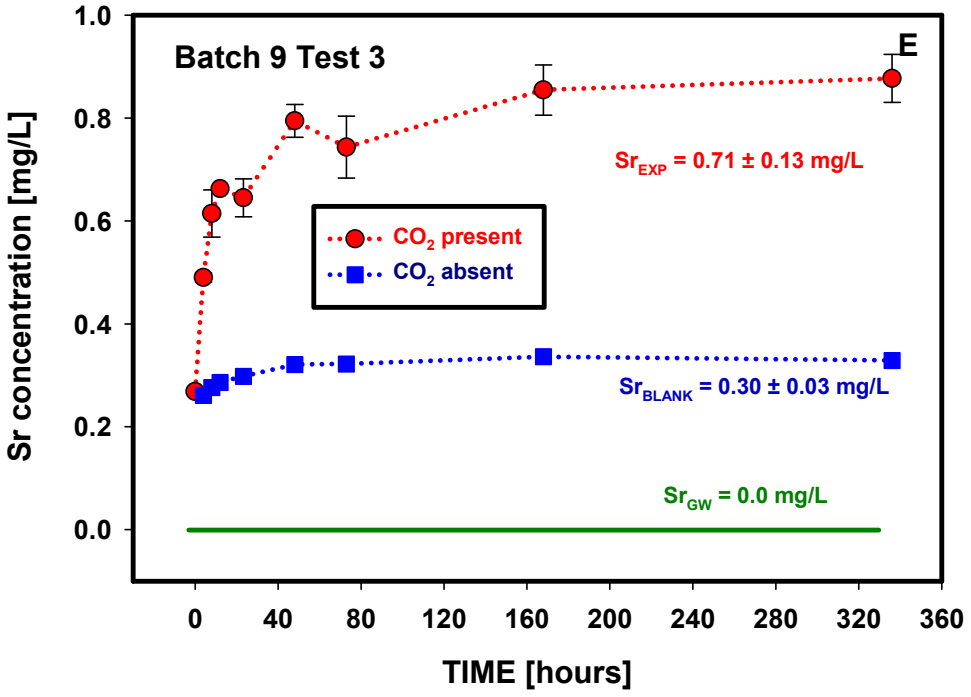

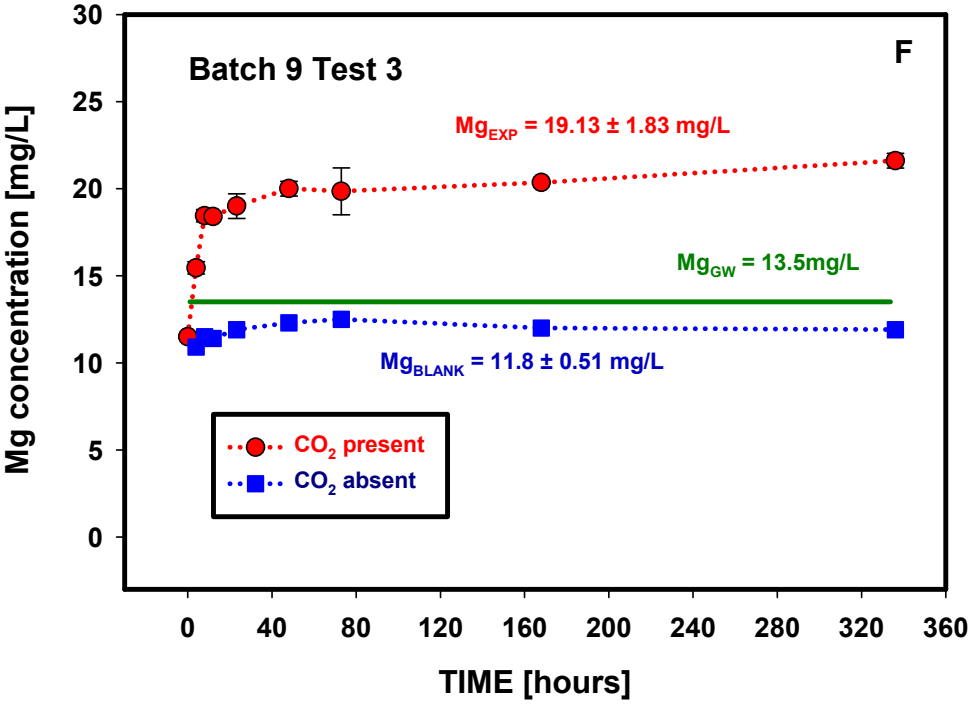

Figure D.29. (contd)

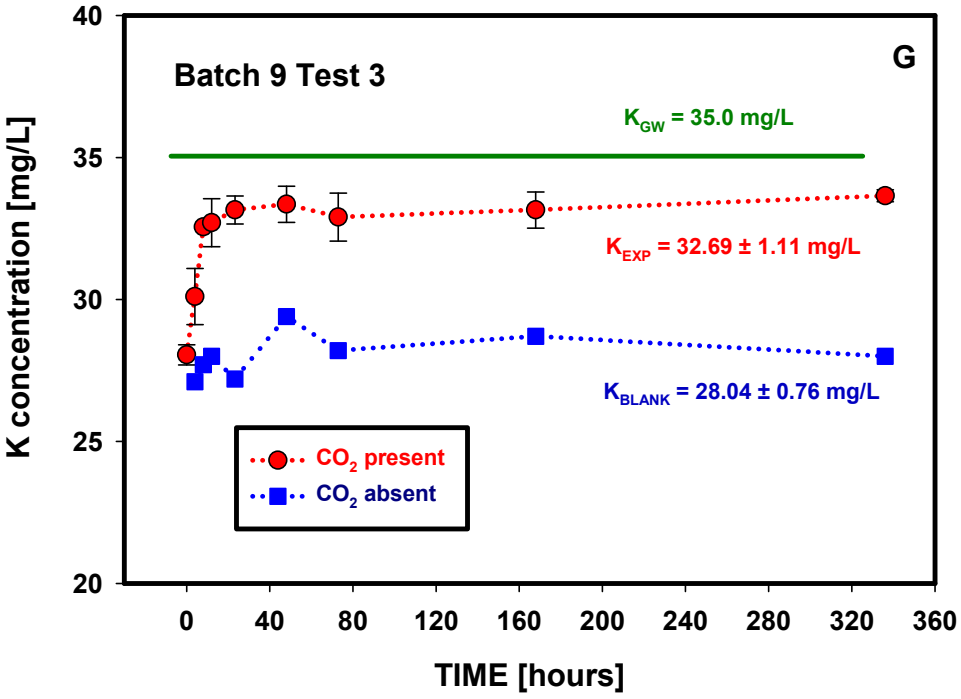

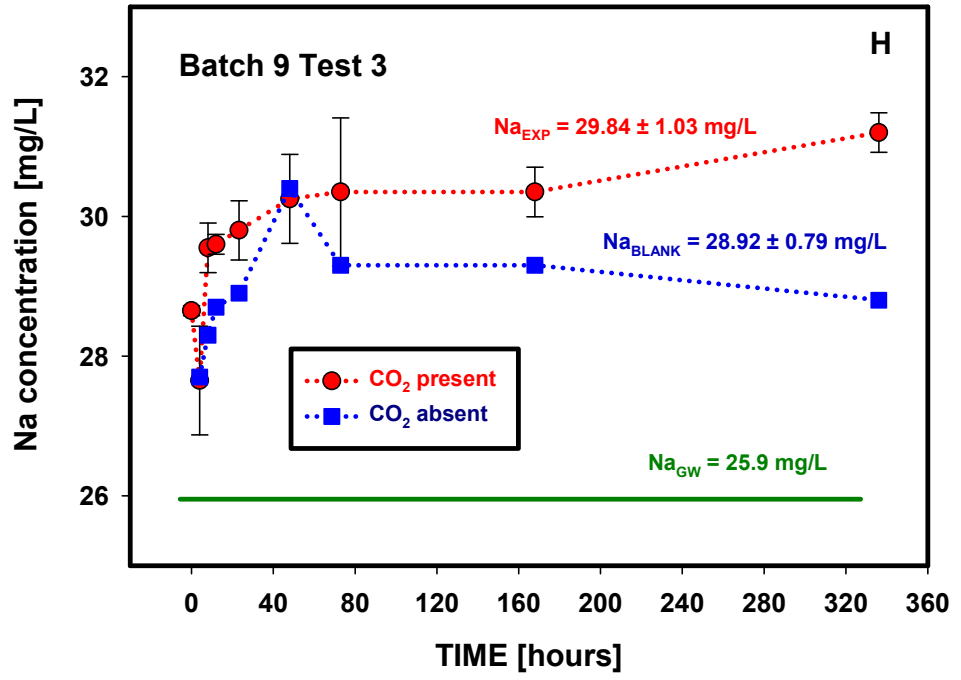

Figure D.29. (contd)

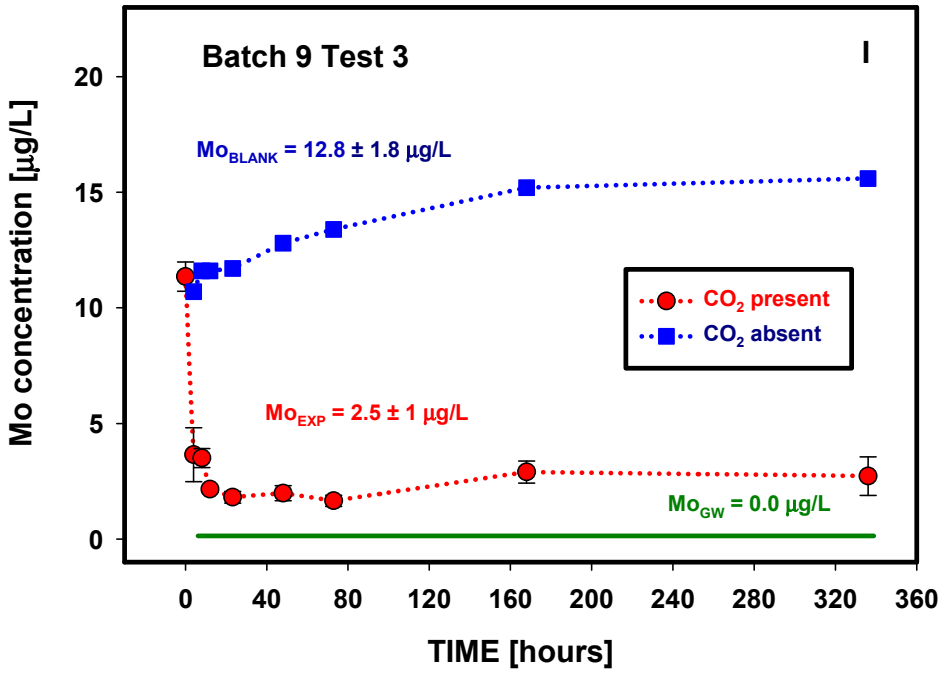

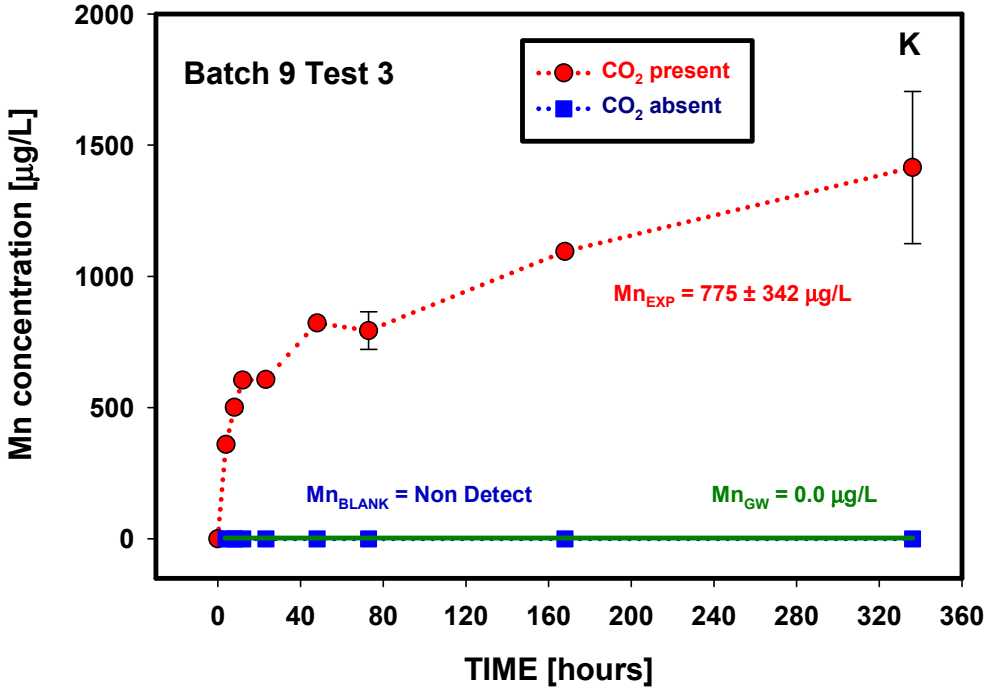

Figure D.29. (contd)

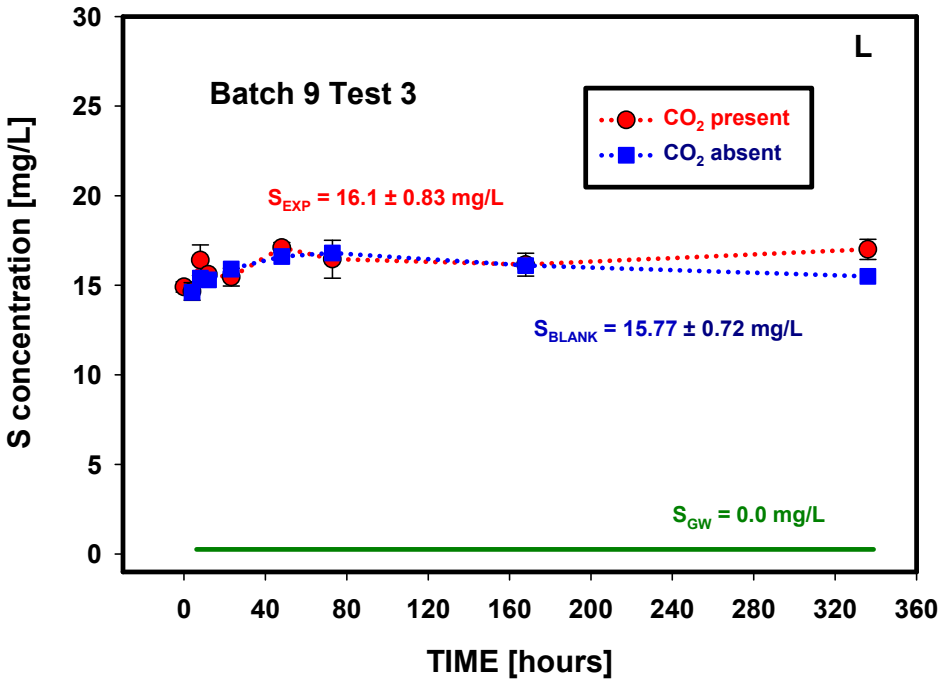

Figure D.29. (contd)

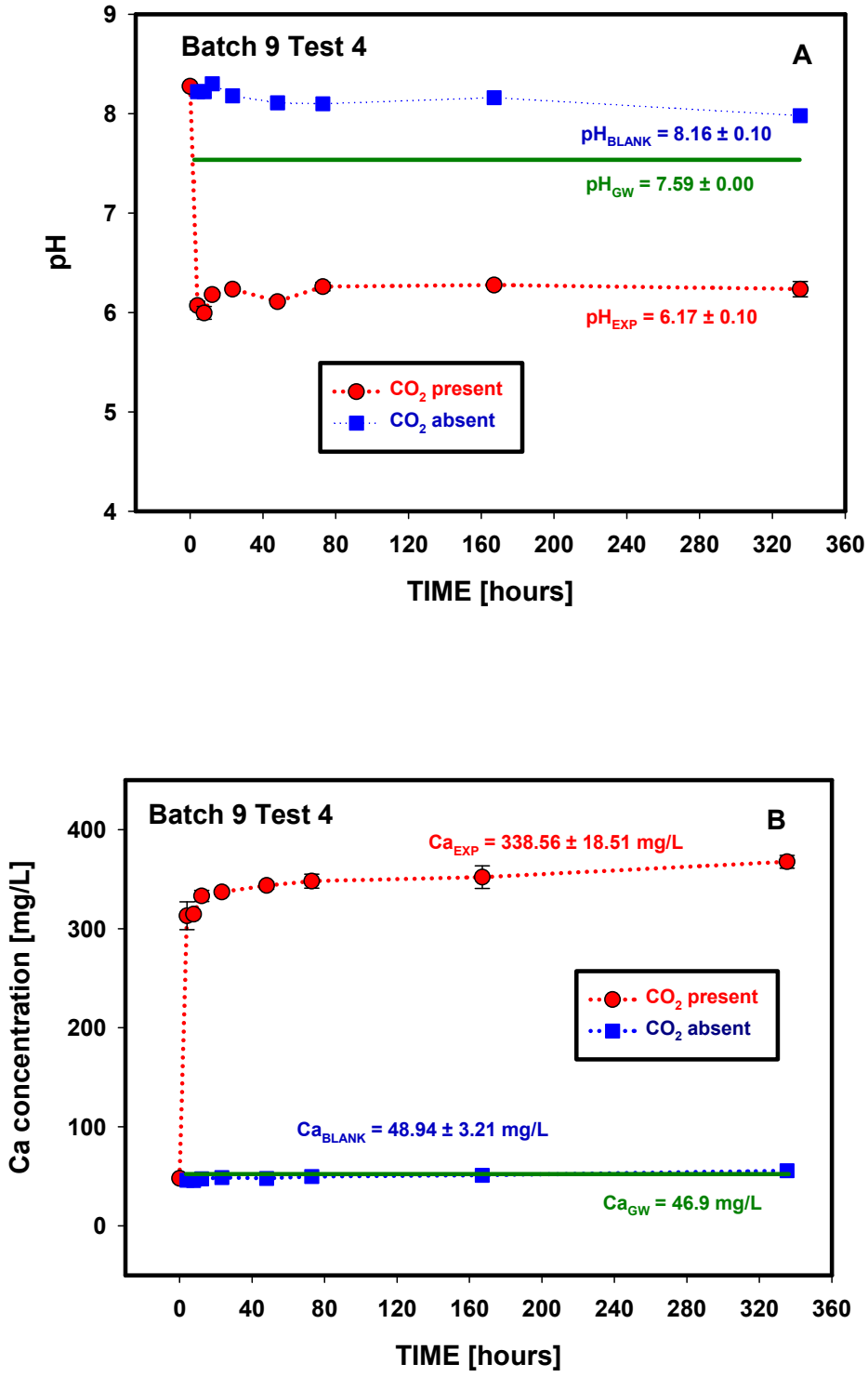

Figure D.30. Changes in pH and elemental composition as a function of time (Batch 9, Test 4, High Plains Aquifer, sediment CAL 2 4).

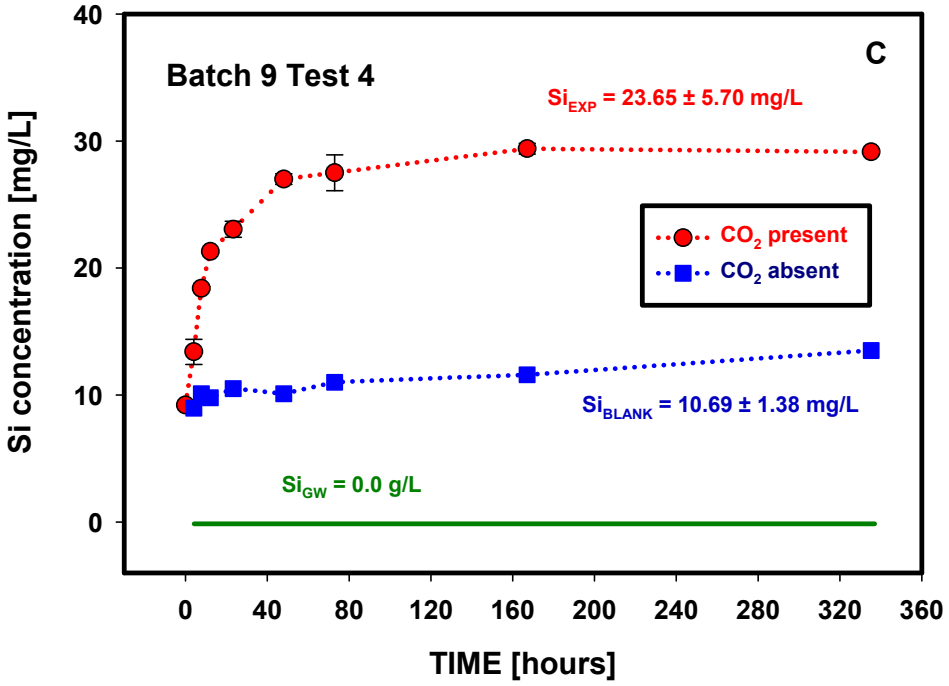

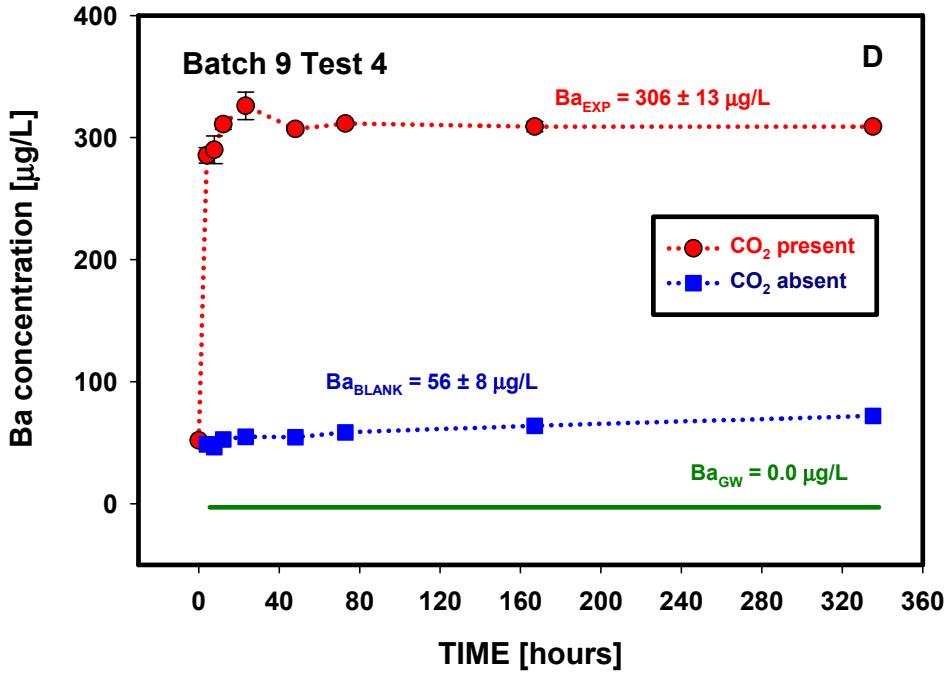

Figure D.30. (contd)

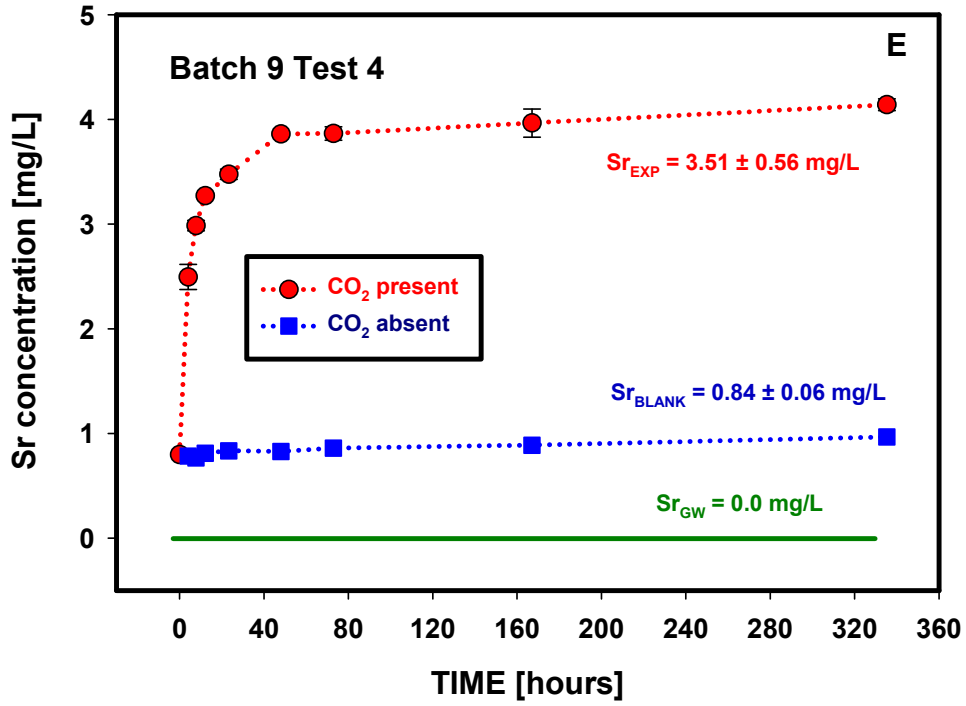

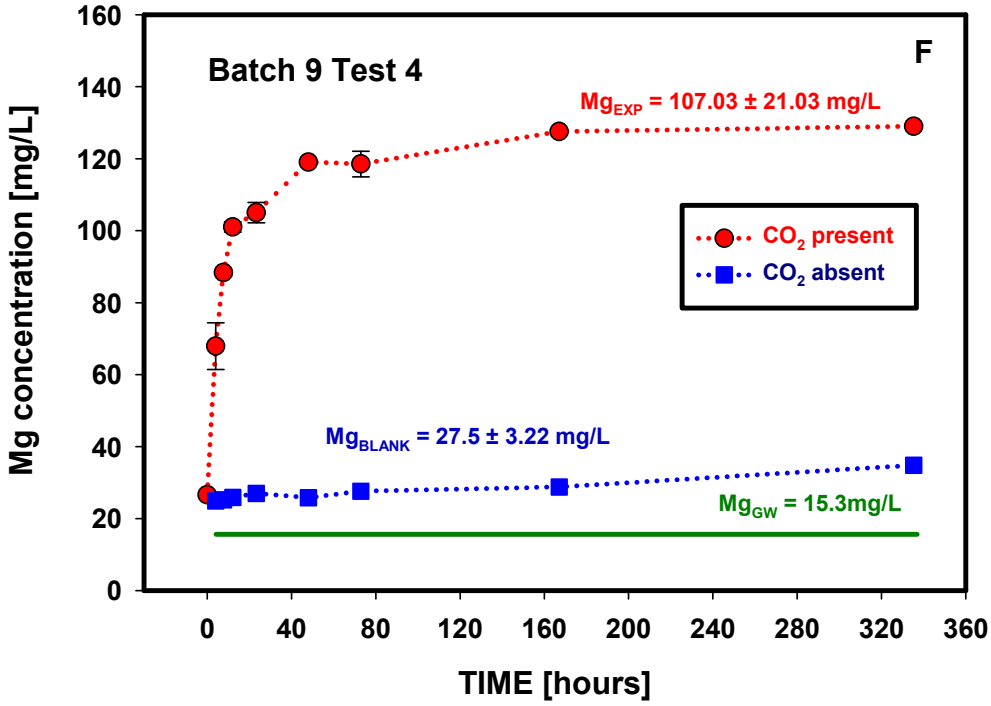

Figure D.30. (contd)

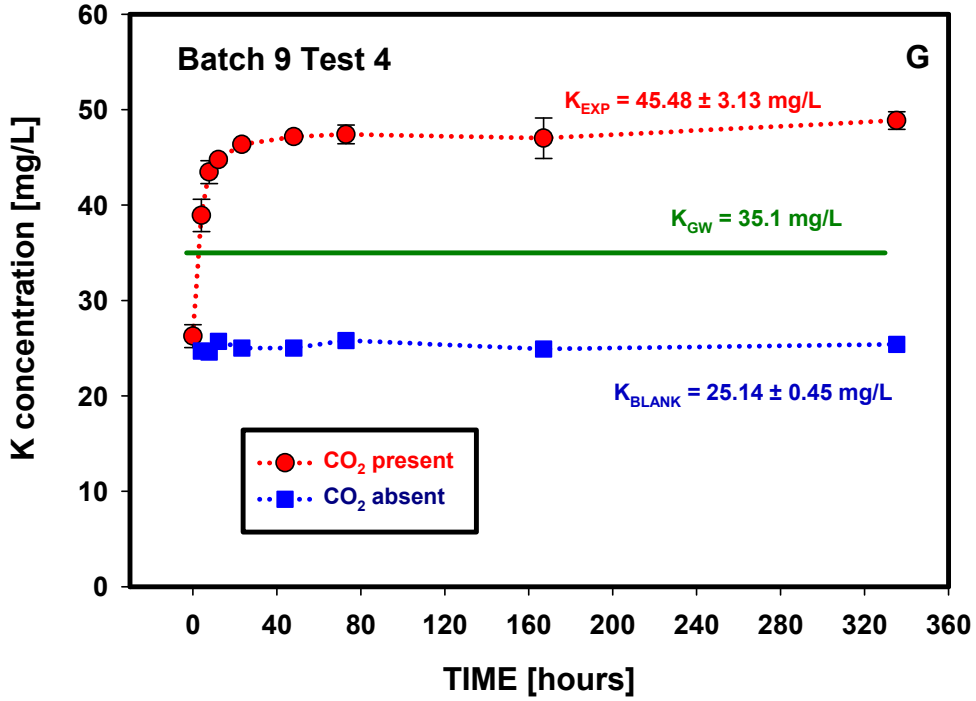

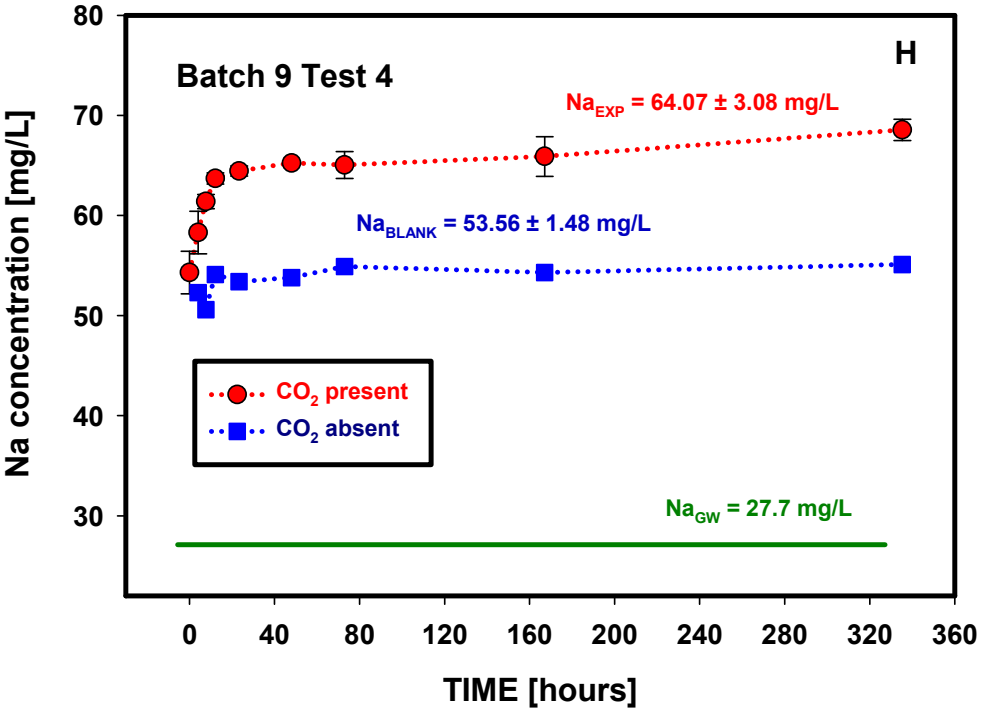

Figure D.30. (contd)

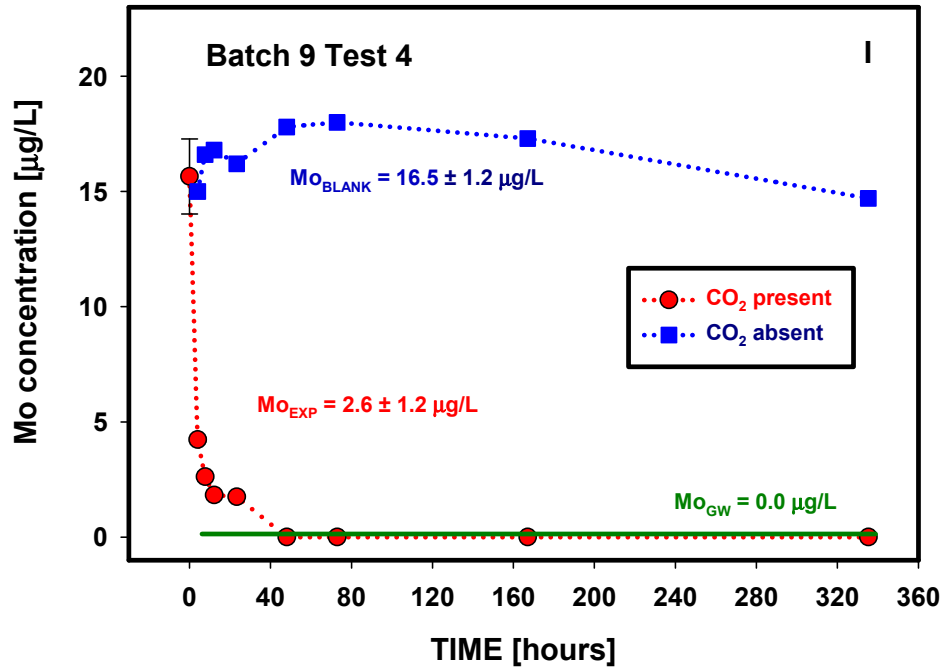

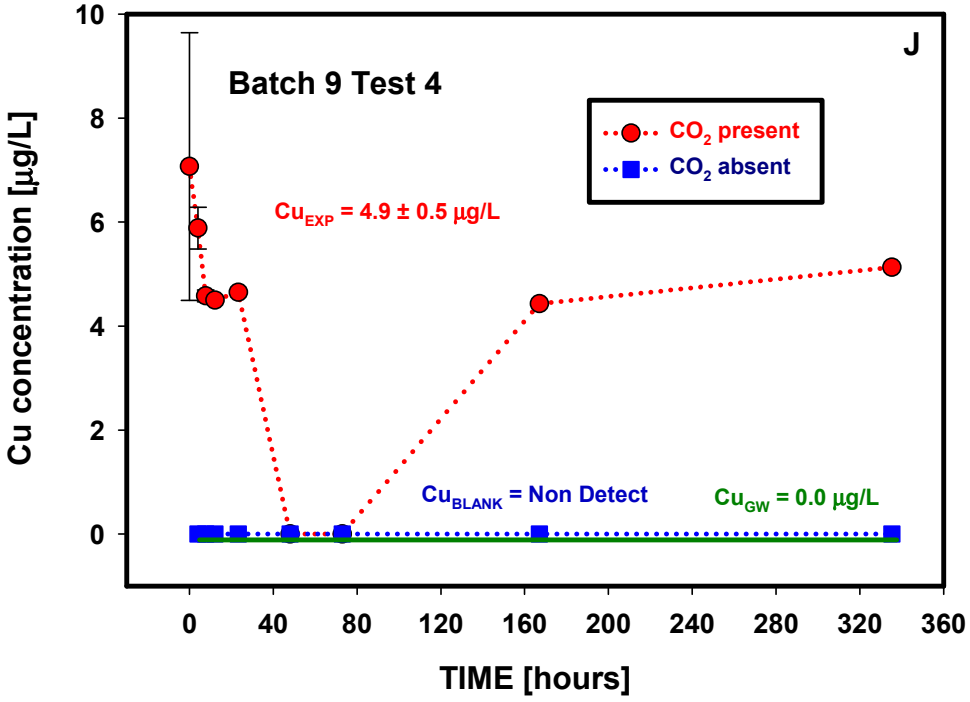

Figure D.30. (contd)

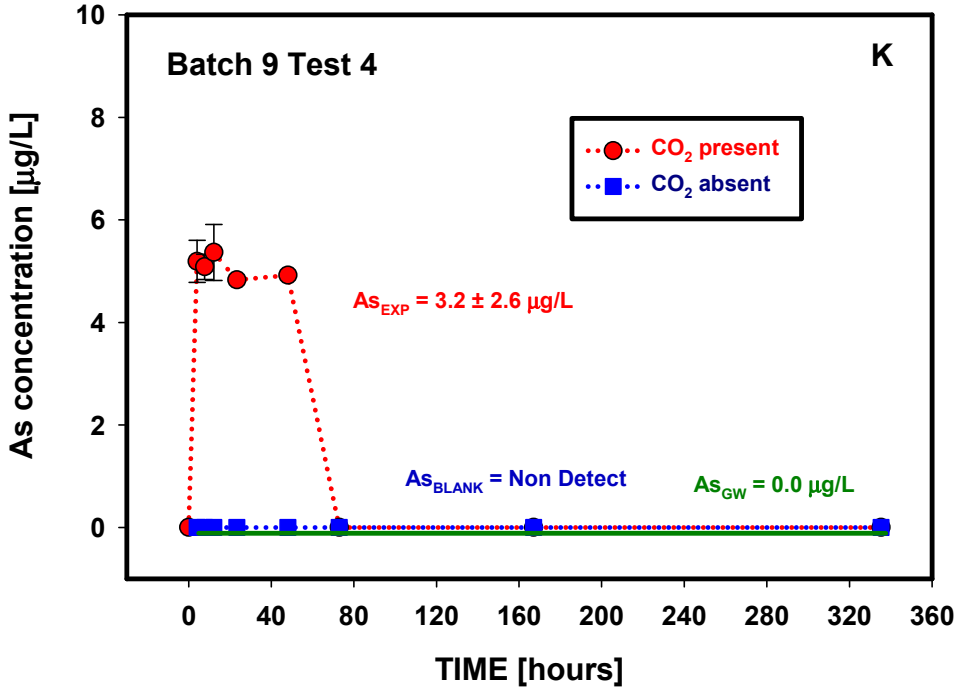

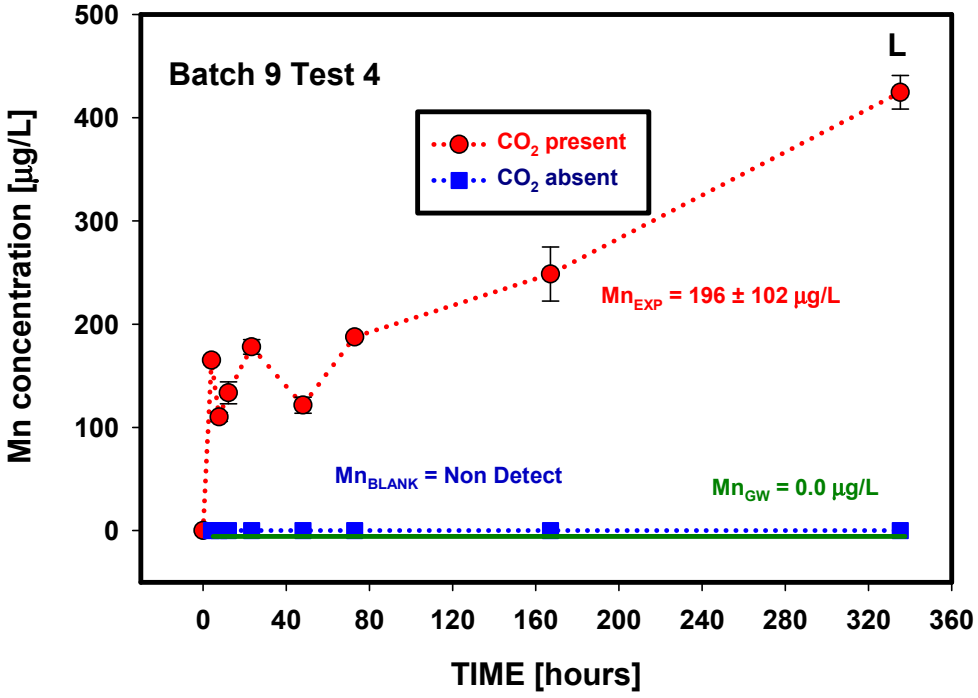

Figure D.30. (contd)

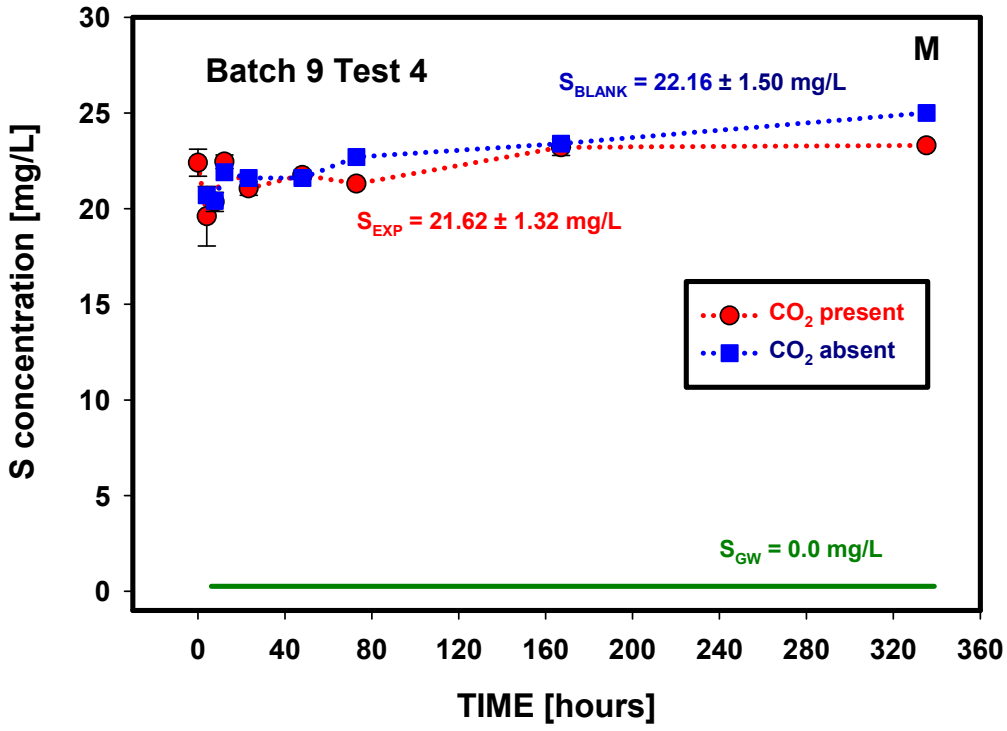

Figure D.30. (contd)

Column Experiments
Set 1: Two column experiments conducted with Edward Aquifer Set B, samples 4 (red) and Accusand (black)

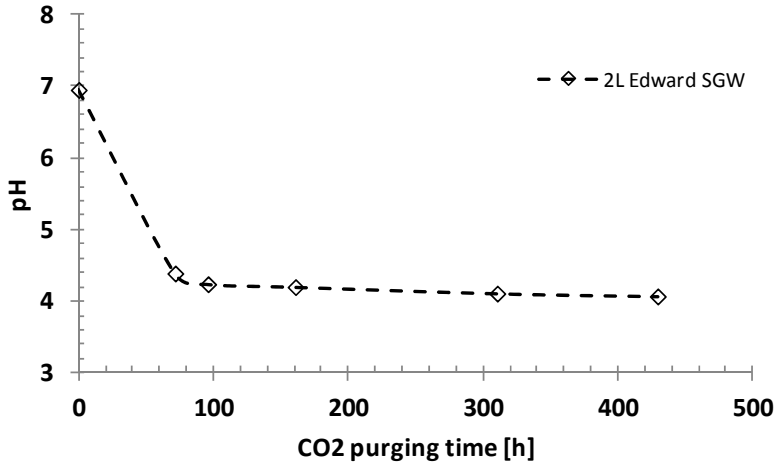

Figure D.31. pH values of inflow reservoir solutions during the CO_2 gas purging processes.

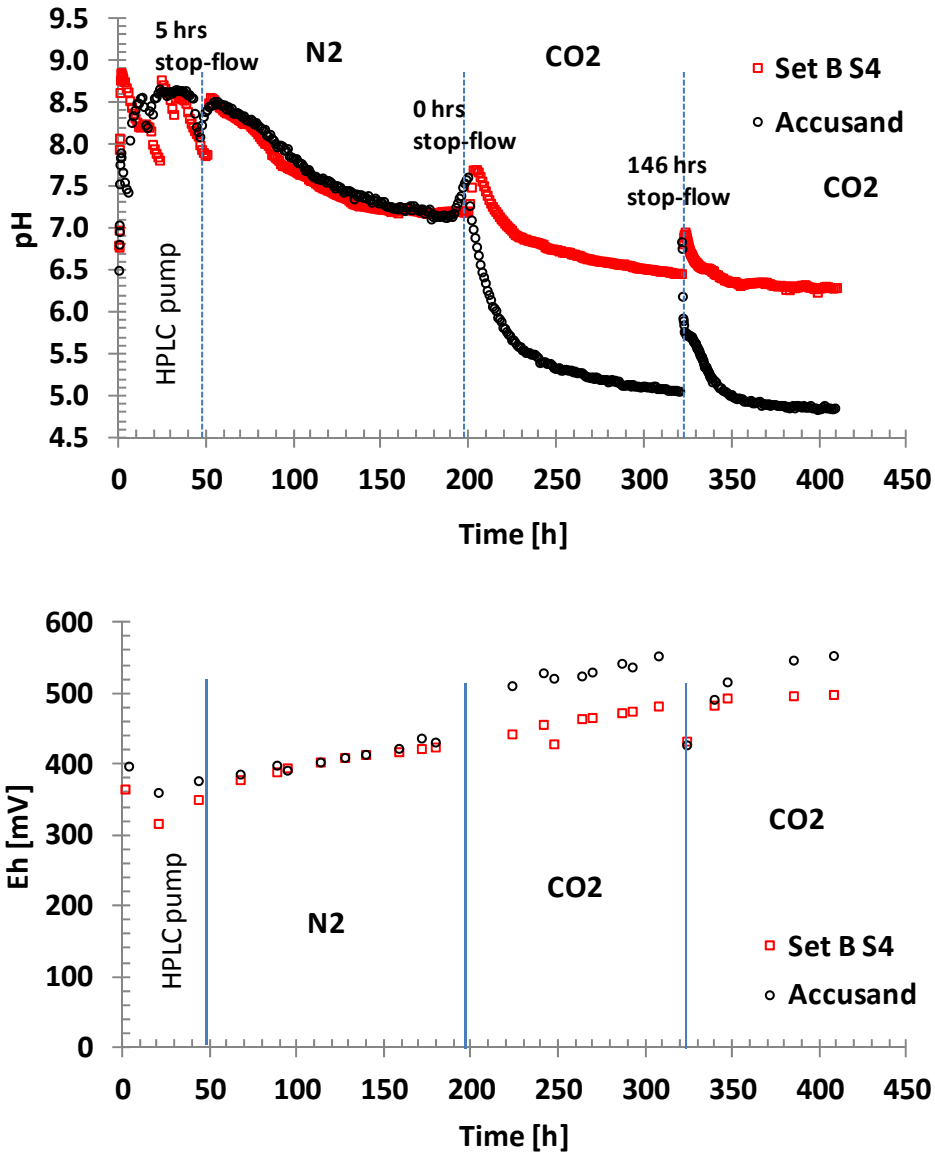

Figure D.32. Changes in effluent pH and Eh during leaching with CO_2 saturated SGW. The pH and Eh measurements were taken on-line. The first column was packed with Accusand material (black) and the second column was packed partially with Accusand and partially with the Edwards Aquifer Set B sample 4 (red). The fluid was injected with a KLOEHN V6 syringe pump (HPLC pumps were used in the initial ~50 hours). One stop flow event of a duration of 146 hours was applied during leaching with the CO_2 gas saturated SGW at about 320 hours of experimental time.

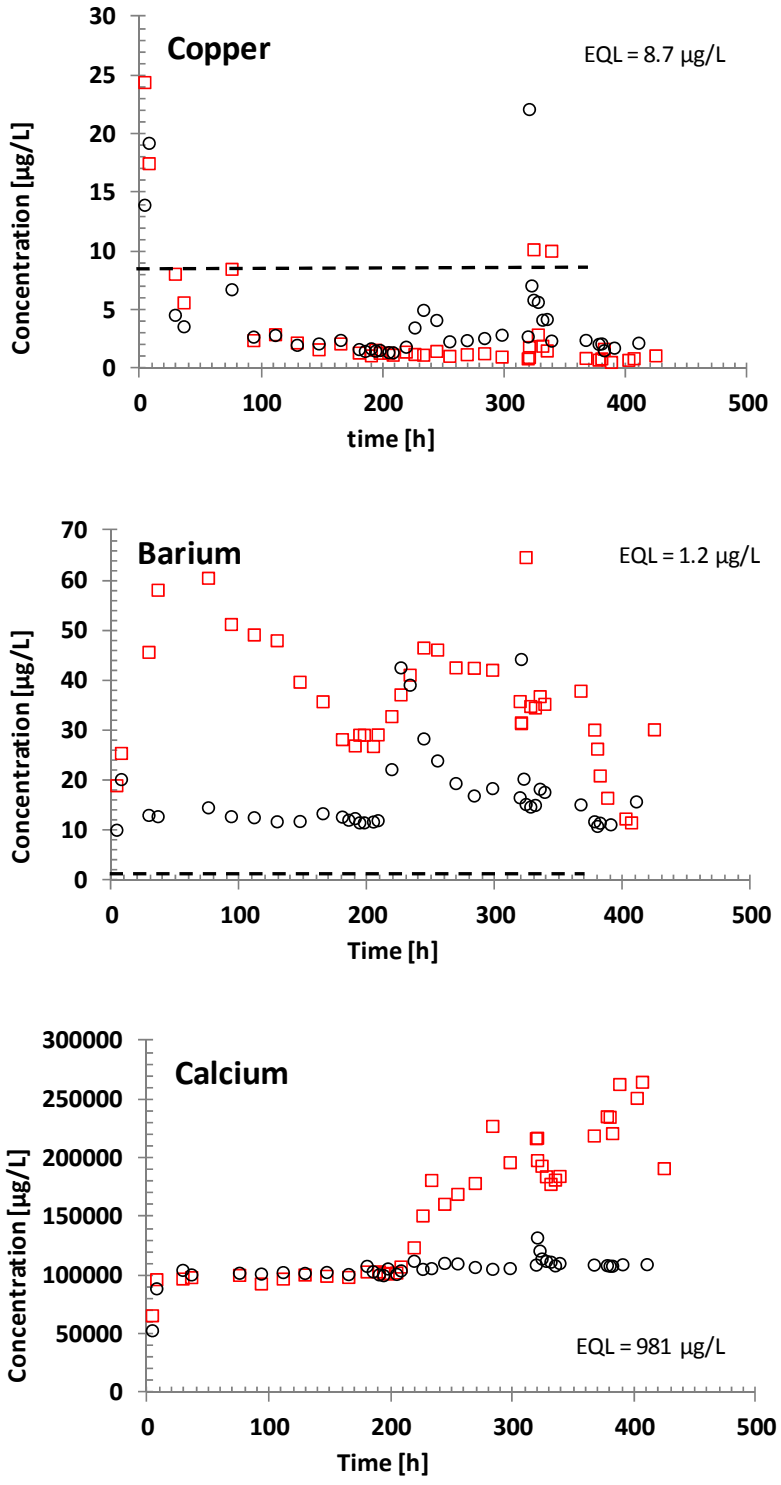

Figure D.33. Column Experiment Set 1. Changes in effluent chemical composition with time. The red squares and the black circles represent Set B sample 4 and Accusand columns, respectively. The EQL (the black dashed lines) indicates the equipment detection limit times the dilution factor. All non-zero concentrations below the EQL line should be considered as nondetect. One stop flow event of a duration of 146 hours was applied during leaching with the CO_2 gas saturated SGW at about 320 hours of experimental time.

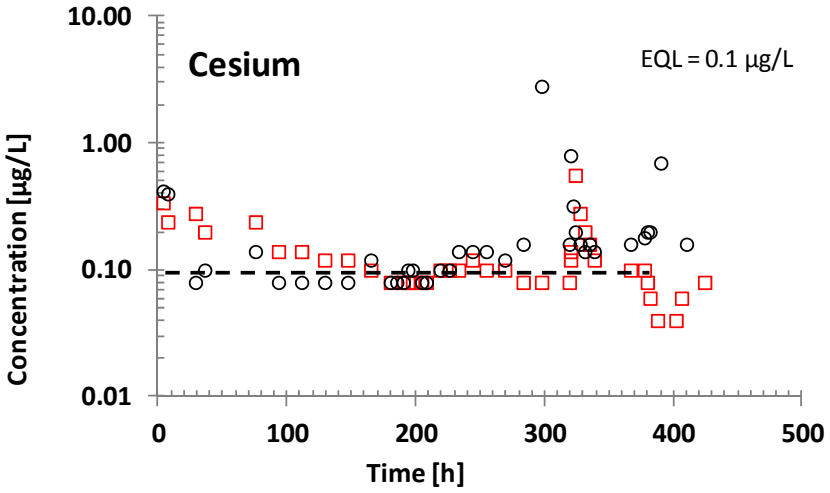

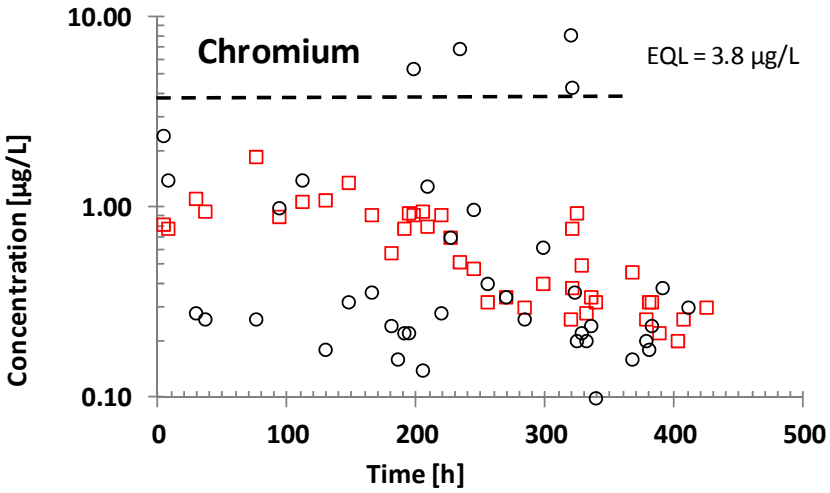

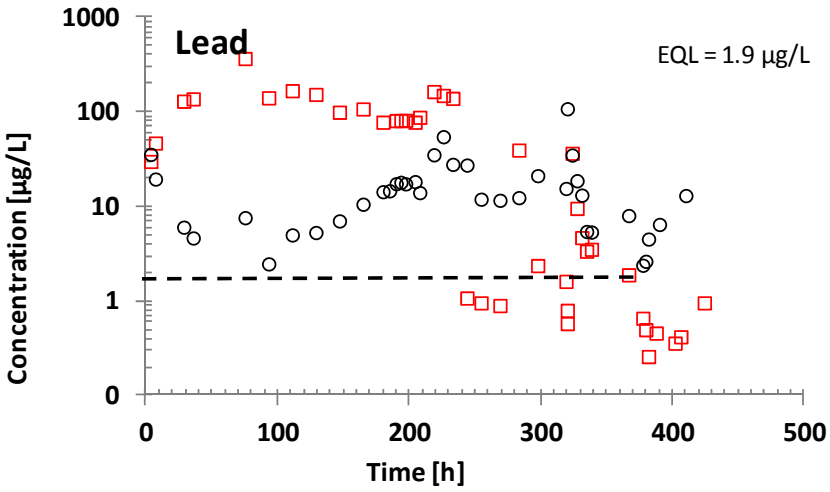

Figure D.33. (contd)

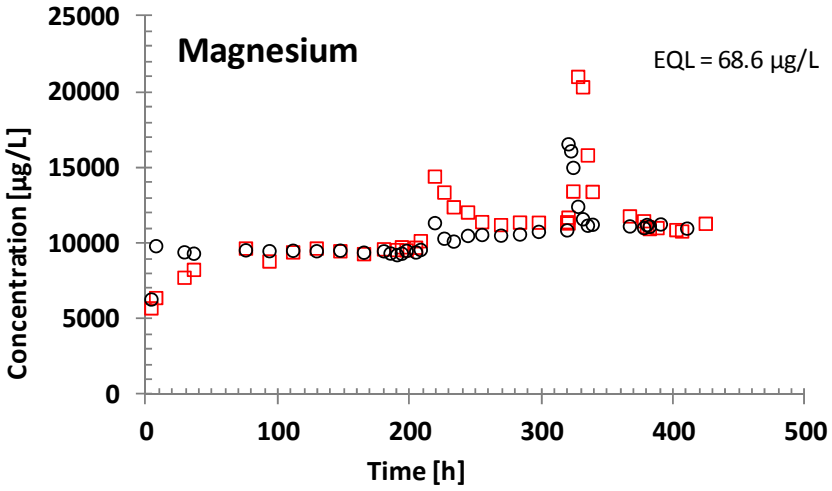

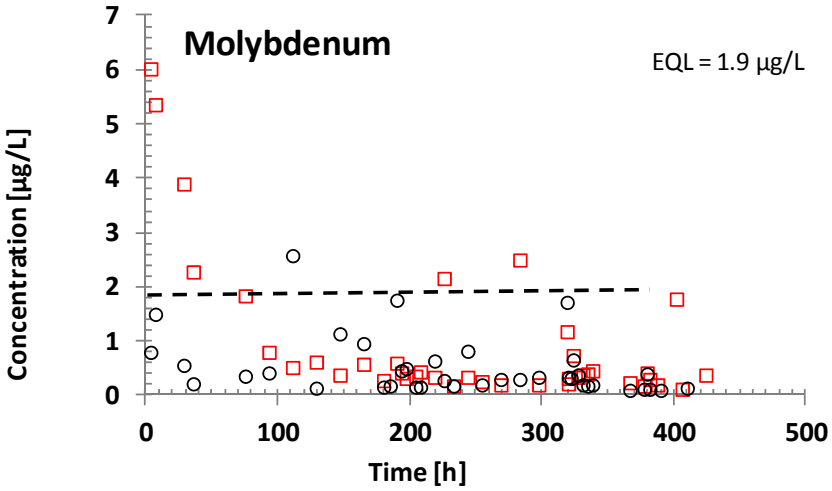

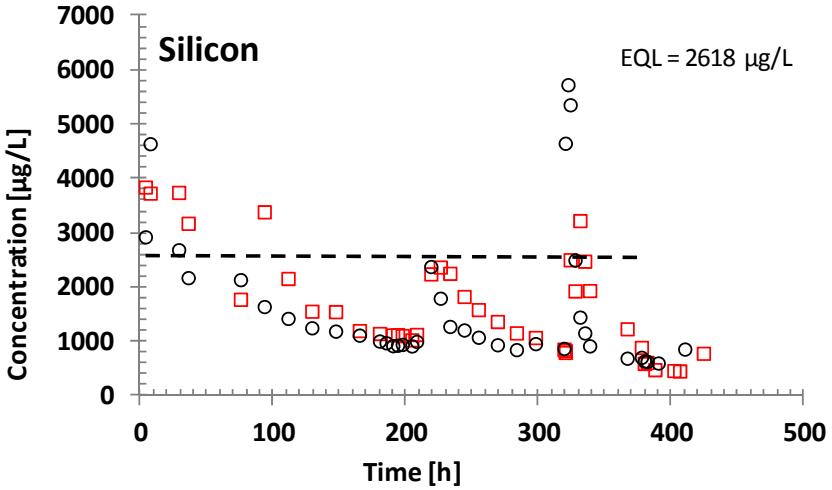

Figure D.33. (contd)

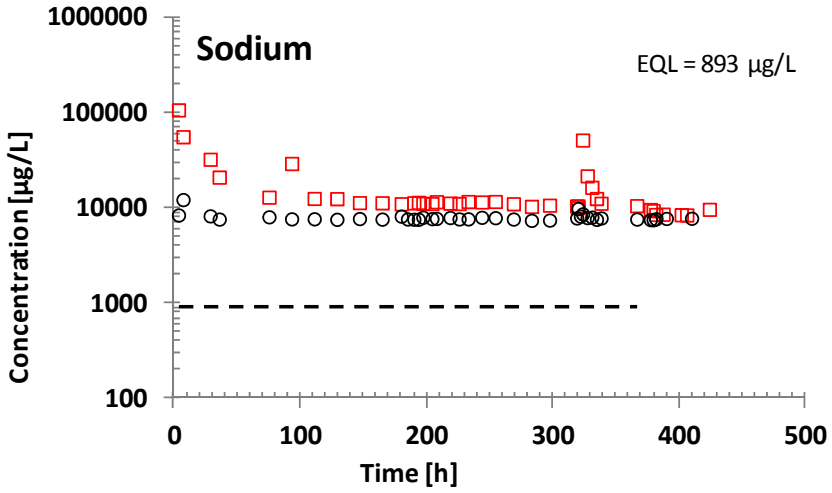

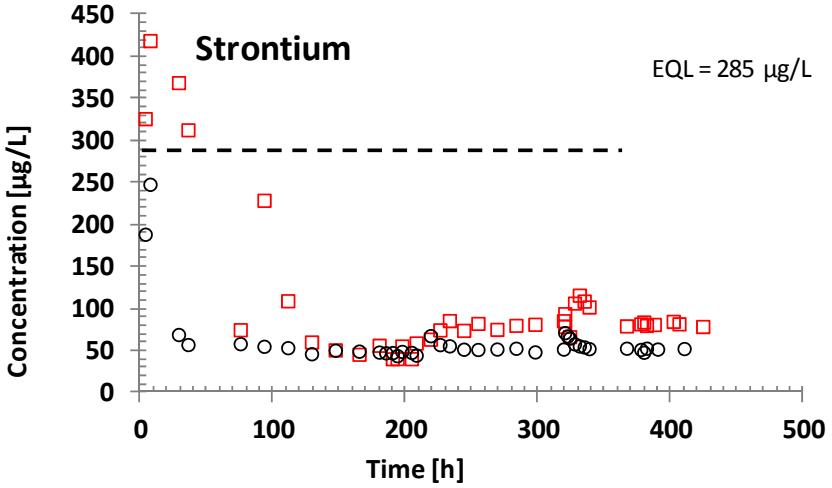

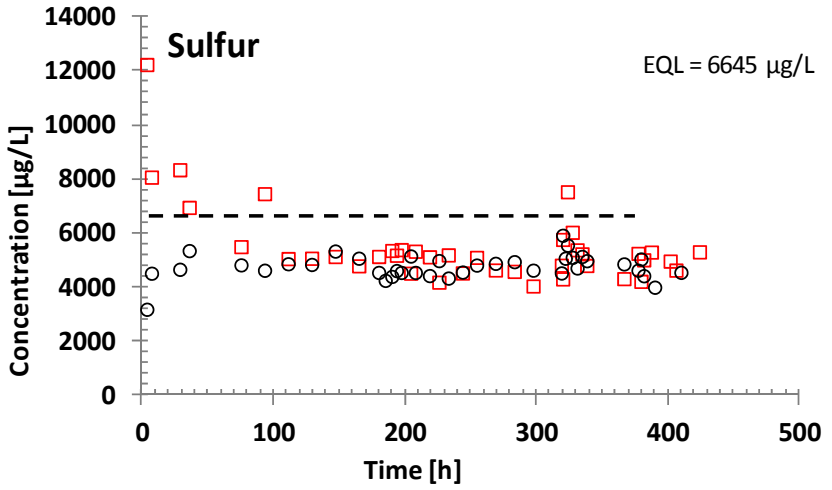

Figure D.33. (contd)

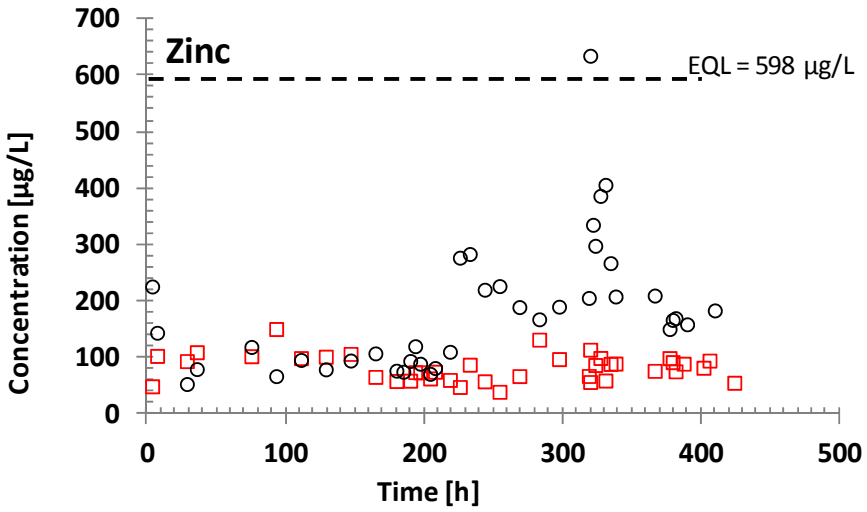

Figure D.33. (contd)

Set 2: Two column experiments conducted with Edward Aquifer Set B, samples 4 (red) and 7 (black)

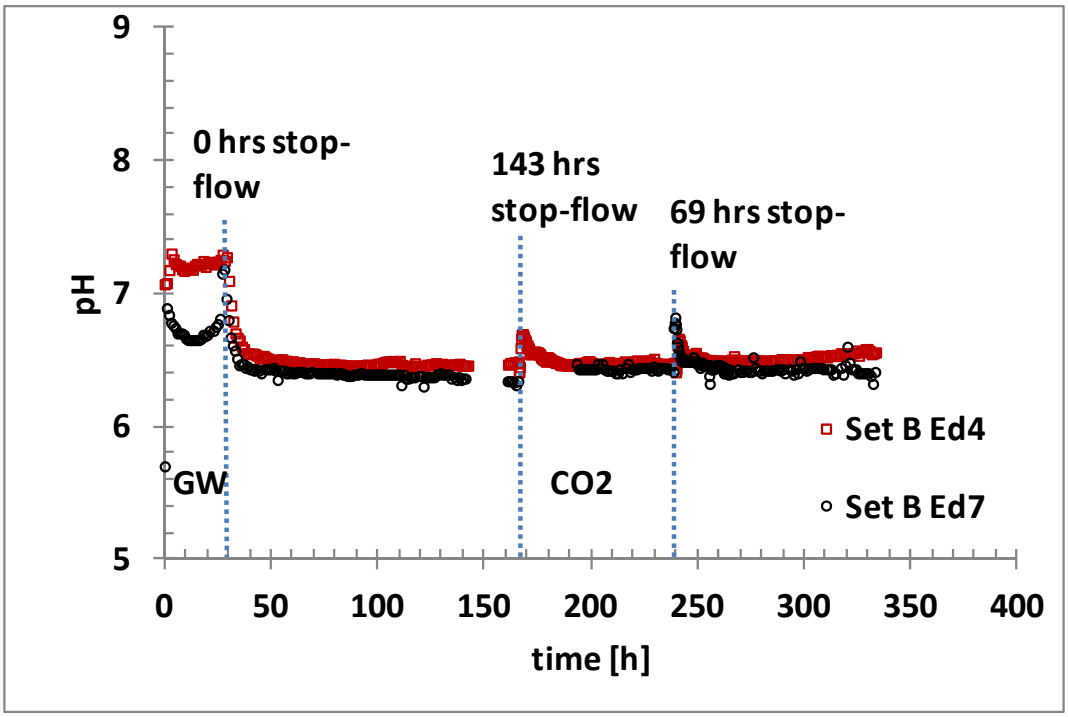

Figure D.34. Changes in effluent pH as a function of time in two column experiments conducted with Edwards Aquifer materials, Set B, sample 4 and 7. The columns were leached with the SGW for about 30 hours and then the input solution was switched to the CO_2 gas saturated SGW. Two stop flow events of a duration of 143 and 69 hours were applied during leaching with the CO_2 gas saturated SGW at about 170 and 240 hours of experimental time.

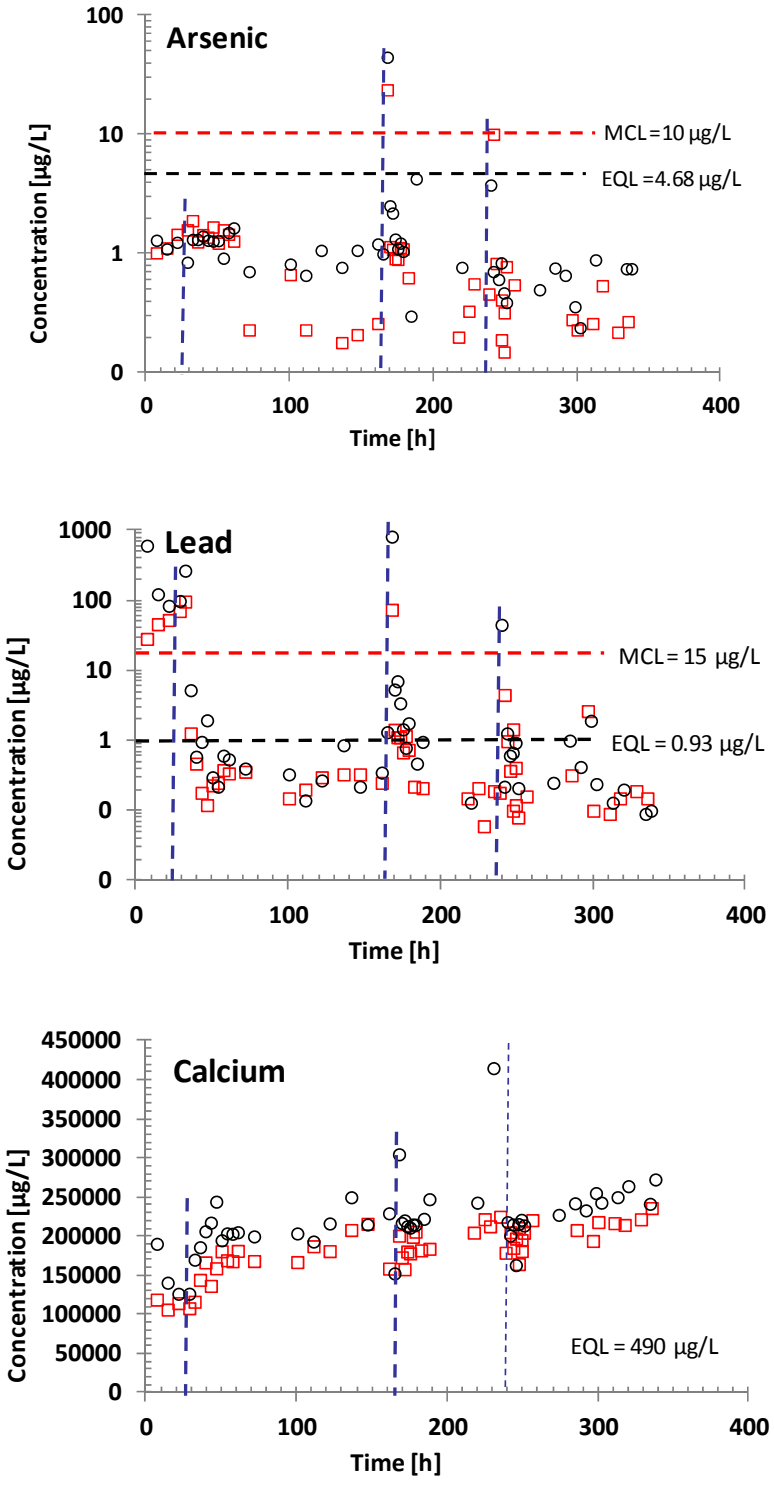

Figure D.35. Changes in effluent chemical concentration as a function of time. Data are from Set 2. There were two column experiments in Set 2 and they were packed with the Edwards Aquifer materials Set B, samples 4 (red) and 7 (black). Two stop flow events of a duration of 143 and 69 hours were applied during leaching with the CO_2 gas saturated SGW at about 170 and 240 hours of experimental time.

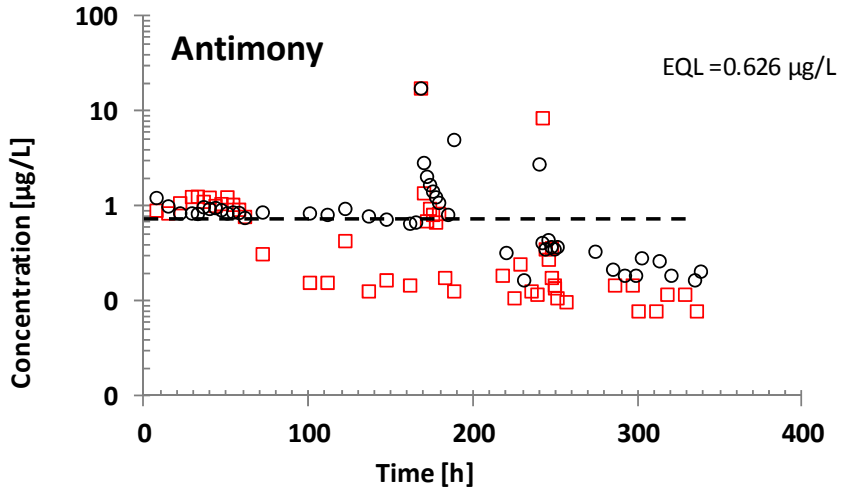

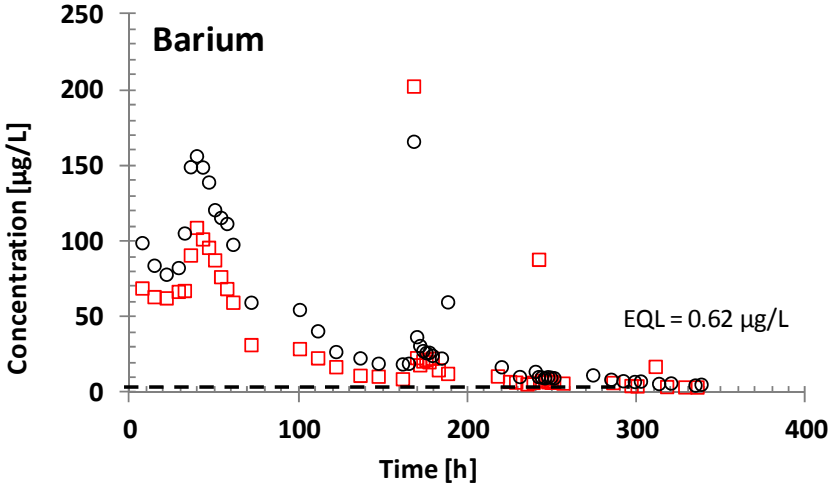

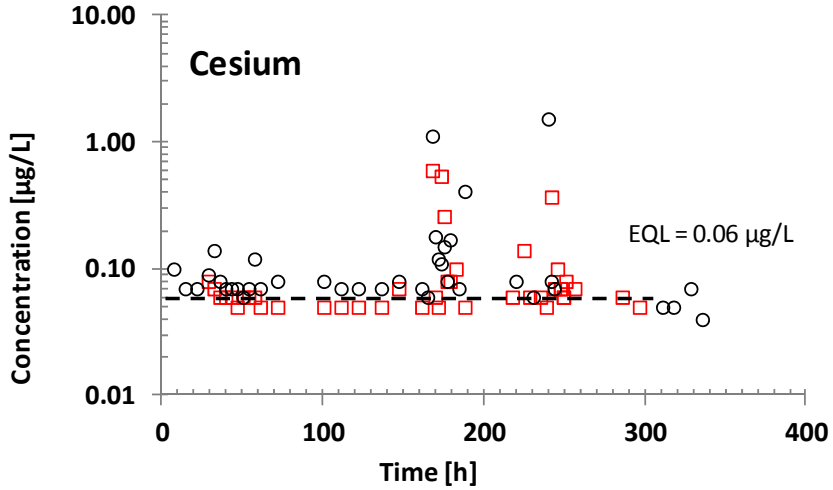

Figure D.35. (contd)

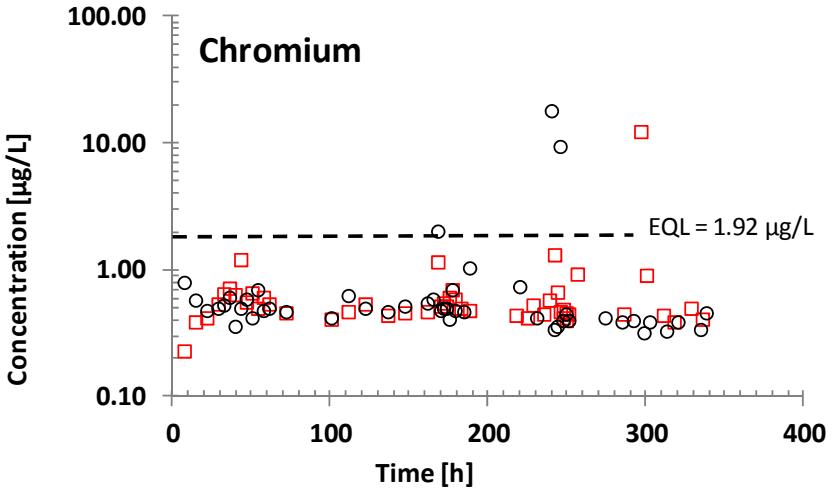

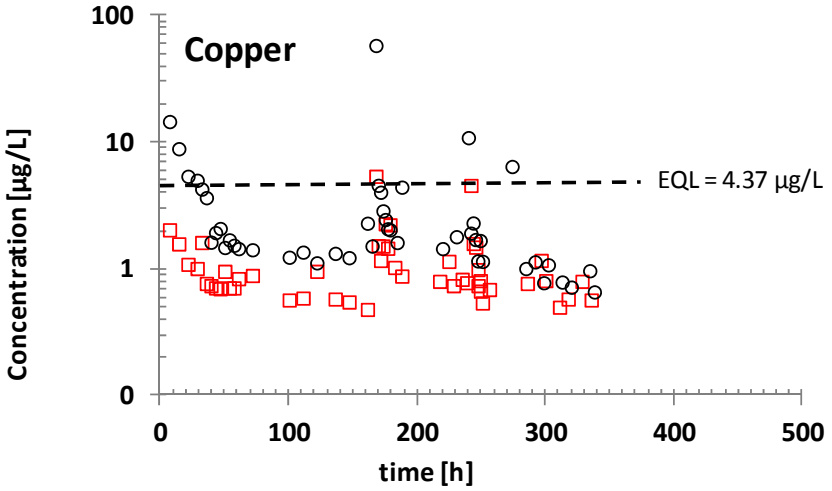

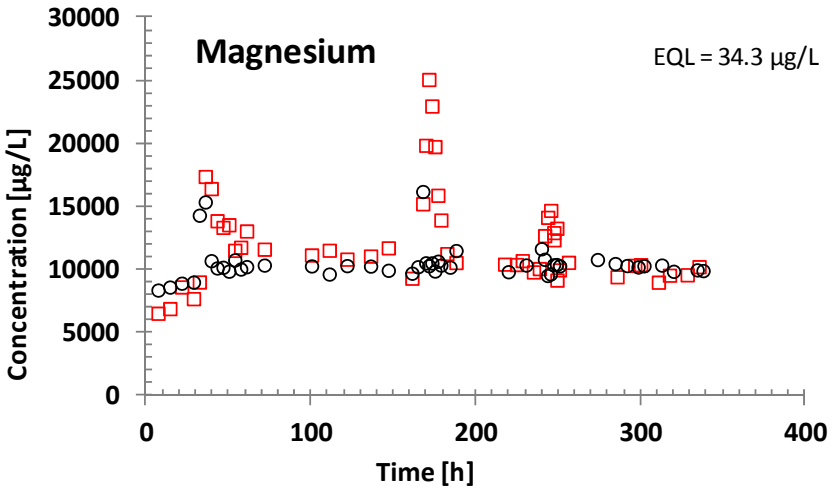

Figure D.35. (contd)

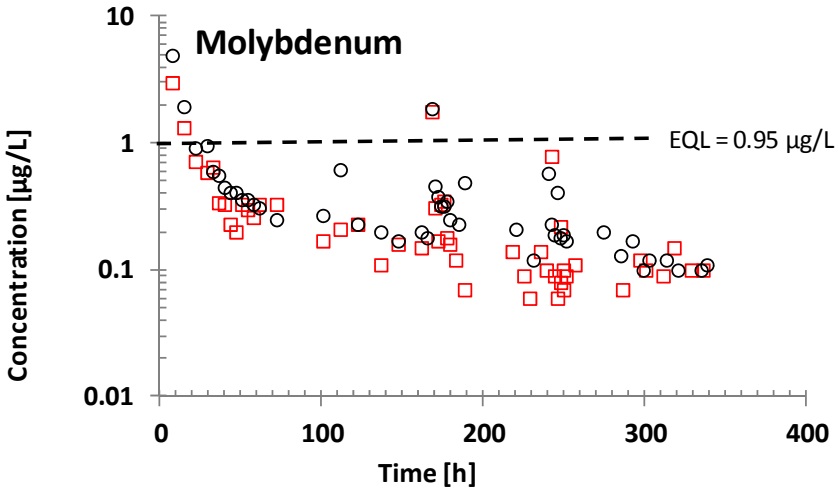

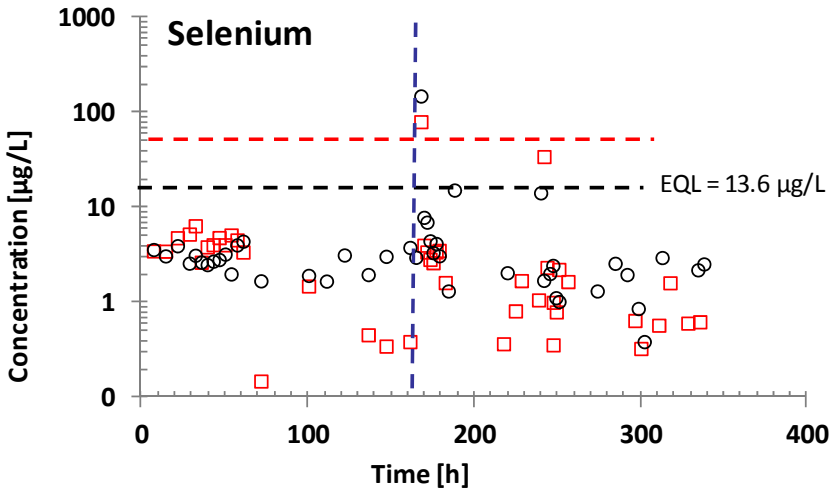

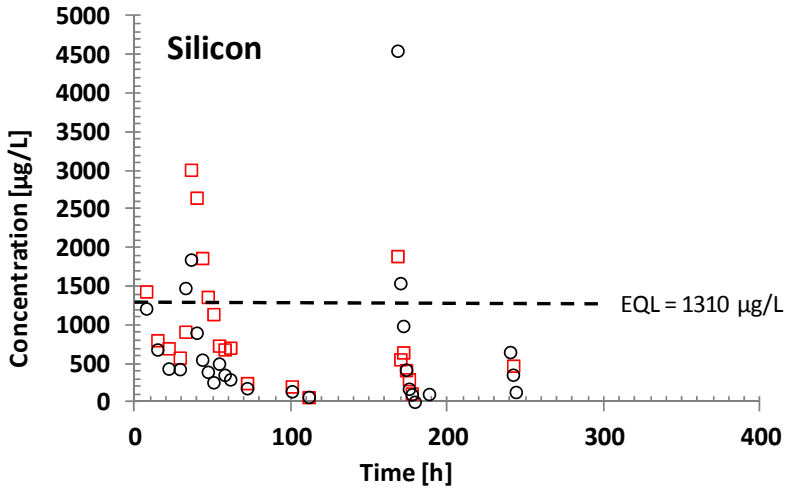

Figure D.35. (contd)

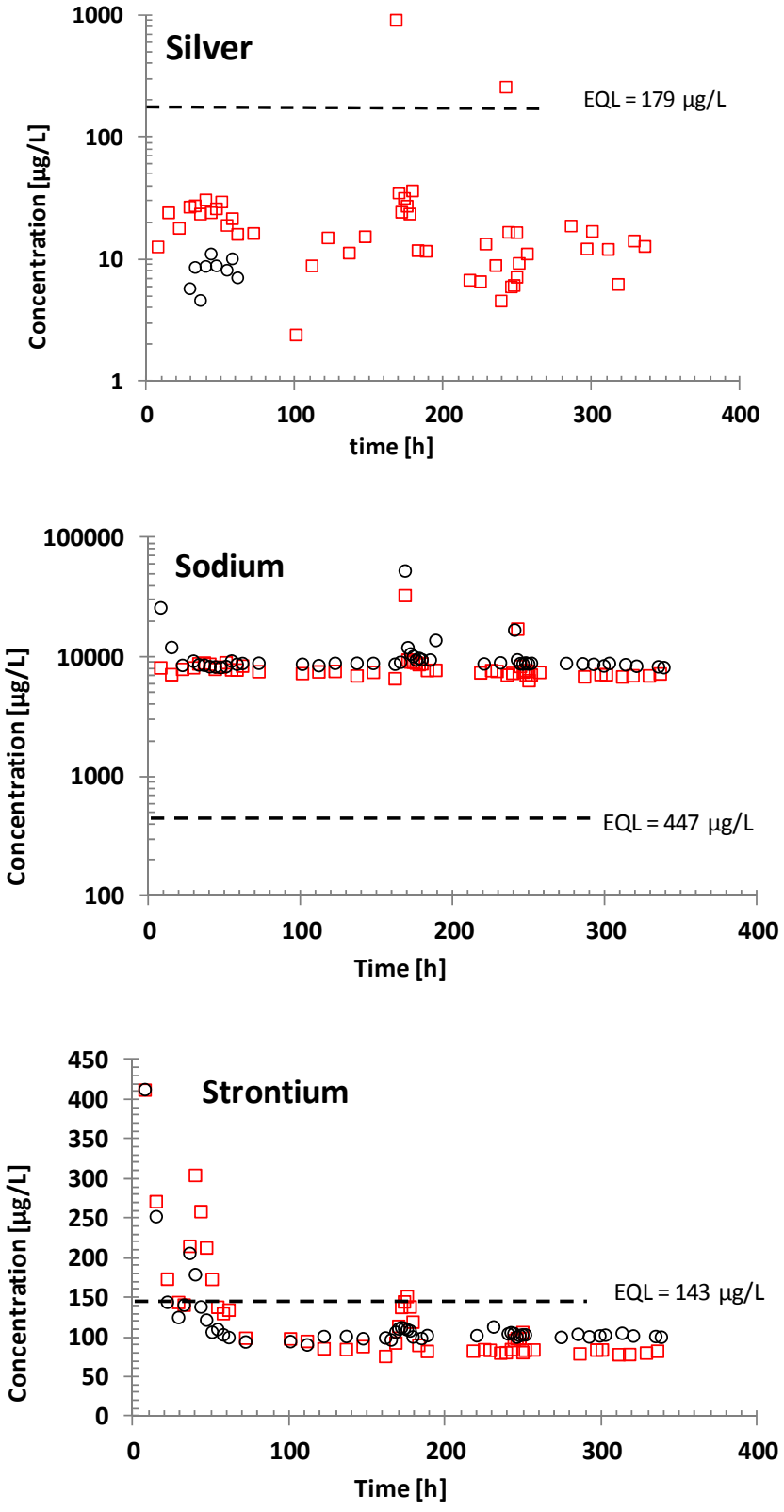

Figure D.35. (contd)

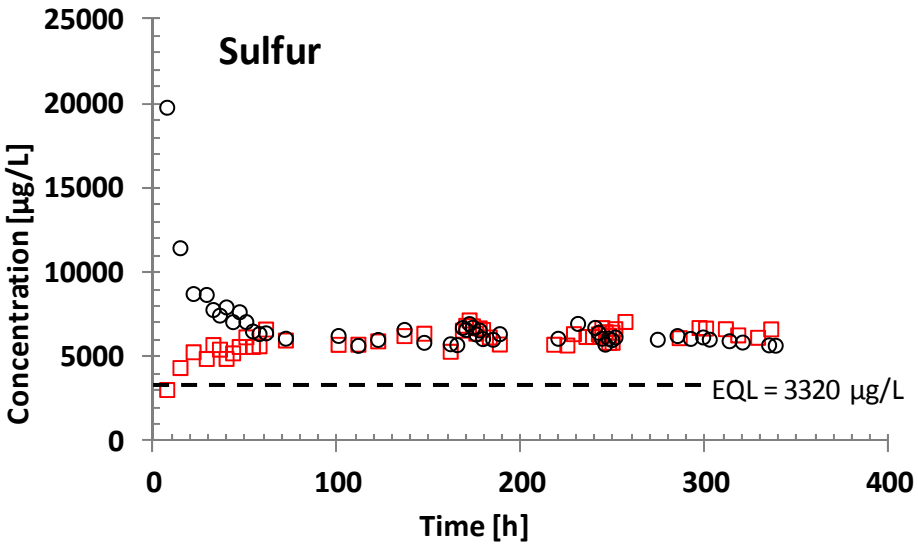

Figure D.35. (contd)

Set 3: Two column experiments conducted with Edward Aquifer Set A, samples 1 (red) and 4 (black)

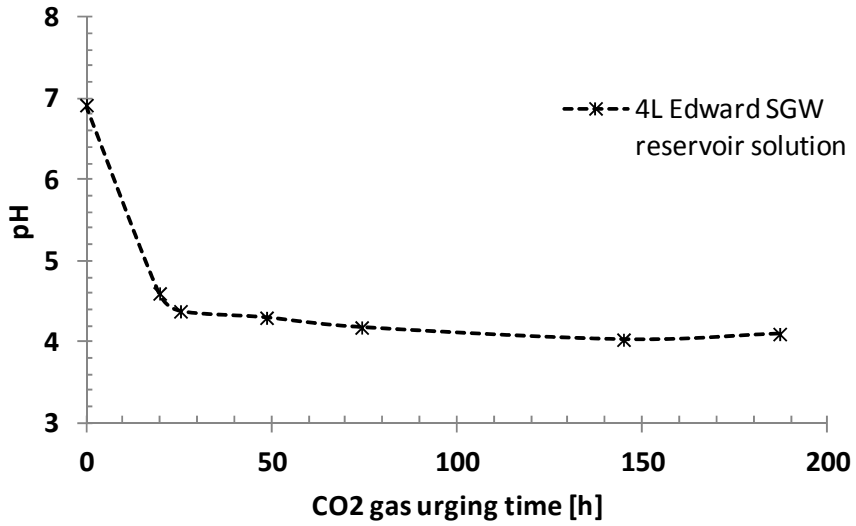

Figure D.36. Changes in SGW pH of the influent 4-L reservoir as a function of time during injection of the CO_2 gas.

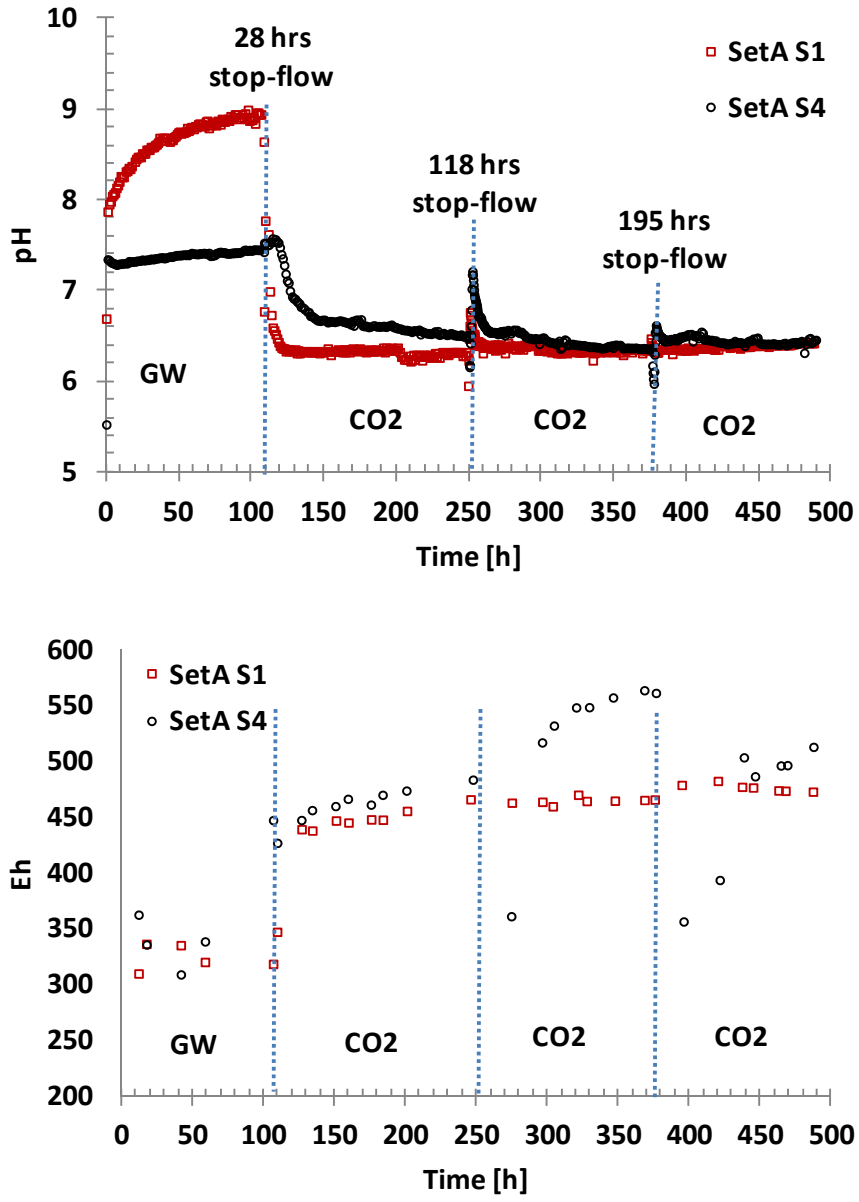

Figure D.37. Changes in effluent pH and Eh as a function of time in two column experiments conducted with Edwards Aquifer materials, Set A, sample 1 (red) and 4 (black). The columns were leached with the SGW for about 110 hours and then the input solution was switched to the CO_2 gas saturated SGW. Two stop-flow events of 118- and 195- hour durations were applied during leaching with the CO_2 saturated SGW.

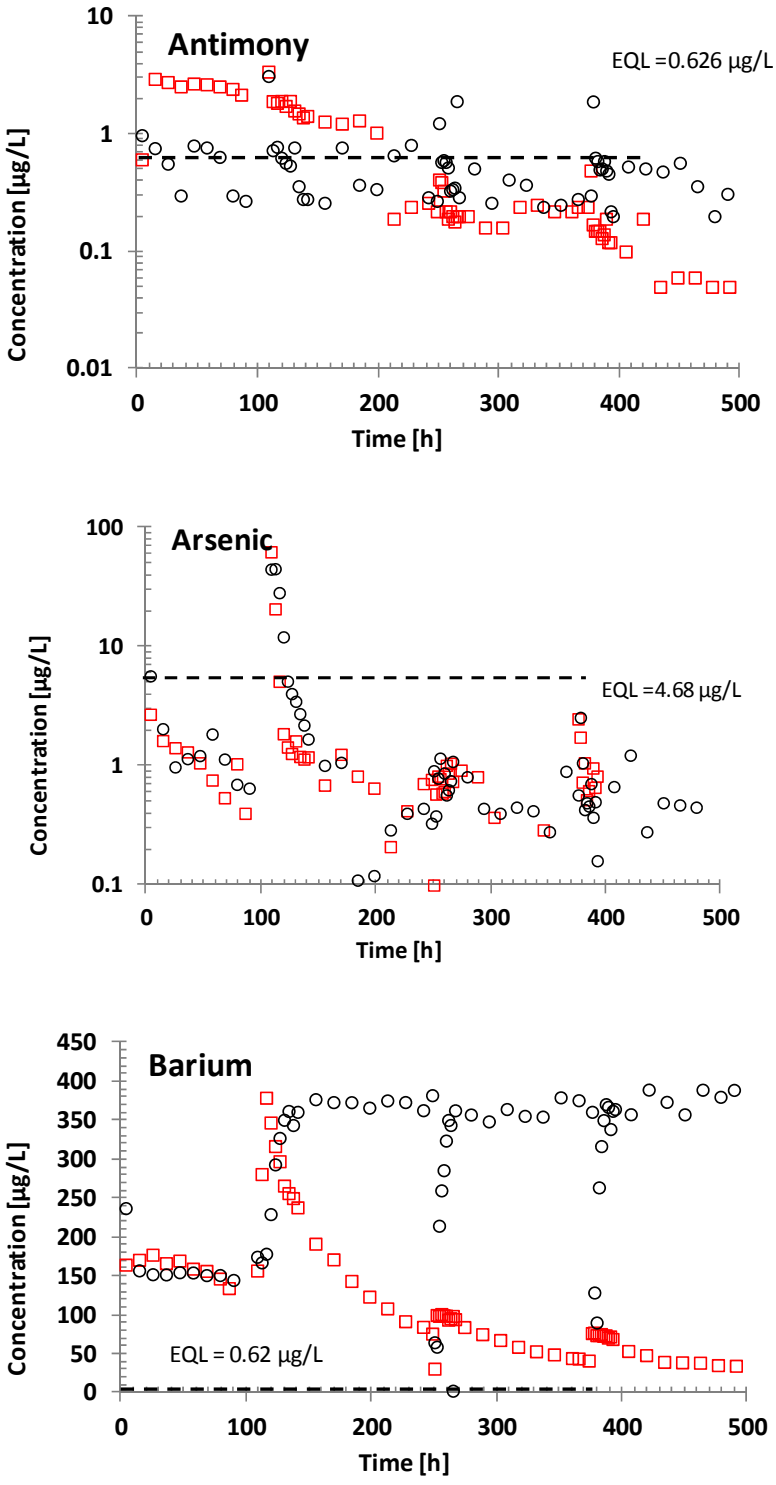

Figure D.38. Changes in effluent elemental composition as a function of time in two column experiments conducted with Edwards Aquifer materials, Set A, sample 1 (red) and 4 (black). The columns were leached with the SGW for about 110 hours and then the input solution was switched to the CO_2 gas saturated SGW. Two stop-flow events of 118- and 195-hour durations were applied during leaching with the CO_2 saturated SGW at 250 and 360 hours of experimental time.

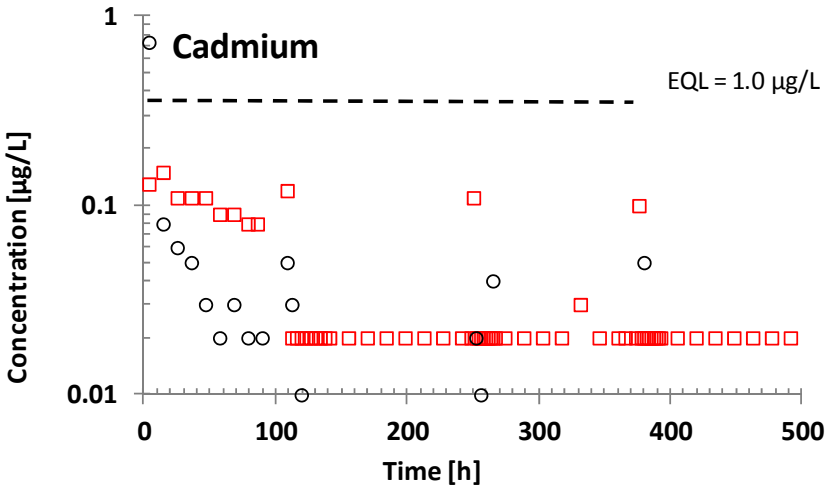

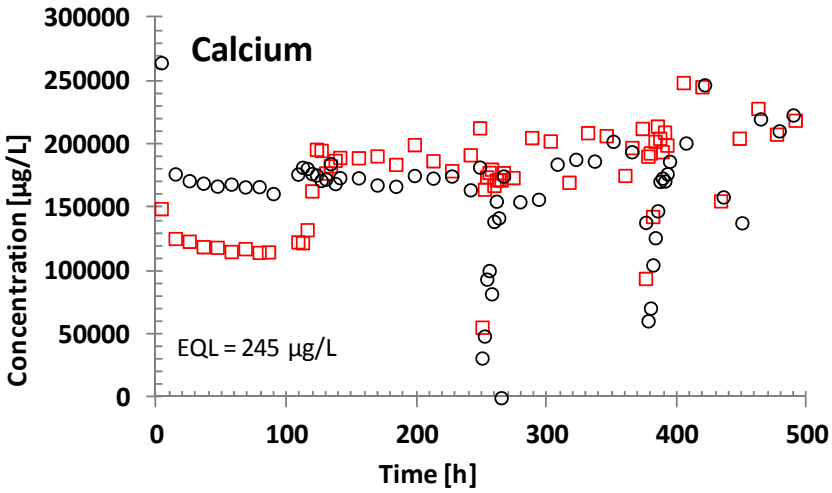

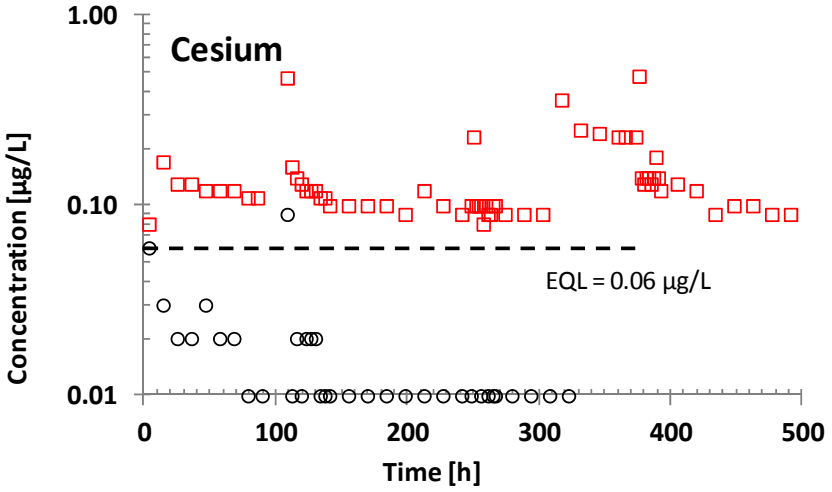

Figure D.38. (contd)

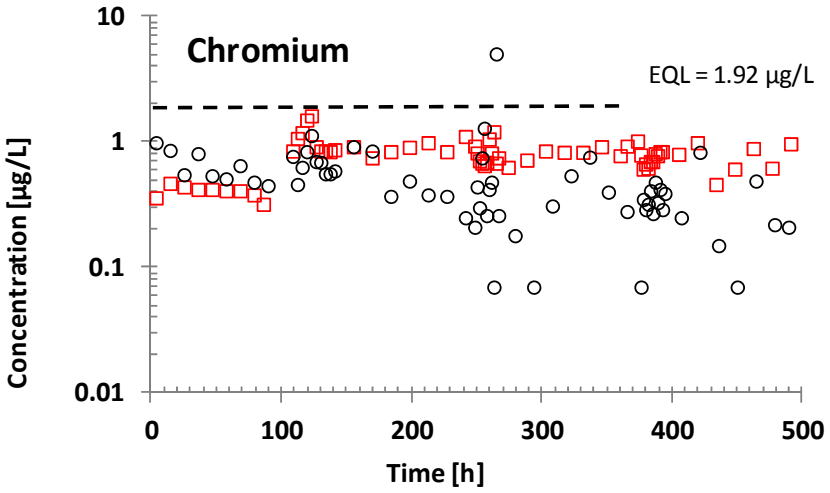

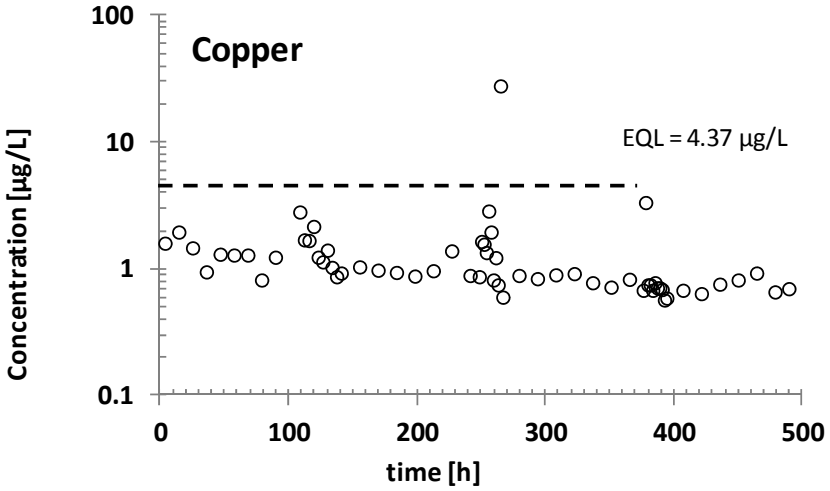

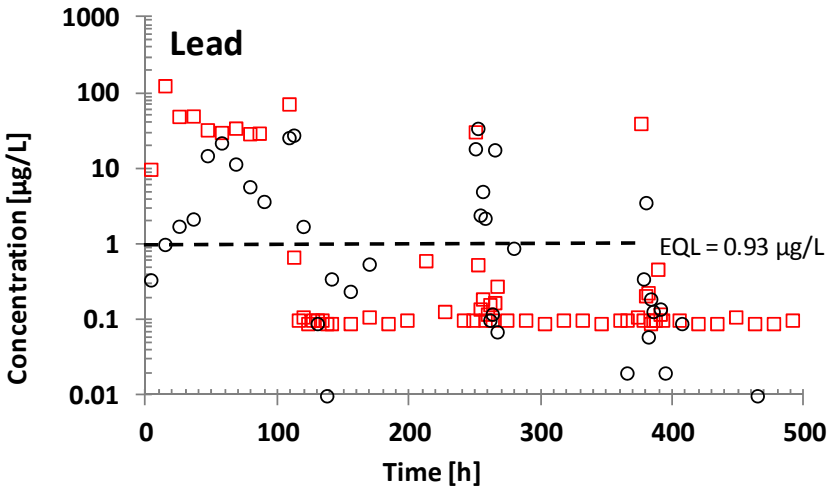

Figure D.38. (contd)

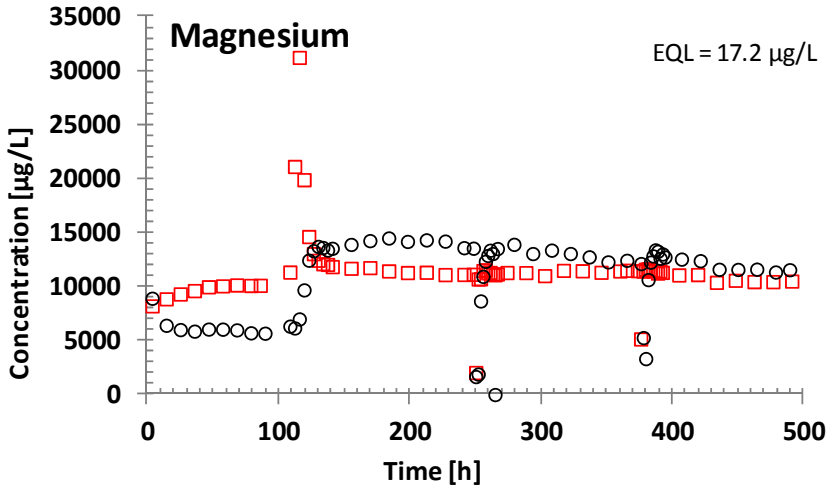

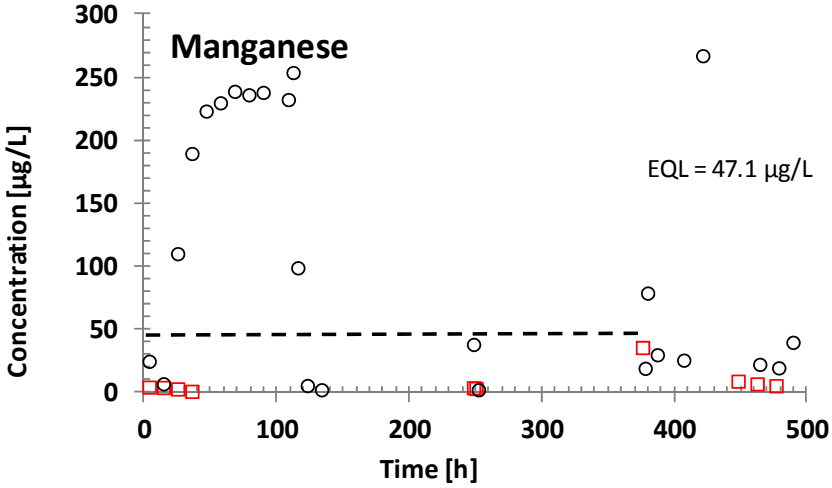

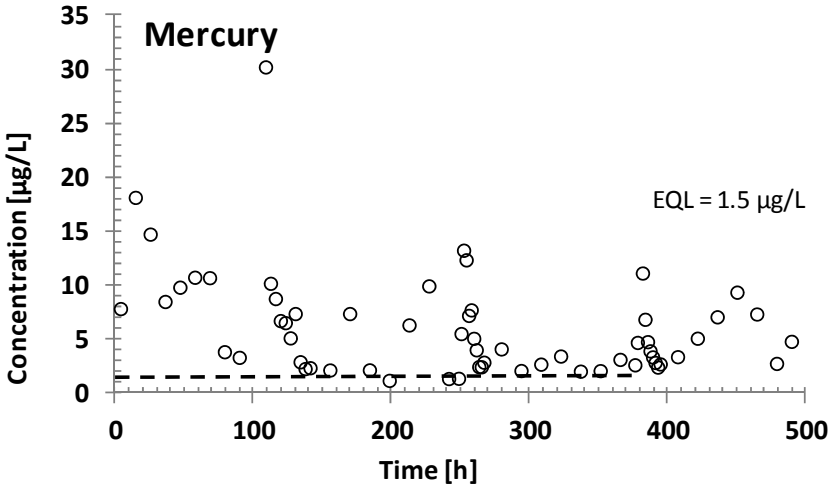

Figure D.38. (contd)

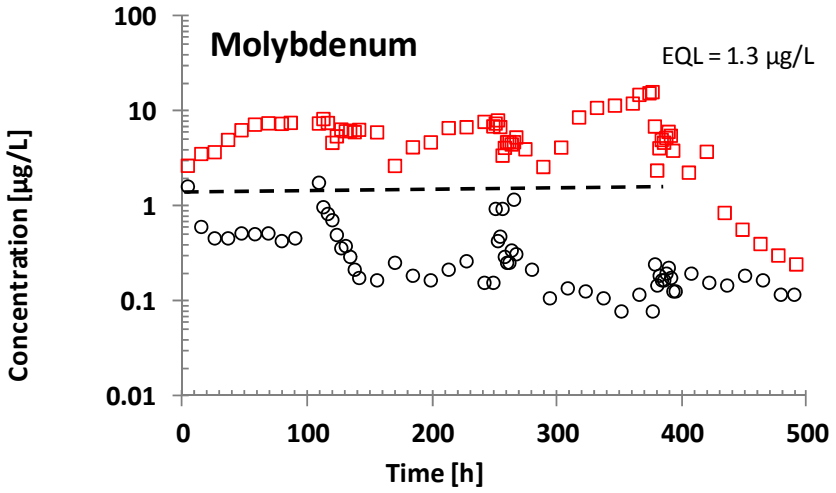

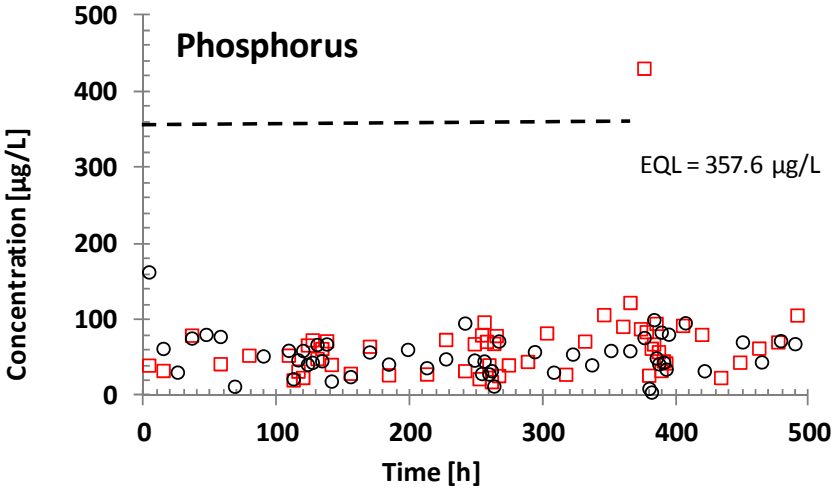

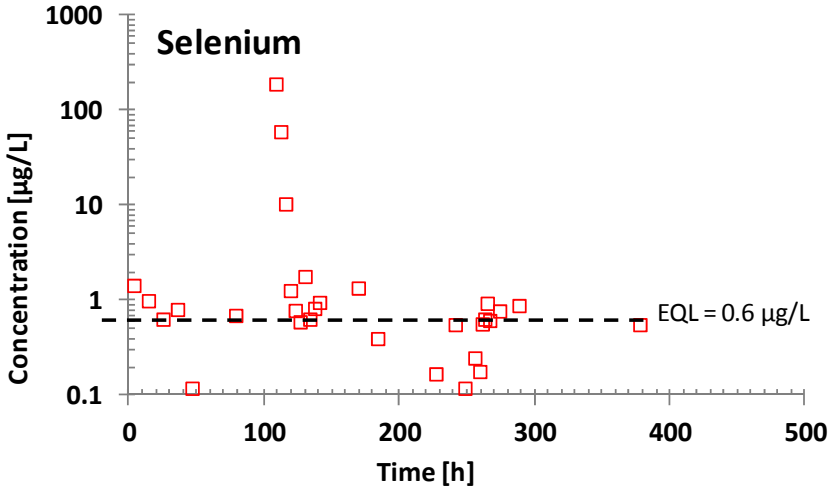

Figure D.38. (contd)

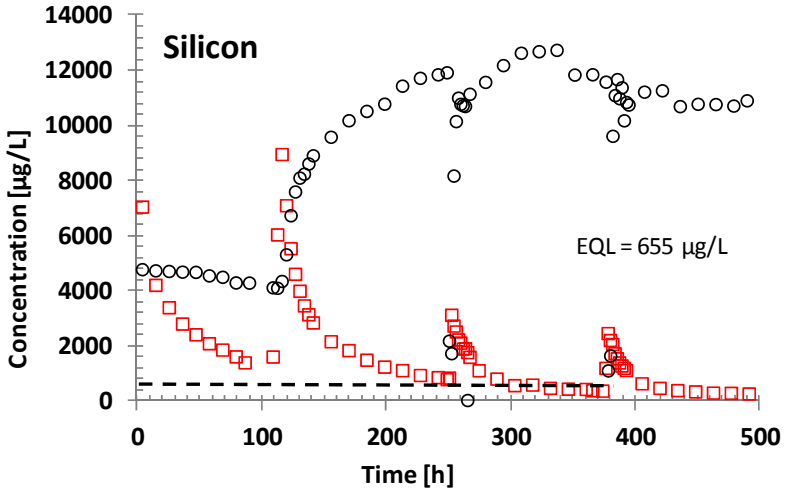

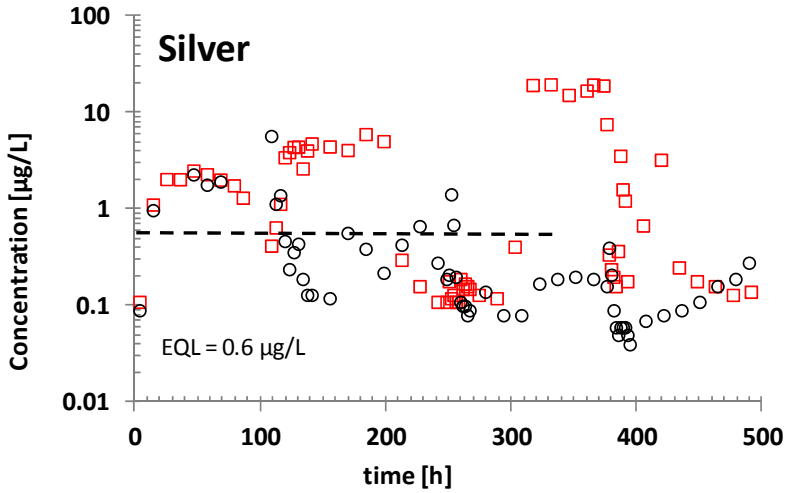

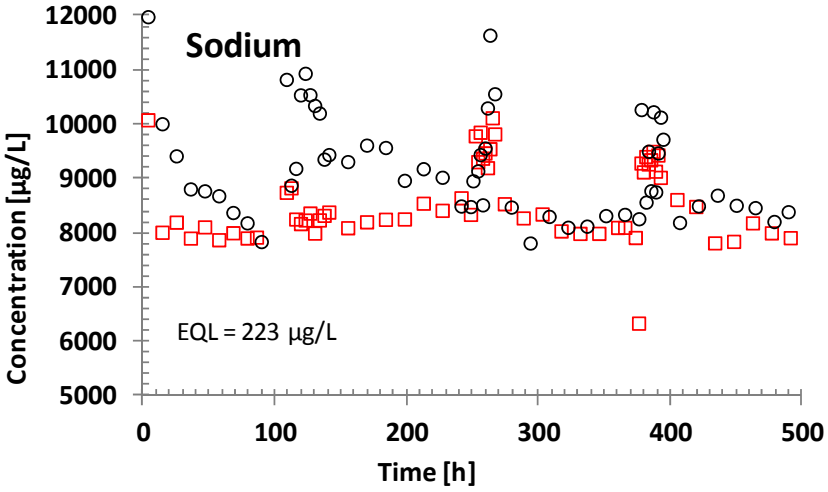

Figure D.38. (contd)

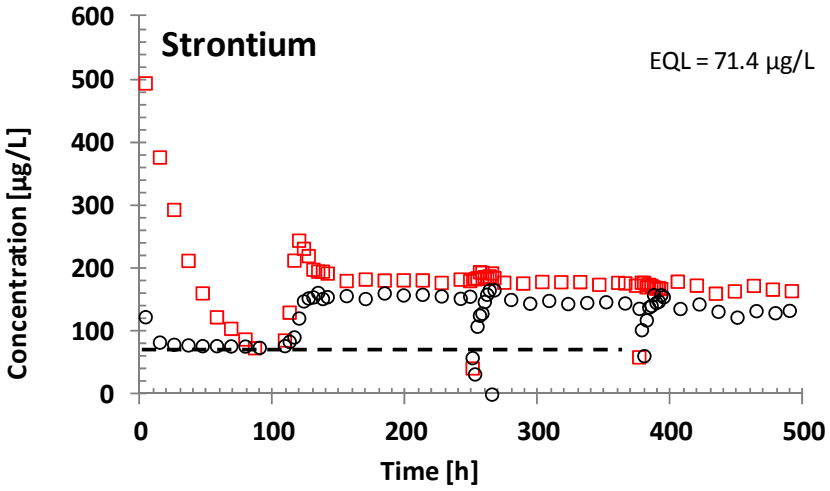

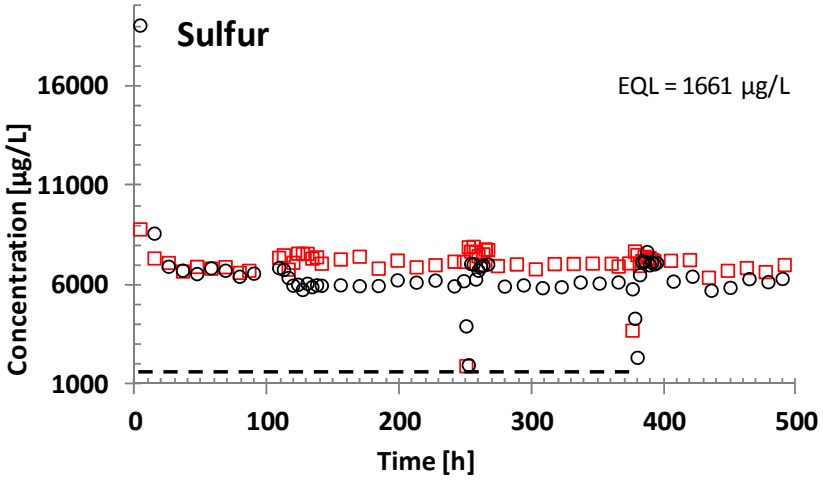

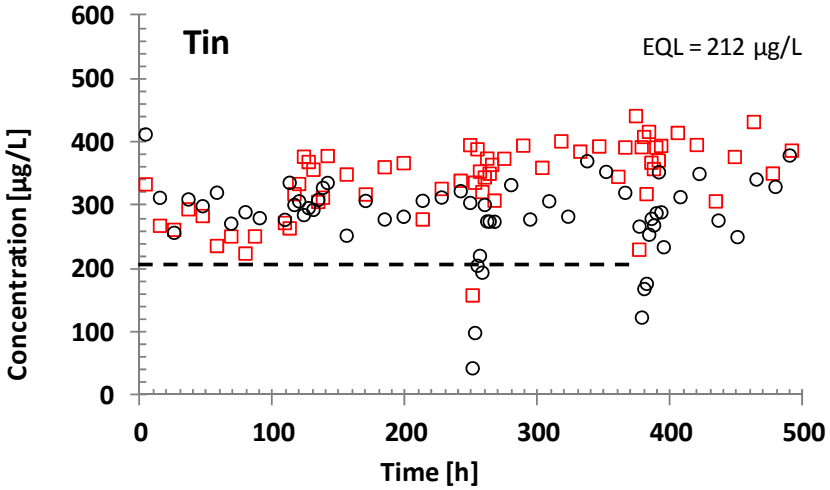

Figure D.38. (contd)

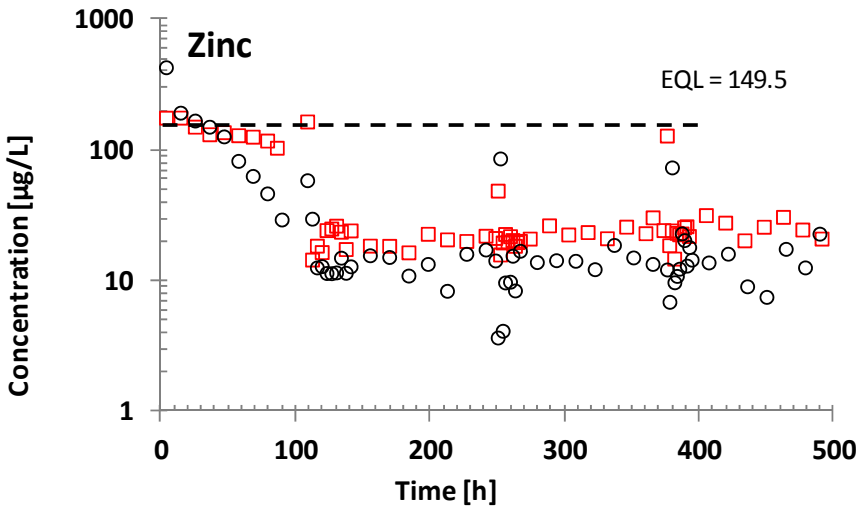

Figure D.38. (contd)

Set 4: Two column experiments conducted with High Plains Aquifer sediments, CNG 110 (black) and CNG 60 (red).

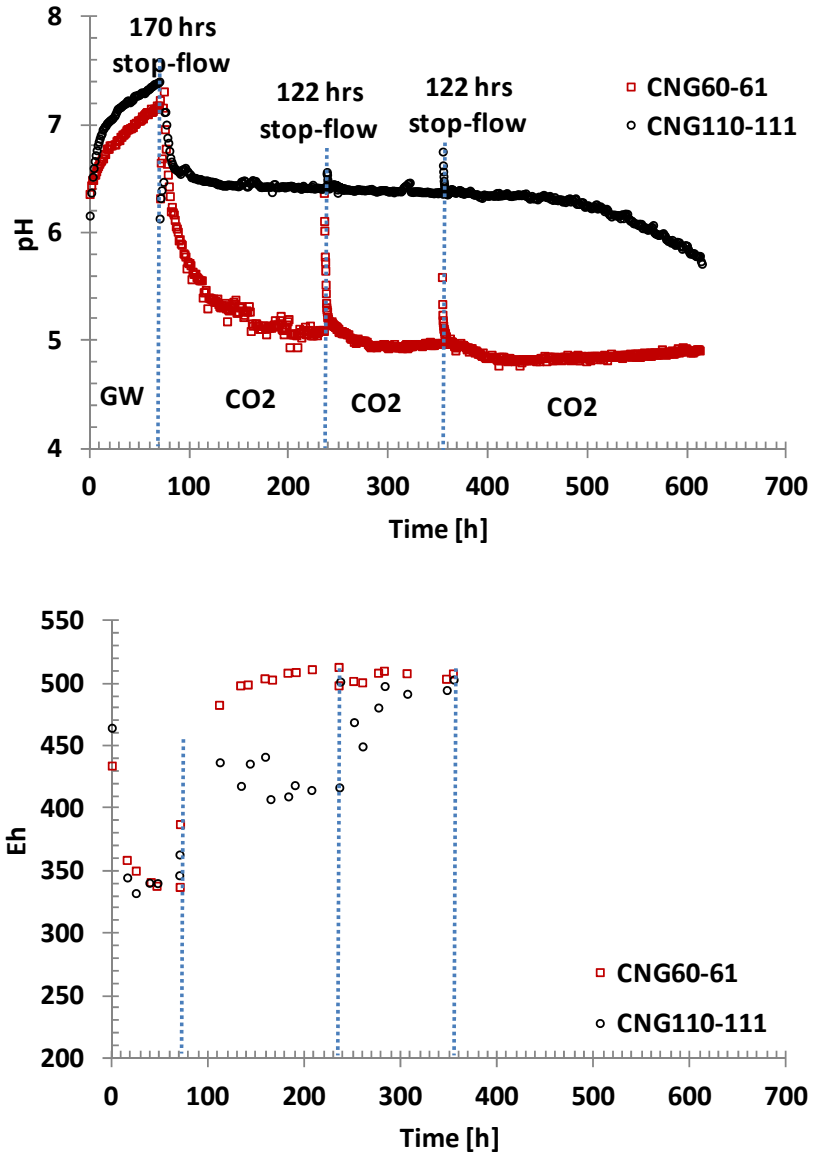

Figure D.39. Changes in effluent pH and Eh as a function of time in two column experiments conducted with the High Plains Aquifer sediments, CNG 110 (black) and CNG 60 (red). The columns were leached with the SGW for about 70 hours and then the input solution was switched to the CO_2 gas saturated SGW. Two stop-flow events of 122- and 122-hour durations were applied during leaching with the CO_2 saturated SGW.

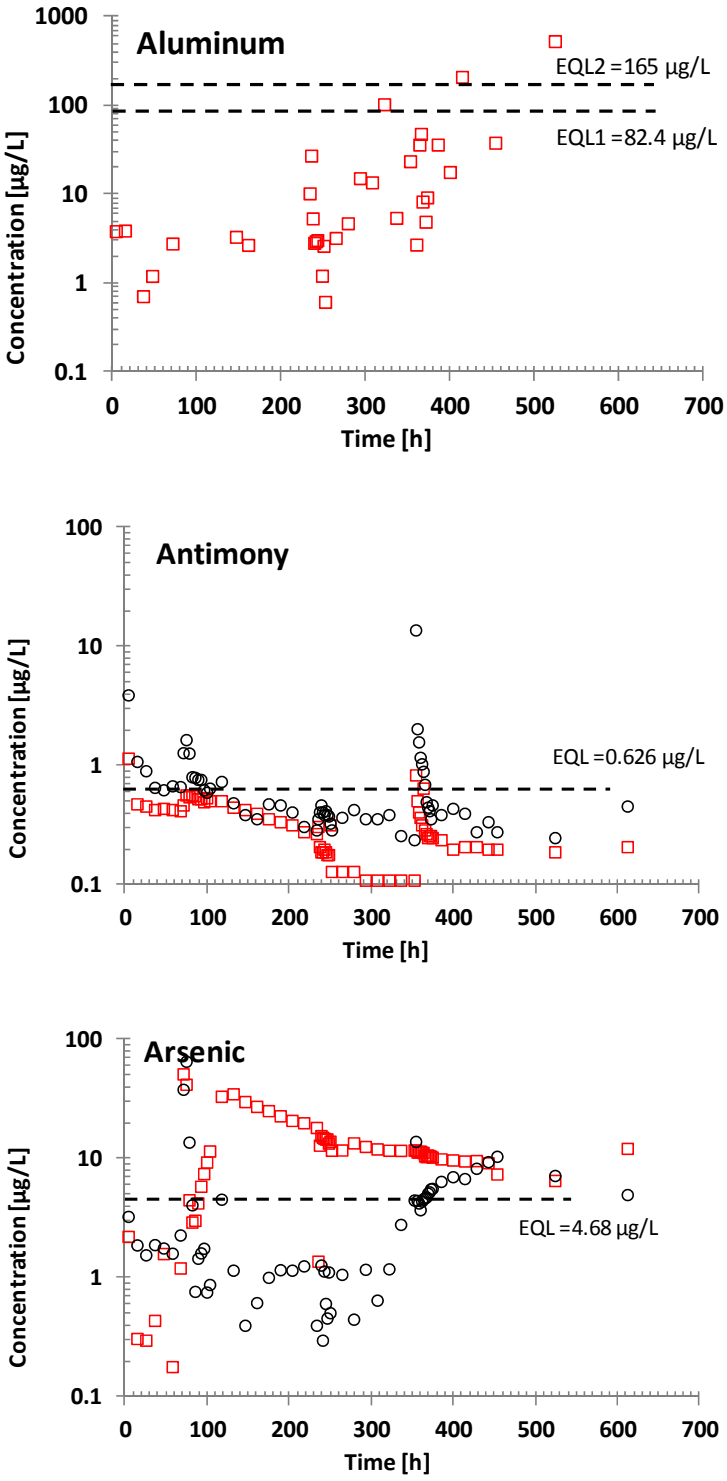

Figure D.40. Changes in effluent chemical composition as a function of time in two column experiments conducted with the High Plains Aquifer sediments, CNG 110 (black) and CNG 60 (red). The columns were leached with the SGW for about 70 hours and then the input solution was switched to the CO_2 gas saturated SGW. Two stop-flow events of 122- and 122-hour durations were applied during leaching with the CO_2 saturated SGW at about 240 and 350 hours of experimental time.

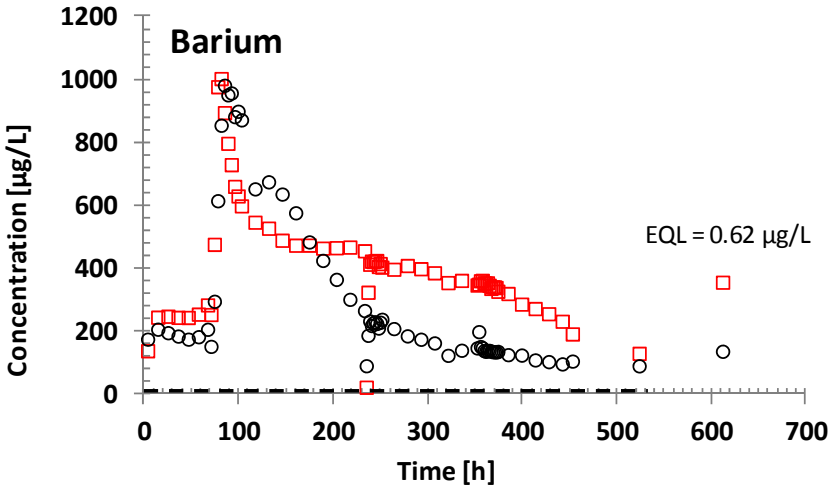

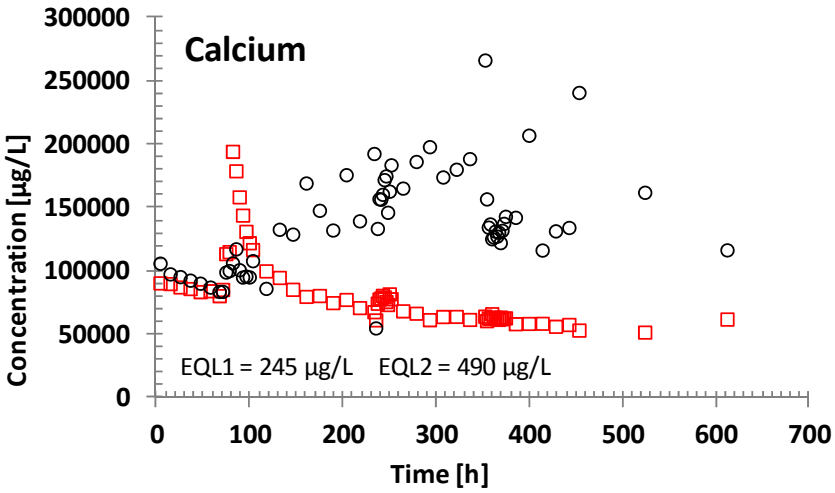

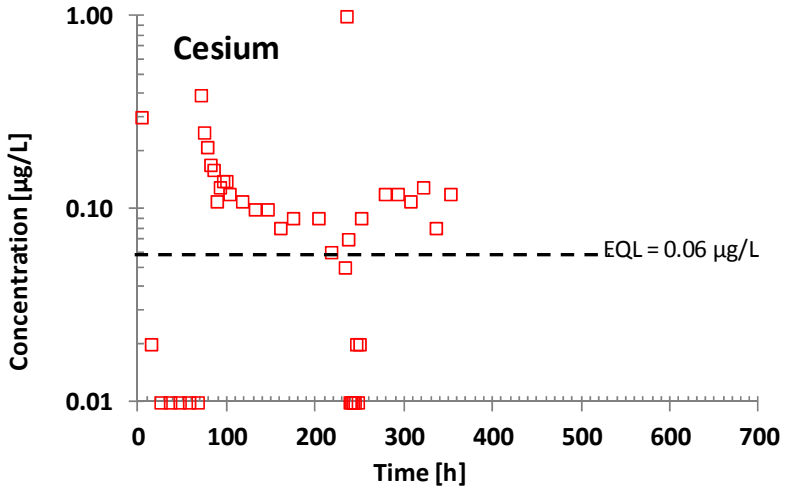

Figure D.40. (contd)

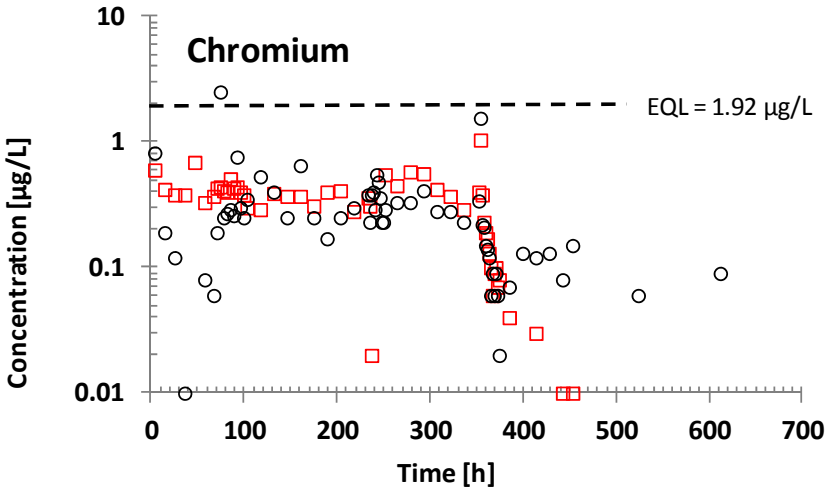

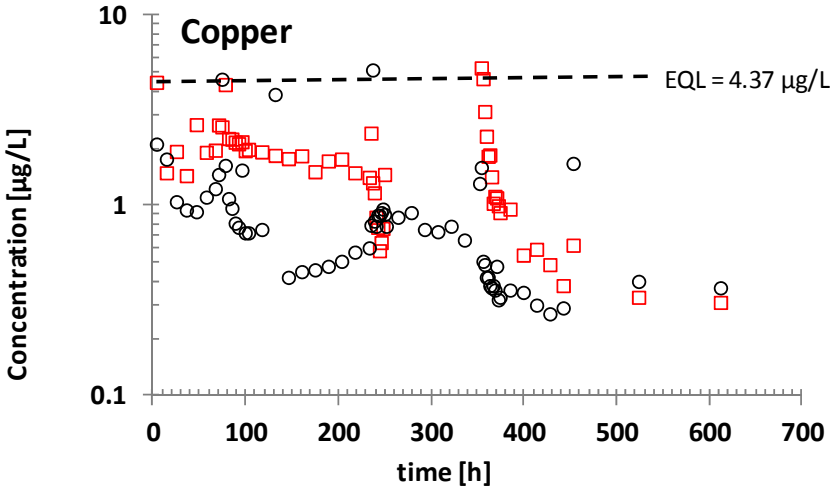

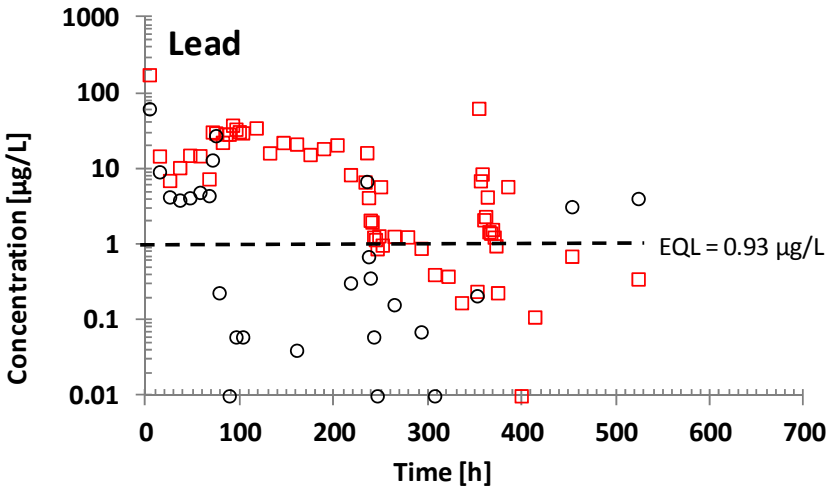

Figure D.40. (contd)

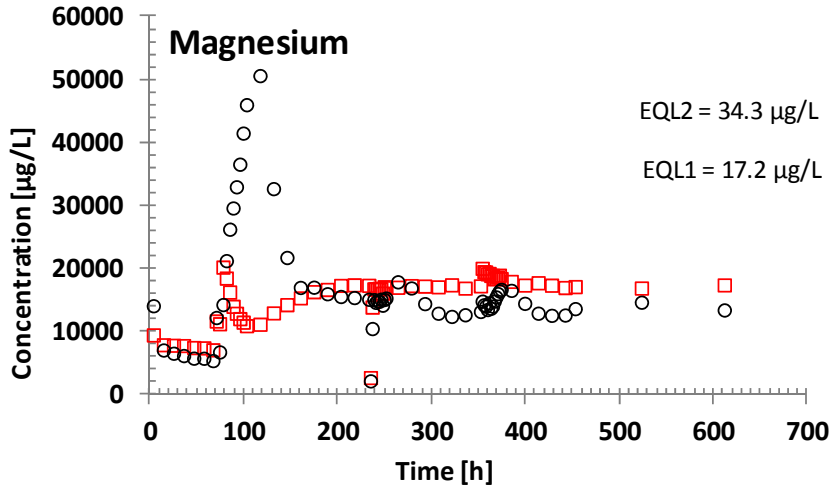

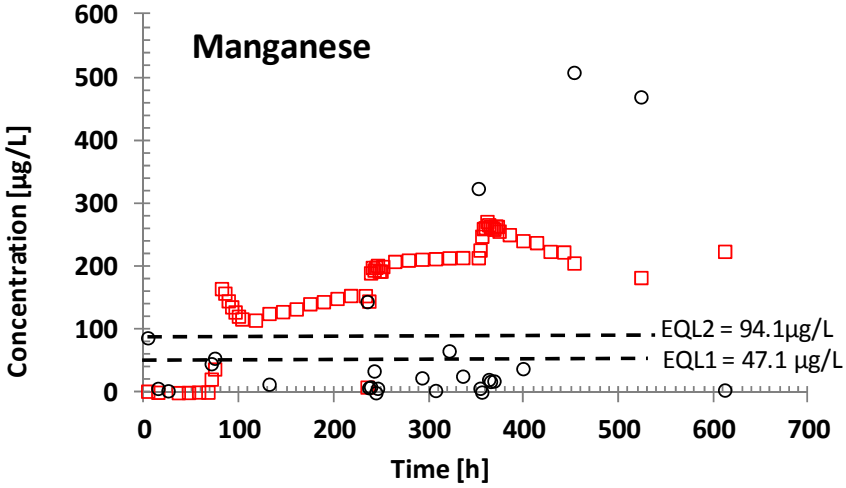

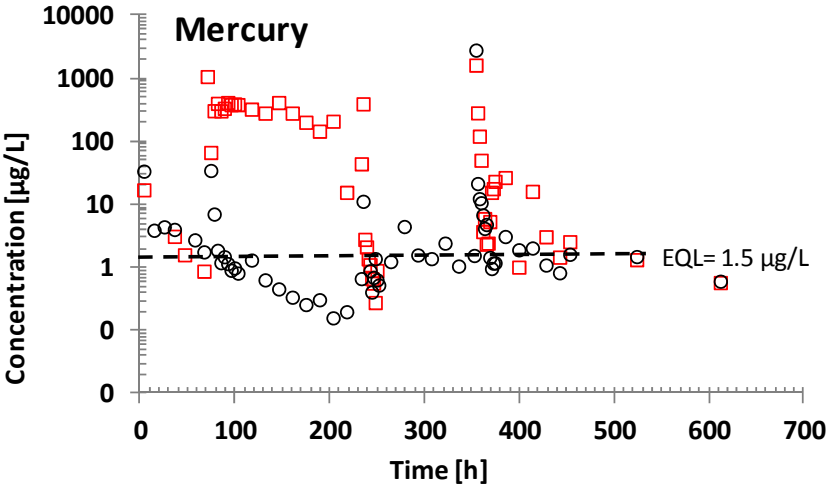

Figure D.40. (contd)

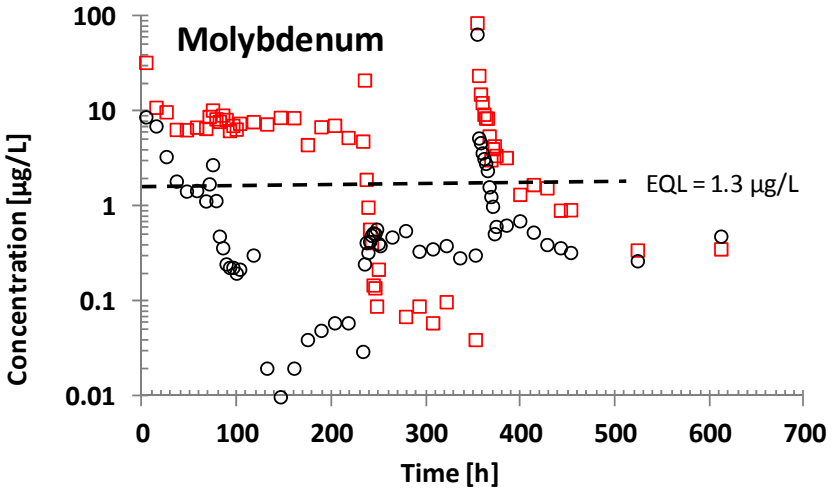

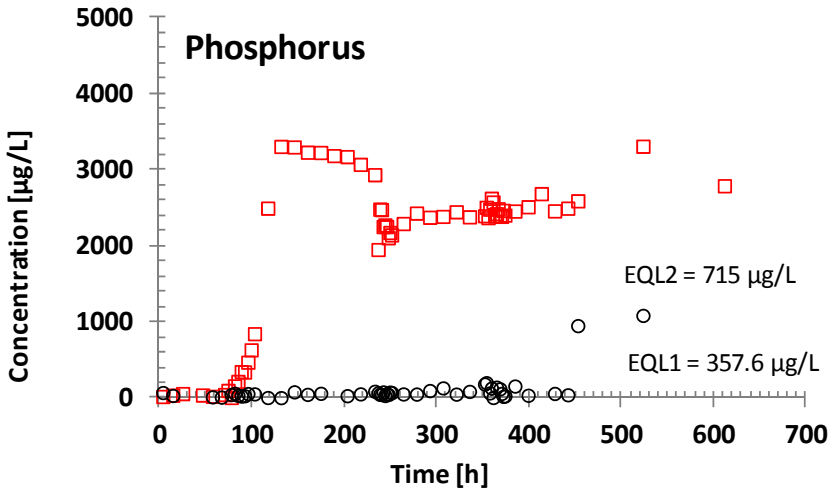

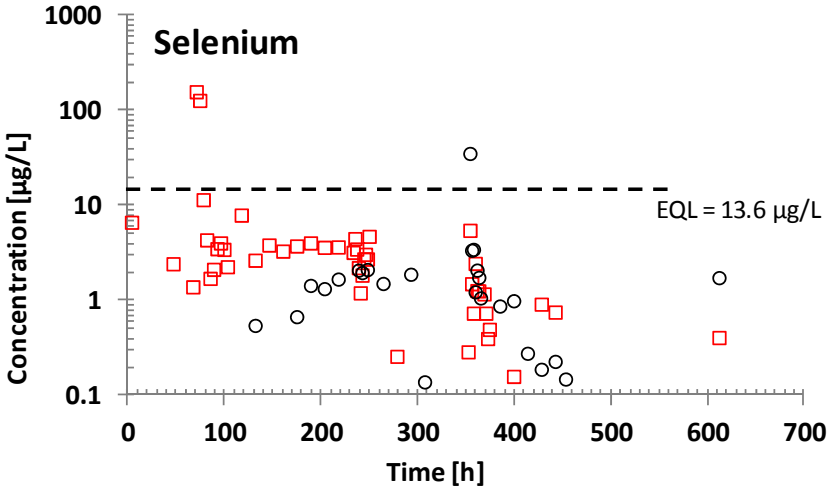

Figure D.40. (contd)

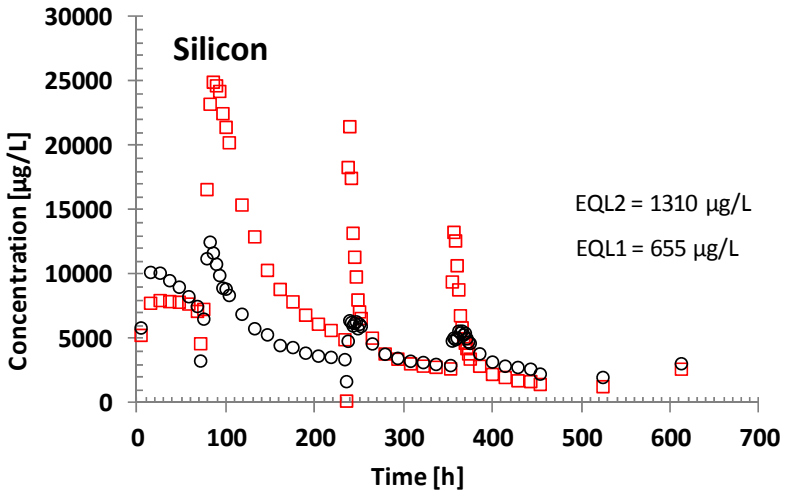

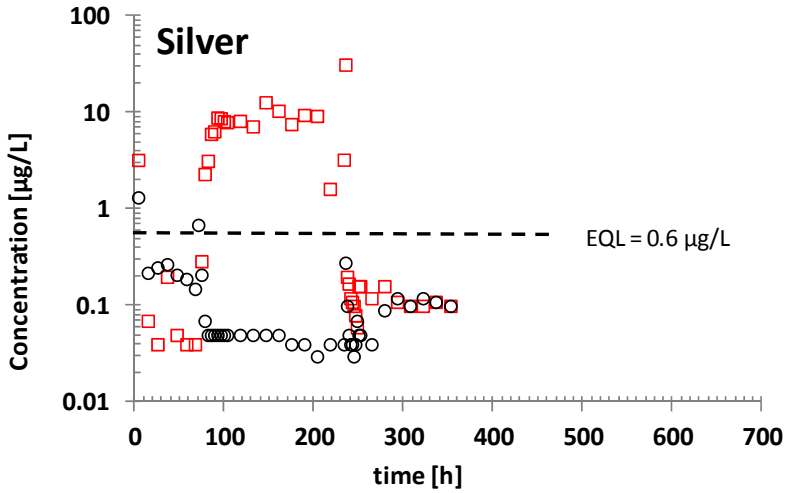

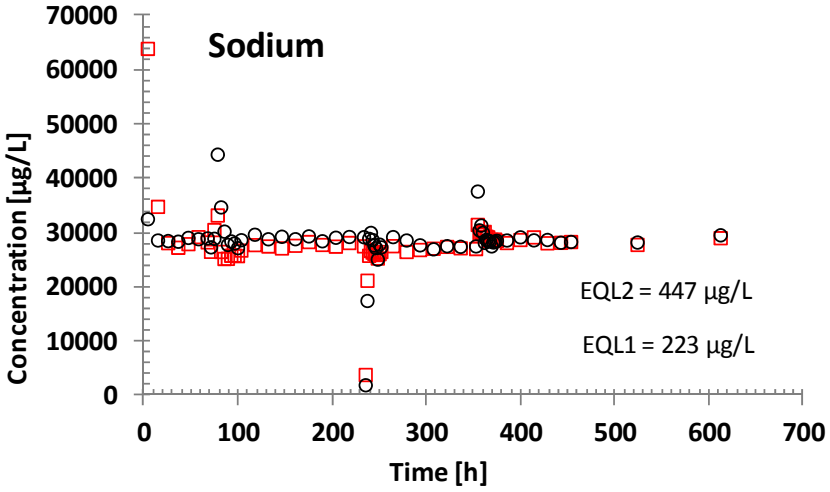

Figure D.40. (contd)

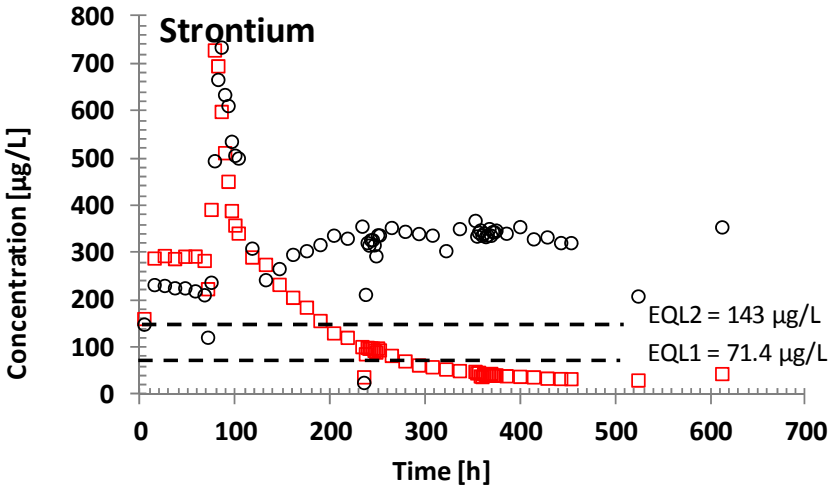

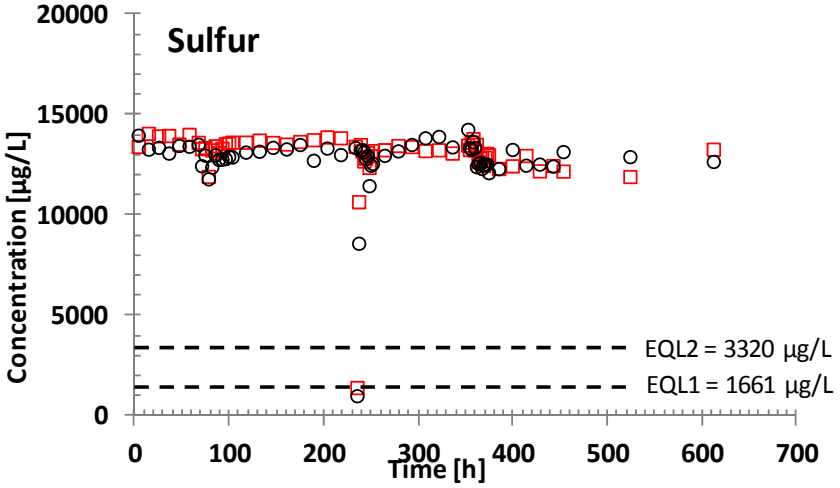

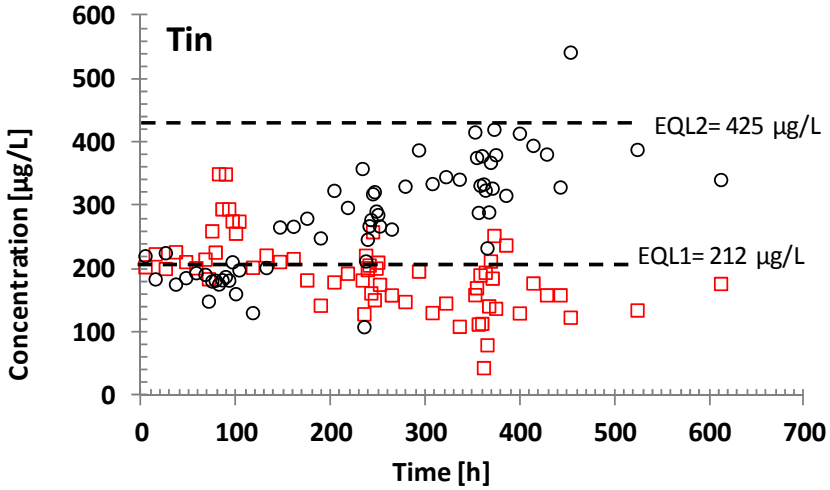

Figure D.40. (contd)

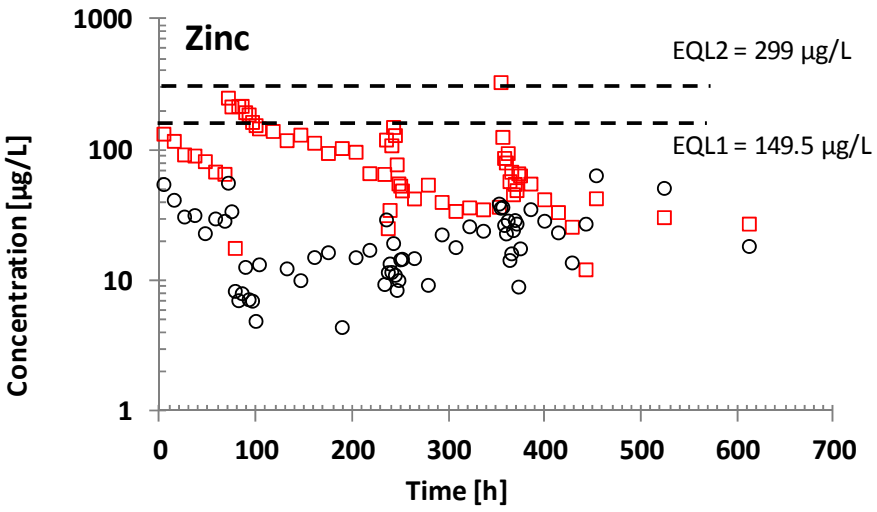

Figure D.40. (contd)

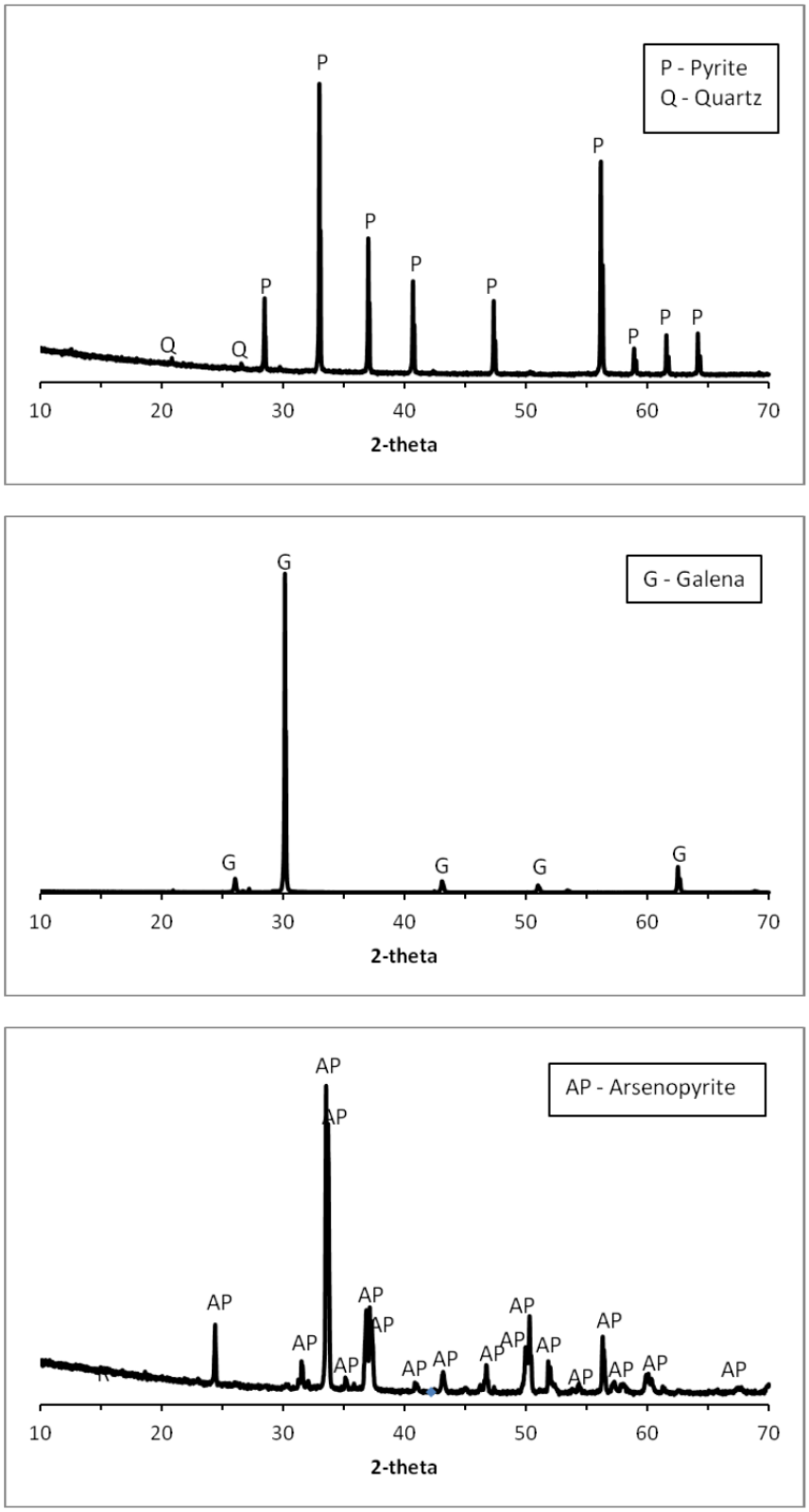

Figure D.41. Mineralogical assessment of the pyrite (FeS_2), arsenopyrite (AsFeS) and galena (PbS) samples used in experiments with microbes. Samples were crushed to a fine powder (under anaerobic conditions) and analyzed by x-ray diffraction.

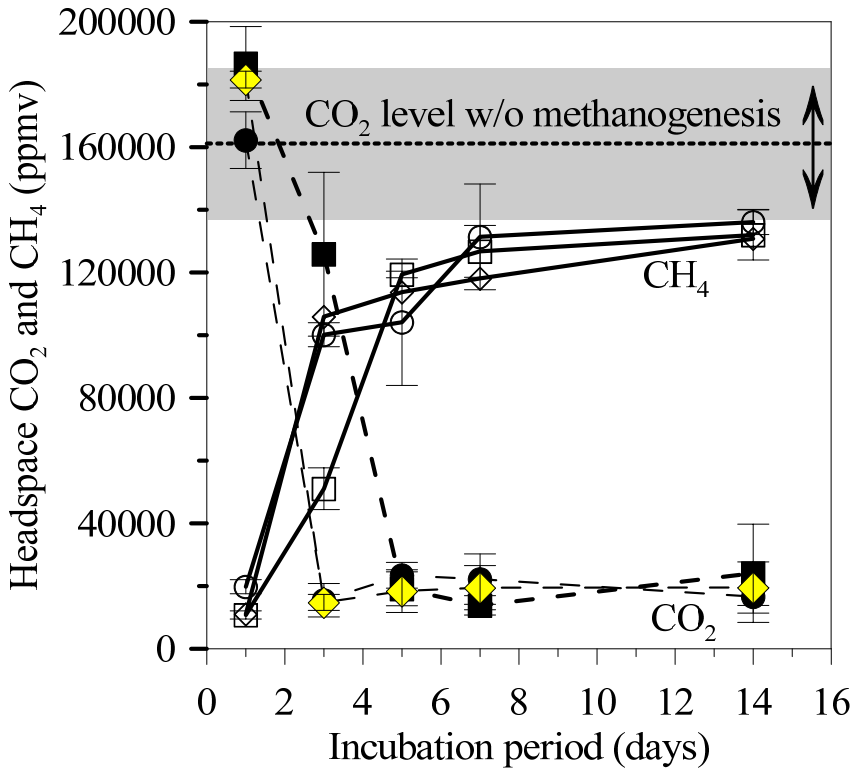

Figure D.42. Concentration of CO_2 (closed symbols) and CH_4 (open symbols) measured in the headspace of methanogen-inoculated treatments with pyrite (circles), arsenopyrite (diamonds), and galena (squares) as the source of metals. Error bars show standard deviation between duplicates and triplicates. Average CO_2 concentration and standard deviation across all uninoculated treatments is depicted by broken line and gray interval, respectively. No CH_4 was measured in uninoculated treatments.

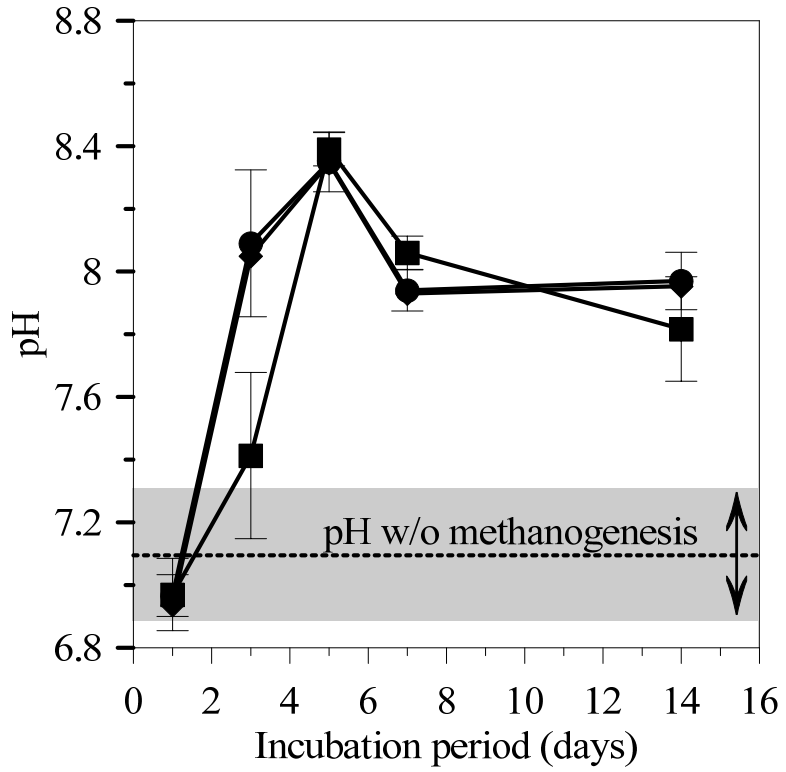

Figure D.43. Changes in solution pH in methanogen-inoculated treatments with pyrite (circles), arsenopyrite (diamonds), and galena (squares) as the source of metals. Error bars show standard deviation between duplicates and triplicates. Average solution pH and standard deviation across all uninoculated treatments is depicted by broken line and gray interval, respectively.

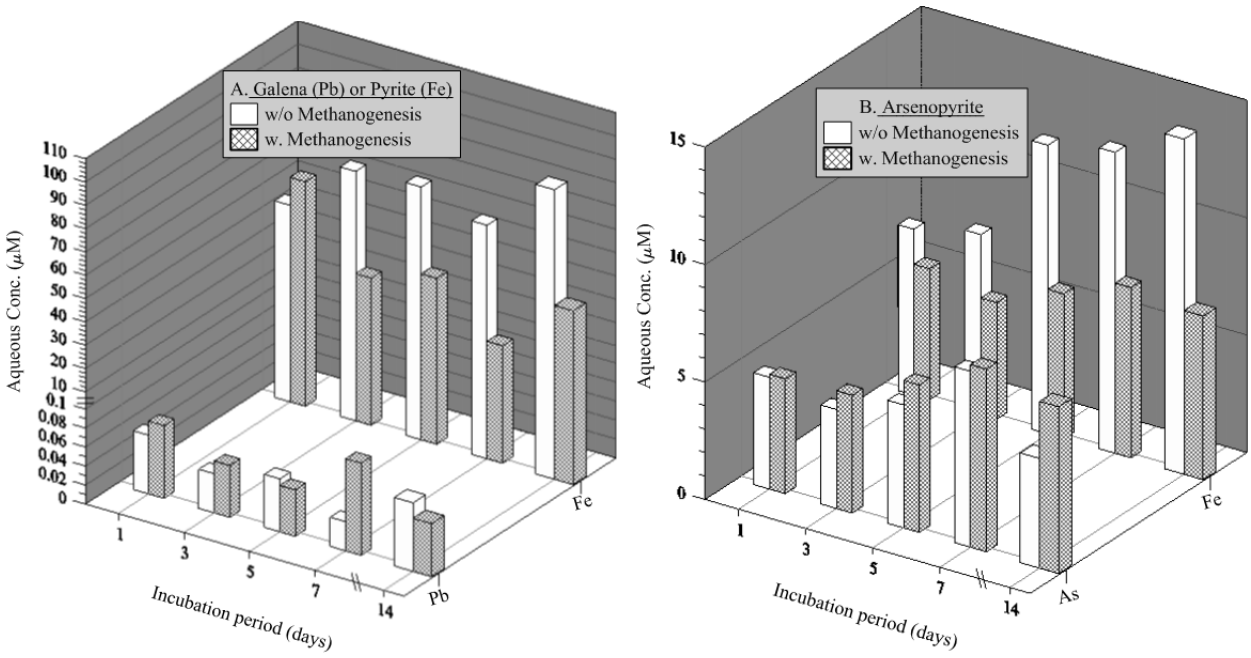

Figure D.44. Aqueous concentrations of Fe, As, and Pb in uninoculated (without methanogenesis – white bars) and methanogen-inoculated (with methanogenesis) treatments. Pyrite, arsenopyrite, and galena were the source of Fe, Fe/As, and Pb, respectively. Values are the average for duplicate or triplicate samples. Standard deviation between samples was within 20% of the respective means.

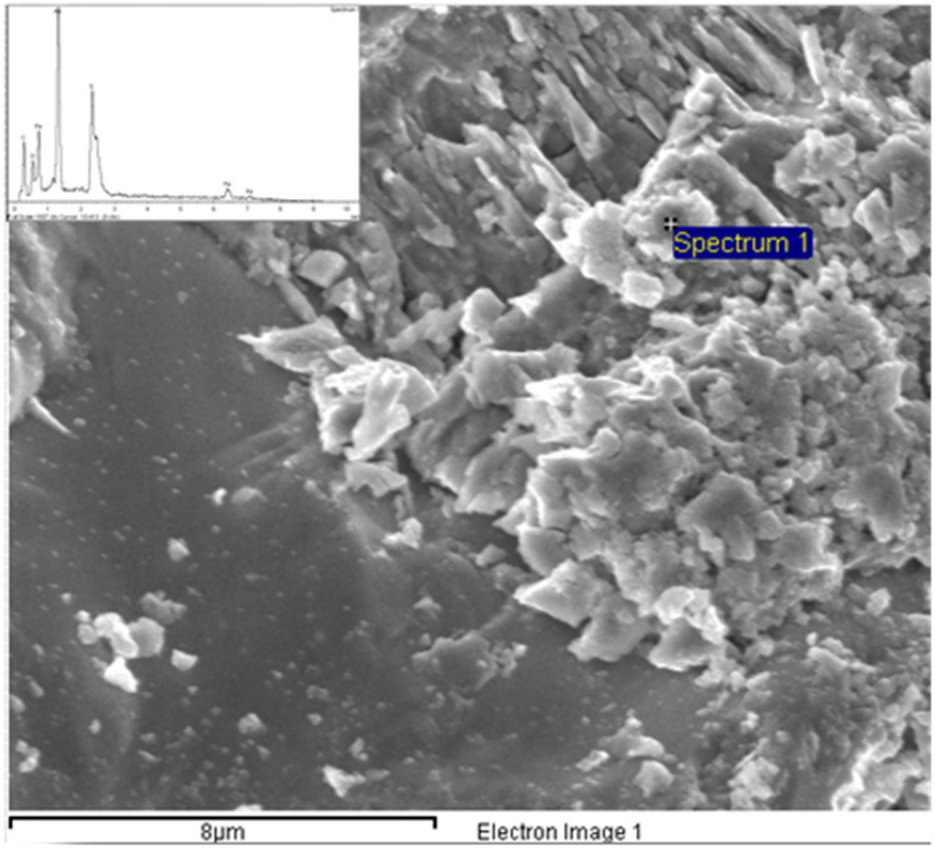

Figure D.45. Methanogenesis-induced precipitation of Fe-rich neophase on FeS_2 surface. Sample was incubated under methanogenic conditions (methanogen + growth solution + H_2/CO_2 headspace) for 14 days. Energy dispersive spectrum (EDS) is shown in the inset.

Pacific Northwest
NATIONAL LABORATORY

Proudly Operated by Battelle *Since 1965*

U.S. DEPARTMENT OF
ENERGY

902 Battelle Boulevard
P.O. Box 999
Richland, WA 99352
1-888-375-PNNL (7665)
www.pnnl.gov